Centro de Investigación y de Estudios Avanzados
del Instituto Politécnico Nacional

Unidad Zacatenco

Departamento de Computación

Nuevos descubrimientos en torno a algoritmos evolutivos multi-objetivo basados en indicadores

T E S I S

Que presenta

Jesús Guillermo Falcón Cardona

Para obtener el grado de

Doctor en Ciencias en Computación

Director de la tesis:

Dr. Carlos Artemio Coello Coello

Ciudad de México Noviembre, 2020

Centro de Investigación y de Estudios Avanzados
del Instituto Politécnico Nacional

Zacatenco Campus

Computer Science Department

New Findings on Indicator-based Multi-Objective Evolutionary Algorithms

Submitted by

Jesús Guillermo Falcón Cardona

as the fulfillment of the requirement for the degree of

Ph.D. in Computer Science

Advisor

Dr. Carlos Artemio Coello Coello

Mexico, Mexico City November 2020

Resumen

Los indicadores de calidad (ICs) son funciones que le asignan un valor real a un conjunto que representa una aproximación a un frente de Pareto generado por un optimizador multi-objetivo, dependiendo de propiedades de calidad específicas. En la comunidad de optimización evolutiva multi-objetivo, los ICs han sido principalmente empleados en dos maneras: (1) para la evaluación de algoritmos evolutivos multi-objetivo (AEMOs), y (2) para guiar el proceso evolutivo de AEMOs, siendo el componente principal de sus mecanismos de selección. Con respecto al primer caso, una de las líneas de investigación más importantes ha sido la búsqueda de nuevos ICs unarios que midan la convergencia hacia el frente de Pareto y que tengan la propiedad de Pareto-compatibilidad, es decir, que sus preferencias sean compatibles con la relación de dominancia de Pareto que es el criterio típicamente empleado al resolver problemas de optimización multi-objetivo (POMs). Actualmente, el indicador de hipervolumen y sus variantes son los únicos ICs unarios Pareto-compatibles. Por otra parte, los ICs han promovido el diseño de nuevos esquemas de selección que permitan a los AEMOs incrementar su presión de selección para resolver POMs que tengan más de tres funciones objetivo (los denominados problemas de optimización con muchos objetivos) y para generar aproximaciones a los frentes de Pareto con diversas distribuciones de soluciones debido a las preferencias específicas de los ICs.

Recientemente, se ha enfatizado que el desempeño de algunos AEMOs del estado del arte depende de la forma del frente de Pareto del POM a resolverse. Desafortunadamente, los mecanismos de búsqueda de estos AEMOs están sobre-especializados para resolver problemas de prueba cuyos frentes de Pareto están altamente correlacionados con la forma de un simplex. En consecuencia, es necesario diseñar AEMOs cuyo desempeño sea invariante a la forma del frente de Pareto.

Esta tesis está enfocada en tratar el problema de dependencia de los AEMOs a las geometrías de los frentes de Pareto y el diseño de nuevos ICs Pareto-compatibles. Con respecto a la dependencia a la forma de los frentes, se propone el uso de múltiples mecanismos de selección basados en indicadores bajo dos esquemas principales: competición y cooperación. La idea subyacente de ambos esquemas es superar las debilidades de un mechanismo de selección basado en un indicador con las fortalezas de otros. Al combinar múltiples mecanismos de selección basados en indicadores se mostró a través de diversas propuestas que es posible generar aproximaciones a los frentes de Pareto con buenas propiedades de convergencia y diversidad, independientemente de la forma geométrica del frente, usando los esquemas competitivo y cooperativo. Por otra parte, se propuso la combinación matemática de uno o más ICs debilmente Pareto-compatibles con al menos uno que sea Pareto-compatible, dando como resultado un nuevo indicador Pareto-compatible. Esta propuesta permite incrementar el número de ICs Pareto-compatibles disponibles para ser usados tanto en la evaluación de AEMOs como en sus mecanismos de selección.

Abstract

Quality indicators (QIs) are set functions that assign a real value to a set that represents the Pareto front approximation generated by a multi-objective optimizer, depending on specific quality properties. In the evolutionary multi-objective optimization community, QIs have been mainly employed in two ways: (1) for the assessment of multi-objective evolutionary algorithms (MOEAs), and (2) to guide the evolutionary process of MOEAs, being the backbone of selection mechanisms. Concerning the former case, one of the most important research paths has been the finding of new unary QIs that measure convergence towards the Pareto front, having the Pareto-compliance property, i.e., their preferences should be compliant with the Pareto dominance relation which has been the typical optimality criterion when solving multi-objective optimization problems (MOPs). Currently, the hypervolume indicator and its variants are the only known unary QIs Pareto-compliant. On the other hand, QIs have promoted the design of new selection mechanisms that allow MOEAs to increase their selection pressure to solve MOPs having more than three objective functions (the so-called many-objective optimization problems) and to generate Pareto front approximations with different distribution properties due to the inner preferenes of QIs.

Some studies have stressed out that the performance of some state-of-the-art MOEAs depends on the Pareto front shape of the MOPs being tackled. Unfortunately, the search mechanisms of these MOEAs are overspecialized to solve benchmark problems with Pareto front shapes highly correlated with the shape of a simplex. In consequence, it is necessary to design MOEAs whose performance is invariant to the Pareto front shape.

In this thesis, we focus on tackling the Pareto front shape dependence of MOEAs and the design of new Pareto-compliant QIs. Regarding the shape dependence, we propose to use multiple indicator-based selection mechanisms under competitive and cooperative schemes. The underlying idea of both schemes is to overcome the weaknesses of an indicator-based selection mechanism with the strengths of the others. When combining multiple indicator-based selection mechanisms, we showed through different proposals that it is possible to generate Pareto front approximations having good convergence and diversity, regardless of the geometrical shape, using both the competitive and the cooperative approaches. On the other hand, we proposed the mathematical combination of one or more weakly Pareto-compliant QIs with at least one Pareto-compliant indicator to produce new Pareto-compliant QIs. This approach allows to increase the number of Pareto-compliant indicators to be used for the assessment of MOEAs or in their selection mechanisms.

Agradecimientos

Primeramente, quiero agradecer a mis padres, Blanca Estela Cardona Ayala y Guillermo Falcón Pacheco, por todo el amor y apoyo a lo largo de este camino. Aunque ha sido difícil la travesía para lograr el máximo objetivo, siempre conté con ellos incondicionalmente. Es por esto que siempre les estaré agradecido. Sin lugar a dudas, esta tesis es por ustedes.

Quiero hacer una mención muy especial a mi director de tesis, el Dr. Carlos A. Coello Coello. Desde mucho antes de que yo entrara al CINVESTAV supe de él y sabía que quería ser su estudiante. Siempre fue y seguirá siendo una gran inspiración para mi carrera científica. De antemano, le agradezco todo el apoyo que he recibido durante estos cinco años.

Por otra parte, quiero dar las gracias a los doctores Adriana Lara, Saúl Zapotecas, Luis Gerardo de la Fraga, y Amilcar Meneses, quienes formaron el comité sinodal que revisó esta tesis tanto para el examen de grado como en el examen predoctoral. Sus comentarios fueron muy valiosos para mejorar la calidad de esta tesis.

Quiero dedicar unas líneas a mi amigo y hermano Julio César Gómez con quien he tenido una muy larga amistad. En todo momento que lo he necesitado, él siempre ha estado conmigo. Es mi deseo que la vida nos siga dando más años y que vengan más experiencias.

Los días del doctorado siempre fueron muy amenos gracias a la grata compañía de muchas personas en el cúbiculo de doctorado. En especial quiero mencionar a los ya doctores Edgar Manoatl, Miriam Pescador, Adrián Sosa, Carlos Henández, y Raquel Hernández. Disfruté mucho las experiencias vividas en el CINVESTAV así como en los congresos donde compartimos momentos.

No quiero olvidar el apoyo de Sofia Reza, Erika Ríos, y Felipa Rosas quienes me ayudaron en todos los trámites para poder asistir a los diversos congresos y estancias de investigación que realicé. Muchas gracias.

Agradezco al CINVESTAV-IPN y al CONACyT por los diversos apoyos económicos para la realización de mis estudios doctorales. Hago una mención especial al CONACyT por la beca de estudios (con número de becario 462466) que me fue asignada. Sin este apoyo económico no hubiese sido posible concluir mis estudios doctorales de forma satisfactoria.

Esta tesis fue derivada de los proyectos titulados "Esquemas de Selección Alternativos para Algoritmos Evolutivos Multi-Objetivo" (Ref. 1920, Convocatoria Fronteras de la Ciencia 2016 de CONACyT) y "Nuevos Esquemas de Selección para Algoritmos Evolutivos Multi-Objetivo basados en Indicadores de Desempeño" (Solicitud no. 4, Convocatoria 2018 del Fondo SEP-Cinvestav). El responsable técnico de ambos proyectos es el Dr. Carlos A. Coello Coello.

Contents

List of Figures

List of Tables

Chapter 1

Introduction

In the engineering, scientific and industrial fields, there exist problems that involve the simultaneous optimization of several, often conflicting, objective functions. These are the so-called multi-objective optimization problems (MOPs). Due to the conflict among the objectives, MOPs do not have a single solution (as in the case of single-objective optimization problems) but a set of them that represent the best possible trade-offs among the objective functions. The solutions of an MOP conform the so-called *Pareto optimal set* (defined in decision variable space), and its image, in objective function space, is called *Pareto optimal front*.

Recently, multi-objective evolutionary algorithms (MOEAs) have become a popular choice for tackling complex MOPs [24]. MOEAs are stochastic population-based metaheuristics that employ the principles of natural selection (i.e., the survival of the fittest individuals in a population) to drive a set of solutions towards the Pareto optimal front. Unlike most of the mathematical programming techniques applied to MOPs that generate a single solution per execution [108], MOEAs generate a Pareto front approximation at each execution, i.e., they are set-based methods. However, MOEAs cannot ensure optimality of solutions due to the use of stochastic mechanisms. For several years, most MOEAs have incorporated the concept of Pareto dominance in their selection mechanisms [63, 31, 154]. Pareto-based MOEAs have shown a good performance when tackling MOPs with two and three objective functions. However, the selection pressure of Pareto-based MOEAs quickly dilutes when solving MOPs having four or more objective functions, i.e., the so-called many-objective optimization problems (MaOPs). This dilution is due to the rapid increase of the size of the search space and also of the number of solutions preferred by the Pareto dominance relation, which eventually causes a Pareto-based selection mechanism to choose solutions at random [77]. Consequently, to improve the performance of MOEAs on MaOPs, three main methodologies have been proposed: (1) the use of reference sets to guide the convergence of MOEAs [30], (2) decomposition of the MOP into multiple single-objective problems to be simutaneously solved [147], and (3) the use of quality indicators (QIs) to design selection mechanisms [8, 18, 100]. In this thesis, we focus on the latter methodology, i.e., the design of new selection mechanisms based on QIs to improve the performance of MOEAs on MaOPs. Additionally, we also propose

new advances on the design of QIs that are compliant with the Pareto dominance relation.

1.1 Motivation

Currently, the difficulties of Pareto-based MOEAs are well known when dealing with multi-objective optimization problems having four or more objectives [77, 89]. As a consequence, indicator-based MOEAs (IB-MOEAs) have become a popular option [152, 8, 15, 43]. These MOEAs employ QIs, which are functions that assess Pareto front approximations [158], depending on certain quality aspects such as convergence and diversity of solutions, to define selection mechanisms. IB-MOEAs transform the MOP into a single-objective optimization problem, i.e., the optimization of a given QI. To this end, IB-MOEAs solve or approximate at each iteration an indicator-based subset selection problem [4].

In the specialized literature, there exists several QIs [133, 84, 95]. QIs focused on assessing convergence or convergence-diversity have been commonly employed to guide the selection process of MOEAs. Zitzler [148] introduced the hypervolume indicator (HV) that rewards the convergence to the Pareto optimal front as well as the extent of solutions along it. HV measures the size of the objective function space dominated by an approximation set and bounded by an anti-optimal reference point. Currently, HV and its variants are the only unary QIs that are known to be Pareto-compliant[1]. Nevertheless, its computation is highly time-consuming as the dimensionality of the approximation set increases. Hence, this high computational cost has prevented its use by IB-MOEAs when tackling MaOPs. Consequently, other less expensive QIs, but with weaker mathematical properties, have been proposed to guide MOEAs' selection mechanisms. For instance: the R2 indicator [17], Inverted Generational Distance plus (IGD^+) [74], the additive ϵ indicator (ϵ^+) [158], and the averaged Hausdorff distance (Δ_p) [118]. In spite of the plethora of QIs currently proposed, no one can assess all the desired features of an approximation set, since each QI exhibits specific preferences over the set of all approximation sets. In other words, each QI guides the search of an MOEA according to its preferences and, thus, each one will produce Pareto front approximations with specific characteristics.

Additionally, a challenging open research topic is the design of more general MOEAs. A wide variety of state-of-the-art MOEAs employ a set of convex weight vectors[2] to guide their selection mechanisms. These weight vectors lie on an $(m-1)$-simplex. However, Ishibuchi *et al.* [75] empirically showed that the use of convex weight vectors overspecializes MOEAs on MOPs whose Pareto fronts are strongly correlated to the simplex shape formed by such weight vectors. In other words, the performance of such MOEAs strongly depends on the Pareto front shape of the MOP

[1] A QI is Pareto-compliant if its resulting values when evaluating approximation sets, are compliant with the Pareto dominance relation.

[2] A vector $\vec{w} \in \mathbb{R}^m$ is a convex weight vector if and only if $\sum_{i=1}^{m} w_i = 1$ and $w_i \geq 0$ for all $i \in \{1, \ldots, m\}$.

being tackled, which makes them unable to solve MOPs with different Pareto front geometries. Hence, IB-MOEAs can be employed to overcome this overspecialization due to the different properties that each QI offers.

1.2 Problem statement

As a consequence of the associated issues with Pareto-based selection mechanisms when dealing with MaOPs, a potential research area is the design of new selection schemes that overcome such problems. IB-MOEAs have shown remarkable results when tackling MaOPs. Since each QI exhibits specific solution preferences, an IB-MOEA based on a single QI will certainly exhibit noteworthy results on MOPs related to such preferences. However, its performance will degrade in problems out of the scope of the QI's preferences. Hence, we focus on the design of selection mechanisms that take advantage of the strengths of multiple indicators to solve low- and high-dimensional MOPs, covering a wide range of difficulties and Pareto front shapes. Regarding problem difficulties, we aim to solve MOPs with the following characteristics:

- **Multi-frontality**: it is related to objective functions that have several locally optimal solutions.
- **Deceptiveness**: this characteristic is associated to objective functions where the search space favors false optimal solutions.
- **Nonseparability**: it implies dependencies beween decision variables.
- **Bias**: An MOP is said to be biased when there is a significant density variation between the Pareto optimal set and the Pareto optimal front.

Additionally, we are interested in solving MOPs with distinct Pareto front shapes, namely, convex, concave, linear, disconnected, degenerate, mixed, simplex-like and non-simplex-like shapes.

1.3 Objectives

The main goal of this thesis is to advance the state-of-the-art of indicator-based MOEAs, through the proposal of new selection mechanisms that combine the search skills of multiple indicator-based selection mechanisms. The specific goals are the following:

- Comprehensively review the state-of-the-art IB-MOEAs with the aim of proposing the first taxonomy that helps the specialized community to classify them.

- Study the advantages and drawbacks of different indicator-based selection mechanisms with the purpose of determining their convergence and distribution properties. This analysis will be a fundamental part to know the practical properties of quality indicators when embedded into selection schemes.

- Analyze multiple indicator-based selection mechanisms in order to produce a hyper-heuristic that selects the best one, according to the problem characteristics.

- Investigate the cooperation between multiple indicator-based selection mechanisms to design an MOEA able to take advantage of the individual strengths of such indicators.

- Propose at least a new quality indicator to assess convergence or convergence-diversity of MOEAs.

- Provide a statistical study of the proposed algorithms using different test problems and real-world applications.

1.4 Research hypothesis

Our new indicator-based selection mechanisms will rely on the following hypotheses:

- Since each QI has different preferences over solutions, it is possible to take advantage of multiple QIs to design selection mechanisms such that the weaknesses of a specific QI could be compensated with the strengths of other(s).

- A more general MOEA, i.e., an MOEA whose performance does not strongly depend on the Pareto front shapes, could be designed on the basis of the combination of the individual search capabilities of indicator-based selection mechanisms.

- Through the mathematical combination of QIs, it is possible to create a family of combined indicators, having specific mathematical properties such as Pareto-compliance.

1.5 Publications and Awards

In this section, we list the current contributions and awards related with this thesis.

Conference publications

1. **Jesús Guillermo Falcón-Cardona** and Carlos A. Coello Coello, *A Multi-Objective Evolutionary Hyper-heuristic based on Multiple Indicator-based Density Estimators*. In Proceedings of the 2018 Genetic and Evolutionary Computation Conference (GECCO'2018), ACM Press, Kyoto, Japan, 2018 pp. 633–640. ISBN: 978-1-4503-5618-3. **Nominated to Best Paper Award**.

2. **Jesús Guillermo Falcón-Cardona** and Carlos A. Coello Coello, *Towards a More General Many-Objective Evolutionary Optimizer using Multi-Indicator Density Estimation*. In Proceedings of the 2018 Genetic and Evolutionary Computation Conference Companion (GECCO'2018), ACM Press, Kyoto, Japan, 2018, pp. 1890–1893. ISBN: 978-1-4503-5764-7. **Nominated to Best Student Paper Award**.

3. **Jesús Guillermo Falcón-Cardona** and Carlos A. Coello Coello, *Towards a More General Many-Objective Evolutionary Optimizer*. In Proceedings of the 15th International Conference on Parallel Problem Solving from Nature (PPSN XV), Springer Lecture Notes in Computer Science Vol. 11101, Coimbra, Portugal, 2018, pp. 335–346. ISBN: 978-3-319-99258-7.

4. A. M. Abdelbar, K. M. Salama, **Jesús Guillermo Falcón-Cardona**, and Carlos A. Coello Coello, *An Adaptive Recombination-Based Extension of the iMOACOR Algorithm*. In Proceedings of the 2018 IEEE Symposium Series on Computational Intelligence (SSCI), Bangalore, India, 2018, pp. 735-742, doi: 10.1109/SSCI.2018.8628657.

5. **Jesús Guillermo Falcón-Cardona**, Carlos A. Coello Coello and Michael T. M. Emmerich, *CRI-EMOA: A Pareto-Front Shape Invariant Evolutionary Multi-Objective Algorithm*. In Proceedings of the 10th International Conference on Evolutionary Multicriterion Optimization (EMO'2019), Springer Lecture Notes in Computer Science Vol. 11411, East Lansing, MI, USA, 2019, pp. 307–318. ISBN: 978-3-030-12597-4.

6. **Jesús Guillermo Falcón-Cardona**, Michael T. M. Emmerich and Carlos A. Coello Coello, *On the Cooperation of Multiple Indicator-based Multi-Objective Evolutionary Algorithms*. In Proceedings of the 2019 IEEE Congress on Evolutionary Computation (CEC'2019), IEEE Press, Wellington, New Zeland, 2019, pp. 2050-2057, doi: 10.1109/CEC.2019.8790315..

7. **Jesús Guillermo Falcón-Cardona** and Carlos A. Coello Coello, *Convergence and Diversity Analysis of Indicator-based Multi-Objective Evolutionary Algorithms*. In Proceedings of the 2019 Genetic and Evolutionary Computation Conference (GECCO'2019), ACM Press, Prague, Czech Republic, 2019, pp. 524–531. ISBN: 978-1-4503-6111-8.

8. **Jesús Guillermo Falcón-Cardona**, Michael T. M. Emmerich and Carlos A. Coello Coello, *On the Construction of Pareto-compliant Quality Indicators*. In Proceedings of the 2019 Genetic and Evolutionary Computation Conference Companion (GECCO'2019), ACM Press, Prague, Czech Republic, 2019, pp. 2024–2027. ISBN: 978-1-4503-6748-6. **Nominated to Best Student Paper Award**.

9. **Jesús Guillermo Falcón-Cardona**, Hisao Ishibuchi and Carlos A. Coello Coello, *Riesz s-energy-based Reference Sets for Multi-Objective Optimization*. In Proceedings of the 2020 IEEE Congress on Evolutionary Computation (CEC'-2020), IEEE Press, Glasgow, Scotland, 2020. **Nominated to Best Paper Award**.

10. **Jesús Guillermo Falcón-Cardona**, Arnaud Liefooghe and Carlos A. Coello Coello, *An Ensemble Indicator-based Density Estimator for Evolutionary Multi-Objective Optimization*. In Proceedings of the 16th International Conference on Parallel Problem Solving from Nature (PPSN XVI), Springer Lecture Notes in Computer Science Vol. 12270, Leiden, The Netherlands, 2020, pp. 201–214. ISBN: 978-3-030-58114-5.

11. **Jesús Guillermo Falcón-Cardona**, Hisao Ishibuchi and Carlos A. Coello Coello, *Exploiting the Trade-off between Convergence and Diverity Indicators*. In Proceedings of the 2020 IEEE Symposium Series on Computational Intelligence (SSCI), Camberra, Australia, 2020. Accepted.

12. **Jesús Guillermo Falcón-Cardona** Edgar Covantes Osuna and Carlos A. Coello Coello, *An Overview of Pair-Potential Functions for Multi-Objective Optimization*. In Proceedings of the 11th International Conference on Evolutionary Multicriterion Optimization (EMO'2021), Springer Lecture Notes in Computer Shenzhen, China, 2021. Under Review.

Journal publications

1. **Jesús Guillermo Falcón-Cardona** and Carlos A. Coello Coello, *A new indicator-based many-objective ant colony optimizer for continuous search spaces*. Swarm Intelligence, 11, 71-100, 2017.

2. **Jesús Guillermo Falcón-Cardona** and Carlos A. Coello Coello, *Indicator-based Multi-Objective Evolutionary Algorithms: A Comprehensive Survey*. ACM Computing Surveys, 53(2), April 2020.

3. **Jesús Guillermo Falcón-Cardona**, Michael T. M. Emmerich and Carlos A. Coello Coello, *On the Combination of Quality Indicators for Multi-Objective Optimization*. Evolutionary Computation Journal, 2020. Under Review.

4. **Jesús Guillermo Falcón-Cardona**, Raquel Hernández Gómez, Carlos A. Coello Coello and Ma. Guadalupe Castillo Tapia, *Parallel Multi-Objective Evolutionary Algorithms: A Comprehensive Survey*. ACM Computing Surveys, 2020. Under Review.

5. **Jesús Guillermo Falcón-Cardona**, Hisao Ishibuchi and Carlos A. Coello Coello and Michael Emmerich, *Studying the Effect of the Cooperation of Indicator-based Multi-Objective Evolutionary Algorithms*. IEEE Transactions on Evolutionary Computation. Under Review.

6. **Jesús Guillermo Falcón-Cardona**, Hisao Ishibuchi and Carlos A. Coello Coello, *Discretizing Pareto Fronts using Pair-Potential Functions*. IEEE Transactions on Evolutionary Computation. To be submitted.

7. **Jesús Guillermo Falcón-Cardona**, Arnaud Liefooghe and Carlos A. Coello Coello, *On the Ensemble of Indicator-based Density Estimators*. IEEE Transactions on Evolutionary Computation. To be submitted.

Book Chapters

Jesús Guillermo Falcón-Cardona, Guillermo Leguizamón, Carlos A. Coello Coello, and Ma. Guadalupe Castillo Tapia, *Multi-Objective Ant Colony Optimization: An Updated Taxonomy and Review of Approaches*. World Scientific Review. Submitted.

Awards

2018 IEEE Computational Intelligence Society Graduate Student Research Grants due to the Project *Advancing Indicator-based Multi-Objective Optimization: Hyper-heuristic and Indicator Design*.

1.6 Structure of this work

Including this introduction, this thesis consists of nine chapters and two appendices. A brief description of each of them is given in the following.

Chapter 2 includes an introduction to evolutionary algorithms and it provides basic mathematical concepts on multi-objective optimization, giving, in each case, a brief review of the related work. All this terminology is necessary for the understanding of the following chapters.

Chapter 3 is devoted to comprehensively review the state-of-the-art of indicator-based Multi-Objective Evolutionary Algorithms. For this purpose, a taxonomy was proposed to classify the current indicator-based mechanisms that have been coupled to MOEAs. The advantages and drawbacks of each proposal are analyzed to provide a reference for their use.

Chapter 4 introduces an empirical study on the convergence and diversity properties of IB-MOEAs when tackling MOPs having different Pareto front shapes and difficulties. Regarding convergence, we found general and particular strengths and weaknesses of IB-MOEAs that particularly depend on the characteristic of the MOP being solved. Concerning diversity, we analyzed the spread and uniformity of solutions related to each IB-MOEA for low-dimensional MOPs, i.e., those having two and three objective functions.

Chapter 5 focuses on the competition of IB-MOEAs when solving an MOP. For this aim, we propose a hyper-heuristic that, depending on an online convergence analysis, selects the best suited indicator-based density estimator (IB-DE) to be executed during a time window. Hence, the IB-DEs compete to be executed as often as possible. This approach is the first one that uses multiple IB-DEs in a MOEA.

Chapter 6 explores the cooperation of IB-MOEAs instead of its competition. The cooperation is due to an MOEA based on the island model, where each individual island executes in isolation a steady-state IB-MOEA with a micro-population. After a given number of generations, a migration process is allowed to increase the diversity of the islands. This approach was compared with respect to panmictic IB-MOEAs, showing that the cooperation combines the strengths of the individual IB-MOEAs, and compensates for their weaknesses.

Chapter 7 proposes the first theoretical development for the combination of quality indicators to produce Pareto-compliant QIs. Based on the proposed mathematical framework, it is possible to construct a family of Pareto-compliant QIs based on the combination of at least one Pareto-compliant QI with one or more weakly Pareto-compliant indicators. This proposal gives an insight of the existence of more Pareto-compliant QIs besides the hypervolume.

The conclusions of this thesis, as well as some possible future research paths, are highlighted in Chapter 9.

Appendix A presents the test problems used throughout all the experiments. Appendix B contains numerical results related to some of the experiments in this document.

Chapter 2

Background

This chapter provides some fundamental concepts and mathematical notation that are adopted throughout this document. Section 2.1 covers the mathematical foundation of multi-objective optimization, defining the multi-objective optimization problem, the most commonly employed optimality criterion, and some special reference vectors. Section 2.2 introduces multi-objective evolutionary algorithms which are bio-inspired metaheuristics designed to solve multi-objective optimization problems. We finish this chapter with a summary in Section 2.3.

2.1 Multi-Objective Optimization

Multi-objective optimization problems (MOPs) arises in several engineering, industrial and scientific applications. MOPs involve the simultaneous optimization of several, often conflicting, objective functions. Due to the conflict among objective functions, the solution to an MOP is defined by a set of solutions that represent the best possible trade-offs among the objectives. In other words, trade-off solutions are solutions in which an objective value cannot be improved without worsening another one. The solution set of an MOP is denoted as the *Pareto set* ($\mathcal{PS}^*$) and its image, in objective function space, is the so-called *Pareto front* ($\mathcal{PF}^*$).

2.1.1 Problem definition

According to Coello *et al.* [24], a multi-objective optimization problem[1] is mathematically defined as:

$$\min_{\vec{x}\in\mathcal{X}} \left\{ \vec{f}(\vec{x}) := [f_1(\vec{x}), f_2(\vec{x}), \ldots, f_m(\vec{x})]^T \} \right\} \tag{2.1}$$

subject to:

$$g_i(\vec{x}) \leq 0 \quad i = 1, 2, \ldots, q \tag{2.2}$$

[1]To transform a minimization problem into a maximization one, we can use: $\max f = -\min(-f)$

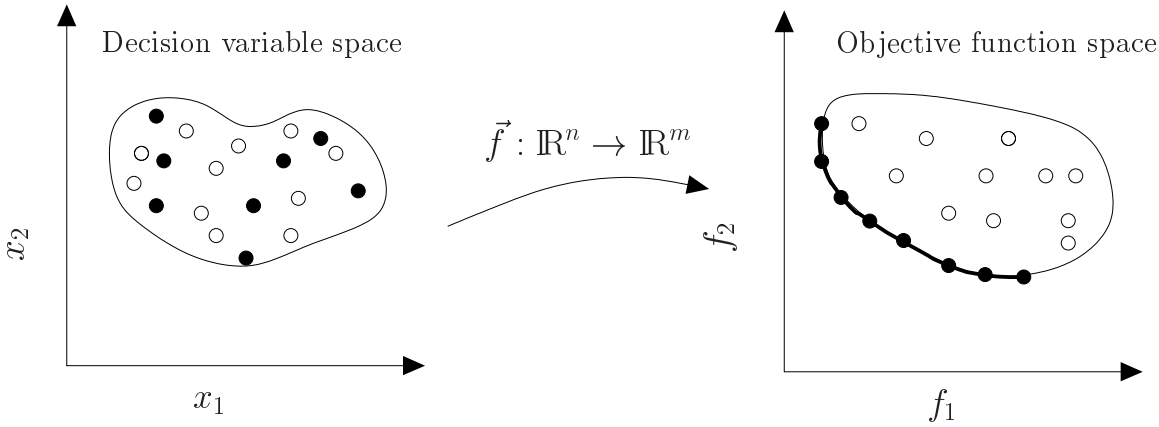

Figure 2.1: Illustration of an optimization problem $\vec{f} : \mathbb{R}^2 \to \mathbb{R}^2$. Black dots in the left-hand side of the figure are solutions in $\mathcal{PS}^*$ and the ones in the right-hand side are their image in $\mathcal{PF}^*$.

$$h_j(\vec{x}) = 0 \quad j = 1, 2, \ldots, p \tag{2.3}$$

where $\vec{x} = (x_1, x_2, \ldots, x_n)^T$ is the n-dimensional vector of decision variables and $\mathcal{X} \subseteq \mathbb{R}^n$ is the decision variable space; $f_k : \mathcal{X} \to \mathbb{R}$, $k = 1, \ldots, m$ are the objective functions and $g_i, h_j : \mathcal{X} \to \mathbb{R}$, $i = 1, \ldots, q$, $j = 1, \ldots, p$ are the constraint functions of the problem which define the feasible region Ω in objective function space. Figure 2.1 exemplifies a bi-objective optimization problem.

2.1.2 Pareto optimality

Unlike single-objective optimization problems where it is straightforward to compare two given solutions $\vec{x}, \vec{y} \in \mathbb{R}^n$ by simply checking their objective values (i.e., if $f(\vec{x}) < f(\vec{y})$ or $f(\vec{y}) < f(\vec{x})$ or $f(\vec{x}) = f(\vec{y})$), regarding MOPs, the comparison is not direct since $\vec{f}(\vec{x})$ and $\vec{f}(\vec{y})$ are in $\mathbb{R}^m$. In consequence, the Pareto dominance relation, which is defined in the following, is employed to compare m-dimensional vectors. In the remaining of this section, let $\vec{x}, \vec{y}, \vec{z} \in \mathcal{X}$ be three vectors of decision variables.

Definition 2.1.1 (Pareto Dominance)**.** *$\vec{x}$ **Pareto dominates** $\vec{y}$ (denoted as $\vec{x} \prec \vec{y}$ or $\vec{f}(\vec{x}) \prec \vec{f}(\vec{y})$) if $f_i(\vec{x}) \leq f_i(\vec{y})$ for all $i = 1, 2, \ldots, m$ and there exists at least one index $j \in \{1, 2, \ldots, m\}$ such that $f_j(\vec{x}) < f_j(\vec{y})$.*

This definition indicates that $\vec{x}$ Pareto dominates $\vec{y}$ if the former is as good as the latter in every objective value and it is better in at least one of them. Pareto dominance is a binary relation that imposes a strict partial order in $\mathbb{R}^m$, i.e., $\prec$ is irreflexive ($\vec{x} \not\prec \vec{x}$), asymmetric ($\vec{x} \prec \vec{y} \Rightarrow \vec{x} \not\prec \vec{y}$), and transitive ($\vec{x} \prec \vec{y} \wedge \vec{y} \prec \vec{z} \Rightarrow \vec{x} \prec \vec{z}$). Four possible results are related to $\prec$: (1) $\vec{x} \prec \vec{y}$, (2) $\vec{y} \prec \vec{x}$, (3) $\vec{x} = \vec{y}$, or

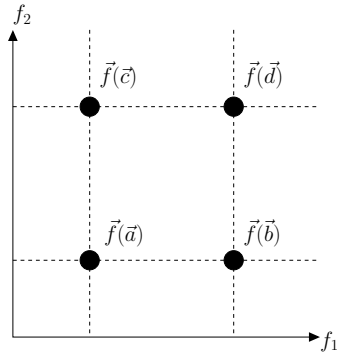

Figure 2.2: Given the images, in the objective function space, of four vectors of decision variables: $\vec{a}, \vec{b}, \vec{c}, \vec{d} \in \mathbb{R}^2$, the following relations are shown: $\vec{a} \prec \vec{b}$, $\vec{a} \prec \vec{c}$, $\vec{a} \prec\prec \vec{d}$, $\vec{c} \prec \vec{d}$, $\vec{b} \prec \vec{d}$, and $\vec{c} \,||\, \vec{b}$.

(4) when $\vec{x} \not\prec \vec{y} \wedge \vec{y} \not\prec \vec{x}$, then $\vec{x}$ and $\vec{y}$ are incomparable or mutually non-dominated, denoted as $\vec{x} \,||\, \vec{y}$.

Based on the Pareto dominance relation, two more binary relations are constructed by relaxing or toughening the conditions, giving rise to the weak Pareto dominance and the strict Pareto dominance, respectively.

Definition 2.1.2 (Weak Pareto Dominance)**.** $\vec{x}$ **weakly Pareto dominates** $\vec{y}$ *(denoted by* $\vec{x} \preceq \vec{y}$ *or* $\vec{f}(\vec{x}) \preceq \vec{f}(\vec{y})$*) if* $f_i(\vec{x}) \leq f_i(\vec{y})$ *for all* $i = 1, 2, \ldots, m$.

Definition 2.1.3 (Strict Pareto Dominance [24])**.** $\vec{x}$ **strictly Pareto dominates** $\vec{y}$ *(denoted by* $\vec{x} \prec\prec \vec{y}$ *or* $\vec{f}(\vec{x}) \prec\prec \vec{f}(\vec{y})$*) if* $f_i(\vec{x}) < f_i(\vec{y})$ *for all* $i = 1, 2, \ldots, m$.

On the one hand, weak Pareto dominance is a binary relation that imposes a partial order in $\mathbb{R}^m$, i.e., $\preceq$ is reflexive ($\vec{x} \preceq \vec{x}$), antisymmetric ($\vec{x} \preceq \vec{y} \wedge \vec{y} \preceq \vec{x} \Rightarrow \vec{x} = \vec{y}$), and transitive ($\vec{x} \preceq \vec{y} \wedge \vec{y} \preceq \vec{z} \Rightarrow \vec{x} \preceq \vec{z}$). On the other hand, strict Pareto dominance imposes a strict partial order as in the case of the Pareto dominance. Figure 2.2 shows the relations of four vectors in a two-dimensional objective space.

In multi-objective optimization, the common optimality criterion is defined in terms of the Pareto dominance relation as follows.

Definition 2.1.4 (Pareto Optimality [24])**.** *A vector of decision variables* $\vec{x}^* \in \mathcal{X}$ *is* **Pareto optimal** *if there does not exist another* $\vec{x} \in \mathcal{X}$ *such that* $\vec{f}(\vec{x}) \prec \vec{f}(\vec{x^*})$.

Thus, a solution is Pareto optimal if its image is not dominated by any other feasible solution's objective vector.

Definition 2.1.5 (Pareto set)**.** *The* **Pareto set** $\mathcal{P}^*$ *is defined by:*

$$\mathcal{PS}^* := \{\vec{x}^* \in \mathcal{X} \mid \vec{x} \text{ is Pareto optimal}\} \tag{2.4}$$

Definition 2.1.6 (Pareto front)**.** *The* **Pareto front** $\mathcal{PF}^*$ *is defined by:*

$$\mathcal{PF}^* := \left\{ \vec{f}(\vec{x}^*) \in \Omega \mid \vec{x}^* \in \mathcal{PS}^* \right\} \tag{2.5}$$

The elements of the Pareto set are the solutions of an MOP and, their image conform the Pareto front. Solutions in $\mathcal{PF}^*$ represent the best possible trade-offs among the objectives. Such solutions cannot be improved in one objective without being worsened in another one. In consequence, when solving an MOP, we thus wish to determine the Pareto set from the set $\mathcal{X}$ that satisfy Eqs. (2.2) and (2.3).

2.1.3 Reference points

The Pareto front of an MOP is bounded by two special reference points: the ideal and nadir vectors. Next, we provide their mathematical definitions.

Definition 2.1.7 (Ideal Vector)**.** *Each component of the* **Ideal Vector** *($\vec{z}^* \in \mathbb{R}^m$) is defined as follows: $z_i^* = \min_{\vec{x} \in \mathcal{X}} f_i(\vec{x})$ for $i = 1, 2, \ldots, m$.*

Definition 2.1.8 (Nadir Vector)**.** *Each component of the* **Nadir Vector** *($\vec{z}^{nad} \in \mathbb{R}^m$) is constructed as follows: $z_i^{nad} = \max_{\vec{x} \in \mathcal{PS}^*} f_i(\vec{x})$ for $i = 1, 2, \ldots, m$.*

The ideal vector is constructed using the minimum of each of the objective functions. This reference point is particularly easy to calculate since to obtain each one if its components, we have to minimize each objective function of the MOP separately. On the other hand, the nadir vector is an anti-optimal point that contains the worst values of the Pareto optimal front. Unlike the ideal vector, the nadir point is difficult to obtain or approximate, since it is necessary to have the Pareto optimal point before [108].

Definition 2.1.9 (Utopian vector)**.** *Given $\vec{z}^*$ and a vector $\vec{\epsilon} = (\epsilon_1, \ldots, \epsilon_m)^T$ (where $\epsilon_i > 0$ for all $i \in \{1, 2, \ldots, m\}$), the* **Utopian Vector** *($\vec{z}^{**}$) is defined as follows: $\vec{z}^{**} = \vec{z}^* - \vec{\epsilon}$.*

The utopian vector is a special reference point that dominates both the ideal and nadir vectors, and, in consequence, al Pareto optimal solutions. Figure 2.3 shows the three reference points for a Pareto front in a two-dimensional objective space.

Finally, there are cases where the objective functions have different scales, i.e., they are incommensurable. Consequently, it is advisable to rescale the objective functions so that their objective value are of approximately the same magnitude. To this aim, the ideal and nadir vectors are employed to normalize the objective values as follows:

$$f_i'(\vec{x}) = \frac{f_i(\vec{x}) - z_i^*}{z_i^{nad} - z_i^*}, i = 1, \ldots, m, \tag{2.6}$$

where the range of each objective function is $[0, 1]$.

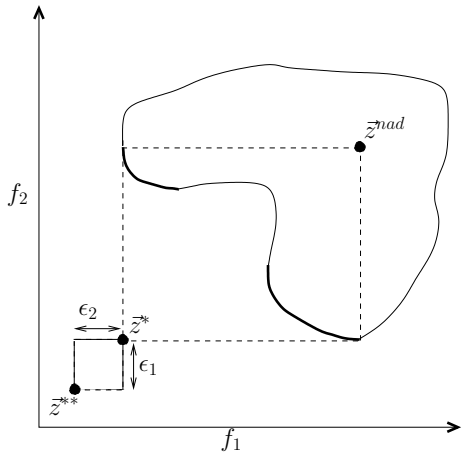

Figure 2.3: Reference points: ideal vector ($\vec{z}^{*}$), nadir vector ($\vec{z}^{nad}$), and utopian vector ($\vec{z}^{**}$).

2.2 Multi-Objective Evolutionary Algorithms

Throughout the years, MOPs have been tackled by mathematical programming techniques [108]. However, and in spite of their efficiency, these methods have several limitations, e.g., they are sensitive to the shape of the Pareto front and continuity and differentiability assumptions are required. Additionally, they usually generate a single solution per execution. These limitations have motivated the development of alternative solution methods to tackle complex MOPs, from which multi-objective evolutionary algorithms (MOEAs) have become a popular choice [24].

MOEAs are population-based and gradient-free metaheuristics that employ the Darwin's principle of natural selection (i.e., the survival of the fittest individuals) to drive a set of solutions towards $\mathcal{PF}^{*}$. In consequence, MOEAs produce a finite Pareto front approximation or approximation set (see Definition 2.2.1) on a single algorithmic execution. However, unlike mathematical programming techniques, MOEAs do not ensure optimality of solutions since their performance is based on heuristic decisions. The vast majority of MOEAs can be classified as *a posteriori* methods [108], i.e., they do not take into account beforehand the preferences of the decision maker, instead, MOEAs produce approximation sets, aiming to achieve the following three goals [150]:

1. **convergence:** to generate solutions as close as possible to the Pareto optimal front,

2. **coverage:** to produce solutions all along the Pareto optimal front,

3. **uniformity:** solutions should be evenly distributed.

Figure 2.4 shows Pareto front approximations having different convergence, coverage and uniformity characteristics. The approximation set is then presented to the decision maker who will choose a solution to the problem being solved, based on

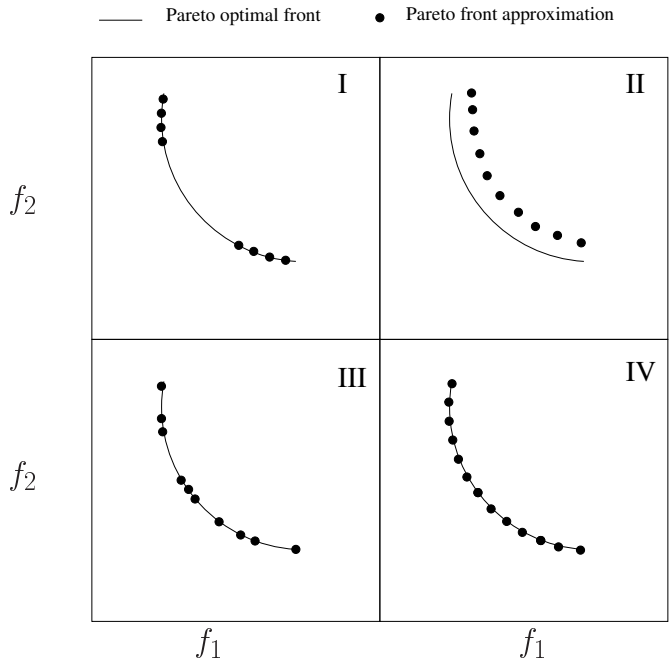

Figure 2.4: (I) Convergent approximation set but not covering the entire Pareto front, (II) evenly distributed approximation set but not convergent, (III) convergent solutions but not evenly distributed, (IV) desired Pareto front approximation: convergent, evenly distributed and covering the whole Pareto optimal front.

his or her preferences. Since 1984, when David Schaffer proposed the first MOEA [117], these metaheuristics have been efficiently employed to tackle complex MOPs [63, 120, 31, 155, 152, 8, 60, 101, 42].

Definition 2.2.1 (Approximation set)**.** *Let $\mathcal{A} \subseteq \Psi$ be a set of m-dimensional objective vectors, where $|\mathcal{A}| = \mu$. $\mathcal{A}$ is called a* ***Pareto front approximation*** *or* ***approximation set*** *if any element of $\mathcal{A}$ does not weakly dominate any other vector in $\mathcal{A}$. The set of all approximation sets for an MOP is denoted as Ψ.*

MOEAs are iterative set-based method whose main goal is to produce Pareto front approximations, exhibiting the three characteristics mentioned before. Each MOEA has a population $P_t = \{\vec{x}^1, \vec{x}^2, \ldots, \vec{x}^\mu\}$ (where t is the iteration number) that has to be evolved using the evolutionary operators: mating or parent selection (π), variation (ν), and survival selection (σ). In the following, let A^N represent a subset of size N of the set A and let $(A, \mathcal{M})$ be a multiset of the set A, where $\mathcal{M} : A \to \mathbb{N}$.

1. $\pi : \mathcal{X}^\mu \to (\mathcal{X}^\mu, \mathcal{M})$. This operator chooses from $\mathcal{X}^\mu$, μ solutions that will shape the mating pool, i.e., the parent solutions employed to create new ones via the variation operators. Since a solution can be chosen zero or more times, the mating pool is represented as the multiset $(\mathcal{X}^\mu, \mathcal{M})$. In the literature, there are

several mating selection mechanisms, but the common strategies are random sampling and binary tournament [24].

2. $\nu : (\mathcal{X}^{\mu}, \mathcal{M}) \rightarrow \mathcal{X}^{\lambda}$. Variation operators produce λ new individuals from the mating pool. Variation operators aim to explore and exploit the decision variable space. A wide range of variation operators have been proposed to handle different encoding representations of the decision vector. Regarding real numbers encoding, the most common choices are: simulated binary crossover (SBX) and polynomial-based mutation [28].

3. Survival selection σ determines the solutions that will conform the next generation. This selection function has two variants: (1) $\sigma_{(\mu,\lambda)} : \mathcal{X}^{\lambda} \rightarrow \mathcal{X}^{\mu}$ in which the best μ ($\mu \leq \lambda$) solutions from $\mathcal{X}^{\lambda}$ replace the parent population, and (2) $\sigma_{(\mu+\lambda)} : (\mathcal{X}^{\mu} \cup \mathcal{X}^{\lambda}) \rightarrow \mathcal{X}^{\mu}$ where the best μ individuals from the union of parent and offspring solutions are chosen. Regarding the latter selection scheme, the simplest case is the steady-state selection, which refers to $\sigma_{\mu+1}$. However, $\sigma_{(\mu+\lambda)}$ is preferred to incorportate elitism which is an important strategy of MOEAs to guide the population towards the Pareto optimal front [24].

Based on the evolutionary operators, an MOEA can be defined by the iterative rule: $P_{t+1} = \sigma\{P_t \cup \nu[\pi(P_t)]\}$. Additionally, some MOEAs use a secondary population (also known as archive) $\mathcal{A}$ that keeps the non-dominated solutions found so far as a way to introduce elitism. The general framework of an MOEA is shown in Algorithm 1. First, the main population $P_{t=0}$ and the archive $\mathcal{A}$ are initialized in lines 1 and 2, respetively. Lines 4 to 11 show the main loop of an MOEA. At each iteration, mating selection is performed to select μ parent solutions from either P_t or $\mathcal{A}$. Variation operators (e.g., crossover and mutation) further explore this set M of parent solutions to create the set $\mathcal{O}$ of λ offspring solutions. Then, the archive $\mathcal{A}$ is updated using the non-dominated offspring solutions in line 7. The next step involves performing the survival selection strategy, using either a (μ, λ) or a $(\mu + \lambda)$ selection rule, to shape the next generation P_{t+1}. Finally, an MOEA returns P_t or $\mathcal{A}$, depending on its specific design. However, both of them contain an approximation to the Pareto optimal front.

2.2.1 Many-Objective Optimization

For several years, most MOEAs have incorporated the concept of *Pareto dominance*[2] in their selection mechanisms [24]. Pareto-based MOEAs have shown a good performance when tackling MOPs with two and three objective functions [155, 31]. However, the selection pressure of Pareto-based MOEAs quickly dilutes when solving MOPs having four or more objective functions, i.e., the so-called many-objective optimization problems (MaOPs). This dilution is due to the rapid increase in the search

[2]A vector $\vec{u}$ Pareto dominates another vector $\vec{v}$ if the former is as good as the latter in every element and it is better in at least one of them.

Algorithm 1: MOEA general framework

```
Generate initial population P_0 of size μ;
Initialize A with the non-dominated solutions from P_0 ;
t ← 0;
while stopping criterion is not fulfilled do
    M ← Select μ parents from P_t or A;
    O ←Generate a set of λ offspring solutions based on M, using variation
     operators;
    Update archive A using O;
    S ← Select survival solutions using a σ_(μ,λ) or σ_(μ+λ) strategy;
    P_{t+1} ← S;
    t ← t + 1;
end
return P_t or A
```

space that produces also an increase of the number of solutions preferred by the Pareto dominance relation, which eventually causes a Pareto-based selection mechanism to choose solutions at random [44, 77]. In recent years, the design of methods that improve the performance of MOEAs on MaOPs has received much interest since these problems are widespread in science and engineering applications [47]. In general, the most popular methodologies to improve the performance of MOEAs on MaOPs are the following:

1. *MOEAs using relaxed Pareto dominance relations:* In this case, the main idea is to employ alternative preference relations that relax the Pareto dominance relation [98]. Relaxed preference relations induce a finer grain order on the solutions belonging to MaOPs, which directly increases the selection pressure of MOEAs. Some examples of these preference relations are the following: the $(1-k)$-dominance relation proposed by Farina and Amato [44], the favour ranking proposed by Drechsler *et al.* [37], and the expansion relation that controls the dominance area of solutions [116].

2. *Decomposition-based MOEAs:* This methodology aims to transform an MOP into multiple single-objective optimization problems (SOPs), using scalarizing functions such as the weighted Tchebycheff function. The distinctive feature of these MOEAs is that all the SOPs are solved in a single run, producing an entire approximation set. The most typical approach within this class is the MOEA based on Decomposition (MOEA/D) [147, 129].

3. *Reference set-based MOEAs:* The Non-dominated Sorting Genetic Algorithm III (NSGA-III) [30] best represents this category. In this case, a reference set is constructed to guide the search process by measuring the quality of the population conforming it. According to Li *et al.* [89], the two main aspects

related to this methodology are: (1) how to construct the reference set when no information about the Pareto optimal front is available, and (2) how to measure the quality of solutions using the reference set.

4. *Indicator-based MOEAs:* These MOEAs employ quality indicators, which are functions that assess approximation sets, to define selection mechanisms. The underlying idea is to optimize the indicator value of the population throughout the evolutionary process. The S-Metric Selection Evolutionary Multi-Objective Algorithm (SMS-EMOA) [8] is the most representative indicator-based MOEA (IB-MOEA). It employs the Hypervolume indicator (HV) [156] that measures the dominated volume of an approximation set, bounded by a reference point that is dominated by all the points in the approximation set. SMS-EMOA imposes a total order among the solutions by calculating their contribution to the hypervolume indicator.

In this thesis, we are interested in the design of IB-MOEAs to advace the state-of-the-art. The following chapter is completely focused on introducing IB-MOEAs and their related mathematical concepts.

2.3 Summary

This chapter introduced the mathematical terminology related to multi-objective optimization. First, we formally defined the multi-objective optimization problem and the most commonly optimality criterion, i.e., the Pareto dominance relation. Additionally, we defined the weak and strict Pareto dominance relations that will be useful for the next chapter. Moreover, we introduced three special reference vectors: the ideal, nadir, and utopian vectors. Then, we described the principal characteristics of an MOEA, emphasizing their main components to define its general algorithmic structure. Finally, we stated the issues that Pareto-based MOEAs have when dealing with MOPs having more than three objective functions, i.e., the so-called many-objective optimization problems. Finally, we briefly illustrated four strategies that MOEAs follow to tackle MaOPs: (1) relaxed Pareto dominance relations, (2) decomposition-based MOEAs, (3) reference set-based MOEAs, and (4) indicator-based MOEAs.

Chapter 3

Indicator-based Multi-Objective Evolutionary Algorithms

This chapter is devoted to formally introduce quality indicators and to provide a comprehensive review of the state-of-the-art related to indicator-based MOEAs. Section 3.1 introduces quality indicators which are functions that evaluate the quality of MOEAs' outcomes. Section 3.2 provides an in-depth review of the state-of-the-art of indicator-based MOEAs following a taxonomy proposed by us. Section 3.3 briefly describes some real-world problems solved by indicator-based MOEAs. Section 3.4 highligths some possible research directions. Finally, a summary of the chapter is outlined in Section 3.5.

3.1 Quality Indicators

Quality indicators (QIs) are functions that assign a real value to one or more approximation sets, depending on certain quality aspects such as convergence and diversity of solutions. The origins of QIs can be traced back to the mid-1990s where some isolated efforts were undertaken to try to (numerically) assess the performance of MOEAs [120, 88, 41, 48]. However, the Ph.D. thesis of David Van Veldhuizen [133] can be considered as the cornerstone of QIs due to his comprehensive review of most of the QIs available at that time. In 2003, Zitzler *et al.* [158] provided the first theoretical analysis of QIs, using a mathematical framework to understand how QIs were related to a set of outperformance relations. In the last few years, Jiang *et al.* [82] and Liefooghe and Derbel [97] have conducted empirical studies aiming to determine the correlation between different QIs and their behavior when assessing a wide variety of Pareto front shapes. Additional reviews of QIs to evaluate the performance of MOEAs have been published by some researchers [122, 115, 141, 52, 39, 145, 45].

Quality indicators are set functions that simultaneously assign a real value to k approximation sets. However, this definition is not enough to describe QIs because they possess several features (see Fig. 3.1). Overall, Knowles and Corne [84], Zitzler *et al.* [151] and Jiang *et al.* [82] have distinguished their following characteristics: cardinal-

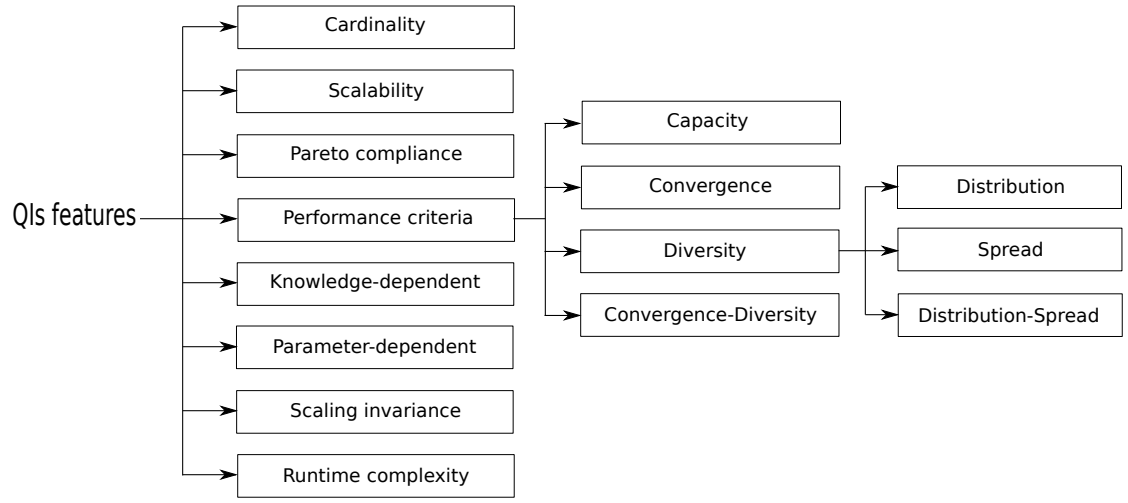

Figure 3.1: Main features of quality indicators.

ity, performance criteria, Pareto compliance, scalability, scaling invariance, knowledge and parameter dependence as well as computational complexity. The cardinality of a QI is the number k of approximation sets that can be simultaneously assessed. Performance criteria are related to what the QI measures: capacity,[1] convergence, diversity (divided into distribution and spread of solutions) or convergence-diversity. Pareto compliance is directly related to convergence QIs. The sensitivity of a QI to the different units and scales of the objective functions determines its scaling invariance. If the computation of the indicator requires knowledge of the MOP being solved, then it is knowledge-dependent. Similarly, a QI is parameter-dependent if it needs user-supplied parameters. A critical aspect in practice is its runtime complexity. Additionally, it is crucial that indicators can properly deal with solution sets to MOPs having a different number of objectives as current MOEAs generate approximation sets in high-dimensional objective spaces, i.e., QIs should be scalable. In this Ph.D. thesis, we focus our attention on unary QIs since they have have been widey employed for the design of selection mechanisms of MOEAs (see Section 3.2 in page 28). Unary QIs[2] are mathematically defined as follows.

Definition 3.1.1 (Unary Quality Indicator)**.** *A unary quality indicator I is a function $I : \Psi \to \mathbb{R}$, which assigns a real value to each approximation set $\mathcal{A} \in \Psi$, where Ψ is the space of all approximation sets for an MOP.*

Regarding QIs that measure the convergence of an approximation set to the Pareto optimal front, an important property is Pareto compliance. First, since QIs evaluate approximation sets produced by MOEAs, the more general notion of quality is the Pareto dominance between sets. Table 3.1 describes five set dominance relations on

[1] According to Jiang *et al.* [82] "capacity QIs quantify the number or ratio of non-dominated solutions in the approximation set that conforms to the predefined requirements".

[2] From this point onwards, unary indicators are denoted as QIs.

Table 3.1: The five relations on approximation sets based on Pareto dominance relations. $\mathcal{A} \prec\prec \mathcal{B} \Rightarrow \mathcal{A} \prec \mathcal{B} \Rightarrow \mathcal{A} \lhd \mathcal{B} \Rightarrow \mathcal{A} \preceq \mathcal{B}$.

Relation	**Description**	**Name**
$\mathcal{A} \prec\prec \mathcal{B}$	$\forall \vec{b} \in \mathcal{B}, \exists \vec{a} \in \mathcal{A} : \vec{a} \prec\prec \vec{b}$	Strictly dominates
$\mathcal{A} \prec \mathcal{B}$	$\forall \vec{b} \in \mathcal{B}, \exists \vec{a} \in \mathcal{A} : \vec{a} \prec \vec{b}$	Dominates
$\mathcal{A} \lhd \mathcal{B}$	$\forall \vec{b} \in \mathcal{B}, \exists \vec{a} \in \mathcal{A} : \vec{a} \preceq \vec{b} \wedge \mathcal{A} \neq \mathcal{B}$	Better
$\mathcal{A} \preceq \mathcal{B}$	$\forall \vec{b} \in \mathcal{B}, \exists \vec{a} \in \mathcal{A} : \vec{a} \preceq \vec{b}$	Weakly dominates
$\mathcal{A} \parallel \mathcal{B}$	$\mathcal{A} \not\preceq \mathcal{B} \wedge \mathcal{B} \not\preceq \mathcal{A}$	Incomparable

the basis of the Pareto dominance relations defined in Section 2.1.2. Hansen and Jaszkiewicz [55] defined the cases in which the evaluation of two approximation sets by a certain indicator is compatible with the result of a Pareto-based outperformance relation applied to these two sets. Hence, an indicator could be compliant or weakly compliant with the outperformance relation $\lhd$ that is defined in Table 3.1. Both properties are defined in the following. Without loss of generality, let us assume that a greater indicator value corresponds to a higher quality.

Property 3.1.1 (Pareto compliance)**.** *Given two approximation sets $\mathcal{A}$ and $\mathcal{B}$, a unary indicator I is $\lhd$-compliant (Pareto compliant) if $\mathcal{A} \lhd \mathcal{B} \Rightarrow I(\mathcal{A}) > I(\mathcal{B})$.*

Property 3.1.2 (Weakly Pareto compliance)**.** *Given two approximation sets $\mathcal{A}$ and $\mathcal{B}$, a unary indicator I is weakly $\lhd$-compliant (weakly Pareto compliant) if $\mathcal{A} \lhd \mathcal{B} \Rightarrow I(\mathcal{A}) \geq I(\mathcal{B})$.*

Since the late 1990s, several QIs have been proposed [95]. Van Veldhuizen [133] proposed different indicators, including the Generational Distance (GD) and Error Ratio (ER), among others. GD measures the average distance from the approximation set to a reference set, while ER reports the number of solutions of the approximation set that do not belong to $\mathcal{PF}^*$. Zitzler and Thiele [156] introduced the hypervolume indicator (HV) that rewards the convergence towards $\mathcal{PF}^*$ as well as the extent of solutions along the Pareto front. Hansen and Jaszkiewicz [55] proposed the R-family indicators (R1, R2 and R3) from a set of outperformance relations and some utility functions. Coello Coello and Cruz Cortés [23] proposed to measure the average Euclidean distances between the true Pareto front (or the reference set) and the approximation produced by an MOEA. Since this is exactly the opposite way in which GD operates, this indicator was called Inverted Generational Distance (IGD) and its use was reported for the first time in [25].[3] More recently, Ishibuchi et al. [74] proposed the Inverted Generational Distance plus (IGD^+) that determines the

[3]The original proposal of IGD was published in a journal but it appeared until 2005, whereas its first reported use was at a conference paper that was published in 2004.

Table 3.2: Summary of properties of QIs. C means Convergence, C/D means Convergence-Diversity, and D denotes Diversity.

Indicator	Performance criteria	Pareto compliance	Knowledge dependent	Parameter dependent	Scaling invariant	Scalable	Runtime complexity
HV	C/D	Strict	Reference point	No	No	Yes	Super-polynomial
R2	C/D	Weak	Reference point	Weight vectors Utility functions	No	Yes	$\theta(m\|\mathcal{Z}\| \cdot \|\mathcal{A}\|)$
GD	C	No	Reference set	$p > 0$	Yes	Yes	$\theta(m\|\mathcal{Z}\| \cdot \|\mathcal{A}\|)$
IGD	C/D	No	Reference set	$p > 0$	Yes	Yes	$\theta(m\|\mathcal{Z}\| \cdot \|\mathcal{A}\|)$
IGD^+	C/D	Weak	Reference set	No	Yes	Yes	$\theta(m\|\mathcal{Z}\| \cdot \|\mathcal{A}\|)$
Δ_p	C/D	No	Reference set	$p > 0$	Yes	Yes	$\theta(m\|\mathcal{Z}\| \cdot \|\mathcal{A}\|)$
ϵ^+	C	Weak	Reference set	No	No	Yes	$\theta(m\|\mathcal{Z}\| \cdot \|\mathcal{A}\|)$
Riesz s-energy	D	No	No	$s > 0$	Yes	Yes	$\theta(m\|\mathcal{A}\|^2)$

distance between an approximation set and a reference set, using a distance measure that adopts Pareto dominance. In spite of the plethora of QIs currently proposed, no one can assess all the desired features of an approximation set, since each QI exhibits a specific preference, and, in this regard, Zitzler *et al.* claimed that it is necessary an infinite number of QI values to characterize the quality of an approximation set [158]. Hence, we should choose a QI depending on the type of conclusions we would like to draw.

In the following, we describe seven convergence QIs (hypervolume indicator, R2, GD, IGD, IGD^+, Δ_p, and ϵ^+) that have mainly promoted the design of MOEAs' selection mechanisms, and one indicator focused on measuring the uniformity of solutions in the large class of rectifiable d-dimensional manifolds. For all definitions, let $\mathcal{A}$ denote an approximation set and $\mathcal{Z}$ be a reference set[4]. The main properties of the adopted QIs are summarized in Table 3.2. For a complete review of QIs, the reader is referred to the survey of Li and Yao [95].

Definition 3.1.2 (Hypervolume indicator [148])**.** *Let Λ denote the Lebesgue measure in $\mathbb{R}^m$, HV is defined as follows:*

$$HV(\mathcal{A}, \vec{z}_{ref}) = \Lambda\left(\bigcup_{\vec{a}\in\mathcal{A}} \{\vec{x} \mid \vec{a} \prec \vec{x} \prec \vec{z}_{ref}\}\right), \tag{3.1}$$

where $\vec{z}_{ref} \in \mathbb{R}^m$ is a reference point which should be dominated by all points in $\mathcal{A}$.

[4]We denote a reference set $\mathcal{Z}$ as a finite subset of solutions from the Pareto optimal front, i.e., $\mathcal{Z} \subseteq \mathcal{PF}^*$.

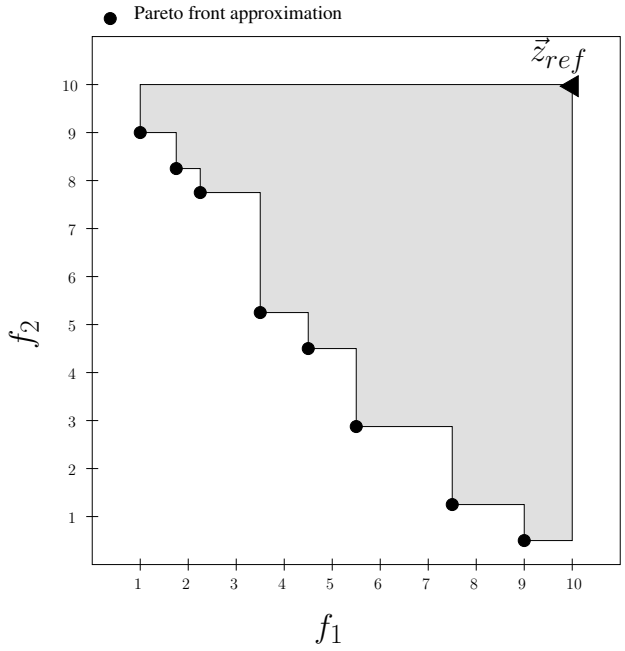

Figure 3.2: Shaded area corresponding to the hypervolume indicator value.

HV is a convergence-diversity QI that measures the extent of volume dominated by $\mathcal{A}$ and bounded by $\vec{z}_{ref}$ (see Figure 3.2). Currently, HV and the closely related logarithmic HV [50], the weighted HV [2], and the free HV [40] are the only known Pareto-compliant QIs. The two main drawbacks of HV are the following. First, under NP $\neq$ P, its computational cost increases super-polynomially as the number of objective functions does [7]. The other issue is related to $\vec{z}_{ref}$ since the preferences of HV strongly depend on it [2, 71]. In other words, the specification of the reference point is dependent on the Pareto front shape. It has been shown that the distribution of points provided by selecton mechanisms based on HV is often concentrated on the boundary and in knee point regions.

Definition 3.1.3 (Unary R2 indicator [17])**.** *The unary R2 indicator is defined as follows:*

$$R2(\mathcal{A}, W) = \frac{1}{|W|} \sum_{\vec{w} \in W} \min_{\vec{a} \in \mathcal{A}} \{u_{\vec{w}}(a)\}, \tag{3.2}$$

where W is a set of m-dimensional weight vectors and $u_{\vec{w}} : \mathbb{R}^m \to \mathbb{R}$ is a utility function, parameterized by $\vec{w} \in W$, that assigns a real value to each solution vector.

The R2 indicator is a convergence-diversity QI that measures the average minimum utility values of the approximation set with respect to a set of weight vectors. Figure 3.3 exemplifies its computation, where each objective vector is associated to a weight vector depending on the optimization of the utility function. Its computational cost is $\Theta(m|W| \cdot |\mathcal{A}|)$. Unlike the hypervolume indicator, the time complexity of R2 scales only linearly with the number of objectives. Its time complexity is, how-

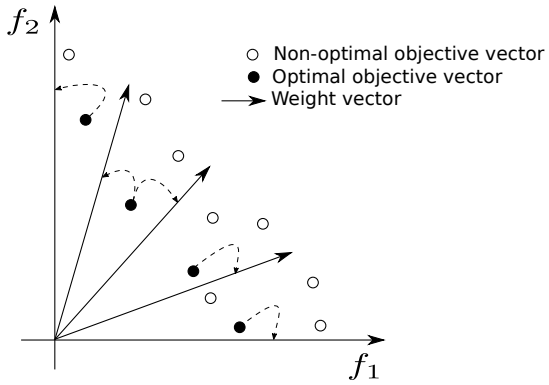

Figure 3.3: Computation of the R2 indicator: optimal objective vectors, according to the utility function, are associated to weight vectors by dashed lines.

ever, proportional to the number of weight vectors[5], which has to grow exponentially in size, if the number of objectives increases and the same sampling resolution is desired. A major conceptual difference with regard to the hypervolume indicator is that the R2 indicator does not require an anti-optimal reference point. Instead it works with an ideal or utopian reference point. Hence, it would be desirable to use the R2 indicator.

A problem, however, arises due to the fact that the R2 indicator is not Pareto-compliant, and it is only weakly Pareto-compliant. This makes it possible that a set might have equal R2 indicator value than another set, although it is dominated in the set order, or that sets degenerate if this indicator is used as a guideline in Pareto optimization. One might argue that these are rare cases, as they always involve shared coordinate values among points, and in most cases the R2 indicator works welll when comparing sets. In fact, in continuous unconstrained optimization such cases this might occur with a low probability, but it is relatively likely in continuous optimization and in cases where box constraints are introduced.

Definition 3.1.4 (Generational Distance [135])**.** *GD evaluates the average distance from each $\vec{a} \in \mathcal{A}$ to its closest reference point $\vec{z} \in \mathcal{Z}$. It is defined as follows:*

$$GD(\mathcal{A}, \mathcal{Z}) = \frac{1}{|\mathcal{A}|} \left(\sum_{\vec{a} \in \mathcal{A}} d(\vec{a}, \mathcal{Z})^p \right)^{1/p}, \tag{3.3}$$

where $p > 0$ is a user-defined parameter (usually set to $p = 2$) and d is the Euclidean distance from $\vec{a} \in \mathcal{A}$ to its nearest member of $\mathcal{Z}$:

$$d(\vec{a}, \mathcal{Z}) = \min_{\vec{z} \in \mathcal{Z}} \sqrt{\sum_{i=1}^{m} (a_i - z_i)^2}. \tag{3.4}$$

[5]The Simplex-Lattice-Design method is usualy employed to construct the set of weight vectors [147]. Using this method, the number of weight vectors is the following combinatorial number: $N = C_{m-1}^{H+m-1}$,where $H \in \mathbb{N}$ is a user-supplied parameter that determines the number of divisions of the space, and m is the number of objectives.

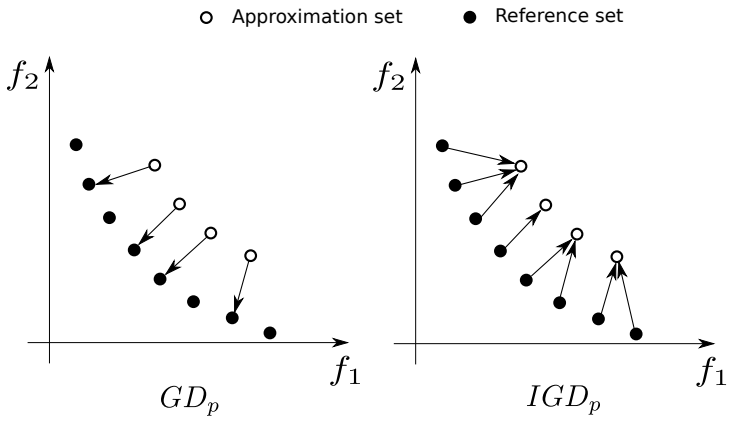

Figure 3.4: Difference between GD and IGD indicators.

Definition 3.1.5 (Inverted Generational Distance [23])**.** *In contrast to GD, IGD measures the average distance from each reference point to its nearest solution in* $\mathcal{A}$ *as follows:*

$$IGD(\mathcal{A}, \mathcal{Z}) = GD(\mathcal{Z}, \mathcal{A}) = \frac{1}{|\mathcal{Z}|}\left(\sum_{\vec{z}\in\mathcal{Z}} d(\vec{z}, \mathcal{A})^p\right)^{1/p}, \tag{3.5}$$

where $p > 0$ *is a parameter usually set to* $p = 2$*.*

Definition 3.1.6 (Inverted Generational Distance plus [74])**.** *The IGD*$^+$*, for minimization, is defined as follows:*

$$IGD^+(\mathcal{A}, \mathcal{Z}) = \frac{1}{|\mathcal{Z}|}\sum_{\vec{z}\in\mathcal{Z}} \min_{\vec{a}\in\mathcal{A}} d^+(\vec{z}, \vec{a}) \tag{3.6}$$

where $d^+(\vec{z}, \vec{a}) = \sqrt{\sum_{k=1}^{m} \left(\max\{a_k - z_k, 0\}\right)^2}$.

GD was proposed by Van Veldhuizen and Lamont [135] and it estimates how far are the elements in $\mathcal{A}$ from those in $\mathcal{Z}$, i.e., it exclusively measures the convergence of the approximation set. Since GD is non-Pareto-compliant, in some cases, it produces misleading results when comparing MOEAs [158, 74]. Additionally, GD is sensitive to the size of the approximation set [9]. For example, an important problem takes place when $\mathcal{A}$ has very few points, but they all are clustered together. In order to overcome this issue, Coello Coello and Cruz Cortés [23] proposed IGD, which unlike GD, measures the average distance from $\mathcal{Z}$ to $\mathcal{A}$. The difference between GD and IGD is shown in Figure 3.4. Unfortunately, IGD is also not Pareto-compliant QI. In furtherance of improving the mathematical properties of IGD, Ishibuchi *et al.* proposed IGD$^+$ [74] that is a variant of it that adopts Pareto dominance in the Euclidean distance. For this purpose, they modified the Euclidean distance as shown in Figure 3.5. Given $\vec{z} \in \mathcal{Z}$ and $\vec{f}(\vec{a}), \vec{f}(\vec{b}) \in \mathcal{A}$, they proposed to measure the distance

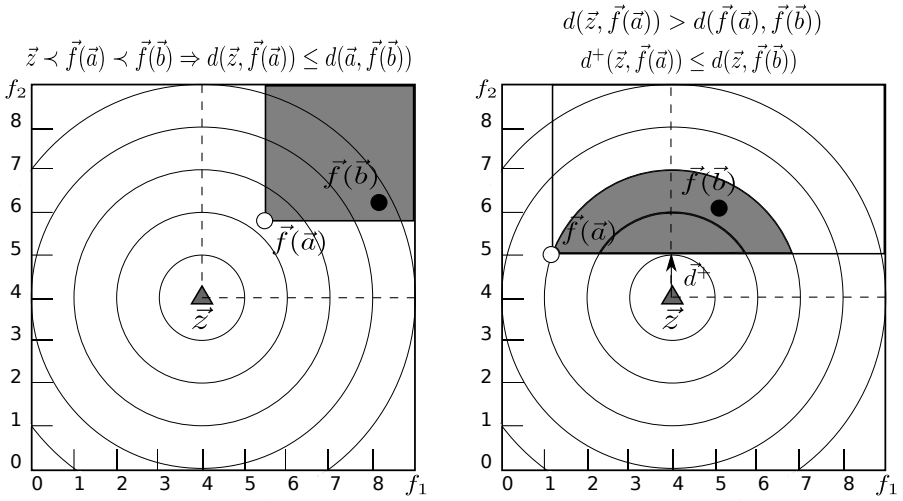

Figure 3.5: Comparison between the typical Euclidean distance employed by IGD in the left-hand side of the figure, and the distance employed by the IGD$^+$ indicator in the right-hand side.

to the dominated region of $\vec{f}(\vec{a})$ from $\vec{z}$ since both are mutually non-dominated, while they employed the usual Euclidean distance from $\vec{z}$ to $\vec{f}(\vec{b})$ since $\vec{z} \prec \vec{f}(\vec{b})$. Due to this modification, IGD$^+$ is weakly Pareto-compliant. Bezerra *et al.* [9] broadly discuss the differences between IGD and IGD$^+$. However, an important issue that GD, IGD, and IGD$^+$ share is how to construct $\mathcal{Z}$ when no information about $\mathcal{PF}^*$ is available [73]. The computational cost of these indicators is $\theta(m|\mathcal{Z}| \cdot |\mathcal{A}|)$.

Definition 3.1.7 (Averaged Hausdorff Distance (Δ_p) indicator [118])**.** *For a given $p > 0$, Δ_p is defined as follows:*

$$\Delta_p(\mathcal{A}, \mathcal{Z}) = \max\{GD_p(\mathcal{A}, \mathcal{Z}), IGD_p(\mathcal{A}, \mathcal{Z})\}. \tag{3.7}$$

Δ_p is composed of two indicators: GD$_p$ and IGD$_p$ which are slight modifications of GD and IGD, respectively. These are defined as follows:

Definition 3.1.8 (GD$_p$ indicator [118])**.**

$$GD_p(\mathcal{A}, \mathcal{Z}) = \left(\frac{1}{|\mathcal{A}|} \sum_{\vec{a} \in \mathcal{A}} d(\vec{a}, \mathcal{Z})^p \right)^{1/p}. \tag{3.8}$$

Definition 3.1.9 (IGD$_p$ indicator [118])**.**

$$IGD_p(\mathcal{A}, \mathcal{Z}) = GD_p(\mathcal{Z}, \mathcal{A}) = \left(\frac{1}{|\mathcal{Z}|} \sum_{\vec{z} \in \mathcal{Z}} d(\vec{z}, \mathcal{A})^p \right)^{1/p}. \tag{3.9}$$

Although the Hausdorff distance is a metric in the mathematical sense on the set of compact subsets of $\mathbb{R}^m$, it tends to penalize outlier solutions that are commonly generated by MOEAs. Consequently, Schütze *et al.* introduced the Δ_p indicator that measures the averaged Hausdorff distance of the approximation set to the reference set [118]. Δ_p is based on the indicators GD_p and IGD_p which are slight modifications of the original GD and IGD indicators that aim to reduce the penalization of outliers. It is worth noting that such averaging of the distances leads to violations of the triangle inequality, and hence, Δ_p is not a metric. Additionally, Δ_p is a non-Pareto-compliant QI, and it assesses convergence and distribution simultaneously. Similarly to GD, IGD and IGD^+, this indicator requires a reference set which is difficult to construct without information of the Pareto optimal front.

Definition 3.1.10 (Unary ϵ^+ indicator [158])**.** *Mathematically, it is defined as follows:*

$$\epsilon^+(\mathcal{A}, \mathcal{Z}) = \max_{\vec{z}\in\mathcal{Z}} \min_{\vec{a}\in\mathcal{A}} \max_{1\leq i\leq m} \{z_i - a_i\}. \tag{3.10}$$

Zitzler *et al.* [158] introduced the unary ϵ-indicator to measure the minimum distance that an approximation set needs to be translated in each dimension to weakly Pareto dominate a reference set. Consequently, ϵ^+ exclusively assesses the convergence of a Pareto front approximation. It is worth emphasizing that ϵ^+ is a weakly Pareto-compliant QI. Although it is a parameterless QI, a reference set is required for its computation. Additionally, ϵ^+ is not very sensitive to small changes of the solutions in $\mathcal{A}$ [14].

Each solution in an approximation set contributes to the total indicator value. This individual contribution is important when designing selection mechanisms to impose a total order among solutions [8]. Hence, for an indicator I in the set $\{\mathrm{HV}, \mathrm{R2}, \mathrm{GD}, \mathrm{IGD}, \mathrm{IGD}^+, \epsilon^+, \Delta_p\}$, the individual contribution is defined as follows.

Definition 3.1.11 (Indicator contribution)**.** *The individual contribution C of a solution $\vec{a} \in \mathcal{A}$ to the indicator value is given by the formula:*

$$C_{\mathcal{I}}(\vec{a}, \mathcal{A}) = |\mathcal{I}(\mathcal{A}) - \mathcal{I}(\mathcal{A} \setminus \{\vec{a}\})|. \tag{3.11}$$

Definition 3.1.12 (Riesz s-energy indicator [56])**.** *For a given $s > 0$, the Riesz s-energy indicator is defined as follows:*

$$E_s(\mathcal{A}) = \sum_{i\neq j} \|\vec{a}_i - \vec{a}_j\|^{-s} \tag{3.12}$$

Riesz s-energy is an indicator that assess the uniformy of solutions, where s is a fixed parameter that controls the degree of uniformity of the solutions in $\mathcal{A}$. As $s \to \infty$, E_s prefers more uniform solutions. Riesz s-energy has been found to lead to uniformly distributed point sets for the large class of rectifiable d-dimensional manifolds. Moreover, s is not a shape-dependent parameter [57]. The individual contribution to E_s is defined in the following.

Definition 3.1.13 (Riesz s-energy individual contribution)**.** *The individual contribution C of a solution $\vec{a} \in \mathcal{A}$ to the Riesz s-energy indicator is as follows:*

$$C_{E_s}(\vec{a}, \mathcal{A}) = \frac{1}{2} \left[E_s(\mathcal{A}) - E_s(\mathcal{A} \setminus \{\vec{a}\}) \right]. \tag{3.13}$$

3.2 IB-MOEAs: state-of-the-art

Multi-Objective Evolutionary Algorithms aim to determine a set of solutions that satisfy specific optimality properties. The Pareto dominance relation [24] has represented the most general optimality notion. However, the degree of freedom to determine what is an optimal solution is still considerable. In consequence, QIs integrated into MOEAs, i.e., the so-called indicator-based MOEAs (IB-MOEAs), introduce additional information that describes the preference of the user and improves the notion of optimality imposed by the Pareto dominance relation [152, 123]. The underlying idea of IB-MOEAs is to optimize an indicator value through the evolutionary process [123]. Since 2003, IB-MOEAs have been developed to overcome the drawbacks of Pareto-based MOEAs, with a particular emphasis on diversity issues and the dilution of selection pressure when tackling MaOPs [136, 89]. In this section, we review the development of IB-MOEAs from the earliest proposals to the current state-of-the-art approaches.

3.2.1 Our Proposed Taxonomy

Currently, several indicator-based mechanisms (IB-Mechanisms) have been designed and integrated into MOEAs. However, there is no clear distinction among them. Consequently, we introduce a taxonomy (see Figure 3.6) to classify IB-Mechanisms based on a comprehensive review of the state-of-the-art approaches. It is worth emphasizing that this is the first taxonomy ever proposed to classify the mechanisms of IB-MOEAs.

Our taxonomy, shown in Figure 3.6, is based on the primary MOEAs' mechanisms described in Section 2.2, i.e., mating selection and selection schemes applied on the main population and the archive. It is worth emphasizing that our taxonomy aims to classify the indicator-based mechanisms that MOEAs have adopted, rather than classifying IB-MOEAs themselves. IB-Mechanisms are divided into two categories: (1) IB-Mating Selection, and (2) IB-Selection. On the one hand, IB-Mating Selection aims to select μ parents to create λ promising offspring solutions. These IB-Mating Selection methods can be variations, for instance, of the commonly employed tournament selection, roulette wheel selection, or proportional selection [10, 24] or new proposals, but applying QIs as the core of the methods. On the other hand, IB-Selection comprises three classes: (1) IB-Environmental Selection (IB-ES), (2) IB-Density Estimation (IB-DE), and (3) IB-Archiving (IB-AR). The main difference between IB-Mating Selection and IB-Selection is that the latter aims to solve or approximate the Indicator-based Subset Selection Problem (IBSSP) [4] that is defined

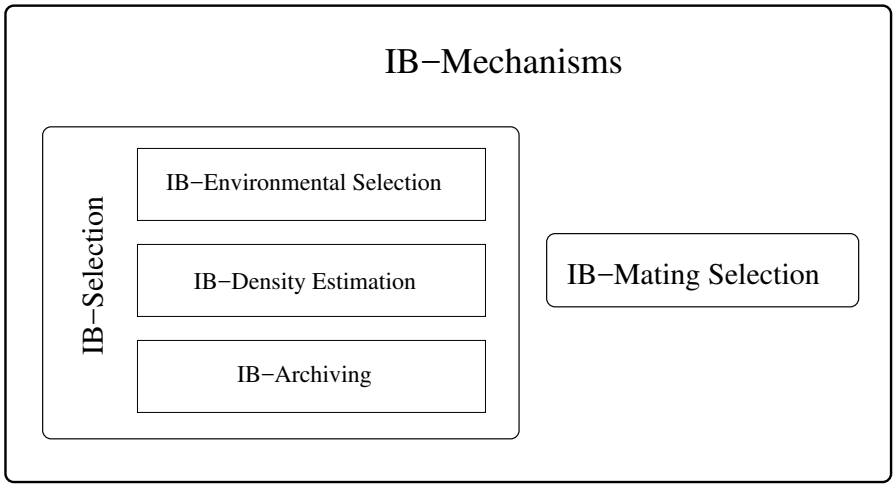

Figure 3.6: IB-Mechanisms are divided into two main categories: (1) IB-Selection, and (2) IB-Mating Selection. Furthermore, the former category is classified in three groups: IB-Environmental Selection, IB-Density Estimation, and IB-Archiving.

as follows:

Definition 3.2.1 (Indicator-based Subset Selection Problem)**.** *Let $Z \subseteq \mathbb{R}^m$ be a space of m-dimensional vectors, and let I be a unary quality indicator. Without loss of generality, we assume that this indicator is to be maximized. Given $R \subseteq Z$, a reference set of cardinality N, and $k \leq N$ a positive subset size, the IBSSP consists in determining the set $S \subseteq R$ of maximal quality:*

$$\underset{\substack{S \subseteq R \\ |S|=k}}{\arg\max}\, I(S). \tag{3.14}$$

In other words, IBSSP aims to select a subset of $k \leq N$ solutions that optimizes the indicator value. The solution space size of IBSSP is $\binom{N}{k}$. Apart from the inherent complexity of computing indicator values, this makes of IBSSP a challenging combinatorial optimization problem. The next question to solve is why IB-Selection is divided into three categories since, at first sight, they seem to overlap.

On the one hand, IB-Archiving corresponds to selection rules that update the external population $\mathcal{A}$. The first proposed IB-MOEA implements an IB-AR scheme based on the hypervolume indicator [85, 87]. In this regard, many MOEAs have an external population whose purpose is to maintain an approximation to the Pareto front, i.e., the global non-dominated solutions generated by the MOEA [24]. Each time a new point is considered for addition to the archive, it must be analyzed for non-dominance concerning the points currently stored. Hence, at the end of the evolutionary process, the archive will only include solutions that are non-dominated for all the objective vectors that have been generated by the MOEA (i.e., the global non-dominated solutions).

On the other hand, IB-ES and IB-DE are exclusively applied to the main population P. These two mechanisms are shown in line 8 of Algorithm 1. However, there is no clear distinction between IB-ES and IB-DE. Environmental selection dictates which solutions should survive at each generation. Thus, this mechanism has particular importance because convergence is closely related to it. Thiele [123] has pointed out that IB-ES can be designed using two algorithmic methodologies: hierarchical selection and selection based on fitness assignment. Hierarchical selection imposes a partial order among the solutions in P just as the non-dominated sorting algorithm [31] does, but it needs a refinement using a density estimator. On the contrary, fitness assignment imposes a total order among the solutions which implies that a density estimator is not required. As we previously mentioned, density estimators refine the partial order imposed by hierarchical environmental selection mechanisms. In this regard, they perform as the second selection criterion to reduce the size of the joint population of parents and offspring, aiming simultaneously to enhance diversity. Although they have different purposes, an IB-DE can perform as an IB-ES under certain conditions. For instance, when the non-dominated sorting algorithm is coupled with an IB-DE [8, 18, 43], the latter will eventually replace the former since it tends to create a single rank of solutions when tackling MaOPs, i.e., it loses selection pressure. Hence, only when an IB-DE is working with an environmental selection mechanism that loses selection pressure, it will perform as the primary selection mechanism. Otherwise, an IB-DE will perform as the second selection criterion.

In the following sections, we will review several IB-Mechanisms that have been proposed until the end of 2018. The review will be done following our taxonomy. For each proposal, we will focus on discussing their properties, advantages, and drawbacks.

3.2.2 IB-Selection

The first IB-MOEA was proposed by Knowles *et al.* [87] in 2003. This algorithm employed an archiving update rule based on the hypervolume indicator. Since then, a plethora of proposals have been published in the specialized literature. In this section, we present a review of the most important MOEAs that use an IB-Selection mechanism. Tables 3.3, 3.4, and 3.5 summarize MOEAs adopting IB-ES, IB-DE, and IB-AR methods, respectively.

3.2.2.1 IB-Environmental Selection

Hypervolume indicator: Zitzler and Künzli [153] proposed the Indicator-Based Evolutionary Algorithm (IBEA) whose general framework is shown in Algorithm 2. The underlying idea of IBEA is to provide a general framework for $(\mu + \lambda)$ environmental selection based on arbitrary binary indicators that are integrated into a fitness function (see line 5). This fitness function measures the loss in quality when each $\vec{x} \in Q$ is removed. According to the authors, the exponential function is employed to amplify the influence of dominating solutions members over dominated ones. This

Table 3.3: IB-Environmental Selection mechanisms. The algorithmic structure of the IB-ES is termed as 'Algorithmic approach' while 'Method' indicates what kind of information is employed to select the solutions. For each approach, we show the test problems and the number of objective functions on which the IB-MOEA was tested on.

Indicator	**Algorithm**	**Algorithmic approach**	**Method**	**Problems**	**# Objetives**	**Year**	**Ref.**
HV	IBEA_{HV}	Greedy	Fitness assignment	ZDT, KUR, DTLZ	2 & 3	2004	[152]
	Iterative-IBEA	Greedy	Fitness assignment	500-item 0/1 Knapsack problem	2 - 4	2007	[76]
	iSMS-EMOA	Greedy	Worst contribution	DTLZ & WFG	3 - 6	2013	[103]
	DIVA	Greedy	Fitness assignment	WFG	2	2014	[130]
	IBEA2	Greedy	Fitness assignment	ZDT, DTLZ, WFG	2 - 5	2016	[81]
	mIBEA	Greedy	Fitness assignment	DTLZ	3	2017	[96]
	aviSMS-EMOA	Greedy	Worst contribution	DTLZ & WFG	3 - 6	2017	[106]
$R2$	$R2$-MOGA	Hierarchical	Worst contribution	ZDT, DTLZ, WFG	2 - 10	2013	[35]
	$R2$-MODE	Hierarchical	Worst contribution	ZDT, DTLZ, WFG	2 - 10	2013	[35]
	$R2$-IBEA	Greedy	Fitness assignment	ZDT & DTLZ	2 - 5	2013	[131]
	MOMBI	Hierarchical	Scalarizing function optimization	DTLZ & WFG	2 - 8	2013	[59]
	MOMBI-II	Hierarchical	Scalarizing function optimization	DTLZ & WFG	3 - 10	2015	[60]
	TS-R2EA	Hierarchical	R2 contribution and fitness assignment	DTLZ & WFG	3 - 15	2018	[91]
	R2-MOEA/D	Decomposition	Worst contribution	DTLZ & WFG	3 - 15	2018	[92]
IGD^+	IGD^+-EMOA	Linear Assignment Problem	Kuhn-Munkres algorithm	DTLZ & WFG	2 - 8	2015	[100]
	IGD^+-EMOA II	Linear Assignment Problem	Kuhn-Munkres algorithm	DTLZ, WFG, MAF, Viennet	2 - 8	2018	[101]
GD	GD-MOEA	Greedy	Minimize distance to $\mathcal{PF}^*$	DTLZ, WFG	3 - 6	2015	[104]
	GDE-MOEA	Greedy	Minimize distance to $\mathcal{PF}^*$ and ϵ dominance	DTLZ, WFG	3 - 6	2015	[105]
ϵ^+	IBEA_{ϵ^+}	Greedy	Fitness assignment	ZDT6, KUR, DTLZ2, DTLZ6	2 - 3	2004	[152]
	AGE	Greedy	Worst contribution	DTLZ	2 - 20	2011	[14]
	AGE-II	Greedy	Worst contribution	DTLZ, WFG	2 - 20	2013	[137]
	Two_Arch2	Greedy	Fitness assignment	DTLZ, WFG	2- 20	2014	[138]
Δ_p	Δ_p-DDE	Greedy	Worst contribution	ZDT, DTLZ	2 - 10	2012	[113]
	Δ_p-MOEA	Greedy Hierarchical	Minimize point-to-set distance	WFG	3 - 6	2016	[107]

fitness function also requires a fitness scaling factor κ that depends on the indicator being used and the MOP. The IB-ES, decribed in lines 6 to 10, is a greedy algorithm that deletes at each iteration the solution having the minimal fitness value while $|Q| > \mu$. To illustrate the effectiveness of IBEA, its authors proposed the IBEA_{HV} that uses a binary hypervolume indicator. IBEA_{HV} was compared to NSGA-II [31] and SPEA2 [155] on the 100-item 0/1 knapsack problem and the low-dimensional continuous MOPs: ZDT6, DTLZ2, DTLZ6 and Kursawe (KUR) [24]. IBEA_{HV} outperformed NSGA-II in almost all MOPs. Interestingly enough, however, the bi-objective KUR problem, which has a disconnected and a concave Pareto front, was the most challenging problem for IBEA_{HV}.

An important disadvantage of IBEA is related to the κ parameter which is dependent on the MOP and the indicator employed. Regarding this drawback, IBEA2 [81] was proposed to adaptively adjust parameter κ. This adaptive mechanism looks for the best κ parameter using the Nelder-Mead method where the objective function is defined as a similarity measure between two sets: one produced by the IB-ES of IBEA_{HV} and another one using a density estimator based on HV [83]. IBEA2 was tested on the ZDT, DTLZ and WFG test problems using for 2 to 5 objective functions, comparing its performance to that of NSGA-II, SPEA2, MOEA/D and IBEA_{HV} in terms of HV. Based on the analysis of the experimental results, IBEA2 was found to be a very good optimizer for MOPs whose Pareto fronts are linear, concave and degenerated. However, it has low performance when tackling MOPs having disconnected, mixed and multifrontal Pareto fronts. Additionally, the results show that due to the use of the adaptive mechanism, IBEA2 is better than IBEA_{HV} in most of the test problems adopted.

Another improvement of the IBEA framework is the modified IBEA (mIBEA), proposed by Li *et al.* [96]. Its main motivation was to improve the bad distribution of points generated by IBEA_{HV}. To this aim, the authors hybridized the IBEA framework with the non-dominated sorting algorithm to exclude dominated solutions at each generation. Due to this modification, the scaling of the objective functions scores is no longer affected by dominated solutions which are far away from the best non-dominated solutions. The uniformity and convergence analysis of solutions showed that mIBEA performs better than IBEA_{HV}. However, the authors did not show an exhaustive performance analysis with respect to other state-of-the-art MOEAs.

In 2007, Ishibuchi *et al.* [76] proposed the Iterative-IBEA[6] that produces at each execution a single solution to maximize the HV value. In other words, it iteratively constructs the final solution set S. At execution k, Iterative-IBEA uses $\text{HV}(S^{(k-1)} \cup \{\vec{u}\})$ as its fitness function (where $S^{(k-1)}$ is the solution set generated in the previous execution, thus, $|S^{(k-1)}| = k-1$). The IB-ES computes the fitness values of the $(\mu+\lambda)$ solutions and deletes the worst λ individuals. If we want a Pareto front approximation of size N, we have to execute Iterative-IBEA the same number of times which implies a high-computational cost due to the use of the hypervolume indicator. This IB-

[6] Although this MOEA is called IBEA, it does not follow the IBEA framework of Algorithm 2.

MOEA was only compared to NSGA-II on the 500-item 0/1 knapsack problem for 2, 3 and 4 objective functions.

Ulrich *et al.* [130] proposed the Diversity Integrating Hypervolume-based Search Algorithm (DIVA) that combines a decision space diversity measure and HV into one single set measure, where the trade-off between the two measures is tunable. DIVA employs a greedy environmental selection that aims to remove the worst contributing solutions to HV to obtain the best μ solutions out of a set of $(\mu + \lambda)$ individuals. DIVA was tested on the WFG test suite for two objective functions. Experimental results showed that DIVA significantly improves diversity compared to HypE [3] (see Section 3.2.2.2, in page 41) due to the integration of the diversity measure into HV. However, its main drawback is related to the high computational cost associated with both HV and the diversity measure adopted.

Since the main limitation of the above-mentioned proposals is the expensive calculation of HV, Menchaca-Mendez and Coello Coello [103] proposed an IB-ES that exploits the locality property of HV.[7] This approach, called iSMS-EMOA, generates at each generation one offspring solution that must compete, regarding its HV contribution, with its nearest neighbor in objective space and $r \geq 1$ randomly chosen solutions from the population (they set $r = 1$). In consequence, it only needs to compute $r + 2$ HV contributions instead of handling the whole population. iSMS-EMOA was compared to SMS-EMOA and HypE on the DTLZ test suite for 3 to 6 objective functions, regarding HV. The stopping criterion of all MOEAs was 50,000 function evaluations or a maximum of four hours of running time (since SMS-EMOA computes the exact HV, it is very time-consuming for many-objective problems). For 3 and 4 objectives, iSMS-EMOA presented a competitive performance compared to SMS-EMOA. However, for 5 and 6 objective functions, iSMS-EMOA completely outperformed the adopted MOEAs since they ran out of running time. Hence, iSMS-EMOA can be considered as a promising approach for solving MaOPs due to its less expensive IB-ES while still relying on the nice mathematical properties of HV.

Finally, in 2017, the same authors proposed an improvement of iSMS-EMOA. denoted as approximate version of the improved SMS-EMOA (aviSMS-EMOA) [106]. The idea of aviSMS-EMOA is to combine the selection scheme of iSMS-EMOA with a recently proposed mechanism to approximate the hypervolume contributions with a minimal error [12]. Due to the exploitation of the locality property and the mechanism to approximate HV contributions, aviSMS-EMOA is able to balance the quality of the outcome set and the running time required to obtain it. In its experimental results, considering the DTLZ and WFG test suites, aviSMS-EMOA was able to outperform both iSMS-EMOA and HypE. However, SMS-EMOA obtained better results since it employs the exact calculation of the hypervolume, but if the trade-off between computational cost and quality is taken into account, then aviSMS-EMOA is a very competitive alternative to the use of SMS-EMOA.

[7] For two dimensions, "given three consecutive points on the Pareto front, moving the middle point will only affect the HV contribution that is dedicated to this point, but the joint HV contribution remains fixed" [2].

Algorithm 2: IBEA general framework

Input: Fitness scaling factor κ
Output: Pareto front approximation

```
Randomly initialize population P of size μ;
while stopping criterion is not fulfilled do
    Create the set O of λ offspring solutions;
    Q ← P ∪ O;
    fitness(x⃗) = Σ_{y⃗∈Q\{x⃗}} −e^{−I({y⃗},{x⃗})/κ}, ∀x⃗ ∈ Q;
    while |Q| > μ do
        x⃗^min ← arg min_{x⃗∈Q} fitness(x⃗);
        Q ← Q \ {x⃗^min};
        Update fitness values of all individuals in Q;
    end
end
return P
```

R2 indicator: In 2013, Phan and Suzuki [131] proposed R2-IBEA following the scheme of IBEA (see Algorithm 2) but adopting a binary version of R2. Additionally, the authors suggested two new mechanisms. First, a hypervolume-based weight vector generation approach that uniformly distributes the weight vectors required by R2, aiming to maximize HV. Additionally, they proposed an adaptive reference point adjustment mechanism that aids R2-IBEA to reduce the bias of the R2 indicator to prefer the knee of the Pareto front therefore promoting the generation of uniform solutions. The performance of R2-IBEA was examined on MOPs from the ZDT and DTLZ test suites (using 3 and 5 objectives), using the HV, GD, IGD and ϵ^+ indicators and it was compared with Pareto-based, indicator-based and decomposition-based MOEAs. Although R2-IBEA had remarkable results in almost all problems in terms of convergence and diversity, it is worth emphasizing its poor performance on multifrontal MOPs, i.e., ZDT4 and DTLZ3 for 2 and 3 objective functions, respectively. For 5-dimensional problems, R2-IBEA obtained the best HV value in problems DTLZ1, DTLZ3, DTLZ4 and DTLZ7. However, the authors did not test their proposal on degenerated problems (DTLZ5 and DTLZ6).

In the same year, Díaz-Manríquez *et al.* [35] proposed a hierarchical IB-ES similar to the non-dominated sorting scheme of NSGA-II. However, instead of computing ranks of non-dominated solutions, they suggested the creation of ranks of contributing solutions to the R2 indicator. The first layer contains solutions that do contribute to R2; then, these solutions are temporarily removed and a new layer is generated. This process continues until there are no more solutions left. The authors embedded this IB-ES into two search engines: a genetic algorithm and a differential evolution algorithm, giving rise to the R2-Multi-Objective Genetic Algorithm (R2-MOGA) and the R2-Multi-Objective Differential Evolution (R2-MODE). Both proposals were compared to NSGA-II, MOEA/D and SMS-EMOA on the ZDT, DTLZ, and WFG test

suites using 2 and 3 objective functions. According to their HV results, R2-MOGA and R2-MODE had a poor performance on these MOPs. Additionally, the authors experimented on MaOPs, comparing R2-MOGA and R2-MODE to SMS-EMOA and HypE using the HV indicator. They employed the DTLZ1-DTLZ4 test instances with 4 to 10 objective functions. These results indicated that their two proposals were competitive with respect to SMS-EMOA and HypE regarding HV. Additionally, the proposed approaches outperformed the HV-based MOEAs adopted in the comparison in terms of computational time.

Hernández Gómez and Coello Coello [59] proposed the $R2$-ranking algorithm which is similar to the one previously described. However, instead of creating ranks of $R2$-contributing solutions, this approach identifies solutions that optimize the set of utility functions involved in the definition of R2. This selection mechanism was implemented in the Many-Objective Metaheuristic Based on the $R2$ Indicator (MOMBI). The authors adopted the DTLZ and WFG test suites in their experiments, assessing the performance of MOMBI, MOEA/D, and SMS-EMOA in terms of HV using MOPs with 2 to 8 objective functions. From the results, it is evident that MOMBI outperformed the other MOEAs on the multifrontal MOPs and those having disconnected and mixed Pareto front shapes, such as DTLZ7 and WFG1, respectively. However, MOMBI was outperformed by the other MOEAs on degenerated MOPs (DTLZ5, DTLZ6, and WFG3) and concave MOPs (DTLZ2 and WFG4-WFG9). Regarding concave MOPs, the distribution of points generated by MOMBI was strongly biased towards the knee of the Pareto front due to the adoption of the weighted Tchebycheff utility function (WTCH). Additionally, a running time analysis showed that MOMBI was less computationally expensive than SMS-EMOA and that it was slightly more costly than MOEA/D.

In furtherance of solving the distribution bias of MOMBI, the same authors proposed MOMBI-II [60] that uses the achievement scalarizing function (ASF) instead of WTCH, where the former promotes a more uniform distribution of points. Additionally, MOMBI-II employs a mechanism to statistically estimate the nadir point that is needed to normalize the population. MOMBI-II was tested on one linear MOP (DTLZ1) and 5 concave MOPs (DTLZ2-DTLZ4, WFG6 and WFG7) using 3 and 5 objective functions and it was compared to numerous MOEAs, using the indicators HV and Δ_p. The results show that due to the use of ASF, MOMBI-II produces evenly distributed solutions in the considered MOPs, outperforming all of the adopted MOEAs. However, the authors did not test MOMBI-II in MOPs having complicated Pareto fronts such as DTLZ5, DTLZ6, WFG3 nor in MOPs having degenerated or disconnected Pareto fronts such as DTLZ7 and WFG2.

In recent years, some studies have emphasized that MOEAs using a set of convex weight vectors,[8] using, for example, the Simplex Lattice Design method [147], may lose diversity when solving MaOPs [60, 30]. This is the case of all the above mentioned R2-based MOEAs (except for R2-IBEA). In consequence, Li *et al.* [91] have enhanced the diversity management of the R2 environmental selection mecha-

[8] A vector $\vec{w}$ is a convex weight vector if and only if $\sum_{i=1}^{m} w_i = 1$ and $\forall i \in \{1, \ldots, m\} w_i \geq 0$.

nisms by taking advantage of the Reference Vector guided Evolutionary Algorithm (RVEA) [20]. This selection mechanism first divides the population into contributing and non-contributing solutions to the R2 indicator, keeping the contributing ones. If the next population is not complete, the remaining solutions are selected from the non-contributing ones, enhancing diversity with the RVEA mechanism that clusters the population into different subregions where a weight vector defines each subregion. Then, the idea is to avoid deleting solutions from isolated subregions, i.e., to remove solutions from the most crowded subregions. The proposed approach, called Two-Stage R2 Evolutionary Algorithm (TS-R2EA), was mainly compared to MOMBI-II and RVEA on the DTLZ and WFG test suites for 3 to 15 objective functions, using the HV and IGD^+ indicators. Statistically, TS-R2EA had a better performance on MaOPs with more than 10 objective functions and on multifrontal problems such as DTLZ1. However, it did not show good results when tackling test problems with irregular Pareto fronts, namely, WFG1, WFG2 and WFG3 which have mixed, disconnected and degenerated Pareto front geometries.

In 2018, Li *et al.* [92] proposed an environmental selection mechanism that combines the R2 indicator with the decomposition strategy of MOEA/D [147]. The motivation of this algorithm (called R2-MOEA/D) is that in some cases a simple R2 selection strategy may lose the diversity of solutions in objective space. Based on the set of weight vectors required by R2, the authors defined subspaces where the solutions are assigned depending on their proximity to each weight vector. Instead of using the scalarizing values for each solution as in MOEA/D, R2-MOEA/D assigns to each solution its contribution to R2. The underlying idea of this hybrid selection scheme is to avoid deleting solutions from isolated subregions even if the pure R2 selection mechanism aims to do it. In this way, a better diversity of solutions is promoted. To the authors' best knowledge this is the first approach that combines an IB-Mechanism with a decomposition strategy. Compared to MOMBI-II, R2-MOEA/D produces better results regarding the Δ_p indicator that assesses convergence and diversity simultaneously. However, due to the use of convex weight vectors, it is likely that the performance of R2-MOEA/D strongly depends on specific Pareto front shapes [75].

IGD^+ indicator: Manoatl and Coello Coello introduced the IGD^+-EMOA which is the only algorithm currently available (to the authors' best knowledge) that uses an environmental selection based on IGD^+ [100]. It transforms the selection process into a Linear Assignment Problem (LAP) such that the best relationship between the reference set and the population is found from the modified Euclidean distance of IGD^+. The authors proposed to use the Kuhn-Munkres' algorithm to solve the LAP. The reference set is a crucial aspect of IGD^+-EMOA. Manoatl and Coello Coello proposed the construction of this set using γ-superspheres [38] to approximate convex, linear or concave geometries of the Pareto front. A γ-supersphere is a type of curve defined as: $\{(y_1, \ldots, y_m) \in \mathbb{R}^m_+ \,|\, y_1^\gamma + \cdots + y_m^\gamma = 1\}$, where $\gamma \in \mathbb{R}^m_+$ is a parameter that controls the geometry of the curve. The authors proposed to find the value of γ by solving a

root-finding problem using Newton's method. However, due to the limitation of geometries that can be approximated using this strategy, IGD$^+$-EMOA cannot properly solve MOPs having degenerated and disconnected Pareto front shapes. IGD$^+$-EMOA II [101], proposed by the same authors, aims to solve the problem of the previous version with difficult Pareto front shapes. Its main contribution is a new method to generate the reference set. This mechanism employs an external archive of non-dominated solutions from which certain ones are selected to be part of the reference set based on their contribution to the hypercube (a concept closely related to the hypervolume). Regarding the experimental results, it is confirmed that the HV-based strategy to build the reference set allows IGD$^+$-EMOA II to solve MOPs having complex Pareto front shapes, for example, the Viennet problems [134] and the MAF test suite [21], making it a very versatile multi-objective optimizer.

GD indicator: Menchaca and Coello Coello [104] proposed the Generational Distance-based Multi-Objective Evolutionary Algorithm (GD-MOEA) that employs an environmental selection scheme based on GD. However, since GD only promotes convergence leaving aside diversity, the authors introduced a mechanism based on Euclidean distances that compensates for this deficiency. At each iteration, the population is divided into non-dominated and dominated solutions. In case that we have less than μ non-dominated solutions, the remaining solutions are selected from the dominated ones using a GD-based environmental selection mechanism in which the non-dominated individuals represent the reference set. The IB-DE aims to choose the nearest dominated solutions to the reference set, diversifying the set by analyzing its nearest neighbors. If the number of non-dominated solutions is greater than μ, then the diversity mechanism is applied. GD-MOEA was compared to MOEA/D and HypE on the DTLZ and WFG test suites using 3 to 6 objective functions, and adopting the hypervolume indicator. The results reported by the authors showed that HypE outperformed GD-MOEA in 75% of the test problems and the latter outperformed MOEA/D in 67% of the MOPs. It is worth noting that GD-MOEA had difficulties to solve multifrontal MOPs such as DTLZ1 and DTLZ3. We can only distinguish a good performance of GD-MOEA on problems DTLZ7 and WFG7 for high-dimensional objective spaces. Regarding running time, GD-MOEA is 168 times faster than HypE and 1.46 times slower than MOEA/D.

Menchaca *et al.* [105] found that the diversity mechanism of GD-MOEA did not sufficiently increase the selection pressure when tackling MaOPs. Thus, they replaced the old diversity mechanism with one based on the additive ϵ-dominance[9] whose aim is to uniformly distribute solutions among the hypercubes produced by this dominance relation. The new algorithm, called GDE-MOEA, controls the ϵ value that divides objective function space. To validate the performance of GDE-MOEA, the authors employed the same experimental setup of GD-MOEA and this algorithm was also

[9]Given $\vec{x}, \vec{y} \in \mathcal{X}$ and $\epsilon > 0$, $\vec{x}$ is said to ϵ^+-dominate $\vec{y}$ (denoted by $\vec{x} \prec_{\epsilon^+} \vec{y}$ or $\vec{f}(\vec{x}) \prec_{\epsilon^+} \vec{f}(\vec{y})$) if for all $i = 1, 2, \ldots, m$ $f_i(\vec{x}) \leq (f_i(\vec{y}) + \epsilon)$ and there exists at least one index $j \in \{1, 2, \ldots, m\}$ such that $f_i(\vec{x}) < (f_i(\vec{y}) + \epsilon)$.

included. From the results, it is clear that GDE-MOEA is a bad option for MOPs similar to DTLZ1 and DTLZ2 since in all cases it was outperformed by the adopted MOEAs. However, with respect to HV, GDE-MOEA was an outstanding optimizer for disconnected problems such as DTLZ7 and WFG2 in which it consistently obtained the best results. In general, GDE-MOEA had better results than GD-MOEA and MOEA/D. Unlike GD-MOEA that was outperformed by HypE, GDE-MOEA had a competitive performance with respect to this HV-based MOEA.

ϵ^+ indicator: When Zitzler and Künzli proposed the IBEA framework (see Algorithm 2), they also showed the effectiveness of the binary ϵ^+ indicator in its selection mechanism, giving rise to IBEA$_{\epsilon^+}$ [153]. The experimental scenario was the same as that of IBEA$_{\text{HV}}$'s. However, IBEA$_{\epsilon^+}$ performed significantly better on the problem DTLZ6 which is a degenerated MOP that other MOEAs cannot properly solve because of the generation of numerous weakly dominated solutions.

The Approximation-Guided Evolutionary Multi-Objective Optimizer (AGE) [14] employs a greedy environmental selection mechanism that reduces the population size based on the worst contribution to the ϵ^+ indicator.[10] An external archive that stores non-dominated solutions is employed as the reference set. AGE does not need additional parameters, unlike IBEA$_{\epsilon^+}$. Furthermore, the authors proposed a fast method to reduce the number of calculations related to the greedy selection mechanism. AGE was comprehensively tested on four MOPs of the DTLZ test suite, varying the number of objective functions from 2 to 20. Experimental results showed that AGE does not perform well on MOPs having 2 and 3 objective functions and it is competitive in MaOPs with respect to SMS-EMOA, IBEA$_{\text{HV}}$ and NSGA-II.

Wagner and Neumann proposed AGE-II [137] that tackles the two main limitations of AGE. First, AGE adopts an unbounded external archive whose update rule is solely based on Pareto dominance, slowing down its execution time. In contrast, AGE-II uses a bounded external archive adopting ϵ dominance in the update rule. However, this introduces the need for a parameter ϵ_{grid} for the ϵ dominance. To improve performance in MOPs with 2 and 3 objective functions, AGE-II proposes a crowding distance-based parent selection that aims to maintain a diverse genetic material for the variation operators. Experimental results based on HV showed that AGE-II outperforms its predecessor, AGE, for MOPs in low- and high-dimensional objective space. Additionally, under time constraints, AGE-II is also able to be competitive or even get better results than SMS-EMOA and IBEA$_{\text{HV}}$. AGE-II presented remarkable results for multifrontal problems, i.e., DTLZ1 and DTLZ3.

The Two Archive algorithm 2 (Two_Arch2) [138] is a hybrid MOEA that uses two subpopulations, one dedicated to maintain convergence and the other to preserve diversity. Two_Arch2 was especially designed to tackle MaOPs. To this purpose, the convergence subpopulation is updated based on the ϵ^+ indicator, using the scheme of IBEA$_{\epsilon^+}$. The current solutions of the convergence subpopulation and the non-dominated solutions from the newly created offspring are merged into a single tem-

[10] In the original paper, the authors denoted the ϵ^+ indicator as the α indicator.

porary population Q. If Q exceeds its maximum allowable size, a greedy selection is performed by calculating the fitness values of all solutions, using the equation on Line 5 of Algorithm 2 with $\kappa = 0.05$. The solution with the lowest fitness value is removed and, then, all fitness values are updated. This process continues until Q reaches its maximum size. The other subpopulation of Two_Arch2 aims to maintain diversity by using an update rule based on a $L_{1/m}$ norm, where m is the number of objective functions. Both subpopulations interact to produce a Pareto front approximation with both convergence and diversity properties. Two_Arch2 was tested on MOPs from the DTLZ and WFG benchmarks, varying the number of objective functions from 2 to 20. The performance of Two_Arch2 was compared with respect to IBEA$_{\epsilon^+}$ and AGE-II, outperforming both algorithms in low- and high-dimensional MOPs.

Δ_p indicator: In 2012, Rodríguez Villalobos and Coello Coello [113] proposed to use the Δ_p indicator in a selection mechanism coupled to differential evolution, giving rise to the Δ_p-DDE algorithm. The selection method used in this case is a greedy algorithm that removes the worst contributing solutions. Since Δ_p is based on GD_p and IGD_p, the authors decided to give more importance to the latter because it rewards both convergence and distribution while the former is specifically focused on convergence. Hence, when the individual Δ_p contributions of all solutions are computed, the first criterion to check is the IGD_p contribution. It is worth noting that unlike other IB-MOEAs using a greedy strategy, Δ_p-DDE only needs to compute all contributions once and then it identifies the best μ solutions. In consequence, this reduces its computational cost. Regarding the reference set, it is constructed by fitting the current non-dominated points of the population into a frame formed by the approximations to the ideal and nadir points, uniformly distributing the points using a distance measure. Regarding HV results on the ZDT and DTLZ test suites, Δ_p-DDE produced poor solution sets for discontinuous problems (such as DTLZ7 and ZDT3) and the degenerated DTLZ5 and DTLZ6 problems. However, it had outstanding results when tackling multifrontal problems such as DTLZ1 and DTLZ3. Unfortunately, Δ_p-DDE was not exhaustively tested on MaOPs, and the authors only considered the many-objective version of DTlZ2 in which SMS-EMOA obtained better results than Δ_p-DDE.

In a further paper, Menchaca *et al.* designed the Δ_p-selection mechanism that was integrated into the Δ_p-MOEA [107]. Unlike Δ_p-DDE which prefers to use IGD$_p$ for selection, Δ_p-MOEA switches between IGD$_p$ and GD$_p$ to select solutions, depending on which of these two QIs best assesses the population. The GD$_p$-selection is the same as GDE-MOEA. The IGD$_p$-based environmental selection is similar to the non-dominated sorting mechanism of NSGA-II but considering the proximity of the solutions to the reference set. Concerning the reference set, it is constructed using the non-dominated solutions and ϵ dominance to assign each solution to a certain hypercube. Δ_p-MOEA was compared to MOEA/D and HypE on the WFG test suite using 3 to 6 objective functions, adopting HV and Δ_p as QIs. Δ_p-MOEA outperforms both MOEAs, only showing poor results for WFG1 whose Pareto front is mixed (i.e.,

it combines convex and concave shapes). Additionally, Δ_p-MOEA performs better on discontinuous MOPs such as WFG2 where Δ_p-DDE fails. It is worth noting that even Δ_p-MOEA has better results than GD-MOEA and GDE-MOEA.

Discussion Due to its strong mathematical properties, the hypervolume seems to be the best option to design environmental selection schemes. It has been proved that the maximization of the HV is related to finding the Pareto optimal set [46]. However, its high computational cost is a critical drawback. From Table 3.3, we observe that none of the HV-ES performs a hierarchical selection; as a matter of fact, all of them are greedy algorithms. The lack of HV-based hierarchical mechanisms is related to the complexity of the hypervolume subset selection problem (HSSP) which is NP-hard [13]. The solution of the HSSP would allow us to find a subset of solutions that maximizes the HV value. However, there is no polynomial-time algorithm able to solve the HSSP unless P = NP. Due to the computational limitations involved, greedy strategies have to be implemented. Nevertheless, Bradstreet *et al.* [11] claim that a greedy strategy does not always produce the desired results. From the HV-selection mechanisms presented before, the one implemented in iSMS-EMOA and aviSMS-EMOA should be strongly considered. The key aspect of both IB-MOEAs is to exploit the locality property of HV to reduce the number of times the HV-contribution is computed. These algorithms considerably reduce the computational time with respect to the other proposals without sacrificing the quality of the generated approximation in a significant way.

Other indicators have been employed to avoid the drawbacks of the HV. The $R2$ indicator is a remarkable option because of its weak Pareto compliance. MOMBI-II and TS-R2EA are perhaps the best $R2$-based algorithms currently available. However, since all $R2$-based MOEAs need to be supplied a set of convex weight vectors, that forms an $(m-1)$-simplex, in order to define the utility functions and to maintain diversity. This requirement is indeed its main drawback. As the dimensionality of the objective space increases, the number N of weight vectors increases in a combinatorial fashion, i.e., $N = C_{m-1}^{h+m-1}$, where h is an integer parameter [17, 93]. Maintaining a relatively small N in MaOPs affects the number of intermediate vectors in the simplex. A two-layer set of weight vectors has been used to overtake this last issue [30]. Another important problem related to the set of weight vectors is a possible overspecialization on Pareto fronts that are strongly coupled with these vectors [75]. Regarding ϵ^+, Δ_p, GD and IGD$^+$, their performance is strongly related to the way in which the reference set is built [73]. Each approach proposes a different way to define the reference set. However, from the experimental results, the method to construct the reference set of IGD$^+$-EMOA II seems the best option currently available since it is based on a HV-based method which is less computationally expensive. Its usage allows IGD$^+$-EMOA II to solve problems having complex Pareto front shapes which directly tackles the problem stated by Ishibuchi *et al.* [75].

Table 3.4: IB-Density Estimators. The 'Method' determines how the solutions are selected. For each IB-MOEA, it is shown in which problems it has been tested on as well as the number of objectives adopted in each case.

Indicator	Algorithm	Method	Problems	# Objectives	Year	Ref.
HV	ESP	Worst contribution	ZDT	2	2003	[66]
	SIBEA	Worst contribution	ZDT	2	2007	[149]
	SMS-EMOA	Worst contribution	ZDT & DTLZ	2 & 3	2007	[8]
	MO-CMA-ES	Worst contribution	ZDT & FON	2	2007	[67]
	SMS-EMOA-Apr	HV contribution using ASF-based approximation	DTLZ	3 & 6	2010	[79]
	HypE	HV approximation	DTLZ, WFG knapsack problem	2, 3, 5, 7, 10, 25, 50	2011	[3]
	FV-MOEA	Worst contribution	ZDT, DTLZ, WFG	2 - 5	2015	[83]
	I-SIBEA	Worst contribution	ZDT & DTLZ	2 & 3	2015	[22]
R2	R2-EMOA	Worst contribution	ZDT, DTLZ	2	2015	[18]
IGD^+	IGD^+-MaOEA	Worst contribution	DTLZ & $DTLZ^{-1}$	3 - 7	2018	[43]
IGD	MyO-DEMR	Worst contribution	DTLZ	2, 3, 5, 8, 10, 15, 20	2013	[34]
	MOEA/IGD-NS	Worst contribution	ZDT & DTLZ	2 - 3	2016	[124]
	MaOEA/IGD	Linear Assignment Problem	DTLZ & WFG	8, 15, 20	2018	[121]
	AR-MOEA	Worst contribution	DTLZ, $DTLZ^{-1}$, WFG, MAF	3, 5, 10	2018	[125]
Δ_p	RIB-EMOA	Worst contribution	DTLZ	3 - 10	2014	[146]

3.2.2.2 IB-Density Estimation

Hypervolume indicator: In 2007, Beume *et al.* introduced the S-Metric Selection Evolutionary Multiobjective Optimization Algorithm (SMS-EMOA) [8] which is a steady-state[11] version of NSGA-II, in which the density estimator originally based on crowding distance is replaced by one that removes the least HV-contributing solution. Algorithm 3 provides the general framework of SMS-EMOA. At each generation, the union set $P \cup \{\vec{a}_{\text{new}}\}$ (where $\vec{a}_{\text{new}}$ is the newly created solution and P is the population) is categorized in layers or ranks $\{R_1, R_2, \cdots, R_k\}$ using the Pareto dominance relation (see line 5). If R_k has more than one solution, then we need to delete in line 8 the solution $\vec{q}_{\text{worst}}$ that has the least HV contribution (this is the HV-based density estimator). In case R_k has one solution, this one is eliminated since it is the worst solution regarding Pareto dominance. Due to the mathematical properties of HV, SMS-EMOA can theoretically solve any MOP, producing convergent and uniformly distributed solutions along the Pareto front (although it prefers the Pareto front knee since solutions in this part of the front have a more substantial HV contribution). An essential aspect of SMS-EMOA is that it can solve MOPs whose Pareto front is degenerated such as DTLZ5, DTLZ6, and WFG3, which are very difficult for other MOEAs, including IB-MOEAs. However, it has some drawbacks. First, when solving MaOPs the number of ranks tends to one, forcing SMS-EMOA to calculate the HV

[11] It implements a $(\mu + 1)$-selection scheme.

Algorithm 3: SMS-EMOA general framework

Output: Pareto front approximation

Randomly initialize population P of size μ;
while *stopping criterion is not fulfilled* **do**
  Create a new offspring solution $\vec{a}_{\text{new}}$;
  $Q \leftarrow P \cup \{\vec{a}_{\text{new}}\}$;
  $\{R_1, \ldots, R_k\} \leftarrow$ non-dominated sorting(Q);
  if $|R_k| > 1$ **then**
    $z_i^{\max} \leftarrow \max_{\vec{q} \in Q} f_i(\vec{q}), \forall i = 1, \ldots, m$;
    $\vec{q}_{\text{worst}} \leftarrow \arg\min_{\vec{q} \in R_k} HV(Q, \vec{z}^{\max}) - HV(Q \setminus \{\vec{q}\}, \vec{z}^{\max})$;
  else
    $\vec{q}_{\text{worst}}$ is equal to the sole solution in R_k;
  end
  $P \leftarrow Q \setminus \{\vec{q}_{\text{worst}}\}$;
end
return P

contributions of the whole population which implies an additional computational cost to the already expensive calculation of HV in high-dimensional objective spaces. Recently, it has been empirically shown that the reference point employed by HV is dependent on the MOP and its geometry [71, 69]. This has a severe impact on the performance of HV-based MOEAs.

Although SMS-EMOA is the most remarkable HV-based MOEA, the underlying idea of its density estimator had been previously presented by Huband *et al.* in 2003 in their Evolution Strategy with Probabilistic Mutation (ESP) algorithm [66]. The only difference between SMS-EMOA and ESP is that the latter is a $(\mu+\lambda)$-Evolution Strategy (ES) which implies that the HV-based density estimator has to compute much more HV contributions than the HV-based density estimator of SMS-EMOA. This is a critical aspect that avoids the use of ESP and that is why all HV-based proposals employ a steady-state scheme. ESP was compared to a variety of other MOEAs, outperforming them on the ZDT test suite due to the use of its HV-based density estimator.

Igel *et al.* [67] proposed the Multi-Objective Covariance Matrix Adaptation Evolution Strategy (MO-CMA-ES) that uses two types of density estimators: one adopting crowding distance (as NSGA-II) and another one which is the same as that adopted in SMS-EMOA and ESP. A steady-state MO-CMA-ES was tested on the ZDT test suite and the Fonseca problem (FON) [24], obtaining similar results to SMS-EMOA.

On the other hand, Zitzler *et al.* [149] defined the weighted HV indicator which allows the user to incorporate preferences through a set of weight vectors (as R2-based MOEAs do), preserving the Pareto compliance of the original HV indicator. A density estimator based on this weighted HV was integrated into the NSGA-II framework that performs a $(\mu + \lambda)$-selection scheme, giving rise to the Simple Indicator-Based

Evolutionary Algorithm (SIBEA). Due to the incorporation of preferences, SIBEA can focus the search on a specific region of the objective space and it can circumvent the bias towards the knee of the Pareto front that is related to traditional HV-based mechanisms. However, SIBEA is restricted to bi-objective MOPs due to the mathematical definition of the weighted HV that makes it computationally expensive. Additionally, due to the $(\mu + \lambda)$-selection scheme, the execution of SIBEA is very time-consuming even for bi-objective MOPs.

Due to the high computational cost of the hypervolume, some authors have proposed its approximation. Bader and Zitzler [3] proposed the Hypervolume Estimation Algorithm for Multiobjective Optimization (HypE). HypE uses Monte Carlo sampling with the aim of approximating the HV contributions. The authors stated that "the main idea is that the actual indicator values are not important, but rather the rankings of solutions induced by the hypervolume indicator" [3]. HypE is a $(\mu + \lambda)$-EA that works under the same framework of NSGA-II. It is worth noting that HypE uses the exact HV contribution for two and three dimensions of the objective space and, in case of MaOPs, it employs the approximation. Additionally, the quality of the solution set is sensitive to the number of samples that the Monte Carlo method adopts. Although the quality of the solutions is a bit lower than those of SMS-EMOA, the computational cost of HypE in MaOPs is considerably lower. HypE was compared to NSGA-II, SPEA2 and IBEA_{HV} on the DTLZ and WFG test suites using 2, 3, 5, 10, 25 and 50 objective functions. According to the hypervolume results, HypE performs better than the adopted MOEAs which implies that the approximation of the ranks produced by HV allows an MOEA to get good results.

Ishibuchi *et al.* [79] proposed an HV approximation approach based on the use of achievement scalarizing functions (ASFs) [110]. They decided to use ASFs because: (1) they have shown to be effective when solving MaOPs, and (2) the accuracy and computational load can be adjusted through the number of weight vectors employed. The idea of the approximation is to measure the distance from the reference vector employed by HV to the solution set using the ASFs. This approximation method was incorporated into SMS-EMOA, giving rise to SMS-EMOA-Apr. The authors claim that this new approach drastically decreased the runtime of SMS-EMOA. Furthermore, they observed that the use of an approximation to HV does not severely deteriorate the quality of the solutions produced. However, SMS-EMOA-Apr was only tested in DTLZ1 and DTLZ2, leaving aside MOPs with interesting properties. It is worth noting that the accuracy of this approximation method strongly depends on the number of weight vectors. As the dimensionality of the objective space increases, it would be necessary to provide even more weight vectors than those commonly employed by R2-based MOEAs which will increase the runtime of the algorithm.

In 2015, Jiang *et al.* [83] presented the Simple and Fast Hypervolume Indicator-Based MOEA (FV-MOEA). The main contribution of this work is a new method to update the exact HV contributions of different solutions based on the locality property of HV. The IB-density estimator using this fast HV calculation was incorporated into the NSGA-II framework. Experimental results confirmed the superiority

of FV-MOEA regarding HV as well as its lower cost with respect to SMS-EMOA and IBEA_{HV}. The distribution of points is similar to other HV-based MOEAs. A possible drawback of FV-MOEA is that the locality property is well-defined for the two-objective case, while it is not entirely stated for $m > 2$ objectives.

Finally, the Interactive Simple Indicator-Based Evolutionary Algorithm (I-SIBEA), introduced by Chugh *et al.* [22], is an interactive MOEA [108], i.e., it asks the decision maker (DM) to provide preference information throughout the evolutionary process. I-SIBEA uses a density estimator based on the weighted HV to reduce the population size, and it collects data from the decision maker, related to preferred and non-preferred solutions. Since I-SIBEA is an interactive MOEA, it asks for preference information through the search process. Due to this interaction, the solution process of I-SIBEA could be complicated, especially when the decision maker does not have a clear idea of his preferences. However, focusing the search on some areas of the objective space could be beneficial when solving MaOPs because of the reduction of the search space. Additionally, the DM can decide how many times s(he) wants to interact with the algorithm and how many solutions s(he) wants to compare while interacting. Therefore, the DM does not need to compare more solutions than s(he) is able to consider at a time. Unfortunately, the comparative study only included ZDT4, DTLZ1 and DTLZ2 problems using 2 and 3 objective functions. These MOPs are not very challenging for most MOEAs.

R2 indicator: Brockhoff *et al.* [18] proposed the $R2$-EMOA that substitutes the HV-based density estimator of SMS-EMOA by one based on the $R2$ indicator. $R2$-EMOA obtained promising results because of the weakly Pareto compliance of the $R2$ indicator and the even distribution of points promoted by the required set of convex weight vectors. Another remarkable feature of $R2$-EMOA is that it is less computationally expensive than SMS-EMOA, allowing it to solve MaOPs at an affordable computational cost. However, the cardinality of the set of weight vectors increases in a combinatorial fashion as the number of objective functions does. Moreover, the performance strongly depends on the utility function that is employed. Each utility function allows $R2$-EMOA to find solutions in different regions of the objective space [110]. The authors performed an empirical analysis of their greedy heuristic strategy, i.e., the R2-based density estimator could produce the μ-optimal distributions associated with the R2 indicator. To this aim, they employed some ZDT and DTLZ problems. The experimental results showed that R2-EMOA produces approximation sets similar to the μ-optimal distributions. However, no comprehensive comparative study is available yet.

IGD^+ indicator: Motivated by the overspecialization of MOEAs using convex weight vectors (as search directions, reference sets or as part of a quality indicator) on certain benchmark problems, Falcón-Cardona and Coello Coello have proposed an MOEA that employs the IGD^+ indicator as its density estimator [43]. Based on an empirical analysis, they found out that an IGD^+-based search could produce

similar Pareto front approximations to those of SMS-EMOA. Hence, they proposed the IGD$^+$-Many-Objective Evolutionary Algorithm (IGD$^+$-MaOEA) that replaces the HV density estimator of SMS-EMOA in Algorithm 3 by the IGD$^+$ contributions of all solutions in the last dominated rank. Additionally, they introduced a method to reduce the computational cost of computing the IGD$^+$ contributions of the entire population. The authors compared IGD$^+$-MaOEA with respect to IGD$^+$-EMOA, NSGA-III, MOEA/D and SMS-EMOA on the DTLZ and DTLZ^{-1} [75] test suites using 3 to 7 objective functions. The DTLZ^{-1} test suite is a slight modification of the original DTLZ test suite, where all the objective functions of the MOPs are multiplied by -1, producing in some cases MOPs whose Pareto front is not correlated to the simplex that a set of convex weight vectors forms. On the basis of the HV results, IGD$^+$-MaOEA is very competitive with respect to the adopted MOEAs in the DTLZ test suite and it outperforms all the other MOEAs when tackling the DTLZ^{-1} test problems. On the basis of these results, the authors claimed that IGD$^+$-MaOEA is a more general many-objective optimizer since its performance does not depend on the Pareto front shapes. An in-depth description of IGD$^+$-MaOEA is given in Chapter 6 since this algorithm is part of this Ph.D. thesis.

IGD indicator: In 2013, Denysiuk *et al.* [34] introduced the Many-Objective Differential Evolution with Mutation Restriction (MyO-DEMR) based on the NSGA-II framework. MyO-DEMR replaces the density estimator of NSGA-II by one based on the individual contributions to the IGD indicator. The reference set $\mathcal{Z}$ is equal to the hyperplane that dominates the set of solutions in the rank R_j that makes the population size to exceed μ solutions. After calculating the individual contribution of each solution in R_j, the contributions are sorted in descending order, and the elements that make the population equal to μ are kept. This strategy differs from the one employed by $R2$-EMOA where each time a solution is removed, all the contributions must be recomputed. Hence, this saves computational time. MyO-DEMR showed competitive results with respect to state-of-the-art algorithms, producing well-covered and well-distributed solutions for problems with up to 20 objectives. However, MyO-DEMR was not tested on MOPs having degenerated and discontinuous Pareto fronts. It is worth noting that MyO-DEMR presented remarkable results for multifrontal MOPs such as DTLZ1 and DTLZ3, although the authors mentioned that this behavior was due to the restriction strategy contained in the differential evolution search engine.

Tian *et al.* [124] proposed an enhanced IGD indicator, called IGD with noncontributing solution detection (IGD-NS). This indicator defines a value on the basis of all noncontributing solutions which penalizes the original IGD value. Noncontributing solutions are the ones which are avoided to be the nearest neighbors of any point in the required reference set. The authors proposed the MOEA/IGD-NS that employs Pareto dominance as its environmental selection mechanism and a density estimator that removes the worst IGD-NS contributing solutions, i.e., it follows the NSGA-II scheme. MOEA/IGD-NS has an external archive that stores non-dominated solutions, improving their diversity with a scheme similar to that of RVEA, i.e., it

clusters solutions in different subregions [20]. This external archive is employed as the reference set of IGD. Evidently, the identification of noncontributing solutions increases the computational cost of MOEA/IGD-NS in comparison to MyO-DEMR. Experimental results on low-dimensional instances of the ZDT and DTLZ test suites showed that MOEA/IGD-NS produces evenly distributed solutions. Nevertheless, the authors claimed that MOEA/IGD-NS could not solve MaOPs because it is complicated to maintain an external archive with both a good convergence and a good diversity. Hence. the performance of the approach is not scalable.

In 2018, Sun *et al.* [121] introduced the IGD Indicator-based Many-Objective Evolutionary Algorithm (MaOEA/IGD). This IB-MOEA first constructs an ideal version of the Pareto front on the basis of the $(m-1)$-dimensional hyperplance that is shaped by the set of approximated extreme points. This hyperplane is employed to classify the population in three groups based on the Pareto dominance relation: (1) rank R_1 contains points that dominate the hyperplane, (2) rank R_2 has points mutually non-dominated with the hyperplane, and (3) points dominated by the hyperplane belong to rank R_3. Unlike the non-dominated sorting procedure that creates different ranks of solutions, the previous classification only generates three ranks of solutions that are added to the next population whenever the population size is not exceeded. It is worth noting that depending on the rank, a distance between a point and the reference set (the hyperplane) is measured: a negative Euclidean distance, a modified Euclidean distance of IGD$^+$ and an Euclidean distance for $R1, R2$ and R_3, respectively. Starting from the rank that exceeds the population, the remaining solutions are selected by transforming the selection problem into a Linear Assignment Problem just as Manoatl and Coello Coello proposed in IGD$^+$-EMOA [100]. The authors were interested in showing the effectiveness of MaOEA/IGD in MaOPs. Thus, they compared it with NSGA-III, MOEA/D, HypE and RVEA on the DTLZ and WFG test suites using 8, 15 and 20 objective functions, adopting the hypervolume indicator. Their experimental results showed that MaOEA/IGD performs better than the other MOEAs on MaOPs with 8 and 20 objective functions and its performance is significantly better for MaOPs DTLZ1, DTLZ7, WFG1, and WFG3, which covers a wide range of Pareto front shapes. However, an important aspect to consider is that its performance mainly depends on the proper construction of the approximated hyperplane. The method to approximate the extreme points that shape the hyperplane is very time-consuming since it involves m additional approximation sets and it may sometimes fail to produce good points.

As in the case of IGD$^+$-MaOEA whose primary motivation is the overspecialization of MOEAs using convex weight vectors on specific benchmark problems, Tian *et al.* presented the Adaptive Reference Set-based MOEA (AR-MOEA) [125] as an alternative to deal with a wider variety of Pareto front shapes. AR-MOEA is an improvement of MOEA/IGD-NS since the latter had a poor performance on MOPs having different Pareto front geometries. Although IGD-NS solves some of the problems of IGD when selecting solutions, the former tends to choose non-contributing solutions that are clustered together and too near to a reference point. Consequently,

the density estimator based on IGD-NS of AR-MOEA also includes an adaptive reference set that approximates the inner geometry of the Pareto front, using an approach similar to that of RVEA [20]. Hence, AR-MOEA takes advantage of both the adaptive reference set and the IGD-NS-based selection. AR-MOEA follows the framework of NSGA-II, i.e., it uses Pareto dominance as its main selection criterion and, additionally, the IGD-NS density estimator is adopted to delete the worst-contributing solution from the last rank of solutions. AR-MOEA was tested on several test problems that cover a wide range of Pareto front shapes. They used the DTLZ, DTLZ^{-1}, WFG and MAF test suites adopting 3, 5 and 10 objective functions. Their experimental results showed that AR-MOEA is a more versatile optimizer since its performance does not depend on the Pareto front shape. For 3-objective functions, AR-MOEA could rank first in terms of HV values only on DTLZ4, WFG3 and MAF4. In case of MaOPs, its performance was competitive with respect to NSGA-III, RVEA and MOMBI-II.

Δ_p indicator: The Reference Indicator-Based Evolutionary Multi-Objective Algorithm (RIB-EMOA) proposed by Zapotecas *et al.* in 2014 [146] is a steady-state MOEA that adopts Δ_p as its second selection criterion. RIB-EMOA follows the SMS-EMOA framework although it tries to save some computations of Δ_p contributions. Regarding the required reference set, the authors proposed to generalize its construction using Lamé superspheres such that specific Pareto front geometries are approximated, namely, linear, concave and convex shapes. Experimental results showed that RIB-EMOA has some difficulties when solving multifrontal MOPs, namely DTLZ1 and DTLZ3 as well as MOPs having degenerated Pareto fronts, e.g., DTLZ5 and DTLZ6. Nevertheless, RIB-EMOA presents better results than IGD$^+$-EMOA (see Section 3.2.2.1) which uses a similar strategy to build the reference set, in MOPs having degenerated and discontinuous Pareto fronts.

Discussion IB-Density estimators are mechanisms that aim to reduce the population size of MOEAs once the main selection criterion has been applied. Unlike mechanisms such as crowding distance or fitness sharing, the advantages of IB-DEs become clear when solving MaOPs because the use of quality indicators increase the selection pressure once the Pareto dominance relation cannot properly rank solutions in several layers. It is worth emphasizing that most of the IB-MOEAs from Table 3.4 are based on the NSGA-II framework (a number of them adopt a steady-state version).

The main issue with HV-based MOEAs is the high computational cost associated with computing exact HV contributions. However, as stated by Ishibuchi *et al.* [79], the use of an approximation to the HV does not severely deteriorate the quality of the solutions and allows a significant reduction in the computational cost required. However, the approximation of HV is currently an open research area. A remarkable approach within this class is FV-MOEA which calculates exact HV contributions using an efficient algorithm based on the locality property of HV. FV-MOEA is indeed

Table 3.5: IB-Archiving methods. The 'Method' determines how the solutions are selected. For each IB-MOEA, it is shown in which problems it has been tested on as well as the number of objectives of the MOPs adopted.

Indicator	Algorithm	Method	Problems	# Objectives	Year	Ref.
HV	LAHC	Worst contribution	General point sequences	2 & 3	2003	[87]
	ϵ-MOPSO$^{UD}_{MRV}$	Worst contribution	ZDT & DTLZ	2 & 3	2009	[80]
Δ_p	Δ_p-EMOA	Worst contribution	DTLZ, ZDT spheres model, DENT	2	2011	[51]
	Δ_p-M-EMOA	Worst contribution	DTLZ & Viennet	3	2012	[128]
	Δ_p-T-EMOA	Worst contribution	DTLZ & Viennet	3	2013	[114]
	SMS-DPPSA	Worst contribution	DTLZ	4	2013	[36]
	PS-EMOA	Worst contribution	DTLZ	4	2013	[36]

capable of producing solutions of the same quality as SMS-EMOA but at a considerably lower computational cost. However, scalability is an issue in this case, since for high-dimensional objective spaces the locality property is difficult to interpret.

Regarding the other approaches, they produce competitive results although the Pareto compliance property is not held in the worst case. $R2$-EMOA produces competitive results but it is necessary to analyze its performance in high-dimensional objective spaces. Its main drawbacks are the need for a set of convex weight vectors whose cardinality increases with the number of objective functions as well as a possible overspecialization on certain Pareto fronts due to the method adopted to generate the weight vectors. The performance of RIB-EMOA, MyO-DEMR and MOEA/IGD-NS is strongly dependent on the construction of the reference set. Hence, it would be useful to analyze the impact that the reference sets have on the performance of these approaches, with the aim of designing an adaptive method that could generalize their use. Two interesting MOEAs within this class are AR-MOEA and IGD$^+$-MaOEA. The motivation of these two IB-MOEAs is to avoid the overspecialization of MOEAs on certain benchmark, i.e., they have traced the path to design more general many-objective optimizers whose performance does not depend on some particular Pareto front shapes. Both algorithms have been tested on different benchmarks that cover a wide range of Pareto front geometries. In the future, it would be interesting to compare both algorithms to determine their advantages and drawbacks.

3.2.2.3 IB-Archiving

Hypervolume indicator: To the authors' best knowledge, the Lebesgue Archiving Hillclimber (LAHC) was the first IB-Mechanism ever proposed [87]. The operation of the archiver $\mathcal{A}$ is very simple. If we try to add a solution $\vec{u}_{\text{new}}$ to the archive and the archive is full, then the solution from $\mathcal{A} \cup \{\vec{u}_{\text{new}}\}$ having the least contribution to HV, is deleted. This is similar to the operation of an HV-based steady-state MOEA, such as SMS-EMOA (see Algorithm 3) although LAHC operates on an external archive. LAHC was tested on general point sequences that intend to approximate different Pareto front geometries. However, the experimental analysis did not include the

implementation of LAHC in an MOEA. In spite of this, it is very likely that some MOEA using LAHC behaves in a similar way to SMS-EMOA, since LAHC operates under a similar principle.

Jiang and Cai [80] introduced the ϵ-MOPSO$^{UD}_{MRV}$ that uses an archive acceptance rule called Minimum Reduced Hypervolume (MRV) that combines HV and ϵ-dominance. The solutions in the archive are placed on the hyperboxes created by the ϵ-dominance mechanism. Considering a hyperbox with more than one solution inside, the update rule will delete the solution having the lowest contribution to the HV. By doing this, convergence and diversity of the archive is promoted. Experimental results showed that the combination of ϵ-dominance and HV in the archive improves both convergence and diversity of the Pareto front approximations. However, ϵ-MOPSO$^{UD}_{MRV}$ was only tested on the ZDT and DTLZ test suites using 2 and 3 objective functions.

Δ_p indicator: Gerstl *et al.* [51] introduced the first MOEA based on the Δ_p indicator. This MOEA, called Δ_p-EMOA, is a modified version of the SMS-EMOA (see Section 3.2.2.2) which is restricted to two-dimensional objective spaces. Δ_p-EMOA adds a Δ_p-based archive to the SMS-EMOA to improve diversity by compensating the distribution bias of the SMS-EMOA's HV-based density estimator. The reference set for Δ_p is constructed from the current population produced by SMS-EMOA which is linearly interpolated, aiming to distribute solutions evenly. Each time a new solution is considered to be added to the archive, the Δ_p contributions of all solutions, including the new one, are calculated, and the one with the worst value is removed. Unfortunately, the authors did not show an exhaustive performance analysis. However, a clear disadvantage of Δ_p-EMOA is its reference set construction method that relies on linear interpolation of the main population which makes the MOEA unable to solve MOPs with more than three objective functions.

In order to scale up Δ_p-EMOA, Trautmann *et al.* proposed Δ_p-M-EMOA [128] which is able to solve three-objective problems. The mechanism to construct the reference set uses the Multi-Dimensional Scaling (MDS) method to perform a dimensionality reduction from m dimensions to two-objective spaces. The solution having the worst Δ_p contribution within a set of grid points inside the ϵ^+-convex hull of the population in MDS space is removed from the archive. The experimental study presented by the authors considered DTLZ1, DTLZ2, DTLZ3 and the Viennet problem with 3 objective functions and to assess performance, the Δ_p indicator was employed. From the experimental results, it is clear that Δ_p-M-EMOA produces Pareto front approximations with more uniform solutions than those generated by SMS-EMOA, NSGA-II and MOEA/D. However, as in the case of the Δ_p-EMOA, the archiving strategy is computationally expensive. It is worth noting, however, that reducing the dimensionality always to two-dimensional objective spaces may lead to the loss of important information, especially when dealing with MaOPs.

Regarding Δ_p-M-EMOA, Rudolph *et al.* [114] claimed that the sequential generation of reference sets in Δ_p-M-EMOA is highly complex. Hence, they proposed

the Δ_p-T-EMOA which follows the direction of Δ_p-EMOA, but it can solve three-dimensional MOPs using a triangulation technique to generate the reference set. Using this technique, they circumvented the dimensionality reduction of Δ_p-M-EMOA. This archiving strategy is considerably faster than that of Δ_p-M-EMOA. An important issue of Δ_p-T-EMOA is the detection of the border of the Pareto front and its inability to solve MaOPs. Δ_p-T-EMOA was compared to Δ_p-M-EMOA, SMS-EMOA, MOEA/D and NSGA-II using the same experimental setup as in Δ_p-M-EMOA. From the experimental results, it is clear that the Δ_p-based archive improves the uniformity of solutions, outperforming all the adopted MOEAs. Additionally, the archive update rule of Δ_p-T-EMOA is less computationally expensive than the one of Δ_p-M-EMOA.

Finally, Domínguez *et al.* [36] proposed two algorithms that can be seen as an improvement of Δ_p-EMOA: Δ_p-M-EMOA and Δ_p-T-EMOA. For this purpose, the core idea is the use of the Part and Selection Algorithm (PSA). Unlike SMS-EMOA, SMS-EMOA with PSA (SMS-EMOA-DPPSA) adds a Δ_p-based external archive to store convergent and evenly spaced solutions that are not outliers. PSA processes the current population to generate a reference set of a given size. Roughly speaking, PSA is similar to a clustering algorithm because it partitions the set of solutions according to a dissimilarity function aiming to group alike solutions. Using the reference set described above, the archiver removes the worst Δ_p contributing solutions until the desired population size is reached. As SMS-DPPSA is a variant of SMS-EMOA, it uses a density estimator based on the hypervolume. Hence, it is highly expensive when solving MaOPs. In order to circumvent this issue, PS-EMOA is introduced. PS-EMOA uses Pareto dominance as its main selection criterion and PSA to get samples of the current archive. The above algorithm is the online version of PS-EMOA. Domínguez *et al.* also proposed an offline version of PS-EMOA that first executes the online version to store all possible non-dominated solutions in the archive and, after that, the Δ_p archiver is run to prune it, optimizing the Δ_p value. When using DTLZ1, DTLZ2 and DTLZ3, both algorithms were able to produce evenly distributed solutions due to the bias of Δ_p. Unfortunately, SMS-DPPSA and PS-EMOA were only well-suited for MOPs having a maximum of four objective functions.

Discussion Unlike IB-ESs or IB-DEs, IB-ARs have received little attention from the EMOO community. It is worth noting that some important reasons for this is the computational overhead associated with the use of unbounded archives [85]. Also, and mainly for pragmatic reasons (e.g., to allow a fair comparison with other MOEAs), most approaches have adopted bounded archives.

In spite of the nice mathematical properties of HV, its high computational cost has prevented its use in more mechanisms. The only two HV-archivers currently available employ the same mechanism, i.e., they remove the solution associated with the lowest HV-contribution. Therefore, there is no real improvement when considering these archivers. Regarding Δ_p-EMOA and its variants, the main drawback is that they are hard-wired to a specific dimensionality of the objective space, i.e., they are not MOEAs intended for general use. Furthermore, the construction of the reference set

Table 3.6: IB-Mating Selection mechanisms. 'Method' is related to the basic algorithm on which the mechanisms are based on and 'Comparison' is related to the information employed to select solutions.

Indicator	Algorithm	Method	Comparison	Year	Ref.
R2	R2-IBEA	Binary tournament	Comparison of binary R2 value	2013	[131]
IGD	MaOEA/IGD	Binary tournament	Comparison of rank and distance value	2018	[121]
	AR-MOEA	Binary tournament	Comparison of IGD-NS contribution	2018	[125]

in all cases is highly complicated, and they do not offer a clear advantage over other IB-MOEAs that adopt a reference set. Clearly, there is a lot of room for improvement in IB-Archiving techniques.

3.2.3 IB-Mating Selection

IB-Mating Selection involves the identification of good parent solutions based on quality indicator values. This type of selection mechanisms does not aim to solve or approximate the indicator-based subset selection problem. Instead, this mechanism tries to produce promising offspring solutions to accelerate the evolutionary process. Unfortunately, the EMOO community has not tuned at all its gaze towards these mechanisms. To the author' best knowledge, there are currently three MOEAs that use IB-Mating Selection. Such methods are summarized in Table 3.6. It is worth emphasizing that none of the authors of the approches has conducted experiments to determine the actual contribution in the search process of these IB-Mating Selection methods. In the following, we will briefly describe the functioning of them that are entirely based on a binary tournament selection scheme.

By adopting a binary tournament selection scheme [24], R2-IBEA iteratively fills its gene pool by selecting those solutions that have a higher value regarding the binary R2 indicator. Since the binary R2 indicator is weakly Pareto-compliant, R2-IBEA always ensures to select solutions that are better in terms of weak Pareto dominance, i.e., the solutions having non-zero contribution. In second place, we have MaOEA/IGD [121] that creates a binary tournament where the comparisons among solutions are made on the basis of their rank and their distance value to the hyperplane (the reference set for the IGD indicator). The first stage is to compare the ranks of solutions, where the lower the rank, the better. In case that both solutions have the same rank, their distance values (negative Euclidean distance, the modified Euclidean distance of IGD^+ or Euclidean distance) are compared and the one having the minimum value is chosen. If there is a tie, a random solution is selected. This IGD-based mating selection scheme aims to choose solutions having a good degree of convergence. Finally, AR-MOEA [125] computes the IGD-NS contribution of those solutions that are selected to compete in the tournament. The one having the larger contribution (the authors called it fitness value) wins the competition and it is added to the gene pool. As in the case of MaOEA/IGD, this mating selection process aims to generate offspring solutions on the basis of the best solutions in terms of convergence.

Table 3.7: Real-world applications solved by IB-MOEAs.

IB-MOEA	Real-world problem	# Objectives	Year	Ref.
SMS-EMOA	Airfoil design optimization	2, 3	2007	[8]
$IBEA_{HV}$ HypE	Permanent magnet motor design	2	2012	[1]
SMS-EMOA	Civil engineering structural design	2	2013	[99]
SMS-EMOA	Power distribution network reconfiguration	2	2014	[142]
MOMBI	Analog integrated circuit optimization	5	2015	[27]
SMS-EMOA	Inventory routing problem	3	2016	[144]
SMS-EMOA	Building spatial design	2	2017	[132]
MOMBI2	Route planning	3	2018	[109]
$IBEA_{HV}$	Software product line	5	2019	[54]

3.3 Real-world Applications

In this section, we make a brief review of real-world applications tackled by IB-MOEAs. Table 3.7 summarizes the most relevant applications, emphasizing the real-world problem, the number of objectives related to the problem, and the publication year which was used to sort the proposals in chronological order.

The airfoil design problem is a very important real-world application whose optimization implies huge potential savings and more secure flight characteristics. When tackling this problem, one aims to maximize the lift to ensure safe and stable flight qualities, while minimizing the drag during the cruising flight, which has a positive impact on the minimization of the energy consumption. SMS-EMOA [8] was tested by its authors on two test cases: (1) airfoil redesign of models NACA0012 and NACA4412, adopting two objective functions, and (2) the minimization of three drag coefficients related to the airfoil RAE2822. A computational fluid dynamics tool, based on the solutions of the Navier-Stokes equations, was employed as the simulation method that evaluates the solutions created by SMS-EMOA. Hence, the objective function evaluation is very time-consuming which encourages the authors to employ metamodels to reduce the computational costs. For both cases, SMS-EMOA was compared to NSGA-II, outperforming it due to the hypervolume-based density estimator, according to the authors. Additionally, SMS-EMOA using a Kriging metamodel was compared to the basic SMS-EMOA, where the former presents better-distributed solutions.

Another application of IB-MOEAs to real-world problems is related to the design of permanent magnet motors. In 2011, Andersen and Santos [1] employed $IBEA_{HV}$ and HypE for the parameter optimization of a permanent magnet motor. The authors defined the problem as a bi-objective MOP, where the goals were to maximize efficiency and minimize cost. For comparison purposes, they used the hypervolume indicator but they fixed one of the components of the reference point to 96% of efficiency since lower values are of no interest. According to the results, both IB-MOEAs produced numerous solutions with efficiency greater or equal to 96% while generating

scarce solutions with lower efficiency. Regarding HV, HypE was slightly better than IBEA_{HV} and it was also less time-consuming.

Civil engineering is a discipline highly related to MOPs that usually involves two main goals: minimizing financial cost and maximizing the final design safety. The structural design of bridges is a clear example of this type of MOPs. In 2013, Luna *et al.* [99] tackled the design of a cable-strayed bridge with two pillars (towers). The bridge had a total length of 162 m and the deck length and width are 90 m and 9 m, respectively. The authors aimed to minimize the total weight of the structure and the summation of the deformations in specific points of the deck and the columns. The bi-objective MOP involved 191 decision variables and 4948 side-constraints. Due to the high computational cost of evaluating the objective functions, the authors proposed a distributed SMS-EMOA, under the master-slave paradigm, in order to parallelize the computation of the objective functions. For comparison purposes, the distributed SMS-EMOA was compared with a distributed NSGA-II, where the former showed better convergence results, according to the empirical attainment surfaces [53]. However, the authors could not conclude which MOEA was better since SMS-EMOA had a strong bias towards the Pareto front's knee and NSGA-II produced a better coverage towards extreme regions.

In 2014, Yang *et al.* [142] proposed to tackle the power distribution network reconfiguration problem (DNRP). Roughly, this problem aims to optimize a distribution system so that the security, efficiency and reliability of the system are enhanced. For this purpose, the network reconfiguration is related to the change of the topology of the power network by operating the switches to minimize power loss. Since DNRP is an NP-hard problem, several metaheuristics have been proposed to solve it. The authors decided to employ SMS-EMOA and NSGA-II to solve the DNRP adopting two objective functions: minimize power loss and voltage profile enhancement. Both SMS-EMOA and NSGA-II were modified to adopt a sequences-based encoding. Based on the use of attainment surfaces, SMS-EMOA was found to outperform NSGA-II since the Pareto front of the MOP was concave, and SMS-EMOA has been found to be able to produce outstanding results when dealing with such Pareto front geometries.

In logistics, the inventory routing problem (IRP) has been typically formulated as a bi-objective MOP. However, Yang *et al.* [144] have recently extended this problem to three objective functions to be minimized: routing cost, inventory cost and stockout cost. Additionally, the authors decided to model the multi-objective IRP with uncertain demand, i.e., in this problem, products are repeatedly delivered from a single supplier to a set of n geographically dispersed customers in a given number of days. To model the uncertain demand, a Poisson distribution was employed. SMS-EMOA and NSGA-II were used to solve different instances of the problem, mainly varying the number of customers from 80 to 200. The experimental results, based on the hypervolume indicator, showed that both MOEAs behave similarly.

De la Fraga and Tlelo-Cuautle [27] proposed the use of MOMBI to improve the optimal sizing of amplifiers design with MOSFETs. This is an analog integrated circuit optimization problem, which involves the optimization of five objectives: maximize

gain, bandwidth and slew rate and minimize power dissipation and setting time. The problem has twelve inequality constraints. Since the original version of MOMBI is unable to deal with constrained MOPs, the authors introduced two modifications to this IB-MOEA: 1) the implementation of a mating selection scheme that takes into account both feasible and infeasible solutions, and 2) they modified the R2 selection mechanism to give more importance to feasible solutions. The authors compared the performance of MOMBI with respect to NSGA-II, and found that the former obtained better results than the latter.

In 2017, Van der Blom *et al.* [132] studied the multi-objective building spatial design problem, aiming to optimize: (1) structural efficiency, and (2) energy efficiency. According to the authors, structural efficiency encompasses the maximal contribution of every individual structural element to the full structure, while energy efficiency allows reductions to both the impact on the environment and on the financial costs. The problem was tackled using a tailored version of SMS-EMOA that uses specific mutation and initialization operators that deal with mixed-integer problems. The authors adopt landscape analysis to identify the main problem's features and to investigate the behavior of the mutation operator. Experimental results, based on the use of attainment surfaces, showed that the tailored version of SMS-EMOA adopted by the authors had a good performance when solving the problem. Additionally, the proposed operators reduced the violation of the constraints of the problem.

Regarding intelligent transport systems, route planning is a problem of remarkable importance. In 2018, Osaba *et al.* [109] focused on tackling a last-mile package delivery routing problem with third-party drop-off points, applied to bike routes in Madrid, Spain. They modelled this as a MOP with three objectives: minimize the travelled distance and maximize both the safety of the biker and the profit. Several MOEAs, including NSGA-II, NSGA-III, MOEA/D and MOMBI2 were adopted to tackle the problem. From the results in three different scenarios, MOMBI2 showed the worst performance according to the hypervolume indicator. However, the authors did not provide any explanation for this poor performance of MOMBI2.

In recent years, software product line (SPL) engineering has attracted the attention of the industry to reduce development costs, improve software quality and shorten time to market. The main goal of SPL is to generate an optimal product that meets specific requirements of stakeholders, i.e., the so-called configuration optimization problem. In 2019, Guo *et al.* [54] proposed to use IBEA_{HV} hybridized with the satisfiability modulo theories (SMT) for solving the five-objective SPL configuration optimization problem. SMT helped IBEA_{HV} to reduce its huge decision variable space and to validate the satisfaction of the constraints defined in the feature model. The proposed hybrid IBEA_{HV} showed effectiveness and capability to scale when solving five large real-world SPLs, ranging from 1,244 to 6,888 features and from 2468 to 343,944 constraints, using the indicators HV, ϵ^+ and IGD.

3.4 Future Research Directions

In spite of the numerous IB-MOEAs that have been proposed, this is a research area with several potential topics for future research. Some of them are briefly described next.

3.4.1 Design of Multi-Indicator-based MOEAs

Currently, IB-MOEAs are based on a single indicator that imposes a certain search bias originated by its own strengths and weaknesses. Hence, a possible research direction is to propose Multi-Indicator-based MOEAs (MIB-MOEAs). The core idea of MIB-MOEAs would be to combine the properties of each indicator-based mechanism to obtain a better global search behavior. Phan and Suzuki [111] were apparently the first to propose a MIB-MOEA (called BIBEA) that boosts existing IB-selection operators, using the AdaBoost algorithm. The proposed multi-indicator selection scheme aims to select the potential parents for crossover. In a further work, Phan *et al.* [112] proposed BIBEA-P which improves BIBEA's parent selection scheme by using an ensemble learning method. The authors also proposed a multi-indicator environmental selection mechanism. An issue of both proposals is that they require supervised offline training, using certain MOPs. Hence, apparently, they would not be able to solve any type of MOP. Unfortunately, the experimental results did not show that the proposals outperformed state-of-the-art MOEAs. Unlike BIBEA and BIBEA-P which are ensemble methods, the Stochastic Ranking-based Multi-Indicator Algorithm (SRA) [90] is an MOEA that aims to balance the search biases of the indicators ϵ^+ and SDE. SRA is a steady-state MOEA that uses the stochastic ranking algorithm as its environmental selection mechanism to sort the population using the two considered indicators as its sorting criteria. After the sorting is done, the worst solution is deleted. The authors showed a comprehensive series of experiments using benchmark problems in low- and high-dimensional objective spaces, comparing their results with those produced by a wide variety of state-of-the-art MOEAs. On the other hand, Hernández Gómez and Coello Coello [61] proposed an MOEA, called MOMBI-III, that combines the convergence effect of an $R2$-selection mechanism and a density estimator based on the Riesz s-energy indicator for improving diversity. Additionally, the $R2$-selection mechanism employs a hyper-heuristic to select the most suitable utility function for the $R2$ indicator. Their experimental results showed that MOMBI-III outperforms several state-of-the-art MOEAs.

The idea of employing MIB-MOEAs is further explored in this Ph.D. thesis in Chapters 5 and 6.

3.4.2 Use of Hyper-heuristics

Due to the No Free Lunch Theorem [140], IB-MOEAs cannot possibly have a good performance in all types of MOPs. With the aim of reducing the effect of the NFL,

hyper-heuristics arise as a good option because they find from among a pool of low-level heuristics, the one that is more suitable for a certain problem [19]. Hence, a hyper-heuristic could decide which is the most effective indicator-based mechanism depending on the MOP being tackled. Such hyper-heuristic is proposed in Chapter 5 where from a pool of density estimators based on the indicators $R2$, IGD^+, ϵ^+ and Δ_p, the most suitable choice is selected for a given problem.

3.4.3 Parallel IB-MOEAs

We believe that it is possible to take advantage of parallelism in at least two ways. First, by designing parallel IB-mechanisms that reduce the computational cost of IB-MOEAs. In this regard, Hernández Gómez and Coello Coello [62] proposed a parallel version of SMS-EMOA based on the island model, where each island has a micro population. This version can substantially reduce the computational cost of SMS-EMOA without sacrificing the population's quality in a significant way, regarding HV. On the other hand, the interactions of subpopulations, using different IB-Mechanisms, in a parallel model (e.g., the island model) could produce new global search behaviors. This research path is exploited in Chapter 6.

3.4.4 QIs and IB-MOEAs' Theory

Currently, the understanding of QIs and IB-MOEAs is far from being complete. Regarding QIs, it is necessary to mathematically analyze them not only in an individual fashion but also when they are combined. An open research direction is to mathematically prove if there are other unary Pareto-compliant QIs besides the hypervolume. Chapter 7 investigates the mathematical combination of QIs to produce new ones having the Pareto compliance property. Additionally, we have to turn our attention to the design of efficient algorithms for the exact hypervolume computation [139] or, at least, a good approximation of it that can be obtained at a relatively low computational cost [78, 119]. Regarding IB-MOEAs, it would be valuable to have a theoretical study that characterizes IB-Selection mechanisms with respect to their speed of convergence, distribution, and spread of solutions. Hence, Chapter 4 provides an empirical study, aiming to characterize steady-state IB-MOEAs. It would also be interesting to propose new selection mechanisms based on existing or on new QIs and investigate their properties from a theoretical point of view. Finally, a theoretical aspect around IB-MOEAs that is worth analyzing is why mechanisms based on non-Pareto-compliant indicators can indeed produce good results, e.g., Δ_p-MOEA or MOEA/IGD-NS. It is clear that from the point of view of quality comparison of MOEAs, Pareto-compliance is required to avoid generating misleading results. However, based on the results of IB-MOEAs using non-Pareto-compliant indicators, convergence of an IB-MOEA is apparently not strictly related to the use of a Pareto-compliant QI. Hence, an interesting topic for future research is to determine if it is really necessary to adopt a Pareto-compliant QI as part of a MOEA in order to produce high-quality results. If not, it is clearly important to know the reasons.

3.5 Summary

This chapter introduced quality indicators and indicator-based MOEAs. QIs are set-functions which measure the quality of approximation sets, regarding convergence, spread, and uniformity of solutions. In the literature, there exist several QIs, however, those focused on assessing convergence have mostly attracted the attention of the evolutionary multi-objective optimization community to compare MOEAs and to design selection mechanisms. Among the plethora of convergence QIs, the most representative ones are the following: HV, R2, GD, IGD, IGD$^+$, ϵ^+, and Δ_p. Additionally, we introduced two QIs that measure the uniformity of solutions: the Riesz s-energy indicator and the Solow-Polasky-Diversity indicator. Moreover, we provided a comprehensive review of the IB-MOEAs' state-of-the-art based on a taxonomy that we proposed. it is worth noting that our taxonomy aims to classify IB-Mechanisms instead of IB-MOEAs, since these IB-Mechanisms can be coupled to any MOEA. Finally, we briefly described some real-world problems solved by IB-MOEAs and some possible future research paths.

Chapter 4

Convergence and Diversity Properties of IB-MOEAs

This chapter introduces an empirical analysis of IB-MOEAs, emphasizing their convergence and diversity properties. Section 4.1 explains the main motivation to produce such analysis. Previous analysis on QIs and IB-MOEAs are outlined in Section 4.2. The experimental design and methodology is specified in Section 4.3. Section 4.4 is devoted to show our experimental results. Finally, a summary of the chapter is presented in Section 4.5.

4.1 Motivation

In the specialized literature there exists a plethora of QIs, each one representing different preferences [95]. Among this large set, QIs focused on measuring convergence to the Pareto optimal front have strongly impacted the development of MOEAs, being the backbone of selection mechanisms (see Chapter 3). An IB-Mechanism presents the same preferences of its baseline QI during the evolutionary process which implies that it has specific strengths and weaknesses depending on the MOP being solved. In spite of the wide range of IB-MOEAs currently available, there is no empirical or theoretical study that compares the strengths and weaknesses of IB-MOEAs in terms of convergence and diversity solutions. Convergence and diversity (divided into spread and uniformity) are the two main characteristics on an MOEA, according to Zitzler *et al.* [150]. Hence, it would be valuable to characterize the convergence and diversity properties of multiple IB-MOEAs when tackling MOPs having different difficulties and Pareto front shapes. In this chapter, we aim to empirically investigate the above mentioned properties of five steady-state IB-MOEAs that employ the indicators HV, R2, IGD^+, ϵ^+, and Δ_p in a density estimator. The purpose of this study is to get a better understanding of the strengths and weaknesses of each IB-MOEAs such that (1) recommendations of IB-MOEAs can be made depending on the characteristics of the problem, and (2) the knowledge obtained from the study could guide the design of hyper-heuristics (see Chapter 5).

4.2 Previous Related Work

In 2008, Brockhoff *et al.* [16] performed a theoretical analysis of hypervolume-based algorithms. The authors aimed to gain insights into the optimization process of HV-based MOEAs by carrying out rigorous running time analyses. The study was focused on convergence and spread properties of the $(\mu+1)$-SIBEA which is a steady-state version of SIBEA [149]. Regarding convergence, they measured the expected running time to achieve a Pareto front approximation sufficiently close to the Pareto optimal front of the LOTZ problem. As a result, they provided theoretical upper bounds to achive the desired degree of convergence. Concerning spread, they assessed this feature by means of the multiplicative ϵ-dominance relation[1]. The idea was to determine the time until the IB-MOEA achieved a good approximation to a large Pareto front, attending the ϵ-dominance that leads to approximation sets with good spread. An important drawback of this study is that the analysis neither covers different Pareto front shapes nor MOPs having a wide variety of difficulties. Hence, more general conclusions cannot be drawn.

Regarding the R2 indicator [17], Brockhoff *et al.* [18] theoretically analyzed its optimal μ-distributions for bi-objective MOPs as a first step. Then, the conclusions that they obtained were enhanced with empirical observations with respect to the optimal μ-distributions on different Pareto front shapes, namely, convex, linear, concave, and disconnected related to the problems ZDT1, DTLZ1, DTLZ2, and DTLZ7 respectively. For this empirical study, they varied the set of weight vectors required by R2, focusing on the number of vectors and the method to generate them. The authors measured the variability of the distribution of points for each combination of test problem, number of weight vectors, and weight distribution. Although this study gives remarkable insights on the preferences of the R2 indicator, it does not consider convergence features.

4.3 Experimental Design

The aim of our experiments is to empirically analyze the convergence and diversity properties of steady-state MOEAs that employ density estimators based on the indicators: HV, R2, IGD^+, ϵ^+, and Δ_p that were introduced in Section 3.1. In other words, we study the above mentioned properties of SMS-EMOA, R2-EMOA, IGD^+-MaOEA, ϵ^+-MaOEA, and Δ_p-MaOEA. All these IB-MOEAs follow the structure of SMS-EMOA. However, Algorithm 4 shows the generic steady-state IB-MOEA that can employ the adopted QIs. The main loop of the generic steady-state IB-MOEA is in lines 2 to 14. At each iteration, a single solution is created from the population P using genetic operators. This solution is then temporarily added to P to form the population Q in line 4, Then, Q is divided into a set of layers $R_1, \ldots, R_t$, using the nondominated sorting algorithm [31], where R_t contains the worst solutions

[1]Given $\vec{x}, \vec{y} \in \mathcal{X}$ and $\epsilon > 0$, $\vec{x}$ ϵ^*-dominates $\vec{y}$, denoted by $\vec{x} \preceq_{\epsilon^*} \vec{y}$ or $\vec{f}(\vec{x}) \preceq_{\epsilon^*} \vec{f}(\vec{y})$ if $f_i(\vec{x}) \leq f_i(\vec{y}) \cdot (1+\epsilon)$ and there exists at least one index $j \in \{1, 2, \ldots, m\}$ such that $f_j(\vec{x}) < f_j(\vec{y}) \cdot (1+\epsilon)$.

according to the Pareto dominance relation. If R_t has more than one solution, an indicator-based density estimator (IB-DE) is executed. First, an IB-DE calculates the individual indicator contributions of all solutions in a given set using Eq. (3.11), and, finally, it deletes the solution having the minimum contribution.

Algorithm 4: Generic steady-state IB-MOEA

Input: Indicator I
Output: Pareto front approximation
Randomly initialize population P;
while *stopping criterion is not fulfilled* **do**
  Generate offspring $\vec{q}$ from population P;
  $Q \leftarrow P \cup \{\vec{q}\}$;
  Obtain $\vec{z}^*$ and $\vec{z}^{\text{nad}}$ from Q and normalize it;
  $\{R_1, \ldots, R_t\} \leftarrow$ non-dominated sorting(Q);
  if $|R_t| > 1$ **then**
    $\vec{r}_{\text{worst}} \leftarrow \arg\min_{\vec{r} \in R_t} C_I(\vec{r}, R_t)$;
  end
  else
    $\vec{r}_{\text{worst}}$ is the single solution in R_t;
  end
  $P \leftarrow Q \setminus \{\vec{r}_{\text{worst}}\}$;
end
return P

For all the experiments that are described in the following, we adopted the Deb-Thiele-Laumanns-Zitzler (DTLZ) [32], Walking-Fish-Group (WFG) [65], Viennet (VIE) [133], Lamé superspheres [38], DTLZ^{-1}, and WFG^{-1} [75] test suites with two and three objective functions. Table 4.1 describes the MOPs employed in the study, emphasizing their Pareto front geometry and whether $\mathcal{PF}^*$ is correlated with the shape of a simplex formed by a set of convex weight vectors[2]. In all cases, we performed 30 independent executions of each algorithm with each test instance.

The goals of our convergence analysis are twofold. First, investigate the percentage of successful executions (denoted as "hit rate") on which an IB-MOEA is sufficiently close (attending a specific criterion) to $\mathcal{PF}^*$, and, on average, how many function evaluations are required to fulfill this condition (convergence speed). Second, we aim to evaluate the final Pareto front approximations generated by the adopted IB-MOEAs, using multiple convergence QIs.

Regarding the first goal, we claim that an IB-MOEA is close enough to a reference set $\mathcal{Z} \subset \mathcal{PF}^*$ if its population (P) at some iteration t meets the following criterion (called ϵ^+-convergence): $\epsilon^+(P_t, \mathcal{Z}) \leq \bar{\epsilon}$, where $\bar{\epsilon}$ is a parameter set to 0.05 and 0.1 for two and three objectives, respectively. If the IB-MOEA has ϵ^+-convergence, that

[2]A vector $\vec{w} \in \mathbb{R}^m$ is a convex weight vector if and only if $\sum_{i=1}^{m} w_i = 1$ and $w_i \geq 0, \forall i = 1, \ldots, m$

Table 4.1: MOPs adopted in our study. For each case, the Pareto front geometry is described, indicating whether it is correlated or not with the shape of a simplex.

MOP	**Pareto front shape**	**Simplex-like**
DTLZ5	Degenerate	×
DTLZ5^{-1}	Convex	×
DTLZ7	Disconnected	×
DTLZ7^{-1}	Disconnected	×
WFG1	Mixed	√
WFG1^{-1}	Mixed	×
WFG2	Disconnected	√
WFG2^{-1}	Slightly concave	×
WFG3	Degenerate	×
WFG3^{-1}	Linear	×
Lamé $\gamma = 0.25$	Highly convex	×
Lamé $\gamma = 0.50$	Convex	√
Lamé $\gamma = 1.00$	Linear	√
Lamé $\gamma = 2.00$	Concave	√
Lamé $\gamma = 5.00$	Highly concave	√
Mirror $\gamma = 0.25$	Highly concave	×
Mirror $\gamma = 0.50$	Concave	×
Mirror $\gamma = 1.00$	Linear	×
Mirror $\gamma = 2.00$	Convex	×
Mirror $\gamma = 5.00$	Highly convex	×
VIE1	Convex	×
VIE2	Mixed (convex and degenerate)	×
VIE3	Degenerate	×

execution is marked as successful; otherwise, the execution is marked as failed. The hit rate (h_r) is the number of successful cases divided by the total number of executions (30 in our experiments). On the basis of h_r, we are interested in determining the strengths and weaknesses of each IB-MOEA, depending on the MOP being tackled. A strength is related to $h_r = 1.0$ (i.e, when in all executions, ϵ^+-convergence was achieved), and a weakness is associated with h_r values in the range $[0, 1)$, where $h_r = 0.0$ indicates that an IB-MOEA is unable to solve the MOP. On the other hand, we consider the speed of convergence as the mean value at which an IB-MOEA reaches ϵ^+-convergence. For each MOP, we investigate which is the fastest IB-MOEA, using the one-tailed Wilcoxon test, with a significance level of $\alpha = 0.05$, to compare the means. Thus, we have statistically significant evidence to draw conclusions.

To analyze the final convergence quality of the IB-MOEAs, we decided to employ the indicators: HV, R2, IGD^+, ϵ^+, and Δ_p. Additionally, we adopted the Hausdorff distance (HD) which is a well-known metric defined as follows:

Definition 4.3.1 (Hausdorff distance)**.** *Given two sets A and B of m-dimensional points, the distance between sets is given by:*

$$\tilde{\delta}(A, B) = \max_{\vec{a} \in A} \min_{\vec{b} \in B} \left\| \vec{a} - \vec{b} \right\|. \tag{4.1}$$

Then, the Hausdorff distance is defined as follows:

$$HD(A, B) = \max(\tilde{\delta}(A, B), \tilde{\delta}(B, A)). \tag{4.2}$$

The reason to use HD is due to its neutrality when assessing the IB-MOEAs, i.e., none of them employ HD in their selection mechanism. Considering the QIs, we opted for a neutral comparison. If we compare a set of IB-MOEAs, using an indicator $\mathcal{I}$, where one of the algorithms uses $\mathcal{I}$ in its selection mechanism, the comparison will be biased to this particular IB-MOEA. Hence, we leave aside that algorithm when comparing with $\mathcal{I}$. For example, if we compare the IB-MOEAs using HV, SMS-EMOA does not take part in the comparison. To obtain statistically significant evidence, we employ the one-tailed Wilcoxon test with $\alpha = 0.05$ for each measure.

Concerning the diversity analysis, we decided to evaluate the diversity of solutions by means of two quality indicators: the Riesz s-energy indicator and the Solow-Polasky-Diversity indicator (SPD) [5]. The first one was introduced in Section 3.1, and SPD is a variant of the Weitzman Diversity [5] that has a lower computational cost. SPD aims to measure the number of species on a population of size N. SPD tends to N, if the distance between all species tends to be very large; and it tends to one, if the species are very similar with respect to each other. SPD depends on a parameter $\theta > 0$ that determines how fast the population tends to N when the distance increases. Using both indicators, we determine which IB-MOEA produces uniformly distributed solutions on each Pareto front. For both QIs, we employ the one-tailed Wilcoxon test as in the final convergence analysis.

4.4 Results

This section aims to present our experimental results. For all experiments, Section 4.4.1 describes the global experimental settings for all the adopted IB-MOEAs and test instances. The next two sections are devoted to describe the convergence and diversity results related to SMS-EMOA, R2-EMOA, IGD$^+$-MaOEA, ϵ^+-MaOEA, and Δ_p-MaOEA.

4.4.1 Experimental Settings

In order to allow a fair comparison, in all the experiments, the IB-MOEAs used the same population size $\mu = C_{m-1}^{H+m-1}$ which is equal to the number of convex weight vectors employed by R2-EMOA. H is a parameter that controls the number of convex weight vectors [147]. Hence, μ is equal to 100 and 105 for two and three objectives, respectively. We adopted a maximum number of function evaluations as the stopping criterion which was set to 50,000 and 60,000 for two and three objectives, respectively. All the IB-MOEAs employed simulated binary crossover and polynomial-based mutation as their genetic operators [31]. For all the objectives, the crossover and mutation probabilities were set to 0.9 and $1/n$, respectively, where n is the number of decision variables. Both the crossover and the mutation distribution indexes were set equal to 20. At each iteration, SMS-EMOA employs the vector of worst objective values of the population as the reference point of HV and the layer R_1 as the reference set in $\{\text{IGD}^+, \epsilon^+, \Delta_p\}$-MaOEA. Regarding the MOPs, the number of decision variables of problems DTLZ, DTLZ^{-1}, and Lamé superspheres is $n = m + K - 1$, where $K = 10$ for DTLZ5 and DTLZ5^{-1}; $K = 20$ for DTLZ7 and its minus version; and, $K = 5$ for the Lamé and Mirror problems that are determined by a different γ value in Table 4.1. Considering the WFG and WFG^{-1} test instances, n was set to 24 and 26 for two and three objective functions, respectively. In both cases, the number of position-related parameters is two. The decision space of the three VIE problems is of dimension two. Finally, for each MOP, we uniformly sampled its $\mathcal{PF}^*$ to generate the reference set required to measure the ϵ^+-convergence. The cardinality of the reference sets was set to 200 and 300 for two- and three-dimensional MOPs. These reference sets are employed by all IB-MOEAs.

4.4.2 Convergence Analysis

Table 4.2 shows the hit rate and speed of convergence for each MOP of all IB-MOEAs. The fastest IB-MOEA is shown in grayscale, and the symbol # is placed when its speed of convergence is significantly better than that of the other IB-MOEAs based on a one-tailed Wilcoxon test, using a significance level of $\alpha = 0.05$. From the table, it is possible to establish the strengths and weaknesses of the IB-MOEAs. We express as a general strength those test instances where all the IB-MOEAs have $h_r = 1.0$ (denoted by the symbol $\surd$), and a general weakness where all the IB-MOEAs have the symbol $\times$ related to $h_r = 0.0$. On the one hand, Lamé and Mirror

problems, DTLZ5 in both 2D and 3D, DTLZ7^{-1} in 2D, WFG2^{-1} in 2D, VIE2 and VIE3 correspond to the general strengths of the adopted IB-MOEAs. On the other hand, DTLZ5^{-1} in 3D, DTLZ7 in 3D, all WFG1 and WFG1^{-1} test instances, WFG2 in 2D and WFG3^{-1} in 3D correspond to the general weaknesses. Figure 4.1 supports our claim of general weaknesses since it shows the IB-MOEAs' median ϵ^+ convergence graphs for all the above-mentioned problems. From this figure, we can see that no IB-MOEA reaches the ϵ^+-convergence condition because in some cases (DTLZ5^{-1} in 3D and DTLZ7 in 3D) the IB-MOEAs get stuck in a higher ϵ^+ value, or the algorithms' behavior is particularly chaotic (WFG1^{-1} in 2D, WFG1^{-1} in 3D and WFG^{-1} in 3D). Considering the 23 MOPs belonging to the DTLZ, DTLZ^{-1}, WFG, WFG^{-1} and VIE test suites (which are more difficult problems than the Lamé superspheres where all the IB-MOEAs achieved ϵ^+-convergence), IGD$^+$-MaOEA ϵ^+-converged in the largest number of MOPs (i.e., 14 problems) although SMS-EMOA and ϵ^+-MaOEA also showed outstanding results since they ϵ^+-converged in 12 and 13 test instances, respectively. Taking into account the total number of MOPs having $h_r = 0.0$ and $h_r \in (0, 1)$, Δ_p-MaOEA and R2-EMOA are the worst IB-MOEAs, having a total of 13 and 15 MOPs under these conditions, respectively. In general, SMS-EMOA presents the best results regarding the speed of convergence because, considering all the MOPs, it was the fastest in 20 out of 43 problems. Additionally, SMS-EMOA and IGD$^+$-MaOEA ϵ^+-converged in a similar number of cases. Consequently, the latter IB-MOEA can be considered to obtain ϵ^+-convergence at a lower computational cost and obtaining similar results to SMS-EMOA. In terms of ϵ^+-convergence, R2-EMOA is the worst IB-MOEA when tackling MOPs having non-simplex-like Pareto fronts. Although in Mirror problems it always presents ϵ^+-convergence, the diversity of solutions is not good, since there is a strong bias to the boundaries of the Pareto fronts. This poor performance is explained by the use of convex weight vectors. Recently, Ishibuchi *et al.* [75] empirically showed that MOEAs using convex weight vectors do not perform very well when tackling MOPs whose Pareto front shapes are not correlated to the geometry of a simplex. In our experiments, most of the problems are not correlated with the simplex shape.

Table 4.2: Hit rate and, in paretheses, the mean value at which IB-MOEAs achieved ϵ^+-convergence (NA means no convergence). The symbols $\surd$ and $\times$ denote hit rate values of 1.0 and 0.0, respectively.

MOP	**Dim.**	**SMS-EMOA**	**R2-EMOA**	**IGD$^+$-MaOEA**	**ϵ^+-MaOEA**	**Δ_p-MaOEA**
DTLZ5	2	$\surd$ (1.7953e+03)	$\surd$ (1.7531e+03)	$\surd$ (1.7720e+03)	$\surd$ (1.7342e+03)	$\surd$ (1.9022e+03)#
	3	$\surd$ (1.2437e+03)#	$\surd$ (1.1537e+03)	$\surd$ (1.1612e+03)	$\surd$ (1.2500e+03)	$\surd$ (1.2542e+03)
DTLZ5^{-1}	2	$\surd$ (4.6186e+03)	0.03 (2.2050e+02)	$\surd$ (4.7308e+03)	$\surd$ (4.6646e+03)	$\surd$ (4.8778e+03)
	3	$\times$ (NA)	$\times$ (NA)	$\times$ (NA)	$\times$ (NA)	$\times$ (NA)
DTLZ7	2	$\surd$ (6.9824e+03)	$\surd$ (7.0057e+03)	$\surd$ (7.1448e+03)	0.97 (6.7282e+03)	$\surd$ (7.3211e+03)#
	3	0.93 (7.8334e+03)	0.90 (1.1067e+04)	0.87 (1.3126e+04)	0.87 (1.5227e+04)	0.93 (1.6307e+04)

Table 4.2 – *Continuation*

MOP	Dim.	SMS-EMOA	R2-EMOA	IGD$^+$-MaOEA	ϵ^+-MaOEA	Δ_p-MaOEA
DTLZ7^{-1}	2	√ (7.1510e+03)	√ (7.4723e+03)	√ (7.1924e+03)	√ (7.2936e+03)	√ (7.1836e+03)
	3	0.93 (8.9018e+03)	√ (1.2634e+04)	0.97 (1.1393e+04)	0.93 (1.2545e+04)	0.93 (1.3663e+04)
WFG1	2	× (NA)	× (NA)	× (NA)	× (NA)	× (NA)
	3	× (NA)	× (NA)	× (NA)	× (NA)	× (NA)
WFG1^{-1}	2	× (NA)	× (NA)	× (NA)	× (NA)	× (NA)
	3	× (NA)	× (NA)	× (NA)	× (NA)	× (NA)
WFG2	2	0.27 (3.0219e+03)	0.33 (6.0751e+03)	0.43 (4.7089e+03)	0.37 (5.6407e+03)	0.37 (4.3414e+03)
	3	√ (1.4918e+04)	0.70 (3.2334e+04)	√ (2.2177e+04)#	√ (2.3527e+04)#	× (NA)
WFG2^{-1}	2	√ (4.3107e+03)	√ (4.4171e+03)	√ (4.4526e+03)	√ (4.5908e+03)#	√ (4.3400e+03)
	3	0.93 (1.6933e+04)	0.43 (1.5769e+04)	√ (2.3580e+04)	√ (2.3414e+04)	× (NA)
WFG3	2	√ (1.0974e+04)	0.13 (3.7698e+03)	√ (1.4113e+04)#	√ (1.3696e+04)#	√ (1.7184e+04)#
	3	√ (2.4031e+04)#	× (NA)	√ (1.6327e+04)	√ (1.6975e+04)	× (NA)
WFG3^{-1}	2	√ (6.8804e+03)	0.13 (2.9965e+03)	√ (7.7343e+03)#	√ (8.5882e+03)#	√ (8.1575e+03)#
	3	× (NA)	× (NA)	× (NA)	× (NA)	× (NA)
VIE1	3	× (NA)	× (NA)	√ (9.6216e+02)#	√ (7.6183e+02)	× (NA)
VIE2	3	√ (1.1300e+02)	√ (8.1733e+01)	√ (8.6866e+01)	√ (1.2800e+02)#	√ (1.1403e+02)#
VIE3	3	√ (5.3703e+02)#	√ (5.3556e+02)#	√ (4.4373e+02)	√ (4.9020e+02)#	√ (4.4970e+02)
LAME $\gamma = 0.25$	2	√ (2.5740e+02)	√ (2.9206e+02)	√ (2.6496e+02)	√ (2.8333e+02)	√ (3.1156e+02)#
	3	√ (7.7591e+02)	√ (7.9923e+02)#	√ (7.8209e+02)	√ (8.0177e+02)#	√ (8.0298e+02)#
LAME $\gamma = 0.50$	2	√ (8.0370e+02)	√ (7.7716e+02)	√ (7.9970e+02)	√ (8.3353e+02)#	√ (8.1173e+02)
	3	√ (6.3380e+02)#	√ (6.8466e+02)#	√ (5.8176e+02)	√ (6.4490e+02)#	√ (7.1123e+02)#
LAME $\gamma = 1.00$	2	√ (1.1465e+03)	√ (1.1300e+03)	√ (1.1749e+03)	√ (1.1643e+03)	√ (1.2303e+03)#
	3	√ (1.3446e+03)	√ (1.3694e+03)	√ (1.4573e+03)	√ (1.4124e+03)	√ (1.7711e+03)#
LAME $\gamma = 2.00$	2	√ (1.2589e+03)	√ (1.3292e+03)	√ (1.2923e+03)	√ (1.2617e+03)	√ (1.3706e+03)
	3	√ (1.6940e+03)	√ (1.8636e+03)#	√ (1.7630e+03)	√ (2.0713e+03)#	√ (2.2545e+03)#
LAME $\gamma = 5.00$	2	√ (1.5477e+03)#	√ (1.3754e+03)	√ (1.2766e+03)	√ (1.4851e+03)	√ (1.3932e+03)
	3	√ (1.8804e+03)	√ (2.0437e+03)	√ (2.1801e+03)	√ (1.9688e+03)	√ (2.3004e+03)#
MIRROR $\gamma = 0.25$	2	√ (1.5231e+03)	√ (1.2931e+03)	√ (1.6226e+03)	√ (1.5719e+03)	√ (1.3624e+03)
	3	√ (1.9233e+03)	√ (2.8885e+03)#	√ (2.0911e+03)	√ (3.8951e+03)#	√ (2.2205e+03)#
MIRROR $\gamma = 0.50$	2	√ (1.0793e+03)	√ (1.1544e+03)	√ (1.1348e+03)	√ (1.1000e+03)	√ (1.3918e+03)#
	3	√ (1.3298e+03)	√ (1.5272e+03)#	√ (1.7857e+03)#	√ (2.4530e+03)#	√ (3.0045e+03)#

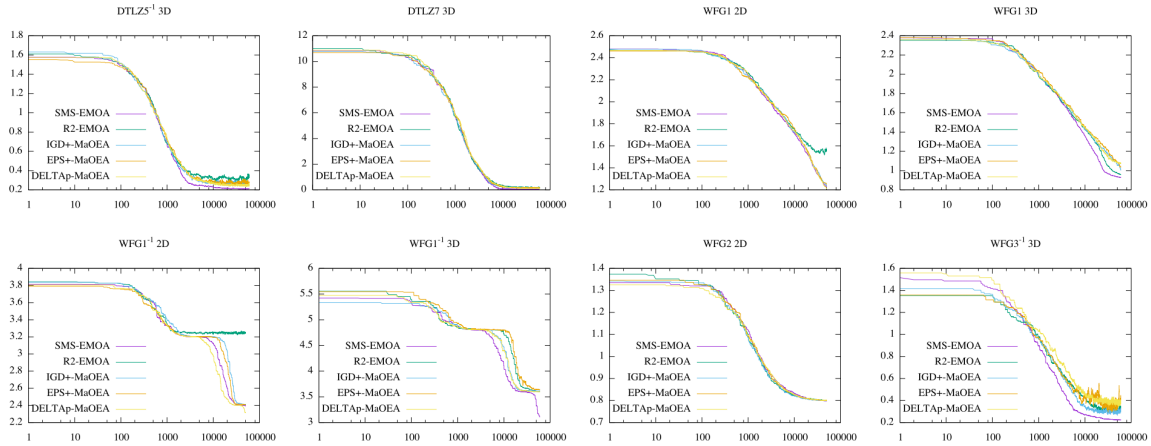

Figure 4.1: Convergence graphs for MOPs which represent general weaknesses for all the adopted IB-MOEAs. The x-axis is related to the number of iterations and the y-axis is the ϵ^+ value.

Table 4.2 – *Continuation*

MOP	**Dim.**	**SMS-EMOA**	**R2-EMOA**	**IGD$^+$-MaOEA**	**ϵ^+-MaOEA**	**Δ_p-MaOEA**
MIRROR $\gamma = 1.00$	2	√ (1.1329e+03)	√ (1.0767e+03)	√ (1.0744e+03)	√ (1.1544e+03)	√ (1.0866e+03)
	3	√ (1.2397e+03)	√ (1.7526e+03)#	√ (1.5057e+03)#	√ (1.5364e+03)#	√ (1.6742e+03)#
MIRROR $\gamma = 2.00$	2	√ (9.7663e+02)	√ (1.0505e+03)	√ (1.0823e+03)#	√ (1.0434e+03)	√ (1.0154e+03)
	3	√ (1.2303e+03)	√ (1.3343e+03)	√ (1.3394e+03)	√ (1.3497e+03)	√ (1.3900e+03)#
MIRROR $\gamma = 5.00$	2	√ (8.6050e+02)	√ (8.3893e+02)	√ (9.1160e+02)#	√ (9.0470e+02)	√ (8.6323e+02)
	3	√ (9.3666e+02)	√ (9.5646e+02)#	√ (8.7250e+02)	√ (9.6340e+02)#	√ (9.1113e+02)

Regarding the final convergence results, Table 4.3 presents the Hausdorff distance results while Tables B.1, B.2, B.3, B.4, and B.5 show the results for HV, R2, IGD$^+$, ϵ^+, and Δ_p, respectively in Appendix B. However, we summarize in Fig. 4.2 the count of the first and second places obtained by the IB-MOEAs on the QIs. Based on HD, Δ_p-MaOEA and SMS-EMOA are the best IB-MOEAs because they obtained very similar results: the former is the best in 16 MOPs while the latter gets the first place in 15 test instances. ϵ^+-MaOEA is ranked as the worst algorithm since it only obtained the first place in one MOP, namely WFG3 in 3D. It is worth noting that although the behavior of Δ_p-MaOEA was not very good with respect to the hit rate and speed of convergence (as it is the case of ϵ^+-MaOEA), it obtains good results on the basis of HD. Based on this and the complete analysis of final convergence, it is possible to see that not always the fastest algorithm obtains the best final convergence performance. Hence, we believe that the hit rate and convergence speed can provide valuable insights about the exploration ability of the corresponding IB-DEs, while the final convergence results help us to determine what is the exploitation (or refinement of the approximated Pareto fronts) ability associated with the IB-DEs. To

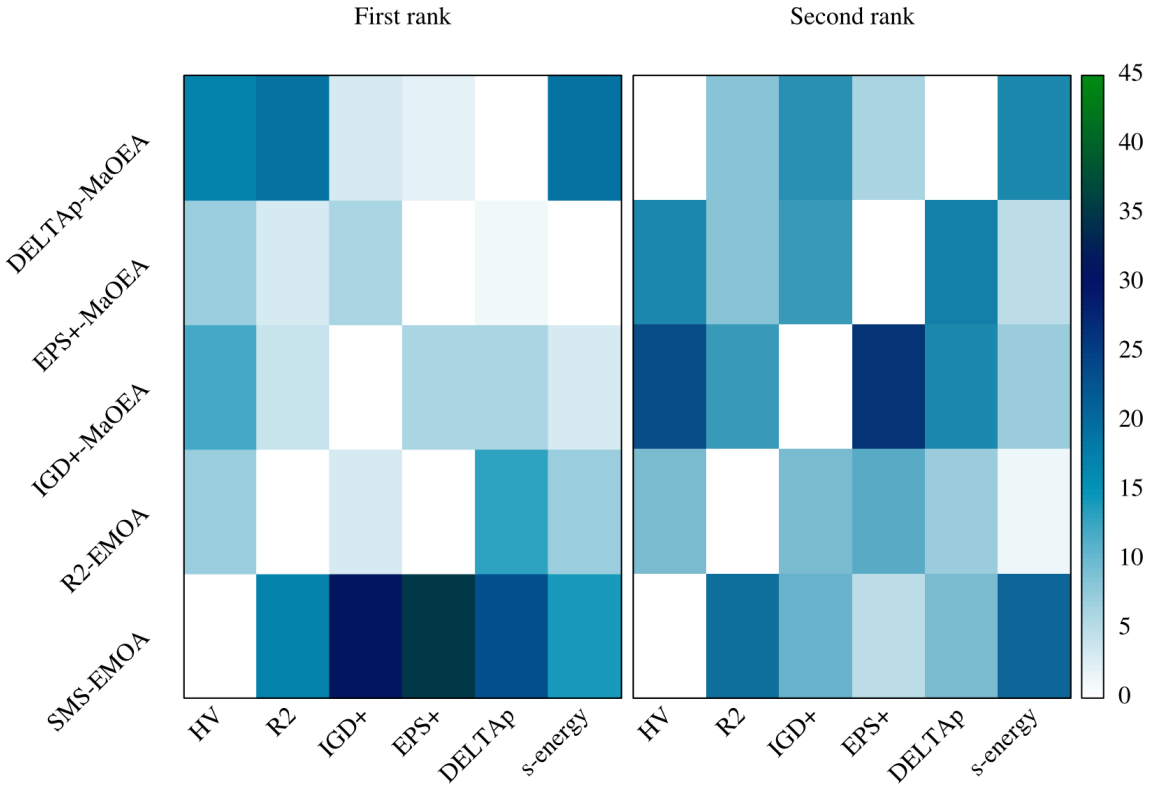

Figure 4.2: Heat map that shows the number of times an IB-MOEA was ranked first or second, according to the indicators HV, R2, IGD^+, ϵ^+, Δ_p, and Riesz s-energy.

support this fact, from Figure 4.2, we observe that SMS-EMOA is the best algorithm for IGD^+, ϵ^+, and Δ_p; while Δ_p-MaOEA is the best for HV and R2. Considering the second places on each QI, we have IGD^+-MaOEa for HV, SMS-EMOA for R2, ϵ^+-MaOEA regarding IGD^+, IGD^+-MaOEA for ϵ^+, and, finally, R2-EMOA for Δ_p. Due to the high correlation between HV and ϵ^+ [97], and HV with IGD^+ [43], it is clear why SMS-EMOA significantly outperforms the other IB-MOEAs on these QIs. Additionally, the first place of SMS-EMOA in Δ_p is due to its good distribution of solutions (which is discussed in the next section) in comparison to the uniformity of solutions produced by R2-EMOA, IGD^+-MaOEA, and ϵ^+-MaOEA. On the other hand, Δ_p-MaOEA obtains the first place in HV because its spread and uniformity of solutions are better than those of the other IB-MOEAs, which is something rewarded by HV. The same arguments hold for the case of R2, which is also highly correlated with HV although it prefers uniformly distributed solutions on linear and concave Pareto fronts.

Based on the results of both experiments, the following conclusions are drawn. The IGD^+-based or the ϵ^+-based density estimators (DEs) can be plugged onto MOEAs to provide a higher probability to obtain ϵ^+-convergence although at a slower rate. HV-DE is better if we are interested in a faster convergence. However, we have to consider that the cost of repeatedly computing HV contributions is time-consuming since the cost of HV increases super-polynomially with the number of objective functions. In order to refine the Pareto fronts produced by the recommended IB-DEs, we can choose Δ_p-DE since it provided excellent final convergence results regarding HD, HV, and R2. On the other hand, due to the use of convex weight vectors, R2-EMOA arises as the worst option when the Pareto front of the MOP is not correlated with the shape of a simplex. This result is supported in [75]. The rest of IB-MOEAs are not strongly sensitive to the Pareto front geometry.

Table 4.3: Mean and, in parentheses, standard deviation of the Hausdorff distance. The two best values are shown in gray scale, where the darker tone corresponds to the best value. A symbol # is placed when the best algorithm performed significantly better than the others based on a one-tailed Wilcoxon test, using a significance level of $\alpha = 0.05$.

MOP	Dim.	SMS-EMOA	R2-EMOA	IGD^+-MaOEA	ϵ^+-MaOEA	Δ_p-MaOEA
DTLZ5	2	3.077574e-02# (1.815526e-03)	9.510878e-03 (1.521790e-04)	6.093201e-02# (9.932257e-03)	5.993075e-02# (1.089149e-02)	1.850188e-02# (2.812982e-03)
	3	3.216520e-02# (1.796077e-03)	7.066692e-02# (3.992978e-02)	5.988385e-02# (1.002451e-02)	5.989544e-02# (1.132659e-02)	1.874597e-02 (3.463474e-03)
$DTLZ5^{-1}$	2	7.843520e-02# (4.729278e-03)	1.699884e+00# (2.473119e-01)	4.344041e-01# (1.048696e-01)	3.853122e-01# (1.114517e-01)	6.256021e-02 (8.528846e-03)
	3	3.829379e-01 (1.460900e-02)	1.444826e+00# (2.827319e-01)	1.192761e+00# (2.420971e-01)	1.156801e+00# (2.427119e-01)	5.146270e-01# (1.033163e-01)
DTLZ7	2	2.202549e-02 (2.005463e-03)	4.852905e-02# (2.302330e-02)	3.065463e-02# (5.417997e-03)	7.589137e-02# (2.481287e-01)	3.470451e-02 (2.569990e-02)
	3	5.261453e-01# (4.365759e-01)	3.669089e-01 (3.613377e-01)	4.845426e-01# (3.995423e-01)	5.441027e-01# (5.347534e-01)	3.366100e-01 (2.958924e-01)
$DTLZ7^{-1}$	2	1.187580e-02 (1.004169e-03)	3.711496e-02# (1.834241e-02)	1.761300e-02# (6.396731e-03)	1.807463e-02# (8.560824e-03)	1.302961e-02# (4.361443e-03)
	3	5.481802e-01# (1.776795e-01)	4.797460e-01 (1.518527e-02)	5.339010e-01# (1.174193e-02)	5.750645e-01# (1.711356e-01)	5.522249e-01# (1.795489e-01)
WFG1	2	2.213367e+00 (3.948808e-01)	2.830692e+00# (4.206011e-01)	2.328385e+00# (5.420895e-02)	2.202644e+00# (4.914847e-01)	2.136225e+00 (4.735624e-01)
	3	2.197492e+00 (4.125112e-01)	2.811781e+00# (3.559170e-01)	3.085727e+00# (2.095829e-01)	3.249765e+00# (1.731195e-01)	3.072379e+00# (2.837441e-01)

Table 4.3 – *Continuation*

MOP	Dim.	SMS-EMOA	R2-EMOA	IGD$^+$-MaOEA	ϵ^+-MaOEA	Δ_p-MaOEA
WFG1^{-1}	2	2.348346e+00# (5.013607e-01)	3.560577e+00# (1.614038e-01)	2.579248e+00# (3.822815e-01)	2.587287e+00# (3.687097e-01)	1.835583e+00 (7.891345e-01)
	3	3.144431e+00 (4.566521e-01)	3.644217e+00# (9.520948e-02)	3.640692e+00# (5.683441e-02)	3.712366e+00# (5.591896e-02)	3.574088e+00# (1.509626e-01)
WFG2	2	7.505522e-01 (4.193102e-01)	7.315594e-01# (3.822844e-01)	6.113520e-01 (4.534472e-01)	6.719010e-01 (4.426562e-01)	6.680274e-01 (4.464939e-01)
	3	1.949492e+00# (1.831101e-01)	1.972061e+00# (8.818055e-02)	2.161069e+00# (1.890187e-01)	2.107503e+00# (1.540904e-01)	1.428000e+00 (3.529359e-01)
WFG2^{-1}	2	2.490296e-02 (1.333398e-03)	1.638632e-01# (8.150410e-02)	4.685722e-02# (8.561709e-03)	4.639651e-02# (7.032178e-03)	4.923717e-02# (8.955797e-03)
	3	1.330635e+00# (8.981255e-02)	7.730115e-01# (6.995659e-02)	9.290884e-01# (1.391188e-01)	9.289295e-01# (8.444951e-02)	6.880378e-01 (7.977693e-02)
WFG3	2	2.707010e-02 (1.121240e-03)	4.011508e-01# (1.575776e-01)	5.339123e-02# (1.394259e-02)	5.038746e-02# (1.123899e-02)	5.753183e-02# (1.266287e-02)
	3	2.108328e+00# (4.214193e-02)	2.124371e+00# (4.720215e-02)	1.490614e+00 (1.557406e-01)	1.445250e+00 (1.461410e-01)	1.723725e+00# (1.199918e-01)
WFG3^{-1}	2	2.466026e-02 (1.343378e-03)	4.682168e-01# (1.769721e-01)	5.507582e-02# (1.385543e-02)	5.835986e-02# (2.302785e-02)	6.257074e-02# (1.894104e-02)
	3	4.196883e-01 (2.153138e-02)	5.821841e-01# (1.038923e-01)	4.439020e-01 (8.330356e-02)	5.805365e-01# (1.639781e-01)	4.858140e-01# (7.909681e-02)
VIE1	3	1.478014e+00# (5.721134e-03)	1.118123e+00# (2.293143e-01)	9.590722e-01 (4.065934e-01)	1.031676e+00 (3.252150e-01)	1.544479e+00# (8.848777e-02)
VIE2	3	7.659238e-02# (1.139953e-02)	4.321739e-01# (1.981138e-01)	5.138187e-01# (2.077573e-01)	5.449889e-01# (2.015539e-01)	6.188452e-02 (1.909836e-02)
VIE3	3	3.597325e+01# (2.535381e-03)	3.580163e+01# (1.483174e-01)	3.570980e+01 (1.239652e-01)	3.580249e+01# (1.644133e-01)	3.596517e+01# (2.413054e-02)
LAME $\gamma = 0.25$	2	7.231123e-02 (1.543747e-03)	7.627063e-01# (9.379871e-02)	4.361314e-01# (5.303411e-02)	4.347943e-01# (7.209262e-02)	1.048069e-01# (1.075039e-02)
	3	3.030839e-01# (6.199006e-02)	8.535220e-01# (2.947354e-01)	7.241131e-01# (2.688209e-02)	7.221472e-01# (3.477759e-02)	1.995764e-01 (3.077426e-02)
LAME $\gamma = 0.50$	2	2.530849e-02# (1.564295e-03)	5.402476e-01# (1.162890e-01)	1.272472e-01# (3.749616e-02)	1.376205e-01# (3.691710e-02)	1.778939e-02 (2.712181e-03)
	3	1.101923e-01# (6.031892e-03)	5.446090e-01# (1.387246e-02)	4.659930e-01# (6.140304e-02)	4.938630e-01# (6.053914e-02)	8.932232e-02 (2.425611e-02)
LAME $\gamma = 1.00$	2	7.589236e-03 (2.965523e-04)	1.007102e-01# (5.897155e-02)	1.313399e-02# (1.948516e-03)	1.329846e-02# (1.638165e-03)	1.973800e-02# (1.835242e-02)
	3	7.173814e-02# (3.872626e-03)	6.206041e-02 (4.862174e-03)	1.050844e-01# (1.151115e-02)	1.179165e-01# (1.197276e-02)	1.111155e-01# (1.292641e-02)
LAME $\gamma = 2.00$	2	3.186574e-02# (1.316612e-03)	1.007065e-02 (3.261561e-04)	6.141609e-02# (9.949159e-03)	5.921995e-02# (8.479438e-03)	1.728853e-02# (2.514175e-03)
	3	1.621467e-01# (4.555663e-03)	9.639930e-02 (2.367559e-04)	1.966129e-01# (2.248088e-02)	1.876308e-01# (2.027803e-02)	1.376867e-01# (1.443447e-02)
LAME $\gamma = 5.00$	2	1.409980e-01# (3.315905e-03)	3.417753e-02 (1.948163e-04)	2.234118e-01# (1.061329e-02)	2.127717e-01# (1.603388e-02)	3.489903e-02# (2.347631e-03)
	3	3.577989e-01# (7.878295e-03)	1.500669e-01 (2.526744e-04)	3.969645e-01# (1.906622e-02)	3.821651e-01# (1.966347e-02)	1.778417e-01# (1.827104e-02)
MIRROR $\gamma = 0.25$	2	1.685054e-01# (3.830728e-03)	4.997593e-02# (5.020421e-05)	2.907454e-01# (1.526963e-02)	2.850196e-01# (1.893000e-02)	4.843340e-02 (1.701295e-03)
	3	2.413126e-01# (4.093401e-03)	9.262397e-02# (9.708269e-03)	3.422523e-01# (1.479797e-02)	3.950458e-01# (1.099417e-01)	4.999952e-02 (5.118307e-03)
MIRROR $\gamma = 0.50$	2	3.741539e-02# (2.082645e-03)	1.035331e-02 (4.401563e-05)	7.385466e-02# (1.007731e-02)	7.193065e-02# (1.092477e-02)	1.851470e-02# (2.759508e-03)
	3	9.976228e-02# (4.064284e-03)	1.124747e-01# (1.086035e-02)	1.379254e-01# (1.743578e-02)	1.642352e-01# (5.671047e-02)	8.372362e-02 (1.921881e-02)
MIRROR $\gamma = 1.00$	2	7.641986e-03 (2.312297e-04)	9.860330e-02# (5.241803e-02)	1.309680e-02# (1.941996e-03)	1.331902e-02# (1.416358e-03)	1.665265e-02# (2.918066e-03)
	3	9.906263e-02 (4.510345e-03)	1.451629e-01# (1.909890e-02)	1.056237e-01 (1.339696e-02)	1.072790e-01# (1.482283e-02)	1.079255e-01# (1.363654e-02)
MIRROR $\gamma = 2.00$	2	2.203991e-02# (1.670770e-03)	4.544187e-01# (7.917778e-02)	9.258290e-02# (2.505483e-02)	1.040329e-01# (3.609639e-02)	1.716760e-02 (2.927445e-03)
	3	1.213664e-01 (4.470778e-03)	3.538615e-01# (3.696266e-02)	3.368791e-01# (4.317780e-02)	3.547486e-01# (4.127689e-02)	1.458980e-01# (1.747558e-02)
MIRROR $\gamma = 5.00$	2	5.878550e-02 (1.711243e-03)	6.881999e-01# (6.701582e-02)	3.174689e-01# (4.997798e-02)	3.425114e-01# (4.141809e-02)	6.861973e-02# (4.090946e-03)
	3	3.402385e-01# (3.222692e-03)	7.875241e-01# (1.882810e-02)	7.533097e-01# (3.185327e-02)	7.785876e-01# (5.575465e-02)	2.116174e-01 (3.172115e-02)

4.4.3 Diversity Analysis

To assess the diversity of solutions in the outcomes of IB-MOEAs, we decided to employ two QIs: the Solow-Polasky Diversity indicator (SPD) [39] and the Riesz s-energy indicator (E_s) [56]. Table 4.4 shows the SPD results while Table B.6 presents the E_s numerical results and Fig. 4.2 summarizes them. Both SPD and E_s values show evidence that Δ_p-MaOEA produces Pareto front approximations with high diversity. In the second place, we have SMS-EMOA for both QIs as well. ϵ^+-MaOEA has the worst diversity results since it does not produce the best value in any of the test cases

adopted. The results of ϵ^+-MaOEA can be explained by the fact that ϵ^+ exclusively assesses convergence while the other indicators adopted in our study simultaneously assess convergence and diversity. Hence, the ϵ^+-based DE only promotes convergence. On the other hand, from Table 4.4, it is easy to see that in most cases where Δ_p-MaOEA obtains the best value, such results are related to MOPs with Pareto fronts not correlated with the form of a simplex, such as DTLZ5 in 3D, DTLZ7 in 3D, WFG2^{-1} in 3D and all the VIE problems. Regarding the Lamé problems, SMS-EMOA has the best results on the convex and linear instances, while R2-EMOA performs better in concave Pareto fronts. This behavior holds on the Mirror problems. In Figure 4.3, we show some Pareto fronts produced by the IB-MOEAs to support our claims. For instance, no IB-MOEA was able to generate the complete front of WFG1 in 2D (that is why this problem was highlighted as a general weakness in the previous section). Also, in the Lamé $\gamma = 2.0$ with three objectives, R2-EMOA produces evenly distributed solutions while for its mirror version, it fails to cover the entire Pareto front. For this latter problem, we can see from the figure that the distributions of both IGD$^+$-MaOEA and ϵ^+-MaOEA are not too uniform and their spread is deficient.

Table 4.4: Mean and, in parentheses, standard deviation of the Solow-Polasky diversity indicator. The two best values are shown in gray scale, where the darker tone corresponds to the best value. A symbol # is placed when the best algorithm performed significantly better than the others based on a one-tailed Wilcoxon test, using a significance level of $\alpha = 0.05$.

MOP	Dim.	SMS-EMOA	R2-EMOA	IGD$^+$-MaOEA	ϵ^+-MaOEA	Δ_p-MaOEA
DTLZ5	2	8.799243e+00# (2.420473e-03)	8.817050e+00 (8.601901e-04)	8.692179e+00# (3.515960e-02)	8.698178e+00# (3.673926e-02)	8.799056e+00# (2.640527e-02)
	3	8.802124e+00# (1.842481e-03)	8.539616e+00# (2.631087e-01)	8.699035e+00# (3.573762e-02)	8.698818e+00# (4.114915e-02)	8.806127e+00 (3.350134e-02)
DTLZ5^{-1}	2	2.742359e+01 (4.815321e-02)	1.321604e+01# (9.843791e-01)	2.363707e+01# (4.646154e-01)	2.387372e+01# (6.603154e-01)	2.722379e+01# (1.251890e-01)
	3	8.788601e+01# (4.577521e-01)	7.726040e+01# (1.951105e+00)	7.816839e+01# (2.541094e+00)	7.747251e+01# (2.386478e+00)	8.936051e+01 (8.589468e-01)
DTLZ7	2	1.075924e+01# (9.485348e-03)	1.055704e+01# (1.764871e-01)	1.066020e+01# (6.687948e-02)	1.041361e+01# (1.293614e+00)	1.085721e+01 (1.688882e-01)
	3	3.659716e+01# (6.215085e+00)	4.027530e+01# (6.216719e+00)	3.504953e+01# (6.740447e+00)	3.403047e+01# (7.516555e+00)	4.140520e+01 (5.385747e+00)
DTLZ7^{-1}	2	6.946015e+00# (4.422645e-03)	6.829293e+00# (1.069516e-01)	6.904642e+00# (4.677685e-02)	6.902470e+00# (4.532370e-02)	6.970949e+00 (3.234239e-02)
	3	2.084053e+01# (3.712756e+00)	2.440047e+01 (1.172822e+00)	2.032370e+01# (5.897520e-01)	1.951134e+01# (3.352975e+00)	2.315315e+01 (4.036582e+00)
WFG1	2	1.154858e+01 (1.062588e+00)	7.966541e+00# (1.461112e+00)	1.095551e+01# (3.125391e-01)	1.122544e+01# (1.345348e+00)	1.174460e+01 (1.270376e+00)
	3	6.254917e+01 (4.372476e+00)	5.412430e+01# (2.518273e+00)	4.603504e+01# (4.082818e+00)	4.426244e+01# (3.908723e+00)	5.570082e+01# (4.245888e+00)
WFG1^{-1}	2	1.203741e+01# (1.365288e+00)	5.778459e+00# (8.738993e-01)	1.084528e+01# (1.389314e+00)	1.078942e+01# (1.273548e+00)	1.334489e+01 (1.901042e+00)
	3	5.665910e+01 (2.887329e+00)	4.855241e+01# (1.400438e+00)	5.763648e+01 (3.496319e+00)	5.725661e+01 (3.691241e+00)	5.752122e+01 (3.486851e+00)
WFG2	2	1.997145e+01 (1.973586e+00)	1.926807e+01# (2.128501e+00)	2.028923e+01# (2.203759e+00)	1.995404e+01# (2.181330e+00)	2.046291e+01 (2.145987e+00)
	3	6.717654e+01# (7.372088e-01)	8.027439e+01# (6.586682e-01)	6.535570e+01# (2.440267e+00)	6.372450e+01# (2.121404e+00)	8.892057e+01 (1.556707e+00)
WFG2^{-1}	2	2.078503e+01 (5.416172e-03)	1.977792e+01# (4.077274e-01)	2.059536e+01# (4.728328e-02)	2.061597e+01# (5.553223e-02)	2.057292e+01# (3.591416e-02)
	3	8.602704e+01# (4.711341e-01)	8.723124e+01# (1.551029e+00)	8.456642e+01# (1.814969e+00)	8.448289e+01# (2.090042e+00)	9.829389e+01 (7.357824e-01)
WFG3	2	2.296039e+01 (1.291320e-02)	1.963773e+01# (1.165537e+00)	2.249084e+01# (1.543758e-01)	2.255296e+01# (1.258089e-01)	2.248167e+01# (1.233345e-01)
	3	5.567263e+01# (5.521267e-01)	6.133350e+01# (2.321322e+00)	5.456024e+01# (2.082674e+00)	5.449212e+01# (2.207354e+00)	6.617536e+01 (2.082402e+00)
WFG3^{-1}	2	2.297874e+01 (6.553550e-03)	1.940599e+01# (1.115155e+00)	2.249152e+01# (1.306431e-01)	2.244912e+01# (1.858592e-01)	2.244101e+01# (1.810237e-01)
	3	8.841161e+01# (3.785907e-01)	7.898779e+01# (1.483873e+00)	9.134386e+01 (6.203059e-01)	9.023680e+01# (8.485443e-01)	8.936711e+01# (7.411444e-01)
VIE1	3	6.805718e+01# (2.521458e-01)	6.740573e+01# (2.310275e+00)	5.453501e+01# (1.807842e+00)	5.552227e+01# (1.601203e+00)	8.005502e+01 (1.007591e+00)

Table 4.4 – *Continuation*

MOP	Dim.	SMS-EMOA	R2-EMOA	IGD$^+$-MaOEA	ϵ^+-MaOEA	Δ_p-MaOEA
VIE2	3	1.154615e+01# (8.125594e-02)	8.685414e+00# (7.102800e-01)	7.650740e+00# (6.617115e-01)	7.504154e+00# (6.006657e-01)	1.206634e+01 (1.333495e-01)
VIE3	3	2.270243e+01# (5.071533e-01)	2.839043e+01# (3.382631e+00)	3.244248e+01# (1.354320e+00)	3.226683e+01# (1.642415e+00)	4.040227e+01 (7.245011e-01)
LAME $\gamma = 0.25$	2	8.941437e+00# (5.772376e-02)	3.466396e+00# (7.335002e-01)	5.424995e+00# (4.050875e-01)	5.319769e+00# (5.079335e-01)	1.034601e+01 (8.009878e-02)
	3	8.305585e+00# (4.656517e-01)	3.211022e+00# (4.651394e+00)	3.245153e+00# (4.269564e-01)	3.169452e+00# (5.650221e-01)	1.526692e+01 (2.753743e-01)
LAME $\gamma = 0.50$	2	9.048334e+00 (2.749814e-03)	4.986518e+00# (6.211100e-01)	7.998533e+00# (3.082688e-01)	7.950827e+00# (2.356451e-01)	9.036493e+00# (4.215163e-02)
	3	1.564823e+01# (7.329384e-02)	7.704771e+00# (2.898069e-01)	9.790586e+00# (9.073317e-01)	9.538096e+00# (7.712106e-01)	1.653927e+01 (3.867472e-01)
LAME $\gamma = 1.00$	2	8.058952e+00 (4.966752e-05)	7.331385e+00# (4.002672e-01)	8.023044e+00# (2.398873e-02)	8.023164e+00# (2.213841e-02)	8.057805e+00# (1.033550e-01)
	3	2.323513e+01 (2.566032e-02)	2.237926e+01# (1.294749e-01)	2.128746e+01# (3.254218e-01)	2.098928e+01# (4.041683e-01)	2.221247e+01# (4.165485e-01)
LAME $\gamma = 2.00$	2	8.798746e+00# (2.632126e-03)	8.816465e+00 (8.420813e-04)	8.686890e+00# (3.921337e-02)	8.694720e+00# (3.146748e-02)	8.783966e+00# (1.916459e-02)
	3	3.186759e+01# (9.079239e-02)	3.339525e+01 (4.378280e-02)	3.023575e+01# (3.969481e-01)	3.043253e+01# (4.591035e-01)	3.098430e+01# (4.273541e-01)
LAME $\gamma = 5.00$	2	8.877808e+00# (4.605688e-02)	9.919260e+00 (1.664460e-03)	7.541355e+00# (1.632247e-01)	7.715249e+00# (1.916045e-01)	9.879156e+00# (3.017395e-02)
	3	2.502635e+01# (1.259251e-01)	4.221664e+01 (1.023175e-02)	2.400398e+01# (6.107517e-01)	2.512005e+01# (7.301891e-01)	3.861530e+01# (7.545026e-01)
MIRROR $\gamma = 0.25$	2	8.841968e+00# (4.921558e-02)	1.036926e+01 (1.776357e-15)	6.736968e+00# (1.987818e-01)	6.823645e+00# (2.712274e-01)	1.030823e+01# (3.404778e-02)
	3	1.093615e+01# (8.161102e-02)	1.416913e+01# (1.578056e-01)	8.310661e+00# (2.339188e-01)	8.203387e+00# (4.731011e-01)	1.477297e+01 (1.127953e-01)
MIRROR $\gamma = 0.50$	2	9.041054e+00# (3.636536e-03)	9.073550e+00 (7.303778e-04)	8.864132e+00# (5.197892e-02)	8.861065e+00# (6.512181e-02)	9.012983e+00# (3.688009e-02)
	3	1.697328e+01 (2.304582e-02)	1.640375e+01# (9.601057e-02)	1.587693e+01# (1.940042e-01)	1.557452e+01# (4.660800e-01)	1.606433e+01# (2.022736e-01)
MIRROR $\gamma = 1.00$	2	8.058956e+00 (4.227378e-05)	7.351128e+00# (3.632428e-01)	8.019590e+00# (2.783349e-02)	8.020846e+00# (2.282434e-02)	8.010456e+0#0 (3.325008e-02)
	3	2.359319e+01 (2.318634e-02)	2.190992e+01# (2.844364e-01)	2.227936e+01# (3.610438e-01)	2.217250e+01# (3.822628e-01)	2.134092e+01# (3.833550e-01)
MIRROR $\gamma = 2.00$	2	8.799740e+00 (1.840336e-03)	4.916376e+00# (3.814669e-01)	7.952831e+00# (2.387585e-01)	7.866694e+00# (2.710103e-01)	8.736439e+00# (4.902078e-02)
	3	3.162068e+01 (3.684369e-02)	2.706497e+01# (6.640911e-01)	2.126063e+01# (1.065545e+00)	2.087369e+01# (1.212016e+00)	2.952776e+01# (5.195778e-01)
MIRROR $\gamma = 5.00$	2	8.713909e+00# (4.863761e-02)	2.961759e+00# (3.079325e-01)	6.252545e+00# (3.950805e-01)	6.073869e+00# (3.581654e-01)	9.810047e+00 (5.141206e-02)
	3	2.442199e+01# (1.206717e-01)	1.850840e+01# (8.730292e-01)	1.260572e+01# (1.243608e+00)	1.200266e+01# (1.300137e+00)	3.611698e+01 (7.843774e-01)

4.5 Summary

In the literature, a wide variety of IB-MOEAs have been proposed, each one exhibiting different convergence and diversity properties associated to the underlying IB-Mechanism. However, a comparison study, focused on the two above mentioned properties, between multiple IB-MOEAs had not been published. In this chapter, we proposed an empirical convergence and diversity analysis of five steady-state IB-MOEAs, using the indicators: HV, R2, IGD$^+$, ϵ^+, and Δ_p as the backbone of density estimators. In other words, we compared SMS-EMOA, R2-EMOA, IGD$^+$-MaOEA, ϵ^+-MaOEA, and Δ_p. Regarding the convergence study, we focused on two goals: (1) investigating the rate at which an IB-MOEA converges to the Pareto optimal front on the basis of the ϵ^+ indicator (we called it ϵ^+-convergence), aiming to determine their strengths and weaknesses, and (2) analyzing the final IB-MOEAs' Pareto front approximations using six convergence measures, i.e., HV, R2, IGD$^+$, ϵ^+, Δ_p, and the Hausdorff distance. On the other hand, we employed the indicators Riesz s-energy and Solow-Polasky-Diversity to measure the divesity of the approximation sets to determine which IB-MOEAs tend to produce evenly distributed solutions in spite of the Pareto front shape. The experimental results indicated that SMS-EMOA,

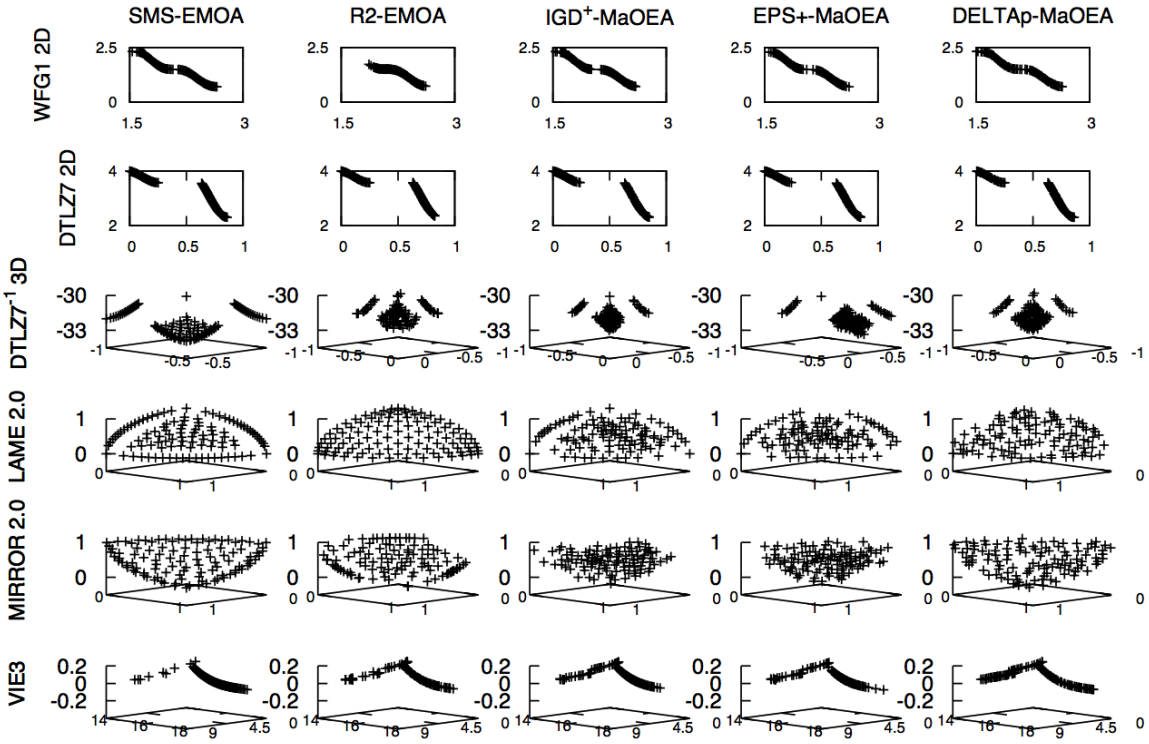

Figure 4.3: Approximated Pareto fronts produced by all the adopted IB-MOEAs. Each approximation set corresponds to the median of the Solow-Polasky Diversity indicator.

IGD$^+$-MaOEA and ϵ^+-MaOEA have remarkable convergence results on MOPs having Pareto front shapes not correlated with a simplex while all IB-MOEAs performed correctly on Lamé superspheres problems whose Pareto fronts are regular. Regarding the diversity analysis, Δ_p-MaOEA tends to produce evenly distributed Pareto front approximations regardless of the Pareto front geometry.

Chapter 5

On the Competition of IB-MOEAs

Commonly, IB-MOEAs have been designed on the basis of a single QI, scarcely exploring the idea of using multiple indicators. In this chapter, we investigate how the competition of multiple IB-Mechanisms, through two proposals, leads to better convergence and diversity results when tackling MOPs. Section 5.1 states the main motivation of our research. Section 5.2 briefly introduces the previous related work. Sections 5.3 and 5.4 are devoted to present our two proposals that exploit the competition of multiple IB-DEs. Finally, a summary of the chapter is provided in Section 5.5.

5.1 Motivation

In the specialized literature, there are several IB-MOEAs (see Chapter 3). A common feature of these IB-MOEAs is that they are mainly based on a single QI, which implies that an IB-MOEA benefits from its strengths and is affected by its weaknesses. For instance, HV-based MOEAs generate a high number of solutions around the Pareto front's knee and on the boundaries for concave Pareto fronts, while they tend to generate evenly distributed solutions for convex and linear Pareto fronts and they also have good performance on degenerate ones [2, 8, 16]. On the contrary, R2-based MOEAs generate well-distributed solutions on concave Pareto fronts but they do not on convex, degenerate or disconnected Pareto fronts since the convex weight vectors, employed by the R2 indicator, do not properly intersect such geometries [18, 59, 75]. In Chapter 4, we investigated the convergence and diversity properties of several steady-state IB-MOEAs, having as the main result their strengths and weaknesses. The aim of this Chapter is to take advantage of the results of Chapter 4 to design two proposals where the competition between multiple IB-DEs is promoted to obtain Pareto front approximations with better convergence and diversity properties.

5.2 Previous Related Work

In this section, we briefly introduce the Multi-Indicator-based MOEAs (MIB-MOEAs) that have been proposed so far.

The first MIB-MOEA was the Boosting Indicator-Based Evolutionary Algorithm (BIBEA) [111] that was proposed by Phan and Suzuki in 2011. BIBEA incorporates a parent selection mechanism that aggregates the indicators HV and ϵ^+ using the AdaBoost algorithm [49]. Through an offline learning process that uses Pareto optimal points of a given MOP, AdaBoost searches for a set of weights that assigns preferences to each of the indicator-based parent tournament selection operators such that the error related to the selection of Pareto or non-Pareto optimal solutions is minimized. Having computed the weights, BIBEA employs them to construct its multi-indicator parent selection mechanism. Unfortunately, the authors only provided an analysis of convergence and diversity of BIBEA, leaving the comparison with other MOEAs out of the study. One year later, Phan et al. [112] introduced a variant of BIBEA, called BIBEA-P. The three main differences concerning BIBEA are the following: (1) AdaBoost is replaced by Pdi-Boosting, (2) a boosting indicator-based environmental selection is added, and (3) a comparison with other MOEAs is presented. The new environmental selection uses the indicator that produces the minimum selection error in the training stage. Thus, it is very similar to BIBEA. The experimental results provided by its authors indicated that BIBEA-P could outperform NSGA-II [29], SMS-EMOA [8], and IBEA [152].

Unlike BIBEA and BIBEA-P which are ensemble methods, the Stochastic Ranking-based Multi-Indicator Algorithm (SRA) [90] is an MOEA that aims to balance the search biases of the indicators ϵ^+ and SDE [94]. SRA is a steady-state MOEA that uses the stochastic ranking algorithm as its environmental selection mechanism to sort the population using the two considered indicators as its sorting criteria. After the sorting is done, the worst solution is deleted. The authors show exhaustive experimentation using benchmark problems in low- and high-dimensional objective spaces, comparing their results with those produced by a wide variety of state-of-the-art MOEAs.

The Stochastic Ranking-based Multi-Indicator Algorithm (SRA) [90] is an MOEA that aims to balance the search biases of the indicators ϵ^+ and SDE. SRA is a steady-state MOEA that uses the stochastic ranking algorithm as its environmental selection mechanism to sort the population using the two considered indicators as its sorting criteria. After the sorting is done, the worst solution is deleted. The authors showed a comprehensive series of experiments using benchmark problems in low- and high-dimensional objective spaces, comparing their results with those produced by a wide variety of state-of-the-art MOEAs.

More recently, Hernández and Coello [61] proposed MOMBI-III which is a hyper-heuristic that selects the best utility function for its environmental selection based on the $R2$ indicator. Additionally, MOMBI-III uses an IB-DE that calculates the contributions to the Riesz s-energy indicator [56] to reduce the joint population of

Figure 5.1: Memoization structure that stores the minimum and second best value per row of the IGD$^+$ cost matrix. We assume that $M = N$.

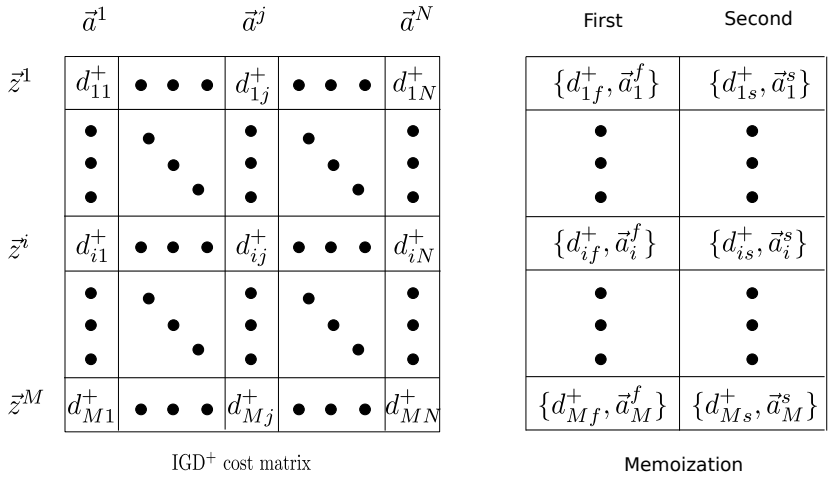

parents and offspring to a specific size. Thus, MOMBI-III combines the effect of $R2$ selection and the Riesz s-energy density estimation.

5.3 Competition through a Hyper-heuristic

In this section, we explore the idea of the competition of multiple IB-DEs by means of a new MOEA which is called Multi-Indicator Hyper-heuristic (MIHPS). First, we outline the framework for the fast computation of the contribution to the indicators $R2$, ϵ^+, Δ_p and IGD$^+$. Then, we describe the hyper-heuristic built from the four IB-DEs and a Markov chain. Finally, we discuss the performance of MIHPS through exhaustive experiments.

5.3.1 Fast Individual Indicator Contribution

The contribution C of a single solution $\vec{a} \in \mathcal{A}$ to an indicator $I \in \{R2, \epsilon^+, \Delta_p, \text{IGD}^+\}$ is defined as follows: $C(\vec{a}, \mathcal{A}) = |I(\mathcal{A}) - I(\mathcal{A} \setminus \{\vec{a}\})|$. For the indicators $R2$, IGD$^+$, ϵ^+ and Δ_p, it can be easily verified that their computation takes $\Theta(mN^2)$, assuming that $|\mathcal{A}| = |\mathcal{Z}| = |W| = N$. Thus, for a single solution, it takes $\Theta(mN^2) + \Theta(m(N-1)^2) = \Theta(mN^2)$ and for all N solutions it takes $\Theta(mN^3)$. For instance, $R2$-EMOA implements this computational-expensive method for calculating the contributions. Hence, we propose a framework for contribution computation of indicators whose definition involves subproblems of maximization or minimization in pursuance of reducing the previously indicated complexity $\Theta(mN^3)$.

Without loss of generality, we focus the analysis on IGD$^+$. However, this analysis can be easily adapted for the other indicators previously mentioned. In the left-hand side of Figure 5.1, we show a cost matrix where $d^+_{ij} = d^+(\vec{a}_j, \vec{z}_i)$ (see Eq. (3.6)). To compute IGD$^+$ using this matrix, we look at the minimum value of each row, sum the

values and divide the result by N. In case a solution $\vec{a}$, associated with one or more of the minimum values, is removed from $\mathcal{A}$, it will be enough to find the second lowest value in the involved rows. Based on this, a memoization structure is shown at the right-hand side of Figure 5.1, where each row stores the minimum value, the second minimum and the corresponding pointers to the associated elements in $\mathcal{A}$. Hence, the memoization structure can be used in furtherance of reducing the cost of computing the contributions.

Algorithm 5 describes how to compute the contributions to IGD^+. First, the $\text{IGD}^+(\mathcal{A}, \mathcal{Z})$ value is calculated and assigned to the variable I_{IGD^+}, using the memoization structure. C_i is the variable which will store the individual contribution of the i^{th} element of $\mathcal{A}$. The main loop is outlined in lines 4-12, where the contribution of each solution is computed taking advantage of the memoization structure. ψ is a temporary variable which accumulates the IGD^+ value of $\mathcal{A} \setminus \{\vec{a}^i\}$. For each element, we only have to determine if it participates in the IGD^+ value; if so, we look for the second best value memoized. The obtained values are added to ψ. Finally, ψ is divided by N and assigned as the contribution of the considered element. The complexity of calculating the IGD^+ value remains as $\Theta(mN^2)$, and the main loop takes $\Theta(N^2)$. Hence, the required time for computing the individual contributions of all solutions in $\mathcal{A}$ is $\Theta(mN^2)$.

Algorithm 5: Fast IGD^+ Individual Contributions

Input: Approximation set $\mathcal{A}$; Reference set $\mathcal{Z}$
Output: IGD^+ individual contributions

```
1  Initialize Memoization;
2  I_IGD+ ← IGD+(A, Z, Memoization);
3  ∀i ∈ {1, ..., |A|}, C_i ← 0;
4  for i = 1 to N do
5      ψ ← 0;
6      for j = 1 to N do
7          if Memoization[j].a⃗_1^f = a⃗^i then
8              ψ ← ψ + Memoization[j].d_js^+;
9          end
10         else
11             ψ ← ψ + Memoization[j].d_jf^+;
12         end
13     end
14     ψ ← ψ/N;
15     C_i ← |I_IGD+ − ψ|;
16 end
17 return {C_i}_{i=1,...,|A|}
```

5.3.2 Hyper-heuristic

On the basis of the selected indicators, four IB-DEs are defined, namely {IGD$^+$-DE, $R2$-DE, ϵ^+-DE, Δ_p-DE}. This set of IB-DEs is the heuristic pool (H_{pool}) from which the hyper-heuristic chooses the most suitable one depending on the MOP being solved. Our proposed hyper-heuristic is a modified version of the work of McClymont and Keedwell [102] where a Markov chain (MC) is employed. The reasons to use an MC are: (1) its low computational cost, (2) the good performance shown in [102], and (3) the related randomness avoids stagnation on a single IB-DE. The hyper-heuristic requires two steps: (1) performance information collection, and (2) heuristic selection. First, once an IB-DE is selected, it is executed during T_w generations. At each generation, the quality of the produced population is measured using the $R2$ indicator, and each sample is stored in a list associated to the IB-DE in H_{pool}. We decided to use the $R2$ indicator because it is highly correlated to the HV [97]. Algorithm 6 outlines the second step which involves the use of the Markov chain (see Figure 5.2), the gathered $R2$ values and a control structure denoted as C_{hh}. At the beginning, in line 1, we check if the current IB-DE has been executed. If so, the counter variable of C_{hh} is augmented by one; otherwise, the transition probability is updated, and a new IB-DE is selected (lines 4 to 19). Let i be the last IB-DE executed and j be the current one. Only the probability p_{ij} is updated. Based on the $R2$ values of the current heuristic, we calculate in line 6 a linear regression model where only the slope b and the standard deviation σ of the data are relevant. Using these two values, in lines 7 to 14, we modified p_{ij} in three cases: (1) adding 2α if the slope is non-negative and $\sigma \geq \bar{\sigma}$, where $\bar{\sigma}$ is a threshold value set to 0.1, (2) adding α if the slope is non-negative but $\sigma < \bar{\sigma}$, and (3) subtracting β if the slope is negative. We set $\alpha = \beta = 0.1$. In line 15, we normalized all values in the i^{th} row of the matrix and, finally, we select a new IB-DE using roulette wheel selection.

5.3.3 MIHPS

The general framework of MIHPS is described by Algorithm 7. MIHPS is similar to SMS-EMOA, but the HV-based DE is replaced by the mechanism described next. MIHPS requires two parameters: a set of weight vectors W for the $R2$ indicator and the time window T_w that determines the number of times a heuristic needs to be executed. The structures C_{hh} and H_{pool} required by Algorithm 6 are initialized in line 1, and the population is randomly initialized using a uniform distribution in line 2. The main loop of MIHPS is shown in lines 3 to 17. First, two randomly-selected solutions of P create a new offspring using SBX and polynomial-based mutation in lines 4 and 5. Then, the union of P and the newly-created solution is assigned to Ψ in furtherance of ranking it using the nondominated sorting algorithm [29] in pursuance of generating a set of layers $\{L_1, \ldots, L_k\}$. L_1 has the nondominated solutions in Ψ, and L_k is composed by the worst individuals regarding the Pareto dominance relation. If the cardinality of L_k is greater than one, an IB-DE is executed. In this case, $\mathcal{Z}$, used by IGD$^+$, ϵ^+ and Δ_p, is set to L_1. Depending on the current IB-DE, the indicator

Algorithm 6: Switch of Heuristics

Input: H_{pool}, C_{hh}, T_w
Output: Update current heuristic being executed

if $C_{hh}.counter < T_w$ **then**
  $C_{hh}.counter \leftarrow C_{hh}.counter + 1$;
end
else
  $i \leftarrow C_{hh}.lastH, j \leftarrow C_{hh}.currentH$;
  $d \leftarrow H_{pool}[j].data$;
  $\{b, \sigma\} \leftarrow ComputeData(d)$;
  if $b \geq 0$ *and* $\sigma \geq \bar{\sigma}$ **then**
    $C_{hh}.p_{ij} \leftarrow C_{hh}.p_{ij} + 2\alpha$;
  end
  else if $b \geq 0$ *and* $\sigma < \bar{\sigma}$ **then**
    $C_{hh}.p_{ij} \leftarrow C_{hh}.p_{ij} + \alpha$;
  end
  else if $b < 0$ **then**
    $C_{hh}.p_{ij} \leftarrow C_{hh}.p_{ij} - \beta$;
    if $C_{hh}.p_{ij} < 0$ **then**
      $C_{hh}.p_{ij} \leftarrow 0$;
    end
  end
  Normalize $C_{hh}.p_{it}, t = 1, \ldots, |H_{pool}|$;
  Clear data of the current heuristic;
  $C_{hh}.lastH \leftarrow C_{hh}.currentH$;
  $C_{hh}.currentH \leftarrow RouletteWheel()$;
  $C_{hh}.counter \leftarrow 0$;
end

Figure 5.2: Markov chain and its corresponding transition matrix. Each element $p_{ij} \in [0, 1]$ of the matrix indicates the probability of going from the i^{th} IB-DE to the j^{th} one. For a row i, $\sum_{j=1}^{4} p_{ij} = 1$. All initial transition probabilities p_{ij} are set to $1/|H_{pool}|$.

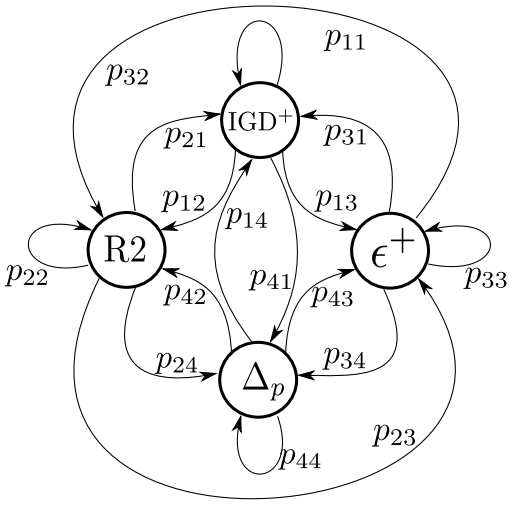

(a) Markov chain

$$\begin{array}{c} \\ \text{IGD}^+ \\ \text{R2} \\ \epsilon^+ \\ \Delta_p \end{array} \begin{array}{c} \begin{array}{cccc} \text{IGD}^+ & \text{R2} & \epsilon^+ & \Delta_p \end{array} \\ \begin{pmatrix} p_{11} & p_{12} & p_{13} & p_{14} \\ p_{21} & p_{22} & p_{23} & p_{24} \\ p_{31} & p_{32} & p_{33} & p_{34} \\ p_{41} & p_{42} & p_{43} & p_{44} \end{pmatrix} \end{array}$$

(b) Transition matrix

contribution of each element in L_k is calculated using the proposed framework in line 10 to identify the worst contributing solution p_{min}. In line 14, the solution p_{min} is deleted from Ψ and the resulting population is set as the population for the next iteration and assessed by the $R2$ indicator. This $R2$-value is added to the list of the current IB-DE executed. Finally, in line 21, Algorithm 6 is invoked to select, if necessary, a new IB-DE. MIHPS returns the main population as the Pareto front approximation.

5.3.4 Experimental Results

In this section, we investigate the performance of MIHPS,[1] considering the nine instances of the Walking-Fish-Group (WFG) [64] test suite for 2, 3, 5, 6 and 10 objective functions. The main properties of the WFG problems are depicted in Table 5.1. We present two experiments: (1) a comparative study that includes the state-of-the-art algorithms MOEA/D[2] [147] (based on decomposition), NSGA-III[3] [30] (based on reference points) and $R2$-EMOA[4] [18] (based on the $R2$ indicator), and (2) an analysis of the IB-DE preference of MIHPS.

[1]The source code is available at `http://computacion.cs.cinvestav.mx/~jfalcon/MIHPS/mihps.html`

[2]Available at `http://dces.essex.ac.uk/staff/zhang/webofmoead.htm`

[3]Available at `http://web.ntnu.edu.tw/~tcchiang/publications/nsga3cpp/nsga3cpp.htm`

[4]We employed the implementation from EMO Project 1.36 available at `http://computacion.cs.cinvestav.mx/~rhernandez/`

Algorithm 7: MIHPS general framework

Input: Set of weight vectors W, T_w
Output: Pareto front Approximation

Initialize C_{hh} and H_{pool};
Randomly initialize population P;
while *stopping criterion is not fulfilled* **do**
  $\{p, q\} \leftarrow Select(P)$;
  offspring $\leftarrow Variation(p, q)$;
  $\Psi \leftarrow P \bigcup \{\text{offspring}\}$;
  $\{L_1, L_2, \ldots, L_k\} \leftarrow$ nondominated-sorting(Ψ);
  if $|L_k| > 1$ **then**
    $\mathcal{Z} \leftarrow L_1$;
    $\{C_i\}_{i=1,\ldots,|\mathcal{A}|} \leftarrow Contribution(L_k, W, \mathcal{Z}, C_{hh}, H_{pool})$;
    Find solution $p_{min} \in L_k$ having the minimum contribution value in $\{C_i\}_{i=1,\ldots,|\mathcal{A}|}$;
  end
  else
    p_{min} is equal to the sole individual in L_k;
  end
  $P \leftarrow \Psi \setminus \{p_{min}\}$;
  $\delta \leftarrow -R2(P, W)$;
  $AddQualityMeasure(C_{hh}, H_{pool}, \delta)$;
  $C_{hh} \leftarrow Switch(C_{hh}, H_{pool}, T_w,)$;
end
return P

Table 5.1: Properties of the WFG test problems

Problem	Separability	Frontality	Geometry
WFG1	separable	unifrontal	convex, mixed
WFG2	non-separable	$f_{1:m-1}$ unimodal f_m multimodal	convex disconected
WFG3	non-separable	unifrontal	linear, degenerated
WFG4	separable	multifrontal	concave
WFG5	separable	deceptive	concave
WFG6	non-separable	unifrontal	concave
WFG7	separable	unifrontal	concave
WFG8	non-separable	unifrontal	concave
WFG9	non-separable	multifrontal, deceptive	concave

Table 5.2: Parameters adopted in our experiments.

Objectives (m)		2	3	5	6	10
Population size		120	120	126	126	220
Objective function evaluations ($\times 10^3$)		50	50	70	80	120
WFG	variables (n)	24	26	30	32	40
WFG	position-related parameters	2	2	4	5	9
Weight-vector partitions (H)		119	14	5	4	3

5.3.4.1 Experimental Settings

The adopted parameter values used by all MOEAs are described in Table 5.2. From this table, the parameter H is related to the Simplex Lattice Design (SLD) [147] that generates the set W of weight vectors required by all the MOEAs. Consequently, $|W| = C_{H-1}^{H+m-1}$. MIHPS and the selected MOEAs employ Simulated Binary Crossover (SBX) and Polynomial-based mutation (PBX) as their variation operators. For two and three objectives, the crossover probability and distribution index were set to 1.0 and 20, respectively; while for high-dimensional objective spaces, these parameters were set to 1.0 and 30. For PBX, its probability and distribution index were set to $1/n$ and 20, respectively. The stopping criterion consisted of reaching a maximum number of function evaluations of the MOP, as depicted in Table 5.2. The parameter T_w of MIHPS is equal to the population size, and the niche size of MOEA/D was set to 20 in all cases.

For performance assessment of the MOEAs, we selected the hypervolume and the Riesz s-energy indicators, defined in Eqs. (3.1) and (3.12), respectively. HV requires a reference point which for WFG1-WFG9 was set to $(2i+1)_{i=1,2,\ldots,m}$, where m is the number of objective functions. The Riesz s-energy indicator needs a parameter $s > 0$ that was set equal to $m - 1$.

We performed 30 independent runs of each of the four compared MOEAs using all the test instances. Tables 5.3, 5.4 and 5.5 show the statistical results for the HV and Riesz s-energy indicators, respectively. In these tables, the two best values among the algorithms are emphasized in grayscale, where the darker tone corresponds to the best value. A sharp symbol (#) is placed when MIHPS performed significantly better than the other approaches based on a one-tailed Wilcoxon rank sum test using a confidence level of 95%.

5.3.4.2 Comparative Results

In this section, we compare MIHPS against MOEA/D, NSGA-III and $R2$-EMOA. The HV results shown in Table 5.3 indicate that for two objective functions, MIHPS is competitive with respect to NSGA-III which obtains the best result in 5 out of

Figure 5.3: Pareto fronts produced by MIHPS. All fronts correspond to the HV's median.

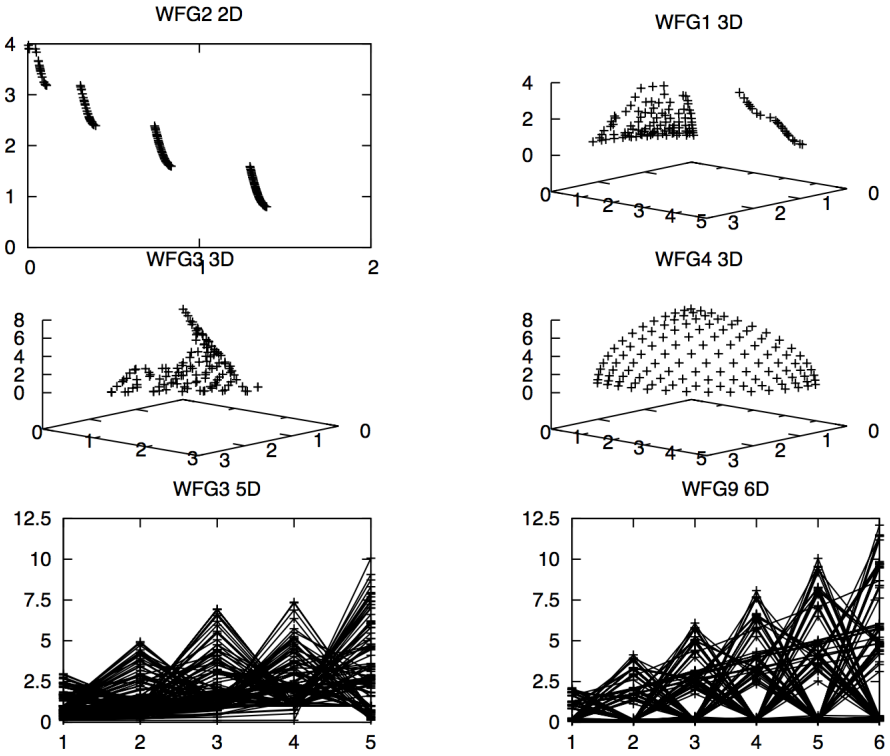

9 problems, while MIHPS gets the best result in 4 test instances and the second best value in the remaining MOPs. In case of three objective functions, MIHPS outperforms the other algorithms, having the best value in 7 instances and the second place in the rest of MOPs. In these two-objective spaces, WFG2, whose Pareto front is disconnected, presents the highest difficulty to MIHPS since it cannot obtain the best HV value. Considering MOPs having 5 and 6 objective functions, MIHPS maintains its good performance because it obtains the best value in 15 out of the 18 instances. In this regard, we observe that in both cases MIHPS obtains the best result in WFG2. Finally, when tackling 10-dimensional MOPs, MIHPS reduces its performance, although it obtains the best value in 55% of the problems. However, in WFG1, MIHPS was outperformed by MOEA/D and NSGA-III. In general, when MIHPS obtains the best value, the difference concerning NSGA-III does not look huge, although the Wilcoxon test states that the difference is indeed statistically significant. For the cases when MIHPS obtains the second place, the differences tend to be significant. Finally, the Riesz s-energy results in Table 5.4 indicate that MIHPS has a competitive performance in low-dimensional MOPs and outperforms all the other MOEAs used in our study when dealing with many-objective problems. Figure 5.3 shows some Pareto front approximations produced by MIHPS that support the Riesz s-energy results.

Table 5.3: Mean and standard deviation (in parentheses) of the hypervolume indicator for the compared MOEAs and MIHPS.

Dim.	MOP	MIHPS	MOEA/D	NSGA-III	R2-EMOA
2	WFG1	5.353823e+00 (4.539967e-01)	5.085414e+00# (2.839145e-01)	6.627788e+00 (3.886166e-01)	4.972801e+00 # (2.120000e-01)
	WFG2	1.087631e+01 (4.043935e-01)	9.812547e+00# (5.469032e-01)	1.091544e+01 (3.990434e-01)	1.076935e+01# (3.672361e-01)
	WFG3	1.090360e+01 (1.338370e-02)	1.076476e+01# (7.102684e-02)	1.090323e+01 (1.312870e-02)	1.085161e+01# (2.379180e-02)
	WFG4	8.650363e+00 (2.063378e-02)	8.497784e+00# (2.407267e-02)	8.650159e+00# (7.209313e-03)	8.592620e+00# (2.586712e-02)
	WFG5	8.157830e+00 (3.768882e-02)	8.105310e+00# (6.867330e-03)	8.185022e+00 (3.730594e-02)	8.133849e+00# (1.887475e-02)
	WFG6	8.350939e+00 (5.352283e-02)	8.164502e+00# (1.036161e-01)	8.373642e+00 (3.334034e-02)	8.328502e+00 (3.833023e-02)
	WFG7	8.664098e+00 (2.142694e-02)	8.558870e+00# (1.836725e-02)	8.670626e+00 (3.901721e-03)	8.625866e+00# (1.282143e-02)
	WFG8	8.067041e+00 (3.917163e-02)	7.927696e+00# (3.876792e-02)	8.062539e+00 (2.129901e-02)	7.979584e+00 # (4.206135e-02)
	WFG9	8.371848e+00 (1.574505e-01)	8.097411e+00# (1.679919e-01)	8.298658e+00# (2.206774e-01)	8.238317e+00# (2.196850e-01)
3	WFG1	5.189445e+01 (1.907972e+00)	4.994533e+01# (2.615320e+00)	4.917540e+01# (1.742752e+00)	4.582011e+01# (1.903103e+00)
	WFG2	9.999710e+01 (2.691156e-01)	9.425491e+01# (1.887090e+00)	1.000303e+02 (2.020421e-01)	9.792476e+01# (4.795771e-01)
	WFG3	7.351098e+01 (8.728010e-01)	6.949014e+01# (2.043137e+00)	7.359113e+01 (3.698540e-01)	7.136640e+01# (7.927364e-01)
	WFG4	7.598303e+01 (1.185769e-01)	7.398207e+01# (3.092256e-01)	7.586556e+01# (1.753519e-01)	7.265719e+01# (3.311758e-01)
	WFG5	7.343176e+01 (3.575197e-01)	7.173103e+01# (4.978797e-01)	7.342821e+01# (1.084695e-01)	7.196333e+01# (4.816689e-01)
	WFG6	7.376195e+01 (3.751150e-01)	7.200035e+01# (6.485353e-01)	7.356399e+01# (3.730537e-01)	7.084095e+01# (6.665309e-01)
	WFG7	7.653560e+01 (7.852050e-02)	7.046696e+01# (2.114407e+00)	7.640131e+01# (8.117286e-02)	7.080832e+01# (1.568479e+00)
	WFG8	8.067041e+00 (3.917163e-02)	7.927696e+00# (3.876792e-02)	8.062539e+00 (2.129901e-02)	7.979584e+00 # (4.206135e-02)
	WFG9	7.386404e+01 (5.158326e-01)	6.675524e+01# (2.213615e+00)	7.319658e+01# (7.798323e-01)	6.578887e+01# (1.219647e+00)
5	WFG1	4.535121e+03 (1.993775e+02)	4.522924e+03 (1.145447e+02)	4.049661e+03# (1.445036e+02)	4.194966e+03# (1.358394e+02)
	WFG2	1.023085e+04 (3.828319e+01)	9.147103e+03# (2.989196e+02)	1.022660e+04 (2.444328e+01)	9.984285e+03# (6.289957e+01)
	WFG3	6.788535e+03 (6.801749e+01)	5.831355e+03# (1.740491e+02)	6.705622e+03# (6.623165e+01)	5.038991e+03# (7.488139e+02)
	WFG4	8.920978e+03 (2.213267e+01)	8.212950e+03# (2.178634e+02)	8.904989e+03# (2.089724e+01)	7.421184e+03# (2.591330e+02)
	WFG5	8.624539e+03 (1.603036e+01)	8.104988e+03# (1.012979e+02)	8.618204e+03# (1.271126e+01)	7.948213e+03# (1.147386e+02)
	WFG6	8.645060e+03 (4.070264e+01)	7.556842e+03# (1.664222e+02)	8.640890e+03 (4.979948e+01)	7.939967e+03# (8.654630e+01)
	WFG7	8.915641e+03 (4.822879e+01)	7.760876e+03# (1.586662e+02)	8.950470e+03 (1.940161e+01)	4.558253e+03# (3.763958e+02)
	WFG8	8.424204e+03 (3.017833e+01)	7.008822e+03# (3.386477e+02)	8.415246e+03 (2.900889e+01)	7.641489e+03# (7.184083e+01)
	WFG9	8.263995e+03 (1.370648e+02)	7.417024e+03# (9.145927e+02)	8.356364e+03 (1.276761e+02)	4.747704e+03# (1.345621e+03)
6	WFG1	5.480387e+04 (1.859254e+03)	5.551582e+04 (1.195407e+03)	4.624351e+04# (7.644434e+02)	4.929380e+04# (1.413982e+03)
	WFG2	1.332612e+05 (6.368992e+02)	1.178550e+05# (3.855927e+03)	1.315301e+05# (8.750023e+02)	1.300786e+05# (1.364547e+03)
	WFG3	8.454601e+04 (1.418348e+03)	6.780238e+04# (3.173871e+03)	7.863759e+04# (1.621669e+03)	4.844251e+04# (1.260649e+03)
	WFG4	1.200307e+05 (4.138230e+02)	9.790915e+04# (4.401103e+03)	1.173793e+05# (4.685098e+02)	9.324355e+04# (5.224468e+03)
	WFG5	1.162325e+05 (1.007331e+02)	1.031395e+05# (1.400494e+03)	1.148425e+05# (2.629454e+02)	1.005002e+05# (2.553915e+03)
	WFG6	1.168731e+05 (6.069773e+02)	8.312614e+04# (1.675956e+03)	1.149958e+05# (6.346863e+02)	1.046326e+05# (1.418536e+03)
	WFG7	1.207436e+05 (6.783023e+02)	8.756181e+04# (1.405257e+03)	1.188896e+05# (7.429985e+02)	5.244257e+04# (3.756718e+03)
	WFG8	1.130648e+05 (5.882422e+02)	6.120502e+04# (1.312103e+04)	1.108116e+05# (5.780063e+02)	9.887326e+04# (1.270952e+03)
	WFG9	1.109319e+05 (1.703241e+03)	8.840778e+04# (1.287881e+04)	1.095528e+05# (1.821095e+03)	3.610090e+04# (2.027429e+03)
10	WFG1	4.263671e+09 (5.387522e+07)	4.626119e+09 (9.082857e+07)	4.333786e+09 (4.767509e+07)	3.619171e+09# (4.265568e+07)
	WFG2	1.346432e+10 (4.695801e+07)	1.153362e+10# (4.307707e+08)	1.343510e+10# (5.838755e+07)	1.290151e+10# (1.470863e+08)
	WFG3	7.253349e+09 (2.738702e+08)	3.407782e+09# (4.406816e+08)	7.851751e+09 (1.420734e+08)	3.849045e+09# (7.035893e+07)
	WFG4	1.263112e+10 (1.101730e+08)	8.323219e+09# (7.081503e+08)	1.263780e+10 (8.783143e+07)	5.596499e+09# (2.750563e+08)
	WFG5	1.240345e+10 (2.216323e+07)	9.239992e+09# (2.118588e+08)	1.237722e+10# (2.716038e+07)	3.990706e+09# (1.057584e+08)
	WFG6	1.253598e+10 (6.372494e+07)	6.359273e+09# (9.586607e+08)	1.250108e+10# (5.551767e+07)	5.453261e+09# (1.016168e+09)

Table 5.3 – *Continuation*

Dim.	MOP	MIHPS	MOEA/D	NSGA-III	R2-EMOA
	WFG7	1.303975e+10 (3.716490e+07)	6.249289e+09# (5.201314e+08)	1.306886e+10 (3.687103e+07)	4.403681e+09# (1.233729e+08)
	WFG8	1.190158e+10 (7.705432e+07)	2.888315e+09# (9.700244e+08)	1.182430e+10# (9.381721e+07)	6.936492e+09# (8.189270e+08)
	WFG9	1.167146e+10 (2.269656e+08)	6.798907e+09# (2.162391e+09)	1.162166e+10# (2.416780e+08)	3.605102e+09# (1.128297e+08)

Table 5.4: Mean and standard deviation (in parentheses) of the Riesz s-energy indicator for the compared MOEAs and MIHPS.

Dim.	MOP	MIHPS	MOEA/D	NSGA-III	R2-EMOA
2	WFG1	1.872714e+07 (5.589395e+07)	2.078402e+09# (6.179776e+09)	4.220447e+08# (1.823807e+09)	3.052235e+07# (3.882580e+07)
	WFG2	1.764804e+07 (4.335797e+07)	1.360580e+11# (4.224067e+11)	7.707419e+08# (3.611565e+09)	3.652743e+07# (1.003287e+08)
	WFG3	3.500463e+05 (2.876591e+04)	4.201784e+05# (6.809222e+03)	6.939978e+06 (3.590074e+07)	4.135505e+05 (2.349694e+05)
	WFG4	7.867810e+05 (1.057606e+06)	3.489431e+05 (7.920373e+03)	5.910070e+05 (5.234480e+05)	9.951450e+05# (8.112717e+05)
	WFG5	3.567459e+05 (1.003470e+05)	4.003092e+05# (3.341154e+03)	3.741169e+05# (2.671847e+04)	1.074483e+06# (2.293603e+06)
	WFG6	8.297581e+05 (9.897593e+05)	6.037467e+07 (2.375227e+08)	8.222445e+05 (1.287128e+06)	1.185283e+07# (5.119626e+07)
	WFG7	6.005176e+05 (4.064338e+04)	3.516485e+05 (2.187221e+03)	4.151943e+05 (2.517076e+05)	2.644334e+08# (1.396116e+09)
	WFG8	9.255261e+05 (1.969640e+06)	3.489084e+05 (6.242702e+03)	6.244380e+07# (9.195854e+07)	1.143237e+06 # (7.077474e+05)
	WFG9	6.781110e+05 (4.898496e+05)	5.372987e+07 (1.257882e+08)	5.781309e+05 (5.713066e+05)	1.237779e+06 (1.588538e+06)
3	WFG1	6.143577e+07 (1.673973e+08)	8.654171e+13# (3.671307e+14)	2.001574e+11# (6.000690e+11)	1.008461e+09 (3.820614e+09)
	WFG2	6.624223e+04 (9.279462e+04)	2.397235e+12# (1.740974e+12)	5.495017e+04 (4.524221e+04)	1.443613e+08# (3.538534e+08)
	WFG3	3.520209e+08 (1.101941e+09)	3.964626e+14# (1.471524e+15)	6.718343e+13# (3.589166e+14)	3.814376e+08 (1.482391e+09)
	WFG4	1.231146e+04 (2.935879e+02)	1.901945e+04# (3.334860e+02)	1.377282e+04# (2.686847e+02)	5.462352e+04# (6.098394e+04)
	WFG5	1.117281e+04 (3.901057e+02)	1.980568e+04# (6.562792e+02)	1.325976e+04# (9.325864e+01)	8.490656e+04# (1.384068e+05)
	WFG6	7.041258e+05 (3.731772e+06)	1.886531e+04 (7.058645e+02)	8.661346e+04 (3.057806e+05)	6.563986e+06# (2.934294e+07)
	WFG7	1.139288e+04 (2.613867e+02)	1.946851e+04# (2.373307e+03)	1.332989e+04# (1.499702e+02)	6.844411e+07# (2.577339e+08)
	WFG8	6.334416e+06 (2.629782e+07)	3.223364e+04 (1.063549e+04)	5.425657e+06 (1.419605e+07)	3.641170e+06 (8.239984e+06)
	WFG9	3.184319e+04 (4.393248e+04)	6.666673e+10# (3.590110e+11)	6.667038e+10# (3.590103e+11)	3.207396e+05# (8.767693e+05)
5	WFG1	9.801655e+08 (4.316843e+09)	8.428701e+21# (3.989661e+22)	1.333338e+19# (7.180219e+19)	6.356396e+11# (3.274853e+12)
	WFG2	3.412454e+04 (1.397693e+05)	9.851610e+21# (3.854359e+22)	3.435707e+11# (1.821926e+12)	3.979127e+08# (9.931633e+08)
	WFG3	1.922689e+15 (1.034797e+16)	1.134485e+23# (6.037710e+23)	5.378389e+19# (1.542099e+20)	1.829545e+13 (8.819243e+13)
	WFG4	2.513006e+02 (1.532131e+01)	1.000468e+44# (5.385078e+44)	3.037938e+06# (8.843297e+06)	3.887261e+02 (6.295909e+02)
	WFG5	1.959483e+02 (9.455351e+00)	4.882370e+35# (9.117700e+35)	2.267384e+12# (1.138301e+13)	4.307820e+02# (1.013691e+03)
	WFG6	1.859204e+02 (1.167860e+01)	1.173885e+36 (4.338642e+36)	1.755902e+10 (8.993706e+10)	1.467884e+03 (5.302806e+03)
	WFG7	2.164027e+02 (3.118630e+01)	2.165757e+46# (7.500306e+46)	5.257040e+09# (2.069378e+10)	8.848340e+05# (2.569514e+06)
	WFG8	1.845485e+02 (1.050481e+01)	9.282909e+30# (4.513332e+31)	2.933885e+09# (1.555046e+10)	8.543378e+12 (4.600747e+13)
	WFG9	2.590924e+02 (7.018357e+01)	1.632844e+34# (7.170632e+34)	1.113532e+05# (3.526911e+05)	6.328721e+05# (1.575043e+06)
6	WFG1	6.047165e+08 (2.970199e+09)	1.146783e+25# (1.045436e+25)	6.666671e+22# (3.590110e+23)	1.078332e+12# (5.048390e+12)
	WFG2	5.221297e+03 (2.543207e+02)	7.565683e+26# (2.720479e+27)	1.905108e+12# (1.025097e+13)	5.201325e+10# (1.625235e+11)
	WFG3	1.653878e+18 (8.797877e+18)	2.000000e+23 (6.000000e+23)	1.333333e+23 (4.988877e+23)	1.204432e+03 (1.089896e+03)
	WFG4	5.609587e+01 (4.538698e+00)	7.653501e+55# (2.292190e+56)	1.354861e+14# (7.296046e+14)	3.297595e+02 (1.563612e+03)
	WFG5	3.818705e+01 (2.517843e+00)	6.406495e+43# (1.354844e+44)	2.530719e+09# (8.470160e+09)	1.927523e+02 (5.843129e+02)
	WFG6	3.465443e+01 (2.886772e+00)	9.787867e+43# (3.027649e+44)	6.666667e+22# (3.590110e+23)	8.009979e+02 (3.432225e+03)
	WFG7	4.038720e+01 (4.437763e+00)	6.635666e+55# (2.699486e+56)	1.087107e+12# (5.838292e+12)	7.460269e+04# (3.384252e+05)
	WFG8	3.997036e+01 (4.850055e+00)	3.528092e+36# (1.620639e+37)	6.666667e+22# (3.590110e+23)	1.833067e+02 (7.276364e+02)
	WFG9	4.452187e+01 (1.485791e+01)	4.653538e+42# (2.441525e+43)	4.219370e+05# (1.138974e+06)	9.827496e+06# (5.228468e+07)

Table 5.4 – *Continuation*

Dim.	MOP	MIHPS	MOEA/D	NSGA-III	R2-EMOA
10	WFG1	6.025963e+07 (4.819117e+07)	1.334400e+59# (7.180024e+59)	2.666667e+39# (1.123487e+40)	3.801374e+13# (1.496857e+14)
	WFG2	1.805484e+04 (4.251975e+03)	1.600000e+60# (8.616264e+60)	6.939858e+30# (3.712175e+31)	3.715520e+20# (2.000830e+21)
	WFG3	1.352050e+04 (7.158030e+04)	3.968305e+49# (1.575951e+50)	4.695580e+39# (1.121605e+40)	1.014720e+01 (1.772339e+00)
	WFG4	3.429733e+00 (2.657303e+00)	7.893333e+111# (4.250690e+112)	4.071902e+00# (1.264681e+00)	2.097761e+01# (2.430840e+01)
	WFG5	1.266066e+00 (1.792841e-01)	2.438414e+72# (5.575768e+72)	3.892117e+00# (2.723236e-01)	2.960655e+02# (3.920714e+02)
	WFG6	1.082768e+00 (1.733274e-01)	6.860262e+71# (3.694218e+72)	3.985430e+00# (3.971706e-01)	1.323056e+06# (6.788670e+06)
	WFG7	1.381504e+00 (2.415390e-01)	2.572763e+102# (9.786282e+102)	3.869951e+00# (4.029032e-01)	3.825779e+01# (6.971002e+01)
	WFG8	3.184230e+00 (2.265388e+00)	2.055197e+62# (6.219703e+62)	3.212638e+01# (1.459811e+02)	9.061778e+03# (4.659196e+04)
	WFG9	2.201585e+00 (2.067237e+00)	4.338407e+70# (1.149034e+71)	8.802783e+00# (8.806394e+00)	2.885282e+01# (3.981606e+01)

5.3.4.3 Selection Bias

The probabilistic selection of an IB-DE performed by MIHPS is biased by its performance, regarding the $R2$ indicator. Consequently, it is straightforward to think that the $R2$-DE will be preferred as it intends to improve the values of $R2$ produced by the population. Our experimental results support this fact, showing that the $R2$-DE is preferred at the end of the search in almost all problem instances. However, the other IB-DEs are used at the beginning of the search. Figure 5.4 shows an example of the previous argument on WFG4 with three objectives. Hence, we considered necessary to determine if the combination of the indicators has an impact on the convergence of MIHPS. For this purpose, we compared MIHPS with a version of it where only $R2$-DE is turned on (denoted as MIHPS-$R2$), using the parameter values shown in Table 5.2. Due to space limitations, Table 5.5 presents the comparison regarding the HV indicator, for low-dimensional instances of the WFG test suite. It can be seen that MIHPS outperforms MIHPS-$R2$ in a statistically significant way because it obtains the best HV value in 15 out of 18 problem instances. For the three problems where MIHPS does not obtain the best result, the difference is not very significant. Hence, these results strongly support that even though $R2$-DE is mostly preferred by MIHPS, the execution of the other IB-DEs contributes to a better convergence, as confirmed by the results shown in Tables 5.3 and 5.4.

5.4 Competition through Ensemble Learning

In this section, we introduce our second approach that exploits the competition of IB-MOEAs. Unlike MIHPS that uses a hyper-heuristic to promote the competition, here we use the AdaBoost algorithm [49] (which is a well-known Ensemble Learning technique) as the backbone of the competition. The main thesis of the AdaBoost algorithm is to construct a stronger mechanism from weaker ones. In our approach, denoted as Ensemble Indicator-Based MOEA (EIB-MOEA), the IB-DEs (which are the weak mechanisms) are combined using the AdaBoost algorithm. The underlying idea is that they have to compete to gain more relative importance in the decision of the ensemble mechanism. In the following, we widely describe the algorithmic

Table 5.5: Mean and standard deviation (in parentheses) of the hypervolume indicator for MIHPS and MIHPS-$R2$.

Dim.	MOP	MIHPS	MIHPS-$R2$
2	WFG1	5.353823e+00 (4.539967e-01)	4.909215e+00# (2.354320e-01)
	WFG2	1.087631e+01 (4.043935e-01)	1.088208e+01 (4.060801e-01)
	WFG3	1.090360e+01 (1.338370e-02)	1.083356e+01# (3.044440e-02)
	WFG4	8.650363e+00 (2.063378e-02)	8.584441e+00# (2.619502e-02)
	WFG5	8.157830e+00 (3.768882e-02)	8.132564e+00# (1.937931e-02)
	WFG6	8.350939e+00 (5.352283e-02)	8.305956e+00# (4.739550e-02)
	WFG7	8.664098e+00 (2.142694e-02)	8.620447e+00# (2.985012e-02)
	WFG8	8.067041e+00 (3.917163e-02)	7.986139e+00# (3.097071e-02)
	WFG9	8.371848e+00 (1.574505e-01)	8.263080e+00# (1.838899e-01)
3	WFG1	5.189445e+01 (1.907972e+00)	5.188408e+01 (1.610899e+00)
	WFG2	1.085075e+01 (3.864759e-01)	1.088208e+01 (4.060801e-01)
	WFG3	7.351098e+01 (8.728010e-01)	7.302124e+01# (3.418580e-01)
	WFG4	7.598303e+01 (1.185769e-01)	7.594650e+01# (1.511291e-01)
	WFG5	7.343176e+01 (3.575197e-01)	7.347454e+01 (9.055205e-02)
	WFG6	7.376195e+01 (3.751150e-01)	7.358466e+01# (3.801285e-01)
	WFG7	7.653560e+01 (7.852050e-02)	7.648279e+01# (7.837593e-02)
	WFG8	7.265162e+01 (2.082143e-01)	7.261357e+01# (1.609685e-01)
	WFG9	7.386404e+01 (5.158326e-01)	7.346278e+01# (9.396951e-01)

Figure 5.4: IB-DE preference on WFG4 with 3 objective functions. Since MIHPS is a steady-state MOEA, the number of generations is equivalent to the number of function evaluations.

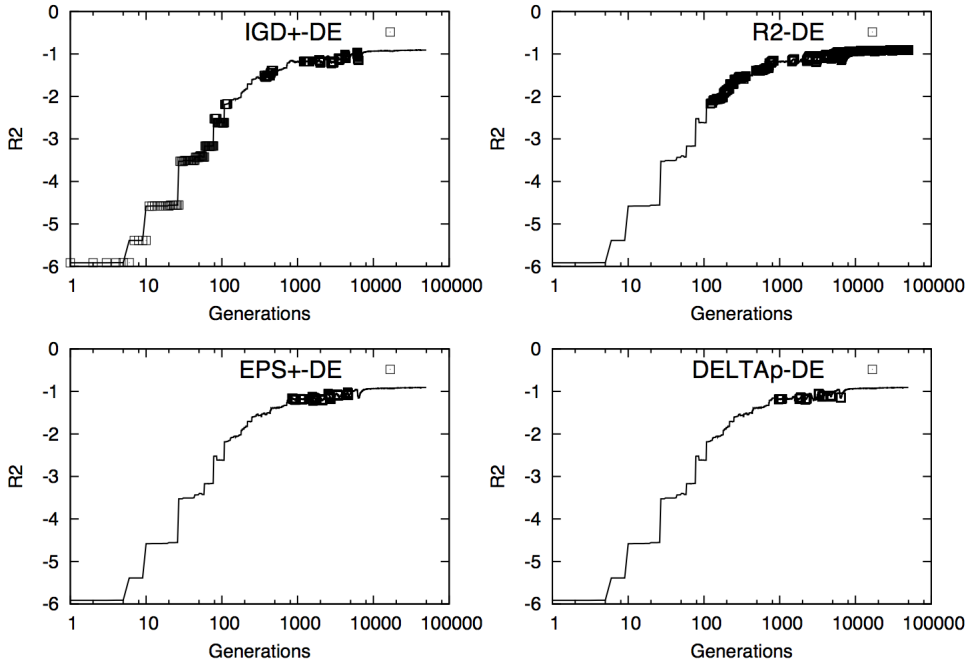

structure of EIB-MOEA, and we also present a discussion of its performance.

5.4.1 General Description

The proposed EIB-MOEA is a steady-state MOEA based on SMS-EMOA [8]. Its general framework is outlined in Algorithm 8. EIB-MOEA requires a set of k indicators $\{I_1, \dots I_k\}$ and a time window frame T_w as input parameters. In Line 2, all the components of the weight vector $\vec{w}$ are set to $1/k$. This weight vector is employed in the ensemble indicator-based density estimator (EIB-DE), and contains the relative importance given to each indicator at the current iteration. Lines 6 to 30 describe the main loop of EIB-MOEA. At each iteration, a single offspring solution $\vec{q}$ is created using variation operators. This newly created solution is added to the population $\mathcal{A}$ to create the temporary population Q. The non-dominated sorting algorithm [31] processes Q to create a set of layers $\{R_1, \dots, R_\ell\}$. If R_ℓ contains more than one solution, the ensemble indicator-based density estimator is executed. First, the population is normalized in Line 13. Then, for each indicator $I_j, j \in \{1, \dots, k\}$, the individual indicator contributions of all solutions in R_ℓ are computed and stored in the vector C_{I_j}. By sorting this vector in ascending order, for each $\vec{r} \in R_\ell$ we obtain $\text{rank}_{I_j}(\vec{F}(\vec{r})) \in \{1, 2, \dots, |R_l|\}$ that returns the ranking of the solution in the sorted C_{I_j}, where rank 1 corresponds to the worst-contributing solution to I_j. In Line

Algorithm 8: EIB-MOEA's general framework

Input: Set of indicators $\{I_1, \ldots, I_k\}$; time window size T_w
Output: Pareto front approximation

Randomly initialize population $\mathcal{A}$;
$w_i = 1/k, i \in \{1, \ldots, k\}$;
Initialize performance matrix $P \in \mathbb{R}^{k \times T_w}$;
Initialize learning matrix $\Psi \in \{0, 1\}^{k \times T_w}$;
$g = 0$;
while *stopping criterion is not fulfilled* **do**
    Create an offspring solution $\vec{q}$ based on $\mathcal{A}$;
    $Q = \mathcal{A} \cup \{q\}$;
    $\{R_1, \ldots, R_\ell\} = NondominatedSorting(Q)$;
    if $|R_\ell| > 1$ **then**
        $z_i^{\min} = \min_{\vec{a} \in \mathcal{A}} f_i(\vec{a}), i \in \{1, \ldots, m\}$;
        $z_i^{\max} = \max_{\vec{a} \in \mathcal{A}} f_i(\vec{a}), i \in \{1, \ldots, m\}$;
        Normalize $\{R_1, \ldots, R_\ell\}$ using $\vec{z}^{\min}$ and $\vec{z}^{\max}$;
        for $j = 1$ *to* k **do**
            $C_{I_j}(\vec{r}, R_\ell) = |I_j(R_\ell) - I_j(R_\ell \setminus \{\vec{F}(\vec{r})\})|, \forall \vec{r} \in R_\ell$;
            Sort C_{I_j} in ascending order;
            $\forall \vec{z} \in R_\ell$, compute $\text{rank}_{I_j}(\vec{F}(\vec{r}))$, using the sorted C_{I_j};
        end
        $\vec{a}_{\text{worst}} = \arg\min_{\vec{r} \in R_\ell} \left\{ H\left(\vec{z} = \vec{F}(\vec{r})\right) = \sum_{j=1}^{k} w_j \text{rank}_{I_j}(\vec{z}) \right\}$;
        Learning$(Q, R_\ell, \{I_1, \ldots, I_k\}, g, \vec{a}_{\text{worst}}, P, \Psi)$;
        $g = g + 1$;
    end
    else
        Let $\vec{a}_{\text{worst}}$ be the sole solution in R_ℓ;
    end
    $\mathcal{A} = Q \setminus \{\vec{a}_{\text{worst}}\}$;
    if $g = T_w$ **then**
        UpdateWeights$(\vec{w}, P, \Psi, T_w, k)$;
        $g = 0$;
    end
end
return $\mathcal{A}$;

19, the worst-contributing solution, using EIB-DE, is obtained. The learning process (see Algorithm 9), which is a fundamental part to update the weight vector $\vec{w}$, is performed in Line 20, and then, the counter g is incremented by one. In Line 25, $\vec{a}_{\text{worst}}$ is eliminated from Q to shape the population for the next generation. In case g is equal to T_w, $\vec{w}$ is updated following Algorithm 10 and g is set to zero. Finally, once the stopping condition is satisfied, $\mathcal{A}$ is returned as the Pareto front approximation.

5.4.2 Learning Process

Algorithm 9: Learning

Input: Population $\mathcal{A}$; worst set R; set of indicators $\{I_1, \ldots, I_k\}$; index t; selected solution $\vec{a}_{\text{worst}}$; performance matrix P; learning matrix Ψ
Output: Updated Ψ

```
1  for j = 1 to k do
2  |  a⃗^j_worst = arg min_{r⃗∈R} |I_j(R) − I_j(R \ {F⃗(r⃗)})|;
3  |  A^j = A \ {a⃗^j_worst};
4  |  P_jt = I_j(A^j);
5  |  if P_jt > P_{j,t−1 mod T_w} ∧ a⃗^j_worst = a⃗_worst then
6  |  |  Ψ_jt = 0;
7  |  end
8  |  else
9  |  |  Ψ_jt = 1;
10 |  end
11 end
12 return Ψ
```

The learning process, described in Algorithm 9, is based on analyzing the behavior of the population using all indicators. For each indicator $I_j, j \in \{1, \ldots, k\}$, we obtain its worst-contributing solution $\vec{a}^j_{\text{worst}}$, where R represents the last layer of solutions with respect to non-dominated sorting. In Line 3, we simulate the elimination of $\vec{a}^j_{\text{worst}}$ from the population $\mathcal{A}$ to generate the set $\mathcal{A}^j$ that is assessed by I_j. This indicator value is stored in the performance matrix at position (j, t), i.e., $P_{jt} = I_j(\mathcal{A}^j)$. It is worth noting that each row of P, represented as P_j, works as a circular array of size T_w. If P_{jt} is greater than the previous sample in P_j (which implies an increase in quality) and $\vec{a}^j_{\text{worst}}$ is the same as the worst-contributing solution to EIB-DE, the selection is marked as successful and a zero value is stored in the learning matrix Ψ in the same position (j, t). Otherwise, we set $\Psi_{jt} = 1$.

5.4.3 Updating the Relative Importance of QIs

After executing EIB-DE and the learning algorithm a total of T_w times, the weight vector has to be updated. Algorithm 10 sketches the update process which is based on

Algorithm 10: UpdateWeights

Input: Weight vector $\vec{w}$; performance matrix P; learning matrix Ψ; time window size T_w; number of indicators k

Output: Updated $\vec{w}$

1 **for** $j = 1$ *to* k **do**
2 $\quad e_j = \frac{w_j}{T_w} \sum_{i=1}^{T_w} \Psi_{ji}$;
3 $\quad$ Validate that $e_j \in (0, 1)$;
4 $\quad \alpha_j = \frac{1}{2} \ln\left(\frac{1-e_j}{e_j}\right)$;
5 $\quad$ Build linear performance model based on P_j;
6 $\quad$ Get the angle θ_j of the linear model;
7 $\quad w_j = \begin{cases} w_j e^{-\alpha_j}, & \theta > 0 \\ w_j e^{\alpha_j}, & \text{otherwise} \end{cases}$;
8 $\quad$ Validate that $w_j > 0$;
9 **end**
10 $w_j = \frac{w_j}{\sum_{i=1}^{k} w_i}, j \in \{1, \ldots, k\}$;
11 **return** $\vec{w}$;

the AdaBoost algorithm [49], whose aim is to minimize the exponential loss. For each indicator $I_j, j \in \{1, \ldots, k\}$, the selection error e_j is calculated using the j^{th} row of the learning matrix Ψ, taking into account that e_j should be in the open interval $(0, 1)$ to avoid numerical problems in the calculation of the factor α_j. Using the indicator values in P_j, a linear model is constructed to obtain its angle θ. In Line 7, we set the weight $w_j = w_j\, e^{-\alpha_j}$ if the θ is strictly positive, which implies an increasing quality of the population due to the use of the density estimator based on I_j. Otherwise, we set $w_j = w_j\, e^{\alpha_j}$. To avoid having the EIB-DE composed of a single indicator, we do not allow the existence of zero weights. At last, all weights are normalized in Line 10 and the updated weight vector is returned.

5.4.4 Experimental Analysis

In this section, we analyze the performance of the proposed approach[5]. First, we compare EIB-MOEA with its average ranking version, i.e, an EIB-MOEA where the weights for the ensemble are the same for all indicators (denoted as avgEIB-MOEA) to show that the adaptive mechanism produces better quality results. Then, we perform an exhaustive analysis where we compare EIB-MOEA with SMS-EMOA, R2-EMOA, IGD$^+$-MaOEA, ϵ^+-MaOEA, and Δ_p-MaOEA, which are all steady-state MOEAs using density estimators based on the HV, R2, IGD$^+$, ϵ^+, and Δ_p indicators, respectively. In all test instances, each MOEA is independently executed 30 times.

[5]The source code of EIB-MOEA is available at `http://computacion.cs.cinvestav.mx/~jfalcon/Ensemble/EIB-MOEA.html`.

5.4.4.1 Parameters Settings

In order to determine the performance of EIB-MOEA and of the IB-MOEAs, we employ the benchmark functions DTLZ1, DTLZ2, DTLZ5, DTLZ7, WFG1, WFG2, WFG3, and WFG4, together with and their corresponding minus versions proposed in [75] for two and three objective functions. We adopted these problems because they all have different search difficulties and Pareto front shapes. The number n of decision variables was set as follows. For DTLZ instances and their minus versions, $n = m + K - 1$, where m is the number of objective functions and $K = 5$ for DTLZ1, $K = 10$ for both DTLZ2 and DTLZ5, and $K = 20$ for DTLZ7. Regarding the WFG and WFG^{-1} test problems, n was set to 24 and 26, for two- and three-objective instances and in both cases the number of position-related parameters was set to 2. For a fair comparison, all the MOEAs employ the same population size $\mu = 120$, and the same variation operators: simulated binary crossover (SBX) and polynomial-based mutation (PBM) [31] for all test instances. The crossover probability is set to 0.9, the mutation probability is $1/n$ (where n is the number of decision variables), and both the crossover and mutation distribution indexes are set to 20. We considered 50,000 function evaluations as the stopping criterion for all MOPs. We employ the achievement scalarizing function for the R2-based density estimator. In every generation, we employ the set of non-dominated solutions as the reference set required by IGD$^+$, ϵ^+, and Δ_p. Regarding EIB-MOEA and avgEIB-MOEA, we set $T_w = \mu$.

5.4.4.2 Experimental Results

For the performance assessment of EIB-MOEA, avgEIB-MOEA and the other IB-MOEAs, we use eight quality indicators: HV, HV relative deviation (HVRD), R2, IGD$^+$, ϵ^+, Δ_p, and, for diversity, we employ Riesz s-energy [56] and the Solow-Polasky Diversity indicator [39]. The indicator values for two- and three-objective instances of the DTLZ and DTLZ^{-1} test problems are shown in Figures 5.5 and 5.6, respectively. The boxplots for the WFG and WFG^{-1} instances with two and three objective functions correspond to Figures 5.7 and 5.8, respectively. Table 5.6 shows the statistical ranks obtained by each algorithm over all benchmark functions with respect to each considered indicator. The rank corresponds to the number of algorithms that significantly outperform the algorithm under consideration with respect to a Mann-Whitney non-parametric statistical test with a p-value of 0.05 and a Bonferroni correction (a lower value is better). Figure 5.9 shows the summary of the statistical ranks. The complete numerical results related to Figure 5.9 are shown in Tables B.7 to B.13 in Appendix B.

Regarding the comparison of EIB-MOEA with avgEIB-MOEA, Figure 5.9 shows that the former gets better statistical ranks for HV, R2, IGD$^+$, ϵ^+, Riesz s-energy, and SPD. From these indicators, the increase in quality is more evident for the hypervolume indicator. This means that the ensemble of multiple indicator-based density estimators allows EIB-MOEA to produce approximation sets closer to the Pareto front. As a consequence, EIB-MOEA is able to obtain good results regarding the

Table 5.6: Statistical ranks obtained by every algorithm on benchmark functions with respect to each considered indicator. Values in **bold face** correspond to the best-performing algorithm for the problem and indicator under consideration.

	DTLZ1 2D	DTLZ1 3D	DTLZ1^{-1} 2D	DTLZ1^{-1} (3D)	DTLZ2 2D	DTLZ2 3D	DTLZ2^{-1} 2D	DTLZ2^{-1} (3D)	DTLZ5 2D	DTLZ5 3D	DTLZ5^{-1} 2D	DTLZ5^{-1} (3D)	DTLZ7 2D	DTLZ7 3D	DTLZ7^{-1} 2D	DTLZ7^{-1} (3D)	WFG1 2D	WFG1 3D	WFG1^{-1} 2D	WFG1^{-1} (3D)	WFG2 2D	WFG2 3D	WFG2^{-1} 2D	WFG2^{-1} (3D)	WFG3 2D	WFG3 3D	WFG3^{-1} 2D	WFG3^{-1} (3D)	WFG4 2D	WFG4 3D	WFG4^{-1} 2D	WFG4^{-1} (3D)	avg
	HV																																
EIB-MOEA	1	2	2	2	1	1	1	**0**	1	1	1	**0**	**0**	**0**	1	1	**0**	**0**	**0**	**0**	**0**	**0**	1	1	**0**	2	**0**	1	**0**	1	1	1	**0.7**
avgEIB-MOEA	1	2	2	2	2	2	1	**0**	2	2	1	**0**	1	1	1	1	1	2	1	1	**0**	**0**	1	2	1	1	2	2	1	2	1	2	**1.3**
SMS-EMOA	**0**	**0**	1	5	**0**	**0**	**0**	4	**0**	**0**	**0**	2	5	1	**0**	**0**	1	**0**	2	1	**0**	2	**0**	**0**	**0**	**0**	**0**	**0**	1	**0**	**0**	**0**	**0.8**
R2-EMOA	**0**	1	**0**	6	3	3	4	6	3	5	4	6	1	3	3	3	1	5	3	1	**0**	3	2	5	3	2	2	3	4	5	3	3	**3.0**
IGD$^+$-MaOEA	4	5	4	**0**	4	4	5	2	4	3	4	3	3	4	5	4	1	3	5	2	**0**	3	5	3	4	2	4	4	3	3	5	3	**3.4**
ϵ^+-MaOEA	4	5	4	1	4	5	4	2	4	3	4	3	3	5	5	4	1	3	5	1	**0**	3	4	3	4	2	4	4	3	3	5	3	**3.4**
Δ_p-MaOEA	4	4	6	4	6	6	3	5	6	6	3	5	6	6	3	4	1	5	1	2	**0**	6	4	6	6	6	6	6	6	6	3	6	**4.6**
	R2																																
EIB-MOEA	2	1	1	**0**	1	3	2	1	1	1	1	1	**0**	**0**	1	5	**0**	**0**	**0**	**0**	**0**	1	1	**0**	**0**	**0**	**0**	1	1	3	1	1	**0.9**
avgEIB-MOEA	1	2	1	1	1	1	1	1	1	1	1	2	**0**	4	1	1	1	2	1	1	**0**	1	1	1	**0**	**0**	1	3	1	2	1	3	**1.2**
SMS-EMOA	1	1	2	5	4	4	1	**0**	4	1	1	**0**	5	1	3	4	1	**0**	2	1	**0**	6	**0**	1	**0**	**0**	1	**0**	3	4	**0**	**0**	**1.8**
R2-EMOA	**0**	**0**	**0**	6	**0**	**0**	4	4	**0**	6	4	3	**0**	3	1	1	1	5	2	1	**0**	**0**	**0**	1	5	4	1	2	**0**	**0**	3	2	**1.8**
IGD$^+$-MaOEA	3	4	5	1	5	5	5	5	5	4	5	5	4	4	1	4	1	3	5	2	**0**	3	4	4	**0**	5	4	4	5	5	5	5	**3.8**
ϵ^+-MaOEA	3	4	5	2	5	5	5	5	5	3	5	5	4	2	1	1	1	3	5	1	1	3	4	5	**0**	5	4	4	5	5	5	5	**3.6**
Δ_p-MaOEA	6	5	4	1	2	1	**0**	1	2	**0**	**0**	4	**0**	2	**0**	**0**	1	3	1	2	**0**	1	4	4	6	**0**	4	6	2	**0**	1	1	**2.0**
	IGD$^+$																																
EIB-MOEA	1	2	2	**0**	1	1	1	**0**	1	1	1	**0**	**0**	**0**	1	1	**0**	1	**0**	**0**	**0**	**0**	1	**0**	**0**	4	1	**0**	**0**	1	1	**0**	**0.7**
avgEIB-MOEA	**0**	2	2	**0**	1	2	1	**0**	1	1	1	**0**	**0**	1	1	1	1	1	1	1	**0**	**0**	1	2	**0**	3	1	2	2	1	1	1	**1.0**
SMS-EMOA	**0**	**0**	**0**	1	**0**	**0**	**0**	**0**	**0**	**0**	**0**	2	6	1	**0**	**0**	1	**0**	2	1	**0**	2	**0**	**0**	**0**	**0**	**0**	**0**	**0**	**0**	**0**	**0**	**0.5**
R2-EMOA	1	1	**0**	5	3	2	4	6	1	6	4	6	2	5	6	3	1	5	3	1	**0**	5	3	5	5	4	1	5	3	3	4	5	**3.4**
IGD$^+$-MaOEA	1	2	4	3	4	4	4	3	4	3	4	3	2	5	3	3	1	1	5	2	**0**	3	3	3	**0**	1	4	2	4	3	4	3	**2.8**
ϵ^+-MaOEA	1	2	4	3	4	4	4	3	4	3	4	3	2	3	3	3	1	2	5	1	**0**	3	3	3	**0**	1	4	3	4	3	3	3	**2.8**
Δ_p-MaOEA	6	6	6	6	6	6	3	3	6	5	3	5	3	4	3	6	1	6	1	1	**0**	6	6	6	6	6	6	6	6	6	3	6	**4.7**
	ϵ^+																																
EIB-MOEA	3	2	2	**0**	1	2	1	**0**	1	1	1	**0**	**0**	**0**	1	**0**	**0**	1	**0**	**0**	**0**	**0**	1	**0**	1	2	2	**0**	1	1	1	**0**	**0.8**
avgEIB-MOEA	2	2	2	**0**	1	2	1	**0**	1	1	1	**0**	**0**	1	1	**0**	1	1	1	1	**0**	**0**	1	**0**	1	2	2	**0**	2	1	1	**0**	**0.9**
SMS-EMOA	1	**0**	1	2	**0**	**0**	**0**	**0**	**0**	**0**	**0**	**0**	6	**0**	**0**	1	1	**0**	2	1	**0**	3	**0**	**0**	**0**	**0**	**0**	**0**	**0**	**0**	**0**	**0**	**0.6**
R2-EMOA	**0**	1	**0**	5	3	1	3	6	1	6	3	6	2	3	6	3	1	3	2	1	**0**	5	4	5	1	5	**0**	3	1	5	4	3	**2.9**
IGD+-MaOEA	4	2	4	2	4	4	3	3	4	4	4	3	2	5	3	3	1	3	5	4	**0**	3	4	3	4	1	4	3	4	3	3	3	**3.2**
EPS+-MaOEA	4	4	4	2	4	4	4	3	4	3	4	3	2	5	3	3	1	2	5	4	**0**	**0**	4	3	4	1	4	3	4	3	3	3	**3.1**
DELTAp-MaOEA	4	4	4	5	6	6	4	3	5	4	3	3	2	2	3	3	1	3	1	4	**0**	6	3	5	4	6	4	6	6	5	3	3	**3.8**
	Δ_p																																
EIB-MOEA	3	3	**0**	**0**	1	1	2	1	1	**0**	2	2	**0**	1	1	**0**	**0**	**0**	**0**	**0**	**0**	1	1	1	**0**	4	**0**	**0**	2	2	2	2	**1.0**
avgEIB-MOEA	**0**	2	**0**	**0**	1	1	2	1	1	**0**	2	**0**	**0**	1	1	**0**	1	2	1	1	1	1	1	1	**0**	4	**0**	**0**	1	1	2	2	**1.0**
SMS-EMOA	**0**	**0**	**0**	4	4	4	1	**0**	4	2	**0**	**0**	6	6	**0**	4	1	**0**	2	1	**0**	3	**0**	6	**0**	2	2	3	2	4	1	**0**	**1.9**
R2-EMOA	**0**	1	**0**	6	**0**	**0**	4	4	**0**	4	4	4	3	4	4	2	1	6	2	1	**0**	4	1	3	3	**0**	**0**	6	**0**	**0**	4	4	**2.3**
IGD$^+$-MaOEA	3	2	4	2	5	5	5	5	5	4	5	5	4	1	4	3	1	3	5	2	**0**	4	4	4	3	1	4	2	5	6	5	5	**3.6**
ϵ^+-MaOEA	3	2	4	2	5	4	5	5	5	4	5	5	4	1	4	2	1	3	5	1	3	4	4	4	3	**0**	4	2	5	4	5	5	**3.5**
Δ_p-MaOEA	2	4	6	5	1	2	**0**	1	1	**0**	**0**	2	**0**	**0**	1	6	1	3	1	1	**0**	**0**	6	**0**	6	4	6	5	2	2	**0**	1	**2.2**
	Riesz s-energy																																
EIB-MOEA	3	1	2	2	2	3	2	1	3	2	2	1	1	2	6	1	**0**	2	**0**	1	2	3	1	4	3	1	1	2	1	1	3	2	**1.9**
avgEIB-MOEA	2	2	2	3	2	4	2	2	3	2	2	1	2	4	2	1	1	3	1	3	2	1	3	2	2	1	1	2	1	1	1	2	**2.0**
SMS-EMOA	1	**0**	1	3	1	1	**0**	**0**	1	**0**	**0**	1	1	1	**0**	**0**	1	1	1	2	**0**	3	**0**	2	**0**	4	**0**	3	**0**	2	**0**	**0**	**0.9**
R2-EMOA	**0**	2	**0**	6	**0**	1	6	6	**0**	6	4	6	6	6	5	6	6	6	2	5	6	6	5	6	1	6	6	6	6	6	4	6	**4.5**
IGD$^+$-MaOEA	4	1	4	**0**	4	2	4	2	5	2	4	2	4	1	3	1	4	2	4	1	4	2	1	1	4	1	3	**0**	4	1	5	2	**2.6**
ϵ^+-MaOEA	4	2	4	1	4	3	4	2	5	2	4	2	4	2	3	1	4	2	4	2	4	2	1	2	4	1	3	1	4	1	5	2	**2.8**
Δ_p-MaOEA	6	2	6	1	5	**0**	1	**0**	2	1	1	**0**	**0**	**0**	1	5	1	**0**	1	**0**	**0**	**0**	6	**0**	6	**0**	5	2	1	**0**	1	**0**	**1.7**
	SPD																																
EIB-MOEA	3	**0**	**0**	**0**	1	1	2	**0**	1	**0**	2	**0**	**0**	1	1	2	**0**	**0**	**0**	**0**	**0**	1	2	1	2	1	2	**0**	1	2	2	1	**0.9**
avgEIB-MOEA	**0**	**0**	**0**	**0**	1	1	2	2	1	**0**	2	**0**	**0**	1	1	**0**	1	2	1	1	**0**	1	2	1	2	1	2	**0**	1	1	2	2	**1.0**
SMS-EMOA	3	1	**0**	**0**	3	3	**0**	**0**	3	1	**0**	3	3	3	1	3	1	**0**	2	2	**0**	4	**0**	3	**0**	3	**0**	5	3	2	**0**	**0**	**1.6**
R2-EMOA	3	**0**	**0**	6	**0**	**0**	4	6	**0**	4	4	6	3	2	1	3	1	6	3	6	1	3	1	6	**0**	6	**0**	6	**0**	5	4	6	**3.0**
IGD$^+$-MaOEA	1	5	**0**	**0**	5	5	5	4	5	4	5	4	3	4	4	5	2	4	5	2	2	4	4	3	4	3	4	2	5	4	5	4	**3.6**
ϵ^+-MaOEA	1	5	**0**	**0**	5	5	5	4	5	4	5	4	3	5	4	5	4	4	5	2	4	4	4	3	4	4	4	3	5	4	5	4	**3.8**
Δ_p-MaOEA	1	**0**	**0**	**0**	2	4	1	**0**	2	**0**	1	**0**	**0**	**0**	**0**	1	1	2	1	2	**0**	**0**	4	**0**	4	**0**	4	4	1	**0**	1	**0**	**1.1**

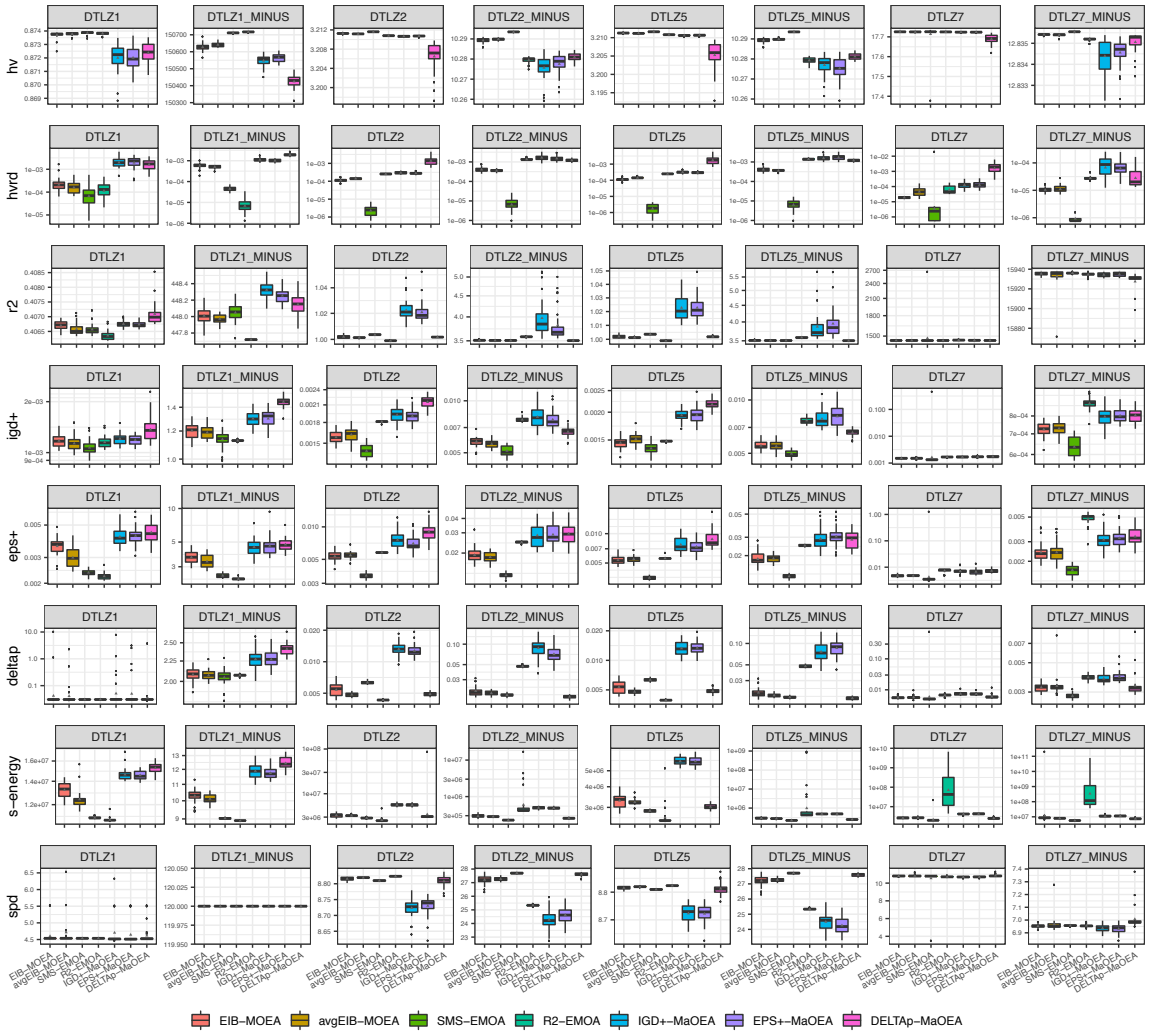

Figure 5.5: Indicator values for two-objective DTLZ benchmark functions.

other convergence indicators, namely R2, IGD^+, ϵ^+, and, to a lower extent, for Δ_p. However, producing better convergent approximation sets is not strictly related to producing higher diversity, as shown by the Riesz s-energy and SPD values, where EIB-MOEA is hardly better than avgEIB-MOEA. Overall, these results support that the adaptive mechanism allows EIB-MOEA to perform better in comparison with the average ranking version. On the other hand, for the comparison of EIB-MOEA against state-of-the-art steady-state IB-MOEAs, Figure 5.9 shows that our proposed approach maintains a robust performance over all the considered QIs. Figures 5.5 to 5.8 illustrate that EIB-MOEA and SMS-EMOA obtained the best HV values. Overall, SMS-EMOA performs better on the original benchmark problems, but the quality of its approximate Pareto fronts is just slightly better than those produced by EIB-MOEA. In contrast, for the DTLZ^{-1} and WFG^{-1} test suites, EIB-MOEA significantly outperforms SMS-EMOA. This evidence is supported by Figure 5.9, where

Figure 5.6: Indicator values for three-objective DTLZ benchmark functions.

we can see that there is a tie between EIB-MOEA and SMS-EMOA in terms of the HV statistical rank. However, we claim that EIB-MOEA has a robust performance since it is significantly better regarding the DTLZ^{-1} and WFG^{-1} test suites, whereas SMS-EMOA is just slightly better on the original benchmark problems. Additionally, for IGD^{+} and ϵ^{+} which are QIs whose preferences are highly correlated to those of HV, Figure 5.9 shows a similar behavior as in the case of HV. This is also supported by the detailed boxplots reported for the different test problems. Regarding the R2 indicator, R2-EMOA presents the best results for MOPs whose Pareto front maps to the simplex shape; e.g., DTLZ1, DTLZ2, and WFG4. This behavior is expected since R2-EMOA uses a set of convex weight vectors [75]. However, for the DTLZ^{-1} and WFG^{-1} test suites, R2-EMOA does not perform well and EIB-MOEA presents the best overall results. This indicates that the ensemble mechanism of EIB-MOEA allows to circumvent the weaknesses of the individual indicator-based density estimators, in

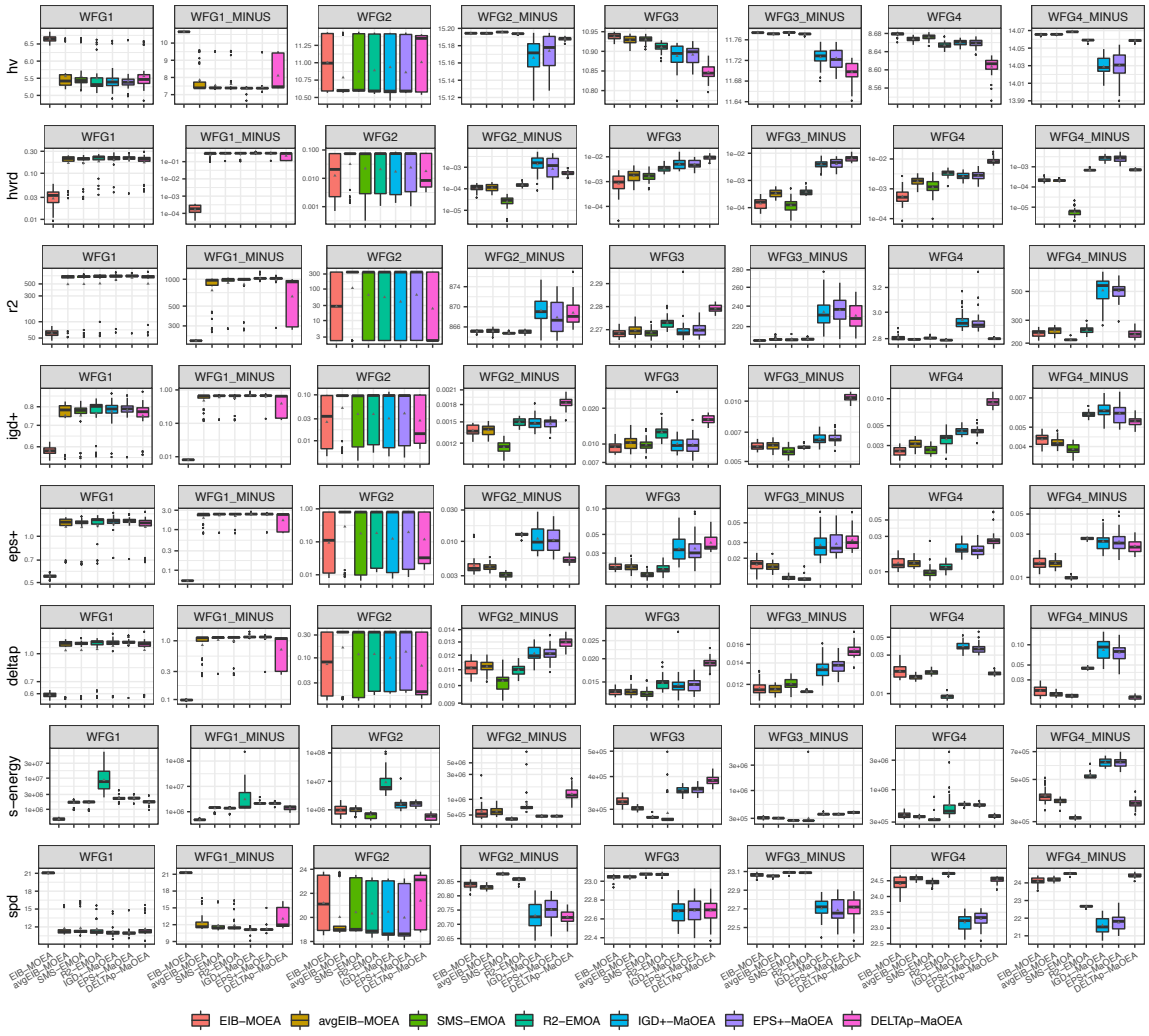

Figure 5.7: Indicator values for two-objective WFG benchmark functions.

this case the one based on R2. Finally, in terms of diversity, Figures 5.5–5.8 show that EIB-MOEA generates well-diversified approximation sets when dealing with MOPs whose Pareto front is irregular; i.e., different from the simplex shape. This is the case, for example, of WFG1, WFG1^{-1}, DTLZ1^{-1}, and DTLZ^{-1}. Nevertheless, EIB-MOEA is able to produce competitive results with respect to Riesz s-energy and SPD, while SMS-EMOA is the best-ranked algorithm for the former indicator and Δ_p-MaOEA is the best for the latter. As such, although EIB-MOEA is able to obtain very good HV values, there is still room for improvement in terms of diversity, e.g. by adding diversity-related indicators into the ensemble controlled by EIB-MOEA.

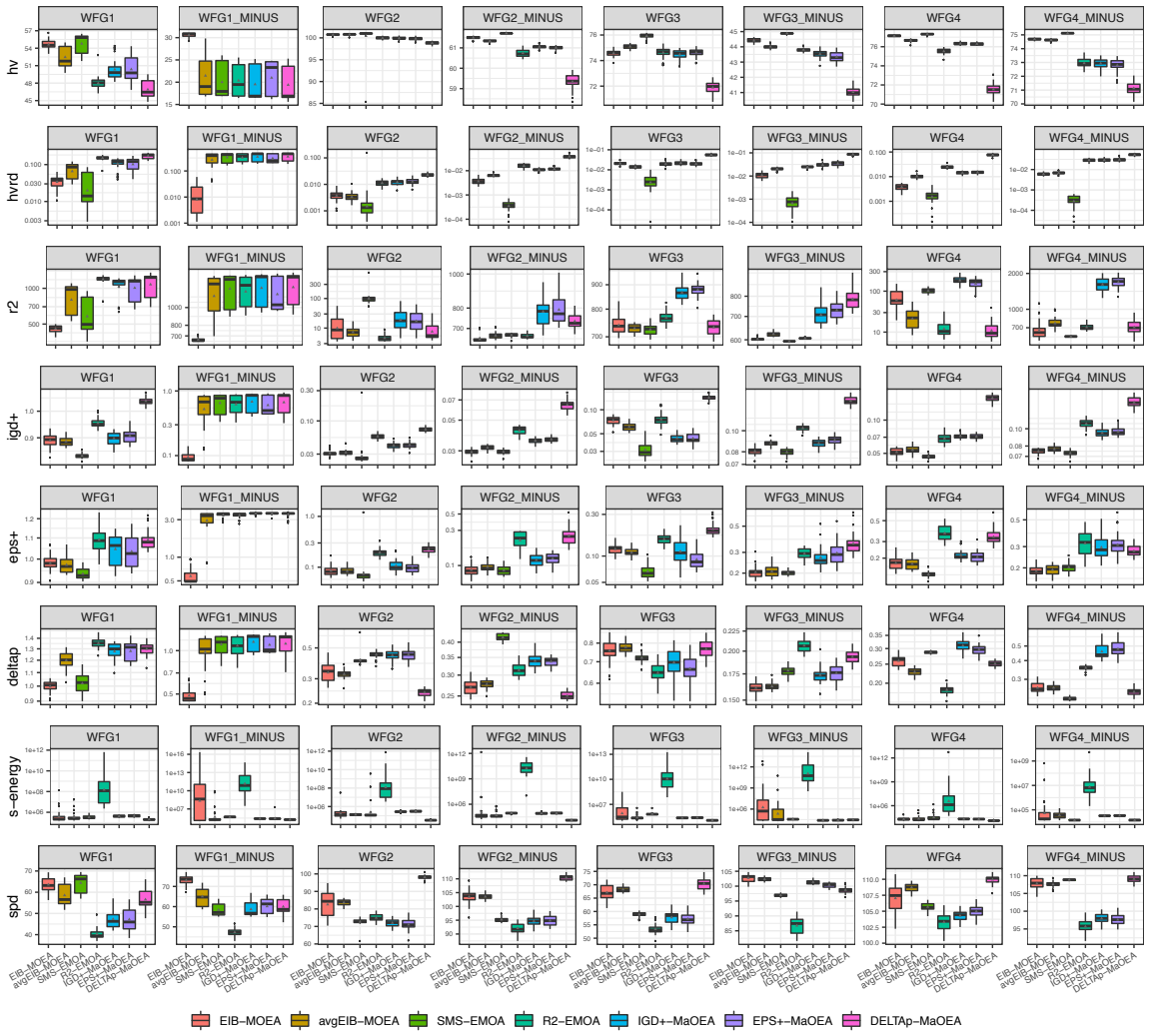

Figure 5.8: Indicator values for three-objective WFG benchmark functions.

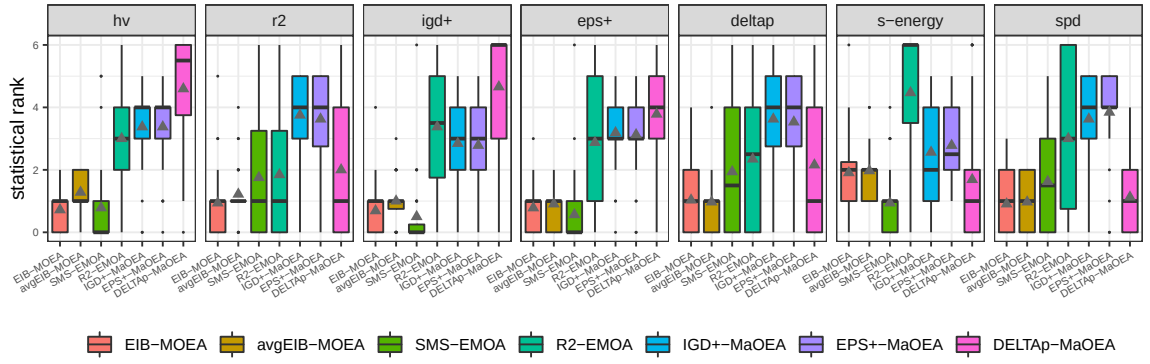

Figure 5.9: Statistical ranks obtained by each algorithm over all benchmark functions with respect to each considered indicator.

5.5 Summary

Traditionally, IB-MOEAs have employed a single indicator as the backbone of selection mechanisms. However, the use of multiple QIs to guide the evolutionary process had not been widely explored. This Chapter aimed to investigate the competition of multiple indicator-based density estimators to improve the performance of steady-state MOEAs. To this aim, we proposed two IB-MOEAs, denoted as MIHPS and EIB-MOEA. On the one hand, MIHPS promotes the competiton between four IB-DEs based on the indicators R2, IGD^+, ϵ^+, and Δ_p. The IB-DEs compete to be executed as much as possible during the evolutionary process, depending on how they help MIHPS' global convergence quality. In other words, the heuristic selection mechanism selects an IB-DE to be executed at T_w generation where the decision is biased by the past performance of the IB-DE. A Markov chain is the core of the heuristic selection mechanism. The experimental results, using the WFG test suite for 3 to 10 objective functions, showed that the indicators IGD^+ and ϵ^+ are better at the early stages of the evolutionary process to speed up convergence, while the R2 indicator is better at the end of the search process to refine convergence and diversity of solutions. The Δ_p indicator did not have a significant impact. Additionally, regarding the comparison of results, MIHPS outperformed NSGA-III, MOEA/D and R2-EMOA on most of the test problems. On the other hand, EIB-MOEA uses the AdaBoost algorithm to ensemble five IB-DEs: the four ones employed by MIHPs and an additional one which is based on the hypervolume indicator. The weight vector employed by AdaBoost is adapted online through a learning mechanism that constantly evaluates the quality of the population, using the five baseline quality indicators. Hence, the IB-DEs compete to obtain a better weight so that they could be preferred more often. EIB-MOEA was tested on the DTLZ, DTLZ^{-1}, WFG, and WFG^{-1} benchmark problems for two and three objective functions. Its performance was compared with respect to the other IB-MOEAs using the five QIs employed in EIB-MOEA. The numerical results using several QIs showed that EIB-MOEA performs more robustly than the other IB-MOEAs.

Chapter 6

On the Cooperation of IB-MOEAs

Section 6.1 introduces our main motivation to explore the cooperation as a solution strategy. Section 6.2 sketches the previous related work. Section 6.3 presents the design of an MOEA whose performance does not depend on the Pareto front shape due to the use of two complementary IB-DEs. Section 6.4 is devoted to describe an MOEA based on the island model where multiple IB-MOEAs cooperate. Finally, a summary of the Chapter is detailed in Section 6.5.

6.1 Motivation

In the previous Chapter, we investigated the competition of IB-Mechanisms as a way of taking advantage of their strengths and to compensate for their weaknesses. In spite of the good performance of MIHPS, we found a selection bias towards the R2-based mechanism in the final stages of the evolutionary process while the density estimators based on the indicators IGD^+, ϵ^+, and Δ_p were preferred at the early stages. Due to the bias to R2-DE, the final Pareto front approximations of MIHPS presented features strongly related to the preferences of the R2 indicator. In this Chapter, we examine the cooperation between IB-Mechanisms and IB-MOEAs to obtain better convergence and diversity results regardless of the MOP being tackled. Regarding the cooperation between IB-Mechanisms, we exploit the idea of Zitzler *et al.* [157] where several indicators are applied succesively to refine the preferences of the previous ones. This way, we succesively apply two IB-DEs, aiming to complement their preferences. Concerning the cooperation between IB-MOEAs, we employ the island model [24] to evolve different subpopulations under the actions of specific IB-Mechanisms to explore different regions of the search space. After some iterations, the subpopulations are merged and the best individuals are saved. Finally, a migration process is performed to increase the diversity of the subpopulations.

6.2 Previous Related Work

Currently, there are different strategies for designing MOEAs, such as the decomposition of a MOP into several single-objective optimization problems [147], the use of reference sets to guide the population towards the Pareto front [30], and the generation of selection mechanisms based on (unary) quality indicators[1] [60]. A wide variety of state-of-the-art MOEAs based on the previously indicated strategies employ a set of convex weight vectors as search directions for the decomposition, in a method to construct reference sets, or as part of the definition of a quality indicator. A vector $\vec{w} \in \mathbb{R}^m$ is a convex weight vector if $\sum_{i=1}^{m} w_i = 1$ and $w_i \geq 0$ for all $i = 1, \ldots, m$. These weight vectors lie on an $(m-1)$-simplex. However, Ishibuchi *et al.* [75] empirically showed that the use of convex weight vectors overspecializes MOEAs on MOPs whose Pareto fronts are strongly correlated to the simplex formed by such weight vectors. In other words, such MOEAs are unable to produce good results when tackling MOPs whose Pareto fronts are not highly coupled with the $(m-1)$-simplex. In consequence, more general MOEAs need to be designed to avoid this overspecialization on specific benchmark problems such as the DTLZ and the WFG test suites.

There are MOEAs that do not use in any of their mechanisms a set of convex weight vectors. An example is the Nondominated Sorting Genetic Algorithm II (NSGA-II) [29] which uses Pareto dominance[2] in its main selection mechanism and crowding distance as its second selection mechanism. However, the selection pressure of NSGA-II dilutes when tackling MOPs having four or more objective functions. Additionally, the crowding distance density estimator cannot produce evenly distributed Pareto fronts in high dimensionality. Another example is the $\mathcal{S}$ Metric Selection Evolutionary Multi-Objective Algorithm (SMS-EMOA) [8] which is a steady-state MOEA that replaces the crowding distance of NSGA-II by the contribution of points to the hypervolume (HV) indicator. The HV is a performance indicator that measures convergence and maximum spread simultaneously. HV is the only unary indicator which is known to be Pareto-compliant[3], but its use in MOEAs with many objectives is limited due to its high computational cost. In 2015, Menchaca-Méndez and Coello proposed an environmental selection mechanism based on the Generational Distance (GD) indicator [105] coupled with a diversity mechanism that adopts ϵ dominance to divide the objective space into hypercubes where the solutions are distributed. A clear disadvantage of GDE-MOEA is the determination of the ϵ value which is required to divide high-dimensional objective spaces and which has an impact on the generation of evenly distributed solutions. Finally, Δ_p-MOEA, proposed by Menchaca *et al.* [107], is an improvement of GDE-MOEA in which instead of using GD in its

[1] A unary indicator I is a function that assigns a real value to set of points $\mathcal{A} = \{\vec{a}^1, \ldots, \vec{a}^N\}$, where $\vec{a}^i \in \mathbb{R}^m$.

[2] Given $\vec{u}, \vec{v} \in \mathbb{R}^m$, $\vec{u}$ Pareto dominates $\vec{v}$ (denoted as $\vec{u} \prec \vec{v}$) if and only if $\forall i = 1, \ldots, m, u_i \leq v_i$ and there exists at least an index $j \in \{1, \ldots, m\} : u_j < v_j$.

[3] Let $\mathcal{A}$ and $\mathcal{B}$ be two non-empty sets of m-dimensional vectors and let I be a unary indicator. I is Pareto-compliant if and only if $\mathcal{A}$ dominates $\mathcal{B}$ implies $I(\mathcal{A}) > I(\mathcal{B})$ (assuming maximization of I).

selection mechanism, it adopts the Δ_p indicator. Δ_p-MOEA improves the diversity of the solutions produced, but it still depends on the calculation of the ϵ value to construct a reference set.

6.3 Cooperation of Multiple IB-DEs

In this section, we explore the idea of the cooperation of multiple IB-Density Estimators in a single MOEA. For this purpose, we present the IGD$^+$-based Many-Objective Evolutionary Algorithm (IGD$^+$-MaOEA), following the framework of the SMS-EMOA [8], as a first step towards a more general optimizer. Then, we propose an extension of IGD$^+$-MaOEA where a Riesz s-energy-based density estimator is incorporated, helping the IGD$^+$-DE to improve the diversity of solutions.

6.3.1 A First Approach

IGD$^+$-MaOEA is a steady state MOEA similar to SMS-EMOA [8]. However, instead of using HV contributions, this approach uses IGD$^+$-DE. Algorithm 11 describes the general framework of IGD$^+$-MaOEA, where the main loop is presented in lines 2 to 13. First, a new solution q is generated by variation operators[4]. q is added to P to create the temporary population Q which is ranked by the nondominated sorting method in line 5. If the layer R_k has more than one solution, then IGD$^+$-DE is executed in line 7, using Algorithm 5 where the set of nondominated solutions R_1 performs as the reference set $\mathcal{Z}$. In case $|R_k| = 1$, the sole solution of R_k is deleted. For both cases, $\vec{u}_{\text{worst}}$ denotes the solution to be deleted. In line 12, the population for the next generation is set. At the end of the evolutionary process, the current population P is returned.

6.3.1.1 Experimental Design

In order to assess the performance of IGD$^+$-MaOEA,[5] we used the Deb-Thiele-Laumanns-Zitzler (DTLZ) test suite and its minus version, DTLZ^{-1} proposed by Ishibuchi *et al.* [75] adopting $m = 3, 4, 5, 6, 7$ objective functions. For all DTLZ and DTLZ^{-1} instances, $n = m + K - 1$, where K is set to 5 for DTLZ1, 10 for DTLZ2-6 and 20 for DTLZ7 [24]. The values of K apply to the corresponding minus problems. The purpose of using DTLZ^{-1} is to show that IGD$^+$-MaOEA is more general than traditional MaOEAs based on the use of convex weight vectors. We compared IGD$^+$-

[4]Simulated binary crossover (SBX) and polynomial-based mutation operators are employed. [31]

[5]The source code is available at `http://computacion.cs.cinvestav.mx/~jfalcon/IGD+-MOEA.html`

Algorithm 11: IGD$^+$-MaOEA general framework

Output: Approximation to the Pareto front

Randomly initialize population P;
while *stopping criterion is not fulfilled* **do**
  $q \leftarrow Variation(P)$;
  $Q \leftarrow P \cup \{q\}$;
  $\{R_1, \ldots, R_k\} \leftarrow NondominatedSorting(Q)$;
  if $|R_k| > 1$ **then**
    $C \leftarrow \text{IGD}^+\text{DE}(\mathcal{A} = R_k, \mathcal{Z} = R_1)$;
    Let $\vec{u}_{\text{worst}}$ the solution with the minimum IGD$^+$ contribution in C;
  end
  else
    Let $\vec{u}_{\text{worst}}$ the sole solution in R_k;
  end
  $P \leftarrow Q \setminus \{\vec{u}_{\text{worst}}\}$;
end
return P

MaOEA with respect to NSGA-III[6], MOEA/D[7], IGD$^+$-EMOA[8] and SMS-EMOA[9] (the latter for only MOPs having 3 and 4 objective functions). Results were compared using the hypervolume indicator. On this regard, we use the following reference points: $(1, 1, \ldots, 1)$ for DTLZ1/DTLZ1^{-1}, $(1, 1, \ldots, 1, 21)$ for DTLZ7/DTLZ7^{-1} and $(2, 2, \ldots, 2)$ for the remaining MOPs.

Since our approach and all the considered MaOEAs are genetic algorithms that use SBX and PBX, we set the crossover probability (P_c), crossover distribution index (N_c), mutation probability (P_m) and the mutation distribution index (N_m) as follows. For MOPs having 3 objective functions $P_c = 0.9$ and $N_c = 20$, while for MaOPs, $P_c = 1.0$ and $N_c = 30$. In all cases, $P_m = 1/n$, where n is the number of decision variables and $N_m = 20$. Table 6.1 shows the population size, objective function evaluations (employed as our stopping criterion) and the parameter H for the generation of the set of convex weight vectors described in [147]. The population size N is equal to the number of weight vectors, i.e., $N = C_{m-1}^{H+m-1}$. In all cases, the neighborhood size T of MOEA/D is set to 20.

[6]We used the implementation available at: `http://web.ntnu.edu.tw/~tcchiang/publications/nsga3cpp/nsga3cpp.htm`.

[7]We used the implementation available at: `http://dces.essex.ac.uk/staff/zhang/webofmoead.htm`

[8] Its author, Edgar Manoatl López provided the source code.

[9]We adopted the implementation of jMetal 4.5.

Table 6.1: Common parameters settings

Objectives	3	4	5	6	7
Population size (N)	120	120	126	126	210
Objective function evaluations ($\times 10^3$)	50	60	70	80	90
Weight-vector partitions (H)	14	7	5	4	4

Table 6.2: Average runtime (in seconds) of IGD$^+$-MaOEA and SMS-EMOA on DTLZ and DTLZ^{-1} benchmarks for 3 objective functions.

MaOEa	**Type**	**DTLZ1**	**DTLZ2**	**DTLZ3**	**DTLZ4**	**DTLZ5**	**DTLZ6**	**DTLZ7**
IGD$^+$-MaOEA	Original	55.87 s	81.66 s	42.44 s	72.80 s	54.92 s	65.31 s	76.26 s
	Minus	78.45 s	91.74 s	68.86 s	92.13 s	93.18 s	102.94 s	81.92 s
SMS-EMOA	Original	963.43 s	2144.43 s	359.28 s	1648.35 s	995.15 s	1944.93 s	1785.38
	Minus	1453.27 s	1868.63 s	1125.25	1906.52 s	1947.56 s	1950.85	1364.88

6.3.1.2 Comparison with MaOEAs based on Convex Weight Vectors

Tables 6.3 and 6.4 show the average HV and the standard deviation (in parentheses) obtained by all the algorithms compared. The two best values among the MaOEAs are highlighted using grayscale, where the darker tone corresponds to the best value. Aiming to have statistical confidence of the results, we performed a one-tailed Wilcoxon test using a significance level of 0.05. Based on the Wilcoxon test, the symbol # is placed when IGD$^+$-MaOEA performs better than other MaOEA in a statistically significant way.

Regarding the original DTLZ problems, in Table 6.3 it is shown that IGD$^+$-MaOEA achieves the best performance in 9 out of 35 problems. Our proposed approach obtained the best HV values in DTLZ3, DTLZ5 and DTLZ6. For DTLZ7, IGD$^+$-MaOEA obtained the second best value when using from 5 to 7 objective functions. Regarding DTLZ1, DTLZ2 and DTLZ4, our proposed approach never obtained the first or the second best HV values among the compared MaOEAs in a statistically significant manner. Nevertheless, it is worth noting that numerically, the differences in all cases are minimal. On the other hand, NSGA-III obtained the best HV values in 7 of the 35 instances, being the best in DTLZ1 and DTLZ7. Overall, IGD$^+$-EMOA obtained the worst place in the performance rank because it only produced the best HV values in 2 instances. Hence, we conclude that IGD$^+$-MaOEA outperforms MOEA/D and IGD$^+$-EMOA and is competitive concerning NSGA-III.

Table 6.4 shows the statistical results for the DTLZ^{-1} test suite. IGD$^+$-MaOEA is the best MaOEA in these problems because it obtained the best HV values in 27 out of 35 instances. Its performance is more evident when tackling the instances having many objectives. In case of three-dimensional problems, it obtained the second best overall HV values, being SMS-EMOA the best optimizer. It is worth noticing that none of the MaOEAs that use convex weight vectors obtained the best HV value in

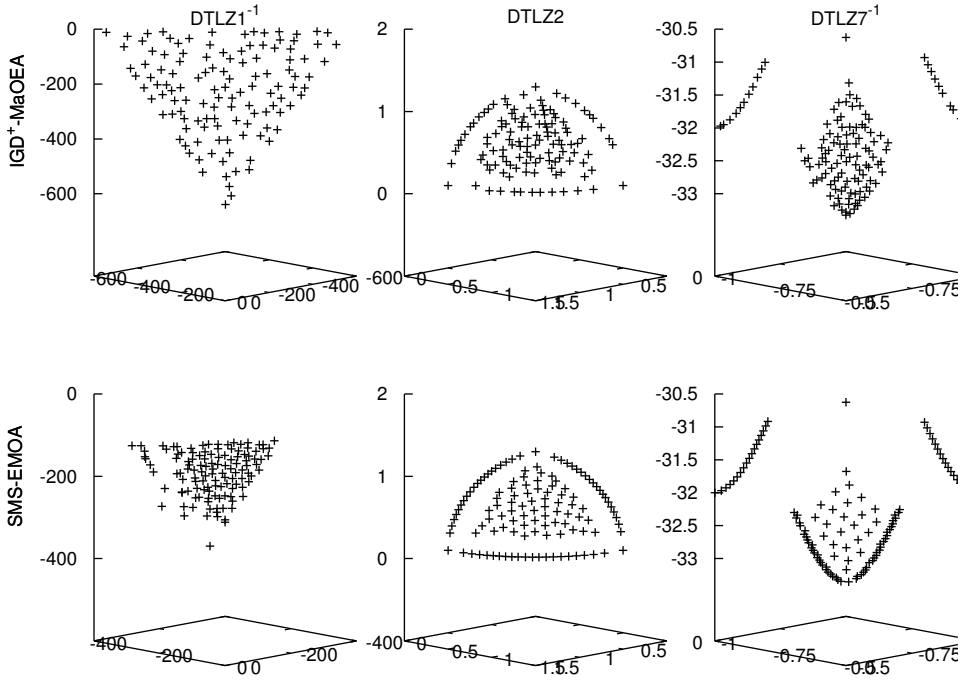

Figure 6.1: Pareto fronts produced by IGD$^+$-MaOEA and SMS-EMOA for DTLZ1^{-1}, DTLZ2 and DTLZ7^{-1} for 3 objective functions. Each front corresponds to the median HV values.

any of the problems. This clearly evidences their overspecialization in MOPs whose Pareto fronts are closely related to the shape of an $(m-1)$-simplex. MOEA/D obtained the second place in 16 problems and NSGA-III in 15. IGD$^+$-EMOA is the worst MaOEA in these problems as it never obtained the best HV values nor the second best ones. Hence, it is evident that the strategy based on weight vectors for the construction of the IGD$^+$-EMOA's reference set has a negative impact on its performance. Moreover, based on the direct comparison between IGD$^+$-MaOEA and IGD$^+$-EMOA, the former can be considered as a better optimizer.

6.3.1.3 Comparison with SMS-EMOA

From Tables 6.3 and 6.4, it is clear that SMS-EMOA outperforms IGD$^+$-MaOEA for the DTLZ benchmark and both are competitive regarding the DTLZ^{-1} instances. However, the aim of SMS-EMOA is to maximize HV and this indicator is being employed for comparison purposes. In spite of this comparison advantage of SMS-EMOA, it is worth noting that the overall HV difference between both algorithms is not very significant. A fact that must be highlighted is that IGD$^+$-MaOEA generates similar distributions to those of SMS-EMOA. This is shown in Fig. 6.1 where the Pareto fronts for DTLZ2 are similar. This distribution is due to the use of the set

Table 6.3: Hypervolume results for the compared MOEAs on the DTLZ problems. We show the mean and standard deviations (in paretheses). The two best values are shown in gray scale, where the darker tone corresponds to the best value. The symbol # is placed when IGD$^+$-MaOEA performs better in a statistically significant way.

MOP	Dim.	IGD$^+$-MaOEA	IGD$^+$-EMOA	NSGA-III	MOEA/D	SMS-EMOA
DTLZ1	3	9.664790e-01 (2.049666e-03)	9.740508e-01 (4.467021e-04)	9.741141e-01 (3.120293e-04)	9.740945e-01 (2.619649e-04)	9.745172e-01 (5.241259e-05)
	4	9.846496e-01 (2.656403e-03)	9.943998e-01 (9.261547e-05)	9.942231e-01 (8.570576e-04)	9.944018e-01 (6.220464e-05)	9.946409e-01 (2.134463e-05)
	5	9.881899e-01 (3.232379e-03)	9.943585e-01 (2.338311e-02)	9.986867e-01 (3.379577e-05)	9.986355e-01 (3.735697e-05)	
	6	9.906617e-01 (2.651917e-03)	9.035094e-01# (7.491169e-02)	9.996492e-01 (2.587221e-05)	9.996231e-01 (1.535746e-05)	
	7	9.948828e-01 (1.318848e-03)	9.264419e-01# (6.287378e-02)	9.999224e-01 (7.339504e-06)	9.998569e-01 (2.567104e-05)	
DTLZ2	3	7.420261e+00 (1.353052e-03)	7.421843e+00 (1.327349e-04)	7.421572e+00 (6.064709e-04)	7.421715e+00 (1.372809e-04)	7.431551e+00 (5.463841e-05)
	4	1.556161e+01 (2.748489e-03)	1.556734e+01 (4.007277e-04)	1.556646e+01 (6.681701e-04)	1.556718e+01 (2.213968e-04)	1.558874e+01 (6.349012e-05)
	5	3.166574e+01 (5.201361e-03)	3.166818e+01 (3.831826e-04)	3.166721e+01 (6.548007e-04)	3.166781e+01 (5.129480e-04)	
	6	6.373545e+01 (5.321646e-03)	6.182623e+01 (4.486397e+00)	6.373806e+01 (1.136133e-03)	6.373808e+01 (6.532194e-04)	
	7	1.278044e+02 (5.835291e-03)	1.117158e+02+ (1.213189e+01)	1.278161e+02 (1.524540e-03)	1.278230e+02 (4.937498e-04)	
DTLZ3	3	7.304310e+00 (5.416726e-01)	5.978405e+00# (2.296587e+00)	6.762070e+00# (1.512456e+00)	7.191410e+00# (9.234976e-01)	7.116381e+00# (1.038033e+00)
	4	1.554332e+01 (1.357241e-02)	1.553667e+01 (2.805291e-02)	1.426614e+01# (3.337968e+00)	1.525936e+01# (9.041126e-01)	1.557833e+01 (4.705930e-03)
	5	3.165020e+01 (9.384670e-03)	3.165404e+01 (6.820552e-03)	2.926244e+01# (5.291705e+00)	2.921654e+01# (6.617692e+00)	
	6	6.371498e+01 (1.113938e-02)	5.883028e+01# (5.646345e+00)	5.837271e+01# (1.552667e+01)	5.395689e+01# (1.319237e+01)	
	7	1.277759e+02 (1.177247e-02)	1.178341e+02# (3.658990e+00)	1.164877e+02# (2.147719e+01)	1.086977e+02# (2.778728e+01)	
DTLZ4	3	6.874113e+00 (7.238869e-01)	7.037545e+00 (7.189670e-01)	7.218780e+00 (4.062937e-01)	7.421636e+00 (1.147608e-04)	6.960992e+00 (5.030399e-01)
	4	1.495718e+01 (1.406114e+00)	1.491851e+01 (1.029726e+00)	1.540943e+01 (3.164949e-01)	1.556707e+01 (2.297960e-04)	1.506728e+01 (6.892799e-01)
	5	3.141161e+01 (5.091958e-01)	3.011363e+01# (1.320577e+00)	3.163040e+01 (1.455720e-01)	3.166733e+01 (4.792449e-04)	
	6	6.342094e+01 (8.053848e-01)	6.220439e+01# (4.109418e-01)	6.374155e+01 (5.870500e-04)	6.373585e+01 (1.078543e-03)	
	7	1.276686e+02 (5.342428e-01)	1.268979e+02# (4.641205e-01)	1.278235e+02 (5.765414e-04)	1.278246e+02 (3.325992e-04)	
DTLZ5	3	6.103250e+00 (3.206747e-04)	4.126358e+00# (1.356638e-01)	6.086240e+00# (3.462620e-03)	6.046024e+00# (2.227008e-04)	6.105419e+00 (1.265596e-05)
	4	1.195066e+01 (1.060364e-02)	8.053758e+00# (6.181680e-02)	1.176583e+01# (3.990838e-02)	1.187250e+01# (4.856384e-03)	1.200938e+01 (7.506854e-04)
	5	2.352758e+01 (5.631168e-02)	1.617222e+01# (1.916164e-01)	2.162912e+01# (9.476133e-01)	2.328373e+01# (1.640165e-02)	
	6	4.655654e+01 (1.477530e-01)	3.216498e+01# (2.350120e-01)	4.222308e+01# (1.270959e+00)	4.584961e+01# (4.179642e-02)	
	7	9.259723e+01 (2.885851e-01)	6.433872e+01# (6.900391e-01)	8.421920e+01# (2.089834e+00)	9.094108e+01# (1.339743e-01)	
DTLZ6	3	5.822452e+00 (9.468474e-02)	5.524093e+00# (8.062048e-01)	5.755154e+00# (7.832234e-02)	5.774939e+00# (8.361881e-02)	5.838678e+00 (7.196085e-02)
	4	1.141949e+01 (1.435037e-01)	9.520791e+00# (5.465663e-01)	5.969793e+00# (6.529944e-01)	1.136532e+01 (1.519071e-01)	1.112687e+01# (1.725538e-01)
	5	2.243194e+01 (2.205059e-01)	1.230783e-02# (1.960431e-02)	6.433325e-02# (1.002102e-01)	2.217372e+01# (3.778954e-01)	
	6	4.395244e+01 (4.872918e-01)	6.039732e+00# (1.208422e+01)	0.000000e+00# (0.000000e+00)	4.349163e+01# (5.731473e-01)	
	7	8.562322e+01 (8.346399e-01)	3.737526e+01# (3.051737e+01)	0.000000e+00# (0.000000e+00)	8.668146e+01 (1.610733e+00)	
DTLZ7	3	1.613138e+01 (1.102308e-01)	1.571995e+01# (7.026627e-02)	1.631926e+01 (1.253568e-02)	1.620770e+01 (1.240925e-01)	1.637100e+01 (7.629934e-02)
	4	1.435812e+01 (1.541455e-01)	1.364183e+01# (1.305431e-01)	1.462787e+01 (3.713300e-02)	1.406944e+01# (5.544544e-02)	1.483349e+01 (1.533320e-01)
	5	1.221977e+01 (5.193563e-01)	1.133320e+01# (1.223979e-01)	1.284401e+01 (3.182259e-02)	6.515913e+00# (1.170945e+00)	
	6	1.035596e+01 (4.758743e-01)	9.287520e+00# (9.704494e-02)	1.082465e+01 (7.434508e-02)	1.366732e+00# (1.894512e+00)	
	7	8.804845e+00 (3.468746e-01)	7.339032e+00# (9.787487e-02)	8.942419e+00 (5.155349e-02)	1.089167e-01# (1.867035e-01)	

Table 6.4: Hypervolume results for the compared MOEAs on the DTLZ^{-1} problems. We show the mean and standard deviations (in paretheses). The two best values are shown in gray scale, where the darker tone corresponds. The symbol # is placed when IGD$^+$-MaOEA performs better in a statistically significant way.

MOP	Dim.	IGD$^+$-MaOEA	IGD$^+$-EMOA	NSGA-III	MOEA/D	SMS-EMOA
DTLZ1^{-1}	3	2.264909e+07 (8.207717e+04)	1.140466e+07# (1.217933e+06)	2.044422e+07# (2.230718e+05)	1.708422e+07# (2.776295e+05)	1.640482e+07# (1.253694e+06)
	4	1.663320e+09 (4.001511e+07)	3.783933e+07# (1.747066e+07)	6.137596e+08# (8.114743e+07)	3.671230e+08# (8.437648e+07)	1.176107e+09# (1.162071e+08)
	5	6.119188e+10 (4.760735e+09)	3.145584e+06# (6.453973e+06)	1.653440e+10# (7.395153e+09)	1.275157e+10# (5.929635e+09)	
	6	1.040799e+12 (2.723386e+11)	5.143618e+05# (1.818714e+06)	3.525438e+11# (1.554685e+11)	6.835890e+10# (4.577981e+10)	
	7	1.879388e+13 (7.487935e+12)	3.352615e+05# (1.083160e+06)	5.717044e+12# (2.906156e+12)	5.582247e+11# (9.246709e+11)	
DTLZ2^{-1}	3	1.210884e+02 (9.009171e-01)	9.369690e+01# (5.010715e+00)	1.226427e+02 (4.332124e-01)	1.241646e+02# (1.767939e-01)	1.261046e+02 (1.456397e-02)
	4	4.674859e+02 (6.158074e+00)	6.908303e+01# (2.593222e-01)	4.670265e+02# (5.036135e+00)	4.782322e+02 (3.762262e-01)	5.109249e+02 (4.731194e-01)
	5	1.655899e+03 (3.942682e+01)	1.817170e+02# (2.352582e+00)	1.529187e+03# (3.829295e+01)	1.570781e+03# (5.466206e+00)	
	6	5.470358e+03 (1.134490e+02)	4.572952e+02# (8.088396e+00)	4.188435e+03# (3.496415e+02)	3.701069e+03# (1.866271e+01)	
	7	1.926684e+04 (4.521928e+02)	1.187017e+03# (1.260695e+01)	1.321225e+04# (1.030901e+03)	1.320162e+04# (6.203137e+01)	
DTLZ3^{-1}	3	5.017451e+09 (1.676399e+07)	3.163373e+09# (3.448716e+08)	4.769399e+09# (4.395958e+07)	4.788299e+09# (5.251105e+07)	3.617983e+09# (1.229064e+08)
	4	5.016984e+12 (2.782494e+10)	1.858417e+11# (1.368270e+11)	3.421113e+12# (1.621812e+11)	3.382020e+12# (8.277136e+10)	2.942443e+12# (1.497601e+11)
	5	4.010397e+15 (5.491013e+13)	2.308672e+10# (5.932196e+10)	1.418461e+15# (2.265638e+14)	2.169617e+15# (3.559794e+13)	
	6	2.671524e+18 (7.441405e+16)	6.882907e+09# (2.710629e+10)	4.952138e+17# (1.783349e+17)	7.151722e+17# (2.068326e+16)	
	7	1.792722e+21 (4.730737e+19)	3.686677e+10# (1.841504e+11)	1.374261e+20# (6.319205e+19)	8.941855e+20# (5.275602e+19)	
DTLZ4^{-1}	3	1.232680e+02 (5.341538e-01)	8.745995e+01# (7.308267e+00)	1.231716e+02# (3.158586e-01)	1.241412e+02 (2.261829e-01)	1.261219e+02 (1.400665e-02)
	4	4.872739e+02 (2.714648e+00)	6.889884e+01# (2.509073e-01)	4.703987e+02# (3.758543e+00)	4.774396e+02# (2.932713e-01)	5.114649e+02 (3.829142e-01)
	5	1.751991e+03 (1.604473e+01)	1.667599e+02# (4.139344e+01)	1.532427e+03# (3.367009e+01)	1.577174e+03# (3.235047e+00)	
	6	5.844499e+03 (5.546305e+01)	4.266016e+02# (3.968221e+02)	4.188345e+03# (2.845836e+02)	3.654612e+03# (4.982487e+00)	
	7	2.024392e+04 (1.637229e+02)	2.470440e+02# (8.390175e+01)	1.311381e+04# (6.546800e+02)	1.295551e+04# (5.175739e+01)	
DTLZ5^{-1}	3	1.189566e+02 (1.131492e+00)	1.045511e+02# (2.925727e+00)	1.212729e+02 (4.506920e-01)	1.230132e+02 (1.173182e-01)	1.248782e+02 (1.400672e-02)
	4	4.524837e+02 (6.184888e+00)	1.458893e+02# (1.837707e+01)	4.617533e+02 (3.033948e+00)	4.737665e+02 (5.201724e-01)	5.067611e+02 (3.943537e-01)
	5	1.590424e+03 (3.260130e+01)	1.247849e+03# (7.727654e+01)	1.526551e+03# (4.186892e+01)	1.532378e+03# (6.612506e+00)	
	6	5.201281e+03 (1.024733e+02)	4.775094e+03# (8.471898e+02)	3.648377e+03# (3.589604e+02)	3.670455e+03# (1.117756e+01)	
	7	1.798605e+04 (3.438881e+02)	3.663675e+03# (2.075826e+03)	1.169538e+04# (9.150133e+02)	1.287945e+04# (5.086978e+01)	
DTLZ6^{-1}	3	1.277596e+03 (8.980299e+00)	5.926270e+02# (4.387564e+01)	1.281204e+03 (4.388455e+00)	1.290813e+03 (6.053013e-01)	1.307600e+03 (1.645502e+00)
	4	9.344785e+03 (1.172155e+02)	7.139870e+02# (1.364398e+02)	8.894185e+03# (9.665925e+01)	8.908490e+03# (7.411574e+00)	9.489564e+03 (6.321189e+01)
	5	5.967159e+04 (9.243485e+02)	4.054599e+03# (5.178149e+02)	4.774990e+04# (2.111510e+03)	5.337501e+04# (1.101944e+02)	
	6	3.401029e+05 (5.077651e+03)	2.826444e+04# (4.152159e+03)	1.871320e+05# (4.124992e+04)	1.611984e+05# (2.134698e+02)	
	7	2.037163e+06 (1.966308e+04)	6.996351e+04# (2.447352e+02)	6.943417e+05# (1.558202e+05)	1.227654e+06# (7.772613e+03)	
DTLZ7^{-1}	3	2.145249e+02 (5.714409e-01)	2.121154e+02# (5.197201e+00)	2.144482e+02 (1.844494e-02)	2.144785e+02 (3.401603e-03)	2.143458e+02# (2.207311e-04)
	4	5.142917e+02 (2.116147e+00)	4.945863e+02# (1.805875e+01)	5.130456e+02# (1.613943e+00)	5.083181e+02# (1.486713e+01)	5.142100e+02# (1.152841e+00)
	5	1.199552e+03 (5.112678e+00)	4.348046e+02# (6.886537e+01)	1.190442e+03# (4.159670e+00)	6.388549e+02# (5.254422e+01)	
	6	2.741875e+03 (1.509787e+01)	7.362027e+02# (1.136842e+02)	2.691994e+03# (7.841504e+00)	9.262902e+02# (3.468054e+00)	
	7	6.176946e+03 (1.308306e+01)	1.355104e+03# (3.306126e+02)	6.016129e+03# (2.260447e+01)	1.621765e+03# (1.220737e+02)	

of nondominated solutions as the reference set in the IGD$^+$-DE algorithm. Hence, this kind of reference set should be strongly considered in order to approximate the performance of HV-based MaOEAs using the IGD$^+$ indicator. Moreover, the average computational cost of IGD$^+$-MaOEA is significantly less compared to SMS-EMOA. This claim is supported by the average running times shown in Table 6.2.

6.3.2 Improving IGD$^+$-MaOEA

In order to overcome the difficulties of MOEAs that do not use weight vectors, we propose here an MOEA that takes advantage of the combination/synergy of the individual effect of two density estimators: one based on the IGD$^+$ indicator [74] and another one based on the Riesz s-energy indicator [56]. The main idea of our Evolutionary Multi-Objective Algorithm based on the Combination of the Riesz s-energy and IGD$^+$ (CRI-EMOA) is to analyze the convergence behavior during the search process in a statistical manner. If convergence stagnates, the generation of evenly distributed solutions is promoted using Riesz s-energy; otherwise, the IGD$^+$-based density estimator will drive the population to $\mathcal{PF}^*$. CRI-EMOA represents an improvement of IGD$^+$-MaOEA since it is able to produce evenly distributed solutions on several Pareto front shapes.

6.3.2.1 CRI-EMOA

Quality indicators can be integrated into MOEAs in three different ways: 1) in the environmental selection mechanism, 2) as an update rule for archives, and 3) as density estimators (DEs). From these approaches, indicator-based DEs (IB-DEs) have been widely used. An IB-DE is the secondary selection mechanism of an MOEA. IB-DEs impose a total order among the solutions of an approximation set by calculating the individual contribution of each solution to the indicator value. Then, the worst-contributing solution is deleted from the population. In this work, we employed IGD$^+$ and Riesz s-energy as IB-DEs. Regarding IGD$^+$, the individual contribution C of a solution $\vec{a} \in \mathcal{A}$ is defined as follows: $C_{\text{IGD}^+}(\vec{a}, \mathcal{A}, \mathcal{Z}) = |\text{IGD}^+(\mathcal{A}, \mathcal{Z}) - \text{IGD}^+(\mathcal{A} \backslash \{\vec{a}\}, \mathcal{Z})|$. On the other hand, for Riesz s-energy, the individual contribution of $\vec{a} \in \mathcal{A}$ is given by: $C_{E_s}(\vec{a}, \mathcal{A}) = \frac{1}{2}[E_s(\mathcal{A}) - E_s(\mathcal{A} \setminus \{\vec{a}\})]$. On the basis of the above equations, IGD$^+$-DEs and E_s-DE are respectively defined as follows: (1) $a_{\text{worst}} = \arg\min_{\vec{a} \in \mathcal{A}} C_{\text{IGD}^+}(\vec{a}, \mathcal{A}, \mathcal{Z})$, and (2) $a_{\text{worst}} = \arg\max_{\vec{a} \in \mathcal{A}} C_{E_s}(\vec{a}, \mathcal{A})$, where a_{worst} denotes the solution having the wost-contributing value.

Algorithm 12 describes our proposed approach, called CRI-EMOA. It is a steady-state MOEA that adopts Pareto dominance in its environmental selection mechanism (using the nondominated sorting algorithm [29] in line 7) and an IB-DE as its secondary selection criterion. The main idea of CRI-EMOA is to exploit the properties of IGD$^+$ and Riesz s-energy by combining the individual effect of the corresponding IB-DEs. In other words, we want to drive the population towards the Pareto front using IGD$^+$-DE and, simultaneously, generating an evenly distributed approximation to the Pareto front through E_s-DE. To this end, CRI-EMOA switches between

Algorithm 12: CRI-EMOA general framework

Input: T_w, $\bar{\beta}$, $\bar{\theta}$
Output: Pareto front Approximation

Randomly initialize population P;
$t \leftarrow 0$;
while *stopping criterion is not fulfilled* **do**
  $q \leftarrow Variation(P)$;
  $Q \leftarrow P \bigcup \{q\}$;
  Normalize Q;
  $\{L_1, L_2, \ldots, L_k\} \leftarrow$ nondominated-sorting(Q);
  $z_i^{\max} = \begin{cases} f_i^* = \max_{\vec{x} \in L_1} f_i(\vec{x}), & f_i^* > z_i^{\max} \\ z_i^{\max}, & \text{otherwise} \end{cases}$;
  $S_{\text{HV}}[t \mod T_w] \leftarrow HV_{appr}(t)$;
  Statistically analyze the last T_w samples in S_{HV} and generate β and θ; **if** $k = 1$ *and* $\beta \leq \bar{\beta}$ *and* $\theta \in [-\bar{\theta}, \bar{\theta}]$ **then**
    $a_{\text{worst}} = \arg\max_{\vec{a} \in L_1} C_{E_s}(\vec{a}, L_1)$;
  end
  else
    if $|L_k| > 1$ **then**
      $a_{\text{worst}} = \arg\min_{\vec{a} \in L_k} C_{\text{IGD}^+}(\vec{a}, L_k, L_1)|$;
    end
    else
      a_{worst} is equal to the sole individual in L_k;
    end
  end
  $P \leftarrow Q \setminus \{a_{\text{worst}}\}$;
  $t \leftarrow t + 1$;
end
return P

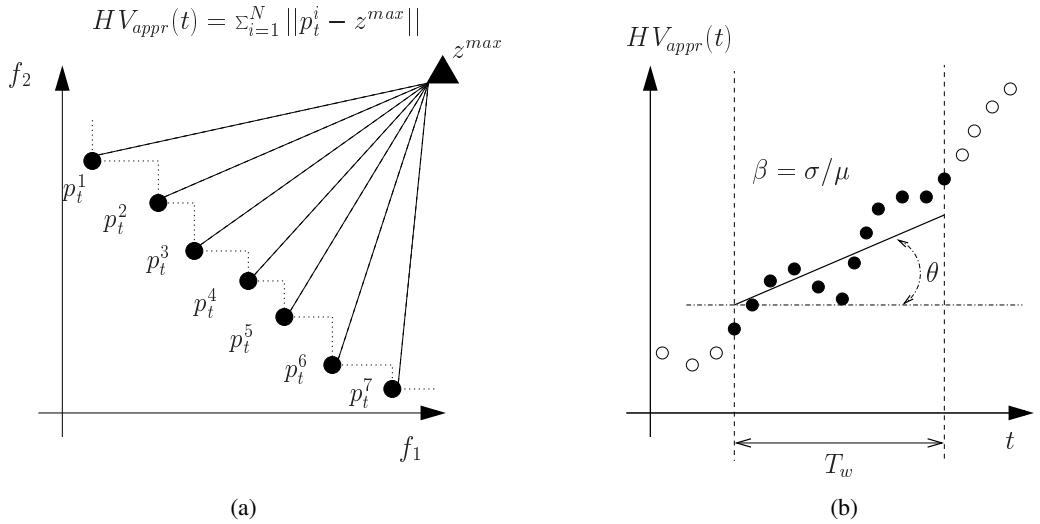

Figure 6.2: (a) The Hypervolume approximation adds up all the distances between the reference point and each nondominated solution, (b) linear model of the convergence behavior created using the last T_w measures of HV_{appr}.

the two IB-DEs depending on a statistical analysis of the convergence behavior of the population, using an approximation to the hypervolume indicator (denoted as HV_{appr}). HV_{appr} is a simplification of the proposal of Ishibuchi *et al.* [78] and it adds up all the distances between an anti-optimal reference point $\vec{z}^{\max}$ and the set of current nondominated solutions in L_1 (see Fig. 6.2a). In line 8, each $z_i^{\max}, i = 1, \ldots, m$ is updated if and only a worse objective value in L_1 is found and, then, $\text{HV}_{\text{appr}}(t)$ is computed such that the obtained value is stored in a circular array S_{HV} of size T_w. After the first T_w generations, S_{HV} will be full, and we can statistically analyze at each iteration the last T_w samples of HV_{appr} as shown in Fig. 6.2b. In line 10, the mean μ and the standard deviation σ of the samples are computed such that the coefficient[10] of variation $\beta = \sigma/\mu$ is calculated. Additionally, the angle θ of a linear regression model of the samples is computed. Based on β and θ, we can exploit the properties of a certain IB-DE. If the number k of ranks produced by the nondominated sorting algorithm is equal to one and it holds that $\beta \leq \bar{\beta}$ and $\theta \in [-\bar{\theta}, \bar{\theta}]$ (where $\bar{\beta}$ and $\bar{\theta}$ are user-supplied parameters), it means that the convergence behavior is stagnated since there is not too much variation of HV_{appr} and the linear model cannot be considered as ascending or descending. In consequence, we have to promote diversity using E_s-DE in line 12. Otherwise, if $|L_k| > 1$, IGD^+-DE is selected in line 15 in furtherance of improving the convergence of the population. In case $|L_k| = 1$, the sole individual in L_k is selected for elimination. Finally, the selected solution a_{worst} is deleted from the population, and a new generation is created.

[10] β is a standardized measure of dispersion that shows the extent of variability to the mean of the population.

6.3.2.2 Experimental Design

In this section, we analyze the performance of CRI-EMOA[11] when compared to several state-of-the-art MOEAs: NSGA-III [30], MOEA/D [147], MOMBI2 [60], Δ_p-MOEA [107] and GDE-MOEA [105]. The adopted MOEAs are classified into two main groups: MOEAs based on convex weight vectors and MOEAs not using convex weight vectors. NSGA-III[12], MOEA/D[13] and MOMBI2[14] belong to the first group while the remaining MOEAs[15] belong to the second group. We adopted MOPs from the DTLZ and WFG test suites, as well as from the minus versions of them, denoted as DTLZ^{-1} and WFG^{-1} that were proposed by Ishibuchi *et al.* [75]. The use of the minus versions of the benchmarks is to determine the performance of the considered MOEAs on MOPs whose Pareto fronts are not correlated to the simplex formed by a set of convex weight vectors. Additionally, the Pareto fronts of these MOPs cover a wide range of geometries such as linear, concave, degenerated, disconnected and mixed. In each case, we employed 3, 5 and 10 objective functions. In order to assess the performance of our proposed CRI-EMOA and the other MOEAs adopted in our comparative study, we applied HV and the Solow-Polasky indicator [39] for assessing convergence and diversity, respectively. For each MOEA in each test instance, we performed 30 independent executions.

For a fair comparison, we set the population size N of all MOEAs, equals to the number of convex weight vectors that some of them employed, i.e., $N = C_{m-1}^{H+m-1}$, where m is the number of objective functions and H is a user-supplied parameter. Hence, in each case, the tuple (m, H, N) was set as follows: (3, 14, 120), (5, 5, 126), and (10, 3, 220). For the considered number of objective functions, we set 50×10^3, 70×10^3, and 120×10^3 function evaluations as our stopping criterion, respectively. Since our approach and all the considered MOEAs are genetic algorithms that use Simulated Binary Crossover and Polynomial-based Mutation as variation operators, we set the crossover probability (P_c), the crossover distribution index (N_c), the mutation probability (P_m), and the mutation distribution index (N_m) as follows. For MOPs having three objective functions $P_c = 0.9$ and $N_c = 20$, while for MaOPs $P_c = 1.0$ and $N_c = 30$. In all cases, $P_m = 1/n$, where n is the number of decision variables, and $N_m = 20$. Regarding both the WFG and the WFG^{-1} test problems with 3, 5 and 10 objectives, we set the number of variables as $n = 26, 30$ and 40, in each case using the following position-related parameters: 2, 4, and 9. Considering the DTLZ and DTLZ^{-1} instances, the number of variables is equal to $n = m + K - 1$,

[11]The source code of CRI-EMOA is available at `http://computacion.cs.cinvestav.mx/~jfalcon/CRI-EMOA.html`.

[12]We used the implementation available at: `http://web.ntnu.edu.tw/~tcchiang/publications/nsga3cpp/nsga3cpp.htm`.

[13]We used the implementation available at: `http://dces.essex.ac.uk/staff/zhang/webofmoead.htm`.

[14]We used the implementation available at `http://computacion.cs.cinvestav.mx/~rhernandez/`.

[15]The source code of Δ_p-MOEA and GDE-MOEA was provided by its author, Adriana Menchaca Méndez.

where $K = 5$ for DTLZ1 and DTLZ1^{-1}, $K = 10$ for DTLZ2, DTLZ5 and their minus versions, and $K = 20$ for DTLZ7 and DTLZ7^{-1}. For MOEA/D, the neighborhood size was set to 20 in all cases. Regarding CRI-EMOA, we employed $T_w = N$, $\bar{\beta} = 0.1$ and $\bar{\theta} = 0.25$ degrees for all instances.

6.3.2.3 Discussion of Results

Tables 6.5 and 6.6 show the mean and standard deviation (in parentheses) obtained by all the compared algorithms for the hypervolume and the Solow-Polasky[16] indicators, respectively. The two best values among the MOEAs are highlighted using gray scale, where the darker tone corresponds to the best value. Aiming to obtain the statistical confidence of our results, we performed a one-tailed Wilcoxon test using a significance level of 0.05. Based on the Wilcoxon test, the symbol # is placed when CRI-EMOA performs better than another MOEA in a statistically significant way.

Regarding the hypervolume indicator, CRI-EMOA is the best algorithm since it obtained the first place in 50% of the test problems. The second place corresponds to NSGA-III because it was the best MOEA in 8 out of 42 problems. However, it is worth emphasizing that for the minus benchmarks, NSGA-III only obtained one first place, specifically for DTLZ7^{-1} with 3 objective functions. In this regard, MOEA/D and MOMBI2 have just one first place in these minus benchmarks, and the remainder of their first places belong to the original DTLZ and WFG test suites. In consequence, it is clear the overspecialization of MOEAs using convex weight vectors on these benchmarks. Considering Δ_p-MOEA and GDE-MOEA, their performance is not so high. In fact, GDE-MOEA never obtains the first place and Δ_p-MOEA is the best algorithm in four test instances.

The Solow-Polasky indicator supports the good results of CRI-EMOA. This indicator measures the number of species present in the population. Thus, a larger value of the indicator is better because it means a good diversity of solutions. Our proposed approach produces well-distributed Pareto fronts in 26 out of 42 test instances (see Fig. 6.3). As a matter of fact, in most cases, when CRI-EMOA obtains the best HV value, it also obtains the best Solow-Polasky value. Hence, this a first insight that the synergy between IGD$^+$ and Riesz s-energy is actually responsible of its good performance in both convergence and diversity. Regarding the other MOEAs, NSGA-III and Δ_p-MOEA tie in second place since they obtained the best indicator value in 5 problems. Once again, NSGA-III can only produce good results for the original DTLZ and WFG problems. The worst algorithm regarding this indicator is MOMBI2.

For DTLZ1 and DTLZ1^{-1}, which have a linear Pareto front, CRI-EMOA does not obtain the best HV value. However, the Solow-Polasky indicator reflects that our approach has a better diversity. The top part of Fig. 6.3 shows the DTLZ1^{-1} fronts produced by all the MOEAs, and it is evident that CRI-EMOA produces an evenly distributed front in comparison with the adopted MOEAs. MOEA/D and MOMBI2 generate numerous solutions in the boundary of the front, while Δ_p-MOEA,

[16]The Solow-Polasky indicator requires a parameter θ that was set to 10.

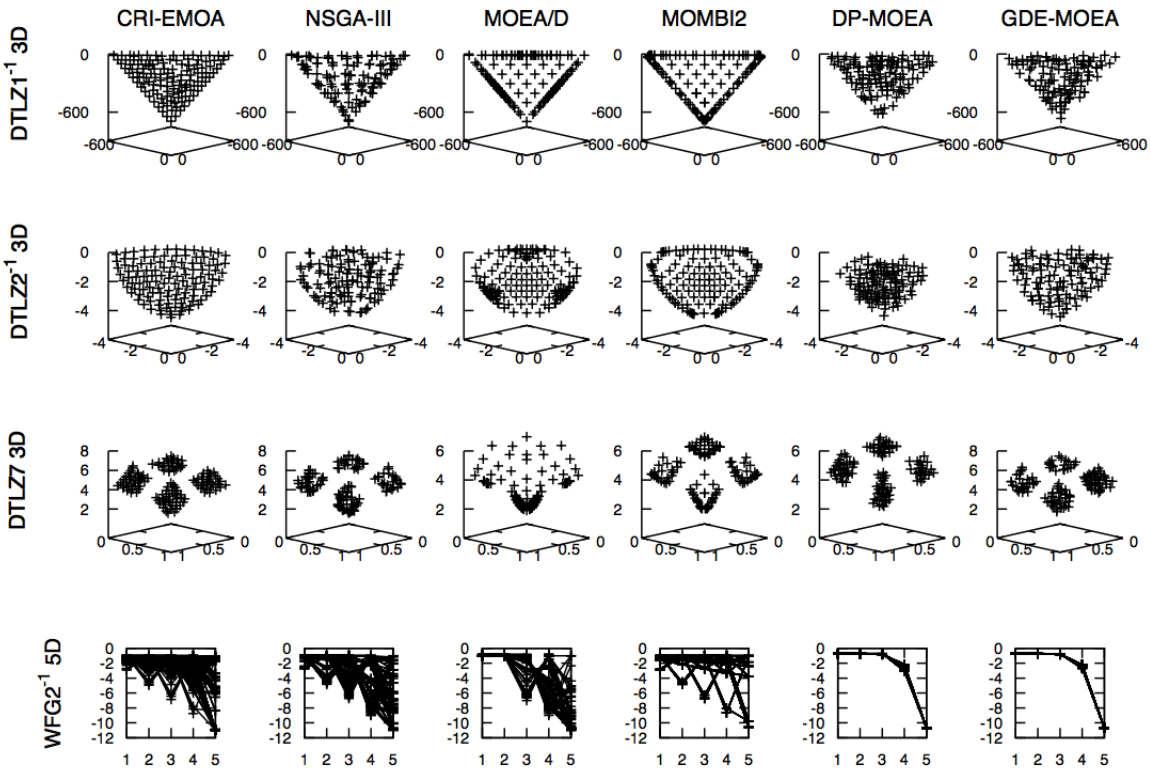

Figure 6.3: Pareto fronts generated by CRI-EMOA and the adopted MOEAs. Each front corresponds to the median of the hypervolume value.

GDE-MOEA and NSGA-III do not produce well-distributed solutions. For convex problems, i.e., DTLZ2^{-1} and DTLZ5^{-1}, it is evident that CRI-EMOA has a good performance. This is because it entirely covers the Pareto front, unlike the other MOEAs which are unable to do the same. This effect is illustrated in the second row of Fig. 6.3. For more complicated problems such as DTLZ7 and WFG2^{-1} that assess the ability of a MOEA to manage subpopulations, it is evident that CRI-MOEA produces better results. In the light of these results, we can claim that CRI-EMOA is a more general optimizer because its performance is not strongly linked to certain types of benchmark problems.

6.4 Cooperation of Multiple IB-MOEAs

Unlike the last section where we investigated the cooperation of multiple IB-DEs, in this section we propose to perform the cooperation of multiple steady-state IB-MOEAs (based on the indicators: HV, R2, IGD$^+$, ϵ^+, and Δ_p) exploiting the island model [24]. In this model, a given number of subpopulations isolatedly evolve, each one in an island. After some iterations, a master island collects all subpopulations to keep the best individuals, according to some criterion, and, then, perform a migration

Table 6.5: Mean and standard deviation (in parentheses) of the Hypervolume indicator. A symbol # is placed when CRI-EMOA performed significantly better than the other approaches based on a one-tailed Wilcoxon test using a significance level of $\alpha = 0.05$. The two best values are shown in gray scale, where the darker tone corresponds to the best value.

MOP	Dim.	CRI-EMOA	NSGA-III	MOEA/D	MOMBI2	Δ_p-MOEA	GDE-MOEA
DTLZ1	3	9.739039e-01 (3.858675e-04)	9.741141e-01 (3.120293e-04)	9.740945e-01 (2.619649e-04)	9.663444e-01# (1.080932e-03)	9.413310e-01# (1.964370e-02)	9.676446e-01# (2.362618e-03)
	5	9.877798e-01 (3.117917e-03)	9.986867e-01 (3.379577e-05)	9.986355e-01 (3.735697e-05)	9.904662e-01 (1.120127e-03)	3.320501e-02# (8.565974e-02)	4.840903e-01# (4.857106e-01)
	10	9.963635e-01 (1.065991e-03)	9.999939e-01 (2.139857e-06)	9.996746e-01 (1.025281e-04)	9.961538e-01 (9.574496e-04)	3.040882e-02# (5.310077e-02)	0.000000e+00# (0.000000e+00)
DTLZ2	3	7.419537e+00 (3.056980e-03)	7.421572e+00 (6.064709e-04)	7.421715e+00 (1.372809e-04)	7.380040e+00# (7.076656e-03)	7.371981e+00# (3.875638e-02)	7.350569e+00# (2.220661e-02)
	5	3.157090e+01 (2.415933e-02)	3.166721e+01 (6.548007e-04)	3.166781e+01 (5.129480e-04)	3.149886e+01# (2.619865e-02)	3.145814e+01# (6.277721e-02)	3.139858e+01# (7.085084e-02)
	10	1.021699e+03 (4.906893e-01)	1.023905e+03 (1.423610e-03)	1.023902e+03 (4.192719e-03)	1.022163e+03 (4.299615e-01)	1.022172e+03 (3.206973e-01)	8.223136e+02# (4.847301e+01)
DTLZ5	3	6.103498e+00 (2.913259e-04)	6.086240e+00# (3.462620e-03)	6.046024e+00# (2.227008e-04)	6.018466e+00# (3.166178e-03)	6.083103e+00# (4.024434e-02)	6.070736e+00# (4.307412e-02)
	5	2.306362e+01 (2.295313e-01)	2.162912e+01# (9.476133e-01)	2.328373e+01 (1.640165e-02)	2.175597e+01# (2.378197e-01)	2.152316e+01# (1.422545e+00)	1.943602e+01# (1.234198e+00)
	10	6.453781e+02 (4.080592e+01)	6.172582e+02# (4.132326e+01)	7.043390e+02 (1.714256e+00)	6.054385e+02# (4.091687e+01)	5.909772e+02# (7.644220e+01)	9.641241e+01# (1.554238e+01)
DTLZ7	3	1.634605e+01 (5.285233e-02)	1.631926e+01# (1.253568e-02)	1.620770e+01# (1.240925e-01)	1.613885e+01# (3.101462e-02)	1.612577e+01# (1.553168e-01)	1.615480e+01# (1.492618e-01)
	5	1.281085e+01 (1.974810e-01)	1.284401e+01 (3.182259e-02)	6.515913e+00# (1.170945e+00)	1.269646e+01# (4.907749e-02)	1.255217e+01# (1.341411e-01)	1.234590e+01# (2.234605e-01)
	10	3.479852e+00 (2.403388e-01)	1.806637e+00# (4.781492e-01)	2.756082e-03# (7.839814e-03)	3.033892e+00# (5.070947e-02)	3.027342e+00# (9.110566e-02)	2.080502e+00# (4.312007e-01)
WFG1	3	5.056544e+01 (1.657420e+00)	4.917540e+01# (1.742752e+00)	4.994533e+01 (2.615320e+00)	5.250059e+01 (1.702362e+00)	3.624458e+01# (9.571499e-01)	3.857628e+01# (9.613983e-01)
	5	4.509188e+03 (1.444159e+02)	4.049661e+03# (1.445036e+02)	4.522924e+03 (1.145447e+02)	4.682300e+03 (7.687667e+01)	3.198417e+03# (8.802857e+01)	3.499936e+03# (7.077142e+01)
	10	5.037589e+09 (8.535179e+07)	4.333786e+09# (4.767509e+07)	4.626119e+09# (9.082857e+07)	5.028893e+09 (6.062765e+07)	3.422833e+09# (2.182108e+07)	3.554077e+09# (4.491835e+07)
WFG2	3	1.000262e+02 (2.196919e-01)	1.000303e+02 (2.020421e-01)	9.425491e+01# (1.887090e+00)	9.995196e+01# (2.218338e-01)	2.860787e+01# (1.562061e-01)	2.878405e+01# (3.147546e-02)
	5	1.008420e+04 (5.737764e+01)	1.022660e+04 (2.444328e+01)	9.147103e+03# (2.989196e+02)	1.021265e+04 (2.425440e+01)	2.356563e+03# (1.302041e+01)	2.352252e+03# (2.298487e+01)
	10	1.348499e+10 (4.708062e+07)	1.343510e+10# (5.838755e+07)	1.153362e+10# (4.307707e+08)	1.346239e+10 (6.456777e+07)	2.433110e+09# (1.405830e+07)	2.417620e+09# (3.423298e+07)
WFG3	3	7.306197e+01 (3.258533e-01)	7.359113e+01 (3.698540e-01)	6.949014e+01 (2.043137e+00)	7.476737e+01 (2.010304e-01)	2.974536e+01 (2.198130e-01)	3.026476e+01 (9.539859e-02)
	5	6.735962e+03 (9.568603e+01)	6.705622e+03 (6.623165e+01)	5.831355e+03# (1.740491e+02)	6.720322e+03 (8.790247e+01)	2.425136e+03# (2.737458e+01)	2.467475e+03# (5.330311e+00)
	10	8.262095e+09 (2.467236e+08)	7.851751e+09# (1.420734e+08)	3.407782e+09# (4.406816e+08)	7.150575e+09# (8.942471e+08)	2.435088e+09# (7.572200e+07)	2.460728e+09# (2.651078e+07)
DTLZ1^{-1}	3	2.237019e+07 (1.096230e+05)	2.044422e+07# (2.230718e+05)	1.708422e+07# (2.776295e+05)	1.754720e+07# (1.024912e+04)	2.249206e+07 (9.308520e+04)	2.178413e+07# (1.919526e+05)
	5	5.990400e+10 (5.969126e+09)	1.653440e+10# (7.395153e+09)	1.275157e+10# (5.929635e+09)	1.829497e+10# (1.178680e+08)	8.421535e+10 (5.019922e+09)	7.834908e+10 (5.592427e+09)
	10	2.331601e+15 (1.332180e+15)	1.690928e+16 (1.594681e+16)	2.068669e+10# (2.776909e+10)	3.254959e+17 (7.964585e+16)	4.163772e+17 (1.784438e+17)	1.959914e+17 (7.692566e+16)
DTLZ2^{-1}	3	1.255756e+02 (1.372903e-01)	1.226427e+02# (4.332124e-01)	1.241646e+02# (1.767939e-01)	1.246298e+02# (1.975120e-02)	1.202429e+02# (1.235826e+00)	1.232392e+02# (4.384877e-01)
	5	1.823404e+03 (5.652832e+00)	1.529187e+03# (3.829295e+01)	1.570781e+03# (5.466206e+00)	1.377041e+03# (2.801096e+00)	1.615070e+03# (3.622796e+01)	1.684100e+03# (2.422012e+01)
	10	3.952305e+05 (6.000728e+03)	2.480210e+05# (3.215706e+04)	1.837497e+05# (3.540744e+03)	1.941735e+05# (4.318334e+03)	4.467775e+05 (1.153133e+04)	4.295481e+05 (1.104582e+04)
DTLZ5^{-1}	3	1.240446e+02 (1.543643e-01)	1.212729e+02# (4.506920e-01)	1.230132e+02# (1.173182e-01)	1.233805e+02# (2.897257e-02)	1.191790e+02# (1.218659e+00)	1.217996e+02# (3.913095e-01)
	5	1.830136e+03 (8.376583e+00)	1.526551e+03# (4.186892e+01)	1.532378e+03# (6.612506e+00)	1.490703e+03# (3.599646e+00)	1.550531e+03# (3.545733e+01)	1.663295e+03# (2.143198e+01)
	10	5.043244e+05 (5.933536e+03)	2.353908e+05# (2.658733e+04)	1.618586e+05# (2.870596e+03)	1.786897e+05# (4.650613e+03)	3.841427e+05# (1.267929e+04)	3.788162e+05# (1.409232e+04)
DTLZ7^{-1}	3	2.139263e+02 (1.705184e+00)	2.144482e+02 (1.844494e-02)	2.144785e+02 (3.401603e-03)	2.144350e+02 (1.484695e-02)	2.141398e+02 (6.446048e-01)	2.117720e+02# (5.620357e+00)
	5	1.193104e+03 (7.463449e+00)	1.190442e+03# (4.159670e+00)	6.388549e+02# (5.254422e+01)	1.197724e+03 (5.760920e+00)	1.195714e+03 (1.560565e+00)	1.167397e+03# (3.067229e+01)
	10	6.493424e+04 (1.799575e+02)	6.282093e+04# (1.236603e+02)	7.555843e+03# (6.397426e+02)	6.278498e+04# (5.606912e+02)	6.374490e+04# (1.597907e+02)	6.336153e+04# (1.579373e+02)
WFG1^{-1}	3	4.721465e+02 (5.118363e+01)	5.214593e+02 (2.613138e+01)	3.653092e+02# (2.305800e+00)	4.717969e+02# (4.848793e+01)	4.289752e+02# (4.089696e+01)	4.226979e+02# (4.328855e+01)
	5	8.957760e+04 (1.295509e+04)	6.766707e+04# (3.634016e+03)	4.312409e+04# (1.486578e+03)	8.604789e+04 (1.028243e+04)	6.687040e+04# (8.125469e+03)	5.398842e+04# (6.022448e+03)
	10	1.920711e+11 (1.254828e+10)	1.167307e+11# (9.811376e+09)	7.403214e+10# (3.748511e+09)	5.753336e+10# (1.586430e+09)	1.037099e+11# (5.197695e+09)	8.712812e+10# (9.507560e+09)
WFG2^{-1}	3	7.318853e+02 (4.584376e-01)	7.256549e+02# (2.471515e+00)	7.318071e+02# (5.137348e-01)	7.277336e+02# (7.218694e-01)	3.548073e+02# (4.631427e-01)	3.549143e+02# (1.951948e-01)
	5	1.638383e+05 (1.165835e+03)	1.470928e+05# (8.586496e+03)	1.122933e+05# (1.197256e+04)	1.499384e+05# (4.291788e+02)	4.315723e+04# (1.487567e+02)	4.156049e+04# (6.526206e+02)
	10	7.365072e+11 (6.254171e+09)	3.658776e+11# (1.973606e+10)	2.462168e+11# (2.934157e+10)	8.919695e+10# (1.091716e+10)	7.359311e+10# (2.277690e+08)	7.165991e+10# (8.580112e+08)
WFG3^{-1}	3	6.701244e+02 (9.728569e-01)	6.581207e+02# (2.461272e+00)	6.559404e+02# (1.399701e-01)	6.678986e+02# (4.368737e-01)	3.901185e+02# (2.837691e+00)	3.929122e+02# (1.663457e+00)
	5	1.460039e+05 (2.618698e+03)	1.271888e+05# (5.065268e+03)	9.818104e+04# (4.519958e+03)	1.345863e+05# (2.667741e+02)	4.822825e+04# (1.017141e+03)	4.912237e+04# (6.555485e+02)
	10	6.613123e+11 (2.015972e+10)	3.003925e+11# (2.070638e+10)	1.932277e+11# (2.123809e+10)	1.572410e+11# (3.994016e+09)	8.120430e+10# (2.177319e+09)	8.405921e+10# (1.518237e+09)

Table 6.6: Mean and standard deviation (in parentheses) of the Solow-Polasky indicator. A symbol # is placed when CRI-EMOA performed significantly better than the other approaches based on a one-tailed Wilcoxon test using a significance level of $\alpha = 0.05$. The two best values are shown in gray scale, where the darker tone corresponds to the best value.

MOP	Dim.	CRI-EMOA	NSGA-III	MOEA/D	MOMBI2	Δ_p-MOEA	GDE-MOEA
DTLZ1	3	9.944608e+00 (7.332450e-01)	9.394548e+00# (2.930251e-01)	9.314418e+00# (3.914884e-02)	9.000566e+00# (2.446366e-02)	7.811889e+00# (9.608413e-01)	9.208526e+00# (7.142910e-01)
	5	1.338590e+01 (5.394744e-01)	1.927839e+01 (2.200570e-01)	1.910784e+01 (2.012103e-01)	1.784107e+01 (5.535436e-02)	1.258001e+02 (3.614573e-01)	7.251588e+01 (4.806114e+01)
	10	1.785253e+01 (8.881198e-01)	4.215677e+01 (2.267717e+00)	3.557264e+01 (6.064497e-01)	3.493408e+01 (2.073537e+00)	2.196627e+02 (4.229255e-01)	1.937667e+02 (5.463117e+00)
DTLZ2	3	3.395527e+01 (9.380927e-02)	3.394704e+01# (1.377030e-02)	3.393654e+01# (1.057577e-03)	3.320388e+01# (3.200128e-02)	3.071966e+01# (5.648283e-01)	3.130480e+01# (3.907121e-01)
	5	9.880242e+01 (3.075202e+00)	1.023559e+02 (2.316020e-01)	1.017397e+02 (4.330518e-03)	1.000214e+02 (9.376416e-02)	9.047203e+01# (1.071667e+00)	8.885177e+01# (1.407456e+00)
	10	2.144437e+02 (8.333968e-01)	2.144143e+02# (4.461039e-02)	2.140218e+02# (1.052798e-02)	2.134074e+02# (2.440550e-01)	2.073661e+02# (1.076644e+00)	2.149790e+02 (1.820800e+00)
DTLZ5	3	8.835302e+00 (8.683488e-03)	8.689954e+00# (4.814112e-02)	4.565503e+01 (6.372947e-01)	8.446415e+00# (1.275105e-02)	8.725615e+00# (1.118233e-01)	9.131640e+00 (8.893988e-01)
	5	5.453458e+01 (3.836635e+00)	7.846618e+01 (3.806546e+00)	2.193721e+01# (7.192604e-01)	1.733111e+01# (1.215347e+00)	6.458870e+01 (4.414063e+00)	9.229364e+01 (3.153601e+00)
	10	1.426916e+02 (1.105651e+01)	1.855864e+02 (4.441145e+00)	7.636613e+00# (7.127440e-02)	2.097795e+01# (1.446842e+01)	1.636387e+02 (1.190412e+01)	2.009986e+02 (2.726407e+00)
DTLZ7	3	4.693189e+01 (4.563587e+00)	4.248938e+01# (8.838503e-01)	3.411613e+01# (6.885687e+00)	3.750968e+01# (4.295088e-01)	3.356066e+01# (8.918332e+00)	3.791999e+01# (1.074318e+01)
	5	7.703740e+01 (2.640331e+01)	9.605921e+01 (4.006295e+00)	2.595428e+01# (3.104755e-01)	7.335971e+01# (1.892378e+00)	1.014229e+02 (7.384253e+00)	8.467007e+01 (2.946531e+01)
	10	2.083721e+02 (1.401193e+01)	3.401405e+01# (4.627073e+01)	6.635493e+00# (8.377910e-01)	1.539631e+02# (1.794040e+01)	2.161036e+02 (1.887145e+00)	1.635677e+02# (5.659825e+01)
WFG1	3	6.266729e+01 (4.306665e+00)	5.624993e+01# (4.311929e+00)	5.053063e+01# (2.764405e+00)	5.406056e+01# (2.296813e+00)	3.936107e+01# (2.712236e+00)	4.901870e+01# (2.752851e+00)
	5	7.766310e+01 (9.797998e+00)	9.244372e+01 (7.266040e+00)	7.480740e+01 (3.832994e+00)	7.292172e+01# (5.425443e+00)	5.404634e+01# (4.708150e+00)	9.197836e+01 (4.116442e+00)
	10	1.153389e+02 (1.285140e+01)	8.917693e+01# (8.545945e+00)	1.552376e+01# (3.169355e+00)	6.819405e+01# (8.992674e+00)	9.420152e+01# (6.434297e+00)	1.681839e+02 (7.642626e+00)
WFG2	3	1.031961e+02 (6.913412e-01)	9.475339e+01# (5.942618e-01)	7.243218e+01# (1.099197e+00)	8.113447e+01# (1.694539e+00)	1.566893e+01# (4.695226e-01)	1.597100e+01# (5.210876e-01)
	5	9.923778e+01 (3.753788e+00)	1.259866e+02 (5.442239e-01)	9.750359e+01# (2.449040e+00)	1.226234e+02 (1.081329e+00)	2.491924e+01# (1.910851e+00)	2.346945e+01# (2.689896e+00)
	10	1.981494e+02 (4.297874e+00)	2.034942e+02 (6.167357e+00)	2.746068e+01# (9.314055e+00)	1.826284e+02# (2.286544e+01)	5.897645e+01# (4.305811e+00)	5.040485e+01# (7.890364e+00)
WFG3	3	7.979549e+01 (8.271398e-01)	5.447458e+01# (3.954759e+00)	6.745390e+01# (1.429561e+00)	4.359786e+01# (9.246690e-01)	2.088260e+01# (5.548807e-01)	2.237972e+01# (2.670741e-01)
	5	1.207901e+02 (1.514908e+00)	9.114798e+01# (4.803291e+00)	1.203892e+02# (1.120195e+00)	3.884532e+01# (5.191645e+00)	3.640185e+01# (1.590306e+00)	3.986356e+01# (1.669298e+00)
	10	2.198151e+02 (1.511883e-01)	1.842494e+02# (6.381996e+00)	1.685512e+02# (8.180955e-01)	1.223302e+02# (2.606946e+01)	7.655449e+01# (7.601122e+00)	9.569073e+01# (5.324356e+00)
DTLZ1^{-1}	3	1.238722e+02 (6.478345e-01)	1.192301e+02# (9.769981e-01)	1.110656e+02# (2.067972e-01)	1.076858e+02# (1.612270e+00)	1.194494e+02# (7.076038e-01)	1.026058e+02# (2.385964e+00)
	5	1.261138e+02 (3.746123e-01)	1.276049e+02 (7.483806e-01)	1.160278e+02# (3.018754e+00)	6.760143e+01# (4.891955e+00)	1.256546e+02# (4.961652e-01)	1.091644e+02# (2.978643e+00)
	10	2.200000e+02 (6.478398e-01)	2.194982e+02# (5.550208e-01)	1.845834e+01# (3.362045e+01)	2.177230e+02# (1.598879e+00)	2.199297e+02# (1.852502e-01)	1.956693e+02# (3.843626e+00)
DTLZ2^{-1}	3	1.129425e+02 (2.079720e-01)	9.168006e+01# (2.394444e+00)	9.466441e+01# (8.426911e-02)	9.433643e+01# (1.896075e-01)	8.857439e+01# (2.604729e+00)	8.818635e+01# (2.087133e+00)
	5	1.259981e+02 (4.099458e-04)	1.134723e+02# (2.970256e+00)	1.247875e+02# (1.631879e-01)	4.888021e+01# (1.111632e+00)	1.185054e+02# (1.679308e+00)	1.078721e+02# (2.347639e+00)
	10	2.249876e+02 (1.368722e+00)	2.075064e+02# (3.824826e+00)	2.079851e+02# (1.899257e+00)	1.810577e+02# (3.309000e+00)	2.118042e+02# (2.291510e+00)	1.931317e+02# (4.552358e+00)
DTLZ5^{-1}	3	1.069995e+02 (2.945855e-01)	8.469885e+01# (1.989703e+00)	7.942908e+01# (2.711812e-01)	8.622124e+01# (1.733700e-01)	8.484735e+01# (2.558670e+00)	8.305258e+01# (1.583665e+00)
	5	1.259747e+02 (3.780629e-03)	1.041424e+02# (3.722763e+00)	1.229014e+02# (1.837627e-01)	4.957223e+01# (1.976910e+00)	1.180479e+02# (1.846989e+00)	1.076183e+02# (2.710724e+00)
	10	2.199997e+02 (6.289321e-05)	1.579241e+02# (1.854156e+01)	1.997485e+02# (1.822188e+00)	1.636386e+02# (7.545337e+00)	2.094613e+02# (2.217251e+00)	1.946215e+02# (3.565477e+00)
DTLZ7^{-1}	3	2.345500e+01 (6.661044e+00)	2.375280e+01 (1.117994e+00)	2.588876e+01 (3.461387e+00)	1.994117e+01# (4.519640e-01)	2.178525e+01# (8.341601e-01)	1.805087e+01# (8.596927e+00)
	5	5.660901e+01 (1.568211e+01)	7.238636e+01 (1.269825e+01)	1.211841e+01# (1.172186e+00)	4.067053e+01# (9.192226e+00)	8.003609e+01 (3.156330e+00)	3.632242e+01# (3.834467e+01)
	10	2.043557e+02 (1.375176e+01)	1.347251e+01# (4.083423e+00)	4.293619e+00# (1.198274e-01)	8.812385e+00# (2.123041e+01)	2.008713e+02# (2.214667e+00)	2.028099e+02# (5.987172e+00)
WFG1^{-1}	3	6.415681e+01 (4.459890e+00)	5.511082e+01# (2.648385e+00)	1.663876e+01# (1.535080e+00)	4.730483e+01# (1.092483e+00)	4.842279e+01# (5.020350e+00)	4.279700e+01# (1.538301e+01)
	5	1.210334e+02 (2.192520e+00)	5.596308e+01# (5.654765e+00)	7.815456e+00# (1.225035e+00)	3.289189e+01# (2.858823e+00)	1.098994e+02# (4.122587e+00)	5.939438e+01# (3.673750e+01)
	10	2.186105e+02 (3.132639e-01)	6.927501e+01# (2.258115e+01)	2.480353e+00# (2.063527e+00)	3.476224e+01# (4.296041e+00)	1.950445e+02# (6.121614e+00)	1.138247e+02# (5.884228e+01)
WFG2^{-1}	3	1.140860e+02 (4.325357e-01)	9.532850e+01# (1.992380e+00)	8.890140e+01# (1.794800e-01)	9.018353e+01# (4.679018e-01)	3.230763e+00# (4.485117e-02)	2.757698e+00# (2.020626e-01)
	5	1.234346e+02 (7.027142e-01)	9.827363e+01# (2.826007e+00)	4.956629e+01# (8.529213e+00)	3.689443e+01# (1.559225e+00)	5.922537e+00# (7.879377e-01)	2.841850e+00# (6.498607e-01)
	10	2.196197e+02 (9.739353e-02)	2.001692e+02# (4.030917e+00)	2.500717e+01# (2.754994e+00)	1.075588e+02# (1.284360e+01)	1.138578e+01# (8.309404e-01)	7.783812e+00# (1.059255e+00)
WFG3^{-1}	3	1.075596e+02 (2.777510e-01)	7.484580e+01# (2.494935e+00)	6.164392e+01# (7.387154e-02)	7.097018e+01# (1.699291e-01)	2.303097e+01# (7.406376e-01)	2.381595e+01# (2.661523e-01)
	5	1.259055e+02 (2.786019e-02)	8.633630e+01# (4.246132e+00)	6.654930e+01# (3.739241e+00)	3.937358e+01# (1.177063e+00)	3.626087e+01# (2.423541e+00)	4.063424e+01# (2.006301e+00)
	10	2.199995e+02 (8.710466e-04)	1.929382e+02# (8.857025e+00)	5.251797e+01# (3.065445e+00)	1.414077e+02# (1.791224e+01)	7.135125e+01# (7.053632e+00)	9.336338e+01 (4.573319e+00)

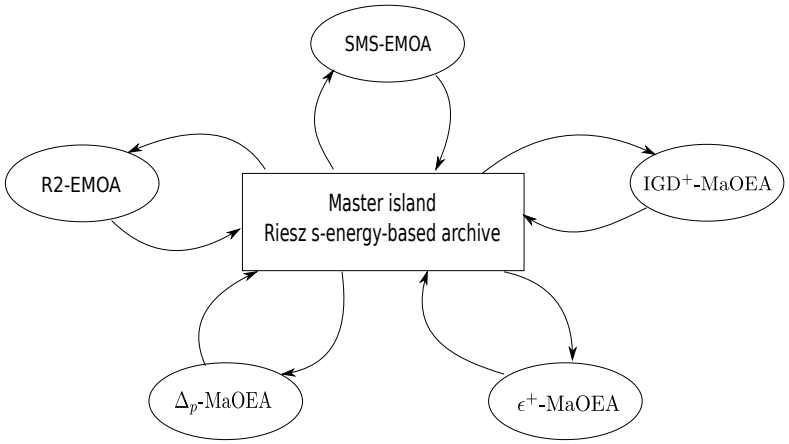

Figure 6.4: cMIB-MOEA is composed of five islands (each one executing a specific IB-MOEA) and a master island that manages a Riesz s-energy-based archive. The communication between the master island and the other islands is bidirectional.

process to increase the diversity of the islands.

6.4.1 Our Proposed Approach

In this section, we describe our proposal, called Cooperative Multi-Indicator-based MOEA (cMIB-MOEA). Our proposed cMIB-MOEA relies on the cooperation of five IB-MOEAs: SMS-EMOA, R2-EMOA, IGD$^+$-MaOEA and two more IB-MOEAs very similar to IGD$^+$-MaOEA but using the indicators ϵ^+ and Δ_p that are denoted as ϵ^+-MaOEA and Δ_p-MaOEA, respectively. To make possible the cooperation between the IB-MOEAs, cMIB-MOEA uses an island model as shown in Fig. 6.4. Additionally, a Riesz s-energy-based archive $\mathcal{A}$ is employed to maintain uniformly distributed solutions coming from the IB-MOEAs. Algorithm 13 outlines the master island that controls each island associated with an IB-DE, and it also manages $\mathcal{A}$. cMIB-MOEA requires as a parameter a set of indicators; in our case, we use HV, R2, IGD$^+$, ϵ^+, and Δ_p. Each indicator is associated with the above mentioned IB-MOEAs. For each indicator $I_j, j = 1, \ldots, k$, a subpopulation P_j of size μ/k is randomly initialized, where μ is the size of $\mathcal{A}$. Additionally, the structures of the j^{th} IB-MOEA are also initialized. Then, in line 5, the set of nondominated solutions extracted from all the subpopulations is used to initialize $\mathcal{A}$. Lines 6 to 15 outline the main loop of cMIB-MOEA. First, all the IB-MOEAs are independently executed during $fmig$ generations, using Algorithm 14, for updating their corresponding subpopulations. In line 9, the current archive is combined with all the subpopulations and, then, the set of nondominated solutions is extracted. If the contents of the archive is greater than μ, a density estimator based on the Riesz s-energy indicator is applied to reduce its size to μ. Finally, in line 15, the migration process, described in Algorithm 15, is executed. cMIB-MOEA returns the archive as its final solution set. In the following, we describe Algorithms 14 and 15.

Algorithm 13: cMIB-MOEA general framework

Input: Number $nmig$ of solutions to migrate; migration frequency $fmig$; Population size μ; Set of indicators $\mathcal{I} = \{I_1, \ldots, I_k\}$

Output: Pareto front approximation

Set archive $\mathcal{A}$ as empty;
for $j = 1$ *to* k **do**
    Randomly initialize subpopulation P_j of size μ/k;
    Initialize the j^{th} IB-MOEA;
end
$\mathcal{A} \leftarrow Nondominated(\bigcup_{j=1}^{k} P_j)$;
while *stopping criterion is not fulfilled* **do**
    for $j = 1$ *to* k **do**
        $P_j \leftarrow$ IB-MOEA$(P_j, I_j, fmig)$;
    end
    $\mathcal{A} \leftarrow \mathcal{A} \cup \left\{\bigcup_{j=1}^{k} P_j\right\}$;
    $\mathcal{A} \leftarrow Nondominated(\mathcal{A})$;
    Obtain $\vec{z}^{*}$ and $\vec{z}^{\text{nad}}$ from $\mathcal{A}$ to normalize $\mathcal{A}$;
    while $|\mathcal{A}| > \mu$ **do**
        $\vec{a}_{\text{worst}} \leftarrow \arg\max_{\vec{a} \in \mathcal{A}} C_{E_s}(\vec{a}, \mathcal{A})$;
        $\mathcal{A} \leftarrow \mathcal{A} \setminus \{\vec{a}_{\text{worst}}\}$;
    end
    $\{P_1, \ldots, P_k\} \leftarrow$ Migration$(nmig, \{P_1, \ldots, P_k\}, \{I_1, \ldots, I_k\})$;
end
return $\mathcal{A}$

Algorithm 14 describes the general framework proposed by Beume *et al.* in SMS-EMOA [8]. However, in this case, we describe it in a generic way so that the IB-MOEA works with a given indicator I from the set $\{\text{HV}, \text{R2}, \text{IGD}^+, \epsilon^+, \Delta_p\}$. Since each IB-MOEA is executed at every step of cMIB-MOEA during $fmig$ generations, this number is the stopping condition of the loop in line 2. At every generation, a single offspring is generated and, then, added to the main population. The joint population Q is ranked, using the nondominated sorting algorithm to produce the layers $R1, \ldots, R_t$, where R_t has the worst solutions according to the Pareto dominance relation. If this layer has more than one solution, all the individual contributions to the indicator I are calculated using equation (3.11) and obtaining the solution $\vec{r}_{\text{worst}}$ with the minimal C value. Then, $\vec{r}_{\text{worst}}$ is deleted from Q and P is updated in line 11.

Algorithm 14: Generic steady-state IB-MOEA

Input: Population P; Indicator I; migration frequency $fmig$
Output: Updated population P

1 $g \leftarrow 0$;
2 **while** $g < fmig$ **do**
3 Generate offspring $\vec{q}$ from population P;
4 $Q \leftarrow P \cup \{\vec{q}\}$;
5 Obtain $\vec{z}^*$ and $\vec{z}^{\text{nad}}$ from Q and normalize it;
6 $\{R_1, \ldots, R_t\} \leftarrow NDsorting(Q)$;
7 **if** $|R_t| > 1$ **then**
8 $\vec{r}_{\text{worst}} \leftarrow \arg\min_{\vec{r} \in R_t} C_I(\vec{r}, R_t)$;
9 **end**
10 **else**
11 $\vec{r}_{\text{worst}}$ is the single solution in R_t;
12 **end**
13 $P \leftarrow Q \setminus \{\vec{r}_{\text{worst}}\}$;
14 $g \leftarrow g + 1$;
15 **end**
16 **return** P

The migration process of cMIB-MOEA is rather simple. If the archive has more than $nmig$ solutions, then migration is possible. To the j^{th} population, we only migrate solutions from $\mathcal{A}$ that were not produced by the j^{th} IB-MOEA. In other words, P_j can receive solutions from all other populations $P_i, i \neq j$. The selection of the $nmig$ solutions to be migrated to P_j is randomized. The selected $nmig$ solutions will replace the worst $nmig$ contributing solutions to the indicator I_j, previously computed. In this case, we employ an elitist replacement scheme.

An essential aspect that it is worth to emphasize is why we employ SMS-EMOA in spite of its high computational cost. Hernández and Coello [58] empirically showed that when using SMS-EMOA with micro-populations, i.e., populations of no more

Algorithm 15: Migration

Input: Number *nmig* of solutions to migrate; Set of subpopulations $\{P_1, \ldots, P_k\}$; Set of indicators $\{I_1, \ldots, I_k\}$
Output: Updated subpopulations

```
if |A| > nmig then
    for j = 1 to k do
        if there are nmig solutions in A that were not produced by the j^th
         IB-MOEA then
            Randomly select nmig solutions from A that were not generated by
             the j^th IB-MOEA;
            Replace from P_j its nmig worst-contributing solutions to I_j, using
             the previously selected solutions;
        end
    end
end
return {P_1, ..., P_k}
```

than 30 individuals, then, the running time of SMS-EMOA remains relatively constant even if the number of objective functions increases. Based on this fact, we set the size of each subpopulation equals to μ/k such that this number does not exceed 30 individuals.

6.4.2 Experimental Results

In this section, we analyze the performance of cMIB-MOEA[17] when compared to panmictic versions of SMS-EMOA, R2-EMOA, IGD$^+$-MaOEA, ϵ^+-MaOEA, and Δ_p-MaOEA. We adopted MOPs from the Deb-Thiele-Laumanns-Zitzler (DTLZ) [32], Walking-Fish-Group (WFG) [65], Lamé superspheres [38], Viennet (VIE) [133], and the DTLZ^{-1} and WFG^{-1} test suites [75]. Table 6.7 summarizes the MOPs that we employed for two and three objective functions, emphasizing their Pareto front shapes. For each test instance, we performed 30 independent executions. The performance of cMIB-MOEA and the adopted IB-MOEAs was compared using the quality indicators HV, R2, IGD$^+$, ϵ^+, Δ_p. However, as each of these QIs prefers the IB-MOEA that uses it as its IB-DE, we decided to leave aside that IB-MOEA for a fair comparison. For example, when comparing performance using HV, we included all the adopted IB-MOEAs except for SMS-EMOA. Additionally, we employed the Hausdorff distance as a neutral convergence measure and the Solow-Polasky indicator for diversity [39].

[17]The source code of cMIB-MOEA is available at `http://computacion.cs.cinvestav.mx/~jfalcon/cMIBMOEA/cMIB-MOEA.html`

6.4.2.1 Parameter Settings

For a fair comparison, cMIB-MOEA and the other IB-MOEAs use the same population size μ as described in Table 6.8. For both two and three objective functions $\mu = C_{m-1}^{H^1+m-1}$, where this combinatorial number determines how many convex weight vectors (as required by R2-EMOA) are generated via the Simplex-Lattice-Design method. All subpopulations are set to $\mu/5$, where five is the number of subpopulations. The stopping criterion of all the MOEAs is the maximum number of function evaluations (MaxFeval). Additionally, Table 6.8 indicates the $fmig$ and $nmig$ parameters of cMIB-MOEA. All the adopted IB-MOEAs utilize Simulated Binary Crossover (SBX) and polynomial-based mutation as their variation operators. In all cases, the crossover probability and the mutation probability were set to 0.9 and $1/n$ (where n is the number of decision variables), respectively. Both the crossover distribution index and the mutation distribution index are equal to 20. Regarding the MOPs, the number of variables of problems DTLZ, DTLZ^{-1}, Lamé and Mirror is $n = m + K - 1$, where $K = 10$ for DTLZ2 and DTLZ5 and their minus versions, $K = 20$ for DTLZ7 and DTLZ7^{-1}, and $K = 5$ in all Lamé and Mirror instances that are determined by a different γ value as shown in Table 6.7. Considering the WFG and WFG^{-1} problems, the number of variables are 24 and 26 for two and three objectives, respectively; in both cases, the number of position-related parameters is two. The decision space of the three Viennet problems is of dimension two.

6.4.2.2 Discussion of Results

The comparison of cMIB-MOEA with the panmictic IB-MOEAs has two main goals: 1) determine that the cooperation between IB-MOEAs produces better global results, and 2) show that cMIB-MOEA is a more general multi-objective optimizer. Regarding the first goal, we compared the performance of cMIB-MOEA with the other IB-MOEAs using the QIs: HV, R2, IGD$^+$, ϵ^+, Δ_p, the Hausdorff distance and the Solow Polasky indicator. From these QIs, the Hausdorff distance is the only neutral convergence measure, i.e., none of the MOEAs uses it as an IB-DE. Table 6.9 shows the mean and standard deviation of all IB-MOEAs on each test instance, regarding the Hausdorff distance. It is worth noting that the reference set required by this metric (and also by IGD$^+$, ϵ^+, and Δ_p) was built uniformly sampling the true Pareto front of all problems, producing sets of size 200 and 300 for two- and three-dimensional MOPs, respectively. From Table 6.9, cMIB-MOEA is the best optimizer since it obtained the best value in 14 out of 39 problems while SMS-EMOA obtained the second best-ranked MOEA, having the best result in 9 out of 39 MOPs. In order to reinforce the evidence that the cooperation between the individual IB-MOEAs benefits cMIB-MOEA, we also compared it using their baseline QIs, i.e., HV, R2, IGD$^+$, ϵ^+, and Δ_p. Tables B.14 to B.19 show the numerical results for the above mentioned QIs, respectively and Fig. 6.6 summarize the results. This figure is a heat map that shows the number of times that each IB-MOEA was ranked first or second according to the above mentioned QIs. Based on this figure, cMIB-MOEA is also the best optimizer

Table 6.7: Adopted MOPs in the study. For each case, the Pareto front geometry is described, indicating if it is correlated with the shape of a simplex.

MOP	**Pareto front shape**	**Simplex-like**
DTLZ2	Concave	Yes
DTLZ2^{-1}	Convex	No
DTLZ5	Degenerate	No
DTLZ5^{-1}	Convex	No
DTLZ7	Disconnected	No
DTLZ7^{-1}	Disconnected	No
WFG1	Mixed	Yes
WFG1^{-1}	Mixed	No
WFG2	Disconnected	Yes
WFG2^{-1}	Slightly concave	No
WFG3	Degenerate	No
WFG3^{-1}	Linear	No
Lamé $\gamma = 0.25$	Highly convex	No
Lamé $\gamma = 1.00$	Linear	Yes
Lamé $\gamma = 5.00$	Highly concave	Yes
Mirror $\gamma = 0.25$	Highly concave	No
Mirror $\gamma = 1.00$	Linear	No
Mirror $\gamma = 5.00$	Highly convex	No
VIE1	Convex	No
VIE2	Mixed (convex and degenerate)	No
VIE3	Degenerate	No

Table 6.8: Parameters adopted in the comparison. H^1 and H^2 are the parameters for the generation of the set of weight vectors of the R2-EMOA used by cMIB-MOEA and the corresponding panmictic version.

Dim.	$\boldsymbol{H^1}$	$\boldsymbol{H^2}$	$\boldsymbol{\mu}$	$\boldsymbol{\mu/5}$	**Maxfeval**	$\boldsymbol{fmig}$	$\boldsymbol{nmig}$
2	19	99	100	20	50,000	20	5
3	5	13	105	21	60,000	21	5

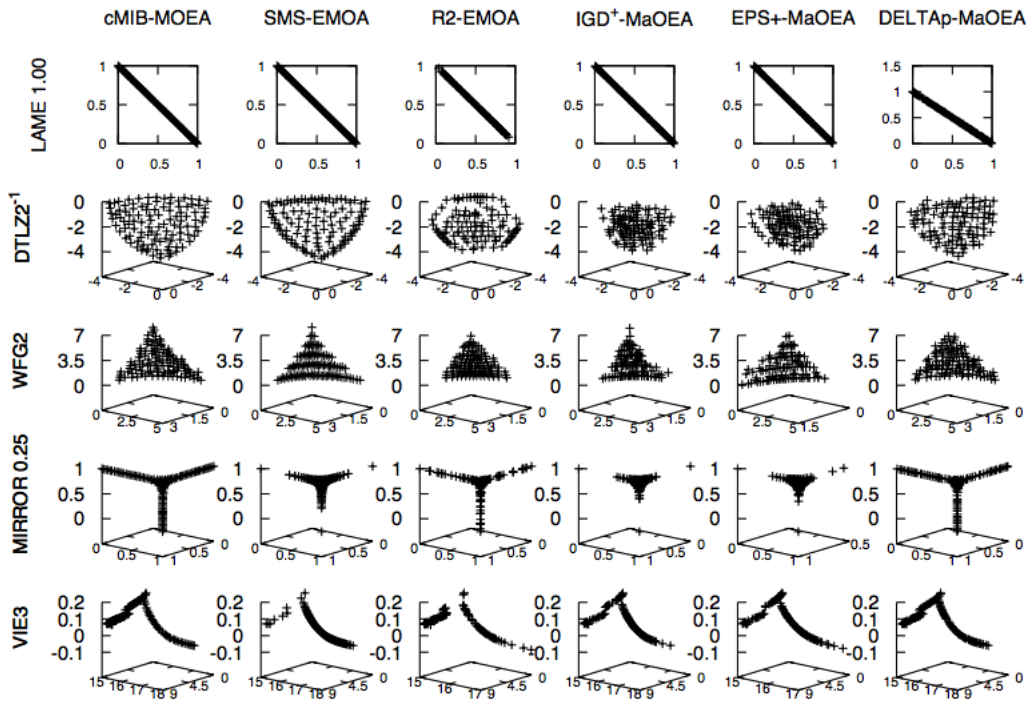

Figure 6.5: Pareto fronts generated by cMIB-MOEA and the adopted IB-MOEAs. Each front corresponds to the median of the Solow Polasky value.

regarding the HV, R2, and Δ_p indicators, and it obtained the second place for IGD$^+$ and ϵ^+. cMIB-MOEA obtained the first place in 27 out of 39 MOPs, regarding HV while for both R2 and Δ_p, it is the best MOEA in 22 test instances. As we explained above, the decision of leaving aside, for example, SMS-EMOA when making an HV-based comparison is to avoid the preference that HV has towards SMS-EMOA and, with the aim of providing unbiased results. In the light of the experimental results, we have the first insight that the cooperation between individual IB-MOEAs instead of using panmictic versions of them, improves the quality of an optimizer. Since each individual IB-MOEA is exploring and exploiting different regions of the Pareto front, according to its QI-based preferences, cMIB-MOEA takes advantage of the strengths of each IB-MOEA to improve the global behavior. Additionally, we performed some experiments in order to determine the impact of the migration process, and we concluded that it helps to improve the search progress. In consequence, we claim that the cooperation is the responsible for getting better results, since cMIB-MOEA is the best optimizer in four out of six convergence measures, i.e., HV, R2, Δ_p, and the Hausdorff Distance and it gets the second place in the remaining ones, i.e., IGD$^+$ and ϵ^+.

The second goal of our experiments is to obtain evidence showing that cMIB-MOEA is a more general optimizer, i.e., that its performance does not depend on the Pareto front shape as it happens with other MOEAs [75]. Once we know that cMIB-MOEA has better convergence results, it is possible to analyze the Pareto fronts of all

the adopted IB-MOEAs using the Solow Polasky Diversity indicator (SPD). Fig. 6.6 reveals that distributions generated by cMIB-MOEA have the best SPD value in 33 out of 39 test instances. In consequence, cMIB-MOEAs outperforms the panmictic versions of SMS-EMOA, R2-EMOA, IGD^+-MaOEA, ϵ^+-MaOEA, and Δ_p-MaOEA, which indicates that its performance is good when dealing with complex Pareto front shapes as shown in Table 6.7. Figure 6.5 shows a comparison of Pareto fronts produced by cMIB-MOEA and the adopted IB-MOEAs. From this figure, we can see that the cMIB-MOEA produces evenly distributed Pareto fronts independently of the associated geometry. This behavior is not as evident in the other IB-MOEAs.

Table 6.9: Mean and standard deviation (in parentheses) of the Hausdorff distance. A symbol # is placed when cMIB-MOEA performed significantly better than the other IB-MOEAs based on a one-tailed Wilcoxon test, using a significance level of $\alpha = 0.05$. The two best values are shown in gray scale, where the darker tone corresponds to the best value.

MOP	Dim.	cMIB-MOEA	SMS-EMOA	R2-EMOA	IGD$^+$-MaOEA	ϵ^+-MaOEA	Δ_p-MaOEA
DTLZ2	2	1.105384e-02 (9.270729e-04)	3.173838e-02# (1.613701e-03)	9.590904e-03 (1.391367e-04)	5.901683e-02# (8.997635e-03)	5.888548e-02# (1.039106e-02)	2.202810e-02# (1.382455e-02)
	3	1.092411e-01 (5.923393e-03)	1.594444e-01# (4.319644e-03)	9.818462e-02 (4.189210e-04)	1.976556e-01# (1.981525e-02)	1.924996e-01# (2.326289e-02)	1.390080e-01# (1.353515e-02)
DTLZ2^{-1}	2	3.788524e-02 (2.808735e-03)	7.352529e-02# (4.638478e-03)	1.631498e+00# (2.864086e-01)	3.803191e-01# (9.505168e-02)	3.970059e-01# (9.754773e-02)	6.172824e-02# (7.946931e-03)
	3	3.699226e-01 (1.824022e-02)	4.168909e-01# (1.539622e-02)	1.384586e+00# (1.464603e-01)	1.289982e+00# (1.636542e-01)	1.288563e+00# (1.892405e-01)	5.732136e-01# (9.746681e-02)
DTLZ5	2	1.144525e-02 (2.091661e-03)	3.121338e-02# (1.973508e-03)	9.483349e-03 (1.314487e-04)	5.586760e-02# (9.183465e-03)	6.197110e-02# (1.253256e-02)	1.841037e-02# (5.364925e-03)
	3	1.222078e-02 (4.516118e-03)	3.331912e-02# (1.979639e-03)	7.259896e-02# (3.636487e-02)	5.756635e-02# (1.250585e-02)	5.937786e-02# (1.155631e-02)	1.846343e-02# (3.622081e-03)
DTLZ5^{-1}	2	3.811842e-02 (2.470698e-03)	7.833632e-02# (4.100489e-03)	1.611194e+00# (2.759175e-01)	3.779225e-01# (1.242316e-01)	4.104359e-01# (1.043483e-01)	6.285257e-02# (1.445305e-02)
	3	3.144057e-01 (1.871137e-02)	3.854935e-01# (1.594254e-02)	1.375219e+00# (2.965503e-01)	1.158505e+00# (1.802020e-01)	1.223359e+00# (2.628891e-01)	5.038938e-01# (1.127651e-01)
DTLZ7	2	6.069350e-02 (2.496451e-01)	2.115424e-02 (1.394340e-03)	5.462852e-02 (6.044331e-02)	7.816969e-02# (2.465541e-01)	3.257727e-02 (7.789854e-03)	3.384385e-02 (2.748613e-02)
	3	3.477614e-01 (4.239738e-01)	6.813853e-01# (4.366072e-01)	3.168888e-01 (2.950831e-01)	4.690831e-01# (3.918240e-01)	6.705290e-01# (6.218506e-01)	6.520370e-01# (5.645169e-01)
DTLZ7^{-1}	2	8.858600e-03 (4.680836e-03)	1.180794e-02# (1.042123e-03)	3.498117e-02# (1.530521e-02)	1.713431e-02# (5.742480e-03)	1.656072e-02# (4.531754e-03)	1.278824e-02# (2.264126e-03)
	3	5.376569e-01 (1.845419e-01)	5.226155e-01 (1.108634e-01)	5.009742e-01 (1.179733e-01)	5.716971e-01# (1.722787e-01)	5.834904e-01# (1.787834e-01)	5.136677e-01 (1.140769e-01)
WFG1	2	1.872677e+00 (6.490135e-01)	2.144039e+00# (4.656587e-01)	2.781527e+00# (4.513154e-01)	2.084150e+00# (5.979649e-01)	2.274507e+00# (2.864709e-01)	2.260408e+00# (2.907941e-01)
	3	2.779055e+00 (3.589481e-01)	2.299031e+00 (2.955950e-01)	2.842268e+00# (3.041895e-01)	3.108680e+00# (3.236080e-01)	3.227137e+00# (1.808980e-01)	3.084785e+00# (3.347422e-01)
WFG1^{-1}	2	2.193076e+00 (6.692088e-01)	2.460818e+00# (3.054873e-01)	3.587648e+00# (3.319739e-02)	2.425968e+00# (5.121160e-01)	2.487955e+00# (5.919251e-01)	2.010333e+00 (7.165466e-01)
	3	3.023132e+00 (7.234743e-01)	3.178590e+00# (4.988111e-01)	3.663829e+00# (3.787046e-02)	3.568923e+00# (1.927237e-01)	3.704674e+00# (4.030209e-02)	3.484878e+00# (2.869542e-01)
WFG2	2	6.510102e-01 (4.642023e-01)	7.509476e-01# (4.184325e-01)	7.049981e-01# (3.837817e-01)	8.250346e-01# (3.655539e-01)	5.792721e-01 (4.581925e-01)	7.594202e-01# (4.075064e-01)
	3	1.478811e+00 (1.087477e-01)	1.992816e+00# (6.342904e-02)	1.977591e+00# (5.231918e-02)	2.117238e+00# (1.639465e-01)	2.142116e+00# (2.007878e-01)	1.461806e+00 (2.294549e-01)
WFG2^{-1}	2	2.872757e-02 (3.355407e-03)	2.506092e-02 (1.060659e-03)	1.617072e-01# (6.794276e-02)	4.626452e-02# (7.036978e-03)	4.659729e-02# (7.037695e-03)	4.722215e-02# (5.741114e-03)
	3	4.547563e-01 (3.543713e-02)	1.343296e+00# (6.894212e-02)	7.481390e-01# (6.541303e-02)	9.564823e-01# (1.533654e-01)	9.681967e-01# (1.663861e-01)	6.546428e-01# (1.130453e-01)
WFG3	2	3.433451e-02 (2.669749e-03)	2.694516e-02 (1.619053e-03)	5.124899e-01# (1.930205e-01)	5.335781e-02# (1.258117e-02)	4.742735e-02# (1.091492e-02)	5.758475e-02# (1.446585e-02)
	3	2.153750e+00 (3.335947e-02)	2.094386e+00 (4.249273e-02)	2.120770e+00 (4.575346e-02)	1.437151e+00 (1.419643e-01)	1.394558e+00 (1.555797e-01)	1.737576e+00 (1.254863e-01)
WFG3^{-1}	2	3.115905e-02 (2.233907e-03)	2.413419e-02 (8.927896e-04)	4.257092e-01# (1.720072e-01)	5.551999e-02# (1.297264e-02)	5.153979e-02# (1.523855e-02)	5.393184e-02# (1.070818e-02)
	3	3.271397e-01 (1.790222e-02)	4.234791e-01# (2.478000e-02)	5.930895e-01# (9.457878e-02)	4.351743e-01# (4.750045e-02)	5.659076e-01# (1.642249e-01)	4.833494e-01# (1.070514e-01)
LAME $\gamma = 0.25$	2	1.022964e-01 (4.251508e-04)	7.199513e-02 (1.597357e-03)	7.790940e-01# (5.055874e-02)	4.493894e-01# (6.963783e-02)	4.163650e-01# (8.842754e-02)	1.076818e-01# (1.009479e-02)
	3	2.181521e-01 (9.166538e-02)	3.306315e-01# (4.715269e-02)	7.909163e-01# (3.595584e-02)	7.110521e-01# (4.389321e-02)	7.342863e-01# (2.043919e-02)	2.176095e-01 (5.148371e-02)

Table 6.9 – *Continuation*

MOP	Dim.	cMIB-MOEA	SMS-EMOA	R2-EMOA	IGD$^+$-MaOEA	ϵ^+-MaOEA	Δ_p-MaOEA
LAME $\gamma = 1.00$	2	1.233049e-02 (1.295561e-02)	7.492362e-03 (2.686326e-04)	9.955142e-02# (5.413129e-02)	1.391223e-02 (2.175235e-03)	1.414534e-02# (2.384110e-03)	1.657829e-02# (4.202435e-03)
	3	8.615970e-02 (1.671945e-02)	7.227939e-02 (4.298681e-03)	6.209480e-02 (4.602889e-03)	1.097183e-01# (1.840681e-02)	1.210148e-01# (2.856508e-02)	1.039719e-01# (1.373382e-02)
LAME $\gamma = 5.00$	2	3.559403e-02 (1.292145e-03)	1.401908e-01# (1.961413e-03)	3.420893e-02 (7.261769e-05)	2.214712e-01# (1.573873e-02)	2.128242e-01# (1.431933e-02)	3.450596e-02 (2.787760e-03)
	3	1.350820e-01 (8.562792e-03)	3.581202e-01# (9.384830e-03)	1.500124e-01# (2.721855e-04)	4.019987e-01# (1.775541e-02)	3.900596e-01# (3.091858e-02)	1.837234e-01# (2.418483e-02)
MIRROR $\gamma = 0.25$	2	4.790673e-02 (2.298588e-03)	1.691297e-01# (4.416528e-03)	4.996473e-02 (3.078737e-05)	2.797045e-01# (1.626290e-02)	2.887144e-01# (2.052701e-02)	4.789617e-02 (2.289451e-03)
	3	4.546330e-02 (4.264168e-03)	2.399739e-01# (3.823196e-03)	9.488459e-02# (1.195802e-02)	3.408904e-01# (1.539832e-02)	4.277988e-01# (1.271120e-01)	4.936646e-02# (5.774740e-03)
MIRROR $\gamma = 1.00$	2	9.824648e-03 (8.012889e-04)	7.610307e-03 (2.856453e-04)	8.211471e-02# (4.629837e-02)	1.297673e-02# (1.605581e-03)	1.339788e-02# (2.260016e-03)	1.584752e-02# (3.354279e-03)
	3	8.149582e-02 (4.428020e-03)	9.869028e-02# (3.037584e-03)	1.355981e-01# (1.433308e-02)	1.017920e-01# (1.173971e-02)	1.077039e-01# (1.064985e-02)	1.177466e-01# (2.897291e-02)
MIRROR $\gamma = 5.00$	2	6.923700e-02 (3.416160e-03)	5.861688e-02 (1.416267e-03)	7.132397e-01# (5.417028e-02)	3.364190e-01# (4.422825e-02)	3.267493e-01# (5.924901e-02)	6.846537e-02 (4.729740e-03)
	3	1.804210e-01 (8.209513e-03)	3.406023e-01# (3.904404e-03)	7.781739e-01# (2.151215e-02)	7.651215e-01# (5.207308e-02)	7.749160e-01# (4.590298e-02)	2.092879e-01# (2.264808e-02)
VIE1	3	1.552675e+00 (7.068297e-02)	1.474508e+00 (5.003594e-03)	1.165155e+00 (2.271376e-01)	1.086031e+00 (3.372768e-01)	1.112837e+00 (3.207447e-01)	1.556628e+00 (9.208280e-02)
VIE2	3	6.330866e-02 (1.959696e-02)	8.020737e-02# (7.431943e-03)	4.439421e-01# (2.447103e-01)	5.004996e-01# (1.673603e-01)	5.041798e-01# (1.984323e-01)	6.229146e-02 (1.629636e-02)
VIE3	3	3.597395e+01 (6.800830e-03)	3.597358e+01 (2.920827e-03)	3.578840e+01 (1.476454e-01)	3.575047e+01 (1.663358e-01)	3.575928e+01 (1.427880e-01)	3.595831e+01 (2.397284e-02)

6.5 Summary

Employing multiple IB-Mechanisms in a single MOEA or multiple IB-MOEAs that work together has been a scarcely explored research topic. In this Chapter, we explored both ideas to design MOEAs whose performance does not depend on the MOP being tackled. On the one hand, we designed the IGD^+-based Many-Objective Evolutionary Optimizer (IGD^+-MaOEA), using an IGD^+-based density estimator. We found that IGD^+-MaOEA performed well on MOPs with different Pareto front shapes. Although IGD^+-MaOEA generates Pareto front approximations similar to those of SMS-EMOA, they are not very uniform. Hence, we proposed to combine the individual effect of the IGD^+-DE with a density estimator based on the Riesz s-energy indicator which promotes uniform distributions on the large class of d-dimensional manifolds. The resulting algorithm was called CRI-EMOA and its performance was found to be superior to that of IGD^+-MaOEA, producing uniformly distributed solutions on several Pareto front shapes. Finally, we explored the cooperation of multiple steady-state IB-MOEAs through the island model. In this approach, SMS-EMOA, R2-EMOA, IGD^+-MaOEa, ϵ^+-MaOEA, and Δ_p-MaOEA evolved micro-populations in an isolated way and after a given number of iterations, a master island gathers all the subpopulations to keep the best ones, according to the Riesz s-energy indicator, in an external archive. The experimental results showed that the weakness of an IB-MOEA were compensated by the strengths of the others, producing better convergence and diversity results than panmictic versions of any of the individual IB-MOEAs employed.

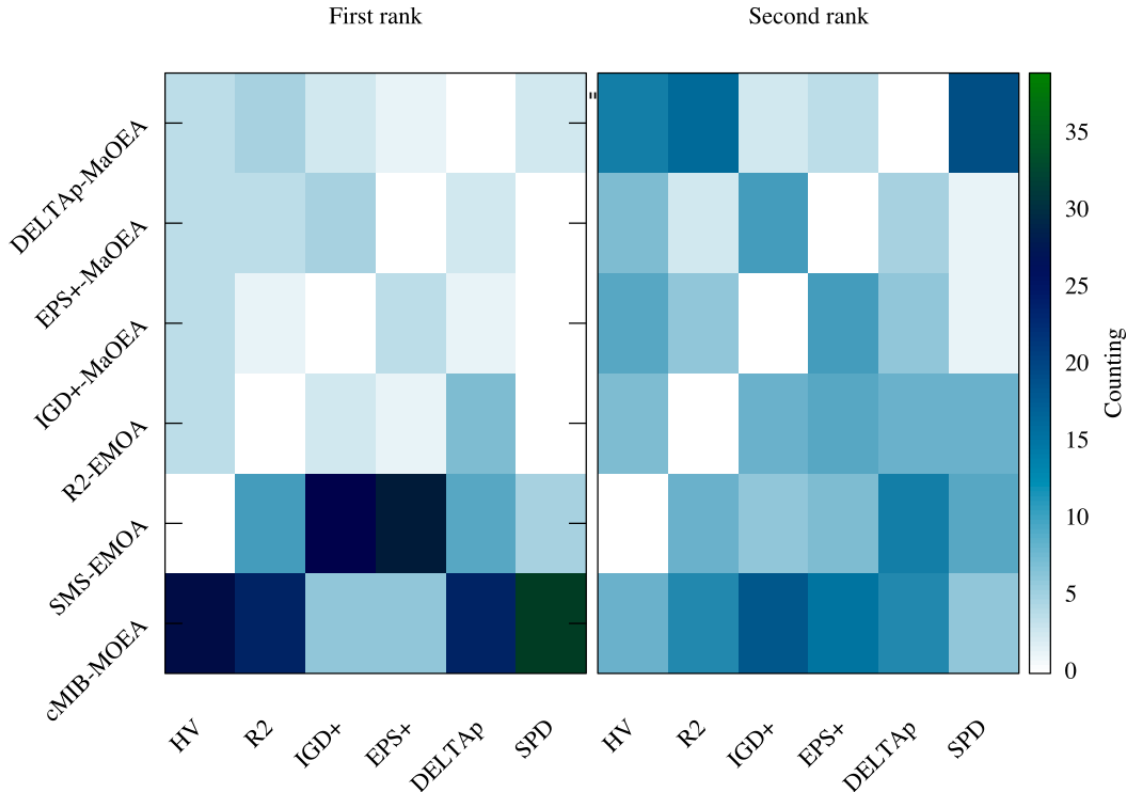

Figure 6.6: Heat map that reveals the number of times an IB-MOEA ranked first or second according to the indicators HV, R2, IGD^+, ϵ^+, Δ_p, and SPD.

Chapter 7

On the Combination of Quality Indicators

This chapter explores the mathematical combination of QIs to produce new ones having the Pareto-compliance property. Section 7.1 highligths the motivation to design new Pareto-compliant QIs. The previous related work on the combination of QIs is briefly described in Section 7.2. The mathematical development on the combination of QIs is depicted in Section 7.3. Section 7.4 presents the results of two experiments: (1) an analysis of preferences, and (2) an empirical study of the optimal μ-distributions. In Section 7.5 we propose an MOEA which exploits the trade-off between a convergence indicator and a diversity one, following the combination scheme of QIs. Finally, a summary of the chapter is introduced in Section 7.6.

7.1 Motivation

For almost two decades, several quality indicators have been proposed to compare MOEAs' approximation sets [95]. Among the plethora of currently available QIs, those focused on assesing convergence towards the Pareto optimal front are the most remarkable. A number of researchers have studied the mathematical properties of convergence QIs [158, 2, 118, 9, 71, 74, 17], being Pareto compliance (see Property 3.1.1) the most important one. Given two approximation sets $\mathcal{A}$ and $\mathcal{B}$, a Pareto-compliant QI (I) ensures that if $\mathcal{A} \lhd \mathcal{B}$, then $I(\mathcal{A}) > I(\mathcal{B})$, i.e., the QI reflects the order structure imposed by $\lhd$. QIs having this property do not produce misleading results, according to the Pareto dominance relation, when evaluating approximation sets. Currently, the hypervolume indicator (see Section 3.1, in page 19) and its variants (i.e., the logarithmic HV [50], the weighted HV [2], and the free HV [40]) are the only Pareto-compliant QIs. Hence, an important research area is to prove the existence of other Pareto-compliant QIs, having different preferences to those of HV.

In this chapter, we investigate the existence of new Pareto-compliant QIs by proposing combinations of QIs. The combination of QIs implies generating new QIs that represent indicators that have preferences that are intermediate to those of the

individual indicators. It is worth mentioning that our proposed framework allows to produce a family of Pareto-compliant QIs based on the combination of one or more weakly Pareto-compliant indicators with at least one Pareto-compliant QI, using a vector-based function that is order-preserving. In consequence, the contributions are the following:

1. The construction of a family of Pareto-compliant QIs whose preferences are essentially different to those of HV.

2. This framework allows to correct weakly Pareto-compliant QIs, such as R2, IGD^+, and ϵ^+, by making them Pareto-compliant.

3. We introduce an empirical study of the approximate optimal μ-distributions of some of the new Pareto-compliant QIs, using a steady-state MOEA.

7.2 Previous Related Work

Knowles *et al.* [86] briefly explained that the combination of indicators, ideally using Pareto-compliant ones, could lead to powerful interpretations in constrast to employing a single QI. However, no mathematical definition was provided to this claim. In a subsequent work, Zitzler *et al.* [151] explained that the combination of indicators could lead to overcome the difficult situation of finding an ideal indicator, i.e., a QI being Pareto-compliant, scaling invariant, and cheap to compute. In consequence, one has to look for a way to combine the resulting indicator values. They first suggested the use of sequence of indicators to evaluate approximation sets. However, it was until 2010 when the use of sequence of indicators was mathematically supported [157]. In this work, Zitzler *et al.* defined new preference relations based on multiple indicators. The backbone of this proposal is to create a chain of refinements of indicator preferences. When one indicator is not able to decide which approximation set is better, the next one in the sequence is employed to refine the preferences, if possible. In consequence, the use of these indicator-based preference relations could increase the sensitivity of an order relation. Furthermore, they proposed to use these preference relations to create a selection mechanism strongly related to the non-dominated sorting algorithm [31].

In Section 3.2.2.1 in page 30, we described the DIVA algorithm [130] that employs an environmental selection mechanism based on a modified hypervolume indicator. Such HV variant is a combination of the original HV with a decision space diversity measure. The resulting indicator, named diversity integrating hypervolume indicator, performs a weak refinement of the order structure imposed by the diversity measure. However, due to the high complexity of the new indicator, it was only employed for bi-objective problems. A remarkable aspect is that the diversity could be significantly increased without worsening the HV value, and there were several cases where the hypervolume indicator is increased if diversity was also optimized.

In 2012, Schütze *et al.* [118] proposed the averaged Hausdorff distance (Δ_p) that can be regarded as a combined indicator. Δ_p combines the indicators GD_p and IGD_p into a single value by selecting the maximum value between both QIs. It is worth noting that Δ_p inherits the non-Pareto compliance of both QIs but it has other interesting properties such as a better management of outlier solutions in approximation sets and a preference for more uniform distributions of solutions.

Based on the use of sequence of indicators to refine order structures, Yen and He [145] proposed a framework for the comparison of MOEAs, using an ensemble of multiple indicators. The method is not a new QI but instead they proposed a double elimination tournament that uses a pool of multiple QIs to evaluate MOEAs and, thus, produce a ranking of them. This method allows that MOEAs having poor performance on some QIs are still able to be selected as the best performing algorithm. The ensemble method uses multiple QIs collectively to obtain a better assessment than what could be obtained from any single indicator.

7.3 Combination of Quality Indicators

In this section, we propose the first guideline to combine several QIs into a single value to generate new combined indicators. Additionally, we provide the mathematical argumentation to ensure that when combining QIs with specific properties, the resulting combined indicator will be Pareto-compliant. This leads not only to new types of indicators but also provides a mechanism to create new Pareto-compliant indicators with very different properties than the HV in terms of distributions of points that they favor, and in terms of parameters to be provided by the user. In the following, we present the mathematical development for the combination of QIs.

Definition 7.3.1 (Combination function)**.** *A combination function* $C : \mathbb{R}^k \to \mathbb{R}$ *assigns a real value to a vector* $\vec{I} = (I_1, I_2, \ldots, I_k)$*, where each* I_j *is the value of a unary indicator.*

Definition 7.3.2 (Combined Indicator)**.** *Given an indicator vector* $\vec{I} = (I_1, I_2, \ldots, I_k)$ *and a combination function* C*, a combined indicator* $\mathcal{I}$ *is defined as follows:* $\mathcal{I} = C(\vec{I})$*.*

A general combined indicator $\mathcal{I}$ is a function that maps a vector of indicator values to a single real value as it is stated in Definitions 7.3.1 and 7.3.2. Figure 7.1 shows how a combined indicator works. For a given MOP, Ψ contains the set of all approximation sets of a specific size. Based on an indicator vector $\vec{I}$, such approximation sets are evaluated and the obtained vector of indicator values is in the quality space Q. Finally, the combined indicator $\mathcal{I}$ maps the vector of indicator values to the real numbers. Based on the above definitions, nothing can be said about the properties of $\mathcal{I}$ at this point. Hence, for getting more important theoretical results, we should say something about the properties of each $I_j, j = 1, \ldots, k$ and the combination function. We are interested in analyzing the Pareto compliance of $\mathcal{I}$. Based on Properties 3.1.1 and 3.1.2, we construct a special vector of indicators that is necessary for the refinement of the combined indicator model.

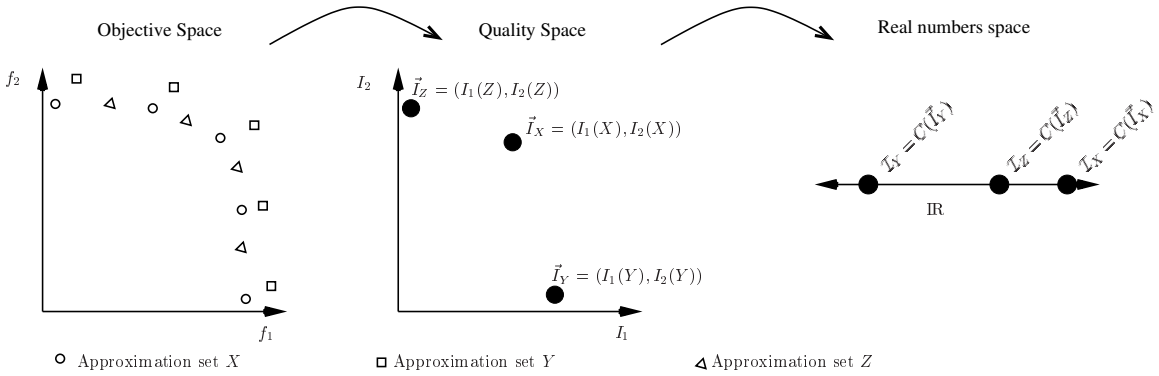

Figure 7.1: The objective space contains the approximation sets X, Y, and Z that are mapped to the quality space using an indicator vector. The points $\vec{I}_X, \vec{I}_Y$, and $\vec{I}_Z$ in quality space are then transformed to a single real value by the combination function $\mathcal{C} : \mathbb{R}^2 \to \mathbb{R}$ to generate the real values $\mathcal{I}_X, \mathcal{I}_Y$, and $\mathcal{I}_Z$.

Definition 7.3.3 (Compliant Indicator Vector)**.** *$\vec{I} = (I_1, I_2, \ldots, I_k) \in Q$ is called a compliant indicator vector (CIV) if $\forall j = 1, \ldots, k, I_j$ is weakly Pareto compliant and there exists at least an index $t \in \{1, \ldots, k\}$ such that I_t is Pareto compliant. $Q \subseteq \mathbb{R}^k$ is denoted as the quality space.*

For the following Theorem, let us assume, without loss of generality, that the unary indicators $I_1, \ldots, I_k$ are to be maximized.

Theorem 7.3.1 (Construction of Pareto-compliant combined indicators)**.** *Let $I_1, \ldots, I_k$ be unary indicators that form a compliant indicator vector $\vec{I}$. A combined indicator $\mathcal{I}(\vec{I})$ is $\lhd$-compliant if it has the order-preserving property:*

$$\forall \vec{u}, \vec{v} \in \mathbb{R}^k, \vec{u} \succ \vec{v} \Rightarrow \mathcal{I}(\vec{u}) > \mathcal{I}(\vec{v}).$$

Proof. Consider two approximation sets $\mathcal{A}$ and $\mathcal{B}$ such that $\mathcal{A} \lhd \mathcal{B}$ and let $\vec{I}^{\mathcal{A}} = \vec{I}(\mathcal{A})$ and $\vec{I}^{\mathcal{B}} = \vec{I}(\mathcal{B})$, where $\vec{I}$ is a CIV. Then, $\mathcal{A} \lhd \mathcal{B} \Rightarrow \vec{I}^{\mathcal{A}} \succ \vec{I}^{\mathcal{B}}$ because the Pareto-compliant indicators get better and the weakly Pareto-compliant ones get better or stay equal. Moreover, by definition $\vec{I}^{\mathcal{A}} \succ \vec{I}^{\mathcal{B}} \Rightarrow \mathcal{I}(\vec{I}^{\mathcal{A}}) > \mathcal{I}(\vec{I}^{\mathcal{B}})$. Hence, by transitivity of $\Rightarrow$, it holds $\mathcal{A} \lhd \mathcal{B} \Rightarrow \mathcal{I}(\vec{I}^{\mathcal{A}}) > \mathcal{I}(\vec{I}^{\mathcal{B}})$, i.e., $\mathcal{I}$ is Pareto-compliant. □

Theorem 7.3.1 provides a sufficient condition for constructing Pareto-compliant combined indicators on the basis of compliant indicator vectors. In other words, a combined indicator preserves the Pareto-compliant property because of the use of order-preserving combination functions.

Remark 7.3.1. *The condition of Theorem 7.3.1 is sufficient but not necessary. For instance, given $\vec{I} = (I_1, I_2, \ldots, I_k)$ where I_1 is Pareto-compliant and the $I_j, j = 2, \ldots, k$ are not Pareto-compliant, the "combined" indicator $\mathcal{I}(\vec{I}) = I_1$ is also Pareto-compliant. Hence, there is a large number of possibilities to construct combined indicators.*

An important question that arises is why it is important to construct new Pareto-compliant indicators. For answering this, let us show by means of an example that weak Pareto compliance is not sufficient as a guideline for constructing meaningful indicators. The example is an indicator which we will call Zero indicator. It is defined as $Z : \Psi \to \mathbb{R}$ with $Z \equiv 0$. Clearly, for every $\mathcal{A}, \mathcal{B} \in \Psi$ such that $\mathcal{A} \prec \mathcal{B}$, it implies $Z(\mathcal{A}) = Z(\mathcal{B})$, i.e., Z is weakly Pareto-compliant. Although indicators such as R2, IGD^+ and ϵ^+ are more complex than Z in a mathematical sense, all of them are weakly Pareto-compliant. Hence, we can see that is not enough to construct a weakly Pareto-compliant QI but Pareto compliance is desirable to avoid misleading results when comparing approximation sets. In consequence, there is a need of new Pareto-compliant indicators and weakly Pareto-compliant QIs can be employed to redefine the preferences of the hypervolume indicator.

There exists many combination functions that have the property of Theorem 7.3.1. However, in this paper, we focus on certain utility functions [108, 110] $u : \mathbb{R}^k \to \mathbb{R}$ that hold the desired property. A utility function (UI) is a model of the decision maker preferences that assigns to each k-dimensional vector a utility value. Thus, a combination function C can be defined in terms of these functions. Generally, UIs employ a convex weight vector $\vec{w} \in \mathbb{R}^k$ such that $\sum_{i=1}^{k} w_i = 1, w_i \geq 0$. This is indeed neccesary to show $u \succ v$, but in general it suffices if only a weight corresponding to one of the Pareto-compliant indicators is strictly positive. Based on the above, a Pareto-compliant utility indicator (PCUI) is defined as follows:

Definition 7.3.4 (Utility indicator)**.** *Given a utility function $u : \mathbb{R}^k \to \mathbb{R}$, an indicator vector $\vec{I} \in \mathbb{R}^k$ that assesses an approximation set $\mathcal{A}$ and a weight vector $\vec{w} \in \mathbb{R}^k$ such that $w_i > 0, i = 1, \ldots, k$, we denote a utility indicator as $u_{\vec{w}}(\vec{I}(\mathcal{A}))$. If u is also order-preserving as required in Theorem 7.3.1, $u_{\vec{w}}(\vec{I}(\mathcal{A}))$ is denoted as a Pareto-compliant utility indicator.*

In this work, we focused our attention on two utility functions that are order-preserving, namely, the weighted sum function (WS) and the augmented Tchebycheff function (ATCH) [108, 110]. However, there is a plethora of utility functions having this property. In the following, we prove that both WS and ATCH are order-preserving functions and, thus, can be employed to define PCUIs.

Definition 7.3.5. *The weighted sum (WS) is defined by the following formula:*

$$WS_{\vec{w}}(\vec{x}) = \sum_{i=1}^{k} w_i x_i, \tag{7.1}$$

where $\vec{x}, \vec{w} \in \mathbb{R}^k$ and $w_i \geq 0, i = 1, \ldots, k$.

Lemma 7.3.1. *Given two CIVs $\vec{x}, \vec{y} \in \mathbb{R}^k$ and a weight vector $\vec{w} \in \mathbb{R}^k, w_i > 0, i = 1, \ldots, k$, then if $\vec{x} \succ \vec{y} \Rightarrow WS_{\vec{w}}(\vec{x}) > WS_{\vec{w}}(\vec{y})$.*

Proof. Let's prove this lemma by induction. Let us consider, without loss of generality, that the first component of both CIVs is related to a Pareto-compliant indicator

and the rest of components are related to weakly Pareto-compliant indicators, i.e., $x_1 > y_1 \wedge x_i \geq y_i, i = 2, \ldots, k$.

Base case: for $k = 2$, we have $x_1 > y_1 \wedge x_2 \geq y_2$. Then $w_1x_1 + w_2x_2 > w_1y_1 + w_2y_2$.

Inductive hypothesis: Given $\vec{x}, \vec{y} \in \mathbb{R}^k$, then $\sum_{i=1}^{k} w_ix_i > \sum_{i=1}^{k} w_iy_i$.

Inductive step: We want to prove that $\sum_{i=1}^{k} w_ix_i + w_{k+1}x_{k+1} > \sum_{i=1}^{k} w_iy_i + w_{k+1}y_{k+1}$. Without loss of generality, let us assume that the $(k+1)$ components are related to a weakly Pareto-compliant indicator, then $x_{k+1} \geq y_{k+1}$ and for every $w_{k+1} > 0$ it follows that $w_{k+1}x_{k+1} \geq w_{k+1}y_{k+1}$. From the above statement and the inductive hypothesis, we have the following:

$$\sum_{i=1}^{k} w_ix_i + w_{k+1}x_{k+1} > \sum_{i=1}^{k} w_iy_i + w_{k+1}y_{k+1}$$
$$\mathrm{WS}_{\vec{w}}(\vec{x}) > \mathrm{WS}_{\vec{w}}(\vec{y})$$

Hence, $\vec{x} \succ \vec{y} \Rightarrow \mathrm{WS}_{\vec{w}}(\vec{x}) > \mathrm{WS}_{\vec{w}}(\vec{y})$.

□

For the Augmented Tchebycheff function, we assume without loss of generality that $\vec{x} \in \mathbb{R}^k_+$. In consequence, the absolute values in the original definition are not necessary. In fact, by not considering the absolute values, the function is order preserving in the whole $\mathbb{R}^k$.

Definition 7.3.6 (Augmented Tchebycheff)**.** *Given $\vec{x}, \vec{w} \in \mathbb{R}^k$ with $w_i \geq 0$, the Augmented Tchebycheff function (ATCH) is defined as follows:*

$$ATCH_{\vec{w}}(\vec{x}) = \max_{i=1,\ldots,k} \{w_ix_i\} + \alpha \sum_{i=1}^{k} x_i \tag{7.2}$$

Lemma 7.3.2. *Given two CIVs $\vec{x}, \vec{y} \in \mathbb{R}^k$ and a weight vector $\vec{w} \in \mathbb{R}^k, w_i > 0, i = 1, \ldots, k$, then if $\vec{x} \succ \vec{y} \Rightarrow ATCH_{\vec{w}}(\vec{x}) > ATCH_{\vec{w}}(\vec{y})$.*

Proof. We can prove this lemma by induction. Let us consider, without loss of generality, that the first component of both CIVs is related to a Pareto-compliant indicator and the rest of components are related to weakly Pareto-compliant indicators, i.e., $x_1 > y_1 \wedge x_i \geq y_i, i = 2, \ldots, k$.

Base case ($k = 2$): Since $\vec{x} \succ \vec{y}$, it is straightforward to see that $A = \alpha(x_1 + x_2) > \alpha(y_1 + y_2) = B$. Let $i^* = \arg\max_{i=1,2} \{w_ix_i\}$ be the index of the maximum value. Then, we have one of the two following cases:

1. if $i^* = 1$, $w_1x_1 > w_1y_1$ and $w_1x_1 \geq w_2x_2 \geq w_2y_2$, or
2. if $i^* = 2$, $w_2x_2 \geq w_2y_2$ and $w_2x_2 \geq w_1x_1 > w_1y_1$.

From these two cases, it is clear that $\max_{i=1,2}\{w_i x_i\} \geq \max_{i=1,2}\{w_i y_i\}$. However, since $A > B$, it follows: $\vec{x} \succ \vec{y} \Rightarrow \max\{w_1 x_1, w_2 x_2\} + A > \max\{w_1 y_1, w_2 y_2\} + B$.

Inductive hypothesis: For $\vec{x}, \vec{y} \in \mathbb{R}^k$, it holds that $A = \alpha \sum_{i=1}^{k} x_i > \alpha \sum_{i=1}^{k} y_i = B$ because $\vec{x} \succ \vec{y}$. Let $i^* = \arg\max_{i=1,\ldots,k}\{w_i x_i\}$ and $j^* = \arg\max_{j=1,\ldots,k}\{w_j y_j\}$ be the indexes related to the maximum values. Due to the construction of $\vec{x}$ and $\vec{y}$, we have one of the two following cases:

1. if $i^* = 1$, $w_1 x_1 > w_1 y_1$ and $w_1 x_1 \geq w_t x_t \geq w_t y_t, t = 2, \ldots, k$, or
2. if $i^* \in \{2, \ldots, k\}$, $w_{i^*} x_{i^*} \geq w_{i^*} y_{i^*}$ and $w_{i^*} x_{i^*} \geq w_1 x_1 > w_1 y_1$ and $w_{i^*} x_{i^*} \geq w_t x_t \geq w_t y_t, t = 2, \ldots, k \wedge t \neq i^*$.

This implies that $w_{i^*} x_{i^*} \geq w_{j^*} y_{j^*}$. However, since $A > B$, then it is clear that $\vec{x} \succ \vec{y} \Rightarrow w_{i^*} x_{i^*} + A > w_{j^*} y_{j^*} + B$.

Inductive step: We want to prove the following:

$$\vec{x} \succ \vec{y} \Rightarrow$$
$$\max_{i=1,\ldots,k+1}\{w_i x_i\} + \alpha \sum_{i=1}^{k+1} x_i > \max_{i=1,\ldots,k+1}\{w_i y_i\} + \alpha \sum_{i=1}^{k+1} y_i.$$

Without loss of generality, let us assume that the $(k+1)$ components are related to a weaky Pareto-compliant indicator, then $x_{k+1} \geq y_{k+1}$. Based on our inductive hypothesis, we know that $A > B$. Taking the summation upper limits equal to $k+1$, the inequality still holds, thus $A = \alpha \sum_{i=1}^{k+1} x_i > \alpha \sum_{i=1}^{k+1} y_i = B$. Additionally, in spite of considering the $k+1$ elements, $\max_{i=1,\ldots,k+1}\{w_i x_i\} \geq \max_{i=1,\ldots,k+1}\{w_i y_i\}$ because one of the above two cases happens. Hence, $\vec{x} \succ \vec{y} \Rightarrow \max_{i=1,\ldots,k+1}\{w_i x_i\} + \alpha \sum_{i=1}^{k+1} x_i > \max_{i=1,\ldots,k+1}\{w_i y_i\} + \alpha \sum_{i=1}^{k+1} y_i$. □

7.4 Experimental Results

In this section, we present the results of two experiments that aim to provide empirical information on the following PCUIs:

- $\text{WS}_{\vec{w}}(\text{HV}, \text{R2})$, $\text{ATCH}_{\vec{w}}(\text{HV}, \text{R2})$,
- $\text{WS}_{\vec{w}}(\text{HV}, \text{IGD}^+)$, $\text{ATCH}_{\vec{w}}(\text{HV}, \text{IGD}^+)$,
- $\text{WS}_{\vec{w}}(\text{HV}, \epsilon^+)$, and $\text{ATCH}_{\vec{w}}(\text{HV}, \epsilon^+)$.

These PCUIs are the Pareto-compliant versions of the indicators R2, IGD^+, and ϵ^+. The first experiment investigates the preferences of the adopted PCUIs by measuring the correlation of preferences between them and their baseline QIs when assessing several MOEAs, having special distribution properties, on the Lamé and Mirror superspheres problems [38]. On the other hand, the second experiment analyzes

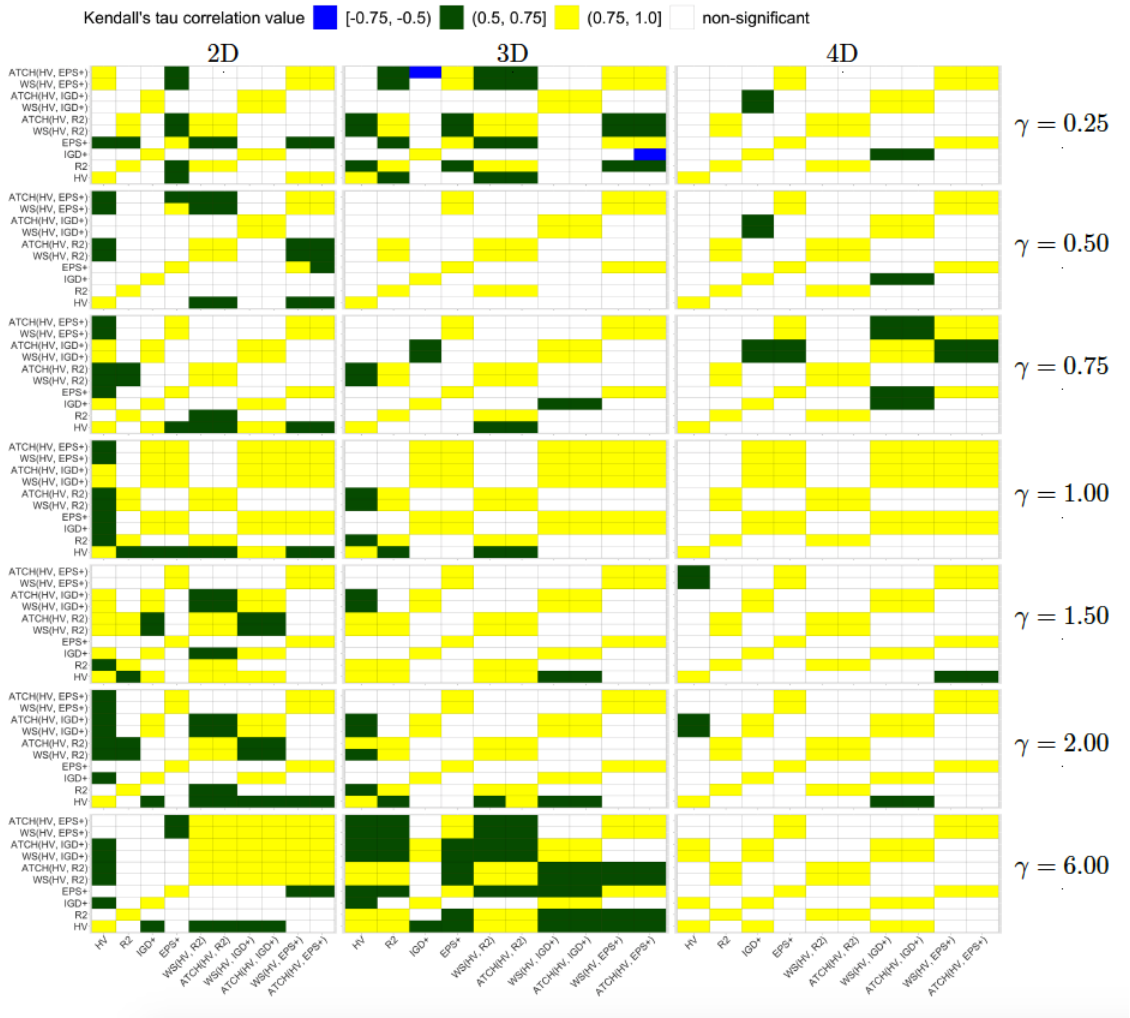

Figure 7.2: Heatmap Kendall rank correlation τ for each pair of set quality indicators, for each Lamé problem on different dimensions of the objective space.

convergence and distribution properties of a steady-state MOEA, similiar to the S-Metric Selection Evolutionary Multi-Objective Algorithm (SMS-EMOA) [8], that uses the PCUIs as part of its density estimator. The proposed algorithm, denoted as PCUI-EMOA, is tested on MOPs from the benchmarks Deb-Thiele-Laumanns-Zitzler (DTLZ) [33], Walking-Fish-Group (WFG) [65], and their minus versions, DTLZ^{-1} and WFG^{-1} [75], respectively.

7.4.1 Analysis of Preferences

We analyzed the correlation of preferences of the six adopted PCUIs when assessing the Pareto fronts of several Lamé and Mirror superspheres problems [38]. The Pareto front geometry of such MOPs is controlled by a parameter γ. Regarding the Lamé problems, when $\gamma \in (0, 1)$, the Pareto front is convex; a linear Pareto front

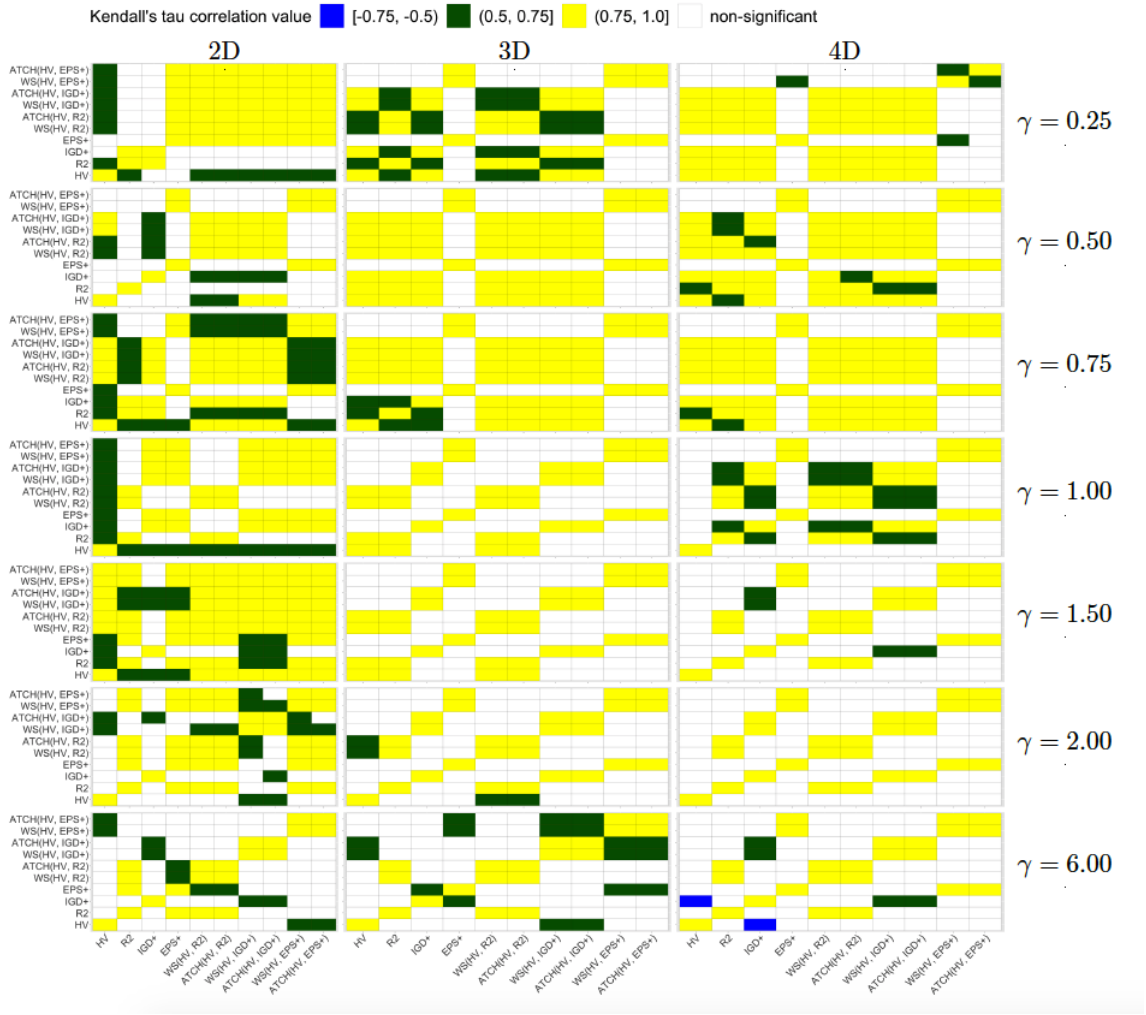

Figure 7.3: Heatmap Kendall rank correlation τ for each pair of set quality indicators, for each Mirror problem on different dimensions of the objective space.

is related to $\gamma = 1$; and when $\gamma \in (1, \infty)$, the Pareto front is concave. In case of the Mirror problems, $\gamma \in (0, 1)$ and $\gamma \in (1, \infty)$ are related to convave and convex Pareto fronts, respectively. For both Lamé and Mirror problems, we employed $\gamma = 0.25, 0.50, 0.75, 1.00, 1.50, 2.00, 6.00$ for 2, 3, and 4 objective functions. Regarding the construction of the Pareto front approximations, we employed MOEAs that exhibit particular distribution characteristics to have a representative sample of the set Ψ (i.e., the set of all approximation sets of a given size for an MOP). For each test instance, 30 independent executions were produced by each MOEA, where all algorithms shared the same settings. For all objective functions, the size of all the produced approximation sets was 120. The adopted MOEAs are classified in five classes as follows:

- Indicator-based MOEAs: SMS-EMOA [8], MOMBI2 [60], IGD$^+$-MaOEA [43] and Δ_p-MaOEA[1].
- Pareto-based MOEAs: NSGA-II [31] and SPEA2 [154].
- Reference set-based MOEAs: NSGA-III [30].
- Decomposition-based MOEAs: MOEA/D [147].
- Image analysis-based MOEAs: MOVAP [62].

Regarding the assessment of the Pareto front approximations generated by the adopted MOEAs, we used the following settings on the QIs and PCUIs. We assumed that we did not know anything about the true Pareto fronts of the adopted MOPs to perform a fair quality comparison. Hence, we employed a very bad reference point for HV, i.e., $\vec{z}_{ref} = \{2i + 1\}_{i=1,\ldots,m}$. A set of convex weight vectors (constructed by the Simplex-Lattice-Design method [147]) was employed as the set W for R2 and as the reference set for IGD$^+$ and ϵ^+. Since the set of weight vectors is in $[0, 1]^m$, we traslated all the approximation sets to $[1, 2]^m$. The vector-angle-distance-scaling (VADS) [110] utility function was employed in R2. Since all these indicators have different scales, the PCUIs could have problems if they used them without normalization. Therefore, before evaluating the PCUIs, it is necessary to evaluate all MOEAs with the baseline QIs and, then, for each indicator, we obtain the maximum and minimum values that will be used by the PCUIs to normalize the indicator values. For all the six adopted PCUIs, the weight vector was set as $\vec{w} = (0.1, 0.9)$, where 0.1 is the weight associated with HV and 0.9 is related to the weakly Pareto-compliant QI. The PCUIs use the same settings for the baseline QIs.

Concerning the correlation analysis, we employed a similar methodology to the one used by Liefooghe and Derbel [97]. We aim to correlate the rankings of MOEAs within each indicator, i.e., by how much do the PCUIs and QIs rank the MOEAs (i.e., the characteristic Pareto front approximations) similarly. For each test instance and QI,

[1]We proposed this algorithm based on the framework of IGD$^+$-MaOEA [43] but using the Δ_p indicator in the density estimator.

the MOEAs are ranked by their mean indicator value. The ranks of MOEAs are then analyzed for correlation with the remaining QIs using the Kendall's τ nonparametric measure of association with a significance value $\alpha = 0.05$. It is worth emphasizing that Kendall's τ quantifies the difference between the proportion of concordant and discordant pairs among all possible pairwise MOEAs. Since $\tau \in [-1, 1]$, where $\tau = -1$ means perfect disagreement and $\tau = 1$ means perfect agreement of ranks, we decided to create intervals of τ values in order to represent them using Heatmaps. Such intervals are the following: $[-1, -0.75)$, $[-0.75, -0.5)$, $[-0.5, -0.25)$, $[-0.25, 0.25]$, $(0.25, 0.5]$, $(0.5, 0.75]$, and $(0.75, 1]$. Figures 7.2 and 7.3 show the results of the nonparametric statistical test for the correlation, using heatmaps for all adopted Lamé and Mirror test instances, respectively.

7.4.1.1 Correlation between PCUIs and baseline QIs

Regarding the correlation analysis on Lamé problems in Fig. 7.2, we have the following conclusions. For 2 objective functions, the more linear the Pareto front (i.e., $\gamma = 0.75, 1.00, 1.50$), the more correlated are the PCUIs with their baseline QIs. For highly convex Pareto fronts there is more correlation with the weakly Pareto-compliant QI (i.e., R2, IGD^+, and ϵ^+) meanwhile for highly concave MOPs, the correlation is stronger with HV. Regarding 3-dimensional MOPs, each class of PCUI shows different behaviors. $\text{WS}_{\vec{w}}(\text{HV}, \text{R2})$ and $\text{ATCH}_{\vec{w}}(\text{HV}, \text{R2})$ are correlated with both HV and R2 for all test problems. For $\text{WS}_{\vec{w}}(\text{HV}, \text{IGD}^+)$ and $\text{ATCH}_{\vec{w}}(\text{HV}, \text{IGD}^+)$, there is independence with both HV and IGD^+ for problems with $\gamma = 0.25$ and 0.50 which means that the PCUIs have preferences completely different. For $\gamma = 0.75$ and 1.00, there is only correlation with IGD^+ and, in the concave cases, the PCUIs are correlated with both HV and IGD^+. Concerning $\text{WS}_{\vec{w}}(\text{HV}, \epsilon^+)$ and $\text{ATCH}_{\vec{w}}(\text{HV}, \epsilon^+)$, both are correlated with ϵ^+ in all cases except for $\gamma = 6.00$. A noteworthy aspect is that for 4-dimensional MOPs, there is a strong tendency of all PCUIs to be exclusively correlated with their weakly Pareto-compliant QI while there is independence with HV. Hence, we could expect that as the dimensionality of the objective space increases, the PCUIs will be more correlated with the weakly Pareto-compliant QI. However, the evaluation results of the PCUIs will be Pareto-compliant.

For the Mirror problems in Fig. 7.3, we have some similar results. In general, for 2 objective functions, the PCUIs are strongly correlated with both baseline QIs except in highly convex and concave MOPs where their preferences are correlated with either HV or the weakly Pareto-compliant QI. It is worth noting that this result is similar to the Lamé problems having 2 objectives. $\text{WS}_{\vec{w}}(\text{HV}, \text{R2})$ and $\text{ATCH}_{\vec{w}}(\text{HV}, \text{R2})$ are correlated with both QIs in all problems except for $\gamma = 6.00$ for MOPs with 3 and 4 objectives. On the other hand, $\text{WS}_{\vec{w}}(\text{HV}, \text{IGD}^+)$ and $\text{ATCH}_{\vec{w}}(\text{HV}, \text{IGD}^+)$ are only correlated with both baseline QIs for convex problems and for linear and concave ones, the correlation is stronger with IGD^+ and there is independence with HV in 3- and 4-dimensional problems. Regarding the PCUIs based on HV and ϵ^+, in all cases there is only correlation with the latter QI in MOPs with 3 and 4 objective functions.

In summary, there are two important points to emphasize. As the dimensionality

of the objective space increases, the PCUIs tend to be strongly correlated with the preferences of their baseline weakly Pareto-compliant QIs and the independence with the preferences of HV is more accentuated. Since the results of the PCUIs are Pareto-compliant, it is relevant that in high-dimensional objective spaces the PCUIs show preferences independent to those of HV because this could encourage the design of new selection mechanisms of MOEAs that would produce approximation sets with different distributions to those of SMS-EMOA but retaining the Pareto-compliance property. In other words, PCUIs could be employed to manipulate the distribution properties of MOEAs while maintaining the Pareto-compliance property. On the other hand, in general, a PCUI inherits from its baseline weakly Pareto-compliant QI the correlation with HV. A reason for this fact is that we are using a combination vector in the PCUIs that favors the weakly Pareto-compliant QI.

7.4.1.2 Correlation between PCUIs

We analyzed the correlation between the preferences of all PCUIs to ensure that the combination does produce different indicators. Concerning both the Lamé and Mirror problems, the correlation analysis indicates that the PCUIs based on the same weakly Pareto-compliant QI are strongly correlated between them. In consequence, the use of WS or ATCH is basically producing the same PCUI. In the next section, we give the reason to this behavior that, in a few words, is due to the formation of a convex Pareto front in the Quality space. Since both WS and ATCH are able to find solutions on convex Pareto fronts, thus, both will present almost the same preferences when they are employed in PCUIs. As a result of this observation, in this correlation analysis we investigated the Pareto-compliant versions of the indicators R2, IGD^+, and ϵ^+.

Another remarkable conclusion is that the preferences of PCUIs based on a different weakly Pareto-compliant QI are, in general, independent. Hence, each class of PCUIs are presenting distinct preferences. This is explained by the analysis of correlation between R2-IGD^+, R2-ϵ^+, and IGD^+-ϵ^+ that are mostly independent. Additionally, each PCUI inherits the preferences of its weakly Pareto-compliant QI. Hence, the PCUI will behave in a similar way to its weakly Pareto-compliant QI but maintaining the Pareto-compliance property.

7.4.1.3 Pareto fronts in Quality Space

In objective space, we find Pareto fronts that represent the solution to an MOP. These Pareto fronts are formed due to the conflict among objective functions. In Quality Space (see Fig. 7.1), it is also possible to find Pareto fronts when the preferences of an indicator are in conflict with the preferences of another QI. Based on the correlation analysis previously explained, we found that when there is independence of preferences between two QIs or when the preferences are negatively correlated (as in the case of HV and IGD^+ for the Mirror problem with $\gamma = 6.00$ in 4D), a Pareto front in the Quality Space Q is formed. Fig. 7.4 shows four examples where it is possible to see

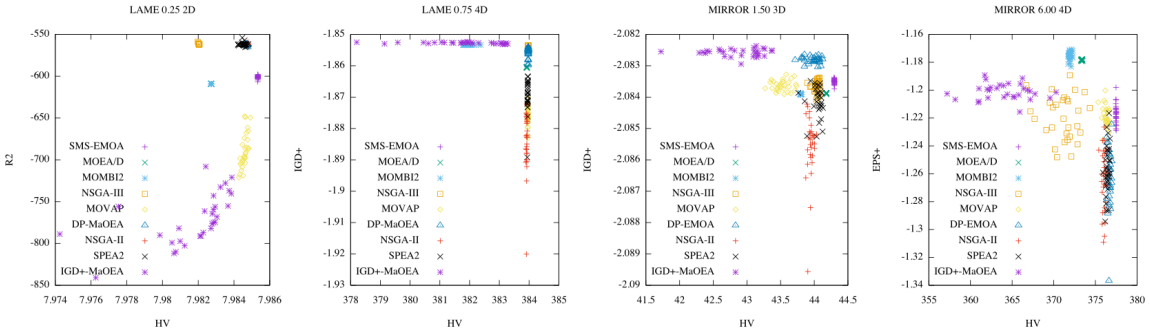

Figure 7.4: From left to right, it is shown the Quality Spaces: HV-R2 for Lamé $\gamma = 0.25$ 2D, HV-IGD$^+$ for Lamé $\gamma = 0.75$ 4D, HV-IGD$^+$ for Mirror $\gamma = 1.50$ 3D, and HV-ϵ^+ for Mirror $\gamma = 6.00$ 4D. All cases tend to show a Pareto front in Quality Space.

the tendency to a Pareto front. These plots present the indicator vectors associated to each execution of the adopted MOEAs in the correlation study for a specific test instance. Since we are maximizing HV, R2, IGD$^+$, and ϵ^+ to use the PCUIs, it is possible to see that all plots introduce convex Pareto front shapes. Hence, this fact supports the observation that there is no critical difference when using WS or ATCH for constructing PCUIs since both order-preserving utility functions are able to find solutions in convex Pareto fronts [108, 110]. The rest of cases of independence on both heatmaps in Figures 7.2 and 7.3 present convex Pareto fronts. In case a PCUI is employed in the selection mechanism of an MOEA, a compromise between the indicators will be found, resulting in new distributions on the Pareto fronts that represent the solution to an MOP. In conclusion, this result supports the fact that PCUIs could be employed to better control the diversity of an MOEA but maintaining Pareto-compliance.

7.4.2 Steady-state Selection

In this section, we investigate the effect of using PCUIs in the selection mechanism of an MOEA. For this purpose, we considered the framework of SMS-EMOA that uses a density estimator (DE) based on HV but, in our case, a PCUI is employed in the DE. Algorithm 16 presents the general framework of our proposed PCUI-EMOA whose main loop is in lines 2 to 12. At each generation, a new solution is created using genetic operators and, then, this newly created solution is added to the population P to create the temporary population Q. Then, in line 5, a set of ranks $R_1, \ldots, R_t$ are created using the nondominated sorting algorithm [31], where R_t has the worst solutions according to the Pareto dominance relation. If R_t has more than one solution, the individual contributions to the PCUI are computed to delete the worst-contributing solution in line 11. Finally, the Pareto front approximation is returned when the stopping criterion is fulfilled.

We focused our attention on studying the final distribution properties of PCUI-

Algorithm 16: PCUI-EMOA general framework

Input: PCUI $u_{\vec{w}}(\vec{I})$, where $\vec{I}(I_1, I_2, \ldots, I_k)$
Output: Approximation to the Pareto front
Randomly initialize population P;
while *stopping criterion is not fulfilled* **do**
  $q \leftarrow Variation(P)$;
  $Q \leftarrow P \cup \{q\}$;
  $\{R_1, \ldots, R_t\} \leftarrow NondominatedSorting(Q)$;
  if $|R_t| > 1$ **then**
    $\vec{p}_{\text{worst}} = \arg\min_{\vec{p} \in R_t} \{u_{\vec{w}}(\vec{I}(R_t)) - u_{\vec{w}}(\vec{I}(R_t \setminus \{p\}))\}$;
  end
  else
    Let $\vec{p}_{\text{worst}}$ be the sole solution in R_t;
  end
  $P \leftarrow Q \setminus \{\vec{p}_{\text{worst}}\}$;
end
return P

EMOA in comparison with four steady-state MOEAs based on the indicators HV, R2, IGD$^+$, and ϵ^+, i.e., SMS-EMOA, R2-EMOA, IGD$^+$-MaOEA, and ϵ^+-MaOEA. The latter is similar to IGD$^+$-MaOEA. Regarding PCUI-EMOA, we employed the six PCUIs of the previous section. Since all the adopted indicator-based MOEAs (IB-MOEAs) share the same structure, the parameters settings are the following. For all objective functions, the population size is 120. All MOEAs use simulated binary crossover and polynomial-based mutation as their genetic operators [31], where, for all cases, the crossover probability is set to 0.9, the mutation probability is $1/n$ (n is the number of decision variables), and both the crossover and mutation distribution indexes are set to 20. PCUI-EMOA employs the combination vector as $\vec{w} = (0.5, 0.5)$ in order to search for distributions similar to both baseline QIs. We tested the adopted MOEAs on 14 MOPs from the benchmarks DTLZ, WFG, DTLZ^{-1}, and WFG^{-1} for 2, 3 and 4 objective functions. We employed the problems DTLZ1, DTLZ2, DTLZ5, DTLZ7, WFG1, WFG2, WFG3 and their minus versions. We selected these MOPs since they possess Pareto fronts with different geometries, namely, linear, concave, convex, degenerate, mixed, disconnected, correlated with the simplex shape and not correlated with it [75].

The distribution analysis is focused on determining if the Pareto front approximations produced by the six PCUI-EMOAs are similar to the IB-MOEAs that use their baseline indicators. For each test instance, the MOEAs were executed $N = 30$ independent times. Thus, each one produces N approximation sets for each MOP. We investigate the similarity between two sets of approximation sets produced by two MOEAs, using a similarity measure based on the Hausdorff distance that we propose in the following:

Definition 7.4.1 (Hausdorff similarity measure)**.** *Given two sets* $\mathbb{A} = \{A_1, \ldots, A_N\}$ *and* $\mathbb{B} = \{B_1, \ldots, B_N\}$*, each one of* N *Pareto front approximations, the Hausdorff*

similarity measure S is given as follows:

$$S(\mathbb{A},\mathbb{B}) = \frac{1}{N}\sum_{i=1}^{N} median(A_i,\mathbb{B}), \tag{7.3}$$

where $median(A_i,\mathbb{B})$ computes all the Hausdorff distances from A_i to every element in $\mathbb{B}$ and returns the median value.

S calculates the degree of similarity between two sets. However, if we are given three sets of approximation sets $\mathbb{A},\mathbb{B}$, and $\mathbb{C}$ and we would like to know if $\mathbb{A}$ is similar to $\mathbb{B}$, to $\mathbb{C}$, to both or to none of them, a classification function is required. Such classifier is given as follows.

Definition 7.4.2 (Classifier)**.** *Given three sets of approximation sets $\mathbb{A},\mathbb{B}$, and $\mathbb{C}$ and a threshold $\epsilon > 0$, the classifier function is given as follows:*

$$C_\epsilon(S(\mathbb{A},\mathbb{B}),S(\mathbb{A},\mathbb{C})) = \begin{cases} -1, & S(\mathbb{A},\mathbb{B}) \leq \epsilon \wedge S(\mathbb{A},\mathbb{C}) > \epsilon \\ 0, & S(\mathbb{A},\mathbb{B}) \leq \epsilon \wedge S(\mathbb{A},\mathbb{C}) \leq \epsilon \\ 1, & S(\mathbb{A},\mathbb{B}) > \epsilon \wedge S(\mathbb{A},\mathbb{C}) > \epsilon \\ 2, & S(\mathbb{A},\mathbb{C}) \leq \epsilon \wedge S(\mathbb{A},\mathbb{B}) > \epsilon \end{cases}$$

where -1 means that $\mathbb{A}$ is exclusively similar to $\mathbb{B}$; 0 means that $\mathbb{A}$ is similar to both $\mathbb{B}$ and $\mathbb{C}$; 1 means that $\mathbb{A}$ is not similar to $\mathbb{B}$ nor $\mathbb{C}$; and, 2 means that $\mathbb{A}$ is exclusively similar to $\mathbb{C}$.

Based on the classification function, we analyzed the similarities between the approximation sets produced by the PCUI-EMOAs and their corresponding IB-MOEAs that use the baseline indicators for the construction of the PCUI. Table 7.1 shows the results for all the considered test instances. Since all PCUI-EMOAs use $\vec{w} = (0.5, 0.5)$ as the combination weight vector for the order-preserving utility functions, our hypothesis is that the Pareto front approximations should be similar to both IB-MOEAs that employ the baseline indicators. This hypothesis is true for several cases related to the DTLZ and DTLZ^{-1} problems. Nevertheless, for most of the WFG and WFG^{-1} problems, the PCUI-EMOAs tend to produce approximation sets with particular distributions that are not similar to the baseline IB-MOEAs. This fact could be explained by independence of preferences between HV and the weakly Pareto-compliant indicators on these MOPs. Considering the linear problems DTLZ1 and DTLZ1^{-1}, it is clear that in most cases the PCUI-EMOAs produce approximation sets similar to the IB-MOEAs using their baseline indicators. This result is explained by the correlation analysis of Sect. 7.4.1 where in almost all cases HV, R2, IGD$^+$, and ϵ^+ are strongly correlated. The most important observation is related to the PCUI-EMOAs based on $\text{WS}_{\vec{w}}(\text{HV},\text{R2})$ and $\text{ATCH}_{\vec{w}}(\text{HV},\text{R2})$. On the one hand, SMS-EMOA [8] produces uniformly distributed solutions in convex and linear Pareto fronts and there is a bias towards the knee and boundaries of concave Pareto fronts. Additionally, SMS-EMOA presents good results in degenerate problems such as DTLZ5 and WFG3. On

Table 7.1: Distribution similarities between each PCUI-EMOA and the IB-MOEAs based on the indicators HV, R2, IGD^+, ϵ^+. For each test instance, it is shown if the distribution of the PCUI-EMOA is similar to one or other baseline indicator, to both or none of them.

MOP	**Dim.**	$WS_{\vec{w}}(HV, R2)$	$ATCH_{\vec{w}}(HV, R2)$	$WS_{\vec{w}}(HV, IGD^+)$	$ATCH_{\vec{w}}(HV, IGD^+)$	$WS_{\vec{w}}(HV, \epsilon^+)$	$ATCH_{\vec{w}}(HV\epsilon^+)$
DTLZ1	2	Both	Both	Both	Both	Both	Both
	3	Both	Both	Both	Both	Both	Both
	4	Both	Both	Both	Both	Both	Both
$DTLZ1^{-1}$	2	Both	Both	Both	Both	Both	Both
	3	Both	Both	Both	Both	Both	Both
	4	HV	HV	Both	Both	HV	None
DTLZ2	2	Both	Both	Both	Both	Both	Both
	3	R2	R2	Both	Both	Both	Both
	4	R2	R2	None	None	None	None
$DTLZ2^{-1}$	2	HV	HV	Both	Both	Both	Both
	3	HV	HV	None	None	None	None
	4	None	None	None	None	None	None
DTLZ5	2	R2	R2	Both	Both	Both	Both
	3	HV	HV	Both	Both	Both	Both
	4	HV	HV	IGD^+	IGD^+	ϵ^+	ϵ^+
$DTLZ5^{-1}$	2	HV	HV	Both	Both	Both	Both
	3	HV	HV	IGD^+	IGD^+	None	None
	4	None	None	None	None	None	None
DTLZ7	2	Both	Both	Both	Both	Both	Both
	3	None	None	IGD^+	IGD^+	ϵ^+	None
	4	None	None	None	None	None	None
$DTLZ7^{-1}$	2	Both	Both	Both	Both	Both	Both
	3	R2	R2	Both	Both	Both	Both
	4	None	None	IGD^+	None	ϵ^+	Both
WFG1	2	None	None	None	None	None	None
	3	None	None	None	None	None	ϵ^+
	4	None	None	IGD^+	IGD^+	ϵ^+	None
$WFG1^{-1}$	2	R2	R2	None	None	None	None
	3	None	None	None	None	None	None
	4	None	None	None	None	None	None
WFG2	2	None	None	None	None	None	None
	3	None	None	None	None	None	None
	4	None	None	None	None	None	None
$WFG2^{-1}$	2	None	None	None	None	None	None
	3	R2	R2	IGD^+	IGD^+	ϵ^+	ϵ^+
	4	None	None	None	None	None	None
WFG3	2	None	None	None	None	None	None
	3	Both	Both	Both	Both	Both	Both
	4	None	None	IGD^+	IGD^+	ϵ^+	ϵ^+
$WFG3^{-1}$	2	R2	R2	None	None	None	None
	3	Both	Both	Both	Both	Both	Both
	4	HV	HV	Both	Both	HV	HV

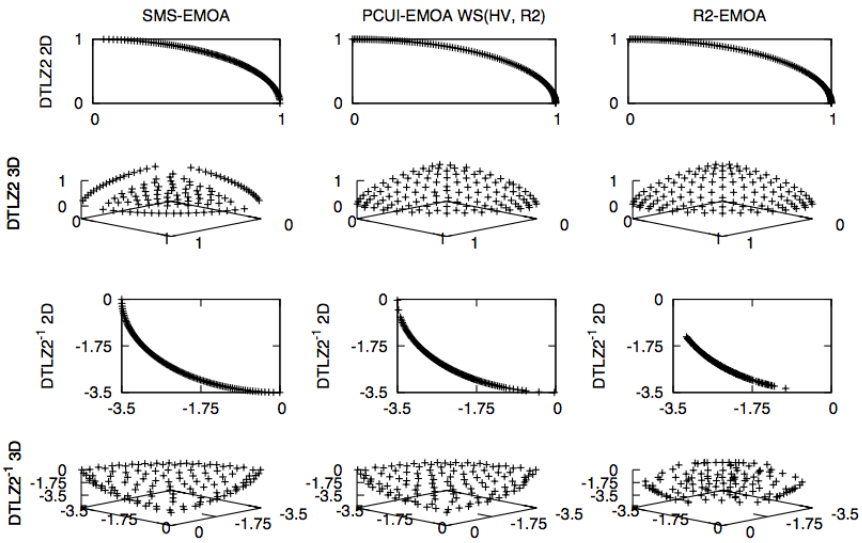

Figure 7.5: Pareto fronts that show the compensation of weaknesses of one indicator with the strengths of other when coupled to PCUI-EMOA.

the other hand, R2-EMOA [18] does not produce uniformly distributed solutions in convex Pareto fronts, but it does in linear and concave ones. Regarding degenerate MOPs, R2-EMOA does not produce good results since its weight vectors do not completely intersect the Pareto front shape. Hence, SMS-EMOA and R2-EMOA have specific strengths and weaknesses depending on the MOP being tackled. Regarding DTLZ2 in two and three objective functions which have concave Pareto fronts, it is possible to see that the distribution of the PCUI-EMOAs based on $\mathrm{WS}_{\vec{w}}(\mathrm{HV}, \mathrm{R2})$ and $\mathrm{ATCH}_{\vec{w}}(\mathrm{HV}, \mathrm{R2})$ are similar to the preferences of R2, i.e., R2-EMOA. When we analyze DTLZ2^{-1} for the same objective funtions, the distributions are similar to those of SMS-EMOA. This also happens for DTLZ5 3D which is degenerate where the distributions are similar to those of SMS-EMOA as well. Hence, we have empirical evidence on the compensation of weaknesses of one indicator with the strengths of the other baseline indicator when employing PCUI-EMOA. Fig 7.5 shows some examples of this compensation.

7.5 Exploiting the Trade-off between Convergence and Diversity Indicators

In section 6.3.2, we proposed the CRI-EMOA algorithm which combines the individual selection effect of two density estimators based on the Riesz s-energy (E_s) [57] and the Inverted Generational Distance plus (IGD^+) [74] indicators. The main idea of CRI-EMOA is to statistically analyze its convergence behavior (based on an approximation to the hypervolume indicator [156]) to decide which indicator-based density estimator

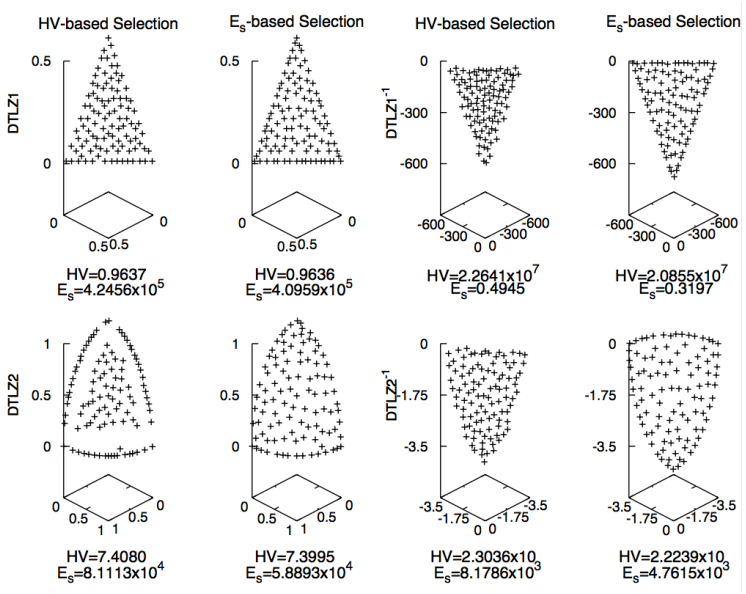

Figure 7.6: Trade-off between the hypervolume indicator and the Riesz s-energy. In all cases, a well-diversified Pareto front does not have the best hypervolume value and viceversa.

(IB-DE) should be executed. If the convergence stagnates, the diversity of solutions is promoted through the E_s-DE. On the other hand, if the convergence either decreases or increases, the IGD$^+$-DE is applied. We empirically showed that the performance of CRI-EMOA is invariant to the Pareto front shape. However, its main drawback concerns its statistical analysis of global convergence since the approximation to the hypervolume indicator (HV) provides noisy results which could lead to not using the correct IB-DE.

Currently, there is a wide range of QIs that aim to assess convergence and diversity of Pareto front approximations [95]. Since the scope of convergence and diversity QIs is different, it is clear that their preferences could be in conflict. In Figure 7.6, we show the Pareto fronts related to some DTLZ [33] and DTLZ^{-1} [75] benchmark problems. For each MOP, we generated two subsets using steady-state selection based on HV and E_s and we measured both indicator values. The QI values show that a high hypervolume value is not strictly related to a well-diversified Pareto front. Hence, there is a trade-off between both QIs that can be exploited by an MOEA to produce Pareto front approximations, optimizing both a convergence indicator and a diversity one.

In this section, we propose to exploit the trade-off between the IGD$^+$[2] and the Riesz s-energy to overcome the drawbacks of CRI-EMOA. To this aim, we mathematically combine IGD$^+$ and E_s in a single indicator which is then embedded into

[2]The decision to use IGD$^+$ instead of HV is because the latter is computationally expensive when dealing with MOPs having more than three objective functions. Additionally, the preferences of IGD$^+$ and HV are highly correlated [70].

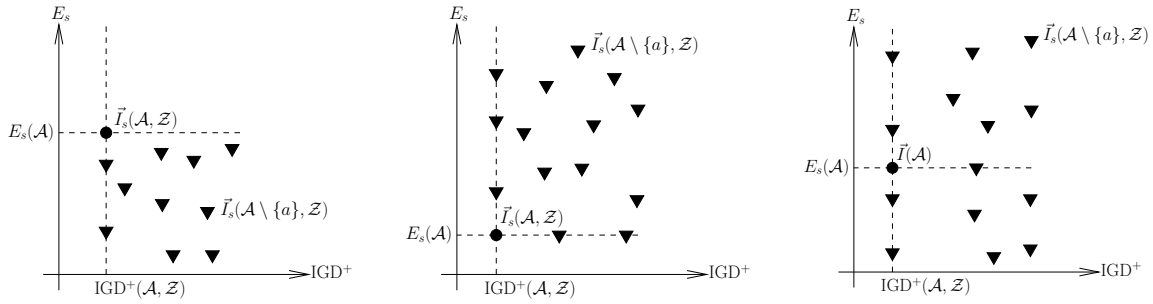

(a) Case 1 (b) Case 2 (c) Case 3

Figure 7.7: Due to the Pareto non-compliance of the Riesz s-energy indicator, there are three cases for selection when using $\mathrm{ATCH}_{\vec{w}}(\vec{I}_s(\mathcal{A},\mathcal{Z}))$.

a density estimator. Our proposed approach, called Pareto front shape invariant evolutionary multi-objective algorithm (PFI-EMOA), is based on the framework of SMS-EMOA [8] but it replaces the HV-DE by our proposed density estimator using the combined indicator. In the following sections, we describe the algorithmic structure of the proposal and the experimental results that show its performance.

7.5.1 Design of the Combined Indicator and Density Estimator

The underlying idea of PFI-EMOA is to unify IGD^+ and E_s in a single QI such that we exploit the trade-off between both indicators and, then, the new QI is embedded in a density estimator. To this aim, we employ the theoretical results, described in the previous sections, to combine IGD^+ and E_s and, thus, to exploit their trade-off. Let $\vec{I}_s(\mathcal{A},\mathcal{Z}) = (\mathrm{IGD}^+(\mathcal{A},\mathcal{Z}), E_s(\mathcal{A}))$ be our indicator vector. From the set of order-preserving functions, we chose the augmented Tchebycheff function (ATCH) that is defined as follows: $\mathrm{ATCH}_{\vec{w}}(\vec{x}) = \max_{i=1,\ldots,k}\{w_i x_i\} + \alpha\sum_{i=1}^{k} x_i$, where $\alpha > 0$ and $\vec{w} \in \mathbb{R}^k$ is a weight vector, holding $\sum_{i=1}^{k} w_i = 1$ and all of its components should be strictly positive such that all the indicators contribute to the ATCH value. Hence, the combined indicator is $\mathrm{ATCH}_{\vec{w}}(\vec{I}_s(\mathcal{A},\mathcal{Z}))$. Since we are combining a weakly Pareto-compliant QI with a non-Pareto-compliant one, according to the theorem 7.3.1 the proposed combined indicator is not Pareto-compliant.

To design a density estimator based on $\mathrm{ATCH}_{\vec{w}}(\vec{I}_s(\mathcal{A},\mathcal{Z}))$, it is necessary to analyze the three cases of Figure 7.7 that arise due to the non-Pareto compliance of E_s. This figure shows the relation between $\vec{I}_s(\mathcal{A},\mathcal{Z})$ and $\vec{I}_s(\mathcal{A}\setminus\{\vec{a}\},\mathcal{Z})$. In Case 1, every time a solution is removed from $\mathcal{A}$, the E_s value gets better, which implies that $\vec{I}_s(\mathcal{A},\mathcal{Z})$ is mutually nondominated with respect to all vectors $\vec{I}_s(\mathcal{A}\setminus\{\vec{a}\},\mathcal{Z})$. Hence, $\mathrm{ATCH}_{\vec{w}}(\vec{I}_s(\mathcal{A}\setminus\{a\},\mathcal{Z}))$ could be less than, greater than or equal to $\mathrm{ATCH}_{\vec{w}}(\vec{I}_s(\mathcal{A},\mathcal{Z}))$. On the other hand, in Case 2, all vectors $\vec{I}_s(\mathcal{A}\setminus\{\vec{a}\},\mathcal{Z})$ are dominated by $\vec{I}_s(\mathcal{A},\mathcal{Z})$

since they all have a greater E_s value. Due to the order-preserving property of ATCH, $\text{ATCH}_{\vec{w}}(\vec{I}_s(\mathcal{A}, \mathcal{Z})) < \text{ATCH}_{\vec{w}}(\vec{I}_s(\mathcal{A} \setminus \{a\}, \mathcal{Z}))$, for all $\vec{a} \in \mathcal{A}$. Finally, case 3 combines cases 1 and 2, thus, $\text{ATCH}_{\vec{w}}(\vec{I}_s(\mathcal{A} \setminus \{a\}, \mathcal{Z}))$ could be less than, greater than or equal to $\text{ATCH}_{\vec{w}}(\vec{I}_s(\mathcal{A}, \mathcal{Z}))$. In the three cases, it is evident that there exist non-contributing solutions to the IGD^+ indicator that must be eliminated every time they appear because they do not contribute to the convergence of the algorithm. In consequence, we delete the worst-contributing solution to the Riesz s-energy indicator in this case. Regarding the rest of solutions, we delete the solution having the minimum $\text{ATCH}_{\vec{w}}(\vec{I}_s(\mathcal{A} \setminus \{a\}, \mathcal{Z}))$ value.

7.5.2 PFI-EMOA: General Description

Algorithm 17: PFI-EMOA general framework

Input: Combination vector $\vec{w} \in \mathbb{R}^2$
Output: Pareto front approximation

Randomly initialize population P;
while *stopping criterion is not fulfilled* **do**
  Create a single offspring solution $\vec{q}$ using variation operators;
  $Q \leftarrow P \cup \{\vec{q}\}$;
  $\{R_1, \ldots, R_k\} \leftarrow$ nondominated-sorting(Q);
  if $|R_k| > 1$ **then**
    $z_i^{\max} \leftarrow \max_{\vec{a} \in Q} a_i, i = 1, \ldots, m$;
    $z_i^{\min} \leftarrow \min_{\vec{a} \in Q} a_i, i = 1, \ldots, m$;
    Normalize $\{R_j\}_{j=1,\ldots,k}$ using $\vec{z}^{\max}$ and $\vec{z}^{\min}$;
    $B \leftarrow \{\vec{b} \mid \text{IGD}^+(R_k \setminus \{\vec{b}\}, R_1) = \text{IGD}^+(R_k, R_1), \forall \vec{b} \in R_k\}$;
    if $|B| > 0$ **then**
      $\vec{a}_{\text{worst}} \leftarrow \arg\max_{\vec{b} \in B} C_{E_s}(\vec{b}, R_k)$;
    end
    else
      $\vec{a}_{\text{worst}} \leftarrow \arg\min_{\vec{r} \in R_k} \text{ATCH}_{\vec{w}}(\vec{I}_s(R_k \setminus \{r\}, R_1))$;
    end
  end
  else
    $\vec{a}_{\text{worst}}$ is the sole solution in R_k;
  end
  $P \leftarrow Q \setminus \{\vec{a}_{\text{worst}}\}$;
end
return P;

Algorithm 17 outlines PFI-EMOA that is a steady-state algorithm based on the framework of SMS-EMOA [8]. In contrast to CRI-EMOA that requires the parameters

$\bar{\beta}$ and $\bar{\theta}$ to control the switching between the IB-DEs, PFI-EMOA only requires a weight vector $\vec{w} \in \mathbb{R}^2$ such that $w_1 + w_2 = 1$ and $w_1, w_2 > 0$ which control the importance of the indicators. Lines 2 to 17 encompass the main loop of PFI-EMOA where the population P (randomly initialized in line 1) is evolved to obtain a Pareto front approximation. At each iteration, the nondominated sorting algorithm [31] classifies P and an offspring solution generated through variation operators[3] in layers $R_1, \ldots, R_k$ according to the Pareto dominance relation. If the cardinality of R_k (which has the worst solutions according to the Pareto dominance) is greater than one, our density estimator is applied; otherwise, the sole solution in R_k is deleted. To execute the density estimator, it is first necessary to normalize the objective values of all solutions. In line 10, the set B of non-contributing solutions to the IGD^+ indicator is computed and if it has one or more solutions, the one having the worst Riesz s-energy contribution is selected. Otherwise, the solution in R_k having the worst trade-off between IGD^+ and E_s is selected in line 14. In lines 10 and 14, R_1 is employed as the reference set of IGD^+. The final step of the loop is to delete in line 17 the selected solution. Finally, P is returned as the Pareto front approximation.

7.5.3 Experimental Results

In this section, we analyze the performance of PFI-EMOA[4] by performing three experiments. First, we turn off the Riesz s-energy indicator in the combined indicator to determine what is its effect on the Pareto front approximations. Then, we compare PFI-EMOA with CRI-EMOA, AR-MOEA [138], RVEA [20], SPEA2+SDE [94], GrEA [143], and Two_Arch2 [138]. We used the WFG [65] and WFG^{-1} [75] benchmark problems with 2 to 6 objective functions to test the convergence and diversity properties of the selected MOEAs. For each test instance, we performed 30 independent executions and to obtain statistical confidence, we performed the Wilcoxon rank-sum test with a confidence value of 95%. To assess the performance of PFI-EMOA, we employed four QIs: IGD^+ and E_s since PFI-EMOA aims to optimize them, and, as neutral QIs, we used HV and the Solow-Polasky-Diversity indicator (SPD) [5]. For each test instance, we merged all the solutions from the MOEAs to produce a subset of mutually nondominated solutions of size $100m$ (where m is the number of objective functions) as the reference set required by IGD^+. In all cases, $s = m - 1$ for E_s as suggested in [61]. Regarding HV, the reference point was set as follows: $\vec{z}_{\text{ref}} = \{2i + 1\}_{i=1,\ldots,m}$ for all the WFG problems, and $\vec{z}_{\text{ref}} = (10, \ldots, 10)$ for all the WFG^{-1} instances. SPD uses $\theta = 10$ for its computation [5]. Finally, we analyze the three possible ways in which PFI-EMOA deletes a solution at each iteration, aiming to determine which combined indicator to adopt.

[3]We employed the simulated binary crossover (SBX) and the polynomial-based mutation (PBX) operators [31].

[4]The source code of PFI-EMOA is available at `http://computacion.cs.cinvestav.mx/~jfalcon/PFI-EMOA.html`.

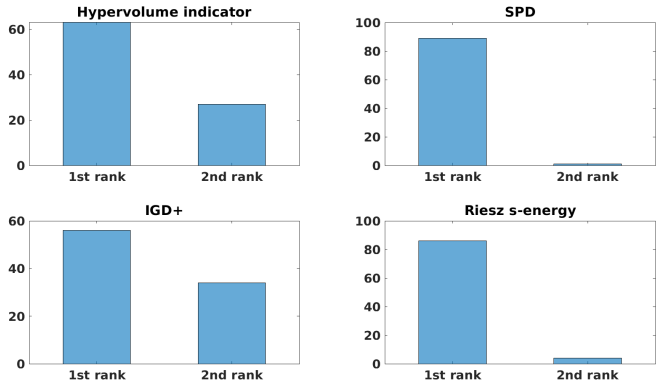

Figure 7.8: For each considered indicator, the number of test instances for which PFI-EMOA is ranked first or second when compared to PFI-EMOA/E_s.

7.5.3.1 Parameters Settings

Let (m, μ, T) be a configuration tuple where m is the number of objective functions, μ is the population size, and T is the maximum number of function evaluations. For a fair comparison, PFI-EMOA and the other MOEAs used the same population size and the same number of function evaluations as their stopping criterion as follows: $(2, 120, 40,000)$, $(3, 120, 50,000)$, $(4, 120, 60,000)$, $(5, 126, 70,000)$, $(6, 126, 80,000)$. Since all the MOEAs employ SBX and PBX as their variation operators, we set the crossover probability (P_c), the crossover distribution index (N_c), the mutation probability (P_m), and the mutation distribution index (N_m) as follows. For MOPs having two and three objective functions $P_c = 0.9$ and $N_c = 20$, while for MOPs with $m > 3$, $P_c = 1.0$ and $N_c = 30$. In all cases, $P_m = 1/n$ where n is the number of decision variables and $N_m = 20$. The number of decision variables n and the number of position-related parameters k of both the WFG and WFG^{-1} test problems are $n = 24+2(m-2)$ and $k = 2(m-1)$. Regarding PFI-EMOA, we set $\vec{w} = (0.5, 0.5)$ for two- and three-dimensional MOPs while $\vec{w} = (0.9, 0.1)$ for MOPs having $m > 3$, where w_1 is related to IGD$^+$ and w_2 to E_s. CRI-EMOA uses $T_w = \mu$, $\bar{\beta} = 0.1$ and $\bar{\theta} = 0.25$ for all MOPs. The size of the convergence archive of Two_Arch2 is equal to the population size and the fractional distance is set to $1/m$ for all the test instances. Concerning RVEA, the rate of change of the penalty is set to 2 and the frequency of employing the reference vector adaptation is equal to 0.1 in all cases. GrEA creates 45, 15, 10, 9, and 9 divisions of the objective space for 2, 3, 4, 5, and 6 objective functions, respectively. We employed the PlatEMO 2.0 [126] to execute AR-MOEA, RVEA, GrEA, SPEA2+SDE, and Two_Arch2 while for CRI-EMOA, we used the source code available at `http://computacion.cs.cinvestav.mx/~jfalcon/CRI-EMOA.html`.

7.5.3.2 Effect of Riesz s-energy

In this experiment, we analyze what is the effect of the Riesz s-energy indicator in the final quality of the Pareto front approximations generated by PFI-EMOA. To this aim, we turned off the E_s-contribution in PFI-EMOA, i.e., we set $\vec{w} = (1, 0)$, where the zero value is related to E_s, and we changed ATCH by the weighted sum function ($\text{WS}_{\vec{w}}(\vec{x}) = \sum_{i=1}^{k} w_i x_i$) in the combined indicator. The reason to use WS instead of ATCH is that even though we set $\vec{w} = (1, 0)$ in ATCH, E_s would be taken into account in the correction factor $\alpha \sum_{i=1}^{k} x_i$ of ATCH. We denote this modified PFI-EMOA as PFI-EMOA/E_s and we compare it with PFI-EMOA in the 90 test instances indicated before, using HV, SPD, IGD$^+$, and E_s. The complete numerical results are available in Tables B.20 to B.23 in Appendix B. In Figure 7.8 we show a summary of the comparison where we stress the number of test instances for which PFI-EMOA is ranked first or second by each QI. Regarding the SPD and E_s values in the figure, it is clear that E_s helps PFI-EMOA to significantly improve the diversity of the Pareto front approximations. On the other hand, PFI-EMOA performs better than PFI-EMOA/E_s in almost 60 out of the 90 test instances for both HV and IGD$^+$. According to the numerical results, PFI-EMOA/E_s is better than PFI-EMOA for WFG1, WFG6, WFG7, WFG8 and WFG9 in terms of HV. This is because PFI-EMOA/E_s is being guided by an IGD$^+$-DE which produces similar distributions to HV (see [70]) and, hence, in the performance comparison HV is rewarding this behavior. In this light, IGD$^+$ prefers PFI-EMOA/E_s in some cases because its preferences are similar to those of HV. However, PFI-EMOA obtained the first rank in both indicators in almost 66.66% of the benchmark problems, which implies that E_s helps to improve the convergence quality as well.

7.5.3.3 Comparison with state-of-the-art MOEAs

We analyzed the convergence and diversity properties of PFI-EMOA with six state-of-the-art MOEAs: GrEA and RVEA are two approaches that aim to balance convergence and diversity during the evolutionary process, and CRI-EMOA, AR-MOEA, SPEA2+SDE, and Two_Arch2 which were specifically designed to have a good performance regardless of the Pareto front shape of the MOP being tackled. Figure 7.9 presents the statistical ranks obtained by the considered MOPs for each quality indicator. The underlying numerical results are shown in Tables B.24 to B.27 in Appendix B. From the figure, it is clear that PFI-EMOA simultaneously optimizes IGD$^+$ and E_s, being the best-ranked algorithm. This is also clear from HV and SPD which are neutral indicators in the comparison, i.e., no algorithm aims to optimize such QIs. Figure 7.10 shows some Pareto front approximations generated by all the MOEAs, where it is possible to see that PFI-EMOA produces the best distributions. An important factor to discuss is the effect of the weight vector $\vec{w}$ in the performance of PFI-EMOA. Based on a wide range of experiments, we observed that for two- and three-dimensional objective spaces, IGD$^+$ and E_s can be equally important (i.e., $\vec{w} = (0.5, 0.5)$) because there are not many mutually nondominated solutions. How-

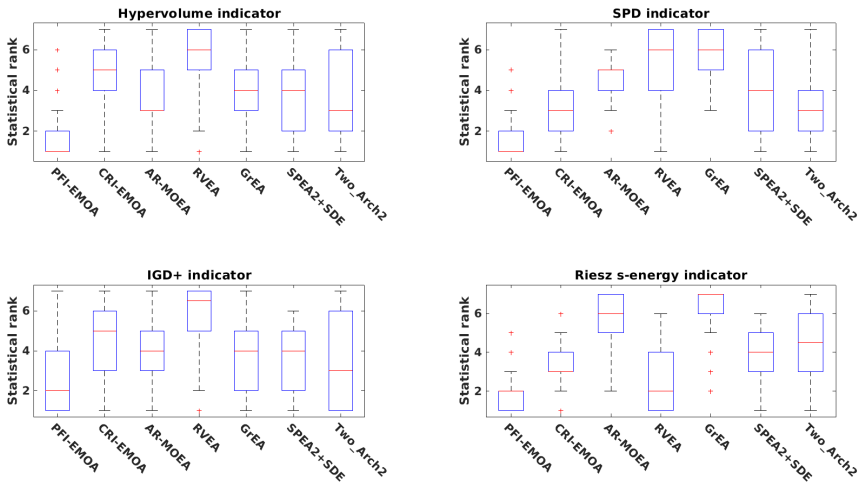

Figure 7.9: Statistical ranks obtained by each algorithm over all benchmark functions with respect to each considered indicator. The lower, the better.

ever, for many-objective problems, the number of mutually nondominated solutions drastically increases, and, in these cases, IGD^+ should apply more selection pressure while E_s helps PFI-EMOA just to refine the ordering of solutions. If we give E_s more importance in high-dimensional spaces, it is more likely to allow dominated solutions to survive.

7.5.3.4 Selection analysis

At each iteration, PFI-EMOA deletes a solution $\vec{a}_{\text{worst}}$ from the population by: (1) selecting the worst-contributing solution to E_s from the set of non-contributing solutions to IGD^+, i.e., by line 12 of Algorithm 17, (2) using the $\text{ATCH}_{\vec{w}}(\vec{I}_s(\mathcal{A}, \mathcal{Z}))$-based density estimator in line 14, and (3) determining the worst solution in terms of the Pareto dominance relation in line 17. These three cases are denoted as C1, C2, and C3. In this section, we analyze the tendency of PFI-EMOA to use these three selection criteria. In Figure 7.11, we present statistical data of the utilization of C1, C2, and C3 for MOPs WFG1-WFG4 and their corresponding inverted instances for 2 to 6 objective functions. For all two-objective test instances (except for WFG1^{-1}), C3 is the most employed selection case, followed by C2, and C1. This is because in two-dimensional objective spaces, it is more likely that the nondominated sorting algorithm creates numerous layers and, therefore, the Pareto-based selection is executed more times. On the other hand, as the dimension of the objective space increases, the number of mutually nondominated solutions increases as well [44]. Consequently, for 3 to 6 objective functions, Figure 7.11 shows that C2 is the most employed selection criterion in a significant manner, followed by C3 and C1. Hence, this result shows that our proposed combined indicator is mostly guiding the search of PFI-EMOA for many-objective problems.

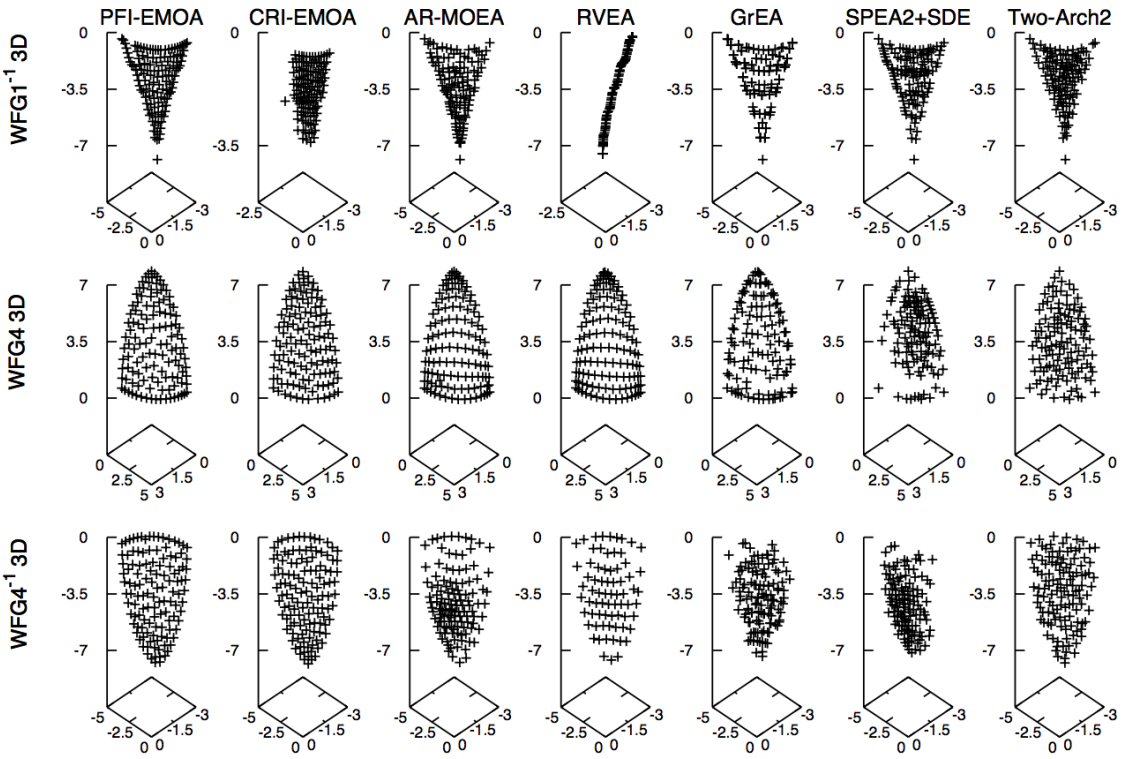

Figure 7.10: Pareto front approximations generated by PFI-EMOA and the selected MOEAs. Each front corresponds to the median of the hypervolume indicator.

7.6 Summary

In recent years, the existence of new Pareto-compliant QIs having different preferences to those of the hypervolume indicator has been an open research area. In this chapter, we proposed an answer to this research question by the combination of quality indicators. Our mathematical development allows to produce a family of Pareto-compliant QIs based on the combination of one or more weakly Pareto-compliant indicators with at least one Pareto-compliant QI, using a vector-based function that is order-preserving. For the combination, we proposed to employ the Pareto-compliant hypervolume indicator and three weakly Pareto-compliant QIs: R2, IGD^+, and ϵ^+. Regarding the order-preserving functions, we employed the weighted sum and the augmented Tchebycheff utility functions as combination functions. Using these elements, we studied six Pareto-compliant utility indicators, focusing on their preferences when assessing approximation sets, and their μ-optimal distributions when they are integrated in the selection mechanism of an MOEA. Experimental results show that the adopted PCUIs (i.e., the Pareto-compliant versions of the indicators R2, IGD^+, and ϵ^+) represent intermediate preferences between the baseline QIs, which clearly broadens the variety of Pareto-compliant QIs. Moreover, this development is an insight to a mathematical proof of the existence of other Pareto-compliant QIs. Regarding the

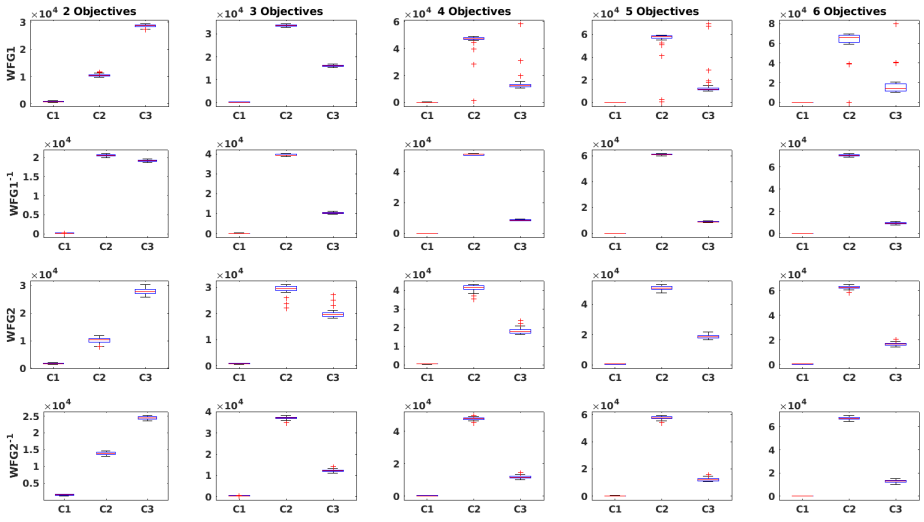

Figure 7.11: Utilization of the three ways to select the worst solution of the population in Algorithm 17.

empirical analysis of μ-optimal distributions, we used the PCUIs as the backbone of an indicator-based density estimator for a steady-state MOEA, named PCUI-EMOA. The results showed that PCUI-EMOA is able to compensate the weaknesses of one of its base indicators with the strengths of the other.

Finally, we proposed PFI-EMOA which exploits the trade-off between IGD^+ and Riesz s-energy, following the mathematical combination of QIs. Even though, the combination of both QIs is not Pareto-compliant, the experimental results showed that PFI-EMOA is able to produce Pareto front approximations, having good convergence and diversity properties simultaneously due to the utilization of the combined indicator. Hence, this result supports that the combination of QIs is a good way to control the search properties of an IB-MOEA.

Chapter 8

Riesz s-energy-based Reference Sets

This chapter explores the construction of reference sets based on the Riesz s-energy to overcome some difficulties on the currently available methods. Section 8.1 explains the motivation to study this problem. Section 8.2 describes the previous related work on the design of reference sets using weight vectors. Section 8.3 introduces our proposed tool to generate reference sets and Section 8.4 presents the results, regarding three experiments. Finally, the summary of the chapter is shown in Section 8.5.

8.1 Motivation

Regarding optimization theory, a reference point is a feasible or infeasible point in objective space that reasonably fulfills the desires of a decision maker [108]. In evolutionary multi-objective optimization, it is usual to employ a set of reference points, also known as a reference set, in two main directions. First, in the context of MOEAs, reference sets have been used to guide the population towards the Pareto front [89]. According to Li *et al.* [89], this class of MOEA uses reference sets based on examined points (i.e., nondominated solutions gathered during the evolutionary process) or virtually generated points in objective space, using, for instance, the method of Das and Dennis [26]. The Nondominated Sorting Genetic Algorithm III (NSGA-III) [30] is a well-known reference set-based MOEA that uses a set of virtual points as its reference set. On the other hand, reference sets play an important role in the assessment of MOEAs. Some quality indicators such as IGD [23] and IGD$^+$ [74] require a reference set for its computation. The idea of these QIs is to determine how close and similar is an approximation set, generated by an MOEA, to the reference set on the basis of a distance function.

Regardless of where the reference set is applied, a critical issue is how to construct it. Currently, the Das and Dennis method, denoted as the Simplex-Lattice-Design (SLD), that generates a set of convex weight vectors fitting the shape of a simplex, has been widely employed to generate reference sets [30]. However, the generation of

a simplex is the main drawback of the SLD method. Ishibuchi *et al.* [75] empirically showed that the performance of MOEAs using convex weight vectors strongly depends on the Pareto front shape of the MOP being tackled. If the weight vectors completely intersect the Pareto front, the MOEA will have a good performance. Otherwise, the MOEA will not be able to completely cover the Pareto front shape and will not be able to produce well-diversified solutions. Concerning the IGD and IGD$^+$ indicators, if a set of convex weight vectors is used as their reference set, both QIs will reward similar approximation sets. Hence, both QIs will produce misleading results since they prefer approximation sets similar to the set of convex weight vectors [72, 68]. Another difficulty of the SLD method is that the cardinality of the set is the combinatorial number $N = \binom{H+m-1}{m-1}$, where m is the dimensionality of the objective space and $H \in \mathbb{N}$ is a user-supplied parameter that controls the number of divisions of the objective space. In the case of high-dimensional objective spaces, the SLD method will generate a number of reference points that, from a practical point of view, is not feasible to handle.

Recently, the Riesz s-energy (E_s) [57] has been employed to improve the diversity of MOEAs [61]. This measure arises from the problem of distributing N points on the unit sphere S^d in $\mathbb{R}^{d+1}$, having the influence of potential theory and the distribution of charges. A relevant application of the Riesz s-energy is the discretization of manifolds (e.g., Pareto fronts). According to Hardin and Saff [56, 57], if a manifold has the d-dimensional Hausdorff measure, the minimization of the Riesz s-energy leads to asymptotically uniformly distributed solutions. Due to these nice mathematical properties, the Riesz s-energy can be used as a diversity indicator and, hence, as part of an MOEA's selection mechanism, aiming to generate well-diversified Pareto front approximations. In this regard, in Chapter 6 we have empirically shown that the use of E_s helps MOEAs to avoid the performance dependence on specific MOPs as pointed out by Ishibuchi *et al.* [75].

In this chapter, we propose a tool to generate reference sets of benchmark problems, using the Riesz s-energy. The underlying idea is to exploit the invariance of E_s to produce discretizations of manifolds with a high degree of diversity. Consequently, we provide reference sets of classical benchmark problems in the EMOO field such that researchers can use them either to guide MOEAs or for the assessment of MOEAs on the basis of QIs such as IGD and IGD$^+$. To this aim, we performed several experiments that show the superiority of our Riesz s-energy-based reference sets in terms of diversity for MOPs having from 2 up to 10 objectives.

8.2 Previous Related Work

In this section, we first describe the Riesz s-energy indicator which is a diversity indicator that has been hardly considered in the evolutionary multi-objective optimization community. Then, we provide a brief description of the construction of reference sets using weight vectors.

8.2.1 Riesz s-energy

Hardin and Saff [56, 57] proposed the discrete Riesz s-energy to measure the evenness of a set of points in d-dimensional manifolds. Mathematically, given an approximation set $\mathcal{A} = \{\vec{a}^1, \ldots, \vec{a}^N\}$, where $\vec{a}^i \in \mathbb{R}^m$, the Riesz s-energy is defined as follows:

$$E_s(\mathcal{A}) = \sum_{\vec{x} \in \mathcal{A}} \sum_{\substack{\vec{y} \in \mathcal{A} \\ \vec{y} \neq \vec{x}}} k_s(\vec{x}, \vec{y}), \tag{8.1}$$

where

$$k_s(\vec{x}, \vec{y}) = \begin{cases} ||\vec{x} - \vec{y}||^{-s}, & s > 0 \\ -\log ||\vec{x} - \vec{y}||, & s = 0 \end{cases} \tag{8.2}$$

The function k_s is the Riesz s-kernel, $|| \cdot ||$ denotes the Euclidean distance, and $s \geq 0$ is a parameter that controls the emphasis on the uniform distribution. As $s \to \infty$, a more uniform distribution is rewarded. It is worth noting that $s \geq 0$ is independent of the geometry of the underlying manifold of $\mathcal{A}$. According to Hardin and Saff [56], the minimization of E_s is related to the solution of the best-packing problem. There are several applications of the Riesz s-energy such as the discretization of a manifold (statistical sampling), quadrature rules, starting points for Newton's method, computer-aided design, interpolation schemes, finite element tessellations, among others [56].

8.2.2 Reference Sets based on Weight Vectors

In the EMOO field, the Simplex-Lattice-Design method to generate weight vectors has been widely used [26, 30, 61]. Its authors, Das and Dennis, proposed to generate uniformly distributed weight vectors in the simplex lattice, where each weight vector $\vec{w} \in \mathbb{R}^m$ has $\sum_{i=1}^{m} w_i = 1$, and $w_i \in \{0, \frac{1}{H}, \frac{2}{H}, \ldots, \frac{H}{H}\}$, i.e., it is a convex weight vector. $H \in \mathbb{N}$ is a user-supplied parameter that determines the number of divisions in each axis. The SLD method generates $N = C_{m-1}^{H+m-1}$ weight vectors in the simplex. This combinatorial number of vectors is an important drawback since as m increases, N grows in an exponential fashion which, from a practical point of view, is not desirable for MOEAs or even to evaluate Pareto front approximations using QIs. To generate reference sets using SLD, the usual way is to determine the best relationship between the set of points from the Pareto front and the weight vectors via a scalarizing function $u : \mathbb{R}^m \to \mathbb{R}$ [108]. For instance, a good scalarizing function is the achivement scalarizing function (ASF) that is defined as follows:

$$u_{\vec{w}}^{\text{ASF}}(\vec{x}, \vec{z}) = \max_{i=1,\ldots,m} \left\{ \frac{|x_i - z_i|}{w_i} \right\}. \tag{8.3}$$

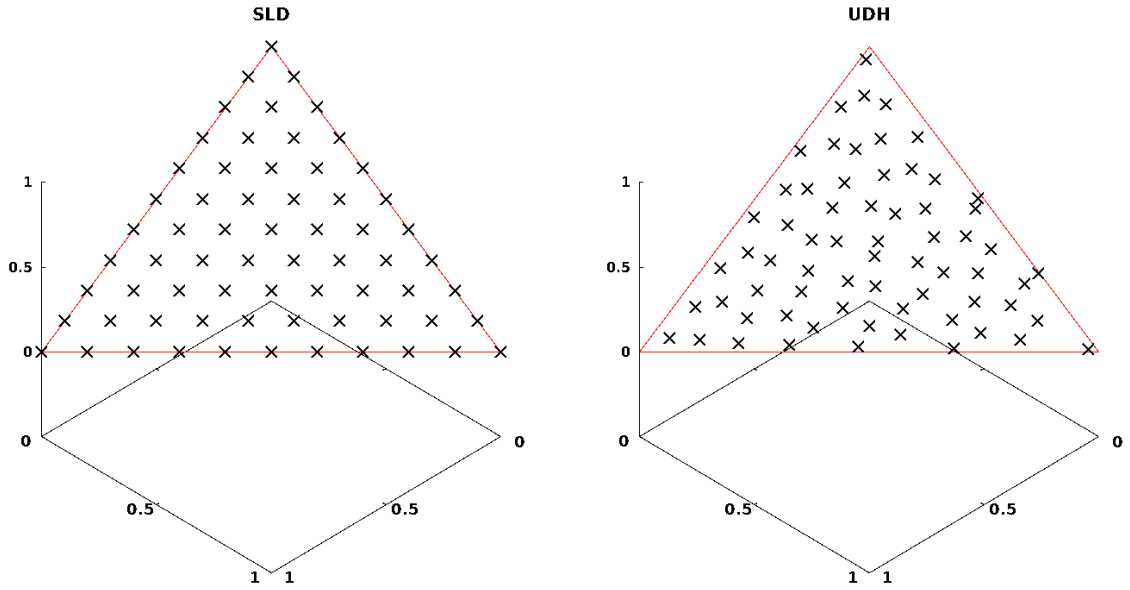

Figure 8.1: Weight vectors generated by SLD and UDH in a three-dimensional space. The contour of the simplex is shown in red.

where $\vec{x}, \vec{z} \in \mathbb{R}^m$ are the solution vectors to be evaluated and a reference point[1], respectively.

Another approach for generating evenly distributed weight vectors is the uniform design using the Hammersley method (UDH) [6]. UDH aims to tackle the three main drawbacks of SLD: (1) the diversity of weight vectors, (2) the generation of too many vectors in the boundary of the simplex, and (3) the nonlinear increase of the set cardinality. Uniform design generates uniformly scattered points in the selected space. According to Molinet Berenguer and Coello Coello [6], in uniform design, a set of points is considered uniformly spread throughout the entire domain if it has a small discrepancy, where the discrepancy is a numerical measure of scatter. Unlike SLD, the combination of the uniform design and the Hammersley method produces more uniform solutions and the cardinality of the set is not subject to a formula. We refer readers to [6] to obtain more details of this method. Figure 8.1 compares the distribution of points between SLD and UDH. It is clear that UDH does not generate several solutions in the boundary of the simplex which is a good property in the case of high-dimensional objective spaces. Similarly to SLD, to generate reference sets using UDH, the best relationship between each weight vector and a point from the Pareto front is found using a scalarizing function.

[1]In multi-objective optimization, $\vec{z}$ is usually the ideal point that has the minimum values for all the objective functions.

8.3 A Tool for Reference Set Construction

In the following, we consider $\mathcal{A} = \{\vec{a}^1, \ldots, \vec{a}^N\}$ as a finite subset of the Pareto front. To generate reference sets based on the Riesz s-energy, a subset $\mathcal{Z}$ of size $\mu < N$ has to be constructed by solving the so-called Riesz s-energy subset selection problem:

$$\mathcal{Z} = \begin{array}{l} \arg\min \\ \mathcal{Z}' \subset \mathcal{A} \\ |\mathcal{Z}'| = \mu \end{array} E_s(\mathcal{Z}'). \tag{8.4}$$

However, the size of the search space of the above problem is $\binom{N}{\mu}$. Hence, solving the Riesz s-energy subset selection problem requires a lot of computational effort. To overcome this difficulty, we follow a heuristic approach to iteratively reduce the cardinality of $\mathcal{A}$ until getting the desired set size. To this aim, we compute the individual contribution C of each solution $\vec{a} \in \mathcal{A}$ to the Riesz s-energy as follows:

$$C(\vec{a}, \mathcal{A}) = \frac{1}{2}[E_s(\mathcal{A}) - E_s(\mathcal{A} \setminus \{\vec{a}\})]. \tag{8.5}$$

Finally, to reduce the cardinality of $\mathcal{A}$, the worst-contributing solution $\vec{a}_{\text{worst}} = \arg\max_{\vec{a} \in \mathcal{A}} C(\vec{a}, \mathcal{A})$ is deleted.

The cost of computing E_s and $C(\vec{a}, \mathcal{A})$ is $\Theta(N^2)$. In consequence, the cost of computing all N individual contributions is $\Theta(N^3)$, following a naïve approach. In Figure 8.2, we propose a memoization structure that allows us to reduce the computational cost of computing the individual contributions to E_s. When $E_s(\mathcal{A})$ is calculated, we take advantage of the dissimilarity matrix by storing all $k_{ij} = k(\vec{a}^i, \vec{a}^j), i \neq j$. The memoization structure is a vector $\vec{r} \in \mathbb{R}^N$, where each $r_t = \sum_{j=1}^{N} k_{tj}$. Based on the components of $\vec{r}$, it is possible to compute $E_s(\mathcal{A})$ as shown in Figure 8.2. To compute $C(\vec{a}^i, \mathcal{A})$, we only need to substract k_{it} from each $r_t, t \neq i$ such that $E_s(\mathcal{A} \setminus \{\vec{a}^i\}) = \sum_{t=1, t\neq i}^{N} r_t$. This update process allows to compute every $C(\vec{a}, \mathcal{A})$ in $\Theta(N)$ and, thus, all individual contributions are computed in $\Theta(N^2)$. Algorithm 18 sketches the above described process.

8.4 Experimental Results

In this section, we compare our Riesz s-energy-based reference sets with reference sets constructed by the SLD, UDH, and a random selection procedure. For both SLD and UDH, we use ASF to find the best relationship between the weight vectors and the solutions in the Pareto fronts. For our experiments, we employed MOPs from the benchmarks: Deb-Thiele-Laumanns-Zitzler (DTLZ) [33], Walking-Fish-Group (WFG) [65], Irregular MOPs (IMOPs) [127], and the Viennet MOPs (VIE) [24]. We employed PlatEMO 2.0 [126] to obtain the Pareto fronts, i.e., the sets $\mathcal{A} = \{\vec{a}^i\}_{i=1,\ldots,N}$. To show the properties of the Riesz s-energy-based reference sets, we performed the following experiments:

Algorithm 18: Riesz s-energy steady state selection

Input: Pareto front approximation $\mathcal{A}$; size of the desired reference set μ
Output: Reference set

```
Compute dissimilarity matrix;
while |A| > μ do
    ā_worst = arg max_{ā∈A} (1/2)[E_s(A) − E_s(A \ {ā})];
    From the dissimilarity matrix, delete the row and column associated to ā_worst;
    Update the memoization structure r⃗;
    A = A \ {ā_worst};
end
return A;
```

$$\begin{bmatrix} 0 & k_{12} & \cdots & k_{1N} \\ k_{21} & 0 & \cdots & k_{2N} \\ \vdots & \vdots & & \vdots \\ k_{N1} & k_{N2} & \cdots & 0 \end{bmatrix} \qquad \begin{bmatrix} r_1 = \sum_{j=1}^{N} k_{1j} \\ r_2 = \sum_{j=1}^{N} k_{2j} \\ \vdots \\ r_N = \sum_{j=1}^{N} k_{Nj} \end{bmatrix}$$

Dissimilarity matrix — Memoization

$$E_s(\mathcal{A}) = \sum_{i=1}^{N} r_i$$

Figure 8.2: Memoization structure that takes advantage of the dissimilarity matrix to reduce the cost associated to the computation of all the individual contributions of a set.

1. We studied the influence of the parameter s in the distribution of solutions, aiming to determine which is its best value.

2. A diversity comparison of the reference sets produced by the four methodologies was performed based on the hypervolume indicator (HV), the Solow-Polasky Diversity (SPD), IGD, and IGD$^+$.

3. We analyzed the effect of all the reference set schemes for the optimal μ-distributions of the IGD and IGD$^+$ indicators.

4. A set of MOEAs is evaluated by IGD and IGD$^+$ using the four types of reference sets to analyze the difference in preferences.

It is worth noting that the source code of the Riesz s-energy steady state selection that implements the fast computation of the individual contributions and the complete numerical results of the proposed experiments are available at `http://computacion.cs.cinvestav.mx/~jfalcon/ReferenceSets.html`.

8.4.1 Influence of the Parameter s

The Riesz s-energy depends on the parameter $s \geq 0$ that controls the uniformity of solutions in the E_s-based optimal distribution. Regarding MOEAs, s has been usually set to $m-1$, where m is the number of objective functions. However, we do not completely know what is the effect of s in the Riesz s-energy optimal μ-distributions. In consequence, we varied the value of s for different MOPs to observe some distribution properties. Figure 8.3 shows the distributions related to $s = 0, 1, 2, 3, 4, 5, 6, 13$ for DTLZ1 3D, DTLZ1 5D, and DTLZ2 3D. From the distributions, there is evidence that the closer s gets to zero, the stronger the preference of the Riesz s-energy for boundary solutions. Regarding the three-objective DTLZ1 and DTLZ2, we can see well-diversified distributions with a slight emphasis on the boundaries when $s = 2$ and there is no clear difference between the distributions with $s > 2$. Hence, this supports the election of $s = m - 1$. Although the interpretation of the parallel coordinates of DTLZ1 5D is difficult, when the "peaks" are crowded, this means that the density of solutions in the boundary is high. It is worth emphasizing that for large values of s, the numerical values of the Riesz s-kernel considerably increase, which can produce numerical instability problems in a computer. Hence, for the experiments in the following sections, we employed $s = m - 1$ as suggested in [61].

8.4.2 Assessing Reference Sets

This experiment aims to provide evidence that our proposed approach produces reference sets having high diversity properties. To this purpose, we generated reference sets of the problems DTLZ1, DTLZ2, DTLZ5, DTLZ6, DTLZ7, WFG1-WFG4 for 2 to 10 objective functions and we also considered the test instances IMOP1-IMOP8 and VIE1-VIE3 that have a fixed number of objective functions. We adopted these

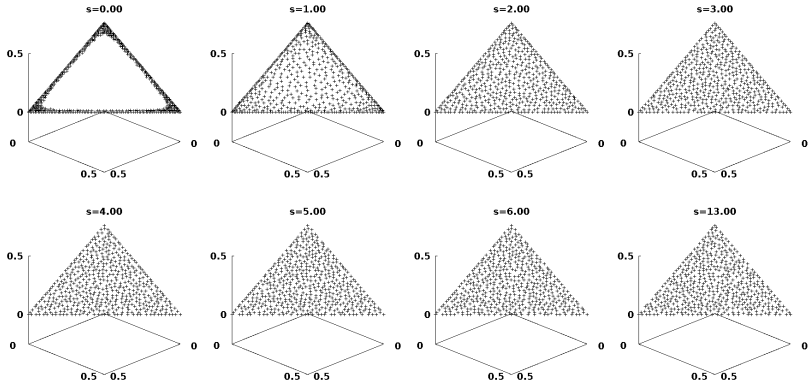

(a) DTLZ1 3D

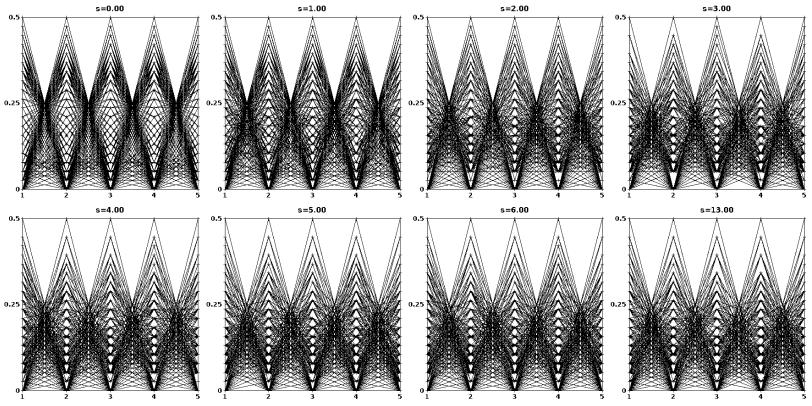

(b) DTLZ1 5D

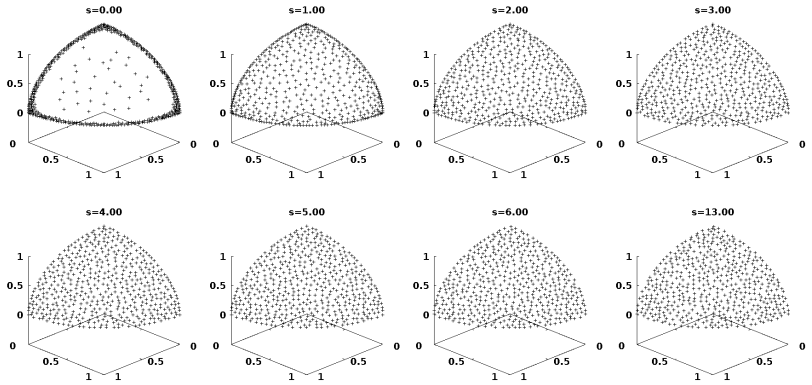

(c) DTLZ2 3D

Figure 8.3: Approximated Riesz s-energy optimal distributions, varying the value of the parameter s.

Table 8.1: Cardinality of the reference sets where H is the parameter of the SLD method.

m	N_1	N_2	N_3	N_4	N_5
2	$50_{H=49}$	$100_{H=99}$	$200_{H=199}$	$300_{H=299}$	$500_{H=499}$
3	$66_{H=10}$	$105_{H=13}$	$210_{H=19}$	$300_{H=23}$	$496_{H=30}$
4	$56_{H=5}$	$120_{H=7}$	$220_{H=9}$	$364_{H=11}$	$560_{H=13}$
5	$35_{H=3}$	$126_{H=5}$	$210_{H=6}$	$330_{H=7}$	$495_{H=8}$
6	$56_{H=3}$	$126_{H=4}$	$252_{H=5}$	-	$462_{H=6}$
7	$28_{H=2}$	$84_{H=3}$	$210_{H=4}$	-	$462_{H=5}$
8	$36_{H=2}$	$120_{H=3}$	-	$330_{H=4}$	$792_{H=5}$
9	$45_{H=2}$	$165_{H=3}$	-	-	$495_{H=4}$
10	$55_{H=2}$	-	$220_{H=3}$	-	$715_{H=4}$

MOPs since all of them cover linear, concave, convex, degenerate, disconnected, and mixed Pareto front shapes. For all test instances, we produced reference sets of different cardinalities that are shown in Table 8.1 (N_1: about 50, N_2: about 100, N_3: about 200, N_4 about 300, and N_5: about 500). As previously mentioned, the Pareto fronts were obtained from PlatEMO 2.0. Tables 8.2, 8.3, 8.4, and 8.5 show the average ranking results for the HV, SPD, IGD, and IGD$^+$ comparisons, respectively. SPD employs $\theta = 10$. IGD and IGD$^+$ employ reference sets of size 2,000 for their computation in each test instance, where these reference sets were directly obtained from PlatEMO. Our proposed reference sets are in all cases the best-ranked approaches considering the SPD indicator which is a pure-diversity QI. On the other hand, HV, IGD, and IGD$^+$, which are convergence-diversity QIs, mostly prefer the Riesz s-energy reference sets. The differences with respect to SPD are due to their own preferences properties, .e.g., HV prefers solutions around the Pareto front's knee. Consequently, there is strong empirical evidence that the Riesz s-energy indicator is able to produce well-diversified reference sets regardless of the geometry of the Pareto fronts and their dimensionality. Figure 8.4 shows a graphical comparison of the four methodologies for the five-objective DTLZ5, WFG1, and WFG3 problems. The Riesz s-energy-based reference sets exhibit better coverage and diversity of solutions in comparison to the random SLD, UDH, and random selection.

8.4.3 IGD and IGD$^+$ optimal μ-distributions

Our aim is to determine which is the effect of the Riesz s-energy-based reference sets to approximate the IGD and IGD$^+$ optimal μ-distribution. Based on the results of the previous section, we hypothesize that their use could improve the diversity proporties of these distributions. For this experiment, we implemented a steady-state MOEA (based on the framework of the SMS-EMOA [8]) that uses a density estimator based on IGD and IGD$^+$. We denoted such algorithms as IGD-MaOEA and IGD$^+$-MaOEA. Both algorithms employed a fixed reference set whose cardinality is given

Table 8.2: Average ranking for Hypervolume comparison.

MOP	**Riesz s-energy**	**Random**	**SLD**	**UDH**
DTLZ1	1.184	2.789	2.289	3.736
DTLZ2	1.973	3.710	1.710	2.605
DTLZ5	1.000	2.421	3.8425	2.736
DTLZ6	1.000	2.263	3.842	2.894
DTLZ7	1.531	3.312	2.562	2.593
WFG1	2.500	2.421	1.657	3.421
WFG2	2.684	2.552	1.447	3.315
WFG3	1.000	2.210	3.736	3.052
WFG4	1.552	3.736	2.210	2.500
IMOP1	1.000	2.200	3.600	3.200
IMOP2	1.000	3.600	2.800	2.600
IMOP3	1.000	2.200	3.600	3.200
IMOP4	1.000	3.200	3.400	2.400
IMOP5	1.000	4.000	2.800	2.200
IMOP6	1.200	1.800	3.600	3.400
IMOP7	1.000	4.000	2.600	2.400
IMOP8	1.000	3.800	3.200	2.000
VIE1	1.000	2.666	3.333	3.000
VIE2	1.000	2.000	3.666	3.333
VIE3	1.333	2.666	2.000	4.000

Table 8.3: Average ranking for Solow-Polasky Diversity comparison.

MOP	**Riesz s-energy**	**Random**	**SLD**	**UDH**
DTLZ1	1.473	2.921	1.763	3.842
DTLZ2	1.184	3.131	2.421	3.263
DTLZ5	1.000	2.289	3.894	2.815
DTLZ6	1.000	2.263	3.842	2.894
DTLZ7	1.000	2.218	3.500	3.281
WFG1	1.000	2.631	2.684	3.684
WFG2	1.000	2.342	2.894	3.763
WFG3	1.000	2.342	3.815	2.842
WFG4	1.000	2.552	2.815	3.631
IMOP1	1.000	2.000	3.800	3.200
IMOP2	1.000	3.600	2.600	2.800
IMOP3	1.000	3.000	2.800	3.200
IMOP4	1.000	2.200	4.000	2.800
IMOP5	1.000	4.000	3.000	2.000
IMOP6	1.000	2.800	3.000	3.200
IMOP7	1.000	4.000	2.000	3.000
IMOP8	1.000	3.200	3.000	2.800
VIE1	1.000	2.000	4.000	3.000
VIE2	1.000	2.000	3.666	3.333
VIE3	1.000	2.000	3.000	4.000

Table 8.4: Average ranking for IGD comparison.

MOP	**Riesz *s*-energy**	**Random**	**SLD**	**UDH**
DTLZ1	2.921	3.078	2.657	1.342
DTLZ2	1.763	3.342	3.026	1.868
DTLZ5	1.263	2.368	3.605	2.763
DTLZ6	1.263	2.421	3.605	2.710
DTLZ7	1.343	2.125	3.562	2.968
WFG1	3.342	2.526	2.078	2.052
WFG2	2.921	2.263	2.210	2.605
WFG3	1.263	2.368	3.605	2.763
WFG4	1.526	2.947	3.263	2.263
IMOP1	1.000	2.000	3.800	3.200
IMOP2	2.200	4.000	2.200	1.600
IMOP3	1.000	3.800	2.400	2.800
IMOP4	1.000	2.000	4.000	3.000
IMOP5	1.000	2.200	3.800	3.000
IMOP6	1.000	2.000	3.200	3.800
IMOP7	1.000	2.400	3.000	3.600
IMOP8	1.000	2.800	3.400	2.800
VIE1	1.000	2.666	2.666	3.666
VIE2	1.000	2.000	3.666	3.333
VIE3	1.000	2.000	3.000	4.000

Table 8.5: Average ranking for IGD$^+$ comparison.

MOP	**Riesz *s*-energy**	**Random**	**SLD**	**UDH**
DTLZ1	2.894	2.842	3.000	1.263
DTLZ2	2.131	4.000	1.368	2.500
DTLZ5	1.000	2.342	3.763	2.894
DTLZ6	1.000	2.342	3.763	2.894
DTLZ7	2.218	2.718	3.187	1.875
WFG1	3.763	3.105	1.973	1.157
WFG2	3.421	3.289	1.921	1.368
WFG3	1.236	2.342	3.605	2.815
WFG4	2.473	3.921	1.184	2.421
IMOP1	1.000	2.200	3.000	3.800
IMOP2	1.000	4.000	2.200	2.800
IMOP3	1.000	3.000	3.200	2.800
IMOP4	1.000	2.000	4.000	3.000
IMOP5	1.200	2.000	4.000	2.800
IMOP6	1.000	2.000	3.200	3.800
IMOP7	1.000	2.600	2.600	3.800
IMOP8	1.800	3.600	2.400	2.200
VIE1	1.000	2.333	4.000	2.666
VIE2	1.000	2.000	3.666	3.333
VIE3	1.000	2.333	2.666	4.000

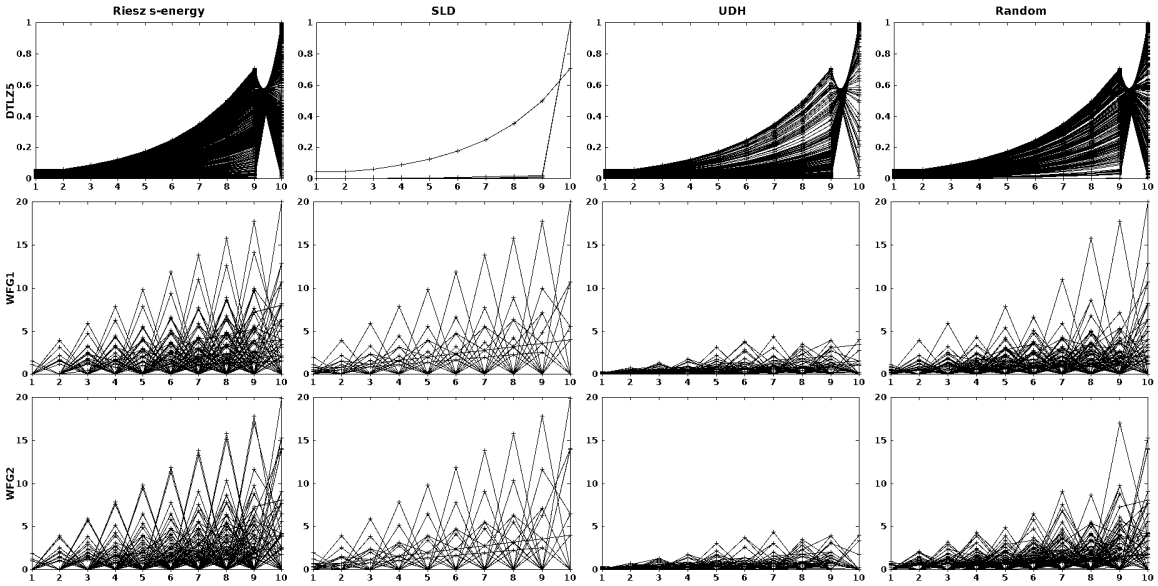

Figure 8.4: Examples of reference sets for the DTLZ5, WFG1, and WFG2 problems with five objective functions.

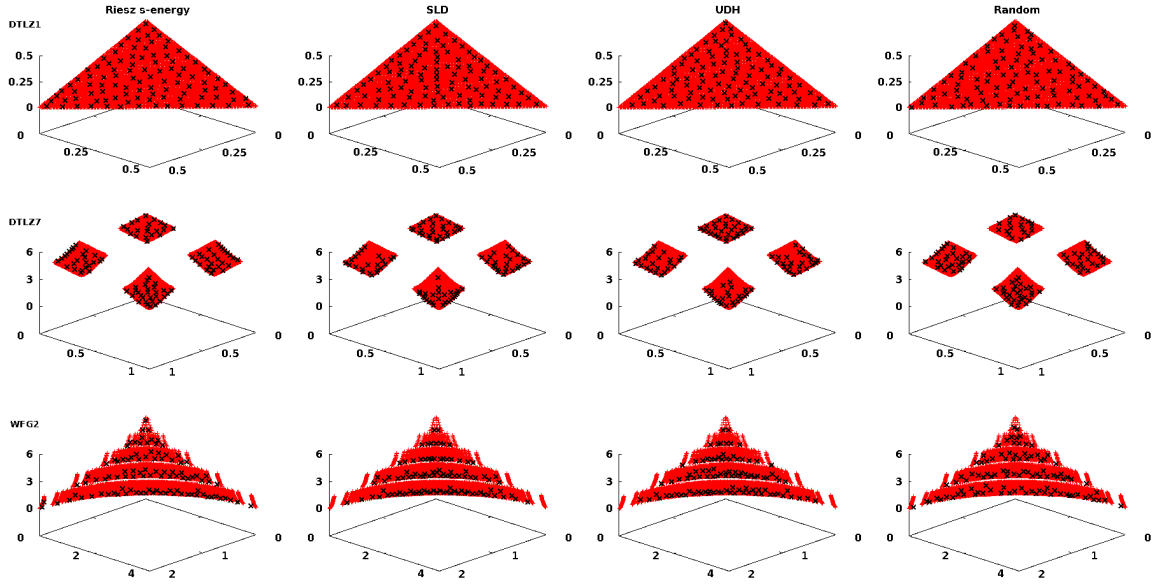

Figure 8.5: Approximated IGD^+ optimal distributions of size 100 of the three-dimensional DTLZ1, DTLZ7, and WFG2 problems. The true Pareto front is shown in red.

by the column N_5 of Table 8.1. We approximated the optimal μ-distributions of the problems DTLZ1, DTLZ2, DTLZ5, DTLZ6, DTLZ7, and WFG1-WFG4 with 2 to 10 objective functions, where μ is the population size of the algorithms and we used $\mu = 20, 50, 100$. To correctly approximate the distributions, we turned off all the difficulties of the problems. For each test instance, the stopping criterion of both algorithms was 100,000 function evaluations.

Tables 8.6 and 8.7 show the average ranking results for IGD-MaOEA and IGD$^+$-MaOEA regarding SPD, IGD, and IGD$^+$ values. Similarly to the previous section, the SPD indicator shows that the use of the Riesz s-energy-based reference sets allows both MOEAs to achieve better distributions in comparison to the use of reference sets based on SLD, UDH, and the random selection. However, the results of both IGD and IGD$^+$ are different from the SPD results, biasing the preference to the UDH-based reference sets. This behavior can be explained as follows. For the calculation of IGD and IGD$^+$, we employed the reference sets produced by the PlatEMO that uses weight vectors to find Pareto optimal solutions. Hence, there is a correlation between such reference sets and the results using UDH. Figure 8.5 presents a comparison of distributions for the DTLZ1, DTLZ7, and WFG2 problems with three-objective functions. As the SPD in Tables 8.6 and 8.7 indicates, the distributions created using the Riesz s-energy-based reference set have better diversity of solutions. Based on these discussions, we can claim that the use of the Riesz s-energy to generate reference sets could help referece set-based MOEAs to generate Pareto front approximations with a higher degree of diversity.

8.4.4 Assessment of MOEAs

In this section, we aim to analyze the preference of the IGD and IGD$^+$ indicators using the four types of reference sets in the IGD- and IGD$^+$-based comparison of different MOEAs. For this aim, we executed several MOEAs on MOPs having 2 to 6 objective functions. Each MOEA was executed 30 independent times on each test instance. Tables B.28, B.29, B.30, and B.31 show the IGD results using references based on Riesz s-energy, SLD, UDG, and Random selection, respectively. Tables B.32, B.33, B.34, and B.35 show the IGD$^+$ results using references based on Riesz s-energy, SLD, UDG, and Random selection, respectively. In this section, Table 8.8 shows the numerical results of the IGD comparison only for the WFG2 problem. We employed the reference sets of cardinality equal to the column N_5 of Table 8.1. The use of different methods to generate reference sets does not radically change the preference of IGD as it is clear in Table 8.8. Further research is required in this direction to determine the effect of the Riesz s-energy-based reference on the IGD and IGD$^+$ comparison.

Table 8.6: SPD, IGD, and IGD$^+$ average ranking results of the IGD optimal μ-distributions using the four types of reference sets.

QI	MOP	Riesz s-energy	Random	SLD	UDH
SPD	DTLZ1	1.962	2.296	1.777	3.962
	DTLZ2	2.333	3.481	2.074	2.111
	DTLZ5	1.370	2.148	3.777	2.703
	DTLZ6	1.592	1.851	3.740	2.814
	DTLZ7	1.380	2.428	3.190	3.000
	WFG1	1.222	2.037	2.962	3.777
	WFG2	1.407	1.814	3.037	3.740
	WFG3	1.296	2.296	3.037	3.370
	WFG4	1.148	2.148	3.481	3.222
IGD	DTLZ1	2.629	3.037	3.148	1.185
	DTLZ2	1.740	3.259	3.370	1.629
	DTLZ5	1.259	2.222	3.703	2.814
	DTLZ6	1.370	2.111	3.703	2.814
	DTLZ7	2.904	2.761	2.476	1.857
	WFG1	3.703	2.814	2.185	1.296
	WFG2	3.629	2.629	1.888	1.851
	WFG3	1.222	2.222	3.666	2.888
	WFG4	2.481	2.629	3.259	1.629
IGD$^+$	DTLZ1	2.851	2.888	3.111	1.148
	DTLZ2	2.592	3.814	1.185	2.407
	DTLZ5	1.148	2.111	3.740	3.000
	DTLZ6	1.370	1.888	3.740	3.000
	DTLZ7	1.428	2.095	3.619	2.857
	WFG1	3.851	3.074	1.925	1.148
	WFG2	3.666	3.333	1.851	1.148
	WFG3	1.296	2.148	3.666	2.888
	WFG4	3.222	3.296	1.333	2.148

8.5 Summary

Currently, reference sets are widely used to guide the population of an MOEA towards the Pareto front or for the assessment of MOEAs through quality indicators. An important issue is how to construct the reference set, having good diversity properties regardless of the dimensionality of the objective space and the geometry of the Pareto front. In this chapter, we proposed to use the Riesz s-energy to construct reference sets due to its nice properties that allow to uniformly sample a d-dimensional manifold. Our experimental results that include the diversity assessment of our reference sets and three other construction methodologies of reference sets indicate the superiority of the Riesz s-energy. This superiority was shown in the construction of approximated optimal μ-distributions for the IGD and IGD$^+$ indicators and for the assessment of state-of-the-art MOEAs.

Table 8.7: SPD, IGD, and IGD$^+$ average ranking results of the IGD$^+$ optimal μ-distributions using the four types of reference sets.

QI	MOP	Riesz s-energy	Random	SLD	UDH
SPD	DTLZ1	1.777	2.481	1.777	3.962
	DTLZ2	1.925	2.333	2.925	2.814
	DTLZ5	1.518	2.555	3.740	2.185
	DTLZ6	1.555	2.296	3.777	2.370
	DTLZ7	1.428	1.809	3.380	3.380
	WFG1	1.259	1.925	3.037	3.777
	WFG2	1.185	1.851	3.074	3.888
	WFG3	1.296	2.444	2.851	3.407
	WFG4	2.000	2.148	2.925	2.925
IGD	DTLZ1	2.481	3.074	3.074	1.370
	DTLZ2	2.296	1.777	3.111	2.814
	DTLZ5	2.333	2.555	3.444	1.666
	DTLZ6	2.370	2.444	3.481	1.703
	DTLZ7	1.952	1.761	3.666	2.619
	WFG1	1.555	1.592	3.185	3.666
	WFG2	1.444	1.629	3.148	3.777
	WFG3	1.185	2.222	3.777	2.814
	WFG4	2.296	1.296	3.407	3.000
IGD$^+$	DTLZ1	2.666	3.074	3.074	1.185
	DTLZ2	2.333	3.629	2.148	1.888
	DTLZ5	1.296	2.296	3.629	2.777
	DTLZ6	1.370	2.185	3.666	2.777
	DTLZ7	2.666	3.190	2.428	1.714
	WFG1	3.740	3.222	1.592	1.444
	WFG2	3.740	3.037	1.925	1.296
	WFG3	1.185	2.185	3.740	2.888
	WFG4	3.074	3.777	1.592	1.555

Table 8.8: Mean and, in parentheses, standard deviation of the IGD comparison, for the WFG2 problem, using the four methods to generate reference sets. The two best values are shown in grayscale, where the darker tone corresponds to the best algorithm. The superscript indicates the rank of the algorithm.

Method	Dim.	IGD$^+$-MaOEA	MOMBI3	AR-MOEA	RVEA	GrEA	SPEA2SDE	Two_Arch2
Riesz s-energy	2	3.234381e-01^{7} (5.975547e-02)	1.580167e-01^{1} (1.562619e-01)	2.425274e-01^{6} (1.389113e-01)	1.628697e-01^{2} (1.133657e-01)	2.116046e-01^{4} (1.402733e-01)	2.054706e-01^{3} (1.545234e-01)	2.407449e-01^{5} (1.416473e-01)
	3	4.184759e-01^{6} (1.524529e-01)	3.353822e-01^{1} (1.640826e-01)	4.106785e-01^{5} (1.896221e-01)	3.597037e-01^{3} (1.858185e-01)	3.934160e-01^{4} (1.304571e-01)	4.731361e-01^{7} (1.426240e-01)	3.387827e-01^{2} (1.946614e-01)
	4	9.748887e-01^{7} (2.014461e-01)	6.478702e-01^{3} (2.399085e-01)	6.169584e-01^{1} (2.333210e-01)	6.909600e-01^{4} (2.427336e-01)	8.551820e-01^{5} (1.974260e-01)	9.490244e-01^{6} (1.679712e-01)	6.207841e-01^{2} (2.577176e-01)
	5	1.556550e+00^{7} (2.180828e-01)	8.046459e-01^{1} (2.501754e-01)	8.353550e-01^{2} (2.332823e-01)	1.237189e+00^{5} (3.040188e-01)	1.152309e+00^{4} (1.611949e-01)	1.530695e+00^{6} (2.194192e-01)	8.896438e-01^{3} (2.928290e-01)
	6	2.147859e+00^{6} (2.503432e-01)	1.265947e+00^{3} (3.529989e-01)	1.233485e+00^{1} (3.172725e-01)	1.963559e+00^{5} (3.526986e-01)	1.686628e+00^{4} (2.801769e-01)	2.278093e+00^{7} (2.432840e-01)	1.252698e+00^{2} (3.298790e-01)
SLD	2	2.956513e-01^{7} (5.532228e-02)	1.426335e-01^{1} (1.445513e-01)	2.198279e-01^{5} (1.299147e-01)	1.574546e-01^{2} (1.007099e-01)	1.894829e-01^{4} (1.318221e-01)	1.869568e-01^{3} (1.424213e-01)	2.212709e-01^{6} (1.290839e-01)
	3	2.790953e-01^{3} (1.789936e-01)	2.749698e-01^{2} (1.981554e-01)	3.770123e-01^{7} (2.174194e-01)	3.242739e-01^{6} (1.958300e-01)	2.749419e-01^{1} (1.567955e-01)	3.217098e-01^{5} (1.847323e-01)	3.153545e-01^{4} (2.156497e-01)
	4	8.156440e-01^{7} (3.160402e-01)	6.355970e-01^{4} (3.662658e-01)	5.993264e-01^{1} (3.674012e-01)	6.045240e-01^{2} (3.345032e-01)	7.095258e-01^{5} (3.111989e-01)	7.208153e-01^{6} (2.656273e-01)	6.244147e-01^{3} (3.755997e-01)
	5	1.333039e+00^{7} (4.444634e-01)	7.221917e-01^{1} (4.213339e-01)	7.631819e-01^{2} (4.415437e-01)	1.028465e+00^{5} (4.727804e-01)	8.547878e-01^{3} (3.092179e-01)	1.213322e+00^{6} (4.193114e-01)	8.743622e-01^{4} (5.053471e-01)
	6	1.687462e+00^{6} (4.759212e-01)	1.109226e+00^{1} (5.243480e-01)	1.166047e+00^{3} (5.466763e-01)	1.668561e+00^{5} (5.778571e-01)	1.413500e+00^{4} (5.366980e-01)	1.859156e+00^{7} (4.830788e-01)	1.133397e+00^{2} (5.686533e-01)
UDH	2	2.919313e-01^{7} (5.461468e-02)	1.408839e-01^{1} (1.426805e-01)	2.171267e-01^{5} (1.281298e-01)	1.563367e-01^{2} (9.891542e-02)	1.872846e-01^{4} (1.299533e-01)	1.847227e-01^{3} (1.404722e-01)	2.185182e-01^{6} (1.273169e-01)
	3	2.708864e-01^{4} (1.694095e-01)	2.722777e-01^{3} (1.868100e-01)	3.654160e-01^{7} (2.079050e-01)	3.177317e-01^{6} (1.848709e-01)	2.709690e-01^{2} (1.475962e-01)	3.122282e-01^{5} (1.743504e-01)	3.073239e-01^{4} (2.058473e-01)
	4	7.117344e-01^{7} (3.442947e-01)	6.117706e-01^{6} (3.712138e-01)	5.899830e-01^{2} (3.619661e-01)	5.401684e-01^{1} (3.481553e-01)	6.079171e-01^{5} (3.394134e-01)	5.969660e-01^{4} (2.934897e-01)	5.908195e-01^{3} (3.861430e-01)
	5	1.064249e+00^{7} (5.660817e-01)	6.771401e-01^{2} (4.442194e-01)	7.016092e-01^{3} (4.810877e-01)	8.099523e-01^{5} (5.401982e-01)	5.844477e-01^{1} (3.717637e-01)	9.007483e-01^{6} (5.296794e-01)	7.878792e-01^{4} (5.560114e-01)
	6	1.113797e+00^{5} (7.729060e-01)	9.476411e-01^{1} (6.455016e-01)	1.065796e+00^{3} (7.050877e-01)	1.334352e+00^{6} (8.255314e-01)	1.066176e+00^{4} (7.819136e-01)	1.375711e+00^{7} (7.944234e-01)	9.829118e-01^{2} (7.250366e-01)
Random	2	3.774162e-01^{7} (7.073652e-02)	1.815207e-01^{2} (1.851105e-01)	2.799561e-01^{6} (1.666496e-01)	1.756049e-01^{1} (1.387162e-01)	2.414035e-01^{4} (1.689005e-01)	2.380349e-01^{3} (1.826005e-01)	2.795021e-01^{5} (1.668415e-01)
	3	3.982291e-01^{5} (1.543673e-01)	3.310771e-01^{1} (1.628366e-01)	4.045044e-01^{6} (1.907077e-01)	3.548877e-01^{3} (1.845288e-01)	3.856882e-01^{4} (1.287517e-01)	4.542812e-01^{7} (1.439465e-01)	3.340118e-01^{2} (1.954608e-01)
	4	8.949975e-01^{7} (2.080101e-01)	6.294227e-01^{3} (2.479606e-01)	6.009273e-01^{2} (2.392728e-01)	6.336071e-01^{4} (2.428153e-01)	7.841559e-01^{5} (2.059607e-01)	8.579769e-01^{6} (1.697523e-01)	6.007684e-01^{1} (2.679241e-01)
	5	1.340366e+00^{7} (2.577005e-01)	7.561532e-01^{1} (2.745982e-01)	7.724436e-01^{2} (2.635507e-01)	1.042620e+00^{5} (3.284797e-01)	9.630800e-01^{4} (1.826575e-01)	1.290533e+00^{6} (2.536782e-01)	8.413921e-01^{3} (3.215030e-01)
	6	1.785146e+00^{6} (2.413379e-01)	1.162767e+00^{3} (3.138277e-01)	1.147089e+00^{2} (2.690098e-01)	1.634505e+00^{5} (3.288890e-01)	1.405960e+00^{4} (2.730746e-01)	1.901939e+00^{7} (2.322959e-01)	1.124687e+00^{1} (3.105391e-01)

Chapter 9

Conclusions and Future Work

The evolutionary multi-objective optimization community has been benefited by quality indicators in two main ways: (1) by using QIs to quantitatively compare MOEAs, and (2) by designing new selection mechanisms that increase the selection pressure of MOEAs, allowing them to solve many-objective optimization problems. Regarding the first aspect, the main concern has been the formulation of new Pareto-compliant QIs, having different preferences to those of the hypervolume indicator. On the other hand, indicator-based mechanisms have been mainly designed on the basis of a single QI which implies that the resulting Pareto front approximations will show characteristics strongly related to the underlying QI. However, the use of multiple QIs to promote the design of selection mechanisms has been scarcely explored. In this thesis, we focus on both aspects, i.e, the design of new Pareto-compliant QIs and multi-indicator-based MOEAs. The main contributions of this thesis are the following:

1. A comprehensive study of the state-of-the-art IB-MOEAs in chapter 3.

2. An empirical analysis of the convergence and diversity properties of steady-state IB-MOEAs is provided in chapter 4.

3. We explored the design of multi-indicator-based MOEAs under two schemes: (1) competition of multiple IB-Density Estimators, using a hyper-heuristic and, additionally, employing ensemble learning (a machine learning technique), and (2) cooperation of multiple IB-Density Estimators whose synergy improves the convergence and diversity results of an MOEA and cooperation between multiple IB-MOEAs, in chapters 5 and 6, respectively.

4. We provided the first mathematical framework for the combination of QIs, giving as main result the formulation of new Pareto-compliant QIs in chapter 7. Based on this mathematical development, we proposed an IB-MOEA that exploits the trade-off between a convergence and a diversity indicator.

5. A tool to construct reference sets, which are widely employed to guide the evolutionary process of an MOEA and in the calculation of QIs such as IGD

and IGD$^+$. This tool is based on the diversity indicator Riesz s-energy that has shown to be invariant to the Pareto front shape.

Regarding the competition of IB-DEs, we proposed two approaches. On the one hand, the approach, called MIHPS, adaptatively selects online the IB-DE that promotes better convergence results, depending on the MOP being solved. For this purpose, a hyper-heuristic based on a Markov chain analyzes the convergence behavior of four IB-DEs based on the indicators R2, IGD$^+$, ϵ^+, and Δ_p. The proposed hyper-heuristic randomly selects an IB-DE to be executed although this decision is biased by the past convergence performance of the IB-DE, giving more chances to be selected to those with the best promotion of convergence. MIHPS outperformed state-of-the-art MOEAs. However, a remarkable point is that the indicators IGD$^+$, ϵ^+, and Δ_p were commonly employed at the initial stages of the evolutionary process, speeding up convergence while R2-DE was employed at the end of the search to refine convergence and diversity of solutions. Despite the good performance of MIHPS, we should emphasize that their Pareto front approximations tend to present characteristics closely related to an R2-based MOEA. On the other hand, the second approach is based on the AdaBoost algorithm (a well-known ensemble method) to construct a stronger density estimator on the basis of five IB-DEs. The proposal, denoted as EIB-MOEA, uses a linear combination of the density estimators to create the new one. The relative importance of each IB-DE is updated according to a learning process that analyzes the convergence behavior of each IB-DE. EIB-MOEA uses the four IB-DEs of MIHPS and a density estimator based on the hypervolume indicator is also considered. The experimental results showed that the ensemble density estimator compensates the weakesses of a baseline IB-DE using the strengths of the others. According to several QIs, the performance of EIB-MOEA is more consistent, producing the best results compared to IB-MOEAs that use the baseline QIs of EIB-MOEA. A critical factor that needs to be studied is the learning process that adapts the weight vector for the linear combination of the IB-DEs. From the proposals, the competition scheme of MIHPS is weakers since it was only able to speed up convergence towards the Pareto front but the desired compensation of the weakness of an IB-Mechanism with the strengths of others was not achievable. In contrast, EIB-MOEA could compensate the weaknesses of the IB-DEs with the strengths of other and, hence, this allowed EIB-MOEA to consistently perform well on different MOPs.

To overcome the main issue of MIHPS, we propose to tackle the design of MIB-MOEAs using a cooperative approach. First, we investigated the idea of the cooperation of two IB-DEs in a single MOEA. The selected indicators were the IGD$^+$ and the Riesz s-energy, where the former is a convergence-diversity QI and the latter is exclusively focused on diversity. We decided to complement the preferences of IGD$^+$ since our IGD$^+$-MaOEA failed to produce evenly distributed solutions in spite of its remarkable convergence results on MOPs having different Pareto front shapes. The synergy or cooperation between both indicators allowed to CRI-EMOA to outperfomed IGD$^+$-MaOEA and other state-of-the-art MOEAs with or without convex

weight vectors. Based on the experimental results, we concluded that CRI-EMOA is a more general optimizer since its performance does not depend on the MOP being solved. On the other hand, we explored the cooperation of multiple IB-MOEA by means of the island model. Our proposed approach, called cMIB-MOEA, isolatedly executes during a given number of iterations five steady-state IB-MOEAs: SMS-EMOA, R2-EMOA, IGD^+-MaOEA, ϵ^+-MaOEA, and Δ_p-MaOEA. Additionally, the master island stores in an external archive the best solutions from the IB-MOEAs, according to their Riesz s-energy contribution which promotes the generation of Pareto fronts evenly distributed. The experimental results showed that cMIB-MOEA is a Pareto-front shape invariant optimizer and it performs better than the panmictic versions of its baseline IB-MOEAs. This result shows that cooperation is a remarkable scheme to take advantage of the strengths of several IB-Mechanisms.

Concerning the design of Pareto-compliant QIs, we proposed a mathematical framework for the combination of QIs. Our main result is a theorem where we demonstrate that the combination of as many weakly Pareto-compliant QIs with at least one Pareto-compliant QI, using an order-preserving combination functions, results in a new Pareto-compliant QI. Hence, the combination of QIs allows to increase the number of Pareto-compliant QIs. For instance, weakly Pareto-compliant QIs such as the R2, IGD^+, and ϵ^+ can be improved by making them Pareto compliant when they are combined with the hypervolume indicator. We performed an analysis of preferences of the new QIs that showed that they have intermediate preferences among their baseline QIs. This result was supported empiricaly by studying the μ-optimal distributions associated to a steady-state MOEA. Thus, the combination of indicators is also a possible way to compensate the weaknesses of an indicator with the strengths of other indicators. This claim was additionally supported by an IB-MOEA that exploits the trade-off between the indicators IGD^+ and Riesz s-energy. Even though the resulting combination of these QIs is not Pareto-compliant, its investigation allowed us to deeply investigate how to extract the good quality properties of both indicators. The experimental results of our approach, denoted as PFI-EMOA, showed that its Pareto front approximations effectively exploit the trade-off between convergence and diversity. Additionally, PFI-EMOA was found to produce better results than CRI-EMOA which is also based on IGD^+ and Riesz s-energy.

As part of our future work, we are interested in the following aspects. We aim to study the properties of the competition and cooperation of multiple IB-Mechanism to extract the best characteristics from both paradigms of MIB-MOEAs. Regarding cMIB-MOEA, it should be parallelized since to the author's best knowledge, there is not a single parallel MIB-MOEA. Since the island model is strongly related to parallel MOEAs, the parallelization seems a logical step to follow. Additionally, it should be tested on many-objective optimization problems. It is necessary to widen the research around EIB-MOEA that showed promising results. The critical parts are the design of the learning mechanism and its high execution time that can be reduced by parallelizing the computation of the multiple density estimators. Finally, more theoretical studies to understand Pareto-compliant combined indicatos are also

necessary. In this regard, we need to better understand the similarities and differences of the preferences of the indicators to properly exploit their trade-off.

Appendix A

Benchmark Problems

In this Appendix, we present the test suites employed throughout the experimental analysis performed in this thesis. The considered benchmark problems, which correspond to real-valued and unconstrained MOPs, are the Deb-Thiele-Laumanns-Zitzler (DTLZ) [33], Walking Fish Group (WFG) [65], their inverted versions denoted as DTLZ^{-1} and WFG^{-1} [75], Lamé superspheres [38], Viennet problems (VIE) [133], and the Irregular MOPs (IMOPs) [127]. In the following, we provide their mathematical definition.

A.1 Deb-Thiele-Laumanns-Zitzler (DTLZ) Test Suite

The DTLZ test suite [33] includes seven unconstrained MOPs which are scalable to any number of decision variables and objective functions. These benchmark problems cover several search difficulties and Pareto front shapes as described in Table A.1. For these MOPs, the total number of decision variables is given by $n = m + k - 1$, where k is the number of distance parameters, and m is the number of objective functions. The distance parameters are defined as $\vec{y} = (x_m, x_{m+1}, \ldots, x_n)^T$, considering the decision vector $\vec{x} = (x_1, \ldots, x_{m-1}, x_m, x_{m+1}, \ldots, x_n)^T$. In [33], the following k-values are recommended: 5 for DTLZ1, 10 for DTLZ2-DTLZ6, and 20 for DTLZ7.

Table A.1: Properties of the DTLZ test suite.

MOP	**Separability**	**Frontality**	**Geometry**	**Bias**
DTLZ1	separable	multifrontal	linear	no
DTLZ2	separable	unifrontal	concave	no
DTLZ3	separable	multifrontal	concave	no
DTLZ4	separable	unifrontal	concave	polynomial
DTLZ5	unknown	unifrontal	arc, degenerated	parameter dependent
DTLZ6	unknown	unifrontal	arc, degenerated	parameter dependent
DTLZ7	separable	unifrontal	disconnected, mixed	no

DTLZ1

This MOP is separable and multifrontal. Its mathematical definition is as follows:

$$
\begin{array}{lrcl}
\text{Minimize} & f_1(\vec{x}) & = & 0.5(1+g(\vec{y}))\prod_{i=1}^{m-1} x_i \\
& f_{j=2:m-1}(\vec{x}) & = & 0.5(1+g(\vec{y})(1-x_{m-j+1})\prod_{i=1}^{m-j} x_i \\
& f_m(\vec{x}) & = & 0.5(1+g(\vec{y})(1-x_1) \\
\text{where} & y_{i=1:k} & = & \{x_m, x_{m+1}, \ldots, x_n\} \\
& g(\vec{y}) & = & 100\left\{k+\sum_{i=1}^{k}\left[(y_i-0.5)^2-\cos\left(20\pi(y_i-0.5)\right)\right]\right\} \\
\text{subject to} & & & \forall i \in \{1,\ldots,n\} 0 \leq x_i \leq 1.
\end{array}
\tag{A.1}
$$

Its Pareto front is linear and all objective function values lie on the linear hyperplane $\sum_{i=1}^{m} f_i = 0.5$.

DTLZ2

This problem is separable and unimodal and its definition is the following:

$$\begin{array}{lrcl} \text{Minimize} & f_1(\vec{x}) & = & (1+g(\vec{y}))\prod_{i=1}^{m-1}\cos\left(x_i\pi/2\right) \\ & f_{j=2:m-1}(\vec{x}) & = & (1+g(\vec{y}))\left(\prod_{i=1}^{m-j}\cos\left(x_i\pi/2\right)\right)\sin\left(x_{m-j+1}\pi/2\right) \\ & f_m(\vec{x}) & = & (1+g(\vec{y}))\sin\left(x_1\pi/2\right) \\ \text{where} & y_{i=1:k} & = & \{x_m, x_{m+1}, \ldots, x_n\} \\ & g(\vec{y}) & = & \sum_{i=1}^{k}(y_i 0.5)^2 \\ \text{subject to} & & & \forall i \in \{1,\ldots,n\} 0 \leq x_i \leq 1. \end{array} \tag{A.2}$$

The Pareto optimal solutions are produced when $\vec{y} = (0.5, 0.5, \ldots)^T$ y all the objective function values must satisfy that $\sum_{i=1}^{m} f_i^2 = 1$.

DTLZ3

This problem is similar to DTLZ2 but it includes multifrontal difficulty.

$$\begin{array}{lrcl} \text{Minimize} & f_1(\vec{x}) & = & (1+g(\vec{y}))\prod_{i=1}^{m-1}\cos\left(x_i\pi/2\right) \\ & f_{j=2:m-1}(\vec{x}) & = & (1+g(\vec{y}))\left(\prod_{i=1}^{m-j}\cos\left(x_i\pi/2\right)\right)\sin\left(x_{m-j+1}\pi/2\right) \\ & f_m(\vec{x}) & = & (1+g(\vec{y}))\sin\left(x_1\pi/2\right) \\ \text{where} & y_{i=1:k} & = & \{x_m, x_{m+1}, \ldots, x_n\} \\ & g(\vec{y}) & = & 100\left\{k+\sum_{i=1}^{k}\left[(y_i-0.5)^2-\cos\left(20\pi(y_i-0.5)\right)\right]\right\} \\ \text{subject to} & & & \forall i \in \{1,\ldots,n\} 0 \leq x_i \leq 1. \end{array} \tag{A.3}$$

The Pareto optimal front corresponds to $\vec{y} = (0.5, 0.5, \ldots)^T$.

DTLZ4

This MOP is concave, separable and unifrontal. Its principal characteristic is the introduced bias that tests the ability of an optimizer to maintain a good distribution

of solutions. It is defined as follows.

$$\begin{array}{lrcl}
\text{Minimize} & f_1(\vec{x}) & = & (1+g(\vec{y}))\prod_{i=1}^{m-1}\cos\left(x_i^{\alpha}\pi/2\right) \\
& f_{j=2:m-1}(\vec{x}) & = & (1+g(\vec{y}))\left(\prod_{i=1}^{m-j}\cos\left(x_i^{\alpha}\pi/2\right)\right)\sin\left(x_{m-j+1}^{\alpha}\pi/2\right) \\
& f_m(\vec{x}) & = & (1+g(\vec{y}))\sin\left(x_1^{\alpha}\pi/2\right) \\
\text{where} & y_{i=1:k} & = & \{x_m, x_{m+1}, \ldots, x_n\} \\
& g(\vec{y}) & = & \sum_{i=1}^{k}(y_i-0.5)^2 \\
\text{subject to} & & & \forall i \in \{1,\ldots,n\} 0 \leq x_i \leq 1.
\end{array} \tag{A.4}$$

The parameter $\alpha = 100$ is suggested in [33].

DTLZ5

This MOP modifies DTLZ2 to make it degenerated. It is defined as follows:

$$\begin{array}{lrcl}
\text{Minimize} & f_1(\vec{x}) & = & (1+g(\vec{y}))\prod_{i=1}^{m-1}\cos\left(\theta_i\pi/2\right) \\
& f_{j=2:m-1}(\vec{x}) & = & (1+g(\vec{y}))\left(\prod_{i=1}^{m-j}\cos\left(\theta_i\pi/2\right)\right)\sin\left(\theta_{m-j+1}\pi/2\right) \\
& f_m(\vec{x}) & = & (1+g(\vec{y}))\sin\left(\theta_1\pi/2\right) \\
\text{where} & y_{i=1:k} & = & \{x_m, x_{m+1}, \ldots, x_n\} \\
& \theta_i & = & \begin{cases} x_i & i=1 \\ \frac{1+2g(\vec{y})}{2(1+g(\vec{y}))}x_i & \forall i \in \{2,3,\ldots,m-1\} \end{cases} \\
& g(\vec{y}) & = & \sum_{i=1}^{k}(y_i-0.5)^2 \\
\text{subject to} & & & \forall i \in \{1,\ldots,n\} 0 \leq x_i \leq 1.
\end{array} \tag{A.5}$$

The Pareto optimal front corresponds to $\vec{y} = (0.5, 0.5, \ldots)^T$ and al the objective values must satisfy $\sum_{i=1}^{m} f_i^2 = 1$.

DTLZ6

By changing the g function in DTLZ5 gives rise to this complex MOP which is unifrontal, degenerated, and it has a stronger bias due to a transformation many-to-

one. It is defined as follows.

$$
\begin{array}{lrcl}
\text{Minimize} & f_1(\vec{x}) & = & (1+g(\vec{y}))\prod_{i=1}^{m-1}\cos\left(\theta_i\pi/2\right) \\
& f_{j=2:m-1}(\vec{x}) & = & (1+g(\vec{y}))\left(\prod_{i=1}^{m-j}\cos\left(\theta_i\pi/2\right)\right)\sin\left(\theta_{m-j+1}\pi/2\right) \\
& f_m(\vec{x}) & = & (1+g(\vec{y}))\sin\left(\theta_1\pi/2\right) \\
\text{where} & y_{i=1:k} & = & \{x_m, x_{m+1}, \ldots, x_n\} \\
& \theta_i & = & \begin{cases} x_i & i=1 \\ \frac{1+2g(\vec{y})}{2(1+g(\vec{y}))}x_i & \forall i \in \{2,3,\ldots,m-1\} \end{cases} \\
& g(\vec{y}) & = & \sum_{i=1}^{k} y_i^{0.1} \\
\text{subject to} & & & \forall i \in \{1,\ldots,n\} 0 \leq x_i \leq 1.
\end{array}
\tag{A.6}
$$

The Pareto optimal front corresponds to $\vec{y} = (0, 0, \ldots)^T$.

DTLZ7

This problem has a set of 2^{m-1} disconnected Pareto optimal regions. It tests the ability of an optimizer to maintain subpopulations in different regions.

$$
\begin{array}{lrcl}
\text{Minimize} & f_{j=1:m-1}(\vec{x}) & = & x_j \\
& f_m(\vec{x}) & = & (1+g(\vec{y}))\left\{m - \sum_{i=1}^{m-1}\left[\frac{f_i}{1+g(\vec{y})}(1+\sin\left(3\pi f_i\right))\right]\right\} \\
\text{where} & y_{i=1:k} & = & \{x_m, x_{m+1}, \ldots, x_n\} \\
& g(\vec{y}) & = & 1 + \frac{9}{k}\sum_{i=1}^{k} y_i \\
\text{subject to} & & & \forall i \in \{1,\ldots,n\} 0 \leq x_i \leq 1.
\end{array}
\tag{A.7}
$$

The Pareto optimal front corresponds to $\vec{y} = (0, 0, \ldots)^T$.

A.2 Walking Fish Group (WFG) Test Suite

The WFG test suite [65] suggests nine MOPs scalable with respect to the number of decision variables and objective functions. Table A.2 summarizes the main properties of the nine WFG instances. In the following, we describe the WFG instances. Here,

Table A.2: Properties of the WFG test suite.

MOP	Separability	Frontality	Geometry	Bias
WFG1	separable	unifrontal	convex, mixed	polynomial, flat
WFG2	non-separable	multifrontal	convex, disconnected	no
WFG3	non-separable	unifrontal	linear, degenerated	no
WFG4	separable	multifrontal	concave	no
WFG5	separable	deceptive	concave	no
WFG6	non-separable	unifrontal	concave	no
WFG7	separable	unifrontal	concave	parameter dependent
WFG8	non-separable	unifrontal	concave	parameter dependent
WFG9	non-separable	multifrontal	concave	parameter dependent

m represents the number of objective functions, and each problem is defined in terms of an underlying vector of parameters $\vec{x} \in \mathbb{R}^m$ that defines the fitness space. All $x_i \in \vec{x}$ have domain $[0, 1]$. x_m is known as the underlying distance parameter, and $x_{1:m-1}$ are the underlying position parameters. The vector $\vec{x}$ is derived, via a series of transition vectors, from a vector of working parameters $\vec{z} \in \mathbb{R}^n$ (also known as vector of variables). The domain of all $z_i \in \vec{z}$ is $[0, 2i]$. It is worth noting that $n \geq m$ and $n = k + l$. The first $k \in \{m-1, 2(m-1), 3(m-1), \dots\}$ working parameters are the position-related parameters and the last $l \in \{1, 2, \dots\}$ working parameters are the distance-related parameters. Each transition vector adds complexity to the underlying problem. The optimizer directly manipulates $\vec{z}$, through which $\vec{x}$ is indirectly manipulated.

WFG1

This problem is separable and unifrontal, but it has a polynomial and flat region. It is strongly biased toward small values of the variables, which makes it very difficult

for some optimizers. It is defined as follows:

$$
\begin{array}{lrcl}
\text{Given} & \vec{z} & = & (z_1, \ldots, z_k, z_{k+1}, \ldots, z_n)^T \\
\text{Minimize} & f_1(\vec{x}) & = & x_m + 2\prod_{i=1}^{m-1}\left(1 - \cos\left(x_i\pi/2\right)\right) \\
& f_{j=2:m-1}(\vec{x}) & = & x_m + 2j\left[\prod_{i=1}^{m-j}\left(1 - \cos\left(x_i\pi/2\right)\right)\right]\left(1 - \sin\left(x_{m-j+1}\pi/2\right)\right) \\
& f_m(\vec{x}) & = & x_m + 2m\left[1 - x_1 - \frac{\cos\left(10\pi x_1 + \pi/2\right)}{10\pi}\right] \\
\text{where} & x_{i=1:m-1} & = & \text{r\_sum}(\left\{y_{(i-1)k/(m-1)+1}, \ldots, y_{ik/(m-1)}\right\}, \\
& & & \{2(i-1)k/(m-1)+1, \ldots, 2ik/(m-1)\}) \\
& x_m & = & \text{r\_sum}(\{y_{k+1}, \ldots, y_n\}, \{2(k+1), \ldots, 2n\}) \\
& y_{i=1:n} & = & \text{b\_poly}(y'_i, 0.02) \\
& y'_{i=1:k} & = & y''_i \\
& y'_{i=k+1:n} & = & \text{b\_flat}(y''_i, 0.8, 0.75, 0.85) \\
& y''_{i=1:k} & = & z_i/(2i) \\
& y''_{i=k+1:n} & = & \text{s\_linear}(z_i/(2i), 0.35)
\end{array}
\tag{A.8}
$$

WFG2

This problem is non-separable and multifrontal. The Pareto optimal front is disconnected, and is given by the following expression.

$$
\begin{array}{lrcl}
\text{Given} & \vec{z} & = & (z_1, \ldots, z_k, z_{k+1}, \ldots, z_n)^T \\
\text{Minimize} & f_1(\vec{x}) & = & x_m + 2\prod_{i=1}^{m-1}\left(1 - \cos\left(x_i\pi/2\right)\right) \\
& f_{j=2:m-1}(\vec{x}) & = & x_m + 2j\left[\prod_{i=1}^{m-j}\left(1 - \cos\left(x_i\pi/2\right)\right)\right]\left(1 - \sin\left(x_{m-j+1}\pi/2\right)\right) \\
& f_m(\vec{x}) & = & x_m + 2m(1 - x_1\cos^2\left(5x_1\pi\right)) \\
\text{where} & x_{i=1:m-1} & = & \text{r\_sum}\left(\left\{y_{(i-1)k/(m-1)+1}, \ldots, y_{ik/(m-1)}\right\}, \{1, \ldots, 1\}\right) \\
& x_m & = & \text{r\_sum}\left(\left\{y_{k+1}, \ldots, y_{k+l/2}\right\}, \{1, \ldots, 1\}\right) \\
& y_{i=1:k} & = & y'_i \\
& y_{i=k+1:k+l/2} & = & \text{r\_nonsep}\left(\left\{y'_{k+2(i-k)-1}, y'_{k+2(i-k)}\right\}, 2\right) \\
& y'_{i=1:k} & = & z_i/(2i) \\
& y'_{i=k+1:n} & = & \text{s\_linear}(z_i/(2i), 0.35)
\end{array}
\tag{A.9}
$$

WFG3

This problem is non-separable but unifrontal. It has a linear and degenerated Pareto optimal front.

$$
\begin{array}{lrcl}
\text{Given} & \vec{z} & = & (z_1, \ldots, z_k, z_{k+1}, \ldots, z_n)^T \\
\text{Minimize} & f_1(\vec{x}) & = & x_m + 2\prod_{i=1}^{m-1} x_i \\
& f_{j=2:m-1}(\vec{x}) & = & x_m + 2j\left(\prod_{i=1}^{m-j} x_i\right)(1 - x_{m-j+1}) \\
& f_m(\vec{x}) & = & x_m + 2m(1 - x_1) \\
\text{where} & x_{i=1} & = & u_i \\
& x_{i=2:m-1} & = & x_m(u_i - 0.5) + 0.5 \\
& x_m & = & \text{r\_sum}\left(\left\{y_{k+1}, \ldots, y_{k+l/2}\right\}, \{1, \ldots, 1\}\right) \\
& u_i & = & \text{r\_sum}\left(\left\{y_{(i-1)k/(m-1)+1}, \ldots, y_{ik/(m-1)}\right\}, \{1, \ldots, 1\}\right) \\
& y_{i=1:k} & = & y'_i \\
& y_{i=k+1:k+l/2} & = & \text{r\_nonsep}\left(\left\{y'_{k+2(i-k)-1}, y'_{k+2(i-k)}\right\}, 2\right) \\
& y'_{i=1:k} & = & z_i/(2i) \\
& y'_{i=k+1:n} & = & \text{s\_linear}(z_i/(2i), 0.35)
\end{array}
\tag{A.10}
$$

WFG4

In this case, the problem is separable, but highly multifrontal. The Pareto optimal front is concave.

$$
\begin{array}{lrcl}
\text{given} & \vec{z} & = & (z_1, \ldots, z_k, z_{k+1}, \ldots, z_n)^T \\
\text{Minimize} & f_1(\vec{x}) & = & x_m + 2\prod_{i=1}^{m-1} \sin(x_i\pi/2) \\
& f_{j=2:m-1}(\vec{x}) & = & x_m + 2j\left(\prod_{i=1}^{m-j} \sin(x_i\pi/2)\right)\cos(x_{m-j+1}\pi/2) \\
& f_m(\vec{x}) & = & x_m + 2m\cos(x_1\pi/2) \\
\text{where} & x_{i=1:m-1} & = & \text{r\_sum}\left(\left\{y_{(i-1)k/(m-1)+1}, \ldots, y_{ik/(m-1)}\right\}, \{1, \ldots, 1\}\right) \\
& x_m & = & \text{r\_sum}\left(\{y_{k+1}, \ldots, y_n\}, \{1, \ldots, 1\}\right) \\
& y_{i=1:n} & = & \text{s\_multi}(z_i/(2i), 30, 10, 0.35)
\end{array}
\tag{A.11}
$$

WFG5

This problem is deceptive and separable. The Pareto front is concave.

$$
\begin{array}{lrcl}
\text{Given} & \vec{z} & = & (z_1, \ldots, z_k, z_{k+1}, \ldots, z_n)^T \\
\text{Minimize} & f_1(\vec{x}) & = & x_m + 2\prod_{i=1}^{m-1} \sin\left(x_i \pi/2\right) \\
& f_{j=2:m-1}(\vec{x}) & = & x_m + 2j\left(\prod_{i=1}^{m-j} \sin\left(x_i \pi/2\right)\right) \cos\left(x_{m-j+1}\pi/2\right) \\
& f_m(\vec{x}) & = & x_m + 2m\cos\left(x_1 \pi/2\right) \\
\text{where} & x_{i=1:m-1} & = & \text{r\_sum}\left(\left\{y_{(i-1)k/(m-1)+1}, \ldots, y_{ik/(m-1)}\right\}, \{1, \ldots, 1\}\right) \\
& x_m & = & \text{r\_sum}\left(\{y_{k+1}, \ldots, y_n\}, \{1, \ldots, 1\}\right) \\
& y_{i=1:n} & = & \text{s\_decept}(z_i/(2i), 0.35, 0.001, 0.05)
\end{array}
\tag{A.12}
$$

WFG6

This MOP is separable and unifrontal. Its Pareto front is concave.

$$
\begin{array}{lrcl}
\text{Given} & \vec{z} & = & (z_1, \ldots, z_k, z_{k+1}, \ldots, z_n)^T \\
\text{Minimize} & f_1(\vec{x}) & = & x_m + 2\prod_{i=1}^{m-1} \sin\left(x_i \pi/2\right) \\
& f_{j=2:m-1}(\vec{x}) & = & x_m + 2j\left(\prod_{i=1}^{m-j} \sin\left(x_i \pi/2\right)\right) \cos\left(x_{m-j+1}\pi/2\right) \\
& f_m(\vec{x}) & = & x_m + 2m\cos\left(x_1 \pi/2\right) \\
\text{where} & x_{i=1:m-1} & = & \text{r\_nonsep}\left(\left\{y_{(i-1)k/(m-1)+1}, \ldots, y_{ik/(m-1)}\right\}, k/(m-1)\right) \\
& x_m & = & \text{r\_nonsep}\left(\{y_{k+1}, \ldots, y_n\}, l\right) \\
& y_{i=1:k} & = & z_i/(2i) \\
& y_{i=k+1:n} & = & \text{s\_linear}(z_i/(2i), 0.35)
\end{array}
\tag{A.13}
$$

WFG7

Having a parameter dependent bias, this problem is also separable and unifrontal. The Pareto front shape is concave.

$$
\begin{array}{lrcl}
\text{Given} & \vec{z} & = & (z_1, \ldots, z_k, z_{k+1}, \ldots, z_n)^T \\
\text{Minimize} & f_1(\vec{x}) & = & x_m + 2\prod_{i=1}^{m-1} \sin\left(x_i\pi/2\right) \\
& f_{j=2:m-1}(\vec{x}) & = & x_m + 2j\left(\prod_{i=1}^{m-j} \sin\left(x_i\pi/2\right)\right)\cos\left(x_{m-j+1}\pi/2\right) \\
& f_m(\vec{x}) & = & x_m + 2m\cos\left(x_1\pi/2\right) \\
\text{where} & x_{i=1:m-1} & = & \text{r\_sum}\left(\left\{y_{(i-1)k/(m-1)+1}, \ldots, y_{ik/(m-1)}\right\}, \{1, \ldots, 1\}\right) \\
& x_m & = & \text{r\_sum}\left(\{y_{k+1}, \ldots, y_n\}, \{1, \ldots, 1\}\right) \\
& y_{i=1:k} & = & y'_i \\
& y_{i=k+1:n} & = & \text{s\_linear}(y'_i, 0.35) \\
& y'_{i=1:k} & = & \text{b\_param}(z_i/(2i), \text{r\_sum}(\{z_{i+1}/(2(i+1)), \ldots, z_n/(2n)\}, \\
& & & \{1, \ldots, 1\}), \frac{0.98}{49.98}, 0.02, 50) \\
& y'_{i=k+1:n} & = & z_i/(2i)
\end{array}
\tag{A.14}
$$

WFG8

This problem also has a parameter dependent bias, but is also non-separable and unifrontal. It has a concave Pareto front.

$$
\begin{array}{lrcl}
\text{Given} & \vec{z} & = & (z_1, \ldots, z_k, z_{k+1}, \ldots, z_n)^T \\
\text{Minimize} & f_1(\vec{x}) & = & x_m + 2\prod_{i=1}^{m-1} \sin\left(x_i\pi/2\right) \\
& f_{j=2:m-1}(\vec{x}) & = & x_m + 2j\left(\prod_{i=1}^{m-j} \sin\left(x_i\pi/2\right)\right)\cos\left(x_{m-j+1}\pi/2\right) \\
& f_m(\vec{x}) & = & x_m + 2m\cos\left(x_1\pi/2\right) \\
\text{where} & x_{i=1:m-1} & = & \text{r\_sum}\left(\left\{y_{(i-1)k/(m-1)+1}, \ldots, y_{ik/(m-1)}\right\}, \{1, \ldots, 1\}\right) \\
& x_m & = & \text{r\_sum}\left(\{y_{k+1}, \ldots, y_n\}, \{1, \ldots, 1\}\right) \\
& y_{i=1:k} & = & y'_i \\
& y_{i=k+1:n} & = & \text{s\_linear}(y'_i, 0.35) \\
& y'_{i=k} & = & z_i/(2i) \\
& y'_{i=k+1:1} & = & \text{b\_param}(z_i/(2i), \text{r\_sum}(\{z_1/2, \ldots, z_{i-1}/(2(i-1))\}, \\
& & & \{1, \ldots, 1\}), \frac{0.98}{49.98}, 0.02, 50)
\end{array}
\tag{A.15}
$$

WFG9

The last problem of the suite is non-separable, multifrontal, deceptive, and has a parameter dependent bias. All these features make it a very difficult problem. Additionally, it has a concave Pareto front.

$$
\begin{array}{lrcl}
\text{Given} & \vec{z} & = & (z_1, \ldots, z_k, z_{k+1}, \ldots, z_n)^T \\
\text{Minimize} & f_1(\vec{x}) & = & x_m + 2\prod_{i=1}^{m-1} \sin\left(x_i \pi/2\right) \\
& f_{j=2:m-1}(\vec{x}) & = & x_m + 2j\left(\prod_{i=1}^{m-j} \sin\left(x_i \pi/2\right)\right) \cos\left(x_{m-j+1}\pi/2\right) \\
& f_m(\vec{x}) & = & x_m + 2m\cos\left(x_1 \pi/2\right) \\
\text{where} & x_{i=1:m-1} & = & \text{r\_nonsep}\left(\left\{y_{(i-1)k/(m-1)+1}, \ldots, y_{ik/(m-1)}\right\}, k/(m-1)\right) \\
& x_m & = & \text{r\_nonsep}\left(\left\{y_{k+1}, \ldots, y_n\right\}, l\right) \\
& y_{i=1:k} & = & \text{s\_decep}(y'_i, 0.35, 0.001, 0.05) \\
& y_{i=k+1:n} & = & \text{s\_multi}(y'_i, 30, 95, 0.35) \\
& y'_{i=1:n-1} & = & \text{b\_param}(z_i/(2i), \text{r\_sum}(\{z_{i+1}/(2(i+1), \ldots, z_n/(2n)\}, \\
& & & \{1, \ldots, 1\}), \frac{0.98}{49.98}, 0.02, 50) \\
& y'_n & = & z_n/(2n)
\end{array}
\tag{A.16}
$$

Transformation Functions

The previous problems are defined in terms of a set of transformation functions, which map parameters with domain $[0, 1]$ onto the range $[0, 1]$. These are three types of transformation functions: **bias, shift, and reduction functions**. Bias and shift functions only employ one parameter, whereas reduction functions can employ many. Bias transformations have a natural impact on the search process by biasing the fitness lanscape. Shift transformations move the location of optimal values, and are used to apply a linear shift, or to produce deceptive and multifrontal problems. Reduction transformations are used to produce non-separability of the problem (dependency between variables). In the following, we define such transformation functions.

Bias: Polynomial

When $\alpha > 1$ or when $\alpha < 1$, y is biased towards zero or towards one, respectively.

$$\text{b\_poly}(y, \alpha) = y^{\alpha} \tag{A.17}$$

where $\alpha > 0$ and $\alpha \neq 1$.

Bias: Flat Region

Values of y between B and C, the area of the flat region, are mapped to the value A.

$$\begin{aligned} \text{b\_flat}(y, A, B, C) = A + \min\left(0, \lfloor y - B \rfloor\right) \cdot \tfrac{A(B-y)}{B} \\ - \min\left(0, \lfloor C - y \rfloor\right) \cdot \tfrac{(1-A)(y-C)}{1-C} \end{aligned} \tag{A.18}$$

where $A, B, C \in [0, 1], B < C, B = 0 \Rightarrow A = 0 \wedge C \neq 1$, and $C = 1 \Rightarrow A = 1 \wedge B \neq 0$.

Bias: Parameter Dependent

A, B, C, the parameter vector $\vec{w} \in [0, 1]^{|\vec{w}|}$, and the reduction function u together determine the degree to which y is biased by being raised to an associated power: values of $u(\vec{w}) \in [0, 0.5]$ are mapped linearly onto $[B, B + (C - B)A]$, and values of $u(\vec{w}) \in [0.5, 1]$ are mapped linearly onto $[B + (C - B)A, C]$.

$$\text{b\_param}(y, u(\vec{w}), A, B, C) = y^{B+(C-B)(A-(1-2u(\vec{w}))\lfloor 0.5-u(\vec{w}) \rfloor + A|)} \tag{A.19}$$

where $A \in (0, 1)$, and $0 < B < C$.

Shift: Linear

$A \in (0, 1)$ is the value for which y is mapped to zero.

$$\text{s\_linear}(y, A) = \frac{|y - A|}{|\lfloor A - y \rfloor + A|} \tag{A.20}$$

Shift: Deceptive

A is the value for which y is mapped to zero, and the global minimum of the transformation. B is the aperture size of the well/basin leading to the global minimum at A, and C is the value of the deceptive minima (there are always two deceptive minima).

$$\begin{aligned} \text{s\_decept}(y, A, B, C) = 1 + (|y - A| - B)(\tfrac{\lfloor y-A+B \rfloor (1-C+\frac{A-B}{B}}{A-B} \\ + \tfrac{\lfloor A+B-y \rfloor (1-C+\frac{1-A-B}{B}}{1-A-B} + \tfrac{1}{B}) \end{aligned} \tag{A.21}$$

where $A \in (0, 1), 0 < B \ll 1, 0 < C \ll 1, A - B > 0$, and $A + B < 1$.

Shift: Multimodal

A controls the number of minima, B controls the magnitude of the hill sizes of the multimodality, and C is the value for which y is mapped to zero. When $B = 0$, $2A + 1$ values of y (one at C) are mapped to zero, and when $B \neq 0$, there are $2A$

local minima, and one global minimum at C. Larger values of A and smaller values of B create more difficult problems.

$$\text{s\_multi}(y, A, B, C) = \frac{1 + \cos\left[(4A+2)\pi\left(0.5 - \frac{|y-C|}{2(\lfloor C-y\rfloor + C)}\right)\right] + 4B\left(\frac{|y-C|}{2(\lfloor C-y\rfloor + C)}\right)^2}{B+2} \tag{A.22}$$

where $A \in \{1, 2, \dots\}, B \geq 0, (4A+2)\pi > 4B$, and $C \in (0, 1)$.

Reduction: Weighted Sum

By varying the constants of the weight vector $\vec{w}$, the optimizers can be forced to treat parameters differently.

$$\text{r\_sum}(\vec{y}, \vec{w}) = \frac{\sum_{i=1}^{|\vec{y}|} w_i y_i}{\sum_{i=1}^{|\vec{y}|} w_i} \tag{A.23}$$

where $|\vec{w}| = |\vec{y}|$, and $w_1, \dots, w_{|\vec{y}|>0}$.

Reduction: Non-separable

A controls the degree of non-separability.

$$\text{r\_nonsep}(\vec{y}, A) = \frac{\sum_{j=1}^{|\vec{y}|}\left(y_j + \sum_{k=0}^{A-2}\left|y_j - y_{1+(j+k)mod|\vec{y}|}\right|\right)}{\frac{|\vec{y}|}{A}\lceil A/2\rceil(1 + 2A - 2\lceil A/2\rceil)} \tag{A.24}$$

where $A \in \{1, \dots, |\vec{y}|$, and $|\vec{y}|modA = 0$

A.3 Inverted DTLZ and WFG Test Suites

Ishibuchi *et al.* [75] proposed to make a slight modification to the DTLZ and WFG instances to generate new Pareto front shapes. This change corresponds to multiply by -1 all the objective functions of the MOPs. The generated problems are referred to as DTLZ^{-1} and WFG^{-1}. The effect is that the Pareto front is inverted though some other properties of the original problems may also change.

A.4 Lamé Superspheres

Emmerich and Deutz [38] proposed the Lamé superspheres test suite where the Pareto fronts of test problems are the intersection of a Lamé supersphere[1] with the positive

[1] An $m-1$-dimensional γ Lamé supersphere (denoted as S_γ^{m-1}) is defined as follows: $S_\gamma^{m-1} = \{(y_1, y_2, \dots, y_m) \in \mathbb{R}^m \mid |y_1|^\gamma + |y_2|^\gamma + \cdots + |y_m|^\gamma = 1\}$, where $\gamma \in \mathbb{R}_+$ is fixed.

$\mathbb{R}^m$-orthant. Besides scalability in the number of objectives and decision variables, the proposed test problems are also scalable in a characteristic denoted by Emmerich and Deutz as resolvability of conflict, which is closely related to convexity/concavity, curvature and the position of knee-points of the Pareto fronts.

For the definition of the test suite, let $\gamma > 0$ be fixed. Let $p_1(\theta_1, \ldots, \theta_{m-1}) = (\cos(\theta_1))^{\frac{2}{\gamma}}$, $p_i(\theta_1, \ldots, \theta_{m-1}) = (\sin(\theta_1)\sin(\theta_2)\cdot\cdots\cdot\sin(\theta_{i_1})\cos(\theta_i))^{\frac{2}{\gamma}}$, where $1 < i < m$, and, finally, $p_m = (\sin(\theta_1)\sin(\theta_2)\cdot\cdots\cdot\sin(\theta_{i_1})\sin(\theta_{m-1}))^{\frac{2}{\gamma}}$, with $0 \leq \theta_j \leq \frac{\pi}{2}$ and $j = 1, \ldots, m-1$ be a parametrization of $S_\gamma^{m-1,+}$. On this basis, the objective functions to be minimized can be defined as follows:

$$f_i(\theta, r) = (1 + g(r))p_i(\theta) \tag{A.25}$$

for $i = 1, \ldots, m$ and where $0 \leq \theta_j \leq \frac{\pi}{2}$ for $j = 1, \ldots, m-1$ and $g : \mathbb{R}_+ \to \mathbb{R}_+$. The variables θ_i with $i = 1, \ldots, m-1$ are viewed as meta-variables and one can, for instance, map the decision variables to θ_i as follows: $\theta_i = \frac{\pi}{2}x_i$ for $i = 1, \ldots, m-1$ with the restriction $0 \leq x_i \leq 1$.

As a unifrontal test problem with $n \geq m$ decision variables, Emmerich and Deutz proposed $g(r) = r, r = \sqrt{x_m^2 + \cdots + x_n^2}$. For a given γ with convex (concave) Pareto front, it can be obtained a problem (denoted as mirror problem) with congruent concave (convex) Pareto front by setting: $f_i(x) = 1/(g(x) + 1)p_i(\theta_1, \ldots, \theta_{m-1}), i = 1, \ldots, m$. In order to make the problem multifrontal, the authors proposed to choose $g(r) = F_{\text{natmin}}(r)$, with $F_{\text{natmin}} = b + (r - a) + 0.5 + 0.5\cos(2\pi(r - a) + \pi)$, where $a = 0.051373$ and $b = 0.0253235$.

A.5 Viennet Test Functions

In this section, we present the mathematical formulations of three Viennet problems (VIE) [24, 133] . These MOPs are three-objective ones, having a two-dimensional decision space.

VIE1

$$\begin{array}{lrcl} \text{Minimize} & f_1(x,y) & = & x^2 + (y-1)^2 \\ & f_2(x,y) & = & x^2 + (y+1)^2 + 1 \\ & f_3(x,y) & = & (x-1)^2 + y^2 + 2 \\ \text{Subject to} & x, y & \in & [-2, 2] \end{array} \tag{A.26}$$

VIE2

$$\begin{aligned} \text{Minimize} \quad f_1(x,y) &= \tfrac{(x-2)^2}{2} + \tfrac{(y+1)^2}{13} + 3 \\ f_2(x,y) &= \tfrac{(x+y-3)^2}{36} + \tfrac{(-x+y+2)^2}{8} - 17 \\ f_3(x,y) &= \tfrac{(x+2y-1)^2}{175} + \tfrac{(2y-x)^2}{17} - 13 \\ \text{Subject to} \quad x,y &\in [-4,4] \end{aligned} \tag{A.27}$$

VIE3

$$\begin{aligned} \text{Minimize} \quad f_1(x,y) &= 0.5(x^2+y^2) + \sin(x^2+y^2) \\ f_2(x,y) &= \tfrac{(3x-2y+4)^2}{8} + \tfrac{(x-y+1)^2}{27} + 15 \\ f_3(x,y) &= \tfrac{1}{x^2+y^2+1} + 1.1e^{-x^2-y^2} \\ \text{Subject to} \quad x,y &\in [-3,3] \end{aligned} \tag{A.28}$$

A.6 Irregular MOPs

In 2019, Tian *et al.* [127] defined the Irregular MOPs (IMOPs) whose main aim is to test the ability of MOEAs to maintain well-diversified solutions. The proposed test suite contains eight benchmark problems (three of them are bi-objective MOPs and the remaining ones are three-objective) with simple landscapes but various irregular Pareto front shapes. Regarding their mathematical defintion, a solution $\vec{x} = (x_1, \ldots, x_{K+L})^T$ consists of two parts, where $x_1, \ldots, x_K$ determine the position of the solution on the Pareto front and $x_{K+1}, \ldots, x_{K+L}$ determine the distance from the solution to the Pareto front. A solution is on the Pareto front only if it satisfies $g = 0$, i.e., $x_{K+1}, \ldots, x_{K+L} = 0.5$; hence the Pareto optimal set satisfies $\mathcal{X} \in [0,1]^K \times \{0.5\}^L$. On the other hand, the decision variables determining the positions of solutions on the Pareto fronts are biased by parameters a_1, a_2, and a_3, which has been recognized as a major factor that makes it difficult to maintain a proper diversity. The values of a_1, a_2, and a_3 should be larger than zero, and an extremely small or large value indicates a great difficulty in diversity preservation. Tian *et al.* recommended the values 5, 5, 0.05, 0.05, and 10 for K, L, a_1, a_2, and a_3, respectively. In the following, we present the mathematical defintion of some functions that are common to all IMOP

problems and, then, we define each IMOP instance.

$$\begin{aligned} \text{Given} \quad \vec{x} &= (x_1, \ldots, x_K, x_{K+1}, \ldots, x_{K+L})^T \\ y_1 &= \left(\frac{1}{K}\sum_{i=1}^{K} x_i\right)^{a_1} \\ y_2 &= \left(\frac{1}{\lceil K/2 \rceil}\sum_{i=1}^{\lceil K/2 \rceil} x_i\right)^{a_2} \\ y_3 &= \left(\frac{1}{\lfloor K/2 \rfloor}\sum_{i=\lceil K/2 \rceil+1}^{K} x_i\right)^{a_3} \\ g &= \sum_{i=K+1}^{K+L}(x_i - 0.5)^2 \end{aligned} \tag{A.29}$$

IMOP1

This problem is a bi-objective MOP with an extremely convex Pareto front shape.

$$\begin{aligned} \text{Minimize} \quad f_1(\vec{x}) &= g + \cos^8\left(\tfrac{\pi}{2}y_1\right) \\ f_2(\vec{x}) &= g + \sin^8\left(\tfrac{\pi}{2}y_1\right) \end{aligned} \tag{A.30}$$

IMOP2

IMOP2 is a bi-objective MOP with a concave Pareto front shape.

$$\begin{aligned} \text{Minimize} \quad f_1(\vec{x}) &= g + \cos^{0.5}\left(\tfrac{\pi}{2}y_1\right) \\ f_2(\vec{x}) &= g + \sin^{0.5}\left(\tfrac{\pi}{2}y_1\right) \end{aligned} \tag{A.31}$$

IMOP3

The Pareto front shape of this bi-objective MOP is represented by five disconnected regions with mixed geometry.

$$\begin{aligned} \text{Minimize} \quad f_1(\vec{x}) &= g + 1 + \tfrac{1}{5}\cos(10\pi y_1) - y_1 \\ f_2(\vec{x}) &= g + y_1 \end{aligned} \tag{A.32}$$

IMOP4

This is a three-objective problem with a degenerated and mixed Pareto front shape.

$$\begin{array}{rrcl} \text{Minimize} & f_1(\vec{x}) & = & (1+g)y_1 \\ & f_2(\vec{x}) & = & (1+g)\left(y_1 + \frac{1}{10}\sin(10\pi y_1)\right) \\ & f_3(\vec{x}) & = & (1+g)(1-y_1) \end{array} \tag{A.33}$$

IMOP5

IMOP5 is a three-objective problem with eight disconnected circular regions.

$$\begin{array}{rrcl} \text{Given} & h_1 & = & 0.4\cos\left(\frac{\pi}{4}\lceil 8y_2\rceil\right) + 0.1y_3\cos(16\pi y_2) \\ & h_2 & = & 0.4\sin\left(\frac{\pi}{4}\lceil 8y_2\rceil\right) + 0.1y_3\sin(16\pi y_2) \\ \text{Minimize} & f_1(\vec{x}) & = & g + h_1 \\ & f_2(\vec{x}) & = & g + h_2 \\ & f_3(\vec{x}) & = & g + 0.5 - h_1 - h_2 \end{array} \tag{A.34}$$

IMOP6

This problem has three objective functions with degenerated Pareto front shape similar to a grid.

$$\begin{array}{rrcl} \text{Given} & r & = & \max\{0, \min\{\sin^2(3\pi y_2), \sin^2(3\pi y_3)\} - 0.5\} \\ \text{Minimize} & f_1(\vec{x}) & = & (1+g)y_2 + \lceil r\rceil \\ & f_2(\vec{x}) & = & (1+g)y_3 + \lceil r\rceil \\ & f_3(\vec{x}) & = & (0.5+g)(2-y_2-y_3) + \lceil r\rceil \end{array} \tag{A.35}$$

IMOP7

IMOP7 is a three-objective MOP with a very challenging Pareto front shape.

$$\begin{array}{lrcl} \text{Given} & h_1 & = & (1+g)\cos\left(\frac{\pi}{2}y_2\right)\cos\left(\frac{\pi}{2}y_3\right) \\ & h_2 & = & (1+g)\cos\left(\frac{\pi}{2}y_2\right)\sin\left(\frac{\pi}{2}y_3\right) \\ & h_3 & = & (1+g)\sin\left(\frac{\pi}{2}y_2\right) \\ & r & = & \min\{\min\{|h_1-h_2|,|h_2-h_3|\},|h_3-h_1|\} \\ \text{Minimize} & f_1(\vec{x}) & = & h_1+10\max\{0,r-0.1\} \\ & f_2(\vec{x}) & = & h_2+10\max\{0,r-0.1\} \\ & f_3(\vec{x}) & = & h_3+10\max\{0,r-0.1\} \end{array} \tag{A.36}$$

IMOP8

This is a three-objective MOP with a Pareto front shape composed of a set of points.

$$\begin{array}{lrcl} \text{Minimize} & f_1(\vec{x}) & = & y_2 \\ & f_2(\vec{x}) & = & y_3 \\ & f_3(\vec{x}) & = & (1+g)\left[3-\sum_{i=2}^{3}\frac{y_i(1+\sin(19\pi y_i))}{1+g}\right] \end{array} \tag{A.37}$$

Appendix B

Numerical results

B.1 Study of IB-MOEAs

Tables B.1 to B.6 show the numerical results of the comparison between SMS-EMOA, R2-EMOA, IGD$^+$-MaOEA, ϵ^+-MaOEA and Δ_p-MaOEA, considering the indicators HV, R2, IGD$^+$, ϵ^+, Δ_p, and Riesz s-energy. These resuls are related to the experiments of Chapter 4.

Table B.1: Mean and, in parentheses, standard deviation of the hypervolume comparison. For each case, the two best values are shown in grayscale, where the darker tone corresponds to the best algorithm. The symbol # is placed when the best algorithm presents a significant difference, according to a one-tailed Wilcoxon test using a significance level of $\alpha = 0.05$.

MOP	Dim.	R2-EMOA	IGD$^+$-MaOEA	ϵ^+-MaOEA	Δ_p-MaOEA
DTLZ5	2	3.209900e+00 (1.735924e-04)	3.209902e+00 (1.530567e-04)	3.209900e+00 (2.258123e-04)	3.204380e+00# (4.629674e-03)
	3	5.989069e+00# (1.615636e-01)	6.101854e+00 (4.956143e-04)	6.101251e+00# (1.197988e-03)	6.087339e+00# (1.006126e-02)
DTLZ5^{-1}	2	9.574429e+00# (1.895817e-01)	1.026361e+01# (6.507777e-03)	1.026606e+01# (6.729446e-03)	1.026987e+01 (2.709873e-03)
	3	2.230222e+01# (8.365740e-02)	2.239088e+01 (1.858588e-01)	2.236659e+01 (1.450860e-01)	2.205768e+01# (9.965789e-02)
DTLZ7	2	1.749789e+01# (2.576291e-01)	1.772215e+01 (1.505239e-03)	1.771032e+01 (6.213428e-02)	1.767321e+01# (4.151049e-02)
	3	1.629005e+01 (8.334426e-02)	1.628256e+01 (9.725591e-02)	1.623511e+01# (1.320388e-01)	1.614994e+01# (9.123708e-02)
DTLZ7^{-1}	2	1.282172e+01# (1.066328e-02)	1.283380e+01# (1.201482e-03)	1.283392e+01# (9.111207e-04)	1.283493e+01 (2.195554e-04)
	3	2.696416e+01 (1.312853e-02)	2.696405e+01 (2.291816e-02)	2.691047e+01 (1.898083e-01)	2.689561e+01# (1.837625e-01)
WFG1	2	4.615522e+00# (4.769032e-01)	5.395035e+00 (1.536161e-01)	5.443496e+00# (4.006494e-01)	5.567246e+00 (3.687579e-01)
	3	5.337528e+01 (1.384148e+00)	5.101235e+01# (1.758679e+00)	5.045367e+01# (1.672276e+00)	4.800171e+01# (1.694798e+00)
WFG1^{-1}	2	5.550982e+00# (3.011860e-01)	7.309929e+00# (5.749252e-01)	7.294646e+00# (5.597702e-01)	8.251784e+00 (9.873184e-01)
	3	2.214750e+01 (3.455999e+00)	2.093763e+01 (3.884015e+00)	2.127560e+01 (3.840611e+00)	1.954952e+01# (3.698654e+00)
WFG2	2	1.082887e+01# (3.940243e-01)	1.093804e+01 (4.131007e-01)	1.088402e+01 (3.966500e-01)	1.087028e+01 (3.936546e-01)
	3	9.987342e+01 (1.764776e-01)	9.980619e+01 (3.365261e-01)	9.969942e+01# (3.580310e-01)	9.874426e+01# (2.339321e-01)
WFG2^{-1}	2	1.479666e+01# (2.773268e-01)	1.516162e+01# (2.416364e-02)	1.517144e+01# (2.045347e-02)	1.518503e+01 (2.843331e-03)
	3	6.111060e+01 (7.531676e-02)	6.092698e+01# (9.699307e-02)	6.085319e+01# (1.001624e-01)	5.917748e+01# (4.110527e-01)
WFG3	2	1.042183e+01# (1.980485e-01)	1.087753e+01 (2.513116e-02)	1.088729e+01 (2.096990e-02)	1.083036e+01# (2.056959e-02)
	3	7.257449e+01# (4.804513e-01)	7.469071e+01# (3.947835e-01)	7.485430e+01 (2.195746e-01)	7.168814e+01# (4.075513e-01)

Table B.1 – *Continuation*

MOP	Dim.	R2-EMOA	IGD$^+$-MaOEA	ϵ^+-MaOEA	Δ_p-MaOEA
WFG3^{-1}	2	1.116798e+01# (2.341934e-01)	1.170957e+01 (2.002401e-02)	1.170302e+01 (2.693215e-02)	1.166511e+01# (2.890196e-02)
	3	4.309221e+01 (4.201694e-01)	4.302405e+01 (2.951300e-01)	4.269899e+01# (5.418257e-01)	4.066105e+01# (4.221531e-01)
VIE1	3	6.098404e+01# (3.129718e-01)	6.085282e+01# (2.058629e-01)	6.089371e+01# (2.168549e-01)	6.151553e+01 (5.181303e-02)
VIE2	3	7.828215e+00# (7.241590e-03)	7.818501e+00# (1.003048e-02)	7.816491e+00# (8.664380e-03)	7.845357e+00 (1.117595e-03)
VIE3	3	2.202150e+02# (3.554071e-01)	2.202696e+02# (1.040812e-01)	2.202766e+02# (1.108682e-01)	2.203585e+02 (2.417736e-02)
LAME $\gamma = 0.25$	2	3.909634e+00# (5.709759e-02)	3.982948e+00# (9.839882e-04)	3.982605e+00# (1.378485e-03)	3.984251e+00 (1.655409e-04)
	3	7.969283e+00# (4.151780e-02)	7.994775e+00# (2.175235e-03)	7.995081e+00# (2.464759e-03)	7.999827e+00 (2.131929e-05)
LAME $\gamma = 0.50$	2	3.645645e+00# (7.434828e-02)	3.822000e+00# (4.413832e-03)	3.821263e+00# (4.064261e-03)	3.828665e+00 (1.914345e-04)
	3	7.862472e+00# (2.513901e-02)	7.932429e+00# (1.887706e-02)	7.924477e+00# (2.395475e-02)	7.980644e+00 (3.398911e-04)
LAME $\gamma = 1.00$	2	3.388040e+00# (6.052368e-02)	3.489914e+00 (3.389927e-03)	3.489934e+00 (3.136226e-03)	3.488181e+00# (4.046927e-03)
	3	7.724104e+00# (1.367839e-02)	7.733053e+00# (2.024301e-02)	7.714423e+00# (3.224908e-02)	7.756926e+00 (1.604649e-02)
LAME $\gamma = 2.00$	2	3.209784e+00# (1.704894e-04)	3.209978e+00 (1.805939e-04)	3.210020e+00 (1.258678e-04)	3.203304e+00# (3.855043e-03)
	3	7.417283e+00 (1.386901e-03)	7.417529e+00 (1.184325e-03)	7.403981e+00# (2.074026e-02)	7.316762e+00# (3.405029e-02)
LAME $\gamma = 5.00$	2	3.046842e+00# (3.362295e-04)	3.047895e+00# (3.110398e-04)	3.048033e+00 (2.516326e-04)	3.040193e+00# (6.242260e-03)
	3	7.099393e+00# (2.193804e-04)	7.106490e+00 (1.243879e-03)	7.062790e+00# (3.582765e-02)	6.894701e+00# (7.498913e-02)
MIRROR $\gamma = 0.25$	2	3.012709e+00# (4.898979e-07)	3.013524e+00# (3.418416e-05)	3.013539e+00 (5.331509e-05)	3.001348e+00# (6.905450e-03)
	3	4.021538e+00# (1.542263e-03)	4.036601e+00 (2.583775e-04)	3.841604e+00# (2.858261e-01)	3.958745e+00# (2.516358e-02)
MIRROR $\gamma = 0.50$	2	3.162196e+00# (1.465601e-04)	3.162629e+00 (1.526524e-04)	3.162604e+00 (1.909101e-04)	3.150500e+00# (7.345288e-03)
	3	4.419776e+00# (4.429657e-03)	4.447563e+00 (3.511804e-03)	4.362379e+00# (1.180306e-01)	4.292338e+00# (4.002761e-02)
MIRROR $\gamma = 1.00$	2	3.392474e+00# (5.463606e-02)	3.489424e+00 (3.938836e-03)	3.489601e+00 (3.227883e-03)	3.486882e+00# (4.914422e-03)
	3	5.303303e+00# (7.188395e-02)	5.426926e+00 (4.196963e-02)	5.408572e+00 (4.969088e-02)	5.299153e+00# (4.594240e-02)
MIRROR $\gamma = 2.00$	2	3.573648e+00# (5.405677e-02)	3.772177e+00# (4.516309e-03)	3.769977e+00# (6.489849e-03)	3.780170e+00 (2.238466e-04)
	3	6.515017e+00# (5.601120e-02)	6.484667e+00# (4.952863e-02)	6.456127e+00# (4.937541e-02)	6.661167e+00 (1.599059e-02)
MIRROR $\gamma = 5.00$	2	3.803607e+00# (5.993229e-02)	3.944249e+00# (2.030429e-03)	3.943153e+00# (2.452780e-03)	3.947422e+00 (2.233225e-04)
	3	7.389603e+00# (5.687905e-02)	7.491070e+00# (3.001289e-02)	7.458097e+00# (4.758334e-02)	7.634448e+00 (4.943987e-03)

Table B.2: Mean and, in parentheses, standard deviation of the R2 comparison. For each case, the two best values are shown in grayscale, where the darker tone corresponds to the best algorithm. The symbol # is placed when the best algorithm presents a significant difference, according to a one-tailed Wilcoxon test using a significance level of $\alpha = 0.05$.

MOP	Dim.	SMS-EMOA	IGD$^+$-MaOEA	ϵ^+-MaOEA	Δ_p-MaOEA
DTLZ5	2	1.005486e+00# (5.104561e-04)	1.029833e+00# (1.059878e-02)	1.028238e+00# (1.001161e-02)	1.003009e+00 (4.284767e-04)
	3	6.109754e+02# (1.551791e-02)	6.109946e+02# (1.023653e-01)	6.110093e+02# (4.498222e-02)	6.103094e+02 (4.117181e-01)
DTLZ5^{-1}	2	3.510697e+00# (1.017290e-03)	4.358365e+00# (9.486050e-01)	4.091429e+00# (6.963809e-01)	3.507580e+00 (1.147293e-03)
	3	4.767704e+01 (5.289497e-01)	6.416130e+02# (1.811837e+02)	6.364461e+02# (1.517197e+02)	1.698762e+02# (4.883579e+01)
DTLZ7	2	1.441503e+03 (2.039131e-02)	1.445657e+03# (3.237280e+00)	1.487451e+03# (2.200021e+02)	1.442743e+03# (2.238336e+00)
	3	2.391873e+03 (4.651224e+02)	2.493480e+03# (3.929539e+02)	2.550239e+03# (5.255527e+02)	2.418017e+03# (2.746513e+02)
DTLZ7^{-1}	2	1.592806e+04# (3.376700e-01)	1.592669e+04# (2.003853e+00)	1.592630e+04# (2.140207e+00)	1.592313e+04 (4.634537e+00)
	3	2.816303e+04# (6.045521e-01)	2.816383e+04# (7.139418e-01)	2.815595e+04# (2.300026e+01)	2.785798e+04 (2.150179e+02)
WFG1	2	6.372488e+02 (1.587253e+02)	7.036806e+02# (3.411281e+01)	6.555643e+02# (1.952589e+02)	6.145524e+02 (1.882392e+02)
	3	5.668730e+02 (2.231981e+02)	1.047378e+03# (1.820088e+02)	1.106070e+03# (1.536457e+02)	1.045511e+03# (2.329230e+02)
WFG1^{-1}	2	9.078785e+02# (2.107915e+02)	1.040345e+03# (1.834798e+02)	1.042570e+03# (1.766694e+02)	6.872446e+02 (3.249294e+02)
	3	1.250145e+03 (2.631020e+02)	1.223268e+03 (2.480948e+02)	1.206985e+03 (2.433435e+02)	1.319739e+03# (2.344599e+02)
WFG2	2	2.535394e+02 (1.514857e+02)	1.979987e+02 (1.711069e+02)	2.211969e+02 (1.665364e+02)	2.214024e+02 (1.667331e+02)
	3	1.191635e+02# (9.955266e+00)	2.864686e+01# (1.829298e+01)	3.380371e+01# (2.565233e+01)	8.832879e+00 (7.201698e+00)
WFG2^{-1}	2	8.683403e+02 (8.965119e-02)	8.737435e+02# (3.692661e+00)	8.724601e+02# (3.251167e+00)	8.743011e+02# (3.753575e+00)
	3	6.739555e+02 (7.026186e+00)	8.204509e+02# (7.473159e+01)	8.776606e+02# (1.245734e+02)	7.410797e+02# (5.329390e+01)
WFG3	2	2.271958e+00 (1.849134e-03)	2.273840e+00# (2.890178e-03)	2.273252e+00# (2.216334e-03)	2.283883e+00# (2.430803e-03)
	3	7.321132e+02 (1.397077e+01)	8.863254e+02# (3.163755e+01)	8.943076e+02# (3.296950e+01)	7.477064e+02# (2.801165e+01)
WFG3^{-1}	2	2.104789e+02 (9.350683e-01)	2.418166e+02# (1.879292e+01)	2.487994e+02# (2.474250e+01)	2.436934e+02# (2.252834e+01)
	3	6.164198e+02 (3.417195e-01)	7.619900e+02# (4.460000e+01)	7.804317e+02# (6.395482e+01)	8.168451e+02# (4.203108e+01)
VIE1	3	2.147352e+03# (3.896644e+00)	2.189517e+03# (3.917203e+01)	2.168234e+03# (3.645915e+01)	2.025592e+03 (1.591550e+01)
VIE2	3	2.009631e+04# (8.860660e-01)	2.019211e+04# (1.059124e+02)	2.023026e+04# (8.755486e+01)	2.009348e+04 (1.356931e+01)
VIE3	3	1.254645e+04# (2.657464e+00)	1.255408e+04# (4.443440e+00)	1.255352e+04# (6.144459e+00)	1.254485e+04 (4.597049e+00)
LAME $\gamma = 0.25$	2	1.290873e-01# (6.666684e-05)	1.286126e-01 (5.713498e-05)	1.286278e-01 (5.860370e-05)	2.003998e-01# (8.848773e-02)
	3	2.126063e-01# (4.733335e-02)	1.206164e-01 (1.715986e-01)	1.158909e-01 (1.425844e-01)	7.010252e+00# (1.429443e+00)
LAME $\gamma = 0.50$	2	4.682969e-01# (6.861085e-05)	4.682036e-01 (1.561540e-04)	4.682564e-01 (1.640181e-04)	4.721240e-01# (8.869523e-04)
	3	5.350178e-01# (2.156048e-02)	5.173003e-01 (5.246649e-02)	5.413574e-01# (5.941437e-02)	1.611826e+00# (9.039626e-01)
LAME $\gamma = 1.00$	2	8.136808e-01 (3.892223e-04)	8.142168e-01# (2.231924e-04)	8.142235e-01# (2.379582e-04)	8.151098e-01# (2.854964e-04)
	3	9.508038e-01 (1.621874e-02)	1.077992e+00# (4.000216e-02)	1.119208e+00# (6.543714e-02)	1.119224e+00# (5.050029e-02)
LAME $\gamma = 2.00$	2	1.005600e+00# (5.002900e-04)	1.030831e+00# (1.079695e-02)	1.028627e+00# (8.567371e-03)	1.002640e+00 (3.468501e-04)
	3	2.033316e+00# (2.731856e-02)	3.125817e+00# (8.623367e-01)	2.895501e+00# (1.444371e+00)	1.580426e+00 (8.071041e-02)
LAME $\gamma = 5.00$	2	1.624360e+00# (4.551037e-02)	6.634684e+00# (1.561829e+00)	5.263233e+00# (1.544037e+00)	1.083729e+00 (5.006587e-04)
	3	9.500838e+01# (1.524563e+00)	1.601928e+02# (1.425093e+01)	1.225680e+02# (2.517442e+01)	2.134192e+00 (4.235226e-01)
MIRROR $\gamma = 0.25$	2	2.330939e+00# (9.724825e-02)	3.711249e+01# (1.105184e+01)	3.384378e+01# (1.398704e+01)	1.098079e+00 (3.902835e-04)
	3	8.782582e+02# (1.056900e+00)	9.160999e+02# (4.445802e+00)	9.355856e+02# (3.915237e+01)	8.614790e+02 (3.254228e-01)
MIRROR $\gamma = 0.50$	2	1.033891e+00# (8.007150e-04)	1.077514e+00# (1.722427e-02)	1.077995e+00# (2.212623e-02)	1.028136e+00 (4.181026e-04)
	3	8.214684e+02 (2.763007e-02)	8.239180e+02# (7.467352e-01)	8.293100e+02# (1.040429e+01)	8.300501e+02# (1.642245e+00)

Table B.2 – *Continuation*

MOP	Dim.	SMS-EMOA	IGD$^+$-MaOEA	ϵ^+-MaOEA	Δ_p-MaOEA
MIRROR $\gamma = 1.00$	2	8.135885e-01 (3.876346e-04)	8.141975e-01# (2.242625e-04)	8.142188e-01# (2.475928e-04)	8.151982e-01# (3.224129e-04)
	3	5.043092e+02 (3.430455e-01)	5.088175e+02# (2.039965e+00)	5.088860e+02# (1.789102e+00)	5.149058e+02# (3.121032e+00)
MIRROR $\gamma = 2.00$	2	5.337165e-01 (9.076267e-05)	5.337376e-01 (1.967854e-04)	5.337958e-01 (2.068919e-04)	5.367964e-01# (7.060632e-04)
	3	1.355486e+02 (4.866807e-01)	1.900996e+02# (1.490261e+01)	1.937577e+02# (1.952611e+01)	1.429503e+02# (3.341191e+00)
MIRROR $\gamma = 5.00$	2	2.517303e-01# (6.956516e-05)	2.514963e-01# (9.396201e-05)	2.514279e-01 (1.114882e-04)	2.667327e-01# (9.571938e-03)
	3	1.566226e+01# (2.742656e-01)	4.194253e+01# (6.795610e+00)	4.529078e+01# (1.092500e+01)	8.935328e+00 (4.235798e+00)

Table B.3: Mean and, in parentheses, standard deviation of the IGD^+ comparison. For each case, the two best values are shown in grayscale, where the darker tone corresponds to the best algorithm. The symbol # is placed when the best algorithm presents a significant difference, according to a one-tailed Wilcoxon test using a significance level of $\alpha = 0.05$.

MOP	Dim.	SMS-EMOA	R2-EMOA	ϵ^+-MaOEA	Δ_p-MaOEA
DTLZ5	2	1.695584e-03 (3.234557e-05)	2.049804e-03# (2.909052e-06)	2.296487e-03# (1.204895e-04)	2.653461e-03# (1.290499e-04)
	3	1.682930e-03 (2.484378e-05)	5.535978e-03# (2.758618e-03)	2.280186e-03# (1.609056e-04)	2.956920e-03# (1.653807e-04)
DTLZ5^{-1}	2	6.196074e-03 (1.238341e-04)	1.363435e-01# (3.622241e-02)	9.322426e-03# (1.176939e-03)	8.141679e-03# (3.756346e-04)
	3	9.366191e-02 (1.227452e-03)	1.143055e-01# (6.081112e-03)	1.021395e-01# (8.539415e-03)	1.098575e-01# (3.663990e-03)
DTLZ7	2	1.628336e-03 (3.495923e-05)	3.007559e-03# (8.823955e-04)	1.717664e-02# (8.137425e-02)	2.082631e-03# (8.069671e-05)
	3	5.215494e-02 (1.349320e-01)	5.307555e-02 (6.426607e-02)	7.405011e-02 (1.490413e-01)	5.000873e-02 (5.317253e-02)
DTLZ7^{-1}	2	7.854840e-04 (2.516270e-05)	1.964593e-03# (7.901776e-04)	9.686953e-04# (3.535944e-05)	1.005376e-03# (3.337688e-05)
	3	2.729009e-02 (6.937086e-02)	1.560221e-02 (1.017142e-03)	2.976307e-02 (6.914669e-02)	3.486042e-02# (6.773933e-02)
WFG1	2	7.653841e-01 (6.019249e-02)	9.347850e-01# (9.304603e-02)	7.795080e-01# (7.628035e-02)	7.555885e-01 (6.994785e-02)
	3	8.169015e-01 (6.624744e-03)	8.689634e-01# (7.137616e-03)	8.880066e-01# (2.515765e-02)	1.015451e+00# (1.648919e-02)
WFG1^{-1}	2	6.030196e-01# (1.606478e-01)	1.210451e+00# (9.050835e-02)	6.915277e-01# (1.606911e-01)	4.381291e-01 (2.519592e-01)
	3	5.800055e-01 (2.198836e-01)	5.339181e-01 (1.778769e-01)	5.863736e-01 (1.977158e-01)	6.518395e-01# (1.962630e-01)
WFG2	2	6.673596e-02 (3.671732e-02)	6.316491e-02# (3.971209e-02)	5.956594e-02 (3.939672e-02)	6.110196e-02 (3.989671e-02)
	3	2.744562e-02 (1.853143e-03)	4.436958e-02# (2.383712e-03)	4.283467e-02# (4.515963e-03)	7.816769e-02# (4.098763e-03)
WFG2^{-1}	2	1.415975e-03 (4.407807e-05)	7.569000e-03# (5.576227e-03)	1.735616e-03# (6.701956e-05)	2.192838e-03# (9.091264e-05)
	3	3.285042e-02 (7.759751e-04)	3.728421e-02# (1.459409e-03)	3.803745e-02# (9.791798e-04)	6.321929e-02# (4.794858e-03)
WFG3	2	1.083253e-02 (1.182583e-03)	3.539072e-02# (1.559783e-02)	1.118421e-02 (1.237053e-03)	1.769827e-02# (1.236446e-03)
	3	2.486311e-02 (3.388914e-03)	1.281786e-01# (1.312570e-02)	3.711180e-02# (4.157123e-03)	1.491613e-01# (1.022267e-02)
WFG3^{-1}	2	6.807507e-03 (1.481638e-04)	3.879721e-02# (1.978041e-02)	7.788440e-03# (4.557040e-04)	1.257812e-02 # (6.267424e-04)
	3	1.007547e-01# (1.213589e-03)	1.102851e-01# (3.463592e-03)	9.842125e-02 (4.620645e-03)	1.393639e-01# (7.116006e-03)
VIE1	3	6.060827e-02# (8.852261e-04)	5.533069e-02# (3.180995e-03)	4.069218e-02 (1.774645e-03)	6.745161e-02# (4.779719e-03)
VIE2	3	2.941424e-03 (1.518446e-04)	4.316030e-03# (8.976983e-04)	4.235757e-03# (7.104672e-04)	2.971846e-03 (1.763561e-04)
VIE3	3	3.437056e+01# (8.163271e-04)	3.437131e+01# (1.112938e-03)	3.436991e+01 (4.075368e-04)	3.437104e+01# (7.149144e-04)
LAME $\gamma = 0.25$	2	2.362458e-04 (1.418313e-05)	1.866296e-02# (1.441148e-02)	7.612490e-04# (2.063942e-04)	6.958310e-04# (8.373615e-05)
	3	3.546617e-04 (1.551129e-05)	6.893500e-03# (6.053915e-03)	1.731868e-03# (3.552169e-04)	1.494761e-03# (2.332077e-04)
LAME $\gamma = 0.50$	2	1.534167e-03 (3.188406e-05)	3.495180e-02# (1.651300e-02)	2.471058e-03# (3.514999e-04)	2.200077e-03# (8.726158e-05)
	3	8.625738e-03 (1.752621e-04)	1.522865e-02# (8.774275e-04)	1.309048e-02# (1.227949e-03)	1.242335e-02# (4.907894e-04)
LAME $\gamma = 1.00$	2	2.523730e-03 (3.262917e-05)	7.892336e-03# (5.038736e-03)	2.759690e-03# (6.658338e-05)	3.266812e-03# (1.206671e-04)
	3	2.539401e-02# (3.813928e-04)	2.456533e-02 (1.106700e-04)	2.876936e-02# (6.219364e-04)	3.216913e-02# (1.003099e-03)
LAME $\gamma = 2.00$	2	1.753442e-03 (4.092261e-05)	2.134488e-03# (3.898561e-06)	2.310598e-03# (7.442727e-05)	2.386799e-03# (8.769657e-05)
	3	1.844746e-02 (4.584678e-04)	2.203263e-02# (7.570671e-05)	2.386517e-02# (1.690704e-03)	3.106458e-02# (1.726688e-03)
LAME $\gamma = 5.00$	2	5.441572e-04 (2.864553e-05)	1.263241e-03# (2.203386e-06)	8.783513e-04# (4.805303e-05)	1.191633e-03# (8.902358e-05)
	3	4.619441e-03 (1.066644e-04)	9.629852e-03# (1.017117e-05)	1.037648e-02# (2.198922e-03)	1.864518e-02# (2.657058e-03)
MIRROR $\gamma = 0.25$	2	2.118677e-04 (1.321315e-05)	7.048073e-04# (6.234310e-07)	4.053672e-04# (3.235797e-05)	6.689731e-04# (6.880326e-05)
	3	6.749016e-04 (3.747716e-05)	3.903468e-03# (4.182137e-04)	9.538769e-03# (1.632313e-02)	2.924400e-03# (3.422683e-04)
MIRROR $\gamma = 0.50$	2	1.501527e-03 (4.173043e-05)	1.849857e-03# (2.106441e-06)	2.064390e-03# (1.113252e-04)	2.191113e-03# (9.214070e-05)
	3	1.114792e-02# (2.167936e-04)	1.457422e-02# (7.071915e-04)	1.105574e-02 (1.441728e-03)	1.480486e-02# (8.323569e-04)

Table B.3 – *Continuation*

MOP	Dim.	SMS-EMOA	R2-EMOA	ϵ^+-MaOEA	Δ_p-MaOEA
MIRROR $\gamma = 1.00$	2	2.535818e-03 (4.574300e-05)	7.752339e-03# (4.184850e-03)	2.752465e-03# (5.530838e-05)	3.285354e-03# (1.416783e-04)
	3	3.095894e-02# (4.319606e-04)	3.514701e-02# (6.350441e-04)	2.865999e-02 (6.004246e-04)	3.204613e-02# (8.245754e-04)
MIRROR $\gamma = 2.00$	2	1.813141e-03 (3.534852e-05)	3.371028e-02# (1.248708e-02)	2.731849e-03# (3.901231e-04)	2.434603e-03# (9.552067e-05)
	3	2.715802e-02 (4.041752e-04)	3.305183e-02# (1.265624e-03)	3.143794e-02# (1.783074e-03)	2.990015e-02# (1.009064e-03)
MIRROR $\gamma = 5.00$	2	5.965585e-04 (3.483584e-05)	3.183511e-02# (1.579689e-02)	1.546184e-03# (3.103224e-04)	1.242003e-03# (9.958487e-05)
	3	7.355287e-03 (1.343513e-04)	2.465969e-02# (3.611979e-03)	2.057858e-02# (3.021821e-03)	1.344849e-02# (8.361468e-04)

Table B.4: Mean and, in parentheses, standard deviation of the ϵ^+ comparison. For each case, the two best values are shown in grayscale, where the darker tone corresponds to the best algorithm. The symbol # is placed when the best algorithm presents a significant difference, according to a one-tailed Wilcoxon test using a significance level of $\alpha = 0.05$.

MOP	Dim.	SMS-EMOA	R2-EMOA	IGD$^+$-MaOEA	Δ_p-MaOEA
DTLZ5	2	4.288867e-03 (1.748715e-04)	6.694033e-03# (9.686364e-05)	9.505733e-03# (1.485828e-03)	1.198187e-02# (2.079283e-03)
	3	3.459100e-03 (8.707749e-05)	3.976550e-02# (3.359484e-02)	8.775400e-03# (1.757153e-03)	1.088393e-02# (2.516491e-03)
DTLZ5^{-1}	2	1.519573e-02 (6.465546e-04)	4.220003e-01# (1.172431e-01)	3.787860e-02# (9.500708e-03)	3.916630e-02# (6.265284e-03)
	3	2.120276e-01 (9.017631e-03)	3.402098e-01# (6.914496e-02)	2.681693e-01# (5.842962e-02)	2.479882e-01# (1.917379e-02)
DTLZ7	2	4.286833e-03 (2.300575e-04)	3.518943e-02# (1.913576e-02)	9.362433e-03# (2.140453e-03)	9.976367e-03# (1.950960e-03)
	3	1.833179e-01 (4.868982e-01)	2.841639e-01# (3.457937e-01)	3.036933e-01# (4.027617e-01)	1.974185e-01# (2.924224e-01)
DTLZ7^{-1}	2	2.066033e-03 (1.796030e-04)	2.427647e-02# (1.493418e-02)	4.022200e-03# (7.868707e-04)	4.848933e-03# (8.986008e-04)
	3	9.121917e-02 (2.427347e-01)	8.612077e-02# (2.753402e-02)	7.167993e-02 (4.720156e-02)	1.377222e-01 (2.326325e-01)
WFG1	2	1.195371e+00 (1.429522e-01)	1.501713e+00# (1.844878e-01)	1.242802e+00# (5.527474e-02)	1.163965e+00 (1.699515e-01)
	3	9.299282e-01 (1.739498e-02)	9.651405e-01# (1.952047e-02)	1.027403e+00# (6.855228e-02)	1.077434e+00# (2.013067e-02)
WFG1^{-1}	2	2.232947e+00# (4.657834e-01)	3.230241e+00# (1.335771e-01)	2.416787e+00# (3.398920e-01)	1.761230e+00 (7.378372e-01)
	3	3.090242e+00 (5.242446e-01)	3.594526e+00# (8.498205e-02)	3.600963e+00# (6.221815e-02)	3.537044e+00# (1.471249e-01)
WFG2	2	5.891101e-01 (3.494691e-01)	5.319518e-01# (3.629393e-01)	4.605487e-01 (3.911434e-01)	5.188458e-01 (3.750637e-01)
	3	7.688937e-02 (7.132705e-03)	1.302322e-01# (1.036749e-02)	1.223313e-01# (2.341651e-02)	2.385037e-01# (3.161913e-02)
WFG2^{-1}	2	4.060333e-03 (4.360840e-04)	1.423319e-01# (9.573484e-02)	1.463893e-02# (6.384099e-03)	7.456600e-03# (1.140392e-03)
	3	1.021728e-01 (1.161072e-02)	1.513375e-01# (3.273466e-02)	1.366452e-01# (2.269532e-02)	3.027704e-01# (1.201660e-01)
WFG3	2	1.934267e-02 (1.493618e-03)	3.191266e-01# (1.285740e-01)	4.032030e-02# (1.239598e-02)	4.541777e-02# (1.047507e-02)
	3	6.123697e-02 (6.271931e-03)	2.345632e-01# (2.667689e-02)	1.162866e-01# (4.476494e-02)	2.221332e-01# (2.426046e-02)
WFG3^{-1}	2	1.455220e-02 (5.709691e-04)	3.595611e-01# (1.618304e-01)	3.617557e-02# (1.147255e-02)	4.553267e-02# (1.581711e-02)
	3	2.270304e-01 (7.841809e-03)	4.143307e-01# (1.767879e-01)	3.415783e-01# (1.054150e-01)	3.987787e-01# (8.988984e-02)
VIE1	3	1.485014e-01# (7.813217e-03)	1.445439e-01# (1.746906e-02)	1.103473e-01 (9.187255e-03)	1.849286e-01# (1.828364e-02)
VIE2	3	1.943703e-02# (9.234191e-04)	1.440070e-02 (3.406558e-03)	1.324500e-02 (3.472923e-03)	1.586703e-02# (2.158368e-03)
VIE3	3	3.200002e+01 (2.617038e-05)	3.200032e+01# (3.592314e-04)	3.200004e+01# (5.262446e-05)	3.200020e+01# (1.473790e-04)
LAME $\gamma = 0.25$	2	1.401967e-03 (1.328685e-04)	4.592090e-02# (2.721952e-02)	2.266333e-03# (3.840171e-04)	1.004937e-02# (2.898355e-03)
	3	3.305233e-03 (3.772316e-04)	1.297557e-02# (1.250013e-02)	3.702267e-03 (9.247918e-04)	1.648257e-02# (3.873501e-03)
LAME $\gamma = 0.50$	2	4.111667e-03 (1.904311e-04)	1.117717e-01# (4.780182e-02)	8.770833e-03# (1.707010e-03)	1.078383e-02# (1.705957e-03)
	3	2.231497e-02 (1.371576e-03)	3.042630e-02# (4.151926e-03)	3.102333e-02# (4.641532e-03)	4.177447e-02# (5.636574e-03)
LAME $\gamma = 1.00$	2	5.366400e-03 (2.096942e-04)	7.129647e-02# (4.163471e-02)	9.287133e-03# (1.377809e-03)	1.126267e-02# (1.393164e-03)
	3	4.667817e-02 (1.925211e-03)	4.881510e-02# (7.817478e-04)	6.681010e-02# (6.607459e-03)	7.434400e-02# (6.467160e-03)
LAME $\gamma = 2.00$	2	4.305133e-03 (1.827293e-04)	7.103300e-03# (1.402636e-04)	9.510567e-03# (1.474281e-03)	1.061927e-02# (1.590049e-03)
	3	4.492820e-02 (2.291838e-03)	6.858377e-02# (2.807471e-04)	6.893733e-02# (8.636191e-03)	8.706860e-02# (1.252971e-02)
LAME $\gamma = 5.00$	2	2.253200e-03 (9.284051e-05)	8.715533e-03# (4.765902e-05)	4.548400e-03# (7.362937e-04)	1.036823e-02# (2.225169e-03)
	3	2.745240e-02 (2.142825e-03)	5.957293e-02# (1.360823e-04)	3.376767e-02# (5.488481e-03)	1.143934e-01# (3.112082e-02)
MIRROR $\gamma = 0.25$	2	1.335467e-03 (1.171585e-04)	8.962733e-03# (2.429531e-05)	2.188233e-03# (3.108442e-04)	1.103240e-02# (3.774229e-03)
	3	9.473000e-03# (3.469447e-18)	3.378247e-02# (4.525699e-03)	7.660567e-03 (1.668890e-03)	3.620283e-02# (1.181870e-02)
MIRROR $\gamma = 0.50$	2	3.982700e-03 (2.457278e-04)	7.289533e-03# (4.789345e-05)	8.277400e-03# (1.235169e-03)	1.221900e-02# (3.236050e-03)
	3	4.599580e-02# (2.917761e-03)	6.777890e-02# (9.194487e-03)	3.533243e-02 (3.934414e-03)	7.450527e-02# (2.358820e-02)

Table B.4 – *Continuation*

MOP	Dim.	SMS-EMOA	R2-EMOA	IGD$^+$-MaOEA	Δ_p-MaOEA
MIRROR $\gamma = 1.00$	2	5.403700e-03 (1.635042e-04)	6.995890e-02# (3.686391e-02)	9.260833e-03# (1.373198e-03)	1.233983e-02# (1.880482e-03)
	3	6.966813e-02 (2.310921e-03)	1.005713e-01# (1.205964e-02)	7.393110e-02# (9.208828e-03)	8.035710e-02# (9.564526e-03)
MIRROR $\gamma = 2.00$	2	4.355267e-03 (1.674833e-04)	1.110318e-01# (4.047145e-02)	9.685933e-03# (1.763040e-03)	1.072607e-02# (1.510878e-03)
	3	6.485817e-02 (3.846548e-03)	8.332627e-02# (1.134454e-02)	7.424183e-02# (9.515501e-03)	7.946677e-02# (6.843873e-03)
MIRROR $\gamma = 5.00$	2	2.360433e-03 (1.042969e-04)	6.453017e-02# (3.761926e-02)	4.671367e-03# (5.648667e-04)	1.143143e-02# (2.576067e-03)
	3	3.662260e-02 (3.165304e-03)	5.111587e-02# (9.700699e-03)	3.925197e-02# (4.871933e-03)	7.637393e-02# (1.472057e-02)

Table B.5: Mean and, in parentheses, standard deviation of the Δ_p comparison. For each case, the two best values are shown in grayscale, where the darker tone corresponds to the best algorithm. The symbol # is placed when the best algorithm presents a significant difference, according to a one-tailed Wilcoxon test using a significance level of $\alpha = 0.05$.

MOP	Dim.	SMS-EMOA	R2-EMOA	IGD$^+$-MaOEA	ϵ^+-MaOEA
DTLZ5	2	7.406892e-03# (2.506466e-04)	4.596968e-03 (4.622463e-06)	1.493306e-02# (2.136301e-03)	1.458711e-02# (2.255226e-03)
	3	6.505713e-03 (1.903906e-04)	1.681478e-02# (6.526178e-03)	1.347136e-02# (2.001874e-03)	1.342005e-02# (2.287723e-03)
DTLZ5^{-1}	2	2.111317e-02 (6.596463e-04)	6.888423e-01# (1.117294e-01)	9.769015e-02# (2.441869e-02)	8.621672e-02# (2.710863e-02)
	3	1.857834e-01 (2.115939e-03)	3.347142e-01# (4.956390e-02)	3.462997e-01# (5.443900e-02)	3.554791e-01# (5.696522e-02)
DTLZ7	2	5.927002e-03 (1.264210e-04)	1.043017e-02# (3.237141e-03)	8.815495e-03# (7.576162e-04)	3.349218e-02# (1.336232e-01)
	3	1.829813e-01# (1.934680e-01)	1.319032e-01 (1.357873e-01)	1.457676e-01 (1.702285e-01)	1.704028e-01 (2.415969e-01)
DTLZ7^{-1}	2	3.291698e-03 (7.041132e-05)	7.715302e-03# (2.717189e-03)	4.669146e-03# (5.792374e-04)	4.766884e-03# (8.250100e-04)
	3	1.182902e-01# (1.150130e-01)	6.555662e-02 (2.508848e-02)	6.850298e-02## (7.558801e-03)	9.903232e-02 (1.203300e-01)
WFG1	2	1.097287e+00 (1.416278e-01)	1.464204e+00# (2.239744e-01)	1.142534e+00 (3.624628e-02)	1.107333e+00 (1.804430e-01)
	3	9.535054e-01 (6.130012e-02)	1.058708e+00# (5.218627e-02)	1.187336e+00# (9.215482e-02)	1.235971e+00# (8.071587e-02)
WFG1^{-1}	2	1.025968e+00 (2.551586e-01)	1.869376e+00# (1.185291e-01)	1.168507e+00# (2.292658e-01)	1.173170e+00# (2.220213e-01)
	3	9.632906e-01 (2.010534e-01)	1.003708e+00 (1.205533e-01)	1.042047e+00# (1.387284e-01)	1.054667e+00# (1.341810e-01)
WFG2	2	2.466787e-01 (1.392414e-01)	2.352225e-01# (1.387027e-01)	1.980112e-01 (1.542363e-01)	2.190145e-01 (1.502228e-01)
	3	3.805331e-01# (5.706660e-03)	3.610311e-01 (5.877678e-03)	4.200883e-01# (4.253271e-02)	4.217750e-01# (4.444525e-02)
WFG2^{-1}	2	1.232389e-02 (2.764109e-04)	3.329214e-02# (1.582048e-02)	1.482709e-02# (6.485688e-04)	1.474882e-02# (5.794326e-04)
	3	4.782631e-01# (1.598683e-02)	3.187479e-01 (8.568225e-03)	3.677384e-01# (2.238619e-02)	3.600088e-01# (1.683329e-02)
WFG3	2	1.428934e-02 (6.784763e-04)	9.597052e-02# (4.967767e-02)	1.695257e-02# (1.103848e-03)	1.648461e-02# (8.490683e-04)
	3	7.379659e-01# (1.831559e-02)	8.802018e-01# (5.775016e-02)	6.705148e-01 (8.163001e-02)	6.459911e-01 (7.522617e-02)
WFG3^{-1}	2	1.310433e-02 (1.839318e-04)	1.187646e-01# (5.556068e-02)	1.605288e-02# (7.680716e-04)	1.643985e-02# (1.731741e-03)
	3	2.060761e-01# (2.925952e-03)	2.240391e-01# (6.151626e-03)	1.845060e-01 (5.815955e-03)	1.931713e-01# (8.850959e-03)
VIE1	3	4.180782e-01# (4.434053e-03)	3.472464e-01# (2.692236e-02)	2.106523e-01 (3.544690e-02)	2.176691e-01 (2.876066e-02)
VIE2	3	1.897265e-02 (1.109635e-03)	1.134802e-01# (5.385696e-02)	1.397716e-01# (6.043678e-02)	1.459694e-01# (5.950758e-02)
VIE3	3	3.463065e+01# (9.341584e-03)	3.442166e+01 (6.298771e-02)	3.439434e+01 (1.509853e-02)	3.440094e+01 (1.393778e-02)
LAME $\gamma = 0.25$	2	2.140526e-02 (8.056726e-04)	3.210521e-01# (4.531988e-02)	1.451217e-01# (2.705175e-02)	1.499476e-01# (3.546758e-02)
	3	7.454173e-02 (1.268640e-02)	3.531762e-01# (8.739043e-02)	2.741324e-01# (1.836154e-02)	2.783684e-01# (2.537823e-02)
LAME $\gamma = 0.50$	2	6.655428e-03 (2.271082e-04)	2.064017e-01# (5.519466e-02)	2.666393e-02# (9.010260e-03)	2.848004e-02# (9.203324e-03)
	3	3.278637e-02 (6.014475e-04)	1.365345e-01# (6.310909e-03)	9.315135e-02# (1.786164e-02)	9.938001e-02# (1.740653e-02)
LAME $\gamma = 1.00$	2	4.139085e-03 (5.140292e-05)	2.302644e-02# (1.650151e-02)	4.726300e-03# (1.547893e-04)	4.736983e-03# (1.106859e-04)
	3	3.977725e-02# (4.900449e-04)	3.832886e-02 (1.816802e-04)	4.500530e-02# (1.132604e-03)	4.632899e-02# (1.112544e-03)
LAME $\gamma = 2.00$	2	7.652167e-03# (3.123124e-04)	4.813167e-03 (9.575336e-06)	1.577385e-02# (2.279521e-03)	1.533650e-02# (1.949915e-03)
	3	7.645934e-02# (1.179189e-03)	5.428870e-02 (3.464988e-05)	7.699633e-02# (3.167635e-03)	7.592208e-02# (3.249837e-03)
LAME $\gamma = 5.00$	2	4.800199e-02# (1.605375e-03)	8.599542e-03 (1.848679e-05)	9.320193e-02# (5.643740e-03)	8.696151e-02# (7.206407e-03)
	3	1.823065e-01# (1.167300e-03)	7.010421e-02 (1.996358e-05)	1.811148e-01# (4.976093e-03)	1.708535e-01# (7.080645e-03)
MIRROR $\gamma = 0.25$	2	5.554415e-02# (1.946736e-03)	1.307076e-02 (5.704684e-06)	1.340588e-01# (8.297530e-03)	1.308626e-01# (1.103825e-02)
	3	8.307629e-02# (1.445734e-03)	2.684718e-02 (2.437578e-03)	1.404159e-01# (6.096533e-03)	1.387284e-01# (1.548361e-02)
MIRROR $\gamma = 0.50$	2	8.925204e-03# (3.297587e-04)	4.980787e-03 (2.763049e-06)	1.954657e-02# (2.529892e-03)	1.956016e-02# (3.023896e-03)
	3	4.302065e-02# (8.371972e-04)	4.323850e-02# (2.300700e-03)	3.891919e-02 (2.228169e-03)	4.044598e-02 (3.641319e-03)

Table B.5 – *Continuation*

MOP	Dim.	SMS-EMOA	R2-EMOA	IGD$^+$-MaOEA	ϵ^+-MaOEA
MIRROR $\gamma = 1.00$	2	4.148358e-03 (6.881384e-05)	2.225160e-02# (1.429510e-02)	4.716280e-03# (1.218065e-04)	4.715821e-03# (1.047166e-04)
	3	5.011539e-02# (7.550655e-04)	5.725235e-02# (1.162920e-03)	4.513631e-02 (9.755519e-04)	4.569586e-02# (1.071872e-03)
MIRROR $\gamma = 2.00$	2	6.037451e-03 (1.610113e-04)	1.761301e-01# (3.542911e-02)	1.949739e-02# (5.895277e-03)	2.222006e-02# (8.953158e-03)
	3	5.853704e-02 (4.979554e-04)	1.002188e-01# (9.411300e-03)	1.150616e-01# (1.127623e-02)	1.192468e-01# (1.132606e-02)
MIRROR $\gamma = 5.00$	2	1.666484e-02 (4.613832e-04)	3.314777e-01# (2.721455e-02)	1.030795e-01# (2.246528e-02)	1.136459e-01# (2.122008e-02)
	3	1.627094e-01 (1.233398e-03)	3.215646e-01# (1.775183e-02)	3.521189e-01# (2.695351e-02)	3.683139e-01# (3.063923e-02)

Table B.6: Mean and, in parentheses, standard deviation of the Riesz s-energy comparison. For each case, the two best values are shown in grayscale, where the darker tone corresponds to the best algorithm. The symbol # is placed when the best algorithm presents a significant difference, according to a one-tailed Wilcoxon test using a significance level of $\alpha = 0.05$.

MOP	Dim.	SMS-EMOA	R2-EMOA	IGD$^+$-MaOEA	ϵ^+-MaOEA	Δ_p-MaOEA
DTLZ5	2	1.642705e+06# (3.667592e+04)	1.426538e+06 (5.331966e+02)	3.284542e+06# (2.324982e+05)	3.246774e+06# (2.476792e+05)	1.779673e+06# (1.334740e+05)
	3	1.137699e+08 (3.334633e+06)	5.415400e+17# (1.075355e+18)	4.139892e+08# (4.414114e+07)	4.211398e+08# (4.947959e+07)	1.559866e+08# (2.553095e+07)
DTLZ5^{-1}	2	1.296325e+05 (2.870240e+03)	6.562904e+08# (2.812100e+09)	2.879533e+05# (1.982203e+04)	2.852587e+05# (1.999574e+04)	1.497304e+05# (8.250750e+03)
	3	2.474935e+04# (1.223894e+03)	6.706334e+16# (3.589393e+17)	4.323645e+04# (7.277478e+03)	4.465221e+04# (6.302722e+03)	2.005661e+04 (1.294014e+03)
DTLZ7	2	1.141697e+06 (2.909429e+04)	7.979252e+09# (3.592319e+10)	2.477841e+06# (2.090567e+05)	2.987530e+06# (2.811123e+06)	1.419812e+06# (1.276149e+05)
	3	1.203024e+06# (2.258313e+06)	6.262355e+10# (2.613354e+11)	1.258730e+06# (1.203218e+06)	1.793360e+06# (3.387314e+06)	5.844906e+05 (5.028749e+05)
DTLZ7^{-1}	2	3.268583e+06 (7.978350e+04)	1.719136e+10# (5.881680e+10)	6.758646e+06# (7.685933e+05)	6.935753e+06# (8.797564e+05)	4.427456e+06# (3.950236e+05)
	3	2.074010e+09 (1.102104e+10)	1.006757e+14# (4.923114e+14)	6.157415e+06 (6.286280e+05)	2.296158e+09 (1.211106e+10)	2.278238e+11 (8.538050e+11)
WFG1	2	8.934498e+05 (1.169571e+05)	7.689052e+09# (3.985797e+10)	1.258394e+06# (9.308691e+04)	1.218884e+06# (2.174472e+05)	9.644694e+05# (1.530521e+05)
	3	2.066124e+05# (8.062808e+04)	1.130505e+10# (6.069368e+10)	2.797654e+05# (5.985555e+04)	3.302417e+05# (6.605761e+04)	1.340369e+05 (2.344808e+04)
WFG1^{-1}	2	7.485416e+05 (9.972770e+04)	5.400936e+08# (1.806448e+09)	1.476324e+06# (8.705842e+05)	1.465063e+06# (7.936464e+05)	7.773445e+05 (1.712791e+05)
	3	2.801482e+05# (6.111701e+04)	3.200017e+12# (1.602124e+13)	1.557129e+05# (2.620210e+04)	2.220459e+05# (2.112907e+05)	1.221268e+05 (1.921651e+04)
WFG2	2	3.874973e+05# (7.320495e+04)	2.838244e+07# (5.909860e+07)	7.776506e+06# (3.713824e+07)	9.252300e+05# (2.389497e+05)	3.477103e+05 (7.772309e+04)
	3	8.313309e+04# (1.118719e+04)	1.059870e+08# (5.418598e+08)	2.160039e+05# (4.144362e+04)	2.559895e+05# (4.871927e+04)	2.351106e+04 (4.102143e+03)
WFG2^{-1}	2	2.430119e+05 (8.966785e+03)	5.970582e+08# (1.930481e+09)	2.745342e+05# (1.306106e+04)	2.728668e+05# (1.041587e+04)	6.723057e+05# (1.619325e+05)
	3	5.603496e+04# (5.153789e+03)	2.510696e+08# (9.183306e+08)	6.257207e+04# (1.236099e+04)	7.165005e+04# (1.894294e+04)	9.309066e+03 (1.365120e+03)
WFG3	2	1.597247e+05 (1.889449e+03)	7.651096e+06# (1.368052e+07)	2.064093e+05# (8.188070e+03)	2.033827e+05# (8.018302e+03)	2.249729e+05# (1.328261e+04)
	3	7.338119e+05# (1.600657e+06)	1.330572e+10# (6.408038e+10)	1.687846e+05# (2.295076e+04)	1.750329e+05# (2.753895e+04)	8.733520e+04 (1.169030e+04)
WFG3^{-1}	2	1.567022e+05 (4.397724e+02)	2.307959e+07# (5.098860e+07)	2.069634e+05# (5.688464e+03)	2.075801e+05# (1.243357e+04)	2.262092e+05# (1.060082e+04)
	3	2.275725e+04# (1.105734e+03)	7.456904e+14# (4.013812e+15)	1.746804e+04 (8.927522e+02)	1.975582e+04# (2.350257e+03)	2.068196e+04# (1.328415e+03)
VIE1	3	9.008727e+04# (2.789419e+03)	4.452919e+11# (2.340388e+12)	1.828579e+05# (1.723622e+04)	1.779405e+05# (1.684371e+04)	3.816533e+04 (2.288552e+03)
VIE2	3	8.100420e+07# (4.999507e+06)	2.989106e+13# (1.477121e+14)	3.648448e+08# (4.188048e+07)	3.707975e+08# (3.646541e+07)	2.581088e+07 (2.971930e+06)
VIE3	3	1.870848e+07# (1.315343e+06)	2.617268e+15# (1.328627e+16)	2.124102e+07# (4.411781e+06)	2.164079e+07# (4.234012e+06)	2.976674e+06 (1.003188e+06)
LAME $\gamma = 0.25$	2	6.461243e+06# (3.726055e+05)	4.804120e+10# (1.351212e+11)	4.867372e+07# (5.073041e+06)	4.917228e+07# (5.697342e+06)	1.233286e+06 (5.791443e+04)
	3	3.391834e+08# (3.931181e+07)	6.955378e+16# (3.587196e+17)	6.518813e+09# (8.951637e+08)	6.589066e+09# (8.928217e+08)	1.610622e+07 (1.154073e+06)
LAME $\gamma = 0.50$	2	1.619967e+06 (3.621627e+04)	8.111698e+08# (1.133423e+09)	4.236560e+06# (3.392327e+05)	4.222500e+06# (3.488763e+05)	1.664322e+06# (6.816516e+04)
	3	3.360179e+06# (1.255342e+05)	3.746806e+10# (1.732736e+11)	1.483810e+07# (2.233503e+06)	1.560206e+07# (2.035800e+06)	3.026936e+06 (2.495049e+05)
LAME $\gamma = 1.00$	2	1.566928e+06 (6.728789e+03)	6.737993e+08# (2.824111e+09)	1.929488e+06# (5.026208e+04)	1.916042e+06# (5.767525e+04)	2.154941e+06# (9.891831e+04)
	3	6.754602e+05 (3.938086e+03)	7.069181e+05# (4.161149e+04)	1.071634e+06# (5.332707e+04)	1.172416e+06# (7.345720e+04)	1.038061e+06# (7.069033e+04)
LAME $\gamma = 2.00$	2	1.645879e+06# (4.514630e+04)	1.426918e+06 (1.538153e+03)	3.295001e+06# (2.012322e+05)	3.316637e+06# (2.097227e+05)	1.771746e+06# (8.377266e+04)
	3	6.711154e+05# (4.032804e+04)	3.385960e+05 (7.212880e+03)	8.504933e+05# (6.904837e+04)	8.538336e+05# (7.664928e+04)	4.786798e+05# (2.746277e+04)
LAME $\gamma = 5.00$	2	7.498451e+06# (1.935681e+07)	1.264608e+06 (5.066119e+04)	1.354972e+07# (1.582782e+06)	1.310267e+07# (1.224850e+06)	1.374215e+06# (4.972939e+04)
	3	2.757830e+09# (1.102707e+10)	2.553093e+05 (1.813380e+03)	3.995109e+06# (4.189985e+05)	3.757314e+06# (5.335883e+05)	2.959040e+05# (2.064500e+04)
MIRROR $\gamma = 0.25$	2	7.282408e+06# (4.617563e+05)	1.218537e+06 (1.212203e+02)	4.777763e+07# (5.168749e+06)	4.775862e+07# (5.655205e+06)	1.289240e+06# (2.506232e+05)
	3	1.229479e+09# (2.321479e+09)	8.703338e+15# (1.321157e+16)	5.348958e+08# (5.767072e+07)	4.541396e+09# (2.071252e+10)	1.871047e+07 (2.487767e+06)
MIRROR $\gamma = 0.50$	2	1.723339e+06# (5.095016e+04)	1.377533e+06 (6.939554e+02)	4.009938e+06# (3.131245e+05)	3.983821e+06# (2.574562e+05)	1.704535e+06# (7.822002e+04)
	3	9.002549e+06# (1.609551e+06)	1.987273e+16# (6.295965e+16)	4.943600e+06# (4.288839e+05)	5.186786e+06# (4.596098e+05)	3.284368e+06 (1.794450e+05)

Table B.6 – *Continuation*

MOP	Dim.	SMS-EMOA	R2-EMOA	IGD$^+$-MaOEA	ϵ^+-MaOEA	Δ_p-MaOEA
MIRROR $\gamma = 1.00$	2	1.565951e+06 (5.566996e+03)	3.323770e+08# (8.349478e+08)	1.911285e+06# (5.389124e+04)	1.914890e+06# (4.255356e+04)	2.201558e+06# (1.204210e+05)
	3	1.398156e+06# (5.171853e+04)	1.619412e+17# (5.073209e+17)	9.744962e+05 (4.674531e+04)	4.168309e+06# (1.685513e+07)	1.112881e+06# (6.507429e+04)
MIRROR $\gamma = 2.00$	2	1.585464e+06 (3.219954e+04)	2.276931e+09# (8.710524e+09)	3.352430e+06# (2.340635e+05)	3.458472e+06# (2.719038e+05)	1.823259e+06# (1.050042e+05)
	3	5.338405e+05# (1.021318e+04)	1.354534e+17# (4.983853e+17)	1.423004e+06# (1.143353e+05)	1.525069e+06# (1.778478e+05)	5.297180e+05 (3.307602e+04)
MIRROR $\gamma = 5.00$	2	3.563192e+06# (1.807682e+05)	2.561909e+10# (5.882747e+10)	1.356737e+07# (1.128377e+06)	1.383275e+07# (1.385592e+06)	1.389883e+06 (6.339161e+04)
	3	9.564379e+05# (3.685362e+04)	3.809270e+09# (1.424536e+10)	8.053827e+06# (1.089352e+06)	8.837185e+06# (1.172617e+06)	3.536266e+05 (7.426666e+04)

B.2 EIB-MOEA

Tables B.7 to B.13 show the numerical results of the comparison between EIB-MOEA, avgEIB-MOEA, SMS-EMOA, R2-EMOA, IGD$^+$-MaOEA, ϵ^+-MaOEA and Δ_p-MaOEA, considering the indicators HV, R2, IGD$^+$, ϵ^+, Δ_p, Riesz s-energy, and Solow-Polasky Diversity indicator. These resuls are related to the experiments of Chapter 5, section 5.4.4.2.

Table B.7: Mean and, in parentheses, standard deviation of the hypervolume comparison. EIB-MOEA stands for the adaptive version and avgEIB-MOEA stands for the average ranking of EIB-MOEA. For each case, the two best values are shown in grayscale, where the darker tone corresponds to the best algorithm. The symbol # is placed when the best algorithm presents a significant difference, according to a one-tailed Wilcoxon test using a significance level of $\alpha = 0.05$.

MOP	Dim.	EIB-MOEA	avgEIB-MOEA	SMS-EMOA	R2-EMOA	IGD$^+$-MaOEA	ϵ^+-MaOEA	Δ_p-MaOEA
DTLZ1	2	8.737764e-01^3# (1.136250e-04)	8.736991e-01^4# (2.665711e-04)	8.738577e-01^1 (1.008001e-04)	8.738131e-01^2# (9.979603e-05)	8.720022e-01^7# (1.018025e-03)	8.720120e-01^6# (8.449071e-04)	8.723735e-01^5# (7.323597e-04)
	3	9.739382e-01^3# (1.821300e-04)	9.738952e-01^4# (2.378834e-04)	9.745094e-01^1 (5.149285e-05)	9.743358e-01^2# (8.570515e-05)	9.664058e-01^6# (2.413026e-03)	9.651634e-01^7# (3.446574e-03)	9.691162e-01^5# (2.482055e-03)
DTLZ1^{-1}	2	1.506408e+05^3# (1.323824e+01)	1.506279e+05^4# (2.428799e+01)	1.507110e+05^2# (1.983985e+00)	1.507168e+05^1 (9.548966e-01)	1.505472e+05^6# (3.494075e+01)	1.505649e+05^5# (2.495414e+01)	1.504247e+05^7# (3.753792e+01)
	3	2.180022e+07^3# (7.514041e+04)	2.176433e+07^4# (1.636252e+05)	1.998268e+07^6# (8.140980e+04)	1.942072e+07^7# (2.264501e+05)	2.225950e+07^1 (1.279257e+05)	2.214927e+07^2# (1.173560e+05)	2.115021e+07^5# (1.875676e+05)
DTLZ2	2	3.211164e+00^3# (4.892288e-05)	3.211255e+00^2# (7.066811e-05)	3.211612e+00^1 (5.643122e-06)	3.210796e+00^4# (5.167044e-05)	3.210650e+00^6# (1.556082e-04)	3.210719e+00^5# (1.161650e-04)	3.206468e+00^7# (3.181915e-03)
	3	7.424117e+00^3# (7.167495e-04)	7.426126e+00^2# (1.003176e-03)	7.431546e+00^1 (4.487141e-05)	7.422032e+00^4# (1.606159e-04)	7.420056e+00^5# (1.082131e-03)	7.414640e+00^6# (9.983771e-03)	7.325874e+00^7# (2.931872e-02)
DTLZ2^{-1}	2	1.028990e+01^2# (5.007866e-04)	1.028925e+01^3# (1.308348e-03)	1.029350e+01^1 (5.662541e-05)	1.027955e+01^5# (1.525186e-03)	1.027565e+01^7# (6.330576e-03)	1.027756e+01^6# (4.964737e-03)	1.028105e+01^4# (1.843947e-03)
	3	2.294408e+01^2# (3.402942e-02)	2.296692e+01^1 (8.768621e-02)	2.264516e+01^5# (1.377448e-02)	2.199164e+01^7# (7.709218e-02)	2.275630e+01^4# (1.049055e-01)	2.276749e+01^3# (7.976193e-02)	2.218083e+01^6# (1.116416e-01)
DTLZ5	2	3.211160e+00^3# (4.593635e-05)	3.211255e+00^2# (7.066811e-05)	3.211612e+00^1 (3.953901e-06)	3.210812e+00^4# (4.304123e-05)	3.210592e+00^6# (1.775941e-04)	3.210652e+00^5# (1.509092e-04)	3.205236e+00^7# (3.663565e-03)
	3	6.104146e+00^3# (2.058559e-04)	6.104321e+00^2# (2.265233e-04)	6.105411e+00^1 (2.729330e-05)	6.097824e+00^6# (1.068114e-03)	6.102903e+00^5# (4.917062e-04)	6.103031e+00^4# (6.311282e-04)	6.088707e+00^7# (1.068745e-02)
DTLZ5^{-1}	2	1.028990e+01^2# (4.523325e-04)	1.028925e+01^3# (1.308348e-03)	1.029352e+01^1 (4.376137e-05)	1.027929e+01^5# (1.504051e-03)	1.027697e+01^6# (5.060453e-03)	1.027533e+01^7# (5.739085e-03)	1.028124e+01^4# (1.661297e-03)
	3	2.299966e+01^2# (3.443112e-02)	2.303049e+01^1 (5.956427e-02)	2.290677e+01^3# (1.976343e-02)	2.220374e+01^7# (7.876260e-02)	2.257175e+01^5# (1.025251e-01)	2.258212e+01^4# (1.490108e-01)	2.227784e+01^6# (8.705157e-02)
DTLZ7	2	1.772483e+01^2# (7.138226e-04)	1.772550e+01^1 (4.574919e-05)	1.771422e+01^6 (6.356944e-02)	1.772455e+01^3# (8.224039e-04)	1.772337e+01^4# (1.159726e-03)	1.772333e+01^5# (1.161732e-03)	1.768915e+01^7# (2.411150e-02)
	3	1.634350e+01^3 (1.079719e-01)	1.636380e+01^1 (8.062365e-02)	1.636149e+01^2 (9.411184e-02)	1.632985e+01^4# (1.049819e-01)	1.628970e+01^5# (1.007615e-01)	1.627456e+01^6# (8.464259e-02)	1.615780e+01^7# (9.618028e-02)
DTLZ7^{-1}	2	1.283540e+01^3# (5.551846e-05)	1.283541e+01^2# (2.775923e-05)	1.283555e+01^1 (4.611330e-06)	1.283519e+01^4# (6.622497e-05)	1.283439e+01^7# (7.783422e-04)	1.283456e+01^6# (6.844252e-04)	1.283506e+01^5# (4.856686e-04)
	3	2.700791e+01^3# (7.826378e-04)	2.700854e+01^2# (1.070110e-03)	2.701652e+01^1 (7.893253e-05)	2.697283e+01^4# (1.426067e-01)	2.694619e+01^5# (1.383594e-01)	2.694209e+01^6# (1.372788e-01)	2.685891e+01^7# (2.611324e-01)
WFG1	2	5.558811e+00^4# (4.417815e-01)	6.650159e+00^1 (9.397065e-02)	5.565514e+00^2# (4.339330e-01)	5.497365e+00^5# (4.246298e-01)	5.448292e+00^6# (3.452536e-01)	5.407837e+00^7# (2.732345e-01)	5.559571e+00^3# (4.234106e-01)
	3	5.246219e+01^3# (1.853296e+00)	5.462174e+01^2 (8.394664e-01)	5.477657e+01^1 (1.654533e+00)	4.798850e+01^6# (1.200120e+00)	5.033596e+01^5# (1.850698e+00)	5.036978e+01^4# (2.287546e+00)	4.689902e+01^7# (1.524285e+00)
WFG1^{-1}	2	7.852046e+00^3# (8.156308e-01)	1.065788e+01^1 (1.128243e-03)	7.538399e+00^5# (5.367997e-01)	7.614634e+00^4# (6.269471e-01)	7.338500e+00^7# (1.467517e-01)	7.439270e+00^6# (3.839397e-01)	8.106008e+00^2# (9.680039e-01)
	3	2.144705e+01^2# (4.296689e+00)	3.056271e+01^1 (5.828320e-01)	2.000915e+01^3# (3.720018e+00)	2.036390e+01^4# (3.623456e+00)	1.952007e+01^6# (3.713256e+00)	2.098848e+01^5# (3.801073e+00)	1.939055e+01^7# (3.680906e+00)
WFG2	2	1.078715e+01^7 (3.566823e-01)	1.100427e+01^2 (4.211115e-01)	1.087355e+01^5 (3.977819e-01)	1.089001e+01^4 (4.085973e-01)	1.093547e+01^3 (4.285781e-01)	1.086123e+01^6 (3.989897e-01)	1.100744e+01^1 (4.117348e-01)
	3	1.007659e+02^1 (1.674324e-01)	1.007135e+02^2 (1.965239e-01)	1.004635e+02^3 (2.853417e+00)	9.996849e+01^4# (2.685782e-01)	9.987732e+01^5# (3.009058e-01)	9.979425e+01^6# (3.624498e-01)	9.881407e+01^7# (2.880843e-01)
WFG2^{-1}	2	1.519433e+01^3# (6.722709e-04)	1.519442e+01^2# (5.840293e-04)	1.519572e+01^1 (2.396223e-04)	1.519380e+01^4# (5.519145e-04)	1.516588e+01^7# (2.291403e-02)	1.517394e+01^6# (1.937666e-02)	1.518789e+01^5# (2.126674e-03)
	3	6.133795e+01^3# (4.281764e-02)	6.150197e+01^2# (6.698304e-02)	6.171171e+01^1 (1.050574e-02)	6.073897e+01^6# (1.879194e-01)	6.105707e+01^4# (8.751900e-02)	6.100724e+01^5# (9.490454e-02)	5.933659e+01^7# (3.955234e-01)
WFG3	2	1.092808e+01^3# (1.252019e-02)	1.093778e+01^1 (8.837058e-03)	1.092987e+01^2# (9.813765e-03)	1.091076e+01^4# (1.226853e-02)	1.088809e+01^6# (3.052675e-02)	1.089143e+01^5# (2.376424e-02)	1.084689e+01^7# (2.017557e-02)
	3	7.509556e+01^2# (1.750046e-01)	7.457472e+01^5# (2.543574e-01)	7.591377e+01^1 (2.087313e-01)	7.461979e+01^4# (4.083305e-01)	7.447021e+01^6# (3.838773e-01)	7.462120e+01^3# (3.479318e-01)	7.188915e+01^7# (4.752644e-01)
WFG3^{-1}	2	1.177146e+01^3# (1.346033e-03)	1.177384e+01^2 (9.480819e-04)	1.177393e+01^1 (1.180483e-03)	1.177103e+01^4# (1.353477e-03)	1.172633e+01^5# (1.832501e-02)	1.172434e+01^6# (2.007880e-02)	1.169751e+01^7# (2.012881e-02)
	3	4.401002e+01^3# (1.192764e-01)	4.441232e+01^2# (1.436889e-01)	4.487959e+01^1 (2.218258e-02)	4.380842e+01^4# (1.033387e-01)	4.353488e+01^5# (2.681933e-01)	4.334837e+01^6# (3.229714e-01)	4.103876e+01^7# (2.775372e-01)
WFG4	2	8.667503e+00^3# (5.109075e-03)	8.678012e+00^1 (4.723931e-03)	8.671948e+00^2# (7.072918e-03)	8.654084e+00^6# (7.356184e-03)	8.659815e+00^4# (6.487625e-03)	8.657943e+00^5# (1.058611e-02)	8.607109e+00^7# (2.216339e-02)
	3	7.663286e+01^3# (1.520104e-01)	7.714138e+01^2# (7.843984e-02)	7.730892e+01^1 (8.178553e-02)	7.552300e+01^6# (2.822633e-01)	7.632573e+01^4# (1.402103e-01)	7.629112e+01^5# (1.385171e-01)	7.154174e+01^7# (6.547193e-01)
WFG4^{-1}	2	1.406566e+01^2# (3.569843e-04)	1.406544e+01^3# (7.840684e-04)	1.406855e+01^1 (5.685331e-05)	1.405888e+01^4# (8.041431e-04)	1.402877e+01^7# (1.141774e-02)	1.403022e+01^6# (1.566796e-02)	1.405848e+01^5# (1.186628e-03)
	3	7.462095e+01^3# (7.685544e-02)	7.468831e+01^2# (7.004690e-02)	7.511780e+01^1 (1.325730e-02)	7.295009e+01^4# (3.557570e-01)	7.292738e+01^5# (3.509286e-01)	7.280354e+01^6# (4.604091e-01)	7.113669e+01^7# (4.533692e-01)

Table B.8: Mean and, in parentheses, standard deviation of the R2 comparison. EIB-MOEA stands for the adaptive version and avgEIB-MOEA stands for the average ranking of EIB-MOEA. For each case, the two best values are shown in grayscale, where the darker tone corresponds to the best algorithm. The symbol # is placed when the best algorithm presents a significant difference, according to a one-tailed Wilcoxon test using a significance level of $\alpha = 0.05$.

MOP	Dim.	EIB-MOEA	avgEIB-MOEA	SMS-EMOA	R2-EMOA	IGD$^+$-MaOEA	ϵ^+-MaOEA	Δ_p-MaOEA
DTLZ1	2	4.065780e-01^3# (2.102674e-04)	4.066969e-01^4# (1.573109e-04)	4.065668e-01^2# (1.789086e-04)	4.063600e-01^1 (1.644603e-04)	4.067548e-01^6# (1.113000e-04)	4.067347e-01^5# (1.049228e-04)	4.070925e-01^7# (3.831973e-04)
	3	4.929948e-01^4# (2.712615e-02)	4.742679e-01^3# (3.779012e-02)	4.601297e-01^2# (5.297765e-03)	3.679229e-01^1 (4.393425e-03)	5.120092e-01^5# (1.697437e-02)	5.297550e-01^7# (5.719085e-02)	5.270813e-01^6# (1.869867e-02)
DTLZ1^{-1}	2	4.479726e+02^2# (5.682474e-02)	4.480097e+02^3# (1.044570e-01)	4.480472e+02^4# (1.078244e-01)	4.477192e+02^1 (6.975623e-03)	4.483245e+02^7# (9.807008e-02)	4.482540e+02^6# (9.629588e-02)	4.481482e+02^5# (1.387686e-01)
	3	5.480104e+02^2# (1.421320e+01)	5.352857e+02^1 (1.388166e+01)	6.645320e+02^6# (2.204913e+01)	1.013609e+03^7# (8.503692e+01)	5.572461e+02^4# (1.412112e+01)	5.651856e+02^5# (1.283468e+01)	5.552950e+02^3# (1.544132e+01)
DTLZ2	2	1.001357e+00^2# (2.119883e-04)	1.001993e+00^4# (1.186192e-03)	1.003588e+00^5# (3.593422e-04)	9.990291e-01^1 (4.099467e-05)	1.022477e+00^7# (8.375910e-03)	1.020907e+00^6# (8.492022e-03)	1.001781e+00^3# (2.464937e-04)
	3	1.501005e+00^2# (2.983463e-02)	1.560594e+00^4# (6.952847e-02)	1.810154e+00^5# (2.088553e-02)	1.036564e+00^1 (1.983280e-02)	2.622435e+00^7# (4.084502e-01)	2.612766e+00^6# (4.463609e-01)	1.512389e+00^3# (1.537589e-01)
DTLZ2^{-1}	2	3.507557e+00^3# (1.365732e-03)	3.510931e+00^4# (6.269280e-03)	3.506810e+00^2# (7.760577e-04)	3.580185e+00^5# (6.278719e-03)	3.996086e+00^7# (4.484729e-01)	3.834550e+00^6# (3.940771e-01)	3.504167e+00^1 (9.602494e-04)
	3	5.986442e+00^3# (4.593506e-01)	6.185196e+00^4# (5.958691e-01)	4.796886e+00^1 (8.261751e-02)	2.821012e+01^5# (3.907643e+00)	2.894792e+02^7# (1.562569e+02)	2.615977e+02^6# (1.176453e+02)	5.856428e+00^2# (8.019856e-01)
DTLZ5	2	1.001263e+00^2# (2.135036e-04)	1.001993e+00^4# (1.186192e-03)	1.003618e+00^5# (3.064076e-04)	9.990258e-01^1 (5.194149e-05)	1.022801e+00^6# (9.475396e-03)	1.022806e+00^7# (8.706925e-03)	1.001831e+00^3# (2.910224e-04)
	3	6.091532e+02^2# (2.859033e-01)	6.092315e+02^4# (9.754946e-02)	6.092222e+02^3# (1.524843e-02)	6.094232e+02^7# (2.418497e-01)	6.092722e+02^5# (7.504547e-02)	6.092818e+02^6# (1.470520e-01)	6.085253e+02^1 (1.109834e+00)
DTLZ5^{-1}	2	3.507672e+00^3# (1.395365e-03)	3.510931e+00^4# (6.269280e-03)	3.506899e+00^2# (8.046600e-04)	3.582293e+00^5# (1.000314e-02)	3.890433e+00^6# (4.697945e-01)	3.973607e+00^7# (4.585739e-01)	3.504155e+00^1 (7.702497e-04)
	3	7.431261e+01^3# (1.007811e+01)	6.471775e+01^2# (2.951850e+01)	4.502220e+01^1 (3.883324e-01)	1.195959e+02^4# (8.285340e+00)	5.408648e+02^7# (1.101386e+02)	5.191219e+02^6# (1.533528e+02)	1.583373e+02^5# (3.265017e+01)
DTLZ7	2	1.442293e+03^3 (3.193226e-01)	1.442292e+03^2 (4.015169e-01)	1.482553e+03^7 (2.233079e+02)	1.442254e+03^1 (3.304472e-01)	1.446681e+03^6# (3.204629e+00)	1.444921e+03^5# (3.066070e+00)	1.442359e+03^4 (1.410000e+00)
	3	2.456687e+03^6 (3.921852e+02)	2.388414e+03^1 (2.894945e+02)	2.417923e+03^2 (3.462270e+02)	2.455591e+03^5 (3.920483e+02)	2.513983e+03^7# (3.909997e+02)	2.454552e+03^4# (3.476300e+02)	2.440820e+03^3# (2.786385e+02)
DTLZ7^{-1}	2	1.593270e+04^2# (1.184134e+01)	1.593534e+04^6# (1.695591e+00)	1.593605e+04^7# (5.878795e-01)	1.593459e+04^4# (1.860548e+00)	1.593432e+04^3# (2.230918e+00)	1.593468e+04^5# (2.270882e+00)	1.592744e+04^1 (1.342423e+01)
	3	2.807692e+04^2# (1.073175e+02)	2.812051e+04^7# (9.335693e-02)	2.812032e+04^6# (8.120430e-02)	2.811869e+04^4# (5.641454e+00)	2.812024e+04^5# (8.421899e-01)	2.811422e+04^3# (1.059925e+01)	2.783239e+04^1 (1.840893e+02)
WFG1	2	6.031466e+02^2# (2.191839e+02)	6.266160e+01^1 (9.439896e+00)	6.042654e+02^3# (2.182262e+02)	6.128952e+02^5# (2.197201e+02)	6.603086e+02^6# (1.657763e+02)	6.828594e+02^7# (1.226561e+02)	6.057479e+02^4# (2.183849e+02)
	3	8.328435e+02^3# (2.291646e+02)	4.574903e+02^1 (2.867298e+01)	6.151453e+02^2# (2.137090e+02)	1.195541e+03^7# (8.950328e+01)	1.056382e+03^5# (1.822665e+02)	1.033514e+03^4# (2.192283e+02)	1.103024e+03^6# (2.265078e+02)
WFG1^{-1}	2	8.219033e+02^3# (2.811589e+02)	2.048781e+02^1 (1.077259e-02)	9.418900e+02^5# (1.830081e+02)	9.182407e+02^4# (2.163618e+02)	1.028153e+03^7# (4.412511e+01)	9.955184e+02^6# (1.363871e+02)	7.332773e+02^2# (3.205969e+02)
	3	1.186750e+03^2# (2.708542e+02)	6.681529e+02^1 (1.820930e+01)	1.290188e+03^3# (2.419775e+02)	1.244385e+03^4# (2.377000e+02)	1.302737e+03^6# (2.449318e+02)	1.205681e+03^5# (2.493480e+02)	1.312981e+03^7# (2.375762e+02)
WFG2	2	2.645326e+02^7 (1.471376e+02)	1.735375e+02^2 (1.741490e+02)	2.299088e+02^5 (1.636744e+02)	2.193529e+02^4# (1.679562e+02)	1.979900e+02^3# (1.740434e+02)	2.317764e+02^6# (1.650208e+02)	1.628041e+02^1 (1.745148e+02)
	3	7.971672e+00^2# (3.653864e+00)	1.483641e+01^4# (1.469776e+01)	1.158276e+02^7# (1.203103e+02)	4.778443e+00^1 (1.364521e+00)	2.489797e+01^6# (1.990841e+01)	2.230000e+01^5# (1.618804e+01)	9.025778e+00^3# (6.237300e+00)
WFG2^{-1}	2	8.651395e+02^4# (5.185009e-01)	8.651168e+02^3# (2.783206e-01)	8.648009e+02^1 (2.021746e-01)	8.650235e+02^2# (3.637121e-01)	8.692601e+02^7# (3.195920e+00)	8.678916e+02^5# (3.167182e+00)	8.688106e+02^6# (2.617558e+00)
	3	6.682861e+02^3# (1.425693e+01)	6.526194e+02^1 (1.385513e+01)	6.703132e+02^4# (7.795940e+00)	6.664781e+02^2# (1.084235e+01)	7.846136e+02^6# (7.079711e+01)	7.951629e+02^7# (8.039122e+01)	7.352142e+02^5# (3.720254e+01)
WFG3	2	2.269730e+00^3# (2.602487e-03)	2.268412e+00^1 (1.826887e-03)	2.268790e+00^2 (2.051273e-03)	2.273049e+00^6# (2.581199e-03)	2.270055e+00^4 (5.219766e-03)	2.270205e+00^5# (3.178676e-03)	2.279190e+00^7# (1.686904e-03)
	3	7.294252e+02^2 (1.489764e+01)	7.414970e+02^4# (3.541837e+01)	7.248444e+02^1 (1.862459e+01)	7.684475e+02^5# (2.398416e+01)	8.673081e+02^6# (3.067601e+01)	8.78716e+02^7# (2.674074e+01)	7.331048e+02^3 (2.667967e+01)
WFG3^{-1}	2	2.086647e+02^4# (1.285162e+00)	2.073999e+02^1 (6.359584e-02)	2.083191e+02^2# (1.181616e+00)	2.086446e+02^3# (9.141489e-01)	2.346617e+02^6# (1.620863e+01)	2.364200e+02^7# (1.508527e+01)	2.308363e+02^5# (1.316663e+01)
	3	6.230901e+02^3# (8.407764e+00)	6.025805e+02^2# (4.607517e+00)	5.941123e+02^1 (4.732728e-01)	6.061898e+02^3# (2.222353e+00)	7.088785e+02^6# (4.777381e+01)	7.306856e+02^6# (4.180492e+01)	7.864977e+02^7# (5.149029e+01)
WFG4	2	2.795035e+00^2# (3.670504e-03)	2.807894e+00^5# (2.081037e-02)	2.805662e+00^4# (8.231490e-03)	2.789017e+00^1 (1.737971e-03)	2.940588e+00^7# (7.809218e-02)	2.931345e+00^6# (9.441640e-02)	2.799895e+00^3# (4.020071e-03)
	3	2.458631e+01^3# (1.365127e+01)	6.962001e+01^4# (3.520504e+01)	1.033363e+02^5# (1.436436e+01)	1.315510e+01^2 (6.527509e+00)	1.886586e+02^7# (4.214053e+01)	1.599418e+02^6# (4.530133e+01)	1.213883e+01^1 (6.873991e+00)
WFG4^{-1}	2	2.498828e+02^4# (1.728954e+01)	2.375707e+02^3# (1.575403e+01)	2.126251e+02^1 (3.682955e+00)	2.523954e+02^5# (1.630160e+01)	5.218592e+02^7# (1.097357e+02)	5.086571e+02^6# (7.708009e+01)	2.356680e+02^2# (1.766228e+01)
	3	7.663080e+02^3# (8.230917e+01)	6.758573e+02^2# (1.301304e+02)	5.909450e+02^1 (6.680946e+00)	7.081071e+02^3# (3.930948e+01)	1.626614e+03^6# (1.983437e+02)	1.701227e+03^7# (1.839032e+02)	7.126793e+02^4# (1.005034e+02)

Table B.9: Mean and, in parentheses, standard deviation of the IGD^+ comparison. EIB-MOEA stands for the adaptive version and avgEIB-MOEA stands for the average ranking of EIB-MOEA. For each case, the two best values are shown in grayscale, where the darker tone corresponds to the best algorithm. The symbol # is placed when the best algorithm presents a significant difference, according to a one-tailed Wilcoxon test using a significance level of $\alpha = 0.05$.

MOP	Dim.	EIB-MOEA	avgEIB-MOEA	SMS-EMOA	R2-EMOA	IGD^+-MaOEA	ϵ^+-MaOEA	Δ_p-MaOEA
DTLZ1	2	1.138816e-03^{2}# (1.187174e-04)	1.178215e-03^{4}# (9.921439e-05)	1.075887e-03^{1} (1.126598e-04)	1.155966e-03^{3}# (9.612310e-05)	1.208357e-03^{6}# (9.283970e-05)	1.189936e-03^{5}# (7.593633e-05)	1.387405e-03^{7}# (2.518266e-04)
	3	1.325667e-02^{4}# (4.838425e-04)	1.327714e-02^{5}# (5.480108e-04)	1.177368e-02^{1} (4.964443e-04)	1.270151e-02^{2}# (3.162440e-04)	1.321498e-02^{3}# (5.500977e-04)	1.339078e-02^{6}# (6.089037e-04)	1.408778e-02^{7}# (6.766080e-04)
DTLZ1^{-1}	2	1.189248e+00^{3}# (4.810848e-02)	1.204831e+00^{4}# (6.255866e-02)	1.139129e+00^{2}# (6.597726e-02)	1.127524e+00^{1} (5.435639e-03)	1.302920e+00^{6}# (7.315995e-02)	1.302302e+00^{5}# (6.962427e-02)	1.451176e+00^{7}# (5.185678e-02)
	3	1.349727e+01^{2}# (4.125129e-01)	1.315492e+01^{1} (5.092481e-01)	1.372287e+01^{3}# (3.498762e-01)	1.706463e+01^{6}# (4.542430e-01)	1.419113e+01^{4}# (6.329394e-01)	1.445832e+01^{5}# (6.851112e-01)	1.924813e+01^{7}# (9.382003e-01)
DTLZ2	2	1.621342e-03^{3}# (1.020741e-04)	1.583488e-03^{2}# (9.515271e-05)	1.403948e-03^{1} (8.209974e-05)	1.811409e-03^{4}# (1.270847e-05)	1.925680e-03^{6}# (1.367207e-04)	1.910354e-03^{5}# (1.301996e-04)	2.155999e-03^{7}# (1.181344e-04)
	3	1.985210e-02^{4}# (8.333919e-04)	1.892805e-02^{2}# (8.507794e-04)	1.657128e-02^{1} (5.743767e-04)	1.972881e-02^{3}# (1.543507e-04)	2.196228e-02^{5}# (8.541667e-04)	2.228655e-02^{6}# (1.258710e-03)	3.473056e-02^{7}# (2.098693e-03)
DTLZ2^{-1}	2	5.624420e-03^{2}# (2.931469e-04)	5.805537e-03^{3}# (3.640741e-04)	5.143650e-03^{1} (3.439863e-04)	7.772299e-03^{5}# (2.521153e-04)	8.147382e-03^{7}# (1.273358e-03)	7.833814e-03^{6}# (9.721202e-04)	6.622056e-03^{4}# (4.371597e-04)
	3	7.958421e-02^{3} (3.116976e-03)	7.938000e-02^{1} (4.061213e-03)	7.951786e-02^{2} (2.623037e-03)	1.254730e-01^{7}# (5.304696e-03)	1.040786e-01^{5}# (9.174636e-03)	1.034832e-01^{4}# (6.865408e-03)	1.058622e-01^{6}# (4.931624e-03)
DTLZ5	2	1.516649e-03^{4}# (9.266965e-05)	1.458232e-03^{2}# (8.852092e-05)	1.376814e-03^{1} (8.110142e-05)	1.482634e-03^{3}# (8.749532e-06)	1.940448e-03^{5}# (1.116637e-04)	1.949409e-03^{6}# (1.739404e-04)	2.169851e-03^{7}# (1.218801e-04)
	3	1.682022e-03^{2}# (9.061864e-05)	1.688898e-03^{3}# (1.155412e-04)	1.452103e-03^{1} (8.947110e-05)	3.023998e-03^{7}# (2.233634e-04)	1.976188e-03^{5}# (1.197024e-04)	1.946427e-03^{4}# (1.259318e-04)	2.628583e-03^{6}# (1.763145e-04)
DTLZ5^{-1}	2	5.492422e-03^{2}# (3.752010e-04)	5.530308e-03^{3}# (3.294430e-04)	4.981403e-03^{1} (2.353366e-04)	7.673906e-03^{5}# (3.243812e-04)	7.873993e-03^{6}# (9.805754e-04)	8.150939e-03^{7}# (1.121745e-03)	6.553539e-03^{4}# (3.207299e-04)
	3	7.406095e-02^{1} (2.489027e-03)	7.409540e-02^{2} (2.775495e-03)	7.681595e-02^{3}# (3.042804e-03)	1.080713e-01^{7}# (4.558661e-03)	9.516004e-02^{5}# (6.676889e-03)	9.435604e-02^{4}# (6.917580e-03)	9.932962e-02^{6}# (4.201786e-03)
DTLZ7	2	1.502308e-03^{1} (7.314812e-05)	1.510247e-03^{2} (7.518022e-05)	1.651585e-02^{7} (8.313686e-02)	1.677737e-03^{3}# (4.863260e-05)	1.695905e-03^{4}# (9.708800e-05)	1.714859e-03^{5}# (7.834030e-05)	1.755186e-03^{6}# (1.015061e-04)
	3	4.749524e-02^{3} (7.582109e-02)	3.298993e-02^{1} (5.646297e-02)	3.658657e-02^{2} (6.719719e-02)	5.021228e-02^{6}# (7.487148e-02)	5.484444e-02^{7}# (7.872036e-02)	4.764429e-02^{4}# (6.822741e-02)	4.821808e-02^{5}# (5.449095e-02)
DTLZ7^{-1}	2	7.302203e-04^{3}# (3.823105e-05)	7.245427e-04^{2}# (3.794532e-05)	6.370590e-04^{1} (4.511613e-05)	8.790273e-04^{7}# (4.437291e-05)	7.968691e-04^{4}# (5.208258e-05)	8.028817e-04^{5}# (4.379660e-05)	8.046368e-04^{6}# (4.910545e-05)
	3	7.101735e-03^{3}# (3.584287e-04)	7.054595e-03^{2}# (5.356348e-04)	5.691448e-03^{1} (2.214618e-04)	1.834142e-02^{6}# (4.626860e-02)	1.830694e-02^{5}# (4.722315e-02)	1.823348e-02^{4}# (4.626704e-02)	4.830946e-02^{7}# (8.667141e-02)
WFG1	2	7.562233e-01^{4}# (8.315992e-02)	5.830305e-01^{1} (1.846339e-02)	7.553260e-01^{3}# (7.992267e-02)	7.675201e-01^{5}# (8.110881e-02)	7.758665e-01^{6}# (6.634075e-02)	7.834092e-01^{7}# (5.242558e-02)	7.548780e-01^{2}# (8.037085e-02)
	3	8.873766e-01^{2}# (1.751364e-02)	8.906524e-01^{3}# (2.457526e-02)	8.380762e-01^{1} (8.077704e-03)	9.540484e-01^{6}# (1.868014e-02)	8.984130e-01^{4}# (2.164659e-02)	9.078633e-01^{5}# (2.460244e-02)	1.041424e+00^{7}# (1.575311e-02)
WFG1^{-1}	2	5.481876e-01^{3}# (2.129948e-01)	8.071802e-03^{1} (2.659464e-04)	6.324440e-01^{5}# (1.371737e-01)	6.118259e-01^{4}# (1.620349e-01)	6.851971e-01^{7}# (4.192718e-02)	6.582995e-01^{6}# (9.926084e-02)	4.838264e-01^{2}# (2.487649e-01)
	3	5.858865e-01^{2}# (2.382798e-01)	9.629440e-02^{1} (1.827569e-02)	6.834385e-01^{3}# (2.007308e-01)	6.542770e-01^{4}# (2.068826e-01)	7.150225e-01^{7}# (2.056066e-01)	6.345212e-01^{3}# (2.087938e-01)	7.043557e-01^{6}# (2.155239e-01)
WFG2	2	7.571457e-02^{7} (3.874006e-02)	5.205202e-02^{2} (4.584202e-02)	6.626901e-02^{5} (4.318253e-02)	6.493902e-02^{4} (4.445997e-02)	5.948470e-02^{3} (4.714510e-02)	6.716520e-02^{6} (4.361916e-02)	5.117229e-02^{1} (4.565861e-02)
	3	3.191545e-02^{2} (3.122939e-03)	3.138270e-02^{1} (3.794308e-03)	3.428869e-02^{3} (4.648446e-02)	5.715154e-02^{6}# (6.085653e-03)	4.118843e-02^{4}# (4.417314e-03)	4.208068e-02^{5}# (4.848321e-03)	7.372309e-02^{7}# (5.593287e-03)
WFG2^{-1}	2	1.378421e-03^{3}# (8.293951e-05)	1.372282e-03^{2}# (7.851190e-05)	1.152447e-03^{1} (6.903412e-05)	1.498181e-03^{6}# (6.291024e-05)	1.492211e-03^{5}# (1.198040e-04)	1.474201e-03^{4}# (7.887042e-05)	1.833578e-03^{7}# (1.058694e-04)
	3	3.163284e-02^{3}# (1.234682e-03)	2.939011e-02^{1} (1.391908e-03)	2.948696e-02^{2} (1.152108e-03)	4.200365e-02^{6}# (2.977206e-03)	3.552751e-02^{4}# (1.425675e-03)	3.632530e-02^{5}# (1.470806e-03)	6.469551e-02^{7}# (6.209421e-03)
WFG3	2	1.038182e-02^{5}# (1.671185e-03)	9.481810e-03^{1} (1.085584e-03)	9.966932e-03^{2} (1.297271e-03)	1.268589e-02^{6}# (1.771434e-03)	1.036496e-02^{4} (3.450778e-03)	1.005910e-02^{3} (1.876482e-03)	1.615870e-02^{7}# (1.283197e-03)
	3	6.143633e-02^{4}# (7.291228e-03)	7.389566e-02^{5}# (8.577341e-03)	3.233225e-02^{1} (8.763235e-03)	7.717283e-02^{6}# (1.585894e-02)	4.431267e-02^{3}# (5.704552e-03)	4.422587e-02^{2}# (6.915511e-03)	1.426049e-01^{7}# (1.093242e-02)
WFG3^{-1}	2	5.999049e-03^{4}# (3.068428e-04)	5.960647e-03^{3}# (2.659767e-04)	5.629306e-03^{1} (3.107375e-04)	5.894956e-03^{2}# (1.203692e-04)	6.487004e-03^{5}# (4.114521e-04)	6.552836e-03^{6}# (4.234703e-04)	1.040981e-02^{7}# (4.394359e-04)
	3	8.772689e-02^{4}# (2.414399e-03)	8.051882e-02^{2} (3.034689e-03)	7.973502e-02^{1} (2.941145e-03)	1.028308e-01^{6}# (3.003894e-03)	8.761892e-02^{3}# (3.783390e-03)	9.052564e-02^{5}# (4.203963e-03)	1.373029e-01^{7}# (5.646360e-03)
WFG4	2	3.147516e-03^{3}# (3.689422e-04)	2.613307e-03^{1} (3.112997e-04)	2.719534e-03^{2} (3.144545e-04)	3.586068e-03^{4}# (6.556709e-04)	4.383503e-03^{6}# (4.811207e-04)	4.379061e-03^{5}# (4.546120e-04)	9.239252e-03^{7}# (1.073468e-03)
	3	5.400605e-02^{3}# (4.268989e-03)	5.158161e-02^{2}# (4.106700e-03)	4.688996e-02^{1} (2.029425e-03)	6.857520e-02^{4}# (6.690078e-03)	7.193515e-02^{6}# (4.118437e-03)	7.116645e-02^{5}# (3.878195e-03)	1.582531e-01^{7}# (1.074525e-02)
WFG4^{-1}	2	4.195580e-03^{2}# (2.591929e-04)	4.349194e-03^{3}# (2.788976e-04)	3.889858e-03^{1} (2.220247e-04)	5.805672e-03^{5}# (1.986764e-04)	6.107114e-03^{7}# (5.389024e-04)	5.908354e-03^{6}# (7.229499e-04)	5.383569e-03^{4}# (3.326486e-04)
	3	7.689889e-02^{3}# (2.465709e-03)	7.477358e-02^{2}# (2.738940e-03)	7.299085e-02^{1} (2.674158e-03)	1.067416e-01^{6}# (6.075198e-03)	9.484515e-02^{4}# (5.080643e-03)	9.663203e-02^{5}# (6.068508e-03)	1.408011e-01^{7}# (9.645817e-03)

Table B.10: Mean and, in parentheses, standard deviation of the ϵ^+ comparison. EIB-MOEA stands for the adaptive version and avgEIB-MOEA stands for the average ranking of EIB-MOEA. For each case, the two best values are shown in grayscale, where the darker tone corresponds to the best algorithm. The symbol # is placed when the best algorithm presents a significant difference, according to a one-tailed Wilcoxon test using a significance level of $\alpha = 0.05$.

MOP	Dim.	EIB-MOEA	avgEIB-MOEA	SMS-EMOA	R2-EMOA	IGD$^+$-MaOEA	ϵ^+-MaOEA	Δ_p-MaOEA
DTLZ1	2	3.029433e-03^{3}# (4.938027e-04)	3.619367e-03^{4}# (5.017904e-04)	2.366967e-03^{2}# (1.238554e-04)	2.237167e-03^{1} (1.250823e-04)	4.201867e-03^{5}# (6.309856e-04)	4.265033e-03^{6}# (6.358441e-04)	4.504067e-03^{7}# (6.773456e-04)
	3	2.818737e-02^{3}# (2.370120e-03)	2.840180e-02^{4}# (2.680628e-03)	2.156677e-02^{1} (7.909133e-04)	2.549273e-02^{2}# (3.669705e-03)	3.272530e-02^{7}# (6.775628e-03)	3.254047e-02^{6}# (5.827186e-03)	3.123333e-02^{5}# (3.400549e-03)
DTLZ1^{-1}	2	3.370583e+00^{3}# (4.409312e-01)	3.676996e+00^{4}# (4.594518e-01)	2.498473e+00^{2}# (1.104765e-01)	2.335057e+00^{1} (4.829008e-02)	4.578842e+00^{5}# (8.471034e-01)	4.727044e+00^{6}# (1.102568e+00)	4.799485e+00^{7}# (6.695103e-01)
	3	3.094822e+01^{2} (2.137831e+00)	3.054857e+01^{1} (3.722525e+00)	3.400585e+01^{3}# (1.529954e+00)	4.389092e+01^{6}# (3.715579e+00)	3.456349e+01^{4}# (4.112826e+00)	3.686079e+01^{5}# (5.511899e+00)	4.788281e+01^{7}# (9.813524e+00)
DTLZ2	2	5.471000e-03^{3}# (4.301869e-04)	5.373733e-03^{2}# (5.167723e-04)	3.537500e-03^{1} (1.787226e-04)	5.779633e-03^{4}# (6.906792e-05)	7.737767e-03^{6}# (1.606539e-03)	7.121767e-03^{5}# (1.355271e-03)	9.186867e-03^{7}# (1.727378e-03)
	3	5.074923e-02^{4}# (4.660551e-03)	4.829913e-02^{3}# (3.542865e-03)	3.991740e-02^{1} (2.926948e-03)	4.598183e-02^{2}# (2.406137e-03)	5.803163e-02^{5}# (8.441366e-03)	6.254920e-02^{6}# (2.739667e-02)	8.392743e-02^{7} (2.082800e-02)
DTLZ2^{-1}	2	1.856653e-02^{2}# (2.006208e-03)	1.945913e-02^{3}# (3.366691e-03)	1.285550e-02^{1} (6.271058e-04)	2.489990e-02^{4}# (4.881354e-04)	2.941133e-02^{5}# (7.710666e-03)	2.949630e-02^{6}# (6.095916e-03)	3.011720e-02^{7}# (6.446450e-03)
	3	1.932722e-01^{2} (2.110411e-02)	1.966413e-01^{3} (2.040695e-02)	1.917019e-01^{1} (1.170197e-02)	3.226318e-01^{7}# (1.189760e-02)	2.607228e-01^{6}# (4.843942e-02)	2.562875e-01^{5}# (4.056330e-02)	2.452603e-01^{4}# (2.326028e-02)
DTLZ5	2	5.504167e-03^{3}# (4.519828e-04)	5.399733e-03^{2}# (5.438064e-04)	3.529433e-03^{1} (1.494714e-04)	5.593167e-03^{4}# (1.544624e-04)	7.838133e-03^{6}# (1.500150e-03)	7.457000e-03^{5}# (1.296672e-03)	8.976667e-03^{7}# (2.134284e-03)
	3	4.964867e-03^{2}# (8.496994e-04)	5.302633e-03^{3}# (9.346047e-04)	2.962867e-03^{1} (1.577387e-04)	1.546253e-02^{7}# (2.947527e-03)	7.631000e-03^{5}# (1.985486e-03)	6.410267e-03^{4}# (1.412308e-03)	8.804833e-03^{6}# (2.491319e-03)
DTLZ5^{-1}	2	1.882933e-02^{3}# (1.686586e-03)	1.878847e-02^{2}# (3.027839e-03)	1.267857e-02^{1} (5.667134e-04)	2.499013e-02^{4}# (5.944780e-04)	2.986223e-02^{6}# (7.848319e-03)	3.121450e-02^{7}# (7.191684e-03)	2.890353e-02^{5}# (5.477040e-03)
	3	1.835070e-01^{2} (2.014381e-02)	1.824071e-01^{1} (1.376932e-02)	1.869102e-01^{3}# (9.885528e-03)	3.014071e-01^{7}# (1.851071e-02)	2.475115e-01^{6}# (5.120556e-02)	2.343574e-01^{5}# (4.539218e-02)	2.200598e-01^{4}# (2.787276e-02)
DTLZ7	2	4.779667e-03^{1} (3.020249e-04)	4.799033e-03^{2} (5.160393e-04)	4.556313e-02^{7} (2.305399e-01)	7.410067e-03^{6}# (1.118633e-03)	7.174833e-03^{4}# (1.636395e-03)	6.898633e-03^{3}# (1.888579e-03)	7.399100e-03^{5}# (1.195047e-03)
	3	2.141649e-01^{4} (4.204887e-01)	1.339988e-01^{1} (3.113922e-01)	1.734326e-01^{2} (3.705064e-01)	2.391101e-01^{5}# (4.102094e-01)	3.089043e-01^{7}# (4.041085e-01)	2.824729e-01^{6}# (3.495371e-01)	1.891735e-01^{3}# (3.025009e-01)
DTLZ7^{-1}	2	2.466800e-03^{3}# (5.838333e-04)	2.458200e-03^{2}# (5.599162e-04)	1.676467e-03^{1} (1.848503e-04)	4.833200e-03^{7}# (5.397443e-04)	3.200867e-03^{4}# (6.858404e-04)	3.292067e-03^{5}# (6.569103e-04)	3.390967e-03^{6}# (6.098407e-04)
	3	2.111490e-02^{1} (1.943197e-03)	2.130607e-02^{2} (3.162668e-03)	2.284907e-02^{3}# (2.054683e-03)	8.283100e-02^{6}# (1.679747e-01)	7.931797e-02^{4}# (1.696813e-01)	8.188160e-02^{5}# (1.686453e-01)	1.814902e-01^{7}# (3.160031e-01)
WFG1	2	1.172790e+00^{4}# (2.016865e-01)	5.487127e-01^{1} (1.625371e-02)	1.169079e+00^{2}# (2.048176e-01)	1.195432e+00^{5}# (1.938614e-01)	1.223734e+00^{6}# (1.499167e-01)	1.244049e+00^{7}# (1.138881e-01)	1.169771e+00^{3}# (1.967495e-01)
	3	9.746622e-01^{2}# (3.744599e-02)	9.824429e-01^{3}# (3.622247e-02)	9.356994e-01^{1} (2.131222e-02)	1.092567e+00^{7}# (5.826752e-02)	1.047950e+00^{5}# (6.736840e-02)	1.037082e+00^{4}# (7.085494e-02)	1.091743e+00^{6}# (5.007468e-02)
WFG1^{-1}	2	2.061609e+00^{3}# (6.030636e-01)	5.526200e-02^{1} (0.000000e+00)	2.290842e+00^{5}# (3.958191e-01)	2.235348e+00^{4}# (4.636545e-01)	2.423669e+00^{7}# (7.039240e-02)	2.356704e+00^{6}# (2.852951e-01)	1.870250e+00^{2}# (7.226348e-01)
	3	3.071724e+00^{2}# (7.124580e-01)	5.890682e-01^{1} (1.504094e-01)	3.424007e+00^{4}# (2.685020e-01)	3.416940e+00^{3}# (2.406362e-01)	3.591879e+00^{6}# (6.973795e-02)	3.597818e+00^{7}# (9.558932e-02)	3.490099e+00^{5}# (2.797429e-01)
WFG2	2	6.155420e-01^{7} (3.395035e-01)	4.057546e-01^{2} (4.012995e-01)	5.358520e-01^{5} (3.788144e-01)	5.125043e-01^{4} (3.853117e-01)	4.604484e-01^{3} (3.998547e-01)	5.386202e-01^{6} (3.787763e-01)	3.868306e-01^{1} (3.959244e-01)
	3	8.485780e-02^{1} (1.347932e-02)	8.759357e-02^{2} (2.240600e-02)	1.052959e-01^{4} (2.063483e-01)	1.965992e-01^{6}# (3.795870e-02)	1.112799e-01^{5}# (3.401757e-02)	1.000486e-01^{3}# (2.419028e-02)	2.278225e-01^{7}# (4.045956e-02)
WFG2^{-1}	2	4.187300e-03^{2}# (6.268132e-04)	4.557367e-03^{3}# (2.156265e-03)	3.101500e-03^{1} (3.293135e-04)	1.271530e-02^{7}# (7.161193e-04)	1.242367e-02^{6}# (6.750211e-03)	1.139070e-02^{5}# (4.937711e-03)	5.313167e-03^{4}# (6.896907e-04)
	3	9.651890e-02^{3}# (1.486332e-02)	8.856503e-02^{2} (1.629729e-02)	8.696420e-02^{1} (1.318886e-02)	2.273629e-01^{6}# (5.443080e-02)	1.207342e-01^{4}# (2.305525e-02)	1.260375e-01^{5}# (2.102257e-02)	2.637524e-01^{7}# (8.201011e-02)
WFG3	2	2.081437e-02^{3}# (2.645154e-03)	2.086490e-02^{4}# (2.344162e-03)	1.685090e-02^{1} (1.507588e-03)	1.981087e-02^{2}# (2.745616e-03)	3.611493e-02^{5}# (1.413570e-02)	3.688543e-02^{6}# (1.768304e-02)	4.102603e-02^{7}# (1.092844e-02)
	3	1.105606e-01^{3}# (1.175578e-02)	1.209671e-01^{5}# (1.705474e-02)	6.778130e-02^{1} (1.329793e-02)	1.573533e-01^{6}# (2.377017e-02)	1.194138e-01^{4}# (4.159749e-02)	9.388627e-02^{2}# (2.370417e-02)	2.064699e-01^{7}# (3.929931e-02)
WFG3^{-1}	2	1.616573e-02^{3}# (2.031856e-03)	1.709220e-02^{4}# (2.631254e-03)	1.206893e-02^{2}# (6.341590e-04)	1.183993e-02^{1} (9.516452e-04)	2.995523e-02^{5}# (1.225320e-02)	3.046000e-02^{6}# (1.035997e-02)	3.307760e-02^{7}# (1.004739e-02)
	3	2.082383e-01^{3} (2.287307e-02)	2.055263e-01^{2} (2.716084e-02)	2.018256e-01^{1} (9.257889e-03)	2.944091e-01^{5}# (3.171431e-02)	2.773118e-01^{4}# (6.408260e-02)	3.035424e-01^{6}# (7.382198e-02)	3.650803e-01^{7}# (9.168717e-02)
WFG4	2	1.328137e-02^{3}# (1.864407e-03)	1.329080e-02^{4}# (2.542630e-03)	1.033350e-02^{1} (3.323581e-03)	1.161453e-02^{2}# (1.470447e-03)	2.114303e-02^{6}# (4.122784e-03)	2.044070e-02^{5}# (4.435727e-03)	2.910173e-02^{7}# (1.093715e-02)
	3	1.756680e-01^{2}# (2.399973e-02)	1.790309e-01^{3}# (2.746987e-02)	1.348170e-01^{1} (9.200762e-03)	3.749806e-01^{7}# (7.914773e-02)	2.173698e-01^{5}# (3.229964e-02)	2.073417e-01^{4}# (3.089131e-02)	3.422943e-01^{6}# (7.074644e-02)
WFG4^{-1}	2	1.451330e-02^{2}# (1.795292e-03)	1.478480e-02^{3}# (2.371127e-03)	9.940333e-03^{1} (3.603529e-04)	2.688500e-02^{7}# (8.272848e-04)	2.579143e-02^{5}# (6.862877e-03)	2.599443e-02^{6}# (8.633918e-03)	2.241183e-02^{4}# (3.728799e-03)
	3	1.937156e-01^{2} (1.890607e-02)	1.893845e-01^{1} (1.898721e-02)	2.029217e-01^{3}# (1.994370e-02)	3.276066e-01^{7}# (7.719444e-02)	3.029892e-01^{5}# (7.104769e-02)	3.188661e-01^{6}# (8.184427e-02)	2.774964e-01^{4}# (3.147925e-02)

Table B.11: Mean and, in parentheses, standard deviation of the Δ_p comparison. EIB-MOEA stands for the adaptive version and avgEIB-MOEA stands for the average ranking of EIB-MOEA. For each case, the two best values are shown in grayscale, where the darker tone corresponds to the best algorithm. The symbol # is placed when the best algorithm presents a significant difference, according to a one-tailed Wilcoxon test using a significance level of $\alpha = 0.05$.

MOP	Dim.	EIB-MOEA	avgEIB-MOEA	SMS-EMOA	R2-EMOA	IGD$^+$-MaOEA	ϵ^+-MaOEA	Δ_p-MaOEA
DTLZ1	2	1.239498e-01^3# (4.139910e-01)	4.071685e-01^7# (1.867255e+00)	3.040709e-02^1 (1.909722e-05)	3.041130e-02^2 (1.981690e-05)	3.532012e-01^6# (1.436518e+00)	2.489119e-01^5# (7.163138e-01)	1.538540e-01^4# (6.742478e-01)
	3	4.334150e-01^6# (1.568254e+00)	1.169981e+00^7# (2.499130e+00)	1.906386e-02^1 (6.948806e-04)	1.968138e-02^2# (1.601801e-04)	2.371820e-02^4# (1.281383e-02)	2.167515e-02^3# (1.416930e-03)	2.817771e-01^5# (7.571135e-01)
DTLZ1^{-1}	2	2.072880e+00^3 (6.343982e-02)	2.081684e+00^4 (8.804044e-02)	2.049846e+00^1 (1.053941e-01)	2.071116e+00^2 (9.417107e-03)	2.279737e+00^6# (1.379096e-01)	2.273862e+00^5# (1.144224e-01)	2.413643e+00^7# (8.474902e-02)
	3	2.194600e+01^2 (5.522435e-01)	2.179119e+01^1 (7.100843e-01)	2.425342e+01^5# (5.597425e-01)	2.895920e+01^7# (7.030148e-01)	2.321045e+01^3# (8.392465e-01)	2.349328e+01^4# (1.015955e+00)	2.634358e+01^6# (1.112528e+00)
DTLZ2	2	4.850849e-03^2# (2.235456e-04)	5.436212e-03^4# (8.098701e-04)	6.335570e-03^5# (2.081659e-04)	4.303931e-03^1 (2.550281e-05)	1.335476e-02^7# (1.993538e-03)	1.284239e-02^6# (1.977466e-03)	4.909886e-03^3# (2.203886e-04)
	3	5.559791e-02^2# (1.720859e-03)	5.661954e-02^3# (2.207755e-03)	6.833190e-02^5# (9.608793e-04)	5.055731e-02^1 (3.329194e-04)	7.034098e-02^6# (2.821212e-03)	7.035274e-02^7# (3.271821e-03)	5.876422e-02^4# (2.471867e-03)
DTLZ2^{-1}	2	1.901430e-02^3# (1.482129e-03)	2.070488e-02^4# (3.764119e-03)	1.782304e-02^2# (8.491022e-04)	4.711470e-02^5# (1.619488e-03)	9.179124e-02^7# (2.854480e-02)	7.550825e-02^6# (2.771971e-02)	1.684486e-02^1 (9.096433e-04)
	3	2.225910e-01^3# (8.959532e-03)	2.242061e-01^4# (1.065479e-02)	1.871562e-01^1 (4.277332e-03)	3.041440e-01^5# (8.392088e-03)	4.606761e-01^7# (6.019753e-02)	4.531561e-01^6# (4.759505e-02)	2.186471e-01^2# (8.267790e-03)
DTLZ5	2	4.790979e-03^2# (2.288816e-04)	5.411999e-03^4# (8.142296e-04)	6.333955e-03^5# (2.145072e-04)	3.926580e-03^1 (2.112764e-05)	1.344507e-02^6# (2.440660e-03)	1.360412e-02^7# (2.230980e-03)	4.874066e-03^3# (2.836410e-04)
	3	5.150870e-03^1 (3.348692e-04)	6.073682e-03^4# (1.378416e-03)	5.930597e-03^3# (2.672396e-04)	1.159951e-02^5# (1.887197e-03)	1.299585e-02^7# (2.508009e-03)	1.243473e-02^6# (1.732408e-03)	5.550695e-03^2 (1.408285e-03)
DTLZ5^{-1}	2	1.863840e-02^3# (1.161723e-03)	2.054576e-02^4# (3.624784e-03)	1.752700e-02^2# (7.255055e-04)	4.783853e-02^5# (2.197859e-03)	8.031004e-02^6# (2.626219e-02)	8.919388e-02^7# (2.438655e-02)	1.699613e-02^1 (8.186813e-04)
	3	1.688187e-01^2 (5.934047e-03)	1.748179e-01^3# (7.802019e-03)	1.680876e-01^1 (4.510447e-03)	2.552100e-01^5# (1.166530e-02)	3.468057e-01^7# (4.510802e-02)	3.433198e-01^6# (5.290872e-02)	1.822088e-01^4# (1.193451e-02)
DTLZ7	2	5.784977e-03^2 (8.625040e-04)	5.666186e-03^1 (5.729535e-04)	2.988837e-02^7 (1.361989e-01)	6.704730e-03^4# (4.880437e-04)	7.500851e-03^6# (8.671025e-04)	7.405602e-03^5# (7.620711e-04)	6.153049e-03^3# (1.223587e-03)
	3	1.454114e-01^4# (1.627106e-01)	1.198168e-01^2# (1.212469e-01)	1.755889e-01^7# (1.272802e-01)	1.567487e-01^6# (1.570315e-01)	1.495984e-01^5# (1.739358e-01)	1.325586e-01^3# (1.514776e-01)	1.033530e-01^1 (1.223117e-01)
DTLZ7^{-1}	2	3.401288e-03^3# (8.963120e-04)	3.262634e-03^2# (2.292845e-04)	2.805258e-03^1 (1.282997e-04)	3.880909e-03^6# (2.000081e-04)	3.806359e-03^5# (3.151503e-04)	3.942231e-03^7# (4.341305e-04)	3.450185e-03^4# (1.062576e-03)
	3	8.090152e-02^1 (3.589643e-03)	8.280975e-02^2# (4.913064e-03)	1.030237e-01^6# (1.529755e-03)	1.028122e-01^4# (8.069147e-02)	1.049907e-01^6# (8.270220e-02)	1.024844e-01^3# (8.042076e-02)	1.357750e-01^7 (1.578792e-01)
WFG1	2	1.069092e+00^2# (2.016845e-01)	5.897665e-01^1 (1.898368e-02)	1.071295e+00^3# (2.005360e-01)	1.083149e+00^5# (1.966695e-01)	1.118394e+00^6# (1.537131e-01)	1.139887e+00^7# (1.130892e-01)	1.071778e+00^4# (1.992611e-01)
	3	1.201312e+00^3# (7.407392e-02)	9.982737e-01^1 (4.193259e-02)	1.021982e+00^2 (7.338975e-02)	1.353354e+00^7# (4.531259e-02)	1.278313e+00^4# (7.731920e-02)	1.281997e+00^5# (8.525051e-02)	1.299570e+00^6# (5.998868e-02)
WFG1^{-1}	2	9.395802e-01^3# (3.376104e-01)	9.803531e-02^1 (1.076016e-03)	1.077265e+00^5# (2.200410e-01)	1.046464e+00^4# (2.591287e-01)	1.169527e+00^7# (5.659772e-02)	1.129379e+00^6# (1.592470e-01)	8.342087e-01^2# (3.924121e-01)
	3	1.002115e+00^2# (2.187432e-01)	4.903245e-01^1 (5.736131e-02)	1.114861e+00^3# (1.480902e-01)	1.093271e+00^3# (1.567656e-01)	1.158333e+00^7# (1.439581e-01)	1.105515e+00^4# (1.428798e-01)	1.131968e+00^6# (1.772848e-01)
WFG2	2	2.675057e-01^7 (1.420481e-01)	1.803695e-01^2 (1.672161e-01)	2.340698e-01^5 (1.582020e-01)	2.253728e-01^4# (1.594381e-01)	2.047652e-01^3# (1.644634e-01)	2.376631e-01^6# (1.564233e-01)	1.698806e-01^1 (1.664895e-01)
	3	3.245992e-01^2# (2.355328e-02)	3.366688e-01^3# (5.574437e-02)	4.100867e-01^4# (4.582813e-02)	4.472541e-01^6# (2.612461e-02)	4.441524e-01^5# (4.032392e-02)	4.497786e-01^7# (4.482843e-02)	2.391306e-01^1 (1.456180e-02)
WFG2^{-1}	2	1.121809e-02^4# (4.545353e-04)	1.113008e-02^3# (4.650995e-04)	1.030633e-02^1 (6.368352e-04)	1.098280e-02^2# (3.489987e-04)	1.214325e-02^5# (5.233527e-04)	1.214631e-02^6# (5.437397e-04)	1.298970e-02^7# (4.304909e-04)
	3	2.773048e-01^3# (1.067945e-02)	2.707268e-01^2# (1.752023e-02)	4.171931e-01^7# (1.288662e-02)	3.137627e-01^4# (1.838819e-02)	3.405671e-01^6# (2.360389e-02)	3.376237e-01^5# (1.318701e-02)	2.506430e-01^1 (8.452348e-03)
WFG3	2	1.346806e-02^3 (9.768714e-04)	1.330196e-02^2# (5.602474e-04)	1.310615e-02^1 (8.018616e-04)	1.487882e-02^6# (1.327967e-03)	1.468168e-02^5# (2.693077e-03)	1.458708e-02^4# (1.384208e-03)	1.894468e-02^7# (1.241600e-03)
	3	7.776444e-01^7# (3.232302e-02)	7.599431e-01^5# (5.769421e-02)	7.200249e-01^4# (2.549175e-02)	6.476556e-01^1 (4.845443e-02)	6.997832e-01^3# (7.096572e-02)	6.690641e-01^2 (6.331834e-02)	7.676176e-01^6# (5.098194e-02)
WFG3^{-1}	2	1.160530e-02^2# (3.524731e-04)	1.168389e-02^3# (5.976255e-04)	1.206808e-02^4# (5.180468e-04)	1.139497e-02^1 (7.388410e-05)	1.357472e-02^5# (1.088330e-03)	1.373123e-02^6# (8.112323e-04)	1.534536e-02^7# (8.017795e-04)
	3	1.626279e-01^2 (3.589644e-03)	1.611946e-01^1 (5.541591e-03)	1.784205e-01^5# (5.424309e-03)	2.066954e-01^7# (8.188066e-03)	1.738570e-01^3# (8.286003e-03)	1.758738e-01^4# (7.941588e-03)	1.934446e-01^6# (7.253771e-03)
WFG4	2	1.599465e-02^2# (1.091338e-03)	1.939648e-02^5# (3.988695e-03)	1.851743e-02^4# (1.372123e-03)	9.180753e-03^1 (5.808510e-04)	3.892197e-02^7# (5.605676e-03)	3.684778e-02^6# (6.002514e-03)	1.773688e-02^3# (1.031926e-03)
	3	2.283584e-01^2# (9.632271e-03)	2.603648e-01^4# (1.684968e-02)	2.874612e-01^5# (3.987403e-03)	1.851471e-01^1 (9.840723e-03)	3.109464e-01^7# (1.902560e-02)	2.969383e-01^6# (1.715060e-02)	2.513435e-01^3# (8.245375e-03)
WFG4^{-1}	2	1.852695e-02^3# (1.402805e-03)	2.100810e-02^4# (3.687464e-03)	1.739347e-02^2# (7.964189e-04)	4.490877e-02^5# (2.011880e-03)	8.908784e-02^7# (3.078176e-02)	8.015681e-02^6# (2.445469e-02)	1.638320e-02^1 (9.762775e-04)
	3	2.641492e-01^3# (1.366662e-02)	2.642737e-01^4# (1.966313e-02)	2.234150e-01^1 (6.009539e-03)	3.577523e-01^5# (1.244170e-02)	4.624059e-01^6# (5.442627e-02)	4.804829e-01^7# (5.324561e-02)	2.474839e-01^2# (1.316654e-02)

Table B.12: Mean and, in parentheses, standard deviation of the Riesz s-energy comparison. EIB-MOEA stands for the adaptive version and avgEIB-MOEA stands for the average ranking of EIB-MOEA. For each case, the two best values are shown in grayscale, where the darker tone corresponds to the best algorithm. The symbol # is placed when the best algorithm presents a significant difference, according to a one-tailed Wilcoxon test using a significance level of $\alpha = 0.05$.

MOP	Dim.	EIB-MOEA	avgEIB-MOEA	SMS-EMOA	R2-EMOA	IGD$^+$-MaOEA	ϵ^+-MaOEA	Δ_p-MaOEA
DTLZ1	2	1.245209e+07^3# (7.981976e+05)	1.323010e+07^4# (6.549903e+05)	1.101146e+07^2# (7.178610e+04)	1.086490e+07^1 (1.564289e+05)	1.464377e+07^6# (6.366370e+05)	1.457581e+07^5# (4.311064e+05)	1.527260e+07^7# (5.765153e+05)
	3	1.422309e+15^7# (7.790303e+15)	4.641884e+09^5# (2.248610e+10)	7.862611e+06^1 (5.202547e+04)	9.188460e+09^6 (3.126318e+10)	1.291945e+07^2# (9.690003e+05)	1.381179e+07^3# (7.940445e+05)	1.490362e+07^4# (1.234168e+07)
DTLZ1^{-1}	2	1.011613e+01^3# (2.578863e-01)	1.029548e+01^4# (4.093859e-01)	9.032038e+00^2# (4.628879e-02)	8.913987e+00^1 (4.576841e-03)	1.189729e+01^6# (5.302761e-01)	1.174751e+01^5# (4.325495e-01)	1.243688e+01^7# (4.686888e-01)
	3	3.360796e+00^5# (8.415703e+00)	4.726578e+03^6 (2.583027e+04)	1.293559e-02^4# (4.824527e-04)	1.055668e+08^7# (4.683271e+08)	8.848949e-03^1 (4.041497e-04)	9.322149e-03^2# (5.140132e-04)	9.561163e-03^3# (5.116497e-04)
DTLZ2	2	3.233501e+06^3# (1.172619e+05)	3.311258e+06^4# (3.256723e+05)	2.862209e+06^2# (6.708421e+04)	2.592471e+06^1 (4.051869e+05)	5.678576e+06^6# (3.676471e+05)	5.632958e+06^5# (3.702106e+05)	5.877482e+06^7# (1.531351e+07)
	3	1.653608e+09^6# (6.284465e+09)	1.252207e+06^4# (1.267528e+06)	9.662145e+05^2# (4.336980e+04)	2.797959e+14^7# (1.443022e+15)	1.228118e+06^3# (8.359941e+04)	1.255653e+06^5# (1.075302e+05)	6.566464e+05^1 (3.496962e+04)
DTLZ2^{-1}	2	2.838515e+05^3# (1.244369e+04)	2.960598e+05^4# (3.007248e+04)	2.268322e+05^1 (4.849151e+03)	1.262202e+06^7# (3.092065e+06)	4.950592e+05^6# (3.968200e+04)	4.863520e+05^5# (3.152357e+04)	2.547450e+05^2# (1.175286e+04)
	3	1.139961e+07^6# (4.697340e+07)	1.165708e+05^2# (2.865988e+05)	1.849636e+04^2# (3.114351e+02)	1.427916e+10^7# (7.289812e+10)	4.908170e+04^4# (5.286262e+03)	4.791515e+04^3# (5.848816e+03)	1.815288e+04^1 (2.249548e+03)
DTLZ5	2	3.234100e+06^4# (1.325770e+05)	3.311258e+06^5# (3.256723e+05)	2.859806e+06^2# (5.225628e+04)	2.636080e+06^1 (5.058904e+05)	5.721084e+06^7# (3.217649e+05)	5.717096e+06^6# (3.502384e+05)	3.027044e+06^3# (1.157903e+05)
	3	6.666695e+16^5# (3.651483e+17)	1.138094e+17^6# (5.065051e+17)	1.960560e+08^1 (5.822459e+06)	4.395397e+18^7# (2.466086e+18)	7.108126e+08^4# (6.328457e+07)	6.799892e+08^3# (8.093547e+07)	2.630113e+08^2# (3.238037e+07)
DTLZ5^{-1}	2	2.802605e+05^3# (9.538761e+03)	2.960598e+05^4# (3.007248e+04)	2.251274e+05^1 (4.726658e+03)	5.923561e+07^7# (2.208819e+08)	4.918868e+05^5# (2.570590e+04)	4.922887e+05^6# (3.219497e+04)	2.524122e+05^2# (9.790368e+03)
	3	5.813590e+08^5# (3.182166e+09)	6.778543e+08^6# (3.558588e+09)	3.824983e+04^2# (2.071020e+03)	2.971018e+14^7# (1.622681e+15)	5.962272e+04^4# (5.706816e+03)	5.953155e+04^3# (6.733471e+03)	2.798130e+04^1 (1.690016e+03)
DTLZ7	2	2.686572e+06^4# (1.491939e+05)	2.659586e+06^3# (2.426333e+05)	2.643110e+06^2 (3.614011e+06)	5.017145e+08^7# (1.312386e+09)	4.205181e+06^5# (2.891552e+05)	4.303217e+06^6# (2.759142e+05)	2.532269e+06^1 (2.081098e+05)
	3	4.904993e+07^5# (1.848661e+08)	5.416497e+07^6# (2.825791e+08)	1.539104e+06^2# (1.526228e+06)	1.635595e+11^7# (4.307163e+11)	1.792668e+06^4# (1.777334e+06)	1.637429e+06^3# (1.441043e+06)	9.882648e+05^1 (1.064137e+06)
DTLZ7^{-1}	2	7.974204e+06^3# (4.257853e+05)	6.675342e+09^7# (3.651460e+10)	5.699772e+06^1 (1.170570e+05)	5.078815e+09^6# (1.468262e+10)	1.129931e+07^4# (1.248592e+06)	1.147446e+07^5# (9.576487e+05)	7.488510e+06^2# (5.583463e+05)
	3	7.071779e+09^4# (2.922335e+10)	2.947026e+12^5# (1.364902e+13)	5.052117e+06^1 (3.408950e+05)	3.021504e+14^7# (1.410176e+15)	9.669742e+07^3# (4.783294e+08)	5.998256e+07^2# (2.815927e+08)	1.237437e+13^6 (4.671126e+13)
WFG1	2	1.635752e+06^3# (2.797918e+05)	4.856344e+05^1 (3.736557e+04)	1.629165e+06^2# (2.815278e+05)	1.297461e+07^7# (1.427410e+07)	2.291195e+06^5# (4.280963e+05)	2.297560e+06^6# (2.726100e+05)	1.729271e+06^4# (2.939444e+05)
	3	1.008502e+06^5# (3.090192e+06)	5.073326e+06^6# (2.427558e+07)	3.577739e+05^2# (1.561550e+05)	2.880554e+10^7# (1.179505e+11)	4.288907e+05^3# (8.532107e+04)	4.659735e+05^4# (1.237011e+05)	2.045881e+05^1 (4.002245e+04)
WFG1^{-1}	2	1.38278e+06^3# (2.211027e+05)	4.846742e+05^1 (2.600416e+04)	1.351266e+06^2# (1.623194e+05)	1.287019e+07^7# (4.232904e+07)	2.191442e+06^6# (3.363223e+05)	2.138012e+06^5# (1.903704e+05)	1.427775e+06^4# (2.779466e+05)
	3	4.616702e+08^5 (1.810607e+09)	7.455249e+14^7# (4.082453e+15)	4.725754e+05^3# (7.569958e+04)	2.766218e+13^6# (9.661958e+13)	2.525371e+05^2# (2.967704e+04)	9.129164e+05^4# (3.668022e+06)	1.736262e+05^1 (2.404343e+04)
WFG2	2	1.040506e+06^3# (2.504316e+05)	1.063879e+06^4# (4.151245e+05)	6.697290e+05^2# (1.456043e+05)	1.628748e+07^7# (2.509368e+07)	1.869108e+06^6# (2.072748e+06)	1.646684e+06^5# (3.438246e+05)	5.861734e+05^1 (1.519271e+05)
	3	1.352298e+05^2# (2.820128e+04)	1.243903e+06^5# (5.832112e+06)	1.275754e+08^6# (6.716331e+08)	2.849513e+10^7# (1.419030e+11)	2.779040e+05^3# (3.549282e+04)	3.221776e+05^4# (6.960950e+04)	3.307969e+04^1 (3.428628e+03)
WFG2^{-1}	2	5.947399e+05^4# (1.059643e+05)	6.486899e+05^5# (4.489979e+05)	4.214349e+05^1 (2.022754e+04)	1.102361e+06^6# (1.522084e+06)	4.769824e+05^2# (1.848529e+04)	4.772484e+05^3# (1.674865e+04)	1.310144e+06^7# (3.781539e+05)
	3	8.466163e+04^3# (1.378030e+05)	4.660980e+10^6# (2.552896e+11)	8.898902e+04^2# (9.048750e+03)	6.310381e+10^7# (9.597681e+10)	8.439016e+04^2# (1.693624e+04)	8.874462e+04^4# (1.568238e+04)	1.304064e+04^1 (1.527657e+03)
WFG3	2	3.025488e+05^3# (5.873878e+03)	3.212196e+05^4# (1.298181e+04)	2.801453e+05^1 (3.429409e+03)	2.935193e+05^2 (5.063639e+04)	3.547582e+05^5# (1.103143e+04)	3.565104e+05^6# (1.172183e+04)	3.886084e+05^7# (1.719335e+04)
	3	3.834840e+05^4# (6.393540e+05)	1.501662e+07^6# (5.846473e+07)	7.602007e+05^3# (5.301992e+05)	1.071802e+12^7# (3.561835e+12)	2.397450e+05^2# (2.847311e+04)	2.560440e+05^3# (3.631517e+04)	1.210822e+05^1 (1.154927e+04)
WFG3^{-1}	2	3.023972e+05^2# (6.640812e+03)	3.077387e+05^3# (1.751452e+04)	2.739928e+05^1 (9.912665e+02)	4.410939e+05^7 (9.288411e+05)	3.585218e+05^4# (1.280312e+04)	3.601615e+05^5# (1.145179e+04)	3.881801e+05^6# (1.664244e+04)
	3	1.873884e+09^3# (1.015554e+10)	2.759154e+11^6# (1.180968e+12)	3.607457e+04^2# (1.712772e+03)	6.213042e+12^7# (2.288251e+13)	2.456917e+04^1 (1.378562e+03)	2.670881e+04^2# (1.831476e+03)	2.933186e+04^3# (2.321941e+03)
WFG4	2	3.679180e+05^2# (1.719485e+04)	3.930429e+05^4# (4.742057e+04)	3.464285e+05^1 (8.459268e+04)	7.075901e+05^7# (7.812602e+05)	5.796439e+05^6# (3.613046e+04)	5.691315e+05^5# (3.311765e+04)	3.763594e+05^3# (2.276421e+04)
	3	3.329852e+04^2# (4.799467e+04)	2.249836e+04^4# (1.170788e+04)	9.120609e+04^6# (2.679777e+05)	1.788700e+11^7# (9.782516e+11)	2.171863e+04^3# (1.580049e+03)	2.062236e+04^2# (1.644799e+03)	1.327554e+04^1 (9.888832e+02)
WFG4^{-1}	2	3.844834e+05^3# (1.402401e+04)	4.115903e+05^4# (3.739372e+04)	3.145898e+05^1 (5.569331e+03)	5.234817e+05^5# (1.987359e+04)	6.156348e+05^7# (2.977823e+04)	6.132561e+05^6# (3.969040e+04)	3.745743e+05^2# (2.204337e+04)
	3	4.253413e+04^3# (2.840019e+04)	2.327135e+07^6# (1.217847e+08)	1.429637e+04^1 (4.214432e+02)	1.991686e+08^7# (9.670294e+08)	3.231753e+04^3# (2.795861e+03)	3.350553e+04^4# (3.292842e+03)	1.431675e+04^2 (1.353587e+03)

Table B.13: Mean and, in parentheses, standard deviation of the Solow-Polasky Diversity comparison. EIB-MOEA stands for the adaptive version and avgEIB-MOEA stands for the average ranking of EIB-MOEA. For each case, the two best values are shown in grayscale, where the darker tone corresponds to the best algorithm. The symbol # is placed when the best algorithm presents a significant difference, according to a one-tailed Wilcoxon test using a significance level of $\alpha = 0.05$.

MOP	Dim.	EIB-MOEA	avgEIB-MOEA	SMS-EMOA	R2-EMOA	IGD$^+$-MaOEA	ϵ^+-MaOEA	Δ_p-MaOEA
DTLZ1	2	4.713609e+00^1 (4.585395e-01)	4.601279e+00^5 (2.499862e-01)	4.535871e+00^6 (1.613867e-03)	4.535618e+00^7 (1.515545e-03)	4.703012e+00^2# (4.597774e-01)	4.642949e+00^3# (3.446648e-01)	4.618029e+00^4# (2.692574e-01)
	3	9.952424e+00^1 (9.889673e-01)	9.473473e+00^3# (4.957191e-01)	9.222998e+00^5# (9.594806e-03)	9.285373e+00^4 (1.284961e-02)	8.562827e+00^6# (2.204085e-01)	8.524605e+00^7# (1.616191e-01)	9.734892e+00^2 (1.003099e+00)
DTLZ1^{-1}	2	1.200000e+02^1 (0.000000e+00)	1.200000e+02^2 (0.000000e+00)	1.200000e+02^3 (0.000000e+00)	1.200000e+02^4 (0.000000e+00)	1.200000e+02^5 (0.000000e+00)	1.200000e+02^6 (0.000000e+00)	1.200000e+02^7 (0.000000e+00)
	3	1.199970e+02^5# (9.667852e-03)	1.199615e+02^6# (1.655009e-01)	1.200000e+02^1 (0.000000e+00)	1.131654e+02^7# (1.688669e+00)	1.200000e+02^2 (0.000000e+00)	1.200000e+02^3 (0.000000e+00)	1.200000e+02^4 (0.000000e+00)
DTLZ2	2	8.819188e+00^2# (9.319932e-04)	8.815375e+00^3# (5.450457e-03)	8.809762e+00^4# (2.048033e-03)	8.823402e+00^1 (3.112817e-04)	8.723287e+00^7# (3.080773e-02)	8.730220e+00^6# (3.168715e-02)	8.807708e+00^5# (1.729533e-02)
	3	3.338078e+01^2# (1.400567e-01)	3.328872e+01^3# (2.526406e-01)	3.258324e+01^4# (7.744708e-02)	3.386086e+01^1 (3.096684e-02)	3.091961e+01^7# (3.887565e-01)	3.096005e+01^6# (3.938666e-01)	3.210546e+01^5# (4.104584e-01)
DTLZ2^{-1}	2	2.726726e+01^3# (1.267071e-01)	2.720710e+01^4# (3.260425e-01)	2.770074e+01^1 (4.170891e-02)	2.533645e+01^5# (4.450670e-02)	2.427690e+01^7# (7.274643e-01)	2.462641e+01^6# (6.628805e-01)	2.759534e+01^2# (1.306324e-01)
	3	1.048545e+02^4# (7.626773e-01)	1.051846e+02^3# (1.578320e+00)	1.055216e+02^2# (1.786256e-01)	8.604883e+01^7# (1.514422e+00)	8.976272e+01^6# (2.252589e+00)	9.022758e+01^5# (2.375920e+00)	1.061348e+02^1 (8.904085e-01)
DTLZ5	2	8.819612e+00^2# (8.971416e-04)	8.815375e+00^3# (5.450457e-03)	8.809725e+00^5# (1.784727e-03)	8.823471e+00^1 (2.828137e-04)	8.723148e+00^6# (3.494596e-02)	8.722128e+00^7# (3.365503e-02)	8.812582e+00^4# (2.234056e-02)
	3	8.817163e+00^2 (7.398640e-03)	8.807216e+00^4 (1.379014e-02)	8.808902e+00^3 (1.998116e-03)	8.736935e+00^5# (2.992169e-02)	8.722295e+00^7# (4.076731e-02)	8.730826e+00^6# (2.628274e-02)	8.827051e+00^1 (8.730976e-02)
DTLZ5^{-1}	2	2.726978e+01^3# (1.165578e-01)	2.720710e+01^4# (3.260425e-01)	2.770609e+01^1 (3.997850e-02)	2.533909e+01^5# (3.148710e-02)	2.449626e+01^6# (6.055237e-01)	2.425656e+01^7# (5.724731e-01)	2.759624e+01^2# (1.083483e-01)
	3	9.947389e+01^4 (6.780544e-01)	9.937371e+01^2 (1.631440e+00)	9.652769e+01^4# (5.310327e-01)	7.976507e+01^7# (1.369811e+00)	8.528248e+01^6# (1.870767e+00)	8.539865e+01^5# (2.438780e+00)	9.879231e+01^3# (1.003202e+00)
DTLZ7	2	1.081500e+01^2 (9.477486e-02)	1.079250e+01^3 (4.272512e-02)	1.054421e+01^7# (1.329476e+00)	1.071951e+01^4# (3.773850e-02)	1.068679e+01^6# (5.661259e-02)	1.069141e+01^5# (5.405478e-02)	1.085069e+01^1 (1.337278e-01)
	3	3.902003e+01^3# (7.644799e+00)	3.969502e+01^2# (5.619235e+00)	3.755375e+01^5# (5.868227e+00)	3.772552e+01^4# (7.075912e+00)	3.611422e+01^7# (7.158260e+00)	3.667995e+01^6# (6.176629e+00)	4.297791e+01^1 (5.789411e+00)
DTLZ7^{-1}	2	6.967050e+00^2# (6.118033e-02)	6.952405e+00^5# (1.347962e-02)	6.956524e+00^3# (3.987003e-03)	6.956419e+00^4# (1.203473e-02)	6.936441e+00^6# (3.022408e-02)	6.931027e+00^7# (3.699790e-02)	7.007207e+00^1 (8.442832e-02)
	3	2.275088e+01^1 (3.859025e-01)	2.245287e+01^3# (2.698668e-01)	2.218304e+01^4# (5.710079e-02)	2.148857e+01^5# (2.786495e+00)	2.023723e+01^7# (2.578102e+00)	2.050485e+01^6# (2.580423e+00)	2.251545e+01^2 (5.805271e+00)
WFG1	2	1.176062e+01^3# (1.485353e+00)	2.105735e+01^1 (1.137963e-01)	1.181182e+01^2# (1.666438e+00)	1.155912e+01^5# (1.207288e+00)	1.117888e+01^6# (9.469125e-01)	1.104606e+01^7# (7.757139e-01)	1.167004e+01^4# (1.381882e+00)
	3	5.853343e+01^3# (4.988708e+00)	6.360126e+01^2 (3.640561e+00)	6.435414e+01^1 (4.296059e+00)	4.025571e+01^7# (2.442696e+00)	4.735498e+01^5# (4.367364e+00)	4.718310e+01^6# (5.486065e+00)	5.655871e+01^4# (4.433774e+00)
WFG1^{-1}	2	1.241816e+01^3# (1.626974e+00)	2.127178e+01^1 (8.996025e-02)	1.178291e+01^5# (1.197487e+00)	1.191431e+01^4# (1.321500e+00)	1.106654e+01^7# (4.455510e-01)	1.127669e+01^6# (7.379574e-01)	1.305902e+01^2# (1.879841e+00)
	3	6.501382e+01^2# (4.527118e+00)	7.302449e+01^1 (2.552368e+00)	5.837913e+01^4# (2.845430e+00)	4.731708e+01^7# (2.007335e+00)	5.868980e+01^5# (3.644109e+00)	6.013493e+01^3# (3.887910e+00)	5.995622e+01^4# (3.744791e+00)
WFG2	2	2.002977e+01^6# (2.000138e+00)	2.119481e+01^2 (2.360414e+00)	2.043245e+01^4# (2.136490e+00)	2.032207e+01^5# (2.166516e+00)	2.046895e+01^3# (2.316731e+00)	1.998198e+01^7# (2.155512e+00)	2.139157e+01^1 (2.300143e+00)
	3	8.363601e+01^2# (1.617491e+00)	8.253917e+01^3# (7.171347e+00)	7.265990e+01^5# (2.310079e+00)	7.491735e+01^4# (2.133336e+00)	7.198862e+01^6# (2.128508e+00)	7.105939e+01^7# (3.509737e+00)	9.813232e+01^1 (1.192229e+00)
WFG2^{-1}	2	2.083093e+01^4# (8.198628e-03)	2.083875e+01^3# (1.393367e-02)	2.087686e+01^1 (3.238531e-03)	2.085755e+01^2# (7.098699e-03)	2.073063e+01^6# (4.825024e-02)	2.075175e+01^5# (4.237807e-02)	2.072645e+01^7# (2.298756e-02)
	3	1.035445e+02^2# (1.063910e+00)	1.034527e+02^3# (2.617298e+00)	9.522378e+01^4# (7.827878e-01)	9.211396e+01^7# (1.933357e+00)	9.469565e+01^6# (1.785066e+00)	9.485389e+01^5# (1.853436e+00)	1.104128e+02^1 (9.478426e-01)
WFG3	2	2.304546e+01^3# (1.386879e-02)	2.304211e+01^4# (2.897781e-02)	2.307287e+01^1 (1.191627e-02)	2.307150e+01^2 (1.535596e-02)	2.267771e+01^7# (1.205283e-01)	2.268870e+01^6# (1.380300e-01)	2.268955e+01^5# (1.180649e-01)
	3	6.826583e+01^2# (1.011265e+00)	6.708241e+01^3# (2.781827e+00)	5.883013e+01^4# (8.993834e-01)	5.337879e+01^7# (1.849752e+00)	5.776904e+01^5# (2.313672e+00)	5.723505e+01^6# (2.211991e+00)	7.035271e+01^1 (2.023566e+00)
WFG3^{-1}	2	2.305213e+01^4# (1.062126e-02)	2.306079e+01^3# (2.124563e-02)	2.308867e+01^1 (8.523389e-03)	2.308702e+01^2 (6.337664e-03)	2.270365e+01^6# (1.086348e-01)	2.268549e+01^7# (1.241366e-01)	2.270963e+01^5# (1.298070e-01)
	3	1.023672e+02^2# (6.850019e-01)	1.027185e+02^1 (1.416504e+00)	9.693100e+01^4# (4.662040e-01)	8.672481e+01^7# (2.791004e+00)	1.013929e+02^3# (7.428073e-01)	1.003597e+02^4# (8.173048e-01)	9.870947e+01^5# (1.026830e+00)
WFG4	2	2.457680e+01^2# (6.208150e-02)	2.439537e+01^5# (2.499154e-01)	2.444812e+01^4# (8.332862e-02)	2.472863e+01^1 (3.400085e-02)	2.318018e+01^7# (2.596626e-01)	2.329061e+01^6# (2.487768e-01)	2.453404e+01^3# (1.022200e-01)
	3	1.087255e+02^2# (6.536196e-01)	1.070237e+02^3# (2.079503e+00)	1.056748e+02^4# (6.272310e-01)	1.032979e+02^7# (1.442731e+00)	1.042833e+02^6# (9.064148e-01)	1.049839e+02^5# (9.499532e-01)	1.099415e+02^1 (6.860651e-01)
WFG4^{-1}	2	2.418805e+01^3# (1.091841e-01)	2.409882e+01^4# (2.230264e-01)	2.452616e+01^1 (5.507526e-02)	2.266931e+01^5# (4.010669e-02)	2.159785e+01^7# (4.924356e-01)	2.174750e+01^6# (4.733697e-01)	2.440109e+01^2# (1.077760e-01)
	3	1.075577e+02^4# (8.162367e-01)	1.077923e+02^3# (1.572622e+00)	1.088426e+02^2 (2.050561e-01)	9.567203e+01^7# (2.014010e+00)	9.794993e+01^5# (1.503817e+00)	9.759686e+01^6# (1.505583e+00)	1.090783e+02^1 (1.004455e+00)

B.3 cMIB-MOEA

Tables B.14 to B.19 show the numerical results of the comparison between cMIB-MOEA, SMS-EMOA, R2-EMOA, IGD$^+$-MaOEA, ϵ^+-MaOEA and Δ_p-MaOEA, considering the indicators HV, R2, IGD$^+$, ϵ^+, Δ_p, and Solow-Polasky Diversity. These resuls are related to the experiments of Chapter 6, section 6.4.2.

Table B.14: Comparison for the hypervolume indicator. The mean and, in parentheses, standard deviation are shown. The two best values are shown in grayscale, where the darker tone corresponds to the best algorithm.

MOP	Dim.	cMIB-MOEA	R2-EMOA	IGD$^+$-MaOEA	ϵ^+-MaOEA	Δ_p-MaOEA
DTLZ2	2	3.210162e+00^1 (1.248254e-04)	3.209810e+00^4# (1.903178e-04)	3.209913e+00^3# (1.647468e-04)	3.209920e+00^2# (1.710046e-04)	3.204510e+00^5# (3.645834e-03)
	3	7.413662e+00^3# (1.311477e-03)	7.418121e+00^1 (9.761419e-05)	7.416422e+00^2# (1.460154e-03)	7.403988e+00^4# (2.140679e-02)	7.316849e+00^5# (2.964130e-02)
DTLZ2^{-1}	2	1.027911e+01^1 (1.108306e-03)	9.624031e+00^5# (2.374198e-01)	1.026687e+01^3# (5.561743e-03)	1.026512e+01^4# (4.994028e-03)	1.027071e+01^2# (2.377370e-03)
	3	2.240389e+01^3# (5.101193e-02)	2.212002e+01^4# (1.120196e-01)	2.259175e+01^1 (7.407921e-02)	2.254567e+01^2# (9.665618e-02)	2.195907e+01^5# (1.171935e-01)
DTLZ5	2	3.210174e+00^1 (1.183556e-04)	3.209855e+00^3# (1.765018e-04)	3.209844e+00^4# (1.708234e-04)	3.209882e+00^2# (2.527762e-04)	3.204797e+00^5# (3.753239e-03)
	3	6.102408e+00^1 (2.812106e-04)	5.974645e+00^5# (1.591283e-01)	6.101791e+00^2# (4.929715e-04)	6.101051e+00^3# (1.834057e-03)	6.087254e+00^4# (8.589120e-03)
DTLZ5^{-1}	2	1.027878e+01^1 (1.052948e-03)	9.643901e+00^5# (2.270272e-01)	1.026547e+01^3# (8.134163e-03)	1.026399e+01^4# (6.846455e-03)	1.027106e+01^2# (2.191922e-03)
	3	2.271210e+01^1 (3.786160e-02)	2.234829e+01^4# (7.368752e-02)	2.240598e+01^2# (1.213057e-01)	2.237449e+01^3# (1.476173e-01)	2.207740e+01^5# (1.056913e-01)
DTLZ7	2	1.771312e+01^2 (6.338443e-02)	1.745588e+01^5# (5.391138e-01)	1.771076e+01^3 (6.300358e-02)	1.772201e+01^1 (1.426308e-03)	1.767071e+01^4# (4.697252e-02)
	3	1.631666e+01^1 (9.866106e-02)	1.629956e+01^2# (6.686372e-02)	1.628276e+01^3# (1.038417e-01)	1.621315e+01^4# (1.521630e-01)	1.609346e+01^5# (1.109553e-01)
DTLZ7^{-1}	2	1.283525e+01^1 (1.155894e-04)	1.282221e+01^5# (8.579096e-03)	1.283372e+01^4# (1.283835e-03)	1.283421e+01^3# (7.914225e-04)	1.283492e+01^2# (2.718326e-04)
	3	2.694964e+01^1 (1.988859e-01)	2.694262e+01^2# (1.399401e-01)	2.691430e+01^4# (1.902287e-01)	2.688537e+01^5# (2.266296e-01)	2.691964e+01^3# (1.353562e-01)
WFG1	2	5.812159e+00^1 (4.739215e-01)	4.711919e+00^5# (5.702726e-01)	5.557041e+00^2# (4.962352e-01)	5.443320e+00^4# (2.707216e-01)	5.467187e+00^3# (2.647421e-01)
	3	5.250059e+01^2 (1.707368e+00)	5.280430e+01^1 (1.655778e+00)	5.238674e+01^3 (2.405678e+00)	5.083102e+01^4# (1.763778e+00)	4.853077e+01^5# (1.458671e+00)
WFG1^{-1}	2	7.814117e+00^2# (8.505052e-01)	5.500073e+00^5# (6.549325e-02)	7.520350e+00^3# (6.758761e-01)	7.407911e+00^4# (8.290113e-01)	8.031382e+00^1 (9.148863e-01)
	3	2.219323e+01^1 (4.627010e+00)	2.059188e+01^5# (3.870421e+00)	2.063307e+01^4# (4.195219e+00)	2.082770e+01^3# (3.967112e+00)	2.154482e+01^2 (3.957917e+00)
WFG2	2	1.087219e+01^2# (4.039260e-01)	1.085551e+01^3# (4.067833e-01)	1.074575e+01^5# (3.352683e-01)	1.096449e+01^1 (4.179559e-01)	1.079275e+01^4# (3.636295e-01)
	3	9.959588e+01^4 (2.875856e+00)	9.990669e+01^1 (1.696087e-01)	9.985689e+01^2 (3.095886e-01)	9.965905e+01^3# (3.253740e-01)	9.871062e+01^5# (2.543823e-01)
WFG2^{-1}	2	1.519246e+01^1 (5.625133e-04)	1.482324e+01^5# (2.644660e-01)	1.515345e+01^4# (2.984115e-02)	1.515557e+01^3# (2.779040e-02)	1.518443e+01^2# (3.345468e-03)
	3	6.101274e+01^2# (8.636979e-02)	6.110828e+01^1 (1.058639e-01)	6.090491e+01^3# (8.692672e-02)	6.085338e+01^4# (1.164159e-01)	5.905973e+01^5# (4.861748e-01)
WFG3	2	1.089079e+01^1 (1.565385e-02)	1.035179e+01^5# (2.032990e-01)	1.087827e+01^3# (1.922049e-02)	1.088722e+01^2 (1.909343e-02)	1.082986e+01^4# (2.193501e-02)
	3	7.492265e+01^1 (3.545610e-01)	7.259043e+01^4# (6.175274e-01)	7.470162e+01^3# (3.631453e-01)	7.481560e+01^2 (3.604198e-01)	7.184839e+01^5# (3.944028e-01)
WFG3^{-1}	2	1.175971e+01^1 (1.560548e-03)	1.120359e+01^5# (2.557854e-01)	1.171173e+01^2# (1.994707e-02)	1.171020e+01^3# (2.550289e-02)	1.167962e+01^4# (2.373243e-02)
	3	4.423134e+01^1 (6.460128e-02)	4.299599e+01^3# (3.557238e-01)	4.323975e+01^2# (1.995049e-01)	4.261920e+01^4# (5.713276e-01)	4.060917e+01^5# (4.294173e-01)
LAME $\gamma = 0.25$	2	3.984508e+00^1 (3.997127e-05)	3.908335e+00^5# (6.218400e-02)	3.982450e+00^4# (1.382638e-03)	3.982839e+00^3# (1.449027e-03)	3.984255e+00^2# (1.979594e-04)
	3	7.999810e+00^2# (1.340338e-05)	7.965122e+00^5# (5.674797e-02)	7.995436e+00^3# (2.010558e-03)	7.994236e+00^4# (2.083512e-03)	7.999817e+00^1 (2.572063e-05)
LAME $\gamma = 1.00$	2	3.494593e+00^1 (6.113332e-05)	3.390690e+00^5# (4.476048e-02)	3.488891e+00^3# (4.488139e-03)	3.489996e+00^2# (3.810590e-03)	3.487793e+00^4# (3.964170e-03)
	3	7.789854e+00^1 (4.756851e-04)	7.726223e+00^4# (1.774686e-02)	7.728385e+00^3# (1.898407e-02)	7.713808e+00^5# (2.762970e-02)	7.762531e+00^2# (8.361664e-03)
LAME $\gamma = 5.00$	2	3.047679e+00^3# (6.607179e-05)	3.046898e+00^4# (2.269920e-04)	3.047935e+00^2 (2.821617e-04)	3.048022e+00^1 (1.575429e-04)	3.039756e+00^5# (5.353281e-03)
	3	7.101947e+00^2# (8.831560e-04)	7.099265e+00^3# (4.564200e-04)	7.106173e+00^1 (1.320166e-03)	7.076194e+00^4# (5.207431e-02)	6.879490e+00^5# (6.192943e-02)
MIRROR $\gamma = 0.25$	2	3.013194e+00^3# (3.364058e-05)	3.012709e+00^4# (4.794633e-07)	3.013533e+00^1 (4.920536e-05)	3.013515e+00^2 (6.628347e-05)	3.001153e+00^5# (7.436136e-03)
	3	4.034491e+00^2# (4.557634e-04)	4.021444e+00^3# (1.476544e-03)	4.036641e+00^1 (2.306522e-04)	3.784857e+00^5# (2.848332e-01)	3.972221e+00^4# (2.108432e-02)
MIRROR $\gamma = 1.00$	2	3.494600e+00^1 (7.585756e-05)	3.408095e+00^5# (4.928017e-02)	3.489873e+00^2# (2.985388e-03)	3.489212e+00^3# (3.562884e-03)	3.484992e+00^4# (5.975681e-03)
	3	5.516597e+00^1 (3.315352e-03)	5.320022e+00^4# (6.273693e-02)	5.430958e+00^2# (3.835292e-02)	5.389980e+00^3# (5.648711e-02)	5.308208e+00^5# (6.376244e-02)
MIRROR $\gamma = 5.00$	2	3.947949e+00^1 (6.013384e-05)	3.796089e+00^5# (5.150682e-02)	3.943382e+00^4# (2.285619e-03)	3.943743e+00^3# (2.981838e-03)	3.947354e+00^2# (2.213637e-04)
	3	7.639415e+00^1 (3.006057e-03)	7.409192e+00^5# (6.688387e-02)	7.481904e+00^3# (4.341704e-02)	7.462161e+00^4# (4.914247e-02)	7.633576e+00^2# (4.198402e-03)
VIE1	3	6.163607e+01^1 (3.607552e-02)	6.091741e+01^3# (2.987945e-01)	6.085508e+01^4# (2.227616e-01)	6.084909e+01^5# (2.605542e-01)	6.150890e+01^2# (7.652368e-02)
VIE2	3	7.846513e+00^1 (7.366847e-04)	7.826301e+00^3# (8.862417e-03)	7.818984e+00^4# (8.942508e-03)	7.816657e+00^5# (1.280338e-02)	7.845769e+00^2# (8.329589e-04)
VIE3	3	2.203028e+02^2# (1.840069e-02)	2.202588e+02^5# (1.988121e-01)	2.202753e+02^4# (1.253037e-01)	2.202902e+02^3 (1.315206e-01)	2.203631e+02^1 (2.059259e-02)

Table B.15: Comparison for the R2 indicator. The mean and, in parentheses, standard deviation are shown. The two best values are shown in grayscale, where the darker tone corresponds to the best algorithm.

MOP	Dim.	cMIB-MOEA	SMS-EMOA	IGD$^+$-MaOEA	ϵ^+-MaOEA	Δ_p-MaOEA
DTLZ2	2	1.001546e+00^1 (2.304413e-04)	1.005628e+00^3# (4.916034e-04)	1.029595e+00^5# (1.041539e-02)	1.028919e+00^4# (1.053044e-02)	1.003043e+00^2# (3.326265e-04)
	3	1.391225e+00^1 (2.656076e-02)	2.025550e+00^3# (2.657776e-02)	3.228428e+00^5# (8.632387e-01)	3.068441e+00^4# (1.370718e+00)	1.591372e+00^2# (9.292731e-02)
DTLZ2^{-1}	2	3.504395e+00^1 (8.425865e-04)	3.510835e+00^3# (1.157573e-03)	4.015808e+00^4# (4.543294e-01)	4.048426e+00^5# (4.231691e-01)	3.507752e+00^2# (1.284154e-03)
	3	4.872409e+00^1 (1.180371e-01)	4.988873e+00^2# (1.095118e-01)	3.316718e+02^4# (1.060464e+02)	3.788705e+02^5# (1.665700e+02)	7.460871e+00^3# (3.001262e+00)
DTLZ5	2	1.001481e+00^1 (2.423728e-04)	1.005444e+00^3# (3.977062e-04)	1.026395e+00^4# (9.720539e-03)	1.031955e+00^5# (1.885062e-02)	1.002940e+00^2# (3.107858e-04)
	3	6.106577e+02^2 (3.168541e-01)	6.109698e+02^3# (1.393868e-02)	6.110280e+02^4# (4.691465e-02)	6.110508e+02^5# (9.308111e-02)	6.104707e+02^1 (4.566731e-01)
DTLZ5^{-1}	2	3.504485e+00^1 (8.427788e-04)	3.510856e+00^3# (8.776468e-04)	4.148450e+00^4# (9.498169e-01)	4.259512e+00^5# (8.578703e-01)	3.507722e+00^2# (1.874279e-03)
	3	6.397156e+01^2# (8.428756e+00)	4.780656e+01^1 (5.065303e-01)	6.464004e+02^5# (1.442356e+02)	6.394942e+02^4# (1.677595e+02)	1.731310e+02^3# (3.452120e+01)
DTLZ7	2	1.482290e+03^4# (2.230660e+02)	1.441488e+03^1 (3.426040e-02)	1.486310e+03^5# (2.224285e+02)	1.445942e+03^3# (3.871828e+00)	1.442185e+03^2 (2.655494e+00)
	3	2.428019e+03^1 (3.972889e+02)	2.583177e+03^3 (5.202847e+02)	2.498875e+03^2# (3.885086e+02)	2.694747e+03^4# (6.161223e+02)	2.714430e+03^5# (5.339504e+02)
DTLZ7^{-1}	2	1.591957e+04^1 (3.140243e+00)	1.592801e+04^5# (4.033573e-01)	1.592681e+04^4# (2.061276e+00)	1.592637e+04^3# (2.509397e+00)	1.592328e+04^2# (3.360946e+00)
	3	2.798789e+04^2 (1.594702e+02)	2.816287e+04^4# (3.123712e-01)	2.816355e+04^5# (7.585267e-01)	2.816239e+04^3# (4.632046e+00)	2.795222e+04^1 (1.548073e+02)
WFG1	2	5.042864e+02^1 (2.528676e+02)	6.093440e+02^3# (1.870415e+02)	6.049682e+02^2# (2.506040e+02)	6.759798e+02^5# (1.245069e+02)	6.647686e+02^4# (1.163336e+02)
	3	8.133871e+02^2# (2.280649e+02)	6.457585e+02^1 (2.278167e+02)	9.119151e+02^3# (2.445134e+02)	1.067014e+03^5# (1.767876e+02)	9.634946e+02^4# (2.222668e+02)
WFG1^{-1}	2	8.479638e+02^2# (2.874410e+02)	9.571928e+02^3# (1.320490e+02)	9.660838e+02^4# (2.301638e+02)	1.002653e+03^5# (2.759513e+02)	7.554245e+02^1 (3.001065e+02)
	3	1.158244e+03^1 (2.829761e+02)	1.228322e+03^3 (2.740211e+02)	1.245600e+03^5# (2.632532e+02)	1.234295e+03^4# (2.532927e+02)	1.197122e+03^2 (2.518037e+02)
WFG2	2	2.204741e+02^2 (1.688453e+02)	2.536255e+02^3 (1.541269e+02)	2.784248e+02^5# (1.404124e+02)	1.864075e+02^1 (1.751323e+02)	2.547736e+02^4 (1.548446e+02)
	3	3.151643e+01^3 (1.374534e+02)	1.170585e+02^5# (1.129157e+01)	3.052979e+01^2# (2.052108e+01)	3.575891e+01^4# (3.207520e+01)	7.692810e+00^1 (4.262271e+00)
WFG2^{-1}	2	8.681702e+02^1 (3.367222e-01)	8.683816e+02^2# (1.292749e-01)	8.749494e+02^5# (3.650107e+00)	8.744175e+02^3# (3.981023e+00)	8.746519e+02^4# (5.043880e+00)
	3	6.631010e+02^1 (6.634425e+00)	6.736255e+02^2# (6.346644e+00)	8.159387e+02^4# (9.278293e+01)	8.684920e+02^5# (1.125040e+02)	7.465999e+02^3# (6.057073e+01)
WFG3	2	2.279509e+00^4# (3.270713e-03)	2.272696e+00^1 (2.664833e-03)	2.273978e+00^3 (2.491350e-03)	2.273341e+00^2 (2.461194e-03)	2.284516e+00^5# (2.729008e-03)
	3	6.610482e+02^1 (1.380583e+01)	7.354023e+02^2# (1.195693e+01)	8.971346e+02^4# (3.378241e+01)	9.104565e+02^5# (3.642940e+01)	7.474012e+02^3# (3.203574e+01)
WFG3^{-1}	2	2.103783e+02^1 (5.755679e-01)	2.103923e+02^2 (6.764117e-01)	2.459381e+02^5# (1.831784e+01)	2.400530e+02^4# (1.330130e+01)	2.384657e+02^3# (1.652563e+01)
	3	6.302704e+02^2# (4.941018e+00)	6.162871e+02^1 (3.865810e-01)	7.475377e+02^3# (5.191735e+01)	7.868629e+02^4# (8.364509e+01)	8.093867e+02^5# (5.045177e+01)
LAME $\gamma = 0.25$	2	1.550956e-01^4# (8.385621e-03)	1.290804e-01^3# (6.942509e-05)	1.286300e-01^2 (5.464076e-05)	1.286264e-01^1 (4.557299e-05)	2.158020e-01^5# (1.414993e-01)
	3	7.671362e+00^5# (1.489027e+00)	2.010007e-01^3# (4.197295e-02)	1.174442e-01^2 (1.175080e-01)	1.146392e-01^1 (6.758444e-02)	6.887707e+00^4# (1.932463e+00)
LAME $\gamma = 1.00$	2	8.140321e-01^2# (2.323290e-04)	8.136003e-01^1 (4.621050e-04)	8.141605e-01^3# (3.056052e-04)	8.142449e-01^4# (2.329007e-04)	8.152456e-01^5# (3.167572e-04)
	3	9.986528e-01^2# (2.658889e-02)	9.516079e-01^1 (2.212431e-02)	1.081104e+00^3# (3.255925e-02)	1.128753e+00^5# (6.577299e-02)	1.107728e+00^4# (3.340503e-02)
LAME $\gamma = 5.00$	2	1.082458e+00^1 (2.010197e-04)	1.611153e+00^3# (3.021595e-02)	6.354600e+00^5# (2.145539e+00)	5.286154e+00^4# (1.622389e+00)	1.083588e+00^2# (4.355950e-04)
	3	1.609724e+00^1 (3.961159e-02)	9.490035e+01^3# (1.915538e+00)	1.680906e+02^5# (1.331664e+01)	1.284311e+02^4# (2.613829e+01)	2.329380e+00^2# (9.749783e-01)
MIRROR $\gamma = 0.25$	2	1.096992e+00^1 (2.291941e-04)	2.326754e+00^3# (9.981433e-02)	3.136659e+01^4# (1.050990e+01)	3.697762e+01^5# (1.489024e+01)	1.098291e+00^2# (4.768486e-04)
	3	8.608823e+02^1 (5.117169e-02)	8.777366e+02^3# (1.058246e+00)	9.153427e+02^4# (3.586311e+00)	9.427186e+02^5# (3.722795e+01)	8.612694e+02^2# (2.425336e-01)
MIRROR $\gamma = 1.00$	2	8.140823e-01^2# (2.724976e-04)	8.137569e-01^1 (4.252025e-04)	8.141436e-01^3# (2.779640e-04)	8.142173e-01^4# (3.169498e-04)	8.150980e-01^5# (2.776934e-04)
	3	5.054924e+02^2# (5.504203e-01)	5.043481e+02^1 (3.086890e-01)	5.087731e+02^4# (2.037821e+00)	5.086982e+02^3# (1.795426e+00)	5.144419e+02^5# (3.013966e+00)
MIRROR $\gamma = 5.00$	2	2.586587e-01^4# (9.234652e-04)	2.517455e-01^3# (7.676020e-05)	2.514530e-01^1 (9.713532e-05)	2.514660e-01^2 (7.746302e-05)	2.672368e-01^5# (7.268805e-03)
	3	5.920852e+00^1 (2.015933e+00)	1.565382e+01^3# (2.624099e-01)	4.066618e+01^4# (9.418834e+00)	4.738339e+01^5# (1.066086e+01)	8.950248e+00^2# (2.769594e+00)
VIE1	3	2.016166e+03^1 (1.358581e+01)	2.147694e+03^3# (4.207376e+00)	2.182004e+03^5# (3.937348e+01)	2.172302e+03^4# (4.109518e+01)	2.021090e+03^2# (1.602570e+01)
VIE2	3	2.009196e+04^1 (1.968038e+00)	2.009629e+04^2# (1.533164e+00)	2.021709e+04^5# (1.149729e+02)	2.021341e+04^4# (1.097454e+02)	2.009695e+04^3 (1.248402e+01)
VIE3	3	1.253957e+04^1 (4.846552e-01)	1.254629e+04^2# (2.273640e+00)	1.255187e+04^4# (8.829199e+00)	1.255283e+04^5# (6.883429e+00)	1.254660e+04^3# (5.922341e+00)

Table B.16: Comparison for the IGD$^+$ indicator. The mean and, in parentheses, standard deviation are shown. The two best values are shown in grayscale, where the darker tone corresponds to the best algorithm.

MOP	Dim.	cMIB-MOEA	SMS-EMOA	R2-EMOA	ϵ^+-MaOEA	Δ_p-MaOEA
DTLZ2	2	2.051386e-03^3# (7.491677e-05)	1.706732e-03^1 (3.985202e-05)	1.991910e-03^2# (2.714430e-06)	2.295901e-03^4# (1.050411e-04)	2.653151e-03^5# (1.695937e-04)
	3	2.456817e-02^4# (5.116531e-04)	1.851793e-02^1 (3.354308e-04)	2.231064e-02^2# (1.263208e-05)	2.429459e-02^3# (1.805971e-03)	3.605669e-02^5# (1.636504e-03)
DTLZ2^{-1}	2	6.849762e-03^2# (2.023959e-04)	6.145464e-03^1 (1.425957e-04)	1.280271e-01^5# (4.537515e-02)	9.571463e-03^4# (9.490564e-04)	7.944673e-03^3# (3.298439e-04)
	3	9.448973e-02^2# (1.931716e-03)	9.096365e-02^1 (1.398727e-03)	1.154588e-01^4# (5.514137e-03)	1.110854e-01^3# (7.329049e-03)	1.158073e-01^5# (5.169046e-03)
DTLZ5	2	2.048534e-03^2# (7.248063e-05)	1.702035e-03^1 (4.034625e-05)	2.050577e-03^3# (3.138008e-06)	2.310930e-03^4# (1.556263e-04)	2.629792e-03^5# (1.064086e-04)
	3	2.159729e-03^2# (7.296220e-05)	1.680575e-03^1 (2.460811e-05)	5.854643e-03^5# (2.410966e-03)	2.261415e-03^3# (9.998578e-05)	2.990658e-03^4# (1.636584e-04)
DTLZ5^{-1}	2	6.918839e-03^2# (1.881795e-04)	6.185955e-03^1 (1.328632e-04)	1.230523e-01^5# (4.290608e-02)	9.775585e-03^4# (1.257897e-03)	7.897810e-03^3# (3.117913e-04)
	3	8.777856e-02^1 (1.911095e-03)	9.359136e-02^2# (1.315148e-03)	1.114440e-01^5# (5.663225e-03)	1.021126e-01^3# (8.221122e-03)	1.090216e-01^4# (4.284055e-03)
DTLZ7	2	1.692386e-02^5# (8.252758e-02)	1.625678e-03^1 (3.672615e-05)	3.276266e-03^4# (3.079752e-03)	2.055926e-03^2# (7.243258e-05)	2.124808e-03^3# (9.822025e-05)
	3	5.483626e-02^2 (7.334253e-02)	7.786350e-02^3 (9.659290e-02)	4.546513e-02^1 (5.347469e-02)	1.035503e-01^4 (1.597579e-01)	1.074210e-01^5# (1.026512e-01)
DTLZ7^{-1}	2	8.753614e-04^2# (2.974193e-05)	7.844796e-04^1 (1.794603e-05)	1.740213e-03^5# (7.294599e-04)	9.843620e-04^3# (5.841218e-05)	9.954293e-04^4# (3.243756e-05)
	3	3.013593e-02^4# (6.982425e-02)	1.846395e-02^1 (5.118612e-02)	2.453773e-02^2# (5.088111e-02)	3.900970e-02^5# (8.462627e-02)	2.599144e-02^3# (4.973959e-02)
WFG1	2	7.114930e-01^1 (8.520883e-02)	7.533249e-01^2# (6.560050e-02)	9.151646e-01^5# (1.110010e-01)	7.790312e-01^4# (5.237431e-02)	7.746876e-01^3# (5.074123e-02)
	3	8.901724e-01^4# (1.366993e-02)	8.209653e-01^1 (8.562743e-03)	8.682323e-01^2# (9.800809e-03)	8.832798e-01^3# (2.241144e-02)	1.022873e+00^5# (1.707475e-02)
WFG1^{-1}	2	5.532384e-01^2# (2.172666e-01)	6.385295e-01^3# (9.907927e-02)	1.225718e+00^5# (1.975224e-02)	6.641492e-01^4# (2.256703e-01)	4.930541e-01^1 (2.358287e-01)
	3	5.122361e-01^1 (2.341601e-01)	5.647885e-01^3 (2.266161e-01)	6.172342e-01^5# (1.991319e-01)	6.078540e-01^4# (2.046416e-01)	5.393766e-01^2 (2.159927e-01)
WFG2	2	6.241035e-02^3# (3.985208e-02)	6.708260e-02^4 (3.746519e-02)	5.993757e-02^2# (4.153727e-02)	5.154300e-02^1 (4.166106e-02)	6.882444e-02^5# (3.631156e-02)
	3	6.258036e-02^4# (4.645224e-02)	2.719234e-02^1 (1.230328e-03)	4.463738e-02^3# (2.200487e-03)	4.304314e-02^2# (4.437784e-03)	7.881098e-02^5# (4.307795e-03)
WFG2^{-1}	2	1.886315e-03^3# (1.151614e-04)	1.432822e-03^1 (4.195084e-05)	7.024113e-03^5# (4.319999e-03)	1.782508e-03^2# (1.093796e-04)	2.219455e-03^4# (1.229911e-04)
	3	4.071443e-02^4# (1.524712e-03)	3.272955e-02^1 (5.473617e-04)	3.752834e-02^2# (1.616625e-03)	3.783211e-02^3# (1.345983e-03)	6.454902e-02^5# (5.160016e-03)
WFG3	2	1.586994e-02^3# (2.237449e-03)	1.141842e-02^2 (1.741934e-03)	4.227060e-02^5# (1.763356e-02)	1.106101e-02^1 (1.151363e-03)	1.819666e-02^4# (1.433415e-03)
	3	6.676228e-02^3# (1.240088e-02)	2.512232e-02^1 (3.849004e-03)	1.268348e-01^4# (1.309652e-02)	3.692504e-02^2# (6.161292e-03)	1.440703e-01^5# (9.309483e-03)
WFG3^{-1}	2	7.993430e-03^3# (2.640529e-04)	6.776838e-03^1 (1.580197e-04)	3.494393e-02^5# (1.840235e-02)	7.661005e-03^2# (3.663796e-04)	1.233720e-02^4# (5.300793e-04)
	3	9.107521e-02^1 (2.270714e-03)	1.007397e-01^3# (1.226368e-03)	1.103550e-01^4# (3.549773e-03)	9.913828e-02^2# (6.202274e-03)	1.401773e-01^5# (5.209819e-03)
LAME $\gamma = 0.25$	2	5.777505e-04^2# (2.481356e-05)	2.302767e-04^1 (1.366405e-05)	1.841172e-02^5# (1.674524e-02)	7.369942e-04^4# (2.124344e-04)	7.040965e-04^3# (1.003481e-04)
	3	1.629087e-03^3# (1.491841e-04)	3.470280e-04^1 (1.718670e-05)	8.139749e-03^5# (8.449632e-03)	1.764726e-03^4# (3.364876e-04)	1.590202e-03^2# (2.544627e-04)
LAME $\gamma = 1.00$	2	2.686095e-03^2# (5.238967e-05)	2.527645e-03^1 (6.058775e-05)	7.531848e-03^5# (3.945578e-03)	2.755762e-03^3# (6.228472e-05)	3.284842e-03^4# (1.064366e-04)
	3	2.716139e-02^3# (4.546322e-04)	2.534859e-02^2# (3.432437e-04)	2.453785e-02^1 (9.417360e-05)	2.883784e-02^4# (7.863894e-04)	3.217983e-02^5# (8.093864e-04)
LAME $\gamma = 5.00$	2	9.872994e-04^3# (4.465187e-05)	5.560965e-04^1 (3.507817e-05)	1.263316e-03^5# (1.937161e-06)	8.894090e-04^2# (5.017955e-05)	1.197684e-03^4# (8.074029e-05)
	3	9.342489e-03^2# (4.416391e-04)	4.620331e-03^1 (1.257326e-04)	9.631733e-03^3# (2.005564e-05)	9.803483e-03^4# (4.842127e-03)	1.911352e-02^5# (2.394936e-03)
MIRROR $\gamma = 0.25$	2	5.164636e-04^3# (2.619580e-05)	2.077012e-04^1 (1.367060e-05)	7.046492e-04^5# (6.690189e-07)	4.180405e-04^2# (4.276393e-05)	6.808126e-04^4# (6.780266e-05)
	3	1.399075e-03^2# (9.135092e-05)	6.711717e-04^1 (2.075480e-05)	3.892399e-03^4# (3.853846e-04)	1.276009e-02^5# (1.657940e-02)	2.906886e-03^3# (3.251959e-04)
MIRROR $\gamma = 1.00$	2	2.702343e-03^2# (6.839164e-05)	2.531253e-03^1 (4.290351e-05)	6.295568e-03^5# (3.195920e-03)	2.780851e-03^3# (7.508472e-05)	3.271675e-03^4# (1.100443e-04)
	3	2.696813e-02^1 (3.831330e-04)	3.089346e-02^3# (3.813775e-04)	3.523520e-02^5# (7.444003e-04)	2.872245e-02^2# (6.585204e-04)	3.254566e-02^4# (9.974744e-04)
MIRROR $\gamma = 5.00$	2	1.011317e-03^2# (4.260323e-05)	5.923403e-04^1 (3.050011e-05)	3.386729e-02^5# (1.272614e-02)	1.479642e-03^4# (4.190104e-04)	1.275268e-03^3# (9.734203e-05)
	3	1.322663e-02^2# (5.497819e-04)	7.379359e-03^1 (2.015195e-04)	2.339586e-02^5# (4.001289e-03)	2.019371e-02^4# (3.084181e-03)	1.362780e-02^3# (7.118328e-04)

Table B.16 – *Continuation*

MOP	Dim.	cMIB-MOEA	SMS-EMOA	R2-EMOA	ϵ^+-MaOEA	Δ_p-MaOEA
VIE1	3	6.105804e-02^{4}# (1.756089e-03)	6.047981e-02^{3}# (8.010301e-04)	5.533114e-02^{2}# (2.861054e-03)	4.092670e-02^{1} (1.599335e-03)	6.626525e-02^{5}# (5.002789e-03)
VIE2	3	3.087631e-03^{3}# (1.448524e-04)	2.958897e-03^{2} (1.545746e-04)	4.229906e-03^{4}# (7.117692e-04)	4.302341e-03^{5}# (1.041948e-03)	2.888633e-03^{1} (1.675692e-04)
VIE3	3	3.437042e+01^{2}# (6.220176e-04)	3.437085e+01^{3}# (9.080185e-04)	3.437162e+01^{5}# (1.158430e-03)	3.436985e+01^{1} (3.008075e-04)	3.437121e+01^{4}# (7.512607e-04)

Table B.17: Comparison for the ϵ^+ indicator. The mean and, in parentheses, standard deviation are shown. The two best values are shown in grayscale, where the darker tone corresponds to the best algorithm.

MOP	Dim.	cMIB-MOEA	SMS-EMOA	R2-EMOA	ϵ^+-MaOEA	Δ_p-MaOEA
DTLZ2	2	7.118000e-03^{3}# (7.789805e-04)	4.293267e-03^{1} (1.831423e-04)	6.793700e-03^{2}# (7.160242e-05)	9.183667e-03^{4}# (1.329228e-03)	1.147553e-02^{5}# (1.984584e-03)
	3	6.447333e-02^{3}# (4.493293e-03)	4.441020e-02^{1} (1.800010e-03)	6.104297e-02^{2}# (2.723207e-04)	6.855230e-02^{4}# (1.055678e-02)	8.840783e-02^{5}# (9.236812e-03)
DTLZ2^{-1}	2	2.520210e-02^{2}# (2.745866e-03)	1.527390e-02^{1} (6.005368e-04)	3.933925e-01^{5}# (1.370061e-01)	3.402283e-02^{3}# (5.698156e-03)	3.746403e-02^{4}# (5.978609e-03)
	3	2.453346e-01^{2}# (1.701314e-02)	2.202564e-01^{1} (9.194547e-03)	3.062821e-01^{5}# (4.637694e-02)	2.837117e-01^{4}# (4.064469e-02)	2.814220e-01^{3}# (2.745633e-02)
DTLZ5	2	7.103667e-03^{3}# (7.790004e-04)	4.338467e-03^{1} (1.575392e-04)	6.688933e-03^{2}# (7.224047e-05)	9.879900e-03^{4}# (1.762974e-03)	1.139320e-02^{5}# (1.645651e-03)
	3	7.001000e-03^{2}# (8.600754e-04)	3.493500e-03^{1} (9.498484e-05)	4.076910e-02^{5}# (3.226959e-02)	8.628433e-03^{3}# (1.604775e-03)	1.000233e-02^{4}# (1.229534e-03)
DTLZ5^{-1}	2	2.603680e-02^{2}# (3.383072e-03)	1.530630e-02^{1} (7.535111e-04)	3.871187e-01^{5}# (1.274061e-01)	3.775327e-02^{4}# (8.705200e-03)	3.594497e-02^{3}# (6.090988e-03)
	3	2.125833e-01^{2} (1.498363e-02)	2.100291e-01^{1} (9.742511e-03)	3.223582e-01^{5}# (6.047533e-02)	2.664104e-01^{4}# (4.015743e-02)	2.523981e-01^{3}# (2.269030e-02)
DTLZ7	2	4.980683e-02^{4}# (2.297414e-01)	4.264967e-03^{1} (2.292047e-04)	3.464380e-02^{3}# (2.861427e-02)	5.045450e-02^{5}# (2.296294e-01)	9.394700e-03^{2}# (1.649633e-03)
	3	2.378955e-01^{1} (4.116585e-01)	3.818311e-01^{4} (5.424236e-01)	2.464458e-01^{2}# (2.855409e-01)	3.127700e-01^{3}# (3.987298e-01)	5.151523e-01^{5}# (5.674773e-01)
DTLZ7^{-1}	2	3.927967e-03^{2}# (6.421533e-04)	2.046867e-03^{1} (1.794485e-04)	2.099557e-02^{5}# (1.308642e-02)	4.307200e-03^{3}# (1.325549e-03)	4.692267e-03^{4}# (9.972819e-04)
	3	1.032207e-01^{3}# (2.436851e-01)	6.723670e-02^{1} (1.825405e-01)	1.131868e-01^{4}# (1.730409e-01)	1.342176e-01^{5}# (2.374613e-01)	9.979253e-02^{2}# (1.715143e-01)
WFG1	2	1.044840e+00^{1} (2.324099e-01)	1.163054e+00^{2}# (1.617913e-01)	1.468806e+00^{5}# (2.125939e-01)	1.169936e+00^{3}# (2.187795e-01)	1.211540e+00^{4}# (1.157397e-01)
	3	9.824879e-01^{3}# (2.514320e-02)	9.371078e-01^{1} (1.779578e-02)	9.683909e-01^{2}# (1.901979e-02)	1.004213e+00^{4}# (6.236634e-02)	1.074509e+00^{5}# (2.420945e-02)
WFG1^{-1}	2	2.084412e+00^{2}# (6.307778e-01)	2.335668e+00^{4}# (2.878350e-01)	3.253147e+00^{5}# (2.520180e-02)	2.282229e+00^{3}# (4.751597e-01)	1.927199e+00^{1} (6.821243e-01)
	3	2.911262e+00^{1} (8.859993e-01)	3.116225e+00^{2} (5.707788e-01)	3.619359e+00^{5}# (3.001984e-02)	3.525182e+00^{4}# (2.019639e-01)	3.447238e+00^{3}# (2.854448e-01)
WFG2	2	5.157696e-01^{2} (3.834060e-01)	5.893385e-01^{3} (3.557487e-01)	5.054610e-01^{1} (3.771995e-01)	6.446593e-01^{5} (3.204999e-01)	5.952168e-01^{4} (3.492576e-01)
	3	2.305098e-01^{5}# (1.868079e-01)	7.432647e-02^{1} (8.183186e-03)	1.265979e-01^{2}# (7.339705e-03)	1.339608e-01^{3}# (3.376467e-02)	2.301112e-01^{4}# (2.923242e-02)
WFG2^{-1}	2	1.208223e-02^{3}# (2.950417e-03)	4.266567e-03^{1} (5.278840e-04)	1.349710e-01^{5}# (8.900526e-02)	1.632620e-02^{4}# (9.210321e-03)	7.451233e-03^{2}# (1.140361e-03)
	3	1.751227e-01^{4}# (3.043722e-02)	1.064725e-01^{1} (1.298674e-02)	1.507995e-01^{3}# (3.184160e-02)	1.431800e-01^{2}# (2.980391e-02)	2.990492e-01^{5}# (9.710719e-02)
WFG3	2	3.053980e-02^{2}# (3.565189e-03)	2.029603e-02^{1} (2.100683e-03)	3.528941e-01^{5}# (1.438062e-01)	4.159363e-02^{3}# (1.538557e-02)	4.577543e-02^{4}# (1.227351e-02)
	3	1.377739e-01^{3}# (1.672905e-02)	6.054853e-02^{1} (6.845133e-03)	2.297785e-01^{5}# (3.776761e-02)	1.222559e-01^{2}# (5.304500e-02)	2.166802e-01^{4}# (2.377122e-02)
WFG3^{-1}	2	2.192823e-02^{2}# (2.446884e-03)	1.448977e-02^{1} (6.780921e-04)	3.029436e-01^{5}# (1.472744e-01)	3.513097e-02^{3}# (1.276027e-02)	3.922603e-02^{4}# (1.077180e-02)
	3	2.017282e-01^{1} (9.641338e-03)	2.300167e-01^{2}# (1.020771e-02)	4.655418e-01^{5}# (1.605946e-01)	3.066389e-01^{3}# (5.053012e-02)	4.186243e-01^{4}# (1.153122e-01)
LAME $\gamma = 0.25$	2	7.898800e-03^{3}# (1.120146e-03)	1.458033e-03^{1} (1.043391e-04)	4.054173e-02^{5}# (3.233630e-02)	2.473433e-03^{2}# (4.791290e-04)	1.021003e-02^{4}# (2.606959e-03)
	3	1.796150e-02^{5}# (2.659497e-03)	3.189433e-03^{1} (5.303600e-04)	1.552300e-02^{3}# (1.416929e-02)	3.503900e-03^{2} (8.562077e-04)	1.605240e-02^{4}# (4.100720e-03)
LAME $\gamma = 1.00$	2	7.161100e-03^{2}# (5.390032e-04)	5.297900e-03^{1} (1.931993e-04)	7.060710e-02^{5}# (3.887146e-02)	9.837433e-03^{3}# (1.564419e-03)	1.173267e-02^{4}# (2.097418e-03)
	3	5.691180e-02^{3}# (3.322721e-03)	4.733873e-02^{1} (1.356723e-03)	4.924030e-02^{2}# (1.063930e-03)	6.932543e-02^{4}# (9.224806e-03)	7.222980e-02^{5}# (4.464222e-03)
LAME $\gamma = 5.00$	2	7.071067e-03^{3}# (8.832482e-04)	2.296067e-03^{1} (1.106015e-04)	8.711600e-03^{4}# (6.077068e-05)	4.722700e-03^{2}# (7.544393e-04)	1.098093e-02^{5}# (2.093217e-03)
	3	5.485860e-02^{3}# (6.479825e-03)	2.763317e-02^{1} (2.345896e-03)	5.948473e-02^{4}# (1.538806e-04)	3.429323e-02^{2}# (5.571235e-03)	1.241889e-01^{5}# (3.825838e-02)
MIRROR $\gamma = 0.25$	2	6.493967e-03^{3}# (9.177931e-04)	1.341167e-03^{1} (1.103143e-04)	8.963833e-03^{4}# (2.559375e-05)	2.265167e-03^{2}# (3.831056e-04)	1.123300e-02^{5}# (3.950065e-03)
	3	1.360733e-02^{3}# (1.542645e-03)	9.473000e-03^{2}# (0.000000e+00)	3.292943e-02^{5}# (4.794966e-03)	7.090067e-03^{1} (1.094930e-03)	2.989373e-02^{4}# (9.291574e-03)
MIRROR $\gamma = 1.00$	2	7.079633e-03^{2}# (5.680806e-04)	5.381300e-03^{1} (2.054346e-04)	5.826527e-02^{5}# (3.313018e-02)	9.175933e-03^{3}# (1.154726e-03)	1.166310e-02^{4}# (2.344770e-03)
	3	5.897270e-02^{1} (2.920122e-03)	6.976930e-02^{2}# (2.049253e-03)	9.519210e-02^{5}# (1.049852e-02)	7.210223e-02^{3}# (9.153865e-03)	8.859713e-02^{4}# (2.517453e-02)
MIRROR $\gamma = 5.00$	2	7.391533e-03^{3}# (8.201517e-04)	2.343367e-03^{1} (1.130790e-04)	7.383200e-02^{5}# (3.049019e-02)	4.603100e-03^{2}# (1.151346e-03)	1.192950e-02^{4}# (2.408357e-03)
	3	7.556350e-02^{4}# (8.816737e-03)	3.660517e-02^{1} (2.501443e-03)	4.871660e-02^{3}# (9.182451e-03)	4.183757e-02^{2}# (6.978066e-03)	8.004303e-02^{5}# (1.233744e-02)

Table B.17 – *Continuation*

MOP	Dim.	cMIB-MOEA	SMS-EMOA	R2-EMOA	ϵ^+-MaOEA	Δ_p-MaOEA
VIE1	3	1.635651e-01^{4}# (1.506110e-02)	1.464426e-01^{2}# (7.435778e-03)	1.486234e-01^{3}# (2.025099e-02)	1.142492e-01^{1} (1.884931e-02)	1.853871e-01^{5}# (2.572549e-02)
VIE2	3	1.709033e-02^{4}# (1.585493e-03)	1.942617e-02^{5}# (1.102125e-03)	1.446717e-02^{2} (3.659380e-03)	1.339830e-02^{1} (2.884166e-03)	1.518050e-02^{3}# (2.322600e-03)
VIE3	3	3.200010e+01^{2}# (4.904139e-05)	3.200002e+01^{1} (2.373464e-05)	3.200033e+01^{5}# (5.110536e-04)	3.200015e+01^{4}# (6.488456e-04)	3.200014e+01^{3}# (1.264007e-04)

Table B.18: Comparison for the Δ_p indicator. The mean and, in parentheses, standard deviation are shown. The two best values are shown in grayscale, where the darker tone corresponds to the best algorithm.

MOP	Dim.	cMIB-MOEA	SMS-EMOA	R2-EMOA	ϵ^+-MaOEA	Δ_p-MaOEA
DTLZ2	2	4.865847e-03^{2}# (7.000612e-05)	7.627592e-03^{3}# (3.405027e-04)	4.556979e-03^{1} (4.495906e-06)	1.523505e-02^{5}# (2.178438e-03)	1.505598e-02^{4}# (2.127147e-03)
	3	5.575933e-02^{2}# (6.313307e-04)	7.596659e-02^{4}# (9.184790e-04)	5.333332e-02^{1} (2.261663e-05)	7.735701e-02^{5}# (3.063697e-03)	7.486625e-02^{3}# (3.139039e-03)
DTLZ2^{-1}	2	1.688265e-02^{1} (2.559978e-04)	2.111639e-02^{2}# (6.960045e-04)	6.614193e-01^{5}# (1.388484e-01)	9.057670e-02^{3}# (2.655218e-02)	9.218387e-02^{4}# (2.513761e-02)
	3	1.911749e-01^{1} (1.766017e-03)	2.020859e-01^{2}# (1.884495e-03)	3.789330e-01^{3}# (2.921503e-02)	4.464288e-01^{4}# (3.936185e-02)	4.582354e-01^{5}# (5.431259e-02)
DTLZ5	2	4.853680e-03^{2}# (1.036004e-04)	7.390486e-03^{3}# (2.129260e-04)	4.595982e-03^{1} (3.746174e-06)	1.420154e-02^{4}# (2.203283e-03)	1.513588e-02^{5}# (3.203857e-03)
	3	4.766987e-03^{1} (9.198269e-05)	6.640421e-03^{2}# (2.454997e-04)	1.755083e-02^{5}# (5.434274e-03)	1.295059e-02^{3}# (2.409442e-03)	1.339318e-02^{4}# (2.245774e-03)
DTLZ5^{-1}	2	1.691565e-02^{1} (3.279980e-04)	2.129329e-02^{2}# (6.167903e-04)	6.394039e-01^{5}# (1.376317e-01)	8.258068e-02^{3}# (3.106901e-02)	9.432772e-02^{4}# (2.784122e-02)
	3	1.632458e-01^{1} (2.129217e-03)	1.861760e-01^{2}# (2.218311e-03)	3.198766e-01^{3}# (4.983340e-02)	3.441954e-01^{4}# (4.178318e-02)	3.580230e-01^{5}# (5.723492e-02)
DTLZ7	2	3.024949e-02^{4} (1.352320e-01)	5.877758e-03^{1} (9.026380e-05)	1.269264e-02^{3}# (1.716582e-02)	3.344423e-02^{5}# (1.346923e-01)	8.909477e-03^{2}# (7.822113e-04)
	3	1.247254e-01^{2} (1.640720e-01)	2.446051e-01^{5}# (1.848096e-01)	1.152919e-01^{1} (1.145019e-01)	1.460901e-01^{3} (1.719175e-01)	2.340722e-01^{4} (2.811636e-01)
DTLZ7^{-1}	2	3.214845e-03^{1} (6.182353e-05)	3.277249e-03^{2}# (5.957530e-05)	6.980895e-03^{5}# (2.537772e-03)	4.553432e-03^{3}# (5.092733e-04)	4.599770e-03^{4}# (4.384120e-04)
	3	9.209468e-02^{2} (1.270279e-01)	1.026235e-01^{4}# (8.424868e-02)	7.902295e-02^{1} (9.033299e-02)	9.883970e-02^{3}# (1.224676e-01)	1.170545e-01^{5}# (1.462014e-01)
WFG1	2	9.647475e-01^{1} (2.251743e-01)	1.069354e+00^{3}# (1.652768e-01)	1.432029e+00^{5}# (2.516870e-01)	1.058814e+00^{2}# (2.269476e-01)	1.122094e+00^{4}# (1.109864e-01)
	3	1.086772e+00^{3}# (5.902545e-02)	9.716990e-01^{1} (5.793072e-02)	1.073782e+00^{2}# (3.832282e-02)	1.149266e+00^{4}# (9.817004e-02)	1.216623e+00^{5}# (7.978088e-02)
WFG1^{-1}	2	9.495171e-01^{1} (3.461358e-01)	1.083860e+00^{3} (1.581793e-01)	1.888999e+00^{5}# (2.684169e-02)	1.080384e+00^{2}# (2.762331e-01)	1.126748e+00^{4}# (3.351547e-01)
	3	9.165714e-01^{1} (2.171926e-01)	9.610582e-01^{2} (2.077366e-01)	1.063768e+00^{4}# (1.313306e-01)	1.038918e+00^{3}# (1.736928e-01)	1.065689e+00^{5}# (1.379979e-01)
WFG2	2	2.154600e-01^{2} (1.538824e-01)	2.465964e-01^{4} (1.415222e-01)	2.233534e-01^{3}# (1.440044e-01)	2.707086e-01^{5}# (1.265877e-01)	1.878335e-01^{1} (1.577465e-01)
	3	2.085460e-01^{1} (7.373908e-02)	3.823700e-01^{3}# (5.058112e-03)	3.604090e-01^{2}# (4.880794e-03)	4.067050e-01^{4}# (3.977859e-02)	4.263901e-01^{5}# (3.865991e-02)
WFG2^{-1}	2	1.233458e-02^{2} (2.608464e-04)	1.232974e-02^{1} (1.988542e-04)	3.161863e-02^{5}# (1.244926e-02)	1.484077e-02^{4}# (6.317017e-04)	1.482789e-02^{3}# (5.515292e-04)
	3	2.236751e-01^{1} (2.941443e-03)	4.789940e-01^{5}# (1.270677e-02)	3.108696e-01^{2}# (1.023628e-02)	3.631718e-01^{4}# (1.791387e-02)	3.627793e-01^{3}# (2.275673e-02)
WFG3	2	1.803316e-02^{4}# (1.633813e-03)	1.458376e-02^{1} (1.017633e-03)	1.271637e-01^{5}# (6.048365e-02)	1.656428e-02^{3}# (8.876076e-04)	1.632980e-02^{2}# (8.836390e-04)
	3	9.918037e-01^{5}# (2.486030e-02)	7.348711e-01^{3}# (2.177252e-02)	8.746770e-01^{4}# (6.261037e-02)	6.420635e-01^{2} (8.066536e-02)	6.117474e-01^{1} (8.049916e-02)
WFG3^{-1}	2	1.407119e-02^{2}# (2.713863e-04)	1.312443e-02^{1} (2.184837e-04)	1.101288e-01^{5}# (5.747052e-02)	1.600926e-02^{4}# (7.478921e-04)	1.571967e-02^{3}# (9.270723e-04)
	3	1.677467e-01^{1} (1.821875e-03)	2.066172e-01^{4}# (2.774801e-03)	2.228437e-01^{5}# (6.948601e-03)	1.829434e-01^{2}# (4.843944e-03)	1.948623e-01^{3}# (1.345422e-02)
LAME $\gamma = 0.25$	2	2.223191e-02^{2}# (5.290881e-04)	2.131835e-02^{1} (6.162224e-04)	3.486028e-01^{5}# (2.752624e-02)	1.535238e-01^{4}# (3.253035e-02)	1.413477e-01^{3}# (4.020552e-02)
	3	4.854347e-02^{1} (1.051667e-02)	7.809791e-02^{2}# (1.041900e-02)	3.182134e-01^{5}# (3.713596e-02)	2.723397e-01^{3}# (2.852863e-02)	2.859797e-01^{4}# (1.981964e-02)
LAME $\gamma = 1.00$	2	4.533726e-03^{2}# (9.161534e-04)	4.114708e-03^{1} (8.413679e-05)	2.235870e-02^{5}# (1.446147e-02)	4.768849e-03^{4}# (1.577171e-04)	4.747712e-03^{3}# (1.416621e-04)
	3	4.175364e-02^{3}# (5.109212e-04)	3.973147e-02^{2}# (4.130875e-04)	3.832683e-02^{1} (1.599377e-04)	4.514587e-02^{4}# (1.415135e-03)	4.673925e-02^{5}# (1.937215e-03)
LAME $\gamma = 5.00$	2	6.882554e-03^{1} (2.226795e-04)	4.752588e-02^{3}# (1.089858e-03)	8.592483e-03^{2}# (1.477560e-05)	9.133275e-02^{5}# (7.094008e-03)	8.727315e-02^{4}# (7.510725e-03)
	3	6.687042e-02^{1} (8.834713e-04)	1.821802e-01^{4}# (1.633360e-03)	7.010146e-02^{2}# (1.455840e-05)	1.833388e-01^{5}# (4.895786e-03)	1.727296e-01^{3}# (8.328334e-03)
MIRROR $\gamma = 0.25$	2	1.013578e-02^{1} (3.640054e-04)	5.548653e-02^{3}# (2.000460e-03)	1.307197e-02^{2}# (5.128982e-06)	1.296021e-01^{4}# (8.901600e-03)	1.336996e-01^{5}# (1.087193e-02)
	3	1.280444e-02^{1} (1.999371e-04)	8.236083e-02^{3}# (1.466539e-03)	2.690547e-02^{2}# (2.154750e-03)	1.386668e-01^{4}# (4.774388e-03)	1.409729e-01^{5}# (1.329555e-02)
MIRROR $\gamma = 1.00$	2	4.372624e-03^{2}# (8.752033e-05)	4.142530e-03^{1} (5.961702e-05)	1.758156e-02^{5}# (1.150480e-02)	4.707470e-03^{3}# (1.151961e-04)	4.757747e-03^{4}# (1.769827e-04)
	3	4.164064e-02^{1} (5.170740e-04)	5.004851e-02^{4}# (6.775633e-04)	5.755019e-02^{5}# (1.379251e-03)	4.500709e-02^{2}# (1.059483e-03)	4.560052e-02^{3}# (1.131002e-03)
MIRROR $\gamma = 5.00$	2	1.245759e-02^{1} (9.391079e-04)	1.655432e-02^{2}# (3.378061e-04)	3.327363e-01^{5}# (2.992005e-02)	1.123032e-01^{4}# (2.055848e-02)	1.047260e-01^{3}# (2.525711e-02)
	3	6.608159e-02^{1} (8.992943e-04)	1.629110e-01^{2}# (1.396769e-03)	3.174197e-01^{3}# (2.007091e-02)	3.533167e-01^{4}# (2.392001e-02)	3.648910e-01^{5}# (2.833919e-02)

Table B.18 – *Continuation*

MOP	Dim.	cMIB-MOEA	SMS-EMOA	R2-EMOA	ϵ^+-MaOEA	Δ_p-MaOEA
VIE1	3	5.290207e-01^{5}# (2.107593e-02)	4.174841e-01^{4}# (4.948423e-03)	3.586087e-01^{3}# (3.049140e-02)	2.184531e-01^{1} (3.764009e-02)	2.282917e-01^{2} (3.269193e-02)
VIE2	3	1.278606e-02^{1} (1.018294e-03)	1.915114e-02^{2}# (8.783006e-04)	1.192974e-01^{3}# (6.950586e-02)	1.338645e-01^{4}# (4.912625e-02)	1.377689e-01^{5}# (5.746942e-02)
VIE3	3	3.437077e+01^{1} (6.286022e-04)	3.462892e+01^{5}# (9.436654e-03)	3.441477e+01^{4}# (4.802292e-02)	3.440457e+01^{3}# (2.525711e-02)	3.439563e+01^{2}# (1.876920e-02)

Table B.19: Comparison for the Solow-Polasky Diversity indicator. The mean and, in parentheses, standard deviation are shown. The two best values are shown in grayscale, where the darker tone corresponds to the best algorithm.

MOP	Dim.	cMIB-MOEA	SMS-EMOA	R2-EMOA	IGD$^+$-MaOEA	ϵ^+-MaOEA	Δ_p-MaOEA
DTLZ2	2	8.821147e+00^1 (1.272405e-03)	8.798568e+00^4# (2.613455e-03)	8.816599e+00^3# (9.463511e-04)	8.691603e+00^6# (3.858349e-02)	8.694854e+00^5# (3.727402e-02)	8.818966e+00^2# (5.961738e-02)
	3	3.356680e+01^1 (1.096942e-01)	3.187029e+01^3# (7.233010e-02)	3.341152e+01^2# (3.763840e-03)	3.017669e+01^6# (4.166380e-01)	3.050420e+01^5# (5.107623e-01)	3.158978e+01^4# (5.301169e-01)
DTLZ2^{-1}	2	2.771195e+01^1 (1.188191e-02)	2.742943e+01^2# (4.669876e-02)	1.356946e+01^6# (1.423211e+00)	2.387310e+01^4# (6.258289e-01)	2.377335e+01^5# (5.411160e-01)	2.723280e+01^3# (1.427658e-01)
	3	9.965279e+01^1 (1.268921e-01)	9.492750e+01^3# (1.440932e-01)	8.417236e+01^4# (1.473444e+00)	8.166996e+01^5# (1.904719e+00)	8.135934e+01^6# (2.084185e+00)	9.522544e+01^2# (7.479462e-01)
DTLZ5	2	8.822442e+00^1 (6.461728e-03)	8.799349e+00^4# (2.187687e-03)	8.816822e+00^2# (8.780230e-04)	8.702784e+00^5# (3.634725e-02)	8.687385e+00^6# (5.813402e-02)	8.804175e+00^3# (2.730395e-02)
	3	8.830416e+00^1 (1.696258e-02)	8.800736e+00^3# (2.589811e-03)	8.491895e+00^6# (2.748910e-01)	8.707356e+00^4# (4.293305e-02)	8.698294e+00^5# (4.037600e-02)	8.806443e+00^2# (2.799272e-02)
DTLZ5^{-1}	2	2.770501e+01^1 (1.842481e-02)	2.740979e+01^2# (4.680747e-02)	1.380627e+01^6# (1.383810e+00)	2.396368e+01^4# (7.138189e-01)	2.361259e+01^5# (5.329063e-01)	2.725310e+01^3# (1.415468e-01)
	3	9.528944e+01^1 (1.731521e-01)	8.781740e+01^3# (4.956846e-01)	7.772504e+01^5# (1.085326e+00)	7.777726e+01^4# (1.854314e+00)	7.746305e+01^6# (2.337139e+00)	8.930511e+01^2# (7.678998e-01)
DTLZ7	2	1.062990e+01^3 (1.346309e+00)	1.076359e+01^2# (6.476192e-03)	1.052425e+01^5# (3.580821e-01)	1.038714e+01^6# (1.303043e+00)	1.062937e+01^4# (9.004919e-02)	1.084149e+01^1 (1.618437e-01)
	3	4.508572e+01^1 (9.006458e+00)	3.332477e+01^5# (8.165612e+00)	4.110640e+01^2# (5.401367e+00)	3.501677e+01^4# (6.910057e+00)	3.196178e+01^6# (9.741718e+00)	3.591174e+01^3# (1.043948e+01)
DTLZ7^{-1}	2	7.006473e+00^1 (3.046232e-02)	6.946288e+00^3# (4.660341e-03)	6.828476e+00^6# (8.469937e-02)	6.900714e+00^5# (3.939213e-02)	6.915919e+00^4# (4.454158e-02)	6.968779e+00^2# (2.800234e-02)
	3	2.502502e+01^1 (5.058758e+00)	2.126198e+01^4# (2.756308e+00)	2.384638e+01^2# (3.249714e+00)	1.954009e+01^5# (3.477691e+00)	1.884096e+01^6# (4.063981e+00)	2.358932e+01^3# (2.971372e+00)
WFG1	2	1.293762e+01^1 (2.195149e+00)	1.175626e+01^2# (1.180110e+00)	8.173223e+00^6# (1.776103e+00)	1.150644e+01^3# (1.587566e+00)	1.113124e+01^5# (8.451126e-01)	1.137984e+01^4# (8.314823e-01)
	3	6.409589e+01^1 (4.680269e+00)	6.155438e+01^2# (4.259137e+00)	5.334642e+01^4# (1.989883e+00)	4.856469e+01^5# (5.024938e+00)	4.500733e+01^6# (4.047860e+00)	5.671619e+01^3# (3.789127e+00)
WFG1^{-1}	2	1.238514e+01^2# (1.776981e-01)	1.171776e+01^3# (8.584777e-01)	5.631747e+00^6# (1.771200e-01)	1.131354e+01^4# (1.254937e+00)	1.099610e+01^5# (1.873225e+00)	1.292010e+01^1 (1.725455e+00)
	3	6.639394e+01^1 (4.760192e+00)	5.662741e+01^5# (3.236413e+00)	4.798510e+01^6# (1.993620e+00)	5.801008e+01^3# (3.764787e+00)	5.702856e+01^4# (3.690761e+00)	5.934036e+01^2# (4.107852e+00)
WFG2	2	2.083195e+01^1 (2.336098e+00)	1.998725e+01^4# (1.987762e+00)	1.947631e+01^5# (2.164075e+00)	1.920171e+01^6# (1.830814e+00)	2.044715e+01^2# (2.245791e+00)	1.999367e+01^3# (2.005542e+00)
	3	9.488862e+01^1 (2.497538e+00)	6.701236e+01^4# (8.437630e-01)	8.054691e+01^3# (7.340269e-01)	6.554756e+01^5# (2.391276e+00)	6.376157e+01^6# (2.324113e+00)	8.924357e+01^2# (1.257948e+00)
WFG2^{-1}	2	2.078970e+01^1 (5.528098e-03)	2.078599e+01^2# (4.228234e-03)	1.984989e+01^6# (3.918397e-01)	2.058007e+01^4# (6.163914e-02)	2.058826e+01^3# (5.090555e-02)	2.056250e+01^5# (4.700077e-02)
	3	1.027510e+02^1 (8.460532e-02)	8.603826e+01^4# (8.144693e-01)	8.831312e+01^3# (1.438748e+00)	8.490830e+01^5# (1.285913e+00)	8.456994e+01^6# (1.955541e+00)	9.838959e+01^2# (6.073728e-01)
WFG3	2	2.295166e+01^2# (1.638104e-02)	2.296180e+01^1 (1.406068e-02)	1.913564e+01^6# (1.209651e+00)	2.251515e+01^4# (1.101178e-01)	2.257362e+01^3# (1.292036e-01)	2.250960e+01^5# (1.638029e-01)
	3	7.567687e+01^1 (1.083666e+00)	5.568496e+01^4# (8.245379e-01)	6.129864e+01^3# (2.053967e+00)	5.413799e+01^5# (2.484887e+00)	5.362586e+01^6# (2.642860e+00)	6.634708e+01^2# (2.042348e+00)
WFG3^{-1}	2	2.295349e+01^2# (7.910825e-03)	2.297868e+01^1 (5.235990e-03)	1.940783e+01^6# (1.377304e+00)	2.249561e+01^5# (1.183683e-01)	2.251769e+01^4# (1.366567e-01)	2.252732e+01^3# (1.491395e-01)
	3	9.657638e+01^1 (1.433283e-01)	8.837430e+01^5# (4.768611e-01)	7.892945e+01^6# (1.971387e+00)	9.164711e+01^2# (6.916358e-01)	9.003548e+01^3# (9.193756e-01)	8.938942e+01^4# (9.023377e-01)
LAME $\gamma = 0.25$	2	1.037823e+01^1 (2.213646e-03)	8.950041e+00^3# (4.312703e-02)	3.013353e+00^6# (8.039508e-01)	5.326372e+00^5# (4.719453e-01)	5.422999e+00^4# (5.402272e-01)	1.036711e+01^2 (7.982199e-02)
	3	1.550826e+01^1 (4.664632e-01)	8.190703e+00^3# (3.434435e-01)	2.832721e+00^6# (1.130079e+00)	3.238244e+00^4# (5.502489e-01)	3.023620e+00^5# (4.745523e-01)	1.539346e+01^2 (3.197087e-01)
LAME $\gamma = 1.00$	2	8.071926e+00^1 (6.577628e-02)	8.058964e+00^2 (5.092004e-05)	7.346984e+00^6# (2.960646e-01)	8.015912e+00^5# (3.191929e-02)	8.023790e+00^4# (2.692432e-02)	8.024318e+00^3# (4.332857e-02)
	3	2.354353e+01^1 (1.750051e-01)	2.322996e+01^2# (2.794359e-02)	2.234300e+01^4# (1.369314e-01)	2.130040e+01^5# (3.909345e-01)	2.092694e+01^6# (4.376669e-01)	2.238878e+01^3# (4.362339e-01)
LAME $\gamma = 5.00$	2	9.925497e+00^1 (7.875456e-04)	8.891586e+00^4# (3.142856e-02)	9.919566e+00^2# (1.125444e-03)	7.593789e+00^6# (1.992855e-01)	7.701974e+00^5# (2.030187e-01)	9.882567e+00^3# (2.275000e-02)
	3	4.322709e+01^1 (1.144778e-01)	2.503881e+01^4# (1.844605e-01)	4.221405e+01^2# (1.391960e-02)	2.377465e+01^6# (6.216880e-01)	2.497272e+01^5# (1.161091e+00)	3.865565e+01^3# (7.262738e-01)
MIRROR $\gamma = 0.25$	2	1.037711e+01^1 (6.673881e-04)	8.843699e+00^4# (5.016676e-02)	1.036926e+01^2# (1.825742e-06)	6.842664e+00^5# (2.157554e-01)	6.750335e+00^6# (2.704904e-01)	1.030594e+01^3# (3.695008e-02)
	3	1.518630e+01^1 (4.423309e-03)	1.097489e+01^4# (8.181314e-02)	1.416100e+01^3# (1.414359e-01)	8.382863e+00^5# (1.829469e-01)	8.117109e+00^6# (4.346317e-01)	1.482451e+01^2# (1.058231e-01)
MIRROR $\gamma = 1.00$	2	8.058111e+00^2# (3.873547e-04)	8.058940e+00^1 (4.816042e-05)	7.458103e+00^6# (3.261540e-01)	8.022796e+00^3# (2.108429e-02)	8.018077e+00^4# (2.525249e-02)	7.997682e+00^5# (4.107385e-02)
	3	2.344203e+01^2# (4.994797e-02)	2.359556e+01^1 (2.184588e-02)	2.192370e+01^5# (2.704394e-01)	2.232280e+01^3# (2.936126e-01)	2.207443e+01^4# (3.786337e-01)	2.144886e+01^6# (3.887247e-01)
MIRROR $\gamma = 5.00$	2	9.826355e+00^1 (3.604948e-02)	8.726723e+00^3# (3.306103e-02)	2.970213e+00^6# (3.839516e-01)	6.122711e+00^5# (3.844550e-01)	6.250719e+00^4# (4.059558e-01)	9.797667e+00^2# (5.189377e-02)
	3	4.160141e+01^1 (2.985432e-01)	2.439618e+01^3# (1.467165e-01)	1.882546e+01^4# (9.146978e-01)	1.275241e+01^5# (1.066539e+00)	1.212362e+01^6# (1.241006e+00)	3.607953e+01^2# (7.339688e-01)
VIE1	3	8.545447e+01^1 (7.503600e-01)	6.810839e+01^3# (2.235645e-01)	6.732149e+01^4# (2.488327e+00)	5.474045e+01^6# (1.926203e+00)	5.537032e+01^5# (1.791954e+00)	8.028319e+01^2# (1.156237e+00)
VIE2	3	1.221494e+01^1 (1.088653e-01)	1.154239e+01^3# (8.328965e-02)	8.808749e+00^4# (7.999777e-01)	7.590036e+00^5# (5.201747e-01)	7.506416e+00^6# (6.423951e-01)	1.210252e+01^2# (1.772663e-01)
VIE3	3	4.588598e+01^1 (1.234293e-01)	2.285092e+01^6# (5.637013e-01)	2.803849e+01^5# (3.651235e+00)	3.228389e+01^4# (1.852805e+00)	3.251593e+01^3# (1.300675e+00)	4.048990e+01^2# (7.029199e-01)

B.4 PFI-EMOA

Tables B.20 to B.23 show the numerical results of the comparison between PFI-EMOA and PFI-EMOA/E_s, considering the indicators HV, SPD, IGD$^+$, and Riesz s-energy. Tables B.24 to B.27 show the numerical results of the comparison between PFI-EMOA and several state-of-the-art MOEAs, on the basis of the indicators HV, SPD, IGD$^+$, and Riesz s-energy. These resuls are related to the experiments of Chapter 7, section 7.5.3.2.

Table B.20: Mean and, in parentheses, standard deviation of the hypervolume comparison. For each case, the two best values are shown in grayscale, where the darker tone corresponds to the best algorithm. The symbol # is placed when the best algorithm presents a significant difference, according to a one-tailed Wilcoxon test using a significance level of $\alpha = 0.05$.

MOP	Dim.	PFI-EMOA	PFI-EMOA/E_s
WFG1	2	2.358163e+01^1 (1.306300e-01)	2.350360e+01^2# (1.659853e-01)
	3	2.131279e+02^2# (1.099155e+00)	2.143017e+02^1 (1.702223e+00)
	4	2.166627e+03^2 (1.861384e+01)	2.192674e+03^1 (1.809109e+01)
	5	2.621782e+04^2 (3.598616e+02)	2.668787e+04^1 (3.481373e+02)
	6	3.726527e+05^2# (3.549169e+03)	3.751032e+05^1 (1.284953e+04)
WFG1^{-1}	2	1.898476e+02^1 (1.083319e-03)	1.898435e+02^2# (1.680470e-03)
	3	2.937552e+03^1 (1.845366e-01)	2.934659e+03^2# (9.522043e-01)
	4	4.612943e+04^1 (1.382122e+01)	4.599780e+04^2# (2.969151e+01)
	5	7.185021e+05^1 (5.046183e+02)	7.163387e+05^2# (1.036210e+03)
	6	1.096231e+07^1 (1.605262e+04)	1.090240e+07^2# (4.472424e+04)
WFG2	2	3.021306e+01^1 (1.211301e+00)	2.984931e+01^2# (1.167372e+00)
	3	2.932859e+02^1 (1.942387e+01)	2.923041e+02^2# (1.892720e+01)
	4	3.248856e+03^1 (2.398926e+02)	3.220061e+03^2# (2.303971e+02)
	5	4.337180e+04^1 (2.656853e+03)	4.288536e+04^2# (2.532732e+03)
	6	6.643667e+05^1 (1.950361e+04)	6.154582e+05^2# (5.062337e+04)
WFG2^{-1}	2	1.943820e+02^1 (1.202957e-03)	1.942593e+02^2# (9.916449e-02)
	3	3.169348e+03^1 (2.762095e-01)	3.151400e+03^2# (8.026644e+00)
	4	5.327203e+04^1 (1.460497e+01)	5.225940e+04^2# (2.589727e+02)
	5	8.908956e+05^1 (8.573290e+02)	8.636435e+05^2# (6.936398e+03)
	6	1.456006e+07^1 (2.641792e+04)	1.390161e+07^2# (2.894509e+05)
WFG3	2	3.087965e+01^1 (2.765609e-02)	3.086723e+01^2# (3.070117e-02)
	3	2.645127e+02^2# (7.650054e-01)	2.646575e+02^1 (1.377059e+00)
	4	2.735330e+03^1 (2.171440e+01)	2.721205e+03^2# (3.241851e+01)
	5	3.339751e+04^1 (4.051637e+02)	3.325327e+04^2# (6.505887e+02)
	6	4.707271e+05^2# (1.028587e+04)	4.791773e+05^1 (1.247914e+04)

Table B.20 – *Continuation*

MOP	Dim.	PFI-EMOA	PFI-EMOA /E_s
WFG3^{-1}	2	1.909592e+02^{1} (2.078171e-03)	1.907834e+02^{2}# (1.334817e-01)
	3	3.016005e+03^{1} (4.292382e-01)	2.980334e+03^{2}# (2.119632e+01)
	4	4.909318e+04^{1} (2.635916e+01)	4.622871e+04^{2}# (8.970768e+02)
	5	8.024166e+05^{1} (1.458510e+03)	7.214877e+05^{2}# (1.680940e+04)
	6	1.289127e+07^{1} (3.602451e+04)	1.110115e+07^{2}# (3.589267e+05)
WFG4	2	2.865515e+01^{1} (1.446041e-02)	2.864851e+01^{2}# (2.558011e-02)
	3	2.860305e+02^{2}# (2.468886e-01)	2.861271e+02^{1} (1.894916e-01)
	4	3.273250e+03^{1} (5.552212e+00)	3.273100e+03^{2}# (4.277927e+00)
	5	4.328951e+04^{1} (8.811447e+01)	4.327103e+04^{2}# (9.284184e+01)
	6	6.538111e+05^{2}# (1.421185e+03)	6.564368e+05^{1} (1.525256e+03)
WFG4^{-1}	2	1.932542e+02^{1} (3.372502e-03)	1.929791e+02^{2}# (1.555176e-01)
	3	3.171981e+03^{1} (8.879317e-01)	3.090446e+03^{2}# (2.018706e+01)
	4	5.522090e+04^{1} (5.660081e+01)	5.117104e+04^{2}# (6.949266e+02)
	5	9.776882e+05^{1} (5.097973e+03)	8.711272e+05^{2}# (1.286628e+04)
	6	1.731875e+07^{1} (1.521168e+05)	1.521064e+07^{2}# (3.185104e+05)
WFG5	2	2.771126e+01^{1} (1.249536e-01)	2.769625e+01^{2}# (8.776815e-02)
	3	2.793949e+02^{1} (6.285803e-01)	2.787009e+02^{2}# (6.648601e-01)
	4	3.194398e+03^{1} (5.480228e+00)	3.185258e+03^{2}# (7.577165e+00)
	5	4.216984e+04^{1} (5.313406e+01)	4.196521e+04^{2}# (1.039120e+02)
	6	6.348109e+05^{2}# (1.326739e+03)	6.354000e+05^{1} (1.063247e+03)
WFG5^{-1}	2	1.931153e+02^{1} (4.037868e-02)	1.928071e+02^{2}# (1.062300e-01)
	3	3.166070e+03^{1} (1.283254e+00)	3.089486e+03^{2}# (1.600152e+01)
	4	5.504353e+04^{1} (6.606727e+01)	5.110834e+04^{2}# (9.357063e+02)
	5	9.741062e+05^{1} (3.472732e+03)	8.695612e+05^{2}# (1.574236e+04)
	6	1.736080e+07^{1} (8.908162e+04)	1.510287e+07^{2}# (3.084432e+05)
WFG6	2	2.820239e+01^{2}# (5.681218e-02)	2.820993e+01^{1} (4.238641e-02)
	3	2.804444e+02^{2}# (6.676875e-01)	2.808396e+02^{1} (5.876715e-01)
	4	3.208056e+03^{2}# (1.060635e+01)	3.212494e+03^{1} (9.426835e+00)
	5	4.237317e+04^{2} (1.524483e+02)	4.248596e+04^{1} (1.323181e+02)
	6	6.416173e+05^{2} (2.293627e+03)	6.428084e+05^{1} (2.252901e+03)
WFG6^{-1}	2	1.932534e+02^{1} (1.246504e-03)	1.929879e+02^{2}# (1.211263e-01)
	3	3.172978e+03^{1} (4.249662e-01)	3.085648e+03^{2}# (2.869449e+01)
	4	5.528790e+04^{1} (7.056636e+01)	5.093447e+04^{2}# (6.727499e+02)
	5	9.817231e+05^{1} (3.908247e+03)	8.619229e+05^{2}# (2.221749e+04)
	6	1.735694e+07^{1} (2.364131e+05)	1.471531e+07^{2}# (4.475530e+05)
WFG7	2	2.867600e+01^{2} (2.633365e-03)	2.867935e+01^{1} (1.782659e-03)
	3	2.867476e+02^{2}# (8.862747e-02)	2.867812e+02^{1} (7.178370e-02)
	4	3.286932e+03^{2}# (2.515918e+00)	3.287296e+03^{1} (1.796567e+00)
	5	4.355668e+04^{1} (3.700878e+01)	4.351630e+04^{2}# (4.209542e+01)
	6	6.587560e+05^{2}# (7.940577e+02)	6.598023e+05^{1} (8.456950e+02)

Table B.20 – *Continuation*

MOP	Dim.	PFI-EMOA	PFI-EMOA / E_s
WFG7^{-1}	2	1.932545e+02^{1} (1.192673e-03)	1.929160e+02^{2}# (1.587545e-01)
	3	3.172054e+03^{1} (8.769530e-01)	3.089406e+03^{2}# (2.409045e+01)
	4	5.522824e+04^{1} (5.943769e+01)	5.084848e+04^{2}# (7.937215e+02)
	5	9.818615e+05^{1} (4.350929e+03)	8.668284e+05^{2}# (2.148612e+04)
	6	1.743776e+07^{1} (1.992002e+05)	1.503978e+07^{2}# (4.112110e+05)
WFG8	2	2.761168e+01^{1} (4.866361e-02)	2.757832e+01^{2}# (1.065341e-01)
	3	2.740005e+02^{2} (6.178329e-01)	2.749070e+02^{1} (5.652913e-01)
	4	3.097026e+03^{2} (9.856048e+00)	3.113827e+03^{1} (7.591942e+00)
	5	4.050054e+04^{2}# (2.133708e+02)	4.061194e+04^{1} (2.172373e+02)
	6	6.054527e+05^{2}# (3.603967e+03)	6.109034e+05^{1} (4.356887e+03)
WFG8^{-1}	2	1.932124e+02^{1} (8.219975e-02)	1.928586e+02^{2}# (1.779677e-01)
	3	3.171616e+03^{1} (2.082455e+00)	3.071790e+03^{2}# (2.060658e+01)
	4	5.506385e+04^{1} (1.215109e+02)	5.003362e+04^{2}# (6.610059e+02)
	5	9.747592e+05^{1} (5.721336e+03)	8.435129e+05^{2}# (1.841625e+04)
	6	1.735779e+07^{1} (1.290705e+05)	1.450183e+07^{2}# (3.813290e+05)
WFG9	2	2.788661e+01^{2}# (2.412829e-01)	2.793995e+01^{1} (1.786772e-01)
	3	2.739934e+02^{2}# (3.095568e+00)	2.751724e+02^{1} (3.706787e+00)
	4	3.034026e+03^{2}# (4.504267e+01)	3.112908e+03^{1} (6.416343e+00)
	5	3.940549e+04^{2}# (6.560557e+02)	4.066591e+04^{1} (1.739304e+02)
	6	5.850666e+05^{2}# (1.025724e+04)	6.087568e+05^{1} (2.568508e+03)
WFG9^{-1}	2	1.931318e+02^{1} (2.606902e-02)	1.928713e+02^{2}# (1.609428e-01)
	3	3.162863e+03^{1} (2.957373e+00)	3.097706e+03^{2}# (2.041798e+01)
	4	5.489133e+04^{1} (1.812425e+02)	5.187682e+04^{2}# (6.151134e+02)
	5	9.790684e+05^{1} (4.851532e+03)	8.951129e+05^{2}# (1.457229e+04)
	6	1.753162e+07^{1} (1.556831e+05)	1.581745e+07^{2}# (3.485680e+05)

Table B.21: Mean and, in parentheses, standard deviation of the Solow-Polasky Diversity comparison. For each case, the two best values are shown in grayscale, where the darker tone corresponds to the best algorithm. The symbol # is placed when the best algorithm presents a significant difference, according to a one-tailed Wilcoxon test using a significance level of $\alpha = 0.05$.

MOP	Dim.	PFI-EMOA	PFI-EMOA/E_s
WFG1	2	2.109587e+01^{1} (1.267764e-01)	2.068337e+01^{2}# (1.381400e-01)
	3	9.624123e+01^{1} (4.190538e-01)	8.053506e+01^{2}# (2.068510e+00)
	4	1.147895e+02^{1} (1.141692e+01)	1.022025e+02^{2}# (2.756173e+00)
	5	1.217847e+02^{1} (1.386415e+01)	1.143859e+02^{2}# (1.979497e+00)
	6	1.169086e+02^{2} (2.531683e+01)	1.175574e+02^{1} (2.186865e+00)
WFG1^{-1}	2	2.128511e+01^{1} (1.079662e-01)	2.080271e+01^{2}# (1.364942e-01)
	3	9.704829e+01^{1} (3.008739e-01)	9.139082e+01^{2}# (9.780176e-01)
	4	1.172789e+02^{1} (1.824988e-01)	1.155877e+02^{2}# (5.475224e-01)
	5	1.254844e+02^{1} (7.973820e-02)	1.247211e+02^{2}# (1.911332e-01)
	6	1.258375e+02^{1} (3.376443e-02)	1.255063e+02^{2}# (1.214112e-01)
WFG2	2	2.173769e+01^{1} (2.370399e+00)	2.014552e+01^{2}# (2.109096e+00)
	3	9.630673e+01^{1} (7.837190e+00)	6.672529e+01^{2}# (7.498575e+00)
	4	1.168621e+02^{1} (2.021163e+00)	7.392259e+01^{2}# (8.673906e+00)
	5	1.256314e+02^{1} (3.621519e-01)	9.137094e+01^{2}# (1.027938e+01)
	6	1.259546e+02^{1} (2.585669e-02)	9.032351e+01^{2}# (1.510624e+01)
WFG2^{-1}	2	2.084620e+01^{1} (3.237860e-03)	2.074116e+01^{2}# (4.444528e-02)
	3	1.126506e+02^{1} (4.984585e-01)	9.586953e+01^{2}# (2.159371e+00)
	4	1.193962e+02^{1} (5.632132e-02)	1.110985e+02^{2}# (1.765287e+00)
	5	1.259041e+02^{1} (2.413802e-02)	1.213066e+02^{2}# (1.490774e+00)
	6	1.259851e+02^{1} (5.896410e-03)	1.236637e+02^{2}# (1.091755e+00)
WFG3	2	2.309424e+01^{1} (2.981853e-03)	2.289741e+01^{2}# (6.264028e-02)
	3	8.000715e+01^{1} (1.507714e+00)	6.171575e+01^{2}# (2.203802e+00)
	4	1.188770e+02^{1} (1.190668e-01)	1.089130e+02^{2}# (1.120645e+00)
	5	1.259751e+02^{1} (1.327177e-02)	1.243581e+02^{2}# (3.353592e-01)
	6	1.259989e+02^{1} (3.626983e-04)	1.256560e+02^{2}# (9.711480e-02)
WFG3^{-1}	2	2.309436e+01^{1} (1.113493e-03)	2.289920e+01^{2}# (8.179739e-02)
	3	1.075989e+02^{1} (2.774600e-01)	1.021571e+02^{2}# (9.680692e-01)
	4	1.196857e+02^{1} (3.132902e-02)	1.190469e+02^{2}# (1.176456e-01)
	5	1.259785e+02^{1} (3.128838e-03)	1.259100e+02^{2}# (2.549723e-02)
	6	1.259985e+02^{1} (1.540491e-04)	1.259851e+02^{2}# (7.900676e-03)
WFG4	2	2.478680e+01^{1} (2.802923e-02)	2.320296e+01^{2}# (3.327672e-01)
	3	1.122361e+02^{1} (2.701175e-01)	1.051179e+02^{2}# (9.220197e-01)
	4	1.198229e+02^{1} (3.447321e-02)	1.195785e+02^{2}# (9.582595e-02)
	5	1.259920e+02^{1} (2.642950e-03)	1.259788e+02^{2}# (2.062169e-02)
	6	1.259995e+02^{1} (3.569417e-04)	1.259974e+02^{2}# (2.180183e-03)

Table B.21 – *Continuation*

MOP	Dim.	PFI-EMOA	PFI-EMOA / E_s
WFG4^{-1}	2	2.476195e+01^{1} (5.823525e-02)	2.192916e+01^{2}# (6.065371e-01)
	3	1.128389e+02^{1} (3.481339e-01)	9.750675e+01^{2}# (1.227338e+00)
	4	1.199063e+02^{1} (1.941758e-02)	1.187814e+02^{2}# (2.256696e-01)
	5	1.259980e+02^{1} (1.426392e-03)	1.259305e+02^{2}# (1.960399e-02)
	6	1.260000e+02^{1} (4.566233e-05)	1.259966e+02^{2}# (1.823110e-03)
WFG5	2	2.420076e+01^{1} (2.043890e-01)	2.286335e+01^{2}# (2.975022e-01)
	3	1.121582e+02^{1} (3.374597e-01)	1.048971e+02^{2}# (9.333345e-01)
	4	1.198163e+02^{1} (3.192123e-02)	1.195265e+02^{2}# (1.166094e-01)
	5	1.259906e+02^{1} (2.481785e-03)	1.259720e+02^{2} (1.360339e-02)
	6	1.259995e+02^{1} (2.504865e-04)	1.259972e+02^{2} (2.045833e-03)
WFG5^{-1}	2	2.396362e+01^{1} (1.997017e-01)	2.148866e+01^{2}# (4.080637e-01)
	3	1.127206e+02^{1} (2.882803e-01)	9.675575e+01^{2}# (1.327218e+00)
	4	1.199016e+02^{1} (2.888783e-02)	1.186736e+02^{2}# (2.829375e-01)
	5	1.259973e+02^{1} (1.356961e-03)	1.259205e+02^{2}# (3.336808e-02)
	6	1.259999e+02^{1} (1.122167e-04)	1.259967e+02^{2} (1.788647e-03)
WFG6	2	2.481786e+01^{1} (9.967893e-03)	2.314950e+01^{2}# (3.635698e-01)
	3	1.121773e+02^{1} (3.207710e-01)	1.046975e+02^{2}# (6.644430e-01)
	4	1.198117e+02^{1} (3.394719e-02)	1.194732e+02^{2}# (1.578850e-01)
	5	1.259921e+02^{1} (3.016284e-03)	1.259654e+02^{2}# (1.826689e-02)
	6	1.259996e+02^{1} (2.424158e-04)	1.259964e+02^{2} (2.497461e-03)
WFG6^{-1}	2	2.480575e+01^{1} (3.458560e-02)	2.188066e+01^{2}# (5.730771e-01)
	3	1.129814e+02^{1} (2.955321e-01)	9.639977e+01^{2}# (1.571255e+00)
	4	1.199089e+02^{1} (1.801891e-02)	1.186947e+02^{2}# (3.419512e-01)
	5	1.259969e+02^{1} (2.627636e-03)	1.259117e+02^{2}# (3.159465e-02)
	6	1.259999e+02^{1} (1.738770e-04)	1.259955e+02^{2}# (4.185310e-03)
WFG7	2	2.482335e+01^{1} (6.973921e-03)	2.325550e+01^{2}# (1.973024e-01)
	3	1.122480e+02^{1} (3.399162e-01)	1.040247e+02^{2}# (9.453753e-01)
	4	1.198259e+02^{1} (3.169245e-02)	1.195084e+02^{2}# (6.803129e-02)
	5	1.259919e+02^{1} (2.687853e-03)	1.259670e+02^{2}# (1.526986e-02)
	6	1.259996e+02^{1} (2.712568e-04)	1.259948e+02^{2}# (5.086754e-03)
WFG7^{-1}	2	2.477204e+01^{1} (7.492573e-02)	2.147636e+01^{2}# (7.703837e-01)
	3	1.130424e+02^{1} (2.987291e-01)	9.580924e+01^{2}# (2.504452e+00)
	4	1.199029e+02^{1} (2.929078e-02)	1.184328e+02^{2}# (2.744961e-01)
	5	1.259975e+02^{1} (2.068697e-03)	1.259061e+02^{2}# (3.932300e-02)
	6	1.259999e+02^{1} (9.938080e-05)	1.259959e+02^{2}# (1.996849e-03)
WFG8	2	2.439797e+01^{1} (1.601730e-01)	2.334875e+01^{2}# (4.391701e-01)
	3	1.130617e+02^{1} (3.077259e-01)	1.066135e+02^{2}# (9.022446e-01)
	4	1.199013e+02^{1} (1.804835e-02)	1.196783e+02^{2}# (6.532412e-02)
	5	1.259973e+02^{1} (1.048783e-03)	1.259821e+02^{2}# (9.277372e-03)
	6	1.259999e+02^{1} (7.768954e-05)	1.259995e+02^{2}# (4.622661e-04)

Table B.21 – *Continuation*

MOP	Dim.	PFI-EMOA	PFI-EMOA /E_s
WFG8^{-1}	2	2.469592e+01^{1} (2.371348e-01)	2.143227e+01^{2}# (4.928724e-01)
	3	1.129982e+02^{1} (2.655534e-01)	9.555520e+01^{2}# (1.957283e+00)
	4	1.199171e+02^{1} (2.646944e-02)	1.183027e+02^{2}# (2.553338e-01)
	5	1.259980e+02^{1} (1.577239e-03)	1.259045e+02^{2}# (4.281167e-02)
	6	1.260000e+02^{1} (3.884477e-05)	1.259943e+02^{2}# (3.835510e-03)
WFG9	2	2.380840e+01^{1} (1.354380e-02)	2.280218e+01^{2}# (2.351005e-01)
	3	1.116045e+02^{1} (3.300699e-01)	1.048471e+02^{2}# (7.809995e-01)
	4	1.198300e+02^{1} (2.992693e-02)	1.195395e+02^{2}# (1.219694e-01)
	5	1.259920e+02^{1} (3.338642e-03)	1.259749e+02^{2}# (1.487836e-02)
	6	1.259995e+02^{1} (3.585904e-04)	1.259979e+02^{2}# (1.529849e-03)
WFG9^{-1}	2	2.370890e+01^{1} (7.841698e-02)	2.166559e+01^{2}# (6.105007e-01)
	3	1.123408e+02^{1} (3.002164e-01)	9.831043e+01^{2}# (1.395372e+00)
	4	1.198990e+02^{1} (2.684260e-02)	1.189106e+02^{2}# (2.027936e-01)
	5	1.259983e+02^{1} (9.185036e-04)	1.259461e+02^{2}# (2.473406e-02)
	6	1.260000e+02^{1} (1.067027e-04)	1.259970e+02^{2}# (2.488200e-03)

Table B.22: Mean and, in parentheses, standard deviation of the IGD^+ comparison. For each case, the two best values are shown in grayscale, where the darker tone corresponds to the best algorithm. The symbol # is placed when the best algorithm presents a significant difference, according to a one-tailed Wilcoxon test using a significance level of $\alpha = 0.05$.

MOP	Dim.	PFI-EMOA	PFI-EMOA/E_s
WFG1	2	9.115576e-01^{1} (1.657392e-02)	9.165581e-01^{2}# (2.040887e-02)
	3	1.010021e+00^{2}# (1.457183e-02)	9.616945e-01^{1} (1.919204e-02)
	4	1.233856e+00^{2}# (2.853462e-02)	1.136010e+00^{1} (2.042304e-02)
	5	1.394397e+00^{2}# (4.166422e-02)	1.263166e+00^{1} (3.394956e-02)
	6	1.662798e+00^{2}# (3.794499e-02)	1.531772e+00^{1} (8.044635e-02)
WFG1^{-1}	2	8.253027e-03^{1} (1.960463e-04)	9.066011e-03^{2}# (3.137002e-04)
	3	4.493124e-02^{1} (9.430771e-04)	4.728925e-02^{2}# (1.607652e-03)
	4	1.073668e-01^{1} (1.288366e-03)	1.094403e-01^{2}# (2.613327e-03)
	5	1.851120e-01^{2}# (3.062433e-03)	1.847807e-01^{1} (3.951598e-03)
	6	2.793072e-01^{1} (3.382326e-03)	2.825421e-01^{2}# (8.235100e-03)
WFG2	2	4.585497e-02^{1} (4.326196e-02)	5.804966e-02^{2}# (4.158314e-02)
	3	1.415265e-01^{2}# (1.301301e-01)	1.368172e-01^{1} (1.304042e-01)
	4	2.351489e-01^{2}# (1.764516e-01)	2.212530e-01^{1} (1.862447e-01)
	5	2.618018e-01^{2}# (1.645899e-01)	2.166972e-01^{1} (1.865107e-01)
	6	3.553141e-01^{1} (9.703401e-02)	4.431394e-01^{2}# (3.205516e-01)
WFG2^{-1}	2	1.128369e-03^{1} (6.392690e-05)	1.318421e-03^{2}# (6.454872e-05)
	3	2.952370e-02^{1} (1.028187e-03)	3.096230e-02^{2}# (9.703427e-04)
	4	8.276346e-02^{1} (2.552918e-03)	8.446090e-02^{2}# (3.243894e-03)
	5	1.606031e-01^{2} (5.424219e-03)	1.532979e-01^{1} (4.193991e-03)
	6	2.759612e-01^{2}# (6.771591e-03)	2.528080e-01^{1} (1.715168e-02)
WFG3	2	7.526473e-03^{2}# (2.480497e-03)	5.343554e-03^{1} (1.311036e-03)
	3	4.939825e-02^{2}# (3.579629e-03)	4.148067e-02^{1} (5.023874e-03)
	4	1.647177e-01^{2}# (6.982687e-03)	1.612803e-01^{1} (9.218358e-03)
	5	3.260741e-01^{2}# (7.906645e-03)	3.142325e-01^{1} (1.595344e-02)
	6	5.276247e-01^{2}# (1.272649e-02)	4.797887e-01^{1} (2.718269e-02)
WFG3^{-1}	2	5.326644e-03^{1} (1.404378e-04)	5.855930e-03^{2}# (1.922720e-04)
	3	7.423873e-02^{1} (1.176798e-03)	8.425089e-02^{2}# (2.880330e-03)
	4	2.073665e-01^{1} (2.120844e-03)	2.404202e-01^{2}# (8.229145e-03)
	5	3.817579e-01^{1} (3.542823e-03)	4.427025e-01^{2}# (1.159040e-02)
	6	5.994293e-01^{1} (4.205715e-03)	6.812734e-01^{2}# (2.291343e-02)
WFG4	2	4.424210e-03^{2}# (4.015850e-04)	4.355761e-03^{1} (3.301835e-04)
	3	5.949619e-02^{1} (2.302430e-03)	6.270175e-02^{2}# (2.175821e-03)
	4	1.691750e-01^{1} (4.999192e-03)	1.813656e-01^{2}# (5.793652e-03)
	5	3.185089e-01^{1} (7.076493e-03)	3.398980e-01^{2}# (1.145266e-02)
	6	4.995284e-01^{2}# (6.694099e-03)	4.918688e-01^{1} (1.367575e-02)

Table B.22 – *Continuation*

MOP	Dim.	PFI-EMOA	PFI-EMOA /E_s
WFG4^{-1}	2	4.181433e-03^{1} (9.975406e-05)	5.725242e-03^{2}# (7.863212e-04)
	3	7.419888e-02^{1} (1.703669e-03)	9.323841e-02^{2}# (5.798459e-03)
	4	2.410928e-01^{1} (5.295466e-03)	2.658655e-01^{2}# (1.052869e-02)
	5	4.715287e-01^{1} (1.086823e-02)	4.827504e-01^{2}# (1.457715e-02)
	6	7.886900e-01^{2}# (1.834395e-02)	7.497597e-01^{1} (2.364108e-02)
WFG5	2	5.557323e-03^{1} (7.773013e-04)	6.224234e-03^{2}# (6.790637e-04)
	3	6.207131e-02^{1} (1.401093e-03)	6.845815e-02^{2}# (2.422769e-03)
	4	1.821591e-01^{1} (3.272253e-03)	1.942494e-01^{2}# (5.173321e-03)
	5	3.336252e-01^{1} (4.999787e-03)	3.524583e-01^{2}# (7.462237e-03)
	6	5.146595e-01^{1} (8.265724e-03)	5.259671e-01^{2}# (1.457718e-02)
WFG5^{-1}	2	4.217165e-03^{1} (2.866826e-04)	5.590409e-03^{2}# (3.917958e-04)
	3	7.403101e-02^{1} (1.808558e-03)	9.166800e-02^{2}# (4.436278e-03)
	4	2.415803e-01^{1} (4.746740e-03)	2.677282e-01^{2}# (1.568455e-02)
	5	4.826800e-01^{1} (1.082775e-02)	4.930232e-01^{2}# (1.672168e-02)
	6	8.070779e-01^{2}# (2.038862e-02)	7.882720e-01^{1} (2.530223e-02)
WFG6	2	1.349166e-02^{2}# (5.321720e-03)	1.309959e-02^{1} (3.952599e-03)
	3	6.686722e-02^{1} (5.798049e-03)	6.805676e-02^{2}# (5.833784e-03)
	4	1.766277e-01^{1} (7.069998e-03)	1.812263e-01^{2}# (8.523306e-03)
	5	3.275480e-01^{2}# (8.132956e-03)	3.219023e-01^{1} (9.453115e-03)
	6	5.007234e-01^{2}# (8.265790e-03)	4.822942e-01^{1} (1.405398e-02)
WFG6^{-1}	2	4.143433e-03^{1} (1.504485e-04)	5.905531e-03^{2}# (8.288877e-04)
	3	7.270920e-02^{1} (1.545596e-03)	9.482316e-02^{2}# (8.486262e-03)
	4	2.439402e-01^{1} (4.319743e-03)	2.762533e-01^{2}# (1.434368e-02)
	5	4.815264e-01^{1} (9.576349e-03)	5.081312e-01^{2}# (2.499539e-02)
	6	8.099175e-01^{1} (1.843198e-02)	8.264962e-01^{2}# (3.675089e-02)
WFG7	2	4.470042e-03^{1} (2.196904e-04)	4.641163e-03^{2}# (2.229314e-04)
	3	6.195437e-02^{1} (1.662629e-03)	6.673388e-02^{2}# (2.011309e-03)
	4	1.811522e-01^{1} (3.725920e-03)	1.900037e-01^{2}# (5.647145e-03)
	5	3.366201e-01^{1} (5.567184e-03)	3.502818e-01^{2}# (1.042166e-02)
	6	5.157974e-01^{1} (7.712192e-03)	5.231531e-01^{2}# (1.339382e-02)
WFG7^{-1}	2	4.113731e-03^{1} (1.561871e-04)	6.388685e-03^{2}# (1.215237e-03)
	3	7.460632e-02^{1} (1.440007e-03)	9.412492e-02^{2}# (9.279220e-03)
	4	2.429791e-01^{1} (4.469558e-03)	2.775691e-01^{2}# (1.539219e-02)
	5	4.804888e-01^{1} (1.133542e-02)	4.985058e-01^{2}# (2.403022e-02)
	6	8.159976e-01^{2}# (1.898564e-02)	7.843564e-01^{1} (3.606954e-02)
WFG8	2	1.251861e-02^{2}# (2.997322e-03)	9.540462e-03^{1} (2.083825e-03)
	3	1.147932e-01^{2}# (4.680982e-03)	1.005640e-01^{1} (2.563882e-03)
	4	2.463152e-01^{2}# (5.972833e-03)	2.417146e-01^{1} (5.116762e-03)
	5	4.194644e-01^{1} (9.043244e-03)	4.239934e-01^{2}# (8.705558e-03)
	6	6.290764e-01^{2}# (1.530398e-02)	6.144222e-01^{1} (2.166864e-02)

Table B.22 – *Continuation*

MOP	Dim.	PFI-EMOA	PFI-EMOA / E_s
WFG8^{-1}	2	4.227838e-03^{1} (3.399110e-04)	6.554587e-03^{2}# (1.087635e-03)
	3	7.640172e-02^{1} (1.507194e-03)	1.005055e-01^{2}# (7.739359e-03)
	4	2.517975e-01^{1} (7.471965e-03)	2.987936e-01^{2}# (1.787688e-02)
	5	5.006291e-01^{1} (1.783633e-02)	5.419246e-01^{2}# (3.028019e-02)
	6	8.407007e-01^{1} (2.593363e-02)	8.508832e-01^{2}# (4.091542e-02)
WFG9	2	1.464817e-02^{2}# (2.493363e-02)	9.517149e-03^{1} (1.849706e-02)
	3	8.250354e-02^{2}# (2.600644e-02)	7.534399e-02^{1} (3.098293e-02)
	4	2.374402e-01^{2}# (3.168753e-02)	1.859514e-01^{1} (7.232942e-03)
	5	3.972840e-01^{2}# (3.735980e-02)	3.389468e-01^{1} (1.260087e-02)
	6	5.930522e-01^{2}# (4.255747e-02)	5.189658e-01^{1} (1.404647e-02)
WFG9^{-1}	2	5.345475e-03^{1} (1.005427e-03)	6.040803e-03^{2}# (8.431295e-04)
	3	7.396514e-02^{1} (4.219944e-03)	8.364456e-02^{2}# (4.289072e-03)
	4	2.435354e-01^{1} (1.067815e-02)	2.436494e-01^{2}# (8.282393e-03)
	5	4.896038e-01^{2}# (1.527524e-02)	4.696935e-01^{1} (1.188562e-02)
	6	8.251119e-01^{2}# (3.446865e-02)	7.397541e-01^{1} (2.319891e-02)

Table B.23: Mean and, in parentheses, standard deviation of the Riesz s-energy comparison. For each case, the two best values are shown in grayscale, where the darker tone corresponds to the best algorithm. The symbol # is placed when the best algorithm presents a significant difference, according to a one-tailed Wilcoxon test using a significance level of $\alpha = 0.05$.

MOP	Dim.	PFI-EMOA	PFI-EMOA/E_s
WFG1	2	3.329147e+04^{1} (3.475418e+02)	3.695642e+04^{2}# (8.521587e+02)
	3	1.351747e+04^{1} (1.914082e+02)	2.317333e+04^{2}# (1.623177e+03)
	4	3.009883e+05^{2}# (1.507010e+06)	2.766205e+04^{1} (5.436916e+03)
	5	8.851787e+07^{2}# (4.497436e+08)	5.231084e+04^{1} (1.639738e+04)
	6	1.561967e+10^{2}# (4.726918e+10)	2.513951e+05^{1} (2.579443e+05)
WFG1^{-1}	2	3.267299e+04^{1} (2.957895e+02)	3.728520e+04^{2}# (6.983310e+02)
	3	1.309073e+04^{1} (1.602760e+02)	1.617819e+04^{2}# (5.460089e+02)
	4	5.142206e+03^{1} (1.627761e+02)	6.974984e+03^{2}# (5.490378e+02)
	5	2.304673e+03^{1} (2.286239e+02)	4.251543e+03^{2}# (5.985307e+02)
	6	1.175779e+03^{1} (1.873441e+02)	3.166476e+03^{2}# (8.436852e+02)
WFG2	2	3.179527e+04^{1} (3.922922e+03)	4.327748e+04^{2}# (4.653409e+03)
	3	1.370907e+04^{1} (4.184925e+03)	4.581436e+04^{2}# (1.321046e+04)
	4	5.338158e+03^{1} (2.719971e+03)	1.333627e+05^{2}# (7.499552e+04)
	5	2.011665e+03^{1} (3.389179e+03)	2.690097e+05^{2}# (2.216914e+05)
	6	3.506277e+02^{1} (1.543069e+02)	1.976637e+07^{2}# (9.439548e+07)
WFG2^{-1}	2	3.658629e+04^{2}# (6.732070e+02)	3.268646e+04^{1} (2.980483e+02)
	3	5.690934e+03^{1} (1.164613e+02)	1.433689e+04^{2}# (1.520422e+03)
	4	1.618620e+03^{1} (4.878747e+01)	1.250230e+04^{2}# (2.745825e+03)
	5	5.351819e+02^{1} (6.167807e+01)	1.610896e+04^{2}# (5.530141e+03)
	6	1.456637e+02^{1} (2.963763e+01)	3.428953e+08^{2}# (1.368595e+09)
WFG3	2	2.769320e+04^{1} (1.642458e+01)	2.929559e+04^{2}# (1.585741e+02)
	3	2.178408e+04^{1} (9.463835e+02)	3.984783e+04^{2}# (3.007675e+03)
	4	3.536110e+03^{1} (1.404055e+02)	1.697921e+04^{2}# (1.594756e+03)
	5	5.347920e+02^{1} (3.757759e+01)	6.489600e+03^{2}# (9.591245e+02)
	6	8.220811e+01^{1} (5.921658e+00)	2.688624e+03^{2}# (5.457807e+02)
WFG3^{-1}	2	2.767287e+04^{1} (6.772505e+00)	2.933093e+04^{2}# (2.950039e+02)
	3	8.749514e+03^{1} (5.507820e+01)	1.076746e+04^{2}# (3.444728e+02)
	4	1.952845e+03^{1} (2.828855e+01)	3.082660e+03^{2}# (1.475517e+02)
	5	4.597061e+02^{1} (1.973765e+01)	8.494335e+02^{2}# (8.894745e+01)
	6	9.826430e+01^{1} (3.820780e+00)	2.114603e+02^{2}# (4.571050e+01)
WFG4	2	2.738152e+04^{1} (2.967730e+02)	3.659051e+04^{2}# (7.425124e+02)
	3	6.138376e+03^{1} (6.943086e+01)	9.420715e+03^{2}# (3.521352e+02)
	4	9.502187e+02^{1} (3.060937e+01)	1.513067e+03^{2}# (1.046281e+02)
	5	1.550559e+02^{1} (1.088390e+01)	2.493811e+02^{2}# (5.576283e+01)
	6	2.172536e+01^{1} (3.866256e+00)	5.281622e+01^{2}# (1.593926e+01)

Table B.23 – *Continuation*

MOP	Dim.	PFI-EMOA	PFI-EMOA / E_s
WFG4^{-1}	2	2.717370e+04^{1} (1.329547e+02)	3.753448e+04^{2}# (1.089048e+03)
	3	6.112216e+03^{1} (7.451382e+01)	1.374494e+04^{2}# (6.624634e+02)
	4	9.137643e+02^{1} (2.205785e+01)	3.763124e+03^{2}# (4.081424e+02)
	5	1.287518e+02^{1} (6.131348e+00)	8.850418e+02^{2}# (9.111736e+01)
	6	1.324126e+01^{1} (1.394781e+00)	1.373948e+02^{2}# (1.960357e+01)
WFG5	2	2.807836e+04^{1} (3.382305e+02)	3.660464e+04^{2}# (8.390293e+02)
	3	6.183227e+03^{1} (7.781398e+01)	9.449485e+03^{2}# (3.950276e+02)
	4	9.611958e+02^{1} (2.879750e+01)	1.593252e+03^{2}# (1.196834e+02)
	5	1.600999e+02^{1} (1.149001e+01)	2.828927e+02^{2}# (4.407339e+01)
	6	2.213267e+01^{1} (3.647382e+00)	5.470417e+01^{2}# (1.585150e+01)
WFG5^{-1}	2	2.820112e+04^{1} (3.350186e+02)	3.811165e+04^{2}# (8.382697e+02)
	3	6.230716e+03^{1} (6.641772e+01)	1.418108e+04^{2}# (7.196550e+02)
	4	9.428973e+02^{1} (3.236175e+01)	3.895740e+03^{2}# (4.504751e+02)
	5	1.408827e+02^{1} (7.738585e+00)	8.937500e+02^{2}# (1.207661e+02)
	6	1.453076e+01^{1} (1.721413e+00)	1.328602e+02^{2}# (2.081667e+01)
WFG6	2	2.722857e+04^{1} (1.657321e+02)	3.686506e+04^{2}# (6.481075e+02)
	3	6.166192e+03^{1} (8.411162e+01)	9.570507e+03^{2}# (2.988953e+02)
	4	9.542430e+02^{1} (3.127038e+01)	1.633857e+03^{2}# (1.618687e+02)
	5	1.499556e+02^{1} (1.055906e+01)	3.046925e+02^{2}# (5.278851e+01)
	6	2.168297e+01^{1} (3.388418e+00)	6.154938e+01^{2}# (1.480770e+01)
WFG6^{-1}	2	2.704979e+04^{1} (7.933718e+01)	3.794797e+04^{2}# (1.103656e+03)
	3	6.080804e+03^{1} (5.769041e+01)	1.429382e+04^{2}# (8.669992e+02)
	4	9.216492e+02^{1} (2.352232e+01)	3.896387e+03^{2}# (5.881994e+02)
	5	1.359236e+02^{1} (1.138177e+01)	9.706790e+02^{2}# (1.389994e+02)
	6	1.506887e+01^{1} (2.963358e+00)	1.534958e+02^{2}# (3.984045e+01)
WFG7	2	2.718184e+04^{1} (1.854674e+02)	3.678763e+04^{2}# (7.630785e+02)
	3	6.146331e+03^{1} (7.235250e+01)	9.865287e+03^{2}# (4.235184e+02)
	4	9.436543e+02^{1} (3.156409e+01)	1.623591e+03^{2}# (7.531799e+01)
	5	1.514071e+02^{1} (1.114274e+01)	3.013311e+02^{2}# (4.257309e+01)
	6	1.975767e+01^{1} (3.896804e+00)	6.874519e+01^{2}# (2.821247e+01)
WFG7^{-1}	2	2.710387e+04^{1} (1.331955e+02)	3.821202e+04^{2}# (1.259617e+03)
	3	6.061254e+03^{1} (6.407758e+01)	1.472851e+04^{2}# (1.235191e+03)
	4	9.125687e+02^{1} (2.837814e+01)	4.445516e+03^{2}# (5.163709e+02)
	5	1.295884e+02^{1} (9.275041e+00)	1.064888e+03^{2}# (2.175854e+02)
	6	1.333349e+01^{1} (1.908695e+00)	1.653037e+02^{2}# (3.148901e+01)
WFG8	2	2.823099e+04^{1} (6.937530e+02)	3.485158e+04^{2}# (1.142719e+03)
	3	6.005994e+03^{1} (5.948055e+01)	8.793487e+03^{2}# (3.784954e+02)
	4	8.798269e+02^{1} (2.183757e+01)	1.410297e+03^{2}# (7.419741e+01)
	5	1.238760e+02^{1} (6.856216e+00)	2.412199e+02^{2}# (3.833624e+01)
	6	1.364717e+01^{1} (2.213803e+00)	3.006035e+01^{2}# (6.885682e+00)

Table B.23 – *Continuation*

MOP	Dim.	PFI-EMOA	PFI-EMOA /E_s
WFG8^{-1}	2	2.720586e+04^{1} (3.749423e+02)	3.868406e+04^{2}# (1.038919e+03)
	3	6.084666e+03^{1} (6.063735e+01)	1.477641e+04^{2}# (1.087389e+03)
	4	9.123298e+02^{1} (2.791790e+01)	4.566795e+03^{2}# (4.646474e+02)
	5	1.275566e+02^{1} (9.608725e+00)	1.047792e+03^{2}# (1.930234e+02)
	6	1.155754e+01^{1} (1.252428e+00)	1.782427e+02^{2}# (3.961740e+01)
WFG9	2	2.852723e+04^{1} (1.954992e+02)	3.677100e+04^{2}# (6.880330e+02)
	3	6.527402e+03^{1} (7.718304e+01)	9.510371e+03^{2}# (3.025597e+02)
	4	1.022240e+03^{1} (2.534339e+01)	1.630732e+03^{2}# (1.283325e+02)
	5	1.685836e+02^{1} (1.314206e+01)	2.927503e+02^{2}# (4.657119e+01)
	6	2.549840e+01^{1} (4.828954e+00)	5.039981e+01^{2}# (1.036941e+01)
WFG9^{-1}	2	2.841594e+04^{1} (2.240574e+02)	3.809430e+04^{2}# (1.078611e+03)
	3	6.515077e+03^{1} (6.803805e+01)	1.338260e+04^{2}# (7.468688e+02)
	4	1.008895e+03^{1} (2.761365e+01)	3.514470e+03^{2}# (3.227571e+02)
	5	1.457236e+02^{1} (8.756088e+00)	7.744400e+02^{2}# (1.412397e+02)
	6	1.434450e+01^{1} (2.447901e+00)	1.196224e+02^{2}# (3.180481e+01)

Table B.24: Mean and, in parentheses, standard deviation of the hypervolume comparison. For each case, the two best values are shown in grayscale, where the darker tone corresponds to the best algorithm. The symbol # is placed when the best algorithm presents a significant difference, according to a one-tailed Wilcoxon test using a significance level of $\alpha = 0.05$.

MOP	Dim.	PFI-EMOA	CRI-EMOA	AR-MOEA	RVEA	GrEA	SPEA2SDE	Two_Arch2
WFG1	2	2.358163e+01^{6}# (1.306300e-01)	2.046098e+01^{7}# (3.141128e-01)	3.069280e+01^{3} (4.945464e-01)	2.527108e+01^{5}# (4.788959e-01)	3.074409e+01^{2} (3.852634e-01)	3.081289e+01^{1} (4.385617e-01)	2.936561e+01^{4}# (5.314418e-01)
	3	2.131279e+02^{6}# (1.099155e+00)	1.900964e+02^{7}# (4.112404e+00)	2.662589e+02^{3}# (5.231819e+00)	2.393566e+02^{5}# (7.274689e+00)	2.778345e+02^{2}# (4.465463e+00)	2.909217e+02^{1} (4.836894e+00)	2.649581e+02^{4}# (4.013693e+00)
	4	2.166627e+03^{6}# (1.861384e+01)	2.009783e+03^{7}# (3.410880e+01)	2.764340e+03^{3}# (5.385023e+01)	2.556760e+03^{5}# (1.073974e+02)	2.925988e+03^{2}# (1.210929e+02)	3.128311e+03^{1} (6.879094e+01)	2.728300e+03^{4}# (7.587119e+01)
	5	2.621782e+04^{6}# (3.598616e+02)	2.473611e+04^{7}# (3.206224e+02)	3.501454e+04^{3}# (8.975453e+02)	3.291392e+04^{5}# (1.352801e+03)	3.747407e+04^{2}# (1.404690e+03)	4.000379e+04^{1} (9.578141e+02)	3.383467e+04^{4}# (9.417310e+02)
	6	3.726527e+05^{6}# (3.549169e+03)	3.600465e+05^{7}# (5.286478e+03)	4.958707e+05^{5}# (1.453065e+04)	4.965261e+05^{4}# (2.572934e+04)	5.569564e+05^{2}# (1.798772e+04)	6.078807e+05^{1} (1.850830e+04)	5.000862e+05^{3}# (1.431099e+04)
WFG1^{-1}	2	1.898476e+02^{4}# (1.083319e-03)	1.632525e+02^{7}# (3.371545e+00)	1.898487e+02^{3}# (1.640256e-02)	1.898418e+02^{5}# (8.694634e-03)	1.898123e+02^{6}# (7.823734e-03)	1.898621e+02^{1} (9.529825e-04)	1.898579e+02^{2}# (4.887755e-03)
	3	2.937552e+03^{1} (1.845366e-01)	2.040377e+03^{7}# (4.970509e+01)	2.934537e+03^{3}# (4.712976e-01)	2.553658e+03^{6}# (2.476118e+02)	2.932665e+03^{4}# (1.396882e+00)	2.935525e+03^{2}# (1.585672e+00)	2.926952e+03^{5}# (4.555382e+00)
	4	4.612943e+04^{1} (1.382122e+01)	2.518002e+04^{7}# (1.315912e+03)	4.587743e+04^{2}# (3.204342e+01)	3.585541e+04^{6}# (3.192731e+03)	4.581516e+04^{3}# (5.236184e+01)	4.576589e+04^{4}# (1.351435e+03)	4.481944e+04^{5}# (1.266004e+02)
	5	7.185021e+05^{1} (5.046183e+02)	3.178923e+05^{7}# (2.296320e+04)	7.024261e+05^{3}# (1.828009e+04)	4.943086e+05^{6}# (6.292266e+04)	7.105943e+05^{2}# (1.033639e+04)	7.022773e+05^{4}# (2.647546e+04)	6.644617e+05^{5}# (3.303038e+03)
	6	1.096231e+07^{1} (1.605262e+04)	3.720331e+06^{7}# (1.350162e+05)	1.030620e+07^{4}# (5.148565e+05)	6.544513e+06^{6}# (8.171779e+05)	1.067695e+07^{2}# (6.348200e+04)	1.047332e+07^{3}# (4.964506e+05)	9.428819e+06^{5}# (1.216308e+05)
WFG2	2	3.021306e+01^{1} (1.211301e+00)	2.976769e+01^{5} (1.142796e+00)	2.963872e+01^{6}# (1.096707e+00)	3.006485e+01^{2}# (1.081642e+00)	2.998183e+01^{3}# (1.187267e+00)	2.992370e+01^{4}# (1.188025e+00)	2.950466e+01^{7}# (1.153611e+00)
	3	2.932859e+02^{4} (1.942387e+01)	2.906137e+02^{6} (1.940231e+01)	2.882384e+02^{7} (1.914522e+01)	2.926309e+02^{5}# (1.804028e+01)	3.004686e+02^{1} (1.478390e+01)	2.965676e+02^{2} (1.738907e+01)	2.940217e+02^{3} (1.858018e+01)
	4	3.248856e+03^{2} (2.398926e+02)	3.171637e+03^{7} (2.386180e+02)	3.236786e+03^{5} (2.363735e+02)	3.241551e+03^{4}# (2.151229e+02)	3.217187e+03^{6}# (2.183348e+02)	3.277465e+03^{1} (2.077758e+02)	3.247401e+03^{3} (2.358248e+02)
	5	4.337180e+04^{1} (2.656853e+03)	4.234738e+04^{5}# (2.830321e+03)	4.289766e+04^{2}# (2.842502e+03)	4.174736e+04^{7}# (2.976394e+03)	4.286052e+04^{3}# (2.009494e+03)	4.205747e+04^{6}# (3.122508e+03)	4.254227e+04^{4}# (3.062807e+03)
	6	6.643667e+05^{1} (1.950361e+04)	6.193593e+05^{5}# (4.947302e+04)	6.335265e+05^{3}# (4.823117e+04)	6.023107e+05^{7}# (5.102523e+04)	6.204792e+05^{4}# (4.688448e+04)	6.135158e+05^{6}# (5.153235e+04)	6.408404e+05^{2}# (4.597410e+04)
WFG2^{-1}	2	1.943820e+02^{1} (1.202957e-03)	1.943728e+02^{3}# (3.575776e-03)	1.943612e+02^{4}# (1.696384e-02)	1.942841e+02^{6}# (1.758052e-02)	1.942616e+02^{7}# (7.272936e-02)	1.943464e+02^{5}# (1.969160e-02)	1.943804e+02^{2}# (1.750704e-03)
	3	3.169348e+03^{1} (2.762095e-01)	3.159506e+03^{3}# (2.141472e+00)	3.165588e+03^{2}# (6.529604e-01)	3.155338e+03^{5}# (3.958395e+00)	3.139335e+03^{7}# (1.074032e+01)	3.152202e+03^{6}# (6.397491e+00)	3.158696e+03^{4}# (2.389596e+00)
	4	5.327203e+04^{1} (1.460497e+01)	5.196805e+04^{4}# (3.395743e+02)	5.265279e+04^{2}# (9.899450e+01)	4.790003e+04^{7}# (9.537227e+01)	5.161422e+04^{5}# (6.354418e+02)	5.236668e+04^{3}# (2.313467e+02)	5.068006e+04^{6}# (6.348535e+02)
	5	8.908956e+05^{1} (8.573290e+02)	8.568351e+05^{5}# (8.615556e+03)	8.630920e+05^{3}# (1.806813e+04)	7.607602e+05^{6}# (4.285927e+04)	8.612392e+05^{4}# (6.928953e+03)	8.656491e+05^{2}# (9.629534e+03)	7.580482e+05^{7}# (1.345222e+04)
	6	1.456006e+07^{1} (2.641792e+04)	1.381013e+07^{4}# (1.465044e+05)	1.401475e+07^{2}# (2.634015e+05)	1.170504e+07^{6}# (4.569074e+05)	1.399424e+07^{3}# (8.642123e+04)	1.337313e+07^{5}# (7.958775e+05)	1.124345e+07^{7}# (2.610765e+05)
WFG3	2	3.087965e+01^{1} (2.765609e-02)	3.082216e+01^{4}# (3.644483e-02)	3.081223e+01^{5}# (7.443832e-02)	3.040946e+01^{7}# (8.861452e-02)	3.083964e+01^{3}# (5.167692e-02)	3.084813e+01^{2}# (3.342685e-02)	3.078780e+01^{6}# (8.078253e-02)
	3	2.645127e+02^{2}# (7.650054e-01)	2.617305e+02^{6}# (6.247729e-01)	2.630607e+02^{4}# (8.447237e-01)	2.595546e+02^{7}# (1.396029e+00)	2.624070e+02^{5}# (1.638489e+00)	2.640380e+02^{3}# (1.924542e+00)	2.663108e+02^{1} (4.960833e-01)
	4	2.735330e+03^{3}# (2.171440e+01)	2.704463e+03^{5}# (3.361874e+01)	2.720903e+03^{4}# (1.602966e+01)	2.753898e+03^{2}# (2.026335e+01)	2.695616e+03^{6}# (5.340386e+01)	2.603373e+03^{7}# (6.168313e+01)	2.799697e+03^{1} (9.894554e+00)
	5	3.339751e+04^{4}# (4.051637e+02)	3.320539e+04^{5}# (4.105242e+02)	3.399829e+04^{2}# (3.145995e+02)	3.163625e+04^{7}# (1.414776e+03)	3.383034e+04^{3}# (5.713333e+02)	3.211027e+04^{6}# (7.667680e+02)	3.502171e+04^{1} (2.831498e+02)
	6	4.707271e+05^{5}# (1.028587e+04)	4.752187e+05^{4}# (1.255037e+04)	4.844601e+05^{3}# (5.085924e+03)	3.791864e+05^{7}# (1.986818e+04)	4.893302e+05^{2}# (6.427895e+03)	4.664634e+05^{6}# (1.508075e+04)	5.058193e+05^{1} (3.824795e+03)

Table B.24 – *Continuation*

MOP	Dim.	PFI-EMOA	CRI-EMOA	AR-MOEA	RVEA	GrEA	SPEA2SDE	Two_Arch2
WFG3^{-1}	2	1.909592e+02^{1} (2.078171e-03)	1.908898e+02^{5} # (1.858483e-02)	1.909478e+02^{3} # (5.998415e-03)	1.905994e+02^{7} # (8.659514e-02)	1.909042e+02^{4} # (4.784569e-03)	1.908512e+02^{6} # (9.183940e-02)	1.909538e+02^{2} # (3.987649e-03)
	3	3.016005e+03^{1} (4.292382e-01)	2.997646e+03^{4} # (4.251279e+00)	3.006767e+03^{2} # (1.889688e+00)	2.988041e+03^{6} # (3.294961e+00)	2.995715e+03^{5} # (7.564430e+00)	2.961025e+03^{7} # (1.622640e+01)	3.004352e+03^{3} # (1.300051e+00)
	4	4.909318e+04^{1} (2.635916e+01)	4.649267e+04^{3} # (7.806956e+02)	4.756107e+04^{3} # (2.021916e+02)	4.447404e+04^{7} # (4.995993e+02)	4.754678e+04^{4} # (5.148836e+02)	4.639039e+04^{6} # (6.425279e+02)	4.791144e+04^{2} # (1.105660e+02)
	5	8.024166e+05^{1} (1.458510e+03)	7.262804e+05^{5} # (1.391514e+04)	7.560497e+05^{3} # (7.646565e+03)	6.601565e+05^{7} # (2.089973e+04)	7.629728e+05^{2} # (1.073046e+04)	7.095923e+05^{6} # (9.195972e+03)	7.451477e+05^{4} # (4.600033e+03)
	6	1.289127e+07^{1} (3.602451e+04)	1.108139e+07^{4} # (4.102871e+05)	1.186341e+07^{3} # (1.012234e+05)	8.263614e+06^{7} # (3.181024e+05)	1.196608e+07^{2} # (1.625987e+05)	1.036545e+07^{6} # (1.943281e+05)	1.107944e+07^{5} # (1.229557e+05)
WFG4	2	2.865515e+01^{1} (1.446041e-02)	2.857537e+01^{6} # (2.841966e-02)	2.860237e+01^{5} # (3.131877e-02)	2.822612e+01^{7} # (4.786554e-02)	2.861402e+01^{4} # (2.092087e-02)	2.864303e+01^{2} # (1.561971e-02)	2.862972e+01^{3} # (3.093790e-02)
	3	2.860305e+02^{1} (2.468886e-01)	2.812318e+02^{7} # (6.013116e-01)	2.838350e+02^{5} # (4.444247e-01)	2.832377e+02^{6} # (5.227227e-01)	2.854012e+02^{3} # (3.411759e-01)	2.855342e+02^{2} # (2.704001e-01)	2.847796e+02^{4} # (4.182312e-01)
	4	3.273250e+03^{1} (5.552212e+00)	3.231477e+03^{5} # (6.772965e+00)	3.223306e+03^{6} # (1.106752e+01)	3.239301e+03^{4} # (1.046810e+01)	3.258949e+03^{2} # (5.228763e+00)	3.258366e+03^{3} # (5.752506e+00)	3.222682e+03^{7} # (7.120927e+00)
	5	4.328951e+04^{1} (8.811447e+01)	4.240232e+04^{3} # (1.378236e+02)	4.230905e+04^{6} # (1.514367e+02)	4.260804e+04^{4} # (2.800209e+02)	4.265085e+04^{3} # (1.370661e+02)	4.289144e+04^{2} # (1.141532e+02)	4.209162e+04^{7} # (1.542492e+02)
	6	6.538111e+05^{1} (1.421185e+03)	6.391051e+05^{6} # (2.553925e+03)	6.391943e+05^{5} # (3.490089e+03)	6.432422e+05^{4} # (4.841465e+03)	6.463927e+05^{3} # (2.703534e+03)	6.478631e+05^{2} # (2.217640e+03)	6.284285e+05^{7} # (4.250163e+03)
WFG4^{-1}	2	1.932542e+02^{1} (3.372502e-03)	1.932485e+02^{3} # (1.008010e-02)	1.932431e+02^{4} # (1.322934e-02)	1.930863e+02^{5} # (1.291359e-01)	1.920802e+02^{7} # (3.670574e-01)	1.930392e+02^{6} # (8.550382e-02)	1.932506e+02^{2} (7.693159e-03)
	3	3.171981e+03^{1} (8.879317e-01)	3.145741e+03^{3} # (7.027295e+00)	3.164521e+03^{3} # (1.897552e+00)	3.151907e+03^{4} # (5.326311e+00)	3.087079e+03^{7} # (1.561030e+01)	3.105734e+03^{6} # (1.496469e+01)	3.167260e+03^{2} # (1.991934e+00)
	4	5.522090e+04^{1} (5.660081e+01)	5.128835e+04^{7} # (5.661836e+02)	5.373573e+04^{3} # (2.627340e+02)	5.197117e+04^{6} # (3.780808e+02)	5.215518e+04^{5} # (3.125833e+02)	5.237373e+04^{4} # (4.317713e+02)	5.482724e+04^{2} # (1.032664e+02)
	5	9.776882e+05^{1} (5.097973e+03)	8.677839e+05^{6} # (1.545042e+04)	9.290448e+05^{3} # (8.619983e+03)	8.473207e+05^{7} # (1.411591e+04)	9.218197e+05^{4} # (1.162314e+04)	9.099767e+05^{5} # (1.296299e+04)	9.702440e+05^{2} # (3.050591e+03)
	6	1.731875e+07^{1} (1.521168e+05)	1.499263e+07^{6} # (2.942231e+05)	1.671505e+07^{3} # (1.917634e+05)	1.455139e+07^{7} # (1.584323e+05)	1.552486e+07^{4} # (2.508976e+05)	1.550013e+07^{5} # (2.294134e+05)	1.714731e+07^{2} # (9.677798e+04)
WFG5	2	2.771126e+01^{4} # (1.249536e-01)	2.769607e+01^{6} # (8.389681e-02)	2.771869e+01^{3} # (1.041691e-01)	2.762536e+01^{7} # (1.014119e-01)	2.770421e+01^{5} # (9.323736e-02)	2.779754e+01^{1} (1.000700e-01)	2.772042e+01^{2} # (9.458660e-02)
	3	2.793949e+02^{1} (6.285803e-01)	2.754168e+02^{7} # (9.248781e-01)	2.771401e+02^{5} # (6.581456e-01)	2.773570e+02^{4} # (7.462558e-01)	2.778225e+02^{3} # (5.877729e-01)	2.781631e+02^{2} # (1.106243e+00)	2.765051e+02^{6} # (7.722893e-01)
	4	3.194398e+03^{1} (5.480228e+00)	3.166240e+03^{4} # (8.692222e+00)	3.159398e+03^{6} # (4.742798e+00)	3.173048e+03^{3} # (8.379721e+00)	3.177742e+03^{2} # (7.359752e+00)	3.165439e+03^{5} # (9.784177e+00)	3.126149e+03^{7} # (1.181161e+01)
	5	4.216984e+04^{1} (5.313406e+01)	4.167777e+04^{5} # (8.825304e+01)	4.160232e+04^{6} # (8.381304e+01)	4.200231e+04^{2} # (9.647357e+01)	4.174264e+04^{3} # (1.237706e+02)	4.171901e+04^{4} # (1.186125e+02)	4.063732e+04^{7} # (2.192150e+02)
	6	6.348109e+05^{2} # (1.326739e+03)	6.292281e+05^{4} # (1.277617e+03)	6.263432e+05^{6} # (1.188843e+03)	6.368867e+05^{1} (9.729577e+02)	6.316714e+05^{3} # (1.703037e+03)	6.283960e+05^{5} # (2.180064e+03)	6.027552e+05^{7} # (5.611793e+03)
WFG5^{-1}	2	1.931153e+02^{1} (4.037868e-02)	1.930708e+02^{4} # (3.639990e-02)	1.931002e+02^{3} # (4.598977e-02)	1.927912e+02^{6} # (4.771357e-02)	1.918370e+02^{7} # (5.072412e-01)	1.928421e+02^{5} # (9.999659e-02)	1.931013e+02^{2} (2.933217e-02)
	3	3.166070e+03^{1} (1.283254e+00)	3.156052e+03^{4} # (1.993229e+00)	3.158319e+03^{3} # (1.075462e+00)	3.144006e+03^{5} # (3.890487e+00)	3.076027e+03^{7} # (1.688717e+01)	3.094555e+03^{6} # (1.529663e+01)	3.161764e+03^{2} # (1.287658e+00)
	4	5.504353e+04^{1} (6.606727e+01)	5.093414e+04^{7} # (7.169273e+02)	5.382243e+04^{3} # (2.844372e+02)	5.159692e+04^{6} # (3.261003e+02)	5.221402e+04^{5} # (4.782467e+02)	5.224917e+04^{4} # (5.085543e+02)	5.477935e+04^{2} # (5.584427e+01)
	5	9.741062e+05^{1} (3.472732e+03)	8.736370e+05^{6} # (1.298232e+04)	9.397978e+05^{3} # (7.995449e+03)	8.367685e+05^{7} # (1.189898e+04)	9.143611e+05^{4} # (9.609424e+03)	9.014003e+05^{5} # (1.476885e+04)	9.724246e+05^{2} # (2.424753e+03)
	6	1.736080e+07^{1} (8.908162e+04)	1.509414e+07^{6} # (2.828775e+05)	1.691446e+07^{3} # (1.257727e+05)	1.447396e+07^{7} # (1.707355e+05)	1.545986e+07^{4} # (2.722908e+05)	1.543885e+07^{5} # (2.399049e+05)	1.729802e+07^{2} # (7.091231e+04)

Table B.24 – *Continuation*

MOP	Dim.	PFI-EMOA	CRI-EMOA	AR-MOEA	RVEA	GrEA	SPEA2SDE	Two_Arch2
WFG6	2	2.820239e+01[3] (5.681218e-02)	2.815398e+01[6]# (7.028054e-02)	2.819166e+01[4] (7.733620e-02)	2.766219e+01[7]# (1.008735e-01)	2.815512e+01[5]# (6.690581e-02)	2.820811e+01[1] (6.864620e-02)	2.820397e+01[2] (7.412731e-02)
	3	2.804444e+02[2] (6.676875e-01)	2.766287e+02[7]# (8.171959e-01)	2.794564e+02[5]# (9.198690e-01)	2.784051e+02[6]# (1.108958e+00)	2.802526e+02[3]# (7.225193e-01)	2.806709e+02[1] (1.001941e+00)	2.796865e+02[4]# (7.665619e-01)
	4	3.208056e+03[1] (1.060635e+01)	3.189160e+03[5]# (1.055731e+01)	3.184524e+03[6]# (8.583426e+00)	3.192370e+03[4]# (1.368715e+01)	3.205077e+03[3] (1.393098e+01)	3.205932e+03[2] (8.611619e+00)	3.166071e+03[7]# (1.258355e+01)
	5	4.237317e+04[1] (1.524483e+02)	4.217763e+04[5]# (1.727764e+02)	4.199870e+04[6]# (2.138915e+02)	4.221597e+04[3]# (2.235060e+02)	4.220943e+04[4]# (1.338486e+02)	4.233418e+04[2] (1.951132e+02)	4.127289e+04[7]# (1.969517e+02)
	6	6.416173e+05[1] (2.293627e+03)	6.380409e+05[5]# (2.636736e+03)	6.370671e+05[6]# (2.729134e+03)	6.395247e+05[3]# (4.245153e+03)	6.397233e+05[2]# (2.654722e+03)	6.394860e+05[4]# (2.971270e+03)	6.152116e+05[7]# (4.966049e+03)
$WFG6^{-1}$	2	1.932534e+02[1] (1.246504e-03)	1.932459e+02[3]# (4.811922e-03)	1.932421e+02[4]# (4.189316e-03)	1.930750e+02[5]# (5.656918e-02)	1.917670e+02[7]# (6.006513e-01)	1.929965e+02[6]# (1.423668e-01)	1.932533e+02[2] (2.922445e-03)
	3	3.172978e+03[1] (4.249662e-01)	3.159048e+03[3]# (2.413866e+00)	3.165844e+03[5]# (1.079791e+00)	3.154104e+03[3]# (8.004119e+00)	3.083645e+03[7]# (1.607450e+01)	3.105698e+03[6]# (1.766090e+01)	3.166403e+03[2]# (1.686542e+00)
	4	5.528790e+04[1] (7.056636e+01)	5.094435e+04[7]# (7.421784e+02)	5.400097e+04[3]# (2.222669e+02)	5.197538e+04[6]# (2.669151e+02)	5.201249e+04[5]# (5.500590e+02)	5.213633e+04[4]# (5.605441e+02)	5.484443e+04[2]# (7.879295e+01)
	5	9.817231e+05[1] (3.908247e+03)	8.615083e+05[5]# (2.065877e+04)	9.500927e+05[3]# (9.286514e+03)	8.445599e+05[7]# (1.294677e+04)	9.158138e+05[4]# (1.337027e+04)	9.068049e+05[5]# (1.249554e+04)	9.737582e+05[2]# (3.569085e+03)
	6	1.735694e+07[1] (2.364131e+05)	1.482018e+07[6]# (4.212915e+05)	1.710839e+07[3]# (1.597870e+05)	1.426384e+07[7]# (3.320943e+05)	1.520662e+07[5]# (3.134574e+05)	1.567143e+07[4]# (3.486910e+05)	1.733708e+07[2] (9.912919e+04)
WFG7	2	2.867600e+01[2]# (2.633365e-03)	2.863257e+01[6]# (1.421740e-02)	2.866278e+01[4]# (5.915648e-03)	2.836974e+01[7]# (2.825133e-02)	2.864606e+01[5]# (2.078786e-03)	2.867368e+01[3]# (2.122810e-03)	2.867977e+01[1] (2.851758e-03)
	3	2.867476e+02[1] (8.862747e-02)	2.838467e+02[7]# (3.939464e-01)	2.856240e+02[5]# (3.358716e-01)	2.851062e+02[6]# (2.522939e-01)	2.866620e+02[4]# (7.859014e-02)	2.865829e+02[3]# (1.183281e-01)	2.865374e+02[4]# (1.061043e-01)
	4	3.286932e+03[2]# (2.515918e+00)	3.266141e+03[6]# (3.184940e+00)	3.259254e+03[7]# (8.629086e+00)	3.272832e+03[4]# (3.660811e+00)	3.290331e+03[1] (1.761158e+00)	3.280974e+03[3]# (2.273181e+00)	3.267262e+03[5]# (4.353991e+00)
	5	4.355668e+04[1] (3.700878e+01)	4.312475e+04[5]# (7.417636e+01)	4.301140e+04[6]# (1.478476e+02)	4.317835e+04[4]# (3.042456e+02)	4.349511e+04[2]# (5.819947e+01)	4.338743e+04[3]# (5.496489e+01)	4.289224e+04[7]# (1.061023e+02)
	6	6.587560e+05[2]# (7.940577e+02)	6.547774e+05[4]# (1.028987e+03)	6.536785e+05[5]# (2.006237e+03)	6.288640e+05[7]# (1.880657e+04)	6.592714e+05[1] (7.550228e+02)	6.566490e+05[3]# (8.125447e+02)	6.434975e+05[6]# (2.898682e+03)
$WFG7^{-1}$	2	1.932545e+02[1] (1.192673e-03)	1.932295e+02[4]# (8.110666e-03)	1.932425e+02[3]# (3.339439e-03)	1.931310e+02[5]# (3.973410e-02)	1.918021e+02[7]# (5.057031e-01)	1.930051e+02[6]# (1.132724e-01)	1.932541e+02[2] (2.162043e-03)
	3	3.172054e+03[1] (8.769530e-01)	3.147451e+03[3]# (3.956933e+00)	3.162895e+03[3]# (1.820225e+00)	3.154199e+03[4]# (4.262133e+00)	3.100626e+03[7]# (1.019935e+01)	3.113952e+03[6]# (1.527764e+01)	3.168146e+03[2]# (1.152210e+00)
	4	5.522824e+04[1] (5.943769e+01)	5.156878e+04[7]# (1.078685e+03)	5.387205e+04[3]# (2.302165e+02)	5.191967e+04[6]# (4.709885e+02)	5.277442e+04[4]# (2.818981e+02)	5.253619e+04[5]# (4.902879e+02)	5.492118e+04[2]# (6.342457e+01)
	5	9.818615e+05[1] (4.350929e+03)	8.617075e+05[6]# (2.157537e+04)	9.447055e+05[3]# (6.656300e+03)	8.534014e+05[7]# (1.134766e+04)	9.296530e+05[4]# (7.837461e+03)	9.062353e+05[5]# (1.506918e+04)	9.751684e+05[2]# (2.459236e+03)
	6	1.743776e+07[1] (1.992002e+05)	1.486115e+07[6] (3.960236e+05)	1.695476e+07[3] (1.271097e+05)	1.421102e+07[7] (2.511975e+05)	1.580084e+07[5] (2.550247e+05)	1.580743e+07[4] (1.534276e+05)	1.736734e+07[2] (9.599265e+04)
WFG8	2	2.761168e+01[4]# (4.866361e-02)	2.755465e+01[6]# (6.104858e-02)	2.758774e+01[5]# (5.916393e-02)	2.696473e+01[7]# (1.191689e-01)	2.763277e+01[3]# (3.866683e-02)	2.767375e+01[1] (4.727180e-02)	2.764668e+01[2] (6.407523e-02)
	3	2.740005e+02[4] (6.178329e-01)	2.714782e+02[7] (5.299624e-01)	2.728673e+02[5] (8.885651e-01)	2.724097e+02[6] (1.756408e+00)	2.748470e+02[3] (1.155890e+00)	2.757875e+02[1] (7.120976e-01)	2.748856e+02[2] (9.188066e-01)
	4	3.097026e+03[3]# (9.856048e+00)	3.078642e+03[6]# (7.165450e+00)	3.094911e+03[4]# (8.872518e+00)	3.088827e+03[5] (2.531246e+01)	3.126620e+03[1] (1.714099e+01)	3.123369e+03[2]# (1.608863e+01)	3.077864e+03[7]# (1.900334e+01)
	5	4.050054e+04[3]# (2.133708e+02)	3.999382e+04[6]# (2.560241e+02)	4.067736e+04[2]# (1.381681e+02)	3.922243e+04[7]# (6.752828e+02)	4.046157e+04[4]# (3.734320e+02)	4.094760e+04[1] (2.538310e+02)	3.947478e+04[6]# (3.567704e+02)
	6	6.054527e+05[3]# (3.603967e+03)	5.982471e+05[5]# (5.252104e+03)	6.174620e+05[1] (3.081155e+03)	5.157317e+05[7]# (4.151858e+04)	6.008340e+05[4]# (7.835316e+03)	6.165158e+05[2]# (4.083860e+03)	5.764996e+05[6]# (7.451143e+03)

Table B.24 – *Continuation*

MOP	Dim.	PFI-EMOA	CRI-EMOA	AR-MOEA	RVEA	GrEA	SPEA2SDE	Two_Arch2
WFG8^{-1}	2	1.932124e+02^{2} (8.219975e-02)	1.931963e+02^{3} # (7.315235e-02)	1.932158e+02^{1} (6.309707e-02)	1.931781e+02^{5} # (7.178004e-02)	1.914309e+02^{7} # (4.731281e-01)	1.929230e+02^{6} # (1.318935e-01)	1.931789e+02^{4} (1.364118e-01)
	3	3.171616e+03^{1} (2.082455e+00)	3.161121e+03^{4} # (4.749265e+00)	3.167285e+03^{3} # (1.573417e+00)	3.154692e+03^{5} # (4.084415e+00)	3.071861e+03^{7} # (1.541978e+01)	3.099827e+03^{6} # (1.761166e+01)	3.168931e+03^{2} # (9.835626e-01)
	4	5.506385e+04^{1} (1.215109e+02)	5.027931e+04^{7} # (8.472145e+02)	5.391900e+04^{3} # (2.925434e+02)	5.183599e+04^{5} # (3.566496e+02)	5.141091e+04^{6} # (5.756170e+02)	5.197004e+04^{4} # (5.357706e+02)	5.495911e+04^{2} # (6.769355e+01)
	5	9.747592e+05^{2} # (5.721336e+03)	8.467807e+05^{6} # (1.564709e+04)	9.451301e+05^{3} # (8.953750e+03)	8.448855e+05^{7} # (1.338975e+04)	9.120066e+05^{4} # (1.127433e+04)	8.984553e+05^{5} # (1.290330e+04)	9.793484e+05^{1} (3.558679e+03)
	6	1.735779e+07^{2} # (1.290705e+05)	1.466467e+07^{6} # (2.341921e+05)	1.702984e+07^{3} # (9.279762e+04)	1.450729e+07^{7} # (1.466244e+05)	1.545844e+07^{5} # (2.782259e+05)	1.551109e+07^{4} # (2.911453e+05)	1.751790e+07^{1} (9.588238e+04)
WFG9	2	2.788661e+01^{1} (2.412829e-01)	2.783867e+01^{2} # (2.329423e-01)	2.752744e+01^{4} # (4.450639e-01)	2.735718e+01^{7} # (2.976044e-01)	2.748815e+01^{5} # (4.525372e-01)	2.765284e+01^{3} (4.400193e-01)	2.741008e+01^{6} # (4.428749e-01)
	3	2.739934e+02^{1} (3.095568e+00)	2.692720e+02^{4} # (2.372594e+00)	2.684009e+02^{7} # (2.893884e+00)	2.684379e+02^{6} # (3.270923e+00)	2.711681e+02^{3} # (4.918302e+00)	2.712731e+02^{2} (5.442192e+00)	2.686752e+02^{5} # (3.744890e+00)
	4	3.034026e+03^{3} (4.504267e+01)	3.065222e+03^{1} (4.543419e+01)	2.975735e+03^{7} # (2.433631e+01)	3.029494e+03^{4} # (4.316095e+01)	3.019458e+03^{5} # (5.665534e+01)	3.046335e+03^{2} (6.182995e+01)	3.007283e+03^{6} # (5.069668e+01)
	5	3.940549e+04^{4} # (6.560557e+02)	4.006788e+04^{1} (6.430478e+02)	3.845740e+04^{6} # (6.395652e+02)	3.964911e+04^{3} # (4.633683e+02)	3.905674e+04^{5} # (8.528322e+02)	3.966090e+04^{2} (9.258593e+02)	3.842404e+04^{7} # (7.556970e+02)
	6	5.850666e+05^{5} # (1.025724e+04)	6.006142e+05^{1} (9.208376e+03)	5.713890e+05^{6} # (9.559904e+03)	5.916348e+05^{2} # (1.057469e+04)	5.860593e+05^{4} # (1.469781e+04)	5.865233e+05^{3} # (1.445993e+04)	5.629328e+05^{7} # (1.284518e+04)
WFG9^{-1}	2	1.931318e+02^{1} (2.606902e-02)	1.930833e+02^{4} # (3.079370e-02)	1.931025e+02^{2} # (3.543100e-02)	1.929770e+02^{5} # (5.597734e-02)	1.915762e+02^{7} # (4.654054e-01)	1.928876e+02^{6} # (1.312428e-01)	1.930941e+02^{3} (7.471159e-02)
	3	3.162863e+03^{1} (2.957373e+00)	3.147168e+03^{4} # (4.742418e+00)	3.148595e+03^{3} # (3.525314e+00)	3.145673e+03^{5} # (4.526151e+00)	3.093612e+03^{7} # (1.619818e+01)	3.110553e+03^{6} # (1.332005e+01)	3.159583e+03^{2} # (2.393704e+00)
	4	5.489133e+04^{1} (1.812425e+02)	5.199964e+04^{6} # (5.971615e+02)	5.323195e+04^{3} # (3.257895e+02)	5.173131e+04^{7} # (3.889458e+02)	5.272235e+04^{4} # (2.968525e+02)	5.258840e+04^{5} # (4.735298e+02)	5.472879e+04^{2} # (8.956164e+01)
	5	9.790684e+05^{1} (4.851532e+03)	9.028535e+05^{6} # (1.285758e+04)	9.281536e+05^{4} # (7.861960e+03)	8.494714e+05^{7} # (8.755335e+03)	9.333918e+05^{3} # (8.307462e+03)	9.221920e+05^{5} # (1.231103e+04)	9.742258e+05^{2} # (3.810570e+03)
	6	1.753162e+07^{1} (1.556831e+05)	1.584612e+07^{6} # (2.804146e+05)	1.669699e+07^{3} # (1.747008e+05)	1.442942e+07^{7} # (3.513051e+05)	1.596942e+07^{5} # (2.764621e+05)	1.622007e+07^{4} # (2.985564e+05)	1.744417e+07^{2} # (1.034792e+05)

Table B.25: Mean and, in parentheses, standard deviation of the Solow-Polasky Diversity comparison. For each case, the two best values are shown in grayscale, where the darker tone corresponds to the best algorithm. The symbol # is placed when the best algorithm presents a significant difference, according to a one-tailed Wilcoxon test using a significance level of $\alpha = 0.05$.

MOP	Dim.	PFI-EMOA	CRI-EMOA	AR-MOEA	RVEA	GrEA	SPEA2SDE	Two_Arch2
WFG1	2	2.109587e+01^{5}# (1.267764e-01)	1.078401e+01^{7}# (4.177875e-01)	2.109409e+01^{6}# (5.747727e-01)	2.849531e+01^{1} (1.891296e+00)	2.116968e+01^{3}# (5.901525e-01)	2.146123e+01^{2}# (4.603296e-01)	2.112926e+01^{4}# (6.415228e-01)
	3	9.624123e+01^{1} (4.190538e-01)	5.009921e+01^{7}# (5.553049e+00)	8.923050e+01^{4}# (2.013415e+00)	9.204647e+01^{2}# (1.862194e+00)	7.001719e+01^{6}# (3.307328e+00)	7.804910e+01^{5}# (2.306423e+00)	8.955420e+01^{3}# (1.968642e+00)
	4	1.147895e+02^{1} (1.141692e+01)	4.546393e+01^{7}# (5.155997e+00)	1.117640e+02^{3}# (1.449512e+00)	1.100211e+02^{4}# (5.392792e+00)	7.765992e+01^{6}# (5.395929e+00)	1.004517e+02^{5}# (1.905167e+00)	1.127574e+02^{2}# (7.324747e-01)
	5	1.217847e+02^{2} (1.386415e+01)	4.510032e+01^{7}# (3.660383e+00)	1.205709e+02^{3}# (1.785242e+00)	1.156241e+02^{4}# (5.915054e+00)	8.649337e+01^{6}# (5.488266e+00)	1.126067e+02^{5}# (1.441473e+00)	1.228084e+02^{1} (4.288330e-01)
	6	1.169086e+02^{3}# (2.531683e+01)	4.396499e+01^{7}# (4.495567e+00)	1.211672e+02^{2}# (2.068992e+00)	1.159857e+02^{5}# (5.673282e+00)	9.754418e+01^{6}# (3.980088e+00)	1.161892e+02^{4}# (2.289272e+00)	1.243155e+02^{1} (4.851602e-01)
WFG1^{-1}	2	2.128511e+01^{5}# (1.079662e-01)	1.134249e+01^{7}# (8.666213e-01)	2.267652e+01^{2} (1.276509e+00)	2.258752e+01^{3} (1.306841e+00)	2.033612e+01^{6}# (9.824305e-01)	2.334140e+01^{1} (1.452136e-01)	2.233376e+01^{4}# (6.339690e-01)
	3	9.704829e+01^{1} (3.008739e-01)	5.013013e+01^{6}# (3.615676e+00)	9.375301e+01^{2}# (1.057932e+00)	3.012829e+01^{7}# (1.684494e+00)	6.219571e+01^{5}# (1.323679e+00)	8.969133e+01^{4}# (1.093058e+00)	9.266408e+01^{3}# (2.448181e+00)
	4	1.172789e+02^{1} (1.824988e-01)	8.624284e+01^{5}# (5.766791e+00)	1.090635e+02^{4}# (1.823636e+00)	1.894470e+01^{7}# (2.838294e+00)	7.049639e+01^{6}# (2.224391e+00)	1.151522e+02^{2}# (2.933069e+00)	1.130992e+02^{3}# (1.073431e+00)
	5	1.254844e+02^{1} (7.973820e-02)	1.072493e+02^{5}# (3.448400e+00)	1.187812e+02^{4}# (1.862869e+00)	1.253860e+01^{7}# (1.866764e+00)	7.303747e+01^{6}# (4.980099e+00)	1.252404e+02^{2} (5.677235e-01)	1.222587e+02^{3}# (9.990105e-01)
	6	1.258375e+02^{2}# (3.376443e-02)	1.144094e+02^{5}# (1.452339e+00)	1.185201e+02^{4}# (2.876537e+00)	8.405859e+00^{7}# (1.589139e+00)	6.786469e+01^{6}# (3.341534e+00)	1.258987e+02^{1}# (6.650953e-02)	1.238273e+02^{3}# (8.558012e-01)
WFG2	2	2.173769e+01^{2}# (2.370399e+00)	2.077414e+01^{3}# (2.239783e+00)	2.015614e+01^{6}# (2.029240e+00)	3.021605e+01^{1} (3.335071e+00)	1.829144e+01^{7}# (1.745310e+00)	2.049107e+01^{5}# (2.205809e+00)	2.050510e+01^{4}# (2.235421e+00)
	3	9.630673e+01^{1} (7.837190e+00)	9.500829e+01^{2} (8.332786e+00)	8.483362e+01^{5}# (9.568292e+00)	9.063847e+01^{4}# (8.697523e+00)	6.137095e+01^{7}# (5.743736e+00)	6.545726e+01^{6}# (6.483635e+00)	9.096248e+01^{3}# (8.536556e+00)
	4	1.168621e+02^{1} (2.021163e+00)	7.772403e+01^{5}# (9.922571e+00)	1.120222e+02^{2}# (4.758859e+00)	1.094680e+02^{4}# (6.592642e+00)	6.753551e+01^{7}# (5.228776e+00)	7.475103e+01^{6}# (7.268518e+00)	1.117605e+02^{3}# (4.516266e+00)
	5	1.256314e+02^{1} (3.621519e-01)	9.232104e+01^{5}# (1.206009e+01)	1.230226e+02^{2}# (2.598129e+00)	1.169787e+02^{4}# (7.232470e+00)	8.311129e+01^{7}# (6.046474e+00)	8.512838e+01^{6}# (1.272955e+01)	1.228170e+02^{3}# (2.337656e+00)
	6	1.259546e+02^{1} (2.585669e-02)	9.457922e+01^{6}# (1.206116e+01)	1.243413e+02^{3}# (1.615741e+00)	1.161330e+02^{4}# (6.638577e+00)	9.867598e+01^{5}# (6.592094e+00)	8.625179e+01^{7}# (1.366109e+01)	1.245005e+02^{2}# (1.318467e+00)
WFG2^{-1}	2	2.084620e+01^{4}# (3.237860e-03)	2.086429e+01^{1} (4.713900e-03)	2.086181e+01^{2} (1.255011e-02)	2.058214e+01^{6}# (9.512646e-02)	2.017158e+01^{7}# (9.144201e-02)	2.064947e+01^{5}# (4.469562e-02)	2.085908e+01^{3}# (5.119023e-03)
	3	1.126506e+02^{2}# (4.984585e-01)	1.141516e+02^{1} (4.081698e-01)	1.081706e+02^{4}# (7.715245e-01)	7.351514e+01^{6}# (5.497253e-01)	6.277653e+01^{7}# (2.938024e+00)	9.492349e+01^{5}# (1.804805e+00)	1.113503e+02^{3}# (6.793987e-01)
	4	1.193962e+02^{1} (5.632132e-02)	1.125821e+02^{3}# (1.278749e+00)	1.111001e+02^{5}# (1.741614e+00)	5.807008e+01^{7}# (1.260565e+00)	7.905963e+01^{6}# (1.041501e+01)	1.123526e+02^{4}# (1.305107e+00)	1.187274e+02^{2}# (2.164009e-01)
	5	1.259041e+02^{1} (2.413802e-02)	1.214523e+02^{4}# (2.117970e+00)	1.157333e+02^{5}# (2.464304e+00)	2.396371e+01^{7}# (6.987370e+00)	8.760720e+01^{6}# (4.287220e+00)	1.237171e+02^{3}# (4.606732e-01)	1.254707e+02^{2}# (1.795677e-01)
	6	1.259851e+02^{1} (5.896410e-03)	1.240410e+02^{4}# (5.878432e-01)	1.184813e+02^{5}# (2.954661e+00)	1.364508e+01^{7}# (2.549729e+00)	9.522875e+01^{6}# (3.675886e+00)	1.253916e+02^{3}# (2.278199e-01)	1.259306e+02^{2}# (3.791872e-02)

Table B.25 – *Continuation*

MOP	Dim.	PFI-EMOA	CRI-EMOA	AR-MOEA	RVEA	GrEA	SPEA2SDE	Two_Arch2
WFG3	2	2.309424e+01^{3}# (2.981855e-03)	2.306051e+01^{4}# (2.193324e-02)	2.310076e+01^{2}# (6.116290e-03)	2.424646e+01^{1} (3.301984e-01)	2.190562e+01^{7}# (8.779586e-02)	2.287970e+01^{6}# (9.314820e-02)	2.305149e+01^{5}# (4.965367e-03)
	3	8.000715e+01^{1} (1.507714e+00)	7.802483e+01^{2}# (1.612272e+00)	6.956504e+01^{4}# (1.778471e+00)	4.841479e+01^{6}# (3.612068e+00)	2.516510e+01^{7}# (1.109962e+00)	5.577842e+01^{5}# (2.600141e+00)	7.370684e+01^{3}# (2.039663e+00)
	4	1.188770e+02^{1} (1.190668e-01)	1.065901e+02^{5}# (1.407858e+00)	1.076944e+02^{3}# (1.800492e+00)	4.699610e+01^{6}# (2.884940e+00)	3.310061e+01^{7}# (1.728509e+01)	1.070839e+02^{4}# (2.133845e+00)	1.156584e+02^{2}# (6.705636e-01)
	5	1.259751e+02^{1} (1.327177e-02)	1.235664e+02^{4}# (6.910675e-01)	1.209988e+02^{5}# (1.525153e+00)	7.881078e+01^{7}# (2.559691e+01)	8.291652e+01^{6}# (1.763917e+01)	1.240269e+02^{3}# (4.649233e-01)	1.251514e+02^{2}# (6.729830e-01)
	6	1.259989e+02^{1} (3.626983e-04)	1.253920e+02^{4}# (2.286863e-01)	1.247397e+02^{5}# (8.014467e-01)	1.118513e+02^{6}# (6.749595e+00)	1.076055e+02^{7}# (4.866472e+00)	1.256426e+02^{2}# (1.037851e-01)	1.254749e+02^{3}# (7.466305e-01)
WFG3^{-1}	2	2.309436e+01^{3}# (1.113493e-03)	2.307066e+01^{4}# (1.100114e-02)	2.310057e+01^{2}# (2.034737e-03)	2.371387e+01^{1} (3.436494e-01)	2.168972e+01^{7}# (2.911961e-02)	2.290031e+01^{6}# (9.340415e-02)	2.304789e+01^{5}# (1.458678e-03)
	3	1.075989e+02^{1} (2.774600e-01)	1.075451e+02^{2} (2.526825e-01)	1.019030e+02^{4}# (6.439382e-01)	3.589187e+01^{7}# (3.424160e-03)	9.982008e+01^{5}# (1.637916e+00)	9.957588e+01^{6}# (9.337679e-01)	1.034684e+02^{3}# (4.328935e-01)
	4	1.196857e+02^{1} (3.132902e-02)	1.189965e+02^{2}# (1.968971e-01)	1.083079e+02^{5}# (2.470791e+00)	2.139834e+01^{7}# (2.838189e+00)	9.166070e+01^{6}# (5.946385e+00)	1.185036e+02^{4}# (2.841274e-01)	1.188650e+02^{3}# (3.181318e-01)
	5	1.259785e+02^{1} (3.128838e-03)	1.259094e+02^{2}# (3.284963e-02)	1.163541e+02^{5}# (2.205594e+00)	1.565761e+01^{7}# (1.597138e+00)	1.147778e+02^{6}# (2.420090e+00)	1.258710e+02^{3}# (2.488838e-02)	1.255944e+02^{4}# (3.818703e-01)
	6	1.259842e+02^{1} (1.540491e-04)	1.259842e+02^{3} (8.559422e-03)	1.203551e+02^{5}# (2.019402e+00)	7.481313e+00^{7}# (1.524498e+00)	1.164029e+02^{6}# (2.121820e+00)	1.259874e+02^{2}# (4.058343e-03)	1.256828e+02^{4}# (3.698431e-01)
WFG4	2	2.478680e+01^{2}# (2.802923e-02)	2.469825e+01^{3}# (6.062453e-02)	2.467201e+01^{4}# (6.275390e-02)	2.570491e+01^{1} (1.592720e-01)	2.313574e+01^{6}# (1.567072e-01)	2.274032e+01^{7}# (3.152869e-01)	2.457010e+01^{5}# (6.487525e-02)
	3	1.122361e+02^{2}# (2.701175e-01)	1.136530e+02^{1} (4.296409e-01)	1.102345e+02^{5}# (4.646873e-01)	1.107686e+02^{4}# (2.450075e-01)	1.004146e+02^{7}# (1.237348e+00)	1.012816e+02^{6}# (1.071597e+00)	1.113785e+02^{3}# (7.676708e-01)
	4	1.198229e+02^{1} (3.447321e-02)	1.196695e+02^{3}# (9.126514e-02)	1.193557e+02^{6}# (9.667877e-02)	1.194098e+02^{5}# (2.450613e-01)	1.182138e+02^{7}# (4.916332e-01)	1.194715e+02^{4}# (7.341455e-02)	1.197027e+02^{2} (3.239148e-01)
	5	1.259920e+02^{1} (2.642950e-03)	1.259864e+02^{3}# (1.224055e-02)	1.258944e+02^{4}# (5.349039e-02)	1.252518e+02^{7}# (6.425851e-01)	1.253856e+02^{6}# (4.798851e-01)	1.259880e+02^{2}# (4.014842e-03)	1.255354e+02^{5} (5.672179e-01)
	6	1.259995e+02^{2}# (3.569417e-04)	1.259985e+02^{3}# (1.446048e-03)	1.259778e+02^{4}# (2.162105e-02)	1.247995e+02^{7}# (9.789724e-01)	1.256434e+02^{5}# (4.441265e-01)	1.259998e+02^{1} (1.355778e-04)	1.250318e+02^{6}# (9.157591e-01)
WFG4^{-1}	2	2.476195e+01^{1} (5.823525e-02)	2.463392e+01^{2}# (1.175339e-01)	2.270143e+01^{5}# (4.375922e-02)	2.274876e+01^{4}# (3.964258e-01)	1.866128e+01^{7}# (7.223139e-01)	2.162790e+01^{6}# (3.859856e-01)	2.455034e+01^{3}# (1.066035e-01)
	3	1.128389e+02^{2}# (3.481339e-01)	1.131103e+02^{1} (3.970161e-01)	1.031121e+02^{4}# (7.072077e-01)	6.963941e+01^{7}# (2.481605e-01)	9.379220e+01^{5}# (1.456486e+00)	9.343232e+01^{6}# (1.127206e+00)	1.110814e+02^{3}# (4.970302e-01)
	4	1.199063e+02^{1} (1.941758e-02)	1.187134e+02^{3}# (3.034379e-01)	1.162426e+02^{6}# (1.496552e+00)	4.121938e+01^{7}# (2.005497e+00)	1.182420e+02^{5}# (8.055880e-01)	1.184327e+02^{4}# (2.609025e-01)	1.198756e+02^{2}# (3.335510e-02)
	5	1.259980e+02^{1} (1.426392e-03)	1.259204e+02^{4}# (2.865137e-02)	1.218180e+02^{6}# (1.285117e+00)	3.362800e+01^{7}# (1.191803e+00)	1.258899e+02^{5}# (2.162719e-01)	1.259386e+02^{3}# (1.309135e-02)	1.259978e+02^{2}# (1.151322e-03)
	6	1.260000e+02^{1} (4.566233e-05)	1.259933e+02^{5}# (3.635211e-03)	1.218208e+02^{6}# (1.494543e+00)	2.751838e+01^{7}# (2.166360e+00)	1.259971e+02^{3}# (5.247005e-03)	1.259984e+02^{2}# (6.164414e-04)	1.259961e+02^{4} (1.135593e-02)
WFG5	2	2.420076e+01^{2}# (2.043890e-01)	2.417540e+01^{4}# (1.350150e-01)	2.419675e+01^{3}# (1.706927e-01)	2.490217e+01^{1} (2.871437e-01)	2.220605e+01^{7}# (1.194087e-01)	2.255248e+01^{6}# (3.012163e-01)	2.409119e+01^{5}# (1.784920e-01)
	3	1.121582e+02^{2}# (3.374597e-01)	1.135241e+02^{1} (3.566099e-01)	1.104561e+02^{4}# (3.266547e-01)	1.094091e+02^{5}# (6.021834e-01)	9.744891e+01^{7}# (1.040139e+00)	1.012279e+02^{6}# (1.290117e+00)	1.109783e+02^{3}# (6.368936e-01)
	4	1.198163e+02^{1} (3.192123e-02)	1.195897e+02^{2}# (1.360919e-01)	1.190255e+02^{6}# (2.724611e-01)	1.193053e+02^{5}# (1.149292e-01)	1.176230e+02^{7}# (7.006338e-01)	1.194421e+02^{4}# (7.866534e-02)	1.194457e+02^{3}# (4.196461e-01)
	5	1.259906e+02^{1} (2.481785e-03)	1.259809e+02^{3}# (1.047856e-02)	1.258423e+02^{5}# (6.062069e-02)	1.259249e+02^{4}# (1.706385e-02)	1.248496e+02^{7}# (8.177616e-01)	1.259864e+02^{2}# (4.777488e-03)	1.253380e+02^{6}# (6.594382e-01)
	6	1.259995e+02^{2}# (2.504865e-04)	1.259977e+02^{3}# (1.713202e-03)	1.259765e+02^{5}# (1.779876e-02)	1.259916e+02^{4}# (1.410610e-03)	1.256264e+02^{6}# (5.143144e-01)	1.259998e+02^{1} (1.276569e-04)	1.255011e+02^{7}# (6.368996e-01)

Table B.25 – *Continuation*

MOP	Dim.	PFI-EMOA	CRI-EMOA	AR-MOEA	RVEA	GrEA	SPEA2SDE	Two_Arch2
WFG5^{-1}	2	2.396362e+01^{1} (1.997017e-01)	2.390198e+01^{2} (1.589013e-01)	2.244721e+01^{4}# (1.068973e-01)	2.240897e+01^{5}# (2.611691e-01)	1.855529e+01^{7}# (6.572637e-01)	2.116966e+01^{6}# (4.594978e-01)	2.377489e+01^{3}# (1.760552e-01)
	3	1.127206e+02^{2} (2.882803e-01)	1.131544e+02^{1}# (2.433931e-01)	1.023449e+02^{4}# (7.345872e-01)	6.944584e+01^{7}# (3.920327e-01)	9.119332e+01^{6}# (2.302628e+00)	9.243098e+01^{5}# (1.263926e+00)	1.105587e+02^{3}# (6.529015e-01)
	4	1.199016e+02^{1} (2.888783e-02)	1.186326e+02^{3}# (3.025300e-01)	1.170577e+02^{5}# (1.679763e+00)	4.025776e+01^{7}# (1.529437e+00)	1.170297e+02^{6}# (1.540021e+00)	1.183161e+02^{4}# (3.187787e-01)	1.197672e+02^{2}# (2.042156e-01)
	5	1.259973e+02^{1} (1.356961e-03)	1.259186e+02^{5}# (3.002682e-02)	1.209158e+02^{6}# (1.310029e+00)	3.381271e+01^{7}# (1.334173e+00)	1.259367e+02^{3}# (8.059995e-02)	1.259303e+02^{4}# (1.893283e-02)	1.259702e+02^{2} (1.281696e-01)
	6	1.259999e+02^{1} (1.122167e-04)	1.259942e+02^{5}# (4.556579e-03)	1.186453e+02^{6}# (1.770611e+00)	2.711092e+01^{7}# (2.131217e+00)	1.259974e+02^{4}# (3.590526e-03)	1.259983e+02^{3}# (5.538740e-04)	1.259999e+02^{2} (5.055250e-04)
WFG6	2	2.481786e+01^{2}# (9.967893e-03)	2.474722e+01^{4}# (3.719593e-02)	2.476149e+01^{3}# (3.100789e-02)	2.785873e+01^{1} (6.108140e-01)	2.306711e+01^{6}# (2.068071e-01)	2.284938e+01^{7}# (4.016680e-01)	2.464008e+01^{5}# (3.646070e-02)
	3	1.121773e+02^{2}# (3.207710e-01)	1.134506e+02^{1} (2.446074e-01)	1.105300e+02^{5}# (3.413109e-01)	1.110898e+02^{4}# (8.306738e-02)	9.855427e+01^{7}# (1.069266e+00)	1.010174e+02^{6}# (1.115250e+00)	1.113760e+02^{3}# (4.396723e-01)
	4	1.198117e+02^{2}# (3.394719e-02)	1.195738e+02^{3}# (1.039988e-01)	1.194609e+02^{5}# (9.710963e-02)	1.195578e+02^{4}# (1.185569e-02)	1.179322e+02^{7}# (1.092179e+00)	1.194247e+02^{6}# (1.301788e-01)	1.198558e+02^{1} (1.739512e-01)
	5	1.259921e+02^{1} (3.016284e-03)	1.259732e+02^{3}# (1.294283e-02)	1.259430e+02^{4}# (2.028008e-02)	1.256913e+02^{6}# (9.621768e-01)	1.245882e+02^{7}# (8.053445e-01)	1.259802e+02^{2}# (5.938133e-03)	1.256968e+02^{5} (5.669729e-01)
	6	1.259996e+02^{2} (2.424158e-04)	1.259973e+02^{3}# (1.369369e-03)	1.259916e+02^{4}# (4.766061e-03)	1.255479e+02^{6}# (6.856558e-01)	1.256759e+02^{5}# (3.842749e-01)	1.259997e+02^{1} (1.717337e-04)	1.254539e+02^{7} (7.750579e-01)
WFG6^{-1}	2	2.480575e+01^{1} (3.458560e-02)	2.464947e+01^{2}# (6.556439e-02)	2.274118e+01^{5}# (1.359576e-02)	2.274735e+01^{4}# (2.132691e-01)	1.814374e+01^{7}# (5.384157e-01)	2.157384e+01^{6}# (6.098047e-01)	2.461247e+01^{3}# (1.031774e-01)
	3	1.129814e+02^{2}# (2.955321e-01)	1.132974e+02^{1} (3.149108e-01)	1.034108e+02^{4}# (4.941460e-01)	6.998426e+01^{7}# (6.060158e-01)	9.123861e+01^{6}# (2.368943e+00)	9.346903e+01^{5}# (1.961992e+00)	1.111479e+02^{3}# (6.629886e-01)
	4	1.199089e+02^{1} (1.801891e-02)	1.186697e+02^{3}# (2.781869e-01)	1.172723e+02^{5}# (1.347991e+00)	3.977623e+01^{7}# (1.662199e+00)	1.167241e+02^{6}# (1.279586e+00)	1.182184e+02^{4}# (2.998126e-01)	1.198209e+02^{2}# (1.585442e-01)
	5	1.259969e+02^{1} (2.627636e-03)	1.259025e+02^{4}# (3.883304e-02)	1.204775e+02^{6}# (1.949389e+00)	3.481445e+01^{7}# (1.441170e+00)	1.258826e+02^{5}# (2.210754e-01)	1.259300e+02^{3}# (2.147438e-02)	1.259957e+02^{2} (1.087041e-02)
	6	1.259999e+02^{1} (1.738770e-04)	1.259941e+02^{4}# (3.179142e-03)	1.178352e+02^{6}# (1.735536e+00)	2.670330e+01^{7}# (3.004001e+00)	1.259909e+02^{5}# (2.212500e-02)	1.259981e+02^{2}# (7.161281e-04)	1.259961e+02^{3} (1.873764e-02)
WFG7	2	2.482335e+01^{2}# (6.973921e-03)	2.475690e+01^{4}# (6.864696e-02)	2.478451e+01^{3}# (1.944659e-02)	2.567376e+01^{1} (1.871121e-01)	2.280030e+01^{6}# (2.460414e-01)	2.258659e+01^{7}# (4.211523e-01)	2.464020e+01^{5}# (4.007583e-02)
	3	1.122480e+02^{2}# (3.399162e-01)	1.138369e+02^{1} (3.177204e-01)	1.107509e+02^{5}# (2.785713e-01)	1.110071e+02^{4}# (5.493356e-02)	9.810256e+01^{7}# (1.632241e+00)	1.010586e+02^{6}# (9.939554e-01)	1.118264e+02^{3}# (4.899654e-01)
	4	1.198259e+02^{1} (3.169245e-02)	1.196000e+02^{3}# (9.220591e-02)	1.194301e+02^{5}# (1.795451e-01)	1.191670e+02^{6}# (7.090217e-01)	1.179153e+02^{7}# (6.668389e-01)	1.194598e+02^{4}# (8.845999e-02)	1.196114e+02^{2} (4.507907e-01)
	5	1.259919e+02^{1} (2.687853e-03)	1.259765e+02^{3}# (1.670540e-02)	1.259149e+02^{4}# (4.883140e-02)	1.237136e+02^{7}# (1.559767e+00)	1.246660e+02^{6}# (7.854836e-01)	1.259859e+02^{2}# (4.024677e-03)	1.257345e+02^{5} (5.027896e-01)
	6	1.259996e+02^{2} (2.712568e-04)	1.259971e+02^{3}# (2.027229e-03)	1.259929e+02^{4}# (1.962180e-03)	1.210653e+02^{7}# (3.859057e+00)	1.256785e+02^{6}# (4.060226e-01)	1.259997e+02^{1} (1.031732e-04)	1.257980e+02^{5} (3.114830e-01)
WFG7^{-1}	2	2.477204e+01^{1} (7.492573e-02)	2.454503e+01^{3}# (1.111417e-01)	2.273542e+01^{4}# (2.771317e-02)	2.272617e+01^{5}# (2.047459e-01)	1.828900e+01^{7}# (5.591708e-01)	2.158839e+01^{6}# (5.377902e-01)	2.458805e+01^{2}# (1.285602e-01)
	3	1.130424e+02^{2}# (2.987291e-01)	1.132926e+02^{1} (2.643000e-01)	1.034386e+02^{4}# (5.828582e-01)	6.953994e+01^{7}# (4.698715e-01)	9.201835e+01^{6}# (2.422617e+00)	9.423779e+01^{5}# (1.877377e+00)	1.113615e+02^{3}# (5.132022e-01)
	4	1.199029e+02^{1} (2.929078e-02)	1.187103e+02^{3}# (4.799481e-01)	1.169475e+02^{6}# (1.318212e+00)	4.125149e+01^{7}# (1.577645e+00)	1.177411e+02^{5}# (1.557643e+00)	1.185845e+02^{4}# (2.556814e-01)	1.198888e+02^{2}# (1.773242e-02)
	5	1.259975e+02^{1} (2.068697e-03)	1.258923e+02^{5}# (4.791840e-02)	1.217071e+02^{6}# (1.559759e+00)	3.303616e+01^{7}# (1.318336e+00)	1.259172e+02^{4}# (1.552581e-01)	1.259458e+02^{3}# (2.308731e-02)	1.259966e+02^{2} (5.745052e-03)
	6	1.259999e+02^{1} (9.938080e-05)	1.259877e+02^{5}# (1.191994e-02)	1.192834e+02^{6}# (2.593158e+00)	2.839062e+01^{7}# (2.769284e+00)	1.259983e+02^{4}# (3.594421e-03)	1.259991e+02^{2}# (3.910873e-04)	1.259988e+02^{3} (4.516876e-03)

Table B.25 – *Continuation*

MOP	Dim.	PFI-EMOA	CRI-EMOA	AR-MOEA	RVEA	GrEA	SPEA2SDE	Two_Arch2
WFG8	2	2.439797e+01^{2}# (1.601730e-01)	2.418730e+01^{4}# (3.682527e-01)	2.425884e+01^{3}# (2.983328e-01)	3.049619e+01^{1} (1.112619e+00)	2.289005e+01^{6}# (2.406462e-01)	2.275991e+01^{7}# (3.741676e-01)	2.377359e+01^{5}# (6.222124e-01)
	3	1.130617e+02^{2}# (3.077259e-01)	1.136160e+02^{1} (3.400146e-01)	1.102710e+02^{4}# (7.532041e-01)	1.075845e+02^{5}# (7.937709e-01)	9.813709e+01^{7}# (1.781766e+00)	1.034702e+02^{6}# (1.205052e+00)	1.113136e+02^{3}# (8.992741e-01)
	4	1.199013e+02^{1} (1.804835e-02)	1.197416e+02^{2}# (6.753678e-02)	1.193228e+02^{5}# (4.360713e-01)	1.192317e+02^{6}# (4.633728e-01)	1.162825e+02^{7}# (1.261056e+00)	1.196279e+02^{3}# (6.584665e-02)	1.196102e+02^{4} (4.153279e-01)
	5	1.259973e+02^{1} (1.048783e-03)	1.259892e+02^{3}# (7.201471e-03)	1.256085e+02^{5}# (4.582224e-01)	1.251827e+02^{6}# (7.793179e-01)	1.247461e+02^{7}# (8.985097e-01)	1.259921e+02^{2}# (2.602916e-03)	1.257965e+02^{4} (3.364029e-01)
	6	1.259999e+02^{1} (7.768954e-05)	1.259995e+02^{3}# (3.914028e-04)	1.252909e+02^{6}# (6.747833e-01)	1.197329e+02^{7}# (3.768799e+00)	1.257497e+02^{5}# (4.488127e-01)	1.259999e+02^{2}# (8.429486e-05)	1.259075e+02^{4} (2.380732e-01)
WFG8^{-1}	2	2.469592e+01^{1} (2.371348e-01)	2.464706e+01^{2}# (1.669531e-01)	2.269366e+01^{5}# (9.470041e-02)	2.276429e+01^{4}# (1.883106e-01)	1.759191e+01^{7}# (6.998997e-01)	2.117162e+01^{6}# (5.608469e-01)	2.449328e+01^{3}# (2.928607e-01)
	3	1.129982e+02^{2}# (2.655534e-01)	1.135309e+02^{1} (2.834510e-01)	1.033283e+02^{4}# (8.475131e-01)	6.981963e+01^{7}# (3.256759e-01)	8.920411e+01^{6}# (2.994162e+00)	9.216301e+01^{5}# (1.691634e+00)	1.113213e+02^{3}# (5.874043e-01)
	4	1.199171e+02^{1} (2.646944e-02)	1.184055e+02^{3}# (3.466429e-01)	1.166992e+02^{5}# (1.502776e+00)	4.092348e+01^{7}# (1.330871e+00)	1.163814e+02^{6}# (1.405091e+00)	1.179598e+02^{4}# (3.505367e-01)	1.198735e+02^{2}# (2.647542e-02)
	5	1.259980e+02^{1} (1.577239e-03)	1.258925e+02^{4}# (3.808580e-02)	1.204254e+02^{6}# (1.967993e+00)	3.455447e+01^{7}# (1.812456e+00)	1.258040e+02^{5}# (2.686210e-01)	1.259033e+02^{3}# (2.432852e-02)	1.259301e+02^{2}# (2.187961e-01)
	6	1.260000e+02^{1} (3.884477e-05)	1.259885e+02^{5}# (9.116978e-03)	1.178581e+02^{6}# (2.217972e+00)	2.759221e+01^{7}# (1.948701e+00)	1.259949e+02^{3}# (1.028751e-02)	1.259975e+02^{4}# (8.331111e-04)	1.259912e+02^{4}# (4.427105e-02)
WFG9	2	2.380840e+01^{2}# (1.354380e-02)	2.375441e+01^{4}# (9.777369e-02)	2.378733e+01^{3}# (5.430909e-02)	2.439499e+01^{1} (4.577117e-01)	2.223639e+01^{7}# (1.573624e-01)	2.241715e+01^{6}# (2.870467e-01)	2.368837e+01^{5}# (5.947863e-02)
	3	1.116045e+02^{2}# (3.300699e-01)	1.129103e+02^{1} (3.192390e-01)	1.095809e+02^{4}# (4.072742e-01)	1.083387e+02^{5}# (3.397103e-01)	9.722533e+01^{7}# (1.902717e+00)	1.016451e+02^{6}# (9.026633e-01)	1.107621e+02^{3}# (6.078575e-01)
	4	1.198300e+02^{1} (2.992693e-02)	1.196327e+02^{2}# (1.081220e-01)	1.188723e+02^{5}# (4.484114e-01)	1.190943e+02^{4}# (1.253889e-01)	1.175969e+02^{7}# (7.962013e-01)	1.194671e+02^{3}# (1.351153e-01)	1.187482e+02^{6}# (5.544526e-01)
	5	1.259920e+02^{1} (3.338642e-03)	1.259812e+02^{3}# (1.014226e-02)	1.256830e+02^{5}# (1.939944e-01)	1.258358e+02^{4}# (4.497539e-02)	1.254129e+02^{6}# (5.207319e-01)	1.259874e+02^{2}# (5.092260e-03)	1.249620e+02^{7}# (7.660655e-01)
	6	1.259995e+02^{2}# (3.585904e-04)	1.259988e+02^{3}# (1.033327e-03)	1.258749e+02^{5}# (1.167310e-01)	1.259723e+02^{4}# (1.066465e-02)	1.258558e+02^{6}# (2.729391e-01)	1.259998e+02^{1} (1.145157e-04)	1.249246e+02^{7}# (8.398425e-01)
WFG9^{-1}	2	2.370890e+01^{1} (7.841698e-02)	2.360701e+01^{2}# (1.077844e-01)	2.245446e+01^{5}# (4.239221e-02)	2.251946e+01^{4}# (1.408323e-01)	1.849896e+01^{7}# (5.056274e-01)	2.144548e+01^{6}# (3.485248e-01)	2.356125e+01^{3}# (1.753061e-01)
	3	1.123408e+02^{2}# (3.002164e-01)	1.125617e+02^{1} (2.434848e-01)	1.016797e+02^{4}# (8.539727e-01)	6.911772e+01^{7}# (4.565947e-01)	9.492851e+01^{5}# (3.012300e+00)	9.484406e+01^{6}# (1.415321e+00)	1.102567e+02^{3}# (5.399876e-01)
	4	1.198990e+02^{1} (2.684260e-02)	1.190906e+02^{3}# (2.430171e-01)	1.167171e+02^{6}# (1.123457e+00)	3.962517e+01^{7}# (1.766247e+00)	1.184856e+02^{5}# (8.545133e-01)	1.187650e+02^{4}# (2.480438e-01)	1.196363e+02^{2}# (2.181985e-01)
	5	1.259983e+02^{1} (9.185036e-04)	1.259638e+02^{3}# (2.559260e-02)	1.230644e+02^{6}# (9.725025e-01)	3.288819e+01^{7}# (1.286149e+00)	1.259554e+02^{4}# (7.050575e-02)	1.259666e+02^{2}# (1.362198e-02)	1.258781e+02^{5}# (2.182330e-01)
	6	1.260000e+02^{1} (1.067027e-04)	1.259984e+02^{4}# (1.575202e-03)	1.231854e+02^{6}# (1.642824e+00)	2.506163e+01^{7}# (1.968895e+00)	1.259988e+02^{3}# (1.830671e-03)	1.259994e+02^{2}# (1.662959e-04)	1.259891e+02^{5}# (2.719487e-02)

Table B.26: Mean and, in parentheses, standard deviation of the IGD$^+$ comparison. For each case, the two best values are shown in grayscale, where the darker tone corresponds to the best algorithm. The symbol # is placed when the best algorithm presents a significant difference, according to a one-tailed Wilcoxon test using a significance level of $\alpha = 0.05$.

MOP	Dim.	PFI-EMOA	CRI-EMOA	AR-MOEA	RVEA	GrEA	SPEA2SDE	Two_Arch2
WFG1	2	9.115576e-01^{6}# (1.657392e-02)	1.007912e+00^{7}# (2.569130e-02)	6.937610e-02^{3} (5.509171e-02)	7.055580e-01^{5}# (5.991814e-02)	6.190270e-02^{2} (4.051828e-02)	5.749991e-02^{1} (4.676162e-02)	2.126311e-01^{4}# (5.817599e-02)
	3	1.010021e+00^{6}# (1.457183e-02)	1.132705e+00^{7}# (2.378500e-02)	3.673443e-01^{4}# (6.324235e-02)	7.023984e-01^{5}# (8.179109e-02)	1.957735e-01^{2}# (4.337701e-02)	7.696161e-02^{1} (3.937960e-02)	3.628441e-01^{3}# (4.973115e-02)
	4	1.233856e+00^{7}# (2.853462e-02)	1.221671e+00^{6}# (1.897300e-02)	5.822389e-01^{4}# (5.741085e-02)	7.763957e-01^{5}# (1.124731e-01)	3.517698e-01^{2}# (8.291925e-02)	1.572294e-01^{1} (5.011420e-02)	5.711432e-01^{3}# (7.963294e-02)
	5	1.394397e+00^{7}# (4.166422e-02)	1.300750e+00^{6}# (1.826167e-02)	6.181026e-01^{3}# (7.478021e-02)	7.303908e-01^{5}# (1.209344e-01)	3.399326e-01^{2}# (9.047963e-02)	1.502983e-01^{1} (5.294909e-02)	6.532155e-01^{4}# (8.007796e-02)
	6	1.662798e+00^{7}# (3.794499e-02)	1.401776e+00^{6}# (1.821361e-02)	8.580047e-01^{5}# (9.066556e-02)	7.756247e-01^{4}# (1.434205e-01)	4.376272e-01^{2}# (8.441897e-02)	1.591565e-01^{1} (6.950354e-02)	7.706958e-01^{3}# (7.748190e-02)
WFG1^{-1}	2	8.253027e-03^{5}# (1.960463e-04)	6.323587e-01^{7}# (1.027720e-01)	6.454689e-03^{3} (1.670126e-03)	7.841979e-03^{4}# (1.774748e-03)	1.340748e-02^{6}# (1.475463e-03)	5.271464e-03^{1} (1.813165e-04)	6.173818e-03^{2}# (1.042758e-03)
	3	4.493124e-02^{1} (9.430771e-04)	9.129636e-01^{7}# (7.267905e-02)	4.982709e-02^{3}# (1.127930e-03)	6.401918e-01^{6}# (4.010451e-01)	5.886510e-02^{5}# (3.197274e-03)	4.683167e-02^{2}# (3.307412e-03)	5.786344e-02^{4}# (1.330295e-02)
	4	1.073668e-01^{1} (1.288366e-03)	1.285351e+00^{7}# (1.382060e-01)	1.327878e-01^{3}# (3.915220e-03)	9.767525e-01^{6}# (3.458756e-01)	1.376204e-01^{4}# (3.782020e-03)	1.272300e-01^{2} (1.045444e-01)	1.959820e-01^{5}# (1.449744e-02)
	5	1.851120e-01^{1} (3.062433e-03)	1.662413e+00^{7}# (1.518566e-01)	2.465158e-01^{3}# (4.847691e-02)	1.238865e+00^{6}# (3.752448e-01)	2.673640e-01^{4}# (5.684531e-02)	2.159745e-01^{2} (8.843243e-02)	4.000797e-01^{5}# (1.916149e-02)
	6	2.793072e-01^{1} (3.382326e-03)	2.067693e+00^{7}# (7.737639e-02)	4.107206e-01^{3}# (8.927876e-02)	1.598812e+00^{6}# (4.250794e-01)	4.282958e-01^{4}# (1.014300e-02)	3.434530e-01^{2} (1.352794e-01)	6.488275e-01^{5}# (2.913807e-02)
WFG2	2	4.585497e-02^{1} (4.326196e-02)	6.118104e-02^{4} (4.124097e-02)	6.874805e-02^{5}# (3.869654e-02)	9.396960e-02^{7}# (3.827834e-02)	5.760244e-02^{3}# (4.113092e-02)	5.672339e-02^{2} (4.225125e-02)	8.114639e-02^{6}# (4.521235e-02)
	3	1.415265e-01^{4} (1.301301e-01)	1.639012e-01^{5}# (1.294658e-01)	1.820658e-01^{7}# (1.244691e-01)	1.646630e-01^{6}# (1.146291e-01)	8.462364e-02^{1} (1.008449e-01)	1.067040e-01^{2} (1.190424e-01)	1.401060e-01^{3}# (1.242149e-01)
	4	2.351489e-01^{5}# (1.764516e-01)	2.602097e-01^{7}# (1.932322e-01)	2.377572e-01^{6}# (1.761734e-01)	2.067051e-01^{2}# (1.694405e-01)	2.207477e-01^{3}# (1.762322e-01)	1.726168e-01^{1} (1.680914e-01)	2.255780e-01^{4}# (1.838343e-01)
	5	2.618018e-01^{4}# (1.645899e-01)	2.534976e-01^{3} (2.086643e-01)	2.365224e-01^{2} (1.946883e-01)	2.621044e-01^{5} (2.231386e-01)	2.023657e-01^{1} (1.486851e-01)	2.683562e-01^{6} (2.298149e-01)	2.697322e-01^{7} (2.149505e-01)
	6	3.553141e-01^{2}# (9.703401e-02)	4.148126e-01^{5} (3.159326e-01)	3.752851e-01^{3}# (2.728342e-01)	4.613669e-01^{7} (3.324552e-01)	3.884635e-01^{4} (3.005179e-01)	4.430212e-01^{6} (3.284689e-01)	3.357483e-01^{1} (2.770340e-01)
WFG2^{-1}	2	1.128369e-03^{1} (6.392690e-05)	1.323915e-03^{3}# (9.231289e-05)	1.381916e-03^{4}# (1.042419e-04)	9.003715e-03^{7}# (1.136059e-03)	2.271142e-03^{6}# (1.539577e-04)	1.492682e-03^{5}# (1.000977e-04)	1.290543e-03^{2}# (7.704822e-05)
	3	2.952370e-02^{1} (1.028187e-03)	3.729886e-02^{4}# (2.353607e-03)	3.070180e-02^{2}# (1.227085e-03)	5.106594e-02^{7}# (4.178392e-03)	5.044887e-02^{6}# (1.999052e-03)	3.084678e-02^{3}# (1.253206e-03)	4.060646e-02^{5}# (3.108791e-03)
	4	8.276346e-02^{1} (2.552918e-03)	9.387057e-02^{3}# (3.930997e-03)	1.138813e-01^{5}# (4.089145e-03)	3.604647e-01^{7}# (3.586464e-03)	1.126034e-01^{4}# (8.292732e-03)	8.406899e-02^{2}# (2.687040e-03)	2.419095e-01^{6}# (4.096590e-02)
	5	1.606031e-01^{2}# (5.424219e-03)	1.678047e-01^{3}# (7.529031e-03)	2.252632e-01^{5}# (3.570871e-02)	5.965623e-01^{6}# (1.335550e-01)	1.891525e-01^{4}# (6.112930e-03)	1.516533e-01^{1} (1.579487e-02)	6.476522e-01^{7}# (7.068499e-02)
	6	2.759612e-01^{2}# (6.771591e-03)	2.568074e-01^{1} (9.328315e-03)	3.474080e-01^{5}# (1.715572e-02)	8.566605e-01^{6}# (6.568290e-02)	3.093773e-01^{3}# (1.315198e-02)	3.335271e-01^{4} (1.302888e-01)	9.590746e-01^{7}# (7.358504e-02)
WFG3	2	7.526473e-03^{1} (2.480497e-03)	1.062874e-02^{3}# (3.030055e-03)	1.373330e-02^{4}# (7.499289e-03)	6.786174e-02^{7}# (1.090328e-02)	1.452694e-02^{5}# (4.664586e-03)	7.936936e-03^{2} (1.905611e-03)	1.666279e-02^{6}# (8.048765e-03)
	3	4.939825e-02^{2}# (3.579629e-03)	6.090213e-02^{5}# (3.483948e-03)	6.023090e-02^{4}# (3.210105e-03)	1.236786e-01^{6}# (1.158731e-02)	1.418986e-01^{7}# (4.033561e-03)	5.526068e-02^{3}# (5.942004e-03)	3.851703e-02^{1} (2.073101e-03)
	4	1.647177e-01^{3}# (6.982687e-03)	1.804736e-01^{5}# (8.732228e-03)	1.619636e-01^{2}# (6.048189e-03)	2.316207e-01^{6}# (2.296604e-02)	5.009097e-01^{7}# (1.290043e-01)	1.747855e-01^{4}# (1.392893e-02)	1.340534e-01^{1} (3.789686e-03)
	5	3.260741e-01^{4}# (7.906645e-03)	3.516200e-01^{5}# (1.980323e-02)	3.103128e-01^{3}# (7.418366e-03)	3.966050e-01^{6}# (1.140583e-01)	4.559994e-01^{7}# (1.874259e-01)	2.915699e-01^{2}# (1.591152e-02)	2.678980e-01^{1} (4.512647e-03)
	6	5.276247e-01^{7}# (1.272649e-02)	5.264958e-01^{6}# (3.579771e-02)	5.011765e-01^{5}# (1.708180e-02)	4.454454e-01^{3}# (1.531355e-02)	4.738197e-01^{4}# (8.649317e-02)	4.092226e-01^{1} (2.009512e-02)	4.231155e-01^{2}# (7.627184e-03)

Table B.26 – *Continuation*

MOP	Dim.	PFI-EMOA	CRI-EMOA	AR-MOEA	RVEA	GrEA	SPEA2SDE	Two_Arch2
WFG3^{-1}	2	5.326644e-03^{4} (1.404378e-04)	6.349626e-03^{4}# (3.326373e-04)	5.710257e-03^{3}# (2.403219e-04)	3.529855e-02^{7}# (5.932595e-03)	1.461514e-02^{6}# (1.396319e-04)	6.534481e-03^{3}# (2.194969e-04)	5.925203e-03^{3}# (1.541175e-04)
	3	7.423873e-02^{1} (1.176798e-03)	9.213128e-02^{6}# (6.668920e-03)	8.831974e-02^{4}# (1.980676e-03)	1.607895e-01^{7}# (3.700455e-03)	8.281114e-02^{2}# (2.224047e-03)	8.902388e-02^{5}# (2.929075e-03)	8.548519e-02^{3}# (2.254097e-03)
	4	2.073665e-01^{1} (2.120844e-03)	2.431236e-01^{2}# (5.990685e-03)	2.466048e-01^{3}# (5.555078e-03)	5.161753e-01^{7}# (4.556797e-02)	2.478207e-01^{4}# (7.436691e-03)	2.484364e-01^{3}# (1.396920e-02)	2.562901e-01^{6}# (5.866830e-03)
	5	3.817579e-01^{1} (3.542823e-03)	4.422589e-01^{3}# (1.355150e-02)	4.463800e-01^{4}# (2.383511e-02)	9.302255e-01^{7}# (7.612517e-02)	4.348050e-01^{2}# (8.098791e-03)	5.014745e-01^{6}# (1.712947e-02)	4.955153e-01^{5}# (1.312144e-02)
	6	5.994293e-01^{1} (4.205715e-03)	6.820098e-01^{4}# (2.131263e-02)	6.646218e-01^{3}# (1.120895e-02)	1.687330e+00^{7}# (2.736539e-01)	6.645105e-01^{2}# (1.232387e-02)	8.572177e-01^{6}# (4.087459e-02)	8.003707e-01^{5}# (1.687493e-02)
WFG4	2	4.424210e-03^{1} (4.015850e-04)	8.718489e-03^{5}# (9.754691e-04)	6.313814e-03^{4}# (6.119144e-04)	5.655824e-02^{7}# (5.753908e-03)	9.293055e-03^{6}# (4.609828e-04)	5.618886e-03^{3}# (3.611814e-04)	5.498526e-03^{2}# (7.404605e-04)
	3	5.949619e-02^{1} (2.302430e-03)	1.008397e-01^{7}# (4.423426e-03)	7.839014e-02^{5}# (3.352612e-03)	9.222435e-02^{6}# (4.480403e-03)	6.762297e-02^{2}# (2.255898e-03)	7.119199e-02^{3}# (2.877037e-03)	7.738151e-02^{4}# (3.426430e-03)
	4	1.691750e-01^{1} (4.999192e-03)	2.102487e-01^{6}# (5.654560e-03)	2.046558e-01^{4}# (7.170724e-03)	1.933080e-01^{3}# (7.048428e-03)	1.783634e-01^{2}# (3.902026e-03)	2.087032e-01^{5}# (6.985246e-03)	2.588292e-01^{7}# (7.039921e-03)
	5	3.185089e-01^{1} (7.076493e-03)	3.911225e-01^{5}# (1.138654e-02)	3.643882e-01^{3}# (6.879134e-03)	3.430251e-01^{2}# (8.657782e-03)	3.657365e-01^{4}# (9.767779e-03)	3.923414e-01^{6}# (1.482802e-02)	5.029441e-01^{7}# (1.446340e-02)
	6	4.995284e-01^{2} (6.694099e-03)	5.680304e-01^{5}# (1.312172e-02)	5.193110e-01^{3}# (1.056805e-02)	4.923158e-01^{1} (8.938393e-03)	5.436524e-01^{4}# (1.235489e-02)	5.935530e-01^{6}# (1.822913e-02)	7.613488e-01^{7}# (2.448185e-02)
WFG4^{-1}	2	4.181433e-03^{3} (9.975406e-05)	4.140590e-03^{2} (1.157656e-04)	6.149821e-03^{5}# (1.308485e-04)	1.710456e-02^{7}# (4.551587e-03)	1.557050e-02^{6}# (3.362479e-03)	5.765401e-03^{4}# (4.531863e-04)	4.140375e-03^{1} (2.309302e-04)
	3	7.419888e-02^{2} (1.703669e-03)	1.118422e-01^{6}# (1.030895e-02)	9.671188e-02^{4}# (2.589462e-03)	1.258003e-01^{7}# (3.673618e-03)	9.742967e-02^{5}# (4.111482e-03)	9.509708e-02^{3}# (4.621729e-03)	7.346373e-02^{1} (1.837968e-03)
	4	2.410928e-01^{2}# (5.295466e-03)	2.653426e-01^{5}# (1.153961e-02)	2.813015e-01^{6}# (9.488745e-03)	4.344256e-01^{7}# (1.529995e-02)	2.492127e-01^{3}# (7.078898e-03)	2.615243e-01^{4}# (8.320218e-03)	2.353415e-01^{1} (6.968164e-03)
	5	4.715287e-01^{4}# (1.086823e-02)	4.921084e-01^{5}# (1.885116e-02)	5.250006e-01^{6}# (1.355840e-02)	8.721702e-01^{7}# (2.940399e-02)	4.574288e-01^{1} (1.466180e-02)	4.687844e-01^{3}# (2.116691e-02)	4.589016e-01^{2}# (7.867407e-03)
	6	7.886900e-01^{4}# (1.834395e-02)	7.607147e-01^{2}# (2.170265e-02)	8.145026e-01^{5}# (2.090082e-02)	1.508629e+00^{7}# (1.001621e-01)	7.480208e-01^{1}# (1.401978e-02)	8.189673e-01^{6}# (1.379196e-02)	7.842176e-01^{3}# (2.123124e-02)
WFG5	2	5.557323e-03^{2} (7.773013e-04)	5.638478e-03^{3} (6.744511e-04)	5.805644e-03^{4}# (6.627338e-04)	2.763413e-02^{7}# (4.285706e-03)	1.055261e-02^{6}# (5.184347e-04)	5.909807e-03^{5} (5.972057e-04)	5.376485e-03^{1} (7.751476e-04)
	3	6.207131e-02^{1} (1.401093e-03)	8.372461e-02^{7}# (4.100055e-03)	7.167499e-02^{4}# (2.235658e-03)	7.684903e-02^{5}# (2.312224e-03)	7.067508e-02^{2}# (1.551295e-03)	7.519620e-02^{4}# (3.508960e-03)	7.981745e-02^{6}# (3.172859e-03)
	4	1.821591e-01^{1} (3.272253e-03)	2.014367e-01^{5}# (4.819805e-03)	1.996863e-01^{4}# (2.870037e-03)	1.939820e-01^{3}# (2.847020e-03)	1.870383e-01^{2}# (3.507577e-03)	2.179652e-01^{6}# (7.487141e-03)	2.586426e-01^{7}# (7.068340e-03)
	5	3.336252e-01^{1} (4.999787e-03)	3.664540e-01^{5}# (8.126899e-03)	3.458265e-01^{3}# (2.651697e-03)	3.356608e-01^{2}# (2.501990e-03)	3.634067e-01^{4}# (5.895290e-03)	3.878581e-01^{6}# (1.563992e-02)	4.998408e-01^{7}# (1.258477e-02)
	6	5.146595e-01^{2}# (8.265724e-03)	5.466442e-01^{5}# (1.053329e-02)	5.162046e-01^{3}# (4.359855e-03)	5.026636e-01^{1} (2.419357e-03)	5.403030e-01^{4}# (9.463663e-03)	6.111180e-01^{6}# (1.338443e-02)	7.638985e-01^{7}# (2.276708e-02)
WFG5^{-1}	2	4.217165e-03^{2}# (2.866826e-04)	5.356974e-03^{3}# (2.798515e-04)	6.693259e-03^{5}# (3.649133e-04)	2.632858e-02^{7}# (3.260104e-03)	1.643279e-02^{6}# (3.239344e-03)	6.332757e-03^{4}# (6.980150e-04)	4.081018e-03^{1} (2.207300e-04)
	3	7.403101e-02^{2}# (1.808558e-03)	8.177232e-02^{3}# (1.872753e-03)	9.119793e-02^{4}# (1.882739e-03)	1.309747e-01^{7}# (4.491158e-03)	1.008603e-01^{6}# (4.058429e-03)	9.796464e-02^{5}# (5.384242e-03)	7.177766e-02^{1} (1.533633e-03)
	4	2.415803e-01^{2}# (4.746740e-03)	2.720218e-01^{6}# (1.177427e-02)	2.554261e-01^{3}# (5.633341e-03)	4.413169e-01^{7}# (1.397046e-02)	2.561094e-01^{4}# (5.977172e-03)	2.652052e-01^{5}# (1.218422e-02)	2.289137e-01^{1} (3.914894e-03)
	5	4.826800e-01^{5}# (1.082775e-02)	4.861584e-01^{6}# (1.341240e-02)	4.779563e-01^{3}# (1.034246e-02)	8.851341e-01^{7}# (2.188512e-02)	4.661163e-01^{2}# (8.881469e-03)	4.822401e-01^{4}# (1.681387e-02)	4.505105e-01^{1} (7.327302e-03)
	6	8.070779e-01^{5}# (2.038862e-02)	7.927281e-01^{4}# (2.323258e-02)	7.804683e-01^{3}# (1.471663e-02)	1.561859e+00^{7}# (7.446946e-02)	7.690523e-01^{2}# (1.817015e-02)	8.318673e-01^{6}# (2.179018e-02)	7.527198e-01^{1} (1.362021e-02)

Table B.26 – *Continuation*

MOP	Dim.	PFI-EMOA	CRI-EMOA	AR-MOEA	RVEA	GrEA	SPEA2SDE	Two_Arch2
WFG6	2	1.349166e-02^{2} (5.321720e-03)	1.569236e-02^{5} (6.371421e-03)	1.467017e-02^{4} (7.326270e-03)	8.536082e-02^{7} # (1.163281e-02)	1.998655e-02^{6} # (6.112283e-03)	1.348620e-02^{1} (6.402939e-03)	1.389190e-02^{3} (5.743855e-03)
	3	6.686722e-02^{1} (5.798049e-03)	9.905996e-02^{7} # (7.864355e-03)	7.710891e-02^{4} # (7.813030e-03)	9.551681e-02^{6} # (1.053350e-02)	7.221665e-02^{2} # (6.173322e-03)	7.376160e-02^{3} # (8.538422e-03)	8.264573e-02^{5} # (7.304869e-03)
	4	1.766277e-01^{1} (7.069998e-03)	1.948790e-01^{3} # (8.146070e-03)	1.986617e-01^{5} # (5.518200e-03)	1.951352e-01^{4} # (9.444854e-03)	1.797443e-01^{2} (9.818330e-03)	2.043893e-01^{6} # (7.697707e-03)	2.584903e-01^{7} # (1.085761e-02)
	5	3.275480e-01^{1} (8.132956e-03)	3.414293e-01^{3} # (1.538064e-02)	3.419320e-01^{4} # (1.036169e-02)	3.334373e-01^{2} # (1.232094e-02)	3.508243e-01^{5} # (9.149092e-03)	3.822278e-01^{6} # (2.235591e-02)	4.984899e-01^{7} # (1.694675e-02)
	6	5.007234e-01^{3} # (8.265790e-03)	5.020381e-01^{4} # (1.059303e-02)	4.967274e-01^{2} # (7.730480e-03)	4.920537e-01^{1} (1.196750e-02)	5.227542e-01^{5} # (1.147084e-02)	5.925072e-01^{6} # (1.667501e-02)	7.685539e-01^{7} # (2.071381e-02)
WFG6^{-1}	2	4.143433e-03^{2} # (1.504485e-04)	4.230211e-03^{3} # (2.377137e-04)	6.200174e-03^{4} # (2.477875e-04)	1.876844e-02^{6} # (2.842980e-03)	1.967970e-02^{7} # (5.409599e-03)	6.488136e-03^{5} # (1.197836e-03)	4.014555e-03^{1} (1.293714e-04)
	3	7.270920e-02^{1} (1.545596e-03)	8.824817e-02^{3} # (4.288234e-03)	9.102456e-02^{4} # (1.788907e-03)	1.182593e-01^{7} # (2.967035e-03)	9.671361e-02^{6} # (4.650470e-03)	9.364567e-02^{5} # (7.075140e-03)	7.644640e-02^{2} # (3.020743e-03)
	4	2.439402e-01^{1} (4.319743e-03)	2.751697e-01^{6} # (1.279790e-02)	2.621845e-01^{4} # (6.523262e-03)	4.366410e-01^{7} # (9.238455e-03)	2.539343e-01^{3} # (6.990756e-03)	2.677781e-01^{5} # (1.251760e-02)	2.446889e-01^{2} (6.104767e-03)
	5	4.815264e-01^{4} # (9.576349e-03)	5.080927e-01^{6} # (2.593346e-02)	4.908822e-01^{5} # (1.088025e-02)	8.861690e-01^{7} # (2.485964e-02)	4.559654e-01^{1} (9.262538e-03)	4.799464e-01^{3} # (1.969327e-02)	4.719365e-01^{2} # (1.101997e-02)
	6	8.099175e-01^{5} # (1.843196e-02)	8.083808e-01^{4} # (3.767518e-02)	8.156947e-01^{6} # (1.670968e-02)	1.567868e+00^{7} # (1.878031e-01)	7.830357e-01^{1} (1.839360e-02)	8.065870e-01^{3} # (4.432657e-02)	7.912882e-01^{2} # (1.441420e-02)
WFG7	2	4.470042e-03^{2} # (2.196904e-04)	5.754277e-03^{5} # (3.612151e-04)	5.540418e-03^{4} # (4.105763e-04)	4.426308e-02^{7} # (3.805068e-03)	9.600506e-03^{6} # (2.738398e-04)	5.377511e-03^{3} # (3.282586e-04)	4.023206e-03^{1} (2.564587e-04)
	3	6.195437e-02^{1} (1.662629e-03)	8.437141e-02^{6} # (3.333225e-03)	7.681583e-02^{5} # (2.434160e-03)	8.830307e-02^{7} # (2.808771e-03)	6.672559e-02^{2} # (1.043647e-03)	7.197466e-02^{4} # (2.698517e-03)	7.075377e-02^{3} # (1.786808e-03)
	4	1.811522e-01^{2} # (3.725920e-03)	2.010539e-01^{4} # (5.511829e-03)	2.071131e-01^{5} # (6.699226e-03)	1.989027e-01^{3} # (3.221350e-03)	1.788520e-01^{1} (2.762027e-03)	2.142562e-01^{6} # (6.885065e-03)	2.451607e-01^{7} # (7.153091e-03)
	5	3.366201e-01^{1} (5.567184e-03)	3.607336e-01^{3} # (7.117635e-03)	3.713236e-01^{5} # (9.838433e-03)	3.632578e-01^{4} # (1.223309e-02)	3.515929e-01^{2} # (8.110017e-03)	3.966845e-01^{6} # (1.140851e-02)	4.784843e-01^{7} # (1.039673e-02)
	6	5.157974e-01^{1} (7.712192e-03)	5.243098e-01^{2} # (9.533940e-03)	5.262793e-01^{3} # (7.909212e-03)	5.954236e-01^{5} # (5.139065e-02)	5.298135e-01^{4} # (8.454317e-03)	6.178954e-01^{6} # (1.369530e-02)	7.329079e-01^{7} # (1.460547e-02)
WFG7^{-1}	2	4.113731e-03^{1} (1.561871e-04)	5.248598e-03^{3} # (4.066950e-04)	6.678928e-03^{5} # (1.882603e-04)	1.567777e-02^{6} # (2.075455e-03)	1.894008e-02^{7} # (4.540549e-03)	6.149201e-03^{4} # (6.871304e-04)	4.216054e-03^{2} # (1.787490e-04)
	3	7.460632e-02^{2} (1.440007e-03)	1.136715e-01^{6} # (6.157050e-03)	1.028489e-01^{5} # (3.633371e-03)	1.258052e-01^{7} # (3.026102e-03)	9.439729e-02^{4} # (2.893575e-03)	9.315789e-02^{3} # (6.203535e-03)	7.450462e-02^{1} (2.288034e-03)
	4	2.429791e-01^{3} # (4.469558e-03)	2.639726e-01^{5} # (1.644771e-02)	2.879118e-01^{6} # (9.548520e-03)	4.343095e-01^{7} # (1.271468e-02)	2.419186e-01^{2} # (5.405457e-03)	2.595722e-01^{4} # (1.200248e-02)	2.346828e-01^{1} (6.197765e-03)
	5	4.804888e-01^{3} # (1.133542e-02)	5.115342e-01^{6} # (1.978384e-02)	5.103842e-01^{5} # (1.333419e-02)	9.924599e-01^{7} # (7.189794e-02)	4.599372e-01^{1} (8.746889e-03)	4.959093e-01^{4} # (3.838073e-02)	4.709358e-01^{2} # (9.995168e-03)
	6	8.159976e-01^{6} # (1.898564e-02)	8.109652e-01^{5} # (3.415690e-02)	8.035471e-01^{4} # (1.400489e-02)	1.453789e+00^{7} # (9.146052e-02)	7.607205e-01^{1} (1.851769e-02)	7.909276e-01^{3} # (2.011566e-02)	7.871133e-01^{2} # (1.465198e-02)
WFG8	2	1.251861e-02^{3} # (2.997322e-03)	1.332597e-02^{6} # (3.527474e-03)	1.331119e-02^{5} # (3.209751e-03)	9.962317e-02^{7} # (1.107783e-02)	1.319596e-02^{4} # (2.604209e-03)	9.498052e-03^{1} (2.532139e-03)	1.172714e-02^{2} # (3.311604e-03)
	3	1.147932e-01^{4} # (4.680982e-03)	1.331758e-01^{6} # (2.907795e-03)	1.164837e-01^{5} # (3.655878e-03)	1.392821e-01^{7} # (1.533339e-02)	9.691851e-02^{1} (9.646200e-03)	9.998499e-02^{2} # (8.724479e-03)	1.127179e-01^{3} # (8.535501e-03)
	4	2.463152e-01^{4} # (5.972833e-03)	2.595017e-01^{6} # (7.879657e-03)	2.440380e-01^{3} # (5.488686e-03)	2.407735e-01^{2} (1.984731e-02)	2.205524e-01^{1} # (1.834547e-02)	2.576853e-01^{5} # (1.782095e-02)	3.100336e-01^{7} # (2.195231e-02)
	5	4.194644e-01^{2} # (9.043244e-03)	4.613402e-01^{5} # (1.334330e-02)	4.260077e-01^{3} # (9.127785e-03)	4.344874e-01^{4} # (3.345079e-02)	4.160290e-01^{1} (2.971354e-02)	4.708708e-01^{6} # (3.071261e-02)	6.010686e-01^{7} # (3.355300e-02)
	6	6.290764e-01^{2} # (1.530398e-02)	6.574238e-01^{4} # (2.752806e-02)	5.973316e-01^{1} (1.313474e-02)	7.751648e-01^{6} # (1.271857e-01)	6.384757e-01^{3} # (4.173567e-02)	7.044443e-01^{5} # (3.850192e-02)	9.373714e-01^{7} # (5.780185e-02)

Table B.26 – *Continuation*

MOP	Dim.	PFI-EMOA	CRI-EMOA	AR-MOEA	RVEA	GrEA	SPEA2SDE	Two_Arch2
WFG8^{-1}	2	4.227838e-03^{1} (3.399110e-04)	4.479470e-03^{3}# (3.376676e-04)	6.301757e-03^{4}# (2.664753e-04)	9.084937e-03^{6}# (1.515302e-03)	2.268571e-02^{7}# (4.942013e-03)	6.515644e-03^{5}# (1.003414e-03)	4.336580e-03^{2} (7.725463e-04)
	3	7.640172e-02^{2} (1.507194e-03)	8.176148e-02^{3}# (1.916650e-03)	9.320715e-02^{4}# (1.710837e-03)	1.177597e-01^{7}# (3.573048e-03)	1.029193e-01^{6}# (5.892969e-03)	9.648210e-02^{5}# (5.739945e-03)	7.606778e-02^{1} (1.903549e-03)
	4	2.517975e-01^{2}# (7.471965e-03)	2.940749e-01^{6}# (1.896114e-02)	2.694556e-01^{4}# (6.743403e-03)	4.284646e-01^{7}# (1.040406e-02)	2.633165e-01^{3}# (1.209761e-02)	2.785268e-01^{5}# (1.981639e-02)	2.375756e-01^{1} (5.964710e-03)
	5	5.006291e-01^{4}# (1.783633e-02)	5.326052e-01^{6}# (2.233903e-02)	4.845645e-01^{3}# (1.173762e-02)	8.710923e-01^{7}# (3.304043e-02)	4.656475e-01^{2} (1.296934e-02)	5.014066e-01^{5}# (3.751152e-02)	4.619614e-01^{1} (1.118402e-02)
	6	8.407007e-01^{6}# (2.593363e-02)	8.351569e-01^{5}# (2.584622e-02)	8.010514e-01^{3}# (1.700031e-02)	1.571765e+00^{7}# (6.443808e-02)	7.805804e-01^{2} (2.490736e-02)	8.124731e-01^{4}# (3.122593e-02)	7.705425e-01^{1} (1.454259e-02)
WFG9	2	1.464817e-02^{1} (2.493363e-02)	1.686115e-02^{2}# (2.449107e-02)	5.217956e-02^{4}# (4.537390e-02)	7.403893e-02^{7}# (2.819597e-02)	5.621813e-02^{5}# (4.654631e-02)	3.935751e-02^{3} (4.533611e-02)	6.407171e-02^{6}# (4.623090e-02)
	3	8.250354e-02^{1} (2.600644e-02)	1.172694e-01^{4}# (2.162647e-02)	1.274936e-01^{5}# (2.567374e-02)	1.342921e-01^{6}# (2.389780e-02)	1.105267e-01^{2}# (4.018560e-02)	1.131351e-01^{3}# (4.160227e-02)	1.344932e-01^{7}# (3.228001e-02)
	4	2.374402e-01^{2}# (3.168753e-02)	2.149083e-01^{1} (3.456943e-02)	2.849030e-01^{6}# (1.988155e-02)	2.428978e-01^{3}# (2.411199e-02)	2.515371e-01^{5}# (3.325347e-02)	2.436469e-01^{4}# (3.955403e-02)	2.905400e-01^{7}# (3.585656e-02)
	5	3.972840e-01^{3}# (3.735980e-02)	3.709297e-01^{1} (4.480525e-02)	4.639012e-01^{6}# (4.405708e-02)	3.771678e-01^{2}# (1.862710e-02)	4.370671e-01^{5}# (4.242064e-02)	4.212732e-01^{4}# (4.495744e-02)	5.464391e-01^{7}# (4.290731e-02)
	6	5.930522e-01^{3}# (4.255747e-02)	5.492311e-01^{2} (4.187362e-02)	6.319476e-01^{5}# (4.052217e-02)	5.453658e-01^{1} (2.944227e-02)	6.141776e-01^{4}# (4.873698e-02)	6.542956e-01^{6}# (5.065795e-02)	8.280847e-01^{7}# (5.225828e-02)
WFG9^{-1}	2	5.345475e-03^{1} (1.005427e-03)	6.870657e-03^{3}# (1.344943e-03)	7.902920e-03^{5}# (1.332872e-03)	1.754235e-02^{6}# (2.495236e-03)	1.835485e-02^{7}# (3.421852e-03)	6.930096e-03^{4}# (1.529482e-03)	5.734532e-03^{2} (2.395579e-03)
	3	7.396514e-02^{2} (4.219944e-03)	9.334023e-02^{5}# (5.699082e-03)	1.078553e-01^{6}# (6.380146e-03)	1.177866e-01^{7}# (4.914609e-03)	9.070154e-02^{4}# (5.642946e-03)	8.645082e-02^{3}# (4.469669e-03)	7.338710e-02^{1} (3.287070e-03)
	4	2.435354e-01^{5}# (1.067815e-02)	2.423833e-01^{4}# (7.623883e-03)	3.257902e-01^{6}# (1.791595e-02)	4.266774e-01^{7}# (1.347292e-02)	2.337112e-01^{2}# (6.901004e-03)	2.395197e-01^{3}# (8.437437e-03)	2.275849e-01^{1} (4.924977e-03)
	5	4.896038e-01^{5}# (1.527524e-02)	4.650081e-01^{4}# (1.093955e-02)	5.496840e-01^{6}# (2.895538e-02)	9.396474e-01^{7}# (7.522888e-02)	4.484572e-01^{1} (8.191394e-03)	4.487435e-01^{2} (1.370391e-02)	4.594881e-01^{3}# (1.170143e-02)
	6	8.251119e-01^{6}# (3.446865e-02)	7.337031e-01^{2} (1.283829e-02)	8.217142e-01^{5}# (2.957798e-02)	1.532614e+00^{7}# (1.173697e-01)	7.411361e-01^{3}# (1.500857e-02)	7.304317e-01^{1} (3.881403e-02)	7.533432e-01^{4}# (1.682142e-02)

Table B.27: Mean and, in parentheses, standard deviation of the Riesz s-energy comparison. For each case, the two best values are shown in grayscale, where the darker tone corresponds to the best algorithm. The symbol # is placed when the best algorithm presents a significant difference, according to a one-tailed Wilcoxon test using a significance level of $\alpha = 0.05$.

MOP	Dim.	PFI-EMOA	CRI-EMOA	AR-MOEA	RVEA	GrEA	SPEA2SDE	Two_Arch2
WFG1	2	3.329147e+04^{2}# (3.475418e+02)	6.754947e+04^{4}# (3.680114e+03)	1.661772e+05^{6}# (2.395327e+05)	2.576149e+04^{1} (1.410316e+03)	7.109447e+05^{7}# (1.086857e+06)	5.731116e+04^{3}# (7.223642e+04)	1.023164e+05^{5}# (1.360420e+05)
	3	1.351747e+04^{1} (1.914082e+02)	5.493856e+04^{5}# (8.101914e+03)	3.180311e+07^{6}# (7.349697e+07)	1.567220e+04^{2}# (8.348782e+02)	6.500165e+08^{7}# (1.146344e+09)	2.515651e+04^{4}# (2.287323e+03)	1.754924e+04^{3}# (1.298446e+03)
	4	3.009883e+05^{4} (1.507010e+06)	3.144886e+05^{5}# (6.377710e+04)	1.504604e+11^{6}# (5.313591e+11)	1.425199e+04^{2}# (5.008393e+03)	7.409456e+19^{7}# (3.778096e+20)	2.934012e+04^{3}# (3.589353e+03)	1.143577e+04^{1} (1.038108e+03)
	5	8.851787e+07^{5} (4.497436e+08)	2.227189e+06^{4}# (4.770309e+05)	2.973104e+15^{6}# (1.180303e+16)	4.498944e+04^{2}# (2.883106e+04)	1.282446e+23^{7}# (6.539217e+23)	5.620016e+04^{3}# (9.102877e+03)	1.453821e+04^{1} (1.884564e+04)
	6	1.561967e+10^{4} (4.726918e+10)	1.687448e+07^{3}# (5.272982e+06)	7.814367e+19^{6}# (1.634315e+20)	6.065625e+05^{2} (9.396643e+05)	1.119756e+24^{7}# (5.708802e+24)	1.176564e+05^{1} (4.353298e+04)	3.032062e+11^{5} (1.514556e+12)
WFG1^{-1}	2	3.267299e+04^{4}# (2.957895e+02)	6.217042e+04^{6}# (3.953956e+03)	3.103843e+04^{3}# (2.329732e+03)	2.372930e+04^{1} (1.931366e+03)	1.015112e+07^{7}# (3.459483e+06)	3.413883e+04^{5}# (5.432191e+02)	3.095237e+04^{2}# (9.081298e+02)
	3	1.309073e+04^{1} (1.602760e+02)	5.479359e+04^{4}# (5.558932e+03)	5.708355e+09^{6}# (1.528475e+10)	1.232232e+06^{5} (2.129221e+06)	6.990013e+11^{7}# (1.245142e+12)	1.695129e+04^{3}# (7.924940e+02)	1.623445e+04^{2}# (1.658018e+03)
	4	5.142206e+03^{1} (1.627761e+02)	5.837701e+04^{4}# (1.297054e+04)	2.618923e+19^{7}# (1.335389e+20)	1.362188e+09^{5}# (4.794495e+09)	6.394689e+18^{6}# (1.931028e+19)	7.390626e+03^{2}# (4.458564e+03)	1.145281e+04^{3}# (1.522438e+03)
	5	2.304673e+03^{1} (2.286239e+02)	7.389865e+04^{4}# (1.816542e+04)	7.408610e+22^{6}# (3.777028e+23)	1.416499e+15^{5} (4.614827e+15)	3.623250e+26^{7}# (1.045776e+27)	2.862597e+03^{2} (1.431926e+03)	1.463387e+04^{3}# (8.676646e+03)
	6	1.175779e+03^{2}# (1.873441e+02)	1.171987e+05^{4}# (8.152397e+04)	3.878611e+23^{6}# (1.883622e+24)	2.604562e+19^{5}# (1.328067e+20)	2.748756e+33^{7}# (4.593899e+33)	8.537133e+02^{1} (3.700405e+02)	1.493407e+04^{3}# (7.192369e+03)
WFG2	2	3.179527e+04^{2}# (3.922922e+03)	3.365921e+04^{3}# (3.692294e+03)	7.521454e+04^{6}# (3.232920e+04)	2.610717e+04^{1} (3.380828e+03)	2.210041e+05^{7}# (7.351507e+04)	4.522768e+04^{5}# (5.645505e+03)	3.561228e+04^{4}# (3.988985e+03)
	3	1.370907e+04^{1} (4.184925e+03)	1.524645e+04^{2}# (4.512056e+03)	7.586888e+06^{6}# (3.774161e+07)	1.814756e+04^{4}# (5.632084e+03)	9.721518e+08^{7}# (4.278675e+09)	5.079232e+04^{5}# (1.394040e+04)	1.739979e+04^{3}# (4.981022e+03)
	4	5.338158e+03^{1} (2.719971e+03)	1.059306e+05^{3}# (5.523293e+04)	1.315672e+06^{6}# (6.641784e+06)	1.673568e+04^{2}# (9.134850e+03)	1.792529e+12^{7}# (2.222096e+12)	1.290905e+05^{4}# (6.724919e+04)	2.515059e+05^{5}# (1.195930e+06)
	5	2.011665e+03^{1} (3.389179e+03)	2.581687e+05^{3}# (2.111430e+05)	1.100909e+08^{5}# (5.453007e+08)	3.164185e+04^{2}# (2.712226e+04)	9.086328e+15^{7}# (1.124474e+16)	4.263964e+05^{4}# (3.577791e+05)	7.120819e+14^{6}# (3.630919e+15)
	6	3.506277e+02^{1} (1.543069e+02)	1.072691e+06^{4}# (9.551549e+05)	1.658837e+04^{2}# (2.809867e+04)	1.036580e+05^{3}# (9.061965e+04)	7.407607e+19^{7}# (1.455314e+20)	1.547492e+06^{5}# (1.214646e+06)	1.782535e+07^{6}# (8.709320e+07)
WFG2^{-1}	2	3.658629e+04^{4}# (6.732070e+02)	3.291241e+04^{2}# (3.525180e+02)	3.317456e+04^{3}# (4.644893e+02)	4.271907e+04^{6}# (1.447826e+03)	2.522214e+05^{7}# (1.111045e+05)	4.128442e+04^{5}# (1.949170e+03)	3.125240e+04^{1} (5.054737e+01)
	3	5.690934e+03^{3}# (1.164613e+02)	5.653957e+03^{2}# (9.468633e+01)	4.331007e+07^{6}# (1.243482e+08)	2.417211e+03^{1} (3.468241e+01)	3.983641e+09^{7}# (1.790933e+10)	1.537371e+04^{5}# (1.540023e+03)	6.887705e+03^{4}# (2.447132e+02)
	4	1.618620e+03^{1} (4.878747e+01)	1.017546e+04^{4}# (1.826814e+03)	3.162063e+12^{7}# (3.559814e+12)	2.575550e+03^{2}# (5.469566e+02)	1.832687e+12^{6}# (2.292284e+12)	1.066830e+04^{5}# (2.158040e+03)	3.478666e+03^{3}# (2.591310e+02)
	5	5.351819e+02^{1} (6.167807e+01)	1.539190e+04^{4}# (7.867586e+03)	6.539873e+16^{6}# (1.495092e+17)	8.478948e+07^{5} (3.532959e+08)	4.982448e+17^{7}# (1.685528e+18)	6.993484e+03^{3}# (1.445280e+03)	2.642557e+03^{2}# (5.562304e+02)
	6	1.456637e+02^{1} (2.963763e+01)	1.488942e+04^{4}# (5.721884e+03)	6.096654e+31^{7}# (3.108685e+32)	3.690201e+07^{5} (1.249188e+08)	6.450567e+21^{6}# (3.122935e+22)	3.818892e+03^{3}# (1.431982e+03)	7.167589e+02^{2}# (2.502608e+02)
WFG3	2	2.769320e+04^{2}# (1.642458e+01)	2.813214e+04^{4}# (1.193740e+02)	2.796458e+04^{3}# (3.567527e+01)	2.688722e+04^{1} (3.106315e+02)	1.968237e+05^{7}# (7.606475e+04)	2.938270e+04^{6}# (2.495499e+02)	2.841648e+04^{5}# (1.079569e+02)
	3	2.178408e+04^{2}# (9.463835e+02)	2.436119e+04^{3}# (1.125912e+03)	1.728860e+10^{6}# (8.724252e+10)	2.158551e+03^{1}# (2.371271e+02)	3.945844e+10^{7}# (1.885363e+11)	5.071474e+04^{4}# (5.047516e+03)	7.434516e+06^{5}# (3.777006e+07)
	4	3.536110e+03^{2}# (1.404055e+02)	2.031542e+04^{4}# (2.034495e+03)	2.329116e+12^{5}# (2.113509e+12)	1.073485e+03^{1}# (4.793957e+02)	6.428354e+13^{6}# (2.673038e+14)	1.936625e+04^{3}# (3.032872e+03)	2.313766e+21^{7}# (1.039721e+22)
	5	5.347920e+02^{1} (3.757759e+01)	9.025751e+03^{3}# (2.084546e+03)	5.970991e+15^{5}# (1.060812e+16)	7.116409e+04^{4}# (1.705082e+05)	3.510411e+20^{6}# (1.785147e+21)	7.310403e+03^{2}# (1.368427e+03)	4.553553e+29^{7}# (2.101665e+30)
	6	8.220811e+01^{1} (5.921658e+00)	4.469481e+03^{4}# (1.626973e+03)	1.481771e+19^{5}# (5.237746e+19)	1.519639e+03^{2}# (2.305453e+03)	1.192669e+20^{6}# (1.660235e+20)	2.613048e+03^{3}# (6.078614e+02)	7.636533e+38^{7}# (3.869110e+39)

Table B.27 – *Continuation*

MOP	Dim.	PFI-EMOA	CRI-EMOA	AR-MOEA	RVEA	GrEA	SPEA2SDE	Two_Arch2
WFG3^{-1}	2	2.767287e+04^{2}# (6.772505e+00)	2.806378e+04^{4}# (9.987171e+01)	2.791164e+04^{3}# (1.531325e+01)	2.739828e+04^{1} (3.928146e+02)	1.131577e+06^{7}# (7.551598e+05)	2.927866e+04^{6}# (2.882322e+02)	2.839891e+04^{5}# (1.090266e+02)
	3	8.749514e+03^{2}# (5.507820e+01)	9.298703e+03^{3}# (6.815595e+01)	5.289999e+07^{6}# (1.849443e+08)	4.756219e+02^{1} (2.595747e+00)	8.749091e+09^{7}# (2.693138e+10)	1.174314e+04^{5}# (3.966289e+02)	1.086368e+04^{4}# (6.714328e+02)
	4	1.952845e+03^{1} (2.828855e+01)	3.190001e+03^{2}# (2.420570e+02)	2.758575e+14^{6}# (8.257632e+14)	8.609555e+03^{4} (4.347588e+04)	1.150686e+15^{7}# (4.651216e+15)	3.925696e+03^{3}# (3.708068e+02)	2.257970e+04^{5}# (7.212509e+04)
	5	4.597061e+02^{2}# (1.973765e+01)	8.855822e+02^{3}# (1.016758e+02)	7.407496e+26^{7}# (3.777097e+27)	2.622523e+01^{1} (1.255872e+02)	1.162606e+21^{6}# (5.900682e+21)	1.195077e+03^{4}# (1.097150e+02)	2.875083e+05^{5}# (9.261705e+05)
	6	9.826430e+01^{2}# (3.820780e+00)	2.295094e+02^{3}# (4.742601e+01)	3.361243e+28^{7}# (1.713904e+29)	1.256767e+00^{1} (3.740545e+00)	5.480686e+20^{6}# (2.459072e+21)	3.097273e+02^{4}# (4.565062e+01)	8.749668e+07^{5}# (4.253893e+08)
WFG4	2	2.738152e+04^{2}# (2.967730e+02)	2.799433e+04^{3}# (3.225225e+02)	3.303148e+04^{5}# (7.401928e+03)	2.653894e+04^{1} (2.504715e+02)	1.549220e+05^{7}# (6.853873e+04)	3.930471e+04^{6}# (9.789088e+02)	2.907154e+04^{4}# (3.084370e+02)
	3	6.138376e+03^{1} (6.943086e+01)	6.154164e+03^{2} (1.056484e+02)	1.482521e+07^{5}# (5.237930e+07)	6.555083e+03^{3}# (1.049231e+02)	3.950736e+07^{6}# (9.892463e+07)	1.110099e+04^{4}# (5.161441e+02)	6.016787e+08^{7}# (3.062939e+09)
	4	9.502187e+02^{1} (3.060937e+01)	1.421054e+03^{4}# (1.014283e+02)	1.374946e+03^{3}# (1.063648e+02)	1.246260e+03^{2}# (5.589868e+01)	1.113040e+05^{7}# (3.504613e+05)	1.878894e+03^{5}# (1.226376e+02)	1.612592e+04^{6}# (4.616727e+04)
	5	1.550559e+02^{1} (1.088390e+01)	2.276452e+02^{2}# (3.272360e+01)	4.072956e+02^{5}# (1.750195e+02)	3.378330e+02^{4}# (8.390641e+01)	7.407408e+14^{7}# (3.777051e+15)	2.769734e+02^{3}# (3.260189e+01)	2.240118e+08^{6}# (9.359818e+08)
	6	2.172536e+01^{1} (3.866256e+00)	4.023884e+01^{3}# (1.253696e+01)	1.505003e+02^{5}# (1.323775e+02)	1.053867e+02^{4}# (5.179285e+01)	7.407407e+18^{6}# (3.777051e+19)	3.014778e+01^{2}# (4.071023e+00)	2.307841e+19^{7}# (1.146509e+20)
WFG4^{-1}	2	2.717370e+04^{1} (1.329547e+02)	2.758885e+04^{2}# (2.369920e+02)	3.750668e+04^{5}# (3.645615e+01)	3.626161e+04^{4}# (6.503841e+02)	2.009748e+05^{7}# (3.444592e+05)	4.020793e+04^{6}# (9.532626e+02)	2.857731e+04^{3}# (3.980160e+02)
	3	6.112216e+03^{2}# (7.451382e+01)	6.525152e+03^{3}# (1.302151e+02)	1.339708e+08^{7}# (1.329266e+08)	2.079469e+03^{1} (3.576370e+01)	4.080868e+07^{6}# (7.814907e+07)	1.556312e+04^{5}# (6.805790e+02)	7.355186e+03^{4}# (2.110337e+02)
	4	9.137643e+02^{2}# (2.205785e+01)	3.939864e+03^{4}# (4.891525e+02)	2.149878e+12^{7}# (2.665047e+12)	8.561453e+01^{1} (1.347415e+01)	1.045519e+06^{6}# (4.265530e+06)	4.174995e+03^{5}# (4.087199e+02)	1.329489e+03^{3}# (5.001050e+01)
	5	1.287518e+02^{2}# (6.131348e+00)	9.525523e+02^{5}# (1.473721e+02)	1.555557e+16^{7}# (1.369870e+16)	2.109787e+01^{1} (9.826047e+00)	4.668426e+03^{6}# (1.926062e+04)	9.099909e+02^{4}# (9.768097e+01)	2.101938e+02^{3}# (1.253173e+01)
	6	1.324126e+01^{2}# (1.394781e+00)	1.820428e+02^{6}# (3.306765e+01)	8.744273e+19^{7}# (1.619580e+20)	1.623982e+00^{1} (3.293752e+00)	6.384560e+01^{4}# (2.701421e+01)	1.371790e+02^{5}# (2.058741e+01)	4.496641e+01^{3}# (6.278653e+01)
WFG5	2	2.807836e+04^{2}# (3.382305e+02)	2.827054e+04^{3}# (2.413131e+02)	2.880835e+04^{4}# (3.300909e+02)	2.755719e+04^{1} (4.622349e+02)	2.176154e+06^{7}# (1.192830e+06)	3.955717e+04^{6}# (1.050573e+03)	2.916054e+04^{5}# (4.090006e+02)
	3	6.183227e+03^{1} (7.781398e+01)	6.268362e+03^{2}# (1.066299e+02)	7.417268e+06^{6}# (3.776986e+07)	6.725000e+03^{3}# (2.538935e+02)	2.219583e+08^{7}# (1.066023e+09)	1.114091e+04^{4}# (5.189750e+02)	1.258180e+05^{5}# (5.900096e+05)
	4	9.611958e+02^{1} (2.879750e+01)	1.538476e+03^{3}# (1.292053e+02)	4.654200e+03^{5}# (1.391990e+04)	1.432058e+03^{2}# (1.330676e+02)	1.199642e+09^{7}# (6.104429e+09)	1.919308e+03^{4}# (1.041772e+02)	2.444804e+08^{6}# (1.246580e+09)
	5	1.600999e+02^{1} (1.149001e+01)	2.580550e+02^{2}# (3.259406e+01)	5.797699e+02^{5}# (4.268547e+02)	3.249902e+02^{4}# (3.758114e+01)	5.903735e+10^{7}# (2.693618e+11)	2.873400e+02^{3}# (3.046862e+01)	3.699359e+07^{6}# (1.339502e+08)
	6	2.213267e+01^{1} (3.647382e+00)	5.083701e+01^{3}# (1.439858e+01)	1.565850e+02^{5}# (1.088815e+02)	7.471331e+01^{4}# (6.584151e+00)	3.149762e+08^{6}# (1.116462e+09)	3.052635e+01^{2}# (3.731194e+00)	3.073500e+20^{7}# (1.567184e+21)
WFG5^{-1}	2	2.820112e+04^{1} (3.350186e+02)	2.872557e+04^{2}# (3.296906e+02)	3.778326e+04^{5}# (1.281274e+03)	3.659900e+04^{4}# (3.686265e+02)	9.061347e+04^{7}# (2.745250e+04)	4.078486e+04^{6}# (1.018590e+03)	2.953288e+04^{3}# (4.634408e+02)
	3	6.230716e+03^{2}# (6.641772e+01)	6.552741e+03^{3}# (5.722114e+01)	1.645674e+08^{7}# (1.337202e+08)	2.120788e+03^{1} (3.275940e+01)	4.506743e+07^{6}# (8.312441e+07)	1.617984e+04^{4}# (7.548820e+02)	2.188919e+04^{5}# (6.755556e+04)
	4	9.428973e+02^{2}# (3.236175e+01)	4.020842e+03^{4}# (4.485819e+02)	2.000287e+12^{7}# (2.244272e+12)	8.189122e+01^{1} (8.821901e+00)	7.407561e+10^{6}# (3.777048e+11)	4.322376e+03^{5}# (4.832251e+02)	1.747523e+03^{3}# (9.713760e+02)
	5	1.408827e+02^{2}# (7.738585e+00)	9.075382e+02^{4}# (1.713065e+02)	1.852004e+16^{7}# (2.771497e+16)	2.193326e+01^{1} (1.745212e+01)	5.349956e+02^{3}# (5.268804e+02)	9.638475e+02^{5}# (1.172247e+02)	3.953571e+03^{6}# (1.903014e+04)
	6	1.453076e+01^{2}# (1.721413e+00)	1.621329e+02^{6}# (3.232821e+01)	2.296319e+20^{7}# (3.557122e+20)	1.673754e+00^{1} (5.135566e+00)	6.640006e+01^{4}# (1.880832e+01)	1.408747e+02^{5}# (2.114105e+01)	2.639361e+01^{3}# (3.730446e+00)

Table B.27 – *Continuation*

MOP	Dim.	PFI-EMOA	CRI-EMOA	AR-MOEA	RVEA	GrEA	SPEA2SDE	Two_Arch2
WFG6	2	2.722857e+04^{2}# (1.657321e+02)	2.774314e+04^{3} # (4.128964e+02)	3.911345e+04^{5}# (1.149097e+04)	2.469132e+04^{1} (4.116497e+02)	1.923978e+05^{7}# (2.178231e+05)	3.951634e+04^{6}# (1.221381e+03)	2.884772e+04^{4}# (2.271773e+02)
	3	6.166192e+03^{1} (8.411162e+01)	6.184606e+03^{2} (8.108355e+01)	7.415719e+06^{6}# (3.777016e+07)	6.493219e+03^{3}# (2.862904e+01)	5.662721e+07^{7}# (1.171655e+08)	1.130783e+04^{4}# (5.661376e+02)	1.758965e+04^{5}# (3.463913e+04)
	4	9.542430e+02^{1} (3.127038e+01)	1.566761e+03^{4}# (1.386909e+02)	1.274476e+03^{3}# (1.013716e+02)	1.178615e+03^{2}# (9.245291e+00)	7.407503e+10^{7}# (3.777050e+11)	1.946541e+03^{5}# (1.810805e+02)	5.368005e+03^{6}# (2.119659e+04)
	5	1.499556e+02^{1} (1.055906e+01)	2.806040e+02^{3}# (3.522875e+01)	2.850053e+02^{4}# (4.599467e+01)	2.663051e+02^{2}# (2.252027e+01)	9.703316e+09^{6}# (4.173126e+10)	3.231157e+02^{5}# (3.077768e+01)	1.230534e+21^{7}# (6.260083e+21)
	6	2.168297e+01^{1} (3.388418e+00)	5.721816e+01^{3}# (1.171178e+01)	7.482801e+01^{5}# (2.201586e+01)	7.021133e+01^{4}# (1.899177e+01)	2.700637e+10^{6}# (9.613278e+10)	3.399054e+01^{2}# (4.908844e+00)	1.325079e+37^{7} (6.756595e+37)
WFG6^{-1}	2	2.704979e+04^{1} (7.933718e+01)	2.771855e+04^{2}# (2.465511e+02)	3.757231e+04^{5}# (5.782969e+01)	3.690763e+04^{4}# (2.893122e+02)	9.385353e+04^{7}# (2.755777e+04)	4.099055e+04^{6}# (1.282638e+03)	2.855593e+04^{3}# (3.944236e+02)
	3	6.080804e+03^{2}# (5.769041e+01)	6.433753e+03^{3}# (7.955461e+01)	1.638914e+08^{7}# (9.509907e+07)	2.079892e+03^{1} (5.937532e+01)	1.765836e+07^{6}# (5.284185e+07)	1.553761e+04^{5}# (1.113860e+03)	7.299757e+03^{4}# (2.024573e+02)
	4	9.216492e+02^{2}# (2.352232e+01)	4.009144e+03^{4}# (4.871205e+02)	1.521602e+12^{7}# (1.527321e+12)	7.305527e+01^{1} (8.479902e+00)	1.327909e+08^{6}# (6.671326e+08)	4.503769e+03^{5}# (4.838584e+02)	1.589306e+03^{3}# (1.218183e+03)
	5	1.359236e+02^{2}# (1.138177e+01)	1.012260e+03^{5}# (1.738054e+02)	2.148191e+16^{7}# (2.771679e+16)	1.493776e+01^{1} (3.375905e+00)	2.463000e+04^{6}# (1.163373e+05)	9.633801e+02^{4}# (1.444157e+02)	2.137626e+02^{3}# (2.673790e+01)
	6	1.506887e+01^{2}# (2.963358e+00)	1.805295e+02^{6}# (4.046069e+01)	1.333761e+20^{7}# (2.036743e+20)	3.066976e+00^{1} (6.978474e+00)	1.133202e+02^{4}# (1.456924e+02)	1.495903e+02^{5}# (2.598245e+01)	5.813959e+01^{3}# (1.684901e+02)
WFG7	2	2.718184e+04^{2}# (1.854674e+02)	2.756178e+04^{3}# (3.255799e+02)	2.915009e+04^{5}# (4.167134e+03)	2.659081e+04^{1} (2.357070e+02)	2.504467e+06^{7}# (2.045401e+06)	3.953500e+04^{6}# (1.090580e+03)	2.885850e+04^{4}# (3.004407e+02)
	3	6.146331e+03^{2}# (7.235250e+01)	6.101543e+03^{1} (7.920343e+01)	8.629830e+03^{4}# (9.814093e+03)	6.525666e+03^{3}# (1.705089e+01)	8.025302e+07^{7}# (1.250583e+08)	1.126607e+04^{5}# (4.845134e+02)	1.364764e+04^{6}# (3.179568e+04)
	4	9.436543e+02^{1} (3.156409e+01)	1.539178e+03^{3}# (1.041407e+02)	1.890065e+03^{4}# (2.213334e+03)	1.159272e+03^{2}# (4.313443e+01)	7.411618e+10^{7}# (3.776969e+11)	1.937259e+03^{5}# (1.242296e+02)	7.407697e+10^{6}# (3.777046e+11)
	5	1.514071e+02^{1} (1.114274e+01)	2.694177e+02^{2}# (5.018289e+01)	3.619018e+02^{5}# (1.905134e+02)	2.942704e+02^{3}# (8.051570e+01)	7.407669e+14^{7}# (3.777046e+15)	2.964290e+02^{4}# (2.266338e+01)	2.673316e+13^{6}# (1.363129e+14)
	6	1.975767e+01^{1} (3.896804e+00)	5.996922e+01^{3}# (1.611642e+01)	6.978337e+01^{4}# (9.096206e+00)	8.185299e+01^{5}# (4.043945e+01)	3.625162e+12^{7}# (1.513479e+13)	3.072941e+01^{2}# (4.015677e+00)	2.219809e+10^{6}# (1.108262e+11)
WFG7^{-1}	2	2.710387e+04^{1} (1.331955e+02)	2.777175e+04^{2}# (2.589943e+02)	3.756454e+04^{5}# (6.595698e+01)	3.718925e+04^{4}# (3.098701e+02)	6.838187e+05^{7}# (8.430500e+05)	4.025651e+04^{6}# (1.156263e+03)	2.867390e+04^{3}# (4.062478e+02)
	3	6.061254e+03^{2}# (6.407758e+01)	6.442682e+03^{3}# (7.161825e+01)	7.423789e+10^{7}# (3.776730e+11)	2.059432e+03^{1} (4.455330e+01)	1.913380e+07^{6}# (6.727451e+07)	1.530339e+04^{5}# (1.047744e+03)	7.734867e+03^{4}# (2.013568e+03)
	4	9.125687e+02^{2}# (2.837814e+01)	3.886133e+03^{4}# (8.064656e+02)	3.045919e+12^{7}# (3.141773e+12)	1.045087e+02^{1} (2.521174e+01)	1.453029e+10^{6}# (7.408538e+10)	3.941917e+03^{5}# (4.171051e+02)	1.277936e+03^{3}# (4.990871e+01)
	5	1.295884e+02^{2}# (9.275041e+00)	1.138939e+03^{5}# (2.767363e+02)	2.377253e+16^{7}# (2.245813e+16)	1.262152e+01^{1} (9.189356e+00)	8.950226e+03^{6}# (4.235050e+04)	8.513486e+02^{4}# (1.403015e+02)	2.014539e+02^{3}# (1.713353e+01)
	6	1.333349e+01^{1} (1.908695e+00)	2.323183e+02^{5}# (8.043987e+01)	3.558406e+25^{7}# (1.814420e+26)	2.677595e+02^{6}# (1.124505e+03)	5.034802e+01^{3}# (1.937768e+01)	1.058978e+02^{4}# (1.531293e+01)	2.871228e+01^{2}# (2.322202e+01)
WFG8	2	2.823099e+04^{2}# (6.937530e+02)	2.904497e+04^{3}# (1.242121e+03)	1.457034e+05^{7}# (3.884738e+05)	2.334008e+04^{1} (3.996896e+02)	1.389509e+05^{6}# (5.630030e+04)	3.771491e+04^{5}# (8.755541e+02)	3.011814e+04^{4}# (1.223460e+03)
	3	6.005994e+03^{2}# (5.948055e+01)	6.234748e+03^{3}# (1.030596e+02)	3.916901e+07^{7}# (1.219626e+08)	5.660040e+03^{1} (1.325979e+02)	3.802519e+07^{6}# (9.459011e+07)	1.012909e+04^{4}# (5.241774e+02)	7.464002e+06^{5}# (3.776115e+07)
	4	8.798269e+02^{1} (2.183757e+01)	1.364422e+03^{3}# (8.655462e+01)	3.377446e+06^{5}# (1.551346e+07)	1.192780e+03^{2}# (4.576416e+01)	2.968538e+11^{7}# (8.948743e+11)	1.677295e+03^{4}# (9.878883e+01)	4.286781e+10^{6}# (2.185785e+11)
	5	1.238760e+02^{1} (6.856216e+00)	2.070816e+02^{2}# (3.027546e+01)	1.481482e+15^{6}# (5.237828e+15)	2.460201e+02^{3}# (3.270985e+01)	7.407414e+14^{5}# (3.777051e+15)	2.493589e+02^{4}# (1.866716e+01)	4.554259e+15^{7}# (2.322226e+16)
	6	1.364717e+01^{1} (2.213803e+00)	2.928840e+01^{3}# (3.398946e+00)	5.185185e+19^{7}# (8.764563e+19)	6.724722e+01^{4}# (3.132273e+01)	4.207912e+09^{6}# (1.677677e+10)	2.604308e+01^{2}# (3.062469e+00)	1.879244e+08^{5}# (9.581635e+08)

Table B.27 – *Continuation*

MOP	Dim.	PFI-EMOA	CRI-EMOA	AR-MOEA	RVEA	GrEA	SPEA2SDE	Two_Arch2
WFG8^{-1}	2	2.720586e+04^{1} (3.749423e+02)	2.725250e+04^{2} (4.180764e+02)	3.759086e+04^{5} # (7.291850e+01)	3.712207e+04^{4} # (3.972344e+02)	2.731098e+05^{7} # (2.707675e+05)	4.074706e+04^{6} # (1.127881e+03)	2.858378e+04^{3} # (4.855377e+02)
	3	6.084666e+03^{2} # (6.063735e+01)	6.360535e+03^{3} # (7.699653e+01)	8.212931e+08^{7} # (3.223479e+09)	2.088056e+03^{1} (2.886352e+01)	3.852268e+07^{6} # (9.823261e+07)	1.639110e+04^{5} # (9.152089e+02)	7.387274e+03^{4} # (9.482307e+02)
	4	9.123298e+02^{2} # (2.791790e+01)	4.440296e+03^{4} # (5.678442e+02)	2.320237e+12^{7} # (2.458732e+12)	8.275710e+01^{1} (1.104412e+01)	7.408231e+10^{6} # (3.777035e+11)	4.850737e+03^{5} # (4.932879e+02)	1.333048e+03^{3} # (5.385237e+01)
	5	1.275566e+02^{2} # (9.608725e+00)	1.127266e+03^{3} # (1.886778e+02)	2.078994e+16^{7} # (2.263096e+16)	1.867739e+01^{1} (7.863187e+00)	6.919681e+06^{6} # (3.520971e+07)	1.134371e+03^{4} # (1.191776e+02)	1.687640e+05^{5} # (6.926182e+05)
	6	1.155754e+01^{2} # (1.252428e+00)	2.141877e+02^{3} # (6.012442e+01)	1.925973e+20^{7} # (3.332504e+20)	2.426521e+00^{1} (9.363979e+00)	7.879693e+01^{3} # (5.486751e+01)	1.712311e+02^{4} # (2.866249e+01)	2.442814e+02^{6} # (1.124433e+03)
WFG9	2	2.852723e+04^{2} # (1.954992e+02)	2.890705e+04^{3} # (2.334989e+02)	3.286778e+04^{5} # (9.097286e+03)	2.818336e+04^{1} (6.124461e+02)	1.998849e+06^{7} # (4.240357e+06)	3.928899e+04^{6} # (8.224846e+02)	2.977973e+04^{4} # (3.566188e+02)
	3	6.527402e+03^{1} (7.718304e+01)	6.636667e+03^{2} # (8.624425e+01)	9.389091e+03^{5} # (1.089021e+04)	6.843179e+03^{3} # (1.871255e+02)	3.755399e+07^{7} # (7.756877e+07)	1.085983e+04^{6} # (3.822755e+02)	8.117192e+03^{4} # (1.644449e+03)
	4	1.022240e+03^{1} (2.534339e+01)	1.551176e+03^{2} # (1.184682e+02)	4.450481e+04^{5} # (2.085226e+05)	1.781017e+03^{3} # (4.040096e+02)	6.885259e+07^{6} # (2.473732e+08)	1.854780e+03^{4} # (1.685190e+02)	2.527759e+10^{7} # (1.288510e+11)
	5	1.685836e+02^{1} (1.314206e+01)	2.661491e+02^{2} # (3.499624e+01)	2.588496e+03^{5} # (3.767943e+03)	5.600174e+02^{4} # (1.279123e+02)	8.899632e+09^{6} # (3.038126e+10)	2.860218e+02^{3} # (3.811534e+01)	5.555992e+12^{7} # (2.829763e+13)
	6	2.549840e+01^{1} (4.828954e+00)	4.056235e+01^{3} # (1.058307e+01)	3.902677e+03^{5} # (1.009911e+04)	1.745747e+02^{4} # (6.118579e+01)	8.042925e+09^{6} # (4.100829e+10)	2.920259e+01^{2} # (4.589707e+00)	5.626269e+12^{7} # (2.867760e+13)
WFG9^{-1}	2	2.841594e+04^{1} (2.240574e+02)	2.897207e+04^{2} # (3.676298e+02)	3.765599e+04^{5} # (8.147602e+01)	3.737840e+04^{4} # (1.360842e+02)	8.905117e+04^{7} # (6.135995e+04)	4.081419e+04^{6} # (1.127566e+03)	2.965729e+04^{3} # (4.187001e+02)
	3	6.515077e+03^{2} # (6.803805e+01)	6.862758e+03^{3} # (9.351415e+01)	1.853270e+08^{7} # (1.532228e+08)	2.192110e+03^{1} (3.132116e+01)	1.486886e+07^{6} # (5.237175e+07)	1.485596e+04^{4} # (8.037095e+02)	2.541840e+04^{5} # (8.909428e+04)
	4	1.008895e+03^{2} # (2.761365e+01)	3.292845e+03^{4} # (4.385135e+02)	2.148273e+12^{7} # (2.876506e+12)	8.843541e+01^{1} (1.423439e+01)	3.816822e+04^{6} # (1.106681e+05)	3.715071e+03^{5} # (4.514395e+02)	2.598521e+03^{3} # (3.614437e+03)
	5	1.457236e+02^{2} # (8.756088e+00)	6.450094e+02^{4} # (1.589134e+02)	2.666668e+16^{7} # (2.309401e+16)	1.716978e+01^{1} (5.899369e+00)	4.917107e+02^{3} # (7.231843e+02)	6.926491e+02^{5} # (1.203884e+02)	6.059355e+05^{6} # (3.082252e+06)
	6	1.434450e+01^{1} (2.447901e+00)	9.653833e+01^{4} # (3.212666e+01)	1.530212e+21^{7} # (6.981445e+21)	1.653672e+02^{6} (8.402137e+02)	5.039339e+01^{2} # (1.157717e+01)	8.911805e+01^{3} # (9.543813e+00)	1.192267e+02^{5} # (3.193888e+02)

B.5 Riesz s-energy-based Reference Sets

Table B.28: IGD comparison using Riesz s-energy-based reference sets.

MOP	Dim.	IGD$^+$-MaOEA	MOMBI3	AR-MOEA	RVEA	GrEA	SPEA2SDE	Two_Arch2
DTLZ1	2	2.089448e-03^{4} (6.191438e-05)	1.791090e-03^{1} (7.981013e-05)	1.844755e-03^{2} (2.183797e-04)	1.949498e-03^{3} (4.042647e-04)	2.373220e-02^{7} (4.916860e-02)	2.119266e-03^{5} (9.090102e-05)	2.749354e-03^{6} (2.431254e-03)
	3	2.208048e-02^{6} (2.081770e-03)	1.909555e-02^{3} (1.345366e-04)	1.838089e-02^{2} (1.123296e-04)	1.831625e-02^{1} (5.287434e-05)	9.607633e-02^{7} (6.191685e-02)	2.085688e-02^{4} (4.319179e-04)	2.138772e-02^{5} (1.100602e-03)
	4	4.751874e-02^{6} (2.525199e-03)	4.065152e-02^{3} (3.440948e-04)	3.922978e-02^{2} (1.242262e-04)	3.917297e-02^{1} (6.950914e-05)	1.853183e-01^{7} (1.051811e-01)	4.513808e-02^{4} (6.953994e-04)	4.539366e-02^{5} (1.410650e-03)
	5	7.050889e-02^{6} (4.987017e-03)	6.079396e-02^{3} (4.329672e-04)	5.975603e-02^{2} (1.384775e-04)	5.964621e-02^{1} (8.224148e-05)	2.112903e-01^{7} (1.125937e-01)	6.558658e-02^{4} (1.808884e-03)	6.602702e-02^{5} (8.478648e-04)
	6	9.274712e-02^{6} (5.521361e-03)	7.807887e-02^{3} (5.211226e-04)	7.800274e-02^{2} (1.754956e-04)	7.782896e-02^{1} (9.479178e-05)	2.521583e-01^{7} (1.147648e-01)	8.414806e-02^{4} (1.594578e-03)	8.605077e-02^{5} (1.086270e-03)
DTLZ2	2	1.302338e-02^{7} (1.810769e-03)	3.952524e-03^{1} (2.381923e-05)	4.002938e-03^{2} (4.026474e-06)	4.279057e-03^{3} (3.818585e-04)	1.296351e-02^{6} (5.144319e-05)	1.290212e-02^{5} (1.793174e-03)	5.262734e-03^{4} (1.617970e-04)
	3	7.483440e-02^{6} (2.239246e-03)	5.236444e-02^{3} (4.061227e-04)	5.064176e-02^{2} (5.824474e-05)	5.061638e-02^{1} (7.433610e-06)	6.362132e-02^{5} (7.403981e-04)	7.525509e-02^{7} (2.577097e-03)	5.771188e-02^{4} (1.401794e-03)
	4	1.486492e-01^{7} (3.249372e-03)	1.257335e-01^{3} (8.466725e-04)	1.231644e-01^{2} (3.886105e-05)	1.231380e-01^{1} (2.307365e-05)	1.321351e-01^{4} (2.541755e-03)	1.482057e-01^{6} (1.736277e-03)	1.375135e-01^{5} (1.711214e-03)
	5	2.192138e-01^{6} (2.438186e-03)	1.959866e-01^{1} (1.109878e-03)	1.979329e-01^{2} (8.161296e-05)	1.979906e-01^{3} (3.124382e-05)	2.073870e-01^{4} (2.292334e-03)	2.195217e-01^{7} (2.180192e-03)	2.179686e-01^{5} (3.012256e-03)
	6	2.876050e-01^{6} (2.628043e-03)	2.661410e-01^{1} (2.522903e-03)	2.753680e-01^{3} (6.017445e-05)	2.753721e-01^{4} (1.295920e-05)	2.746988e-01^{2} (2.715344e-03)	2.843956e-01^{5} (3.305577e-03)	2.894944e-01^{7} (3.002071e-03)
DTLZ5	2	1.302451e-02^{7} (1.810830e-03)	3.960333e-03^{1} (2.667089e-05)	4.002413e-03^{2} (4.762785e-06)	4.461144e-03^{3} (3.793162e-04)	1.293564e-02^{6} (1.048915e-04)	1.290254e-02^{5} (1.366578e-03)	5.286801e-03^{4} (2.001845e-04)
	3	1.337850e-02^{5} (2.253218e-03)	6.663289e-03^{3} (8.624361e-04)	4.760384e-03^{1} (1.121422e-04)	7.349159e-02^{7} (4.069251e-03)	2.713455e-02^{6} (1.427747e-03)	1.334548e-02^{4} (2.027280e-03)	6.258316e-03^{2} (7.552371e-04)
	4	5.343629e-02^{5} (8.944921e-03)	1.124954e-02^{1} (1.202328e-03)	4.443838e-02^{2} (4.736701e-03)	2.441796e-01^{7} (1.169739e-02)	1.084788e-01^{6} (2.526689e-02)	5.021159e-02^{4} (1.241304e-02)	4.893602e-02^{3} (7.005499e-03)
	5	8.481340e-02^{4} (1.148538e-02)	2.389239e-02^{1} (2.002760e-03)	8.476252e-02^{3} (1.057987e-02)	1.950917e-01^{7} (2.652963e-02)	1.707054e-01^{6} (4.804539e-02)	7.737015e-02^{2} (1.566848e-02)	8.592142e-02^{5} (1.695925e-02)
	6	1.360608e-01^{5} (1.921019e-02)	2.834215e-02^{1} (1.726586e-03)	1.092749e-01^{2} (1.960697e-02)	2.131587e-01^{6} (8.211121e-02)	2.292988e-01^{7} (4.119523e-02)	1.170219e-01^{3} (1.250381e-02)	1.220557e-01^{4} (1.956886e-02)
DTLZ6	2	1.262486e-02^{6} (1.496859e-03)	3.953468e-03^{1} (2.384364e-05)	3.997476e-03^{2} (1.555166e-06)	3.997634e-03^{3} (1.714650e-06)	1.299020e-02^{7} (3.597908e-05)	1.254688e-02^{5} (1.526436e-03)	4.858450e-03^{4} (1.812535e-04)
	3	1.363481e-02^{4} (2.413381e-03)	1.398662e-02^{5} (2.178690e-03)	4.423650e-03^{1} (6.994653e-05)	7.493332e-02^{7} (7.109270e-03)	2.743975e-02^{6} (1.060777e-04)	1.260222e-02^{3} (2.106209e-03)	6.908154e-03^{2} (2.851768e-04)
	4	6.294665e-02^{4} (9.961326e-03)	1.436266e-02^{1} (4.872402e-05)	5.075887e-02^{2} (1.638417e-02)	1.765063e-01^{6} (2.550966e-02)	2.694540e-01^{7} (8.870388e-02)	5.381495e-02^{3} (9.000521e-03)	6.480255e-02^{5} (9.858556e-03)
	5	9.773779e-02^{2} (2.554251e-02)	1.971851e-02^{1} (1.757630e-03)	1.144989e-01^{4} (3.148296e-02)	1.405998e-01^{5} (3.063237e-02)	4.357039e-01^{7} (4.451880e-02)	9.900752e-02^{3} (1.744984e-02)	1.461538e-01^{6} (3.048729e-02)
	6	1.709875e-01^{4} (4.747296e-02)	2.707554e-02^{1} (8.549567e-03)	1.337705e-01^{2} (4.066839e-02)	1.673345e-01^{3} (4.668915e-02)	4.212604e-01^{7} (2.966874e-02)	1.842708e-01^{5} (4.483190e-02)	2.173143e-01^{6} (7.500563e-02)
DTLZ7	2	7.295611e-03^{3} (4.446757e-04)	5.389777e-03^{2} (4.083368e-04)	8.815713e-02^{7} (2.333703e-01)	1.912464e-02^{5} (2.424845e-03)	4.706542e-02^{6} (1.953304e-02)	7.854046e-03^{4} (6.695653e-04)	4.746991e-03^{1} (2.984687e-05)
	3	7.538527e-02^{1} (7.468422e-03)	9.320378e-02^{2} (9.682894e-03)	1.555873e-01^{6} (1.805867e-01)	1.172991e-01^{4} (2.109160e-03)	1.322836e-01^{5} (1.017100e-02)	9.406036e-02^{3} (1.430101e-02)	1.638879e-01^{7} (1.974674e-01)
	4	3.506022e-01^{7} (2.634156e-01)	1.821806e-01^{1} (5.328736e-03)	2.689578e-01^{5} (1.820541e-01)	3.476320e-01^{6} (3.312690e-03)	2.193189e-01^{2} (9.636622e-03)	2.420618e-01^{4} (5.562708e-02)	2.322999e-01^{3} (1.885733e-01)
	5	7.068673e-01^{7} (3.084326e-01)	3.873009e-01^{4} (1.109504e-01)	3.753053e-01^{3} (8.171595e-03)	6.833454e-01^{6} (1.067084e-02)	3.603832e-01^{1} (1.262884e-02)	4.239247e-01^{5} (7.074494e-02)	3.614106e-01^{2} (1.023814e-01)
	6	8.890220e-01^{6} (6.160838e-01)	6.521523e-01^{4} (2.567409e-01)	4.983465e-01^{1} (7.238941e-03)	1.304902e+00^{7} (5.968126e-02)	6.733887e-01^{5} (7.642582e-02)	5.029945e-01^{2} (2.821023e-02)	5.324190e-01^{3} (8.330644e-02)

Table B.28 – *Continuation*

MOP	Dim.	IGD$^+$-MaOEA	MOMBI3	AR-MOEA	RVEA	GrEA	SPEA2SDE	Two_Arch2
WFG1	2	9.815933e-01^{7} (1.598339e-02)	9.611372e-01^{6} (1.623934e-02)	1.670971e-01^{3} (4.857506e-02)	7.680590e-01^{5} (5.838414e-02)	1.502504e-01^{2} (3.694645e-02)	1.495466e-01^{1} (4.123950e-02)	2.932184e-01^{4} (5.322271e-02)
	3	1.130426e+00^{6} (1.438844e-02)	1.140983e+00^{7} (1.619618e-02)	5.387619e-01^{4} (5.958864e-02)	8.619522e-01^{5} (7.625500e-02)	3.852891e-01^{2} (3.651878e-02)	3.188146e-01^{1} (3.924647e-02)	5.370950e-01^{3} (4.581859e-02)
	4	1.336544e+00^{6} (2.911380e-02)	1.348022e+00^{7} (2.373965e-02)	7.986170e-01^{4} (5.209901e-02)	1.003595e+00^{5} (1.114822e-01)	6.776057e-01^{2} (1.084705e-01)	5.507430e-01^{1} (4.510787e-02)	7.966680e-01^{3} (7.205885e-02)
	5	1.562904e+00^{7} (3.773918e-02)	1.544909e+00^{6} (2.329497e-02)	9.725649e-01^{3} (5.869319e-02)	1.172323e+00^{5} (1.136791e-01)	9.044077e-01^{2} (7.165720e-02)	8.252224e-01^{1} (7.194093e-02)	1.027123e+00^{4} (6.853655e-02)
	6	1.845417e+00^{7} (2.188176e-01)	1.786655e+00^{6} (1.331439e-01)	1.242482e+00^{3} (6.516171e-02)	1.360731e+00^{4} (9.336883e-02)	1.172335e+00^{1} (8.097826e-02)	1.396186e+00^{5} (1.083598e-01)	1.228551e+00^{2} (5.078279e-02)
WFG2	2	3.234381e-01^{7} (5.975547e-02)	1.580167e-01^{1} (1.562619e-01)	2.425274e-01^{6} (1.389113e-01)	1.628697e-01^{2} (1.133657e-01)	2.116046e-01^{4} (1.402733e-01)	2.054706e-01^{3} (1.545234e-01)	2.407449e-01^{5} (1.416473e-01)
	3	4.184759e-01^{6} (1.524529e-01)	3.353822e-01^{1} (1.640826e-01)	4.106785e-01^{5} (1.896221e-01)	3.597037e-01^{3} (1.858185e-01)	3.934160e-01^{4} (1.304571e-01)	4.731361e-01^{7} (1.426240e-01)	3.387827e-01^{2} (1.946614e-01)
	4	9.748887e-01^{7} (2.014461e-01)	6.478702e-01^{3} (2.399085e-01)	6.169584e-01^{1} (2.333210e-01)	6.909600e-01^{4} (2.427336e-01)	8.551820e-01^{5} (1.974260e-01)	9.490244e-01^{6} (1.679712e-01)	6.207841e-01^{2} (2.577176e-01)
	5	1.556550e+00^{7} (2.180828e-01)	8.046459e-01^{1} (2.501754e-01)	8.353550e-01^{2} (2.332823e-01)	1.237189e+00^{5} (3.040188e-01)	1.152309e+00^{4} (1.611949e-01)	1.530695e+00^{6} (2.194192e-01)	8.896438e-01^{3} (2.928290e-01)
	6	2.147859e+00^{6} (2.503432e-01)	1.265947e+00^{3} (3.529989e-01)	1.233485e+00^{1} (3.172725e-01)	1.963559e+00^{5} (3.526986e-01)	1.686628e+00^{4} (2.801769e-01)	2.278093e+00^{7} (2.432840e-01)	1.252698e+00^{2} (3.298790e-01)
WFG3	2	1.491241e-02^{2} (1.160607e-03)	1.381540e-02^{1} (2.105770e-03)	2.080606e-02^{4} (7.467208e-03)	7.627550e-02^{7} (1.091442e-02)	2.850218e-02^{6} (3.110011e-03)	1.639522e-02^{3} (1.464193e-03)	2.384463e-02^{5} (7.875931e-03)
	3	6.468043e-02^{1} (6.948613e-03)	8.523700e-02^{3} (9.606614e-03)	1.449330e-01^{6} (1.091034e-02)	2.417642e-01^{7} (2.633635e-02)	8.449592e-02^{2} (7.773747e-03)	8.675018e-02^{4} (3.675278e-02)	8.691274e-02^{5} (6.135290e-03)
	4	2.500166e-01^{2} (7.969293e-02)	2.832488e-01^{4} (2.694103e-02)	4.062067e-01^{6} (2.958270e-02)	3.609293e-01^{5} (3.547953e-02)	2.189971e-01^{1} (4.596407e-02)	7.708139e-01^{7} (2.556026e-01)	2.690389e-01^{3} (1.835735e-02)
	5	4.938219e-01^{4} (1.190170e-01)	4.242641e-01^{1} (3.132450e-02)	7.083330e-01^{5} (5.442897e-02)	8.469952e-01^{6} (2.577748e-01)	4.742363e-01^{3} (5.740639e-02)	1.014580e+00^{7} (3.123520e-01)	4.732048e-01^{2} (3.592822e-02)
	6	7.484271e-01^{4} (2.698599e-01)	4.737831e-01^{1} (5.072037e-02)	1.176710e+00^{5} (4.268719e-02)	1.835864e+00^{7} (4.635325e-01)	6.711787e-01^{2} (5.708565e-02)	1.395589e+00^{6} (4.409781e-01)	7.208129e-01^{3} (5.068438e-02)
WFG4	2	4.178574e-02^{5} (9.409248e-03)	1.356010e-02^{1} (5.981262e-04)	1.498094e-02^{2} (1.026112e-03)	6.545790e-02^{7} (6.050327e-03)	3.301469e-02^{4} (2.183808e-03)	5.130570e-02^{6} (9.741055e-03)	1.760508e-02^{3} (6.697624e-04)
	3	3.142255e-01^{6} (1.497645e-02)	2.199127e-01^{2} (2.571116e-03)	2.189026e-01^{1} (9.566860e-04)	2.251180e-01^{3} (1.621123e-03)	2.594524e-01^{5} (7.730174e-03)	3.641452e-01^{7} (2.075551e-02)	2.301305e-01^{4} (6.741925e-03)
	4	7.693196e-01^{6} (2.610138e-02)	6.458779e-01^{1} (4.851493e-03)	6.664885e-01^{3} (2.000156e-03)	6.647960e-01^{2} (1.290079e-03)	6.848551e-01^{5} (1.105126e-02)	8.696583e-01^{7} (3.444149e-02)	6.783869e-01^{4} (1.130205e-02)
	5	1.348548e+00^{6} (3.371853e-02)	1.236545e+00^{2} (1.346287e-02)	1.292884e+00^{5} (2.977323e-03)	1.286164e+00^{4} (4.077745e-03)	1.222092e+00^{1} (1.147777e-02)	1.452643e+00^{7} (4.299448e-02)	1.256269e+00^{3} (1.950905e-02)
	6	2.119445e+00^{7} (6.617552e-02)	1.878557e+00^{4} (2.663774e-02)	1.980655e+00^{5} (3.760755e-03)	1.952130e+00^{4} (1.395892e-02)	1.904284e+00^{2} (2.674602e-02)	2.105803e+00^{6} (4.045887e-02)	1.932132e+00^{3} (1.954336e-02)

Table B.29: IGD comparison using SLD-based reference sets.

MOP	Dim.	IGD$^+$-MaOEA	MOMBI3	AR-MOEA	RVEA	GrEA	SPEA2SDE	Two_Arch2
DTLZ1	2	2.105033e-03^{4} (6.613826e-05)	1.794184e-03^{1} (7.876173e-05)	1.844850e-03^{2} (2.152859e-04)	1.948025e-03^{3} (4.022104e-04)	2.299250e-02^{7} (4.817066e-02)	2.128214e-03^{5} (8.549475e-05)	2.782740e-03^{6} (2.484284e-03)
	3	2.165740e-02^{6} (2.022873e-03)	1.935637e-02^{3} (1.466965e-04)	1.867502e-02^{2} (1.357317e-04)	1.858912e-02^{1} (6.820966e-05)	9.218526e-02^{7} (5.970679e-02)	2.042788e-02^{4} (3.420215e-04)	2.165432e-02^{5} (1.284013e-03)
	4	4.711092e-02^{6} (2.245100e-03)	4.414981e-02^{3} (3.185905e-04)	4.250321e-02^{2} (9.049470e-05)	4.247653e-02^{1} (3.845019e-05)	1.796068e-01^{7} (1.037246e-01)	4.479389e-02^{4} (5.938980e-04)	4.622342e-02^{5} (1.914541e-03)
	5	6.963928e-02^{6} (5.103530e-03)	6.864613e-02^{3} (3.470896e-04)	6.901021e-02^{4} (1.680519e-04)	6.905676e-02^{5} (1.585963e-04)	2.097054e-01^{7} (1.121214e-01)	6.436659e-02^{1} (1.772027e-03)	6.508468e-02^{2} (8.739552e-04)
	6	9.360804e-02^{6} (5.859124e-03)	8.429082e-02^{1} (6.013267e-04)	8.648162e-02^{4} (2.936423e-04)	8.658946e-02^{5} (1.543829e-04)	2.549342e-01^{7} (1.151138e-01)	8.467258e-02^{2} (1.768606e-03)	8.578660e-02^{3} (1.278358e-03)
DTLZ2	2	1.428725e-02^{7} (2.112492e-03)	3.894532e-03^{1} (1.611915e-05)	3.895745e-03^{2} (6.397115e-06)	4.162856e-03^{3} (3.698834e-04)	1.369920e-02^{5} (4.789562e-05)	1.415355e-02^{6} (2.096217e-03)	5.635183e-03^{4} (1.948716e-04)
	3	7.863121e-02^{6} (2.822361e-03)	5.021347e-02^{3} (4.386479e-04)	4.617511e-02^{2} (5.793091e-05)	4.607270e-02^{1} (6.976607e-06)	6.472099e-02^{5} (6.027448e-04)	7.957810e-02^{7} (3.067364e-03)	5.913830e-02^{4} (1.707328e-03)
	4	1.422338e-01^{6} (4.417829e-03)	1.111591e-01^{3} (9.074089e-04)	1.055082e-01^{2} (6.752039e-05)	1.054939e-01^{1} (9.272021e-06)	1.197331e-01^{4} (2.005333e-03)	1.428401e-01^{7} (3.460037e-03)	1.411828e-01^{5} (2.721276e-03)
	5	2.018549e-01^{5} (3.190564e-03)	1.984994e-01^{2} (1.379287e-03)	1.999245e-01^{3} (1.381132e-04)	2.002417e-01^{4} (1.471749e-05)	1.916328e-01^{1} (2.260732e-03)	2.051801e-01^{6} (3.067455e-03)	2.192992e-01^{7} (4.414625e-03)
	6	2.842296e-01^{6} (3.581530e-03)	2.702062e-01^{4} (1.808991e-03)	2.634259e-01^{2} (1.740168e-04)	2.635084e-01^{3} (8.929137e-06)	2.583249e-01^{1} (2.669884e-03)	2.823496e-01^{5} (3.525272e-03)	2.944463e-01^{7} (5.364660e-03)
DTLZ5	2	1.428759e-02^{7} (2.111868e-03)	3.894359e-03^{1} (1.611280e-05)	3.894842e-03^{2} (7.318221e-06)	4.338392e-03^{3} (3.689696e-04)	1.367472e-02^{5} (9.818511e-05)	1.417084e-02^{6} (1.604365e-03)	5.659347e-03^{4} (2.472919e-04)
	3	1.826160e-02^{5} (3.122512e-03)	6.008330e-03^{2} (9.919591e-04)	4.614101e-03^{1} (2.582520e-04)	6.383745e-02^{7} (4.115847e-03)	2.613500e-02^{6} (1.425032e-03)	1.698871e-02^{4} (2.360358e-03)	6.778596e-03^{3} (9.509727e-04)
	4	5.916376e-02^{5} (8.705794e-03)	8.784738e-03^{1} (8.767716e-04)	3.605886e-02^{2} (7.179256e-03)	1.734704e-01^{7} (1.112295e-02)	8.478607e-02^{6} (2.002448e-02)	5.684686e-02^{4} (1.181072e-02)	4.125320e-02^{3} (6.805201e-03)
	5	5.649650e-02^{2} (8.601730e-03)	1.019727e-02^{1} (4.045653e-03)	6.253901e-02^{4} (1.470886e-02)	1.209428e-01^{7} (2.350321e-02)	9.506279e-02^{6} (4.737310e-02)	5.787228e-02^{3} (9.555190e-03)	6.916106e-02^{5} (1.709988e-02)
	6	7.207885e-02^{5} (3.135330e-02)	2.719133e-02^{1} (5.723693e-03)	6.528479e-02^{4} (2.443908e-02)	1.983400e-01^{7} (5.698256e-02)	1.197466e-01^{6} (6.712109e-02)	5.740448e-02^{2} (2.102445e-02)	5.765080e-02^{3} (1.829699e-02)
DTLZ6	2	1.384439e-02^{7} (1.745747e-03)	3.899493e-03^{3} (2.207042e-05)	3.885160e-03^{2} (1.454807e-06)	3.884755e-03^{1} (1.391840e-06)	1.372383e-02^{5} (3.346306e-05)	1.375317e-02^{6} (1.750315e-03)	5.120835e-03^{4} (2.199204e-04)
	3	1.806334e-02^{5} (3.270200e-03)	1.720498e-02^{4} (2.117758e-03)	4.176088e-03^{1} (1.155095e-04)	6.806786e-02^{7} (6.927011e-03)	2.634660e-02^{6} (9.553813e-05)	1.589625e-02^{3} (2.214583e-03)	7.646760e-03^{2} (3.774442e-04)
	4	6.575393e-02^{5} (9.316944e-03)	9.396992e-03^{1} (2.346192e-04)	4.392828e-02^{2} (1.849869e-02)	1.305184e-01^{6} (1.776228e-02)	2.106169e-01^{7} (6.844508e-02)	6.009381e-02^{4} (8.957063e-03)	5.336345e-02^{3} (9.147300e-03)
	5	6.174258e-02^{2} (1.386731e-02)	7.902286e-03^{1} (3.121439e-03)	6.211884e-02^{3} (1.741400e-02)	9.945523e-02^{6} (3.421735e-02)	3.799132e-01^{7} (5.318739e-02)	8.041058e-02^{4} (2.751768e-02)	9.585861e-02^{5} (2.609986e-02)
	6	8.080190e-02^{3} (6.515671e-02)	1.317016e-02^{1} (7.311685e-03)	7.834605e-02^{2} (3.982017e-02)	1.621213e-01^{6} (1.007629e-01)	4.846232e-01^{7} (3.865549e-02)	9.906237e-02^{4} (5.198567e-02)	1.495756e-01^{5} (1.114708e-01)
DTLZ7	2	8.179780e-03^{3} (2.344475e-03)	4.390935e-03^{2} (1.095911e-04)	7.924717e-02^{7} (2.103389e-01)	2.288758e-02^{5} (4.458330e-03)	3.227182e-02^{6} (1.214687e-02)	8.825837e-03^{4} (1.477552e-03)	4.154940e-03^{1} (3.110700e-05)
	3	8.221633e-02^{3} (1.004281e-02)	4.966691e-02^{1} (1.540801e-03)	1.519452e-01^{6} (2.025357e-01)	9.961943e-02^{5} (3.922994e-03)	9.642789e-02^{4} (1.031000e-02)	6.279279e-02^{2} (2.738905e-03)	1.686278e-01^{7} (2.177986e-01)
	4	4.402732e-01^{7} (3.300004e-01)	1.229572e-01^{1} (3.958065e-03)	2.692569e-01^{5} (2.645075e-01)	2.846096e-01^{6} (6.939889e-03)	1.825118e-01^{3} (1.390538e-02)	1.451266e-01^{2} (9.063439e-02)	2.505911e-01^{4} (2.586099e-01)
	5	9.306829e-01^{7} (4.596335e-01)	3.351663e-01^{3} (1.978481e-01)	2.993521e-01^{1} (1.236186e-02)	6.722837e-01^{6} (1.697709e-02)	3.828967e-01^{4} (6.511358e-02)	2.998197e-01^{2} (1.677318e-01)	4.077007e-01^{5} (1.547213e-01)
	6	1.044141e+00^{6} (7.196644e-01)	6.730634e-01^{4} (3.519208e-01)	5.132445e-01^{2} (1.250598e-02)	1.372258e+00^{7} (2.778470e-02)	8.866828e-01^{5} (1.291525e-01)	3.167569e-01^{1} (1.001102e-01)	5.949022e-01^{3} (9.761684e-02)

Table B.29 – *Continuation*

MOP	Dim.	IGD$^+$-MaOEA	MOMBI3	AR-MOEA	RVEA	GrEA	SPEA2SDE	Two_Arch2
WFG1	2	9.997051e-01^{7} (1.623290e-02)	9.764581e-01^{6} (1.650243e-02)	1.486454e-01^{3} (5.437827e-02)	7.844861e-01^{5} (6.020357e-02)	1.384461e-01^{2} (4.108061e-02)	1.356167e-01^{1} (4.618819e-02)	2.902729e-01^{4} (5.786901e-02)
	3	1.171754e+00^{6} (1.427740e-02)	1.191713e+00^{7} (1.691433e-02)	5.592764e-01^{4} (6.543920e-02)	9.023024e-01^{5} (8.222220e-02)	3.870833e-01^{2} (4.304779e-02)	2.799868e-01^{1} (3.667666e-02)	5.546854e-01^{3} (5.012469e-02)
	4	1.383210e+00^{6} (2.153405e-02)	1.407223e+00^{7} (2.532734e-02)	8.212173e-01^{4} (6.015574e-02)	1.027004e+00^{5} (1.132940e-01)	6.468711e-01^{2} (9.589369e-02)	4.588415e-01^{1} (3.478161e-02)	8.191027e-01^{3} (8.010305e-02)
	5	1.579611e+00^{6} (2.653842e-02)	1.591354e+00^{7} (2.607309e-02)	9.614821e-01^{3} (6.917742e-02)	1.116530e+00^{5} (1.136095e-01)	8.141854e-01^{2} (7.067225e-02)	6.666583e-01^{1} (4.848128e-02)	1.024211e+00^{4} (7.611928e-02)
	6	1.803986e+00^{7} (1.250632e-01)	1.785883e+00^{6} (7.249904e-02)	1.190504e+00^{4} (7.891645e-02)	1.218071e+00^{5} (9.438285e-02)	1.014634e+00^{1} (7.046485e-02)	1.030694e+00^{2} (6.729838e-02)	1.178734e+00^{3} (5.921499e-02)
WFG2	2	2.956513e-01^{7} (5.532228e-02)	1.426335e-01^{1} (1.445513e-01)	2.198279e-01^{5} (1.299147e-01)	1.574546e-01^{2} (1.007099e-01)	1.894829e-01^{4} (1.318221e-01)	1.869568e-01^{3} (1.424213e-01)	2.212709e-01^{6} (1.290839e-01)
	3	2.790953e-01^{3} (1.789936e-01)	2.749698e-01^{2} (1.981554e-01)	3.770123e-01^{7} (2.174194e-01)	3.242739e-01^{6} (1.958300e-01)	2.749419e-01^{1} (1.567955e-01)	3.217098e-01^{5} (1.847323e-01)	3.153545e-01^{4} (2.156497e-01)
	4	8.156440e-01^{7} (3.160402e-01)	6.355970e-01^{4} (3.662658e-01)	5.993264e-01^{1} (3.674012e-01)	6.045240e-01^{2} (3.345032e-01)	7.095258e-01^{5} (3.111989e-01)	7.208153e-01^{6} (2.656273e-01)	6.244147e-01^{3} (3.755597e-01)
	5	1.333039e+00^{7} (4.444634e-01)	7.221917e-01^{1} (4.213339e-01)	7.631819e-01^{2} (4.415437e-01)	1.028465e+00^{5} (4.727804e-01)	8.547878e-01^{3} (3.092179e-01)	1.213322e+00^{6} (4.193114e-01)	8.743622e-01^{4} (5.053471e-01)
	6	1.687462e+00^{6} (4.759212e-01)	1.109226e+00^{1} (5.243480e-01)	1.166047e+00^{3} (5.466763e-01)	1.668561e+00^{5} (5.778571e-01)	1.413500e+00^{4} (5.366980e-01)	1.859156e+00^{7} (4.830788e-01)	1.133397e+00^{2} (5.686533e-01)
WFG3	2	1.462885e-02^{2} (1.083936e-03)	1.385251e-02^{1} (2.106883e-03)	2.080766e-02^{4} (7.453229e-03)	7.658615e-02^{7} (1.095048e-02)	2.861892e-02^{6} (3.102222e-03)	1.632436e-02^{3} (1.458564e-03)	2.385527e-02^{5} (7.873175e-03)
	3	6.249591e-02^{1} (7.519862e-03)	8.210067e-02^{3} (8.705019e-03)	1.438565e-01^{6} (1.142762e-02)	2.342781e-01^{7} (2.805292e-02)	8.169807e-02^{2} (7.790922e-03)	1.029380e-01^{5} (6.389944e-02)	8.377634e-02^{4} (5.124442e-03)
	4	2.913261e-01^{4} (1.983063e-01)	2.707651e-01^{3} (2.360861e-02)	3.918231e-01^{6} (1.954030e-02)	3.320896e-01^{5} (3.535364e-02)	1.949949e-01^{1} (4.256587e-02)	1.360517e+00^{7} (4.182111e-01)	2.408205e-01^{2} (2.603809e-02)
	5	6.689214e-01^{5} (4.101911e-01)	3.662505e-01^{2} (6.650767e-02)	6.566053e-01^{4} (9.661710e-02)	1.252424e+00^{6} (6.889855e-01)	2.968479e-01^{1} (5.770258e-02)	1.979413e+00^{7} (5.843479e-01)	4.174528e-01^{3} (5.842410e-02)
	6	9.858892e-01^{5} (6.442344e-01)	4.452399e-01^{2} (9.877424e-02)	9.467361e-01^{4} (4.208576e-02)	2.905209e+00^{7} (7.278719e-01)	4.295792e-01^{1} (1.105180e-01)	2.523046e+00^{6} (7.144186e-01)	5.666343e-01^{3} (1.551667e-01)
WFG4	2	4.328060e-02^{5} (9.206486e-03)	1.296474e-02^{1} (5.940737e-04)	1.438491e-02^{2} (1.047880e-03)	6.479297e-02^{7} (5.822631e-03)	3.265908e-02^{4} (2.303408e-03)	5.166226e-02^{6} (9.569634e-03)	1.781773e-02^{3} (7.805056e-04)
	3	3.166516e-01^{6} (1.558682e-02)	2.047145e-01^{3} (2.728383e-03)	1.909962e-01^{1} (1.257440e-03)	1.970797e-01^{2} (1.848695e-03)	2.478813e-01^{5} (6.604254e-03)	3.551733e-01^{7} (1.878834e-02)	2.276834e-01^{4} (7.030028e-03)
	4	6.972186e-01^{6} (2.486093e-02)	5.321694e-01^{3} (4.480562e-03)	5.131167e-01^{2} (1.392172e-03)	5.117304e-01^{1} (1.186286e-03)	5.838627e-01^{4} (8.908132e-03)	7.859281e-01^{7} (3.303323e-02)	6.638801e-01^{5} (1.581938e-02)
	5	1.242242e+00^{6} (2.633308e-02)	1.192837e+00^{2} (1.292896e-02)	1.221320e+00^{5} (3.791522e-03)	1.218581e+00^{4} (6.083245e-03)	1.093165e+00^{1} (2.047093e-02)	1.343622e+00^{7} (3.511972e-02)	1.214282e+00^{3} (2.159133e-02)
	6	1.993920e+00^{6} (6.077512e-02)	1.709406e+00^{4} (3.090699e-02)	1.644267e+00^{3} (4.709165e-03)	1.611945e+00^{1} (1.624295e-02)	1.638098e+00^{2} (2.186162e-02)	2.037696e+00^{7} (3.242708e-02)	1.892298e+00^{5} (3.746259e-02)

Table B.30: IGD comparison using UDH-based reference sets.

MOP	Dim.	IGD$^+$-MaOEA	MOMBI3	AR-MOEA	RVEA	GrEA	SPEA2SDE	Two_Arch2
DTLZ1	2	2.104001e-03^{4} (6.538460e-05)	1.790883e-03^{1} (7.934803e-05)	1.844774e-03^{2} (2.144821e-04)	1.949600e-03^{3} (4.009148e-04)	2.279802e-02^{7} (4.791675e-02)	2.129326e-03^{5} (8.470121e-05)	2.784240e-03^{6} (2.491050e-03)
	3	2.180187e-02^{5} (1.983796e-03)	1.985293e-02^{3} (1.450950e-04)	1.890580e-02^{2} (1.076211e-04)	1.882461e-02^{1} (4.884626e-05)	8.922194e-02^{7} (5.812102e-02)	2.056978e-02^{4} (3.164549e-04)	2.221140e-02^{6} (1.339592e-03)
	4	4.498874e-02^{5} (2.211853e-03)	4.485093e-02^{4} (3.461127e-04)	4.306628e-02^{3} (1.372368e-04)	4.299797e-02^{2} (8.780134e-05)	1.711773e-01^{7} (1.026380e-01)	4.278653e-02^{1} (6.191603e-04)	4.620351e-02^{6} (2.295570e-03)
	5	6.500721e-02^{3} (3.536077e-03)	6.757143e-02^{6} (5.803085e-04)	6.612251e-02^{5} (2.428150e-04)	6.605767e-02^{4} (1.715846e-04)	1.957060e-01^{7} (1.084983e-01)	6.104552e-02^{1} (7.990691e-04)	6.479471e-02^{2} (1.262957e-03)
	6	8.510700e-02^{3} (4.661531e-03)	8.638569e-02^{4} (8.005577e-04)	8.654040e-02^{6} (2.714653e-04)	8.644306e-02^{5} (1.891581e-04)	2.342789e-01^{7} (1.128673e-01)	7.688359e-02^{1} (1.046104e-03)	8.041820e-02^{2} (1.434306e-03)
DTLZ2	2	1.430354e-02^{7} (2.117884e-03)	3.897536e-03^{2} (1.334732e-05)	3.896139e-03^{1} (5.309725e-06)	4.168120e-03^{3} (3.730410e-04)	1.371766e-02^{5} (4.854304e-05)	1.417070e-02^{6} (2.101485e-03)	5.615731e-03^{4} (1.961018e-04)
	3	8.011346e-02^{6} (2.779649e-03)	5.258585e-02^{3} (3.989993e-04)	5.026954e-02^{2} (6.206709e-05)	5.023988e-02^{1} (9.262625e-06)	6.607947e-02^{5} (6.678335e-04)	8.067890e-02^{7} (3.151655e-03)	5.882569e-02^{4} (1.712779e-03)
	4	1.540394e-01^{6} (4.096395e-03)	1.257352e-01^{3} (1.025580e-03)	1.229519e-01^{1} (7.530109e-05)	1.229896e-01^{2} (1.767541e-05)	1.323112e-01^{4} (2.030561e-03)	1.540894e-01^{7} (2.671936e-03)	1.375148e-01^{5} (2.095761e-03)
	5	2.131297e-01^{5} (2.457061e-03)	1.917376e-01^{3} (1.323695e-03)	1.888933e-01^{1} (1.038258e-04)	1.889097e-01^{2} (2.440092e-05)	1.986589e-01^{4} (2.284830e-03)	2.137853e-01^{6} (2.802623e-03)	2.176629e-01^{7} (3.463716e-03)
	6	2.720624e-01^{6} (3.674766e-03)	2.509993e-01^{3} (3.307487e-03)	2.490588e-01^{1} (1.230400e-04)	2.490738e-01^{2} (1.384473e-05)	2.612117e-01^{4} (1.971625e-03)	2.702818e-01^{5} (3.144097e-03)	2.914915e-01^{7} (4.718551e-03)
DTLZ5	2	1.430283e-02^{7} (2.117994e-03)	3.897561e-03^{2} (1.334108e-05)	3.895421e-03^{1} (5.685666e-06)	4.346473e-03^{3} (3.699411e-04)	1.369238e-02^{5} (9.689323e-05)	1.418611e-02^{6} (1.610562e-03)	5.637905e-03^{4} (2.527389e-04)
	3	1.707916e-02^{5} (3.303011e-03)	5.933840e-03^{3} (7.177504e-04)	4.702368e-03^{1} (1.316538e-04)	6.585503e-02^{7} (4.213063e-03)	2.643290e-02^{6} (1.687038e-03)	1.553562e-02^{4} (2.507702e-03)	5.827482e-03^{2} (6.114171e-04)
	4	6.238160e-02^{5} (1.247110e-02)	9.720415e-03^{1} (1.036402e-03)	4.078942e-02^{2} (6.513234e-03)	1.861242e-01^{7} (8.683859e-03)	1.012938e-01^{6} (2.641793e-02)	5.981193e-02^{4} (1.524708e-02)	4.360515e-02^{3} (6.524138e-03)
	5	1.000723e-01^{5} (1.513420e-02)	1.809549e-02^{1} (1.996416e-03)	7.236595e-02^{2} (1.024732e-02)	1.411700e-01^{6} (1.703092e-02)	1.485686e-01^{7} (3.968749e-02)	9.555092e-02^{4} (2.203790e-02)	7.776082e-02^{3} (1.298050e-02)
	6	1.284837e-01^{5} (1.853917e-02)	2.198422e-02^{1} (1.884705e-03)	9.634929e-02^{2} (1.951145e-02)	1.550730e-01^{6} (4.072535e-02)	1.984735e-01^{7} (3.539563e-02)	1.169874e-01^{4} (1.479330e-02)	1.002111e-01^{3} (1.578166e-02)
DTLZ6	2	1.386032e-02^{7} (1.752139e-03)	3.901333e-03^{3} (2.109547e-05)	3.889446e-03^{2} (1.378302e-06)	3.888447e-03^{1} (1.212097e-06)	1.374128e-02^{5} (3.336276e-05)	1.376813e-02^{6} (1.755453e-03)	5.088982e-03^{4} (2.227692e-04)
	3	1.682659e-02^{5} (3.562052e-03)	1.650742e-02^{4} (2.433004e-03)	4.313459e-03^{1} (9.887454e-05)	7.072576e-02^{7} (7.151626e-03)	2.648861e-02^{6} (7.460570e-05)	1.441732e-02^{3} (2.203353e-03)	6.365853e-03^{2} (2.290715e-04)
	4	6.927269e-02^{5} (1.273207e-02)	1.211516e-02^{1} (6.865126e-05)	5.147050e-02^{2} (2.185329e-02)	1.405467e-01^{6} (1.672307e-02)	2.233620e-01^{7} (7.138413e-02)	6.145249e-02^{4} (1.038850e-02)	5.593125e-02^{3} (6.640641e-03)
	5	1.052638e-01^{2} (2.819787e-02)	1.508979e-02^{1} (5.950863e-04)	1.057422e-01^{3} (3.432979e-02)	1.225612e-01^{5} (3.148192e-02)	3.271223e-01^{7} (2.970348e-02)	1.094091e-01^{4} (1.789853e-02)	1.266652e-01^{6} (2.559378e-02)
	6	1.586835e-01^{3} (3.790597e-02)	2.218765e-02^{1} (7.182403e-03)	1.189968e-01^{2} (3.961025e-02)	1.644646e-01^{4} (9.011012e-02)	3.254433e-01^{7} (1.647256e-02)	1.704340e-01^{6} (3.896388e-02)	1.682607e-01^{5} (5.704716e-02)
DTLZ7	2	8.190962e-03^{3} (2.350615e-03)	4.389390e-03^{2} (1.081673e-04)	7.893278e-02^{7} (2.094086e-01)	2.290728e-02^{5} (4.473273e-03)	3.232469e-02^{6} (1.217282e-02)	8.840420e-03^{4} (1.482964e-03)	4.169597e-03^{1} (3.202894e-05)
	3	8.363103e-02^{3} (1.116519e-02)	4.863955e-02^{1} (1.733852e-03)	1.481581e-01^{6} (1.950484e-01)	9.721717e-02^{4} (3.788232e-03)	9.775715e-02^{5} (1.187671e-02)	6.179119e-02^{2} (3.252352e-03)	1.642929e-01^{7} (2.099979e-01)
	4	4.165808e-01^{7} (2.878092e-01)	1.288376e-01^{1} (4.607723e-03)	2.655544e-01^{5} (2.290308e-01)	3.232149e-01^{6} (5.409461e-03)	1.922120e-01^{3} (1.388249e-02)	1.444126e-01^{2} (8.033230e-02)	2.354110e-01^{4} (2.297699e-01)
	5	8.427254e-01^{7} (4.126784e-01)	3.411339e-01^{4} (1.640564e-01)	3.178975e-01^{2} (1.749643e-02)	7.435439e-01^{6} (1.391916e-02)	3.408975e-01^{3} (4.657011e-02)	2.876229e-01^{1} (1.501907e-01)	3.698213e-01^{5} (1.414299e-01)
	6	1.050844e+00^{6} (7.322262e-01)	6.933550e-01^{4} (3.481261e-01)	4.951398e-01^{2} (8.791478e-03)	1.319851e+00^{7} (4.689997e-02)	9.243628e-01^{5} (1.299648e-01)	3.459427e-01^{1} (7.898416e-02)	5.513499e-01^{3} (1.187095e-01)

Table B.30 – *Continuation*

MOP	Dim.	IGD$^+$-MaOEA	MOMBI3	AR-MOEA	RVEA	GrEA	SPEA2SDE	Two_Arch2
WFG1	2	9.995969e-01^{7} (1.623497e-02)	9.763610e-01^{6} (1.649875e-02)	1.479085e-01^{3} (5.461913e-02)	7.845304e-01^{5} (6.020356e-02)	1.380036e-01^{2} (4.126817e-02)	1.350382e-01^{1} (4.645501e-02)	2.901154e-01^{4} (5.803134e-02)
	3	1.171455e+00^{6} (1.424267e-02)	1.192703e+00^{7} (1.689253e-02)	5.590643e-01^{4} (6.607070e-02)	9.039749e-01^{5} (8.226646e-02)	3.861391e-01^{2} (4.369279e-02)	2.741631e-01^{1} (3.748917e-02)	5.541495e-01^{3} (5.038931e-02)
	4	1.381217e+00^{6} (2.011319e-02)	1.415983e+00^{7} (2.594767e-02)	8.368441e-01^{4} (6.103652e-02)	1.035249e+00^{5} (1.122962e-01)	6.216970e-01^{2} (9.250225e-02)	4.252575e-01^{1} (4.157799e-02)	8.170520e-01^{3} (8.196023e-02)
	5	1.567048e+00^{6} (2.724633e-02)	1.623513e+00^{7} (2.886271e-02)	9.870873e-01^{3} (7.745140e-02)	1.092909e+00^{5} (1.256361e-01)	7.138178e-01^{2} (8.266161e-02)	5.356754e-01^{1} (4.279697e-02)	1.010935e+00^{4} (8.256865e-02)
	6	1.718205e+00^{6} (3.792894e-02)	1.788013e+00^{7} (2.472841e-02)	1.194626e+00^{5} (9.378792e-02)	1.114765e+00^{4} (1.324858e-01)	8.277348e-01^{2} (6.795462e-02)	6.114815e-01^{1} (3.986218e-02)	1.104238e+00^{3} (7.431463e-02)
WFG2	2	2.919313e-01^{7} (5.461468e-02)	1.408839e-01^{1} (1.426805e-01)	2.171267e-01^{5} (1.281298e-01)	1.563367e-01^{2} (9.891542e-02)	1.872846e-01^{4} (1.299533e-01)	1.847227e-01^{3} (1.404722e-01)	2.185182e-01^{6} (1.273169e-01)
	3	2.708864e-01^{1} (1.694095e-01)	2.722777e-01^{3} (1.868100e-01)	3.654160e-01^{7} (2.079050e-01)	3.177317e-01^{6} (1.848709e-01)	2.709690e-01^{2} (1.475962e-01)	3.122282e-01^{5} (1.743504e-01)	3.073239e-01^{4} (2.058473e-01)
	4	7.117344e-01^{7} (3.442947e-01)	6.117706e-01^{6} (3.712138e-01)	5.899830e-01^{2} (3.619661e-01)	5.401684e-01^{1} (3.481553e-01)	6.079171e-01^{5} (3.394134e-01)	5.969660e-01^{4} (2.934897e-01)	5.908195e-01^{3} (3.861430e-01)
	5	1.064249e+00^{7} (5.660817e-01)	6.771401e-01^{2} (4.442194e-01)	7.016092e-01^{3} (4.810877e-01)	8.099523e-01^{5} (5.401982e-01)	5.844477e-01^{1} (3.717637e-01)	9.007483e-01^{6} (5.296794e-01)	7.878792e-01^{4} (5.560114e-01)
	6	1.113797e+00^{5} (7.729060e-01)	9.476411e-01^{1} (6.455016e-01)	1.065796e+00^{3} (7.050877e-01)	1.334352e+00^{6} (8.255314e-01)	1.066176e+00^{4} (7.819136e-01)	1.375711e+00^{7} (7.944234e-01)	9.829118e-01^{2} (7.250366e-01)
WFG3	2	1.463773e-02^{2} (1.108013e-03)	1.383263e-02^{1} (2.115273e-03)	2.080142e-02^{4} (7.454714e-03)	7.664481e-02^{7} (1.096167e-02)	2.856387e-02^{6} (3.105537e-03)	1.634282e-02^{3} (1.468121e-03)	2.384749e-02^{5} (7.874976e-03)
	3	6.326711e-02^{1} (7.540131e-03)	8.077802e-02^{2} (9.259171e-03)	1.447415e-01^{6} (1.137622e-02)	2.378028e-01^{7} (2.862860e-02)	8.188007e-02^{3} (7.948279e-03)	9.685550e-02^{5} (5.378009e-02)	8.222067e-02^{4} (5.602901e-03)
	4	2.686415e-01^{4} (1.406470e-01)	2.670417e-01^{3} (2.459902e-02)	4.079721e-01^{6} (2.150377e-02)	3.459219e-01^{5} (2.658070e-02)	2.017880e-01^{1} (3.690319e-02)	1.126512e+00^{7} (3.754496e-01)	2.622612e-01^{2} (2.383120e-02)
	5	5.771395e-01^{4} (2.657603e-01)	3.908960e-01^{2} (3.740205e-02)	7.213344e-01^{5} (8.076784e-02)	1.059808e+00^{6} (5.162318e-01)	3.905464e-01^{1} (6.135811e-02)	1.582581e+00^{7} (5.214689e-01)	4.308436e-01^{3} (4.148384e-02)
	6	9.118128e-01^{4} (5.369695e-01)	4.529826e-01^{1} (5.856998e-02)	1.126506e+00^{5} (5.809888e-02)	2.645335e+00^{7} (7.655539e-01)	5.809699e-01^{2} (6.015858e-02)	2.242909e+00^{6} (7.229874e-01)	6.615284e-01^{3} (8.196570e-02)
WFG4	2	4.333672e-02^{5} (9.231403e-03)	1.293716e-02^{1} (5.741800e-04)	1.436097e-02^{2} (1.030724e-03)	6.490014e-02^{7} (5.834536e-03)	3.270648e-02^{4} (2.325403e-03)	5.173797e-02^{6} (9.588134e-03)	1.778041e-02^{3} (7.851977e-04)
	3	3.206998e-01^{6} (1.556406e-02)	2.136592e-01^{2} (2.678301e-03)	2.093994e-01^{1} (9.044902e-04)	2.157568e-01^{3} (1.586962e-03)	2.519616e-01^{5} (6.222226e-03)	3.587229e-01^{7} (1.933174e-02)	2.271295e-01^{4} (6.638268e-03)
	4	7.533792e-01^{6} (2.306992e-02)	6.241435e-01^{1} (6.913984e-03)	6.304691e-01^{3} (1.800922e-03)	6.296049e-01^{2} (1.309564e-03)	6.535199e-01^{4} (1.076207e-02)	8.301913e-01^{7} (3.253923e-02)	6.538811e-01^{5} (1.126711e-02)
	5	1.268636e+00^{6} (2.373649e-02)	1.137825e+00^{3} (1.177701e-02)	1.141203e+00^{4} (2.753808e-03)	1.135959e+00^{2} (5.238171e-03)	1.122776e+00^{1} (1.520901e-02)	1.367669e+00^{7} (4.065393e-02)	1.217746e+00^{5} (2.163537e-02)
	6	1.880565e+00^{6} (4.499399e-02)	1.648014e+00^{2} (2.019612e-02)	1.649912e+00^{3} (3.111378e-03)	1.634902e+00^{1} (9.674348e-03)	1.677103e+00^{4} (2.410792e-02)	1.935898e+00^{7} (3.489776e-02)	1.872551e+00^{5} (3.152566e-02)

Table B.31: IGD comparison using Random-based reference sets.

MOP	Dim.	IGD$^+$-MaOEA	MOMBI3	AR-MOEA	RVEA	GrEA	SPEA2SDE	Two_Arch2
DTLZ1	2	2.122990e-03^{4} (7.940192e-05)	1.782186e-03^{1} (7.851859e-05)	1.841916e-03^{2} (2.215992e-04)	1.945354e-03^{3} (4.032621e-04)	2.157760e-02^{7} (4.596346e-02)	2.130533e-03^{5} (1.100075e-04)	2.786915e-03^{6} (2.482308e-03)
	3	2.187158e-02^{6} (2.037187e-03)	1.909761e-02^{3} (2.261250e-04)	1.839792e-02^{2} (1.214705e-04)	1.832317e-02^{1} (5.325760e-05)	9.660762e-02^{7} (6.246358e-02)	2.065250e-02^{4} (5.572669e-04)	2.132224e-02^{5} (1.177309e-03)
	4	4.574340e-02^{6} (2.412565e-03)	4.234757e-02^{3} (3.226809e-04)	4.123308e-02^{2} (1.477262e-04)	4.120908e-02^{1} (9.972120e-05)	1.797464e-01^{7} (1.033585e-01)	4.381816e-02^{4} (7.529776e-04)	4.532635e-02^{5} (1.754092e-03)
	5	6.956190e-02^{6} (4.866533e-03)	6.168459e-02^{3} (4.717930e-04)	6.022851e-02^{2} (2.013091e-04)	6.015984e-02^{1} (9.399737e-05)	2.081580e-01^{7} (1.111492e-01)	6.454068e-02^{4} (1.512158e-03)	6.590035e-02^{5} (8.664959e-04)
	6	9.013723e-02^{6} (5.242620e-03)	8.178911e-02^{2} (6.962494e-04)	8.213932e-02^{4} (1.840747e-04)	8.202686e-02^{3} (1.615146e-04)	2.478781e-01^{7} (1.150074e-01)	8.143976e-02^{1} (1.508169e-03)	8.404330e-02^{5} (1.154784e-03)
DTLZ2	2	1.448590e-02^{7} (2.239081e-03)	3.831364e-03^{1} (7.423334e-05)	3.855591e-03^{2} (9.530790e-06)	4.140627e-03^{3} (3.867660e-04)	1.268673e-02^{5} (5.258891e-05)	1.429285e-02^{6} (2.249932e-03)	5.502863e-03^{4} (4.260694e-04)
	3	7.525690e-02^{6} (2.560540e-03)	5.264496e-02^{3} (4.344583e-04)	5.068683e-02^{1} (8.205260e-05)	5.069278e-02^{2} (8.826590e-06)	6.295778e-02^{5} (9.300094e-04)	7.585390e-02^{7} (2.951273e-03)	5.741122e-02^{4} (1.554334e-03)
	4	1.534782e-01^{7} (3.666671e-03)	1.281519e-01^{3} (1.076111e-03)	1.251547e-01^{1} (4.805905e-05)	1.251613e-01^{2} (1.669892e-05)	1.350142e-01^{4} (2.753644e-03)	1.521949e-01^{6} (1.945796e-03)	1.366307e-01^{5} (2.190958e-03)
	5	2.202984e-01^{6} (2.383384e-03)	2.022198e-01^{1} (1.143805e-03)	2.070041e-01^{2} (1.187318e-04)	2.070689e-01^{3} (5.039779e-05)	2.089316e-01^{4} (2.581359e-03)	2.209064e-01^{7} (2.778935e-03)	2.127213e-01^{5} (2.936400e-03)
	6	2.930731e-01^{7} (3.544477e-03)	2.726326e-01^{1} (2.023051e-03)	2.849727e-01^{4} (6.534213e-05)	2.849938e-01^{5} (1.195779e-05)	2.786298e-01^{2} (3.054638e-03)	2.897298e-01^{6} (4.972952e-03)	2.849452e-01^{3} (3.081391e-03)
DTLZ5	2	1.463158e-02^{7} (2.357089e-03)	3.901883e-03^{2} (7.514204e-05)	3.802491e-03^{1} (1.486225e-05)	4.283735e-03^{3} (3.737555e-04)	1.344353e-02^{5} (7.072189e-05)	1.457066e-02^{6} (1.803868e-03)	5.839425e-03^{4} (4.259825e-04)
	3	1.251831e-02^{4} (2.352814e-03)	6.627389e-03^{3} (8.753998e-04)	4.727304e-03^{1} (1.240792e-04)	7.418447e-02^{7} (4.123474e-03)	2.724457e-02^{6} (1.338618e-03)	1.267335e-02^{5} (2.207933e-03)	6.073985e-03^{2} (7.013437e-04)
	4	4.887975e-02^{5} (1.002653e-02)	1.114920e-02^{1} (1.280711e-03)	4.459400e-02^{2} (4.429804e-03)	2.547589e-01^{7} (1.172795e-02)	1.143330e-01^{6} (2.801673e-02)	4.604125e-02^{3} (1.318709e-02)	4.785857e-02^{4} (6.899095e-03)
	5	9.463367e-02^{5} (1.235552e-02)	2.382399e-02^{1} (1.629128e-03)	8.282416e-02^{2} (9.807849e-03)	2.026203e-01^{7} (2.788055e-02)	1.639583e-01^{6} (4.142744e-02)	8.711550e-02^{3} (1.708381e-02)	9.203252e-02^{4} (1.866585e-02)
	6	1.332148e-01^{5} (1.915836e-02)	2.868598e-02^{1} (1.797062e-03)	1.074462e-01^{2} (1.975547e-02)	2.208085e-01^{6} (7.765713e-02)	2.290993e-01^{7} (4.539119e-02)	1.136131e-01^{3} (1.401603e-02)	1.170587e-01^{4} (1.984056e-02)
DTLZ6	2	1.411906e-02^{6} (2.165436e-03)	3.959571e-03^{1} (7.651533e-05)	3.973875e-03^{3} (3.298187e-06)	3.973086e-03^{2} (3.320816e-06)	1.422714e-02^{7} (2.124404e-05)	1.385103e-02^{5} (1.992895e-03)	5.033930e-03^{4} (3.169876e-04)
	3	1.241366e-02^{4} (2.327192e-03)	1.390128e-02^{5} (2.266968e-03)	4.307963e-03^{1} (7.370992e-05)	7.473719e-02^{7} (7.443258e-03)	2.745766e-02^{6} (1.007741e-04)	1.136412e-02^{3} (2.016142e-03)	5.793192e-03^{2} (2.423585e-04)
	4	5.730148e-02^{4} (1.075894e-02)	1.511476e-02^{1} (3.831532e-05)	5.139590e-02^{3} (1.606651e-02)	1.782400e-01^{6} (2.766511e-02)	2.754999e-01^{7} (9.400649e-02)	4.851601e-02^{2} (8.506237e-03)	6.313529e-02^{5} (9.128902e-03)
	5	1.060486e-01^{2} (2.404918e-02)	2.002524e-02^{1} (1.277262e-03)	1.139849e-01^{4} (2.931459e-02)	1.421332e-01^{5} (2.899086e-02)	3.971114e-01^{7} (3.990401e-02)	1.062282e-01^{3} (1.623989e-02)	1.512574e-01^{6} (3.046521e-02)
	6	1.688888e-01^{4} (5.224841e-02)	2.777954e-02^{1} (9.571481e-03)	1.369949e-01^{2} (4.013581e-02)	1.685560e-01^{3} (4.564005e-02)	4.610656e-01^{7} (2.965938e-02)	1.837964e-01^{5} (4.665568e-02)	2.197566e-01^{6} (8.410053e-02)
DTLZ7	2	6.199217e-03^{3} (4.977229e-04)	4.825427e-03^{2} (1.796284e-04)	8.175801e-02^{7} (2.156622e-01)	2.075383e-02^{5} (3.142458e-03)	3.965549e-02^{6} (1.644958e-02)	6.451670e-03^{4} (5.807875e-04)	4.314813e-03^{1} (6.263863e-05)
	3	7.175638e-02^{1} (7.318123e-03)	9.142992e-02^{3} (9.401353e-03)	1.570927e-01^{6} (1.837583e-01)	1.190905e-01^{4} (1.760888e-03)	1.287546e-01^{5} (9.937362e-03)	9.085404e-02^{2} (1.485350e-02)	1.646925e-01^{7} (2.000097e-01)
	4	3.420749e-01^{6} (2.621617e-01)	1.780235e-01^{1} (4.950090e-03)	2.650455e-01^{5} (1.800469e-01)	3.485712e-01^{7} (3.225877e-03)	2.105102e-01^{2} (9.272506e-03)	2.338799e-01^{4} (5.493927e-02)	2.305593e-01^{3} (1.861635e-01)
	5	6.713107e-01^{6} (3.010521e-01)	3.771722e-01^{3} (1.050315e-01)	3.777018e-01^{4} (1.050504e-02)	6.757838e-01^{7} (1.028425e-02)	3.353557e-01^{1} (1.136474e-02)	4.046187e-01^{5} (6.725444e-02)	3.549662e-01^{2} (9.647183e-02)
	6	8.601724e-01^{6} (5.983783e-01)	6.380195e-01^{4} (2.452621e-01)	5.022950e-01^{1} (7.346007e-03)	1.285793e+00^{7} (6.397577e-02)	6.406006e-01^{5} (6.934588e-02)	5.025682e-01^{2} (2.436701e-02)	5.157199e-01^{3} (7.997373e-02)

Table B.31 – *Continuation*

MOP	Dim.	IGD$^+$-MaOEA	MOMBI3	AR-MOEA	RVEA	GrEA	SPEA2SDE	Two_Arch2
WFG1	2	1.002648e+00^{7} (1.632348e-02)	9.792325e-01^{6} (1.659367e-02)	1.470348e-01^{3} (5.503004e-02)	7.863076e-01^{5} (6.035175e-02)	1.375227e-01^{2} (4.152123e-02)	1.343223e-01^{1} (4.700598e-02)	2.902030e-01^{4} (5.829729e-02)
	3	1.136517e+00^{6} (1.420485e-02)	1.149619e+00^{7} (1.633180e-02)	5.413890e-01^{4} (6.067192e-02)	8.682814e-01^{5} (7.747433e-02)	3.833152e-01^{2} (3.765997e-02)	3.121191e-01^{1} (3.841919e-02)	5.390806e-01^{3} (4.621482e-02)
	4	1.336982e+00^{6} (2.790633e-02)	1.353490e+00^{7} (2.398687e-02)	7.999979e-01^{4} (5.272473e-02)	1.001218e+00^{5} (1.092992e-01)	6.582631e-01^{2} (9.763480e-02)	5.162693e-01^{1} (4.119925e-02)	7.949905e-01^{3} (7.310513e-02)
	5	1.541753e+00^{7} (3.129558e-02)	1.540692e+00^{6} (2.432350e-02)	9.579831e-01^{3} (6.031332e-02)	1.131261e+00^{5} (1.116244e-01)	8.527538e-01^{2} (6.686541e-02)	7.586958e-01^{1} (6.276162e-02)	1.005769e+00^{4} (7.045287e-02)
	6	1.779792e+00^{7} (1.908900e-01)	1.763171e+00^{6} (1.073076e-01)	1.207521e+00^{4} (6.929092e-02)	1.272285e+00^{5} (9.037398e-02)	1.081753e+00^{1} (5.982785e-02)	1.181419e+00^{2} (7.885151e-02)	1.186210e+00^{3} (4.963618e-02)
WFG2	2	3.774162e-01^{7} (7.073652e-02)	1.815207e-01^{2} (1.851105e-01)	2.799561e-01^{6} (1.666496e-01)	1.756049e-01^{1} (1.387162e-01)	2.414035e-01^{4} (1.689005e-01)	2.380349e-01^{3} (1.826005e-01)	2.795021e-01^{5} (1.668415e-01)
	3	3.982291e-01^{5} (1.543673e-01)	3.310771e-01^{1} (1.628366e-01)	4.045044e-01^{6} (1.907077e-01)	3.548877e-01^{3} (1.845288e-01)	3.856882e-01^{4} (1.287517e-01)	4.542812e-01^{7} (1.439465e-01)	3.340118e-01^{2} (1.954608e-01)
	4	8.949975e-01^{7} (2.080101e-01)	6.294227e-01^{3} (2.479606e-01)	6.009273e-01^{2} (2.392728e-01)	6.336071e-01^{4} (2.428153e-01)	7.841559e-01^{5} (2.059607e-01)	8.579769e-01^{6} (1.697523e-01)	6.007684e-01^{1} (2.679241e-01)
	5	1.340366e+00^{7} (2.577005e-01)	7.561532e-01^{1} (2.745982e-01)	7.724436e-01^{2} (2.635507e-01)	1.042620e+00^{5} (3.284797e-01)	9.630800e-01^{4} (1.826575e-01)	1.290533e+00^{6} (2.536782e-01)	8.413921e-01^{3} (3.215030e-01)
	6	1.785146e+00^{6} (2.413379e-01)	1.162767e+00^{3} (3.138277e-01)	1.147089e+00^{2} (2.690098e-01)	1.634505e+00^{5} (3.288890e-01)	1.405960e+00^{4} (2.730746e-01)	1.901939e+00^{7} (2.322959e-01)	1.124687e+00^{1} (3.105391e-01)
WFG3	2	1.473045e-02^{2} (1.253819e-03)	1.367228e-02^{1} (2.154499e-03)	2.066393e-02^{4} (7.527483e-03)	7.667406e-02^{7} (1.090051e-02)	2.785171e-02^{6} (3.192421e-03)	1.626991e-02^{3} (1.507106e-03)	2.375770e-02^{5} (7.946248e-03)
	3	6.426376e-02^{1} (6.701034e-03)	8.552151e-02^{4} (9.550733e-03)	1.451036e-01^{6} (1.114694e-02)	2.415049e-01^{7} (2.658850e-02)	8.390307e-02^{3} (8.440924e-03)	8.338311e-02^{2} (3.493215e-02)	8.745456e-02^{5} (6.083818e-03)
	4	2.476505e-01^{2} (7.531784e-02)	2.843194e-01^{4} (2.836978e-02)	4.061399e-01^{6} (3.016321e-02)	3.654616e-01^{5} (3.724553e-02)	2.173250e-01^{1} (4.637897e-02)	7.449449e-01^{7} (2.483868e-01)	2.704088e-01^{3} (1.848067e-02)
	5	5.006421e-01^{4} (1.250219e-01)	4.230010e-01^{1} (3.193003e-02)	7.054437e-01^{5} (5.381508e-02)	8.471321e-01^{6} (2.636997e-01)	4.738057e-01^{3} (5.380156e-02)	1.022703e+00^{7} (3.098661e-01)	4.735939e-01^{2} (3.825077e-02)
	6	7.485660e-01^{4} (2.700150e-01)	4.714959e-01^{1} (4.986751e-02)	1.183463e+00^{5} (4.473611e-02)	1.839107e+00^{7} (4.659606e-01)	6.668699e-01^{2} (5.692689e-02)	1.396437e+00^{6} (4.446633e-01)	7.176782e-01^{3} (5.102730e-02)
WFG4	2	4.405420e-02^{5} (9.578138e-03)	1.291359e-02^{1} (5.747429e-04)	1.401849e-02^{2} (1.014851e-03)	6.492384e-02^{7} (5.993645e-03)	3.203918e-02^{4} (2.142574e-03)	5.301939e-02^{6} (9.503734e-03)	1.760558e-02^{3} (7.560191e-04)
	3	3.125406e-01^{6} (1.353258e-02)	2.212421e-01^{1} (3.343262e-03)	2.222415e-01^{2} (1.000000e-03)	2.285326e-01^{3} (1.497585e-03)	2.549867e-01^{5} (6.102548e-03)	3.591950e-01^{7} (1.955898e-02)	2.287701e-01^{4} (7.892822e-03)
	4	7.680410e-01^{6} (2.345173e-02)	6.511462e-01^{1} (5.973003e-03)	6.670848e-01^{3} (1.737322e-03)	6.659637e-01^{2} (1.645958e-03)	6.851125e-01^{5} (1.257369e-02)	8.616618e-01^{7} (3.063757e-02)	6.721455e-01^{4} (1.031061e-02)
	5	1.356434e+00^{6} (4.204681e-02)	1.232194e+00^{2} (9.390111e-03)	1.294797e+00^{5} (3.094746e-03)	1.285049e+00^{4} (5.110980e-03)	1.227034e+00^{1} (1.628082e-02)	1.469415e+00^{7} (4.490817e-02)	1.248896e+00^{3} (2.142048e-02)
	6	2.185299e+00^{7} (8.034014e-02)	1.932639e+00^{2} (2.713730e-02)	2.061355e+00^{5} (4.459170e-03)	2.031766e+00^{4} (1.702154e-02)	1.941442e+00^{3} (3.173691e-02)	2.144181e+00^{6} (4.915705e-02)	1.889961e+00^{1} (2.254923e-02)

Table B.32: IGD$^+$ comparison using Riesz s-energy-based reference sets.

MOP	Dim.	IGD$^+$-MaOEA	MOMBI3	AR-MOEA	RVEA	GrEA	SPEA2SDE	Two_Arch2
DTLZ1	2	1.315106e-03^{2} (1.191745e-04)	1.274471e-03^{1} (1.945049e-04)	1.400592e-03^{4} (3.508159e-04)	1.523608e-03^{5} (5.461475e-04)	1.096880e-02^{7} (2.423192e-02)	1.329244e-03^{3} (1.135653e-04)	1.666720e-03^{6} (7.232445e-04)
	3	1.379706e-02^{6} (1.190706e-03)	1.243473e-02^{2} (2.777026e-04)	1.251461e-02^{3} (4.819439e-04)	1.224954e-02^{1} (2.894994e-04)	4.887621e-02^{7} (3.351176e-02)	1.310816e-02^{4} (2.837088e-04)	1.326195e-02^{5} (5.537059e-04)
	4	2.941292e-02^{6} (1.260346e-03)	2.637023e-02^{3} (6.413878e-04)	2.599136e-02^{2} (3.682155e-04)	2.592727e-02^{1} (3.258087e-04)	1.133172e-01^{7} (7.901422e-02)	2.818731e-02^{5} (4.066981e-04)	2.812254e-02^{4} (6.961008e-04)
	5	4.258102e-02^{6} (2.177878e-03)	3.929584e-02^{1} (5.934402e-04)	3.990212e-02^{4} (4.300546e-04)	3.980790e-02^{3} (3.470306e-04)	1.370225e-01^{7} (8.572904e-02)	3.976893e-02^{2} (7.949098e-04)	4.015993e-02^{5} (5.904879e-04)
	6	5.541926e-02^{6} (3.215957e-03)	4.984632e-02^{1} (9.135478e-04)	5.058892e-02^{4} (4.662482e-04)	5.037164e-02^{3} (2.653475e-04)	1.690983e-01^{7} (9.395538e-02)	4.987463e-02^{2} (9.100300e-04)	5.138853e-02^{5} (6.659857e-04)
DTLZ2	2	1.918250e-03^{4} (9.145256e-05)	1.612092e-03^{2} (1.391267e-05)	1.719602e-03^{3} (4.018355e-06)	1.999980e-03^{6} (3.203280e-04)	3.814607e-03^{7} (2.912230e-05)	1.950516e-03^{5} (6.130340e-05)	1.463745e-03^{1} (9.575196e-06)
	3	2.182024e-02^{4} (5.844749e-04)	2.115762e-02^{3} (3.381309e-04)	2.109249e-02^{2} (6.912420e-05)	2.108097e-02^{1} (3.984605e-05)	2.229260e-02^{6} (2.127113e-04)	2.213477e-02^{5} (6.431949e-04)	2.261587e-02^{7} (5.271828e-04)
	4	5.108211e-02^{5} (1.565725e-03)	5.092431e-02^{4} (7.086080e-04)	5.068333e-02^{3} (9.385952e-05)	5.053746e-02^{2} (2.426846e-05)	4.971953e-02^{1} (6.319572e-04)	5.169899e-02^{6} (1.218326e-03)	6.558799e-02^{7} (1.458590e-03)
	5	7.654930e-02^{1} (1.648893e-03)	7.919183e-02^{5} (8.346402e-04)	7.682977e-02^{3} (1.432557e-04)	7.657499e-02^{2} (3.342115e-05)	8.159644e-02^{6} (1.423647e-03)	7.888085e-02^{4} (2.019538e-03)	1.148141e-01^{7} (2.096857e-03)
	6	1.062454e-01^{4} (3.418538e-03)	1.060659e-01^{3} (1.988972e-03)	1.003329e-01^{2} (2.187523e-04)	1.001340e-01^{1} (1.312887e-05)	1.132509e-01^{6} (1.348091e-03)	1.068658e-01^{5} (1.818846e-03)	1.614929e-01^{7} (4.618435e-03)
DTLZ5	2	1.921191e-03^{5} (9.102807e-05)	1.619193e-03^{2} (1.704701e-05)	1.720129e-03^{3} (2.318668e-06)	2.167896e-03^{6} (3.305087e-04)	3.800352e-03^{7} (5.047249e-05)	1.917341e-03^{4} (7.469776e-05)	1.461620e-03^{1} (1.539252e-05)
	3	1.930775e-03^{2} (9.466951e-05)	2.581669e-03^{5} (3.080253e-04)	2.015362e-03^{4} (6.773987e-05)	4.132391e-02^{7} (1.063939e-02)	1.071981e-02^{6} (3.484422e-04)	1.957823e-03^{3} (7.997941e-05)	1.619857e-03^{1} (3.671396e-05)
	4	1.300133e-02^{3} (1.336435e-03)	4.132098e-03^{1} (3.985028e-04)	2.617665e-02^{5} (2.723561e-03)	1.109932e-01^{7} (6.561773e-03)	3.576332e-02^{6} (8.299198e-03)	1.107175e-02^{2} (1.768170e-03)	1.995155e-02^{4} (3.301913e-03)
	5	2.972371e-02^{3} (4.601417e-03)	9.261654e-03^{1} (8.376877e-04)	4.919774e-02^{5} (7.654815e-03)	1.384860e-01^{7} (2.403185e-02)	7.589660e-02^{6} (2.325411e-02)	2.228012e-02^{2} (4.242486e-03)	4.118428e-02^{4} (1.317443e-02)
	6	5.564352e-02^{4} (1.308130e-02)	9.454966e-03^{1} (1.065935e-03)	5.503626e-02^{3} (1.409919e-02)	1.147123e-01^{7} (5.755834e-02)	9.252837e-02^{6} (2.014597e-02)	3.092925e-02^{2} (4.224748e-03)	6.023479e-02^{5} (1.813327e-02)
DTLZ6	2	1.865800e-03^{5} (5.471654e-05)	1.608156e-03^{2} (1.150373e-05)	1.716699e-03^{4} (7.382414e-07)	1.716695e-03^{3} (9.582500e-07)	3.839385e-03^{7} (1.819382e-05)	1.880363e-03^{6} (9.096315e-05)	1.489254e-03^{1} (1.148906e-05)
	3	1.919405e-03^{4} (1.082674e-04)	3.998451e-03^{5} (6.756355e-04)	1.789669e-03^{2} (2.853219e-05)	3.752398e-02^{7} (9.218614e-03)	1.108027e-02^{6} (4.187398e-05)	1.873012e-03^{3} (1.043861e-04)	1.535139e-03^{1} (2.429523e-05)
	4	1.491437e-02^{3} (2.453129e-03)	5.162280e-03^{1} (4.662082e-05)	1.933820e-02^{4} (4.362820e-03)	9.301527e-02^{6} (2.527540e-02)	1.013511e-01^{7} (2.854072e-02)	1.278988e-02^{2} (2.206656e-03)	2.456968e-02^{5} (5.962803e-03)
	5	3.404915e-02^{3} (1.032632e-02)	7.482953e-03^{1} (6.136425e-04)	5.048388e-02^{4} (1.168938e-02)	8.152975e-02^{6} (2.582855e-02)	1.282906e-01^{7} (2.424013e-02)	3.197944e-02^{2} (6.521894e-03)	6.606002e-02^{5} (2.274363e-02)
	6	5.170562e-02^{3} (1.702365e-02)	8.832567e-03^{1} (2.459217e-03)	5.445812e-02^{4} (1.712856e-02)	8.961514e-02^{5} (5.115611e-02)	1.208239e-01^{7} (3.237188e-02)	4.847581e-02^{2} (1.023371e-02)	9.484188e-02^{6} (4.036558e-02)
DTLZ7	2	1.701381e-03^{3} (4.798039e-05)	1.458304e-03^{2} (1.198377e-05)	5.221855e-02^{7} (1.429800e-01)	1.457612e-02^{6} (2.222293e-03)	5.444343e-03^{5} (6.682679e-04)	1.772585e-03^{4} (7.512223e-05)	1.457792e-03^{1} (1.614774e-05)
	3	2.248160e-02^{3} (1.273651e-03)	1.989779e-02^{1} (5.629805e-04)	6.299389e-02^{6} (8.190250e-02)	4.394690e-02^{5} (3.425914e-03)	2.972096e-02^{4} (1.141289e-03)	2.127644e-02^{2} (5.442816e-04)	6.912031e-02^{7} (8.759172e-02)
	4	1.587422e-01^{7} (1.457477e-01)	6.280124e-02^{1} (1.431086e-03)	1.198799e-01^{5} (1.072472e-01)	1.267021e-01^{6} (4.904090e-03)	6.807694e-02^{3} (2.358152e-03)	6.353756e-02^{2} (2.559696e-02)	1.101067e-01^{4} (1.057153e-01)
	5	3.389732e-01^{7} (2.003695e-01)	1.381937e-01^{3} (5.414849e-02)	1.522105e-01^{4} (5.880187e-03)	2.911907e-01^{6} (7.261932e-03)	1.300904e-01^{2} (8.337313e-03)	1.155509e-01^{1} (3.715789e-02)	1.776774e-01^{5} (4.330194e-02)
	6	5.441396e-01^{6} (4.948542e-01)	3.130660e-01^{3} (1.961850e-01)	2.606749e-01^{2} (8.437207e-03)	5.876689e-01^{7} (2.989967e-02)	3.343243e-01^{5} (4.296388e-02)	1.656091e-01^{1} (2.713237e-02)	3.303298e-01^{4} (5.010319e-02)

Table B.32 – *Continuation*

MOP	Dim.	IGD$^+$-MaOEA	MOMBI3	AR-MOEA	RVEA	GrEA	SPEA2SDE	Two_Arch2
WFG1	2	9.793911e-01^{7} (1.596660e-02)	9.593739e-01^{6} (1.620050e-02)	1.452407e-01^{3} (5.365707e-02)	7.655580e-01^{5} (5.851993e-02)	1.344482e-01^{2} (4.059125e-02)	1.307083e-01^{1} (4.606835e-02)	2.841574e-01^{4} (5.634618e-02)
	3	1.121368e+00^{6} (1.404076e-02)	1.135157e+00^{7} (1.622555e-02)	5.232150e-01^{4} (6.254782e-02)	8.497097e-01^{5} (8.078124e-02)	3.547011e-01^{2} (4.339385e-02)	2.382123e-01^{1} (4.317288e-02)	5.204426e-01^{3} (4.801244e-02)
	4	1.308667e+00^{6} (1.968814e-02)	1.331212e+00^{7} (2.433815e-02)	7.487103e-01^{3} (5.636082e-02)	9.459847e-01^{5} (1.129640e-01)	5.380248e-01^{2} (8.607241e-02)	3.448084e-01^{1} (5.458486e-02)	7.516678e-01^{4} (7.844946e-02)
	5	1.481228e+00^{6} (2.396086e-02)	1.500035e+00^{7} (2.408499e-02)	8.488380e-01^{3} (7.582662e-02)	9.829516e-01^{5} (1.197903e-01)	6.235135e-01^{2} (9.216612e-02)	4.141101e-01^{1} (5.877446e-02)	9.208895e-01^{4} (8.084310e-02)
	6	1.636166e+00^{6} (2.383526e-02)	1.652862e+00^{7} (2.505590e-02)	1.024162e+00^{5} (8.726157e-02)	9.810712e-01^{3} (1.408584e-01)	7.024805e-01^{2} (8.667091e-02)	4.145433e-01^{1} (7.807036e-02)	1.007817e+00^{4} (7.241468e-02)
WFG2	2	9.092437e-02^{6} (1.660951e-02)	4.513274e-02^{1} (4.129429e-02)	7.179207e-02^{4} (3.765631e-02)	9.817470e-02^{7} (3.720898e-02)	6.089241e-02^{3} (3.992604e-02)	5.998587e-02^{2} (4.106502e-02)	8.424027e-02^{5} (4.416742e-02)
	3	9.849634e-02^{2} (1.083767e-01)	1.153133e-01^{3} (1.181832e-01)	1.926087e-01^{7} (1.204643e-01)	1.774956e-01^{6} (1.108148e-01)	9.568655e-02^{1} (9.818096e-02)	1.173758e-01^{4} (1.155888e-01)	1.497853e-01^{5} (1.210333e-01)
	4	2.984366e-01^{7} (2.264895e-01)	2.713570e-01^{4} (2.239741e-01)	2.869859e-01^{6} (2.086796e-01)	2.509425e-01^{2} (1.996335e-01)	2.627061e-01^{3} (2.085643e-01)	2.110597e-01^{1} (1.970498e-01)	2.744214e-01^{5} (2.172370e-01)
	5	4.614344e-01^{7} (3.151141e-01)	2.385384e-01^{1} (2.505686e-01)	3.020600e-01^{3} (2.582285e-01)	3.355526e-01^{4} (2.944246e-01)	2.501222e-01^{2} (1.956551e-01)	3.494217e-01^{6} (3.015552e-01)	3.490289e-01^{5} (2.865534e-01)
	6	4.632068e-01^{4} (3.669761e-01)	3.197776e-01^{1} (3.353457e-01)	4.271781e-01^{3} (3.503793e-01)	5.626294e-01^{7} (4.068243e-01)	4.852030e-01^{5} (3.593748e-01)	5.538416e-01^{6} (3.946442e-01)	4.104749e-01^{2} (3.422352e-01)
WFG3	2	1.164928e-02^{1} (1.814116e-03)	1.204553e-02^{2} (2.724495e-03)	2.013017e-02^{4} (7.712359e-03)	7.480213e-02^{7} (1.097124e-02)	2.020727e-02^{5} (4.828298e-03)	1.376824e-02^{3} (2.094420e-03)	2.302906e-02^{6} (8.383162e-03)
	3	4.451503e-02^{1} (7.765677e-03)	7.587075e-02^{5} (1.024452e-02)	1.281018e-01^{6} (1.176235e-02)	1.984578e-01^{7} (2.967561e-02)	4.732991e-02^{3} (5.947972e-03)	4.722713e-02^{2} (9.194676e-03)	6.766012e-02^{4} (7.942428e-03)
	4	1.538379e-01^{2} (2.582636e-02)	2.413323e-01^{4} (2.876190e-02)	3.558739e-01^{7} (3.195197e-02)	2.605909e-01^{6} (4.357395e-02)	1.275220e-01^{1} (3.177552e-02)	2.585907e-01^{5} (7.369275e-02)	1.802611e-01^{3} (1.928211e-02)
	5	2.894925e-01^{1} (3.927768e-02)	3.478904e-01^{4} (3.490353e-02)	6.014443e-01^{7} (5.270989e-02)	5.479799e-01^{6} (1.175889e-01)	3.339513e-01^{3} (5.543478e-02)	4.083721e-01^{5} (8.779585e-02)	3.102710e-01^{2} (3.770947e-02)
	6	4.221565e-01^{2} (9.670011e-02)	3.746859e-01^{1} (5.015730e-02)	9.899732e-01^{6} (5.286161e-02)	1.225693e+00^{7} (1.761805e-01)	5.034674e-01^{4} (4.860052e-02)	5.992873e-01^{5} (1.654779e-01)	4.810420e-01^{3} (5.047181e-02)
WFG4	2	6.538266e-03^{2} (6.038909e-04)	5.653182e-03^{1} (3.128042e-04)	8.028339e-03^{5} (6.132762e-04)	5.829601e-02^{7} (5.755702e-03)	1.087977e-02^{6} (4.469931e-04)	7.262789e-03^{3} (3.918419e-04)	7.270021e-03^{4} (7.546731e-04)
	3	8.069800e-02^{1} (2.975895e-03)	8.267272e-02^{2} (1.935872e-03)	9.566127e-02^{6} (3.508376e-03)	1.103269e-01^{7} (4.549205e-03)	8.509159e-02^{3} (2.531183e-03)	8.962965e-02^{4} (3.097112e-03)	9.545943e-02^{5} (2.953623e-03)
	4	2.185689e-01^{3} (6.011827e-03)	2.089468e-01^{1} (4.072786e-03)	2.538468e-01^{6} (7.476719e-03)	2.414136e-01^{4} (7.824828e-03)	2.172938e-01^{2} (4.206098e-03)	2.480055e-01^{5} (7.911208e-03)	2.969056e-01^{7} (6.300573e-03)
	5	3.939453e-01^{2} (9.667173e-03)	3.657162e-01^{1} (7.181790e-03)	4.282060e-01^{4} (7.839477e-03)	4.053227e-01^{3} (1.214431e-02)	4.298828e-01^{5} (9.033431e-03)	4.501605e-01^{6} (1.500148e-02)	5.729968e-01^{7} (1.376346e-02)
	6	5.557967e-01^{1} (1.542404e-02)	5.880903e-01^{2} (1.210419e-02)	6.286933e-01^{5} (1.319711e-02)	6.072554e-01^{3} (1.348123e-02)	6.216838e-01^{4} (1.061534e-02)	6.688346e-01^{6} (1.626703e-02)	8.647572e-01^{7} (2.715403e-02)

Table B.33: IGD$^+$ comparison using SLD-based reference sets.

MOP	Dim.	IGD$^+$-MaOEA	MOMBI3	AR-MOEA	RVEA	GrEA	SPEA2SDE	Two_Arch2
DTLZ1	2	1.324784e-03^{2} (1.166224e-04)	1.281843e-03^{1} (1.926809e-04)	1.406360e-03^{4} (3.463456e-04)	1.529153e-03^{5} (5.417406e-04)	1.068844e-02^{7} (2.387148e-02)	1.339097e-03^{3} (1.128652e-04)	1.687216e-03^{6} (7.421359e-04)
	3	1.367914e-02^{6} (1.155580e-03)	1.284705e-02^{2} (2.673481e-04)	1.298048e-02^{4} (4.863961e-04)	1.270659e-02^{1} (2.878416e-04)	4.738439e-02^{7} (3.245371e-02)	1.294193e-02^{3} (2.726926e-04)	1.362693e-02^{5} (5.714842e-04)
	4	2.945992e-02^{6} (1.149005e-03)	2.880318e-02^{5} (5.504727e-04)	2.860285e-02^{3} (3.246396e-04)	2.858063e-02^{2} (2.839546e-04)	1.115387e-01^{7} (7.911385e-02)	2.833671e-02^{1} (3.889856e-04)	2.874887e-02^{4} (1.044422e-03)
	5	4.267152e-02^{3} (2.130159e-03)	4.651938e-02^{4} (4.964399e-04)	4.794493e-02^{5} (4.302081e-04)	4.798548e-02^{6} (3.578852e-04)	1.365891e-01^{7} (8.561191e-02)	3.986799e-02^{1} (6.821450e-04)	4.017883e-02^{2} (5.120154e-04)
	6	5.576372e-02^{4} (3.282202e-03)	5.407313e-02^{3} (9.511759e-04)	5.622222e-02^{6} (4.991559e-04)	5.621102e-02^{5} (2.776537e-04)	1.684646e-01^{7} (9.309274e-02)	5.038363e-02^{1} (9.467802e-04)	5.121838e-02^{2} (8.255511e-04)
DTLZ2	2	1.944141e-03^{5} (1.008731e-04)	1.494155e-03^{2} (1.273175e-05)	1.570011e-03^{3} (2.949596e-06)	1.839207e-03^{4} (3.073737e-04)	3.663605e-03^{7} (2.680076e-05)	1.968726e-03^{6} (7.479067e-05)	1.425516e-03^{1} (9.110028e-06)
	3	2.097086e-02^{5} (6.403667e-04)	1.897835e-02^{3} (3.239845e-04)	1.883315e-02^{1} (6.851970e-05)	1.883338e-02^{2} (3.658613e-05)	2.096621e-02^{4} (2.031590e-04)	2.140335e-02^{6} (6.569152e-04)	2.146972e-02^{7} (4.849077e-04)
	4	4.379890e-02^{5} (1.937651e-03)	4.252194e-02^{4} (1.008419e-03)	4.161484e-02^{3} (1.084509e-04)	4.139451e-02^{2} (2.568251e-05)	4.079150e-02^{1} (8.895260e-04)	4.480197e-02^{6} (1.652864e-03)	6.184025e-02^{7} (1.858341e-03)
	5	6.148742e-02^{1} (2.145631e-03)	6.970621e-02^{5} (2.138919e-03)	7.011503e-02^{6} (2.568019e-04)	6.958346e-02^{4} (1.927827e-05)	6.739870e-02^{3} (1.311758e-03)	6.384888e-02^{2} (1.970779e-03)	1.033590e-01^{7} (3.109157e-03)
	6	7.947403e-02^{3} (6.166047e-03)	9.035057e-02^{5} (4.664475e-03)	7.083285e-02^{2} (3.512231e-04)	7.063832e-02^{1} (1.063158e-05)	9.181964e-02^{6} (1.633243e-03)	8.142613e-02^{4} (3.521258e-03)	1.397463e-01^{7} (9.217855e-03)
DTLZ5	2	1.944101e-03^{5} (1.008608e-04)	1.494124e-03^{2} (1.272313e-05)	1.570155e-03^{3} (2.554965e-06)	1.999130e-03^{6} (3.174297e-04)	3.651802e-03^{7} (4.558717e-05)	1.941732e-03^{4} (8.123141e-05)	1.425172e-03^{1} (1.186956e-05)
	3	1.985037e-03^{4} (1.688243e-04)	2.034810e-03^{5} (3.490842e-04)	1.410596e-03^{1} (9.497471e-05)	3.092609e-02^{7} (8.134728e-03)	8.849264e-03^{6} (2.919408e-04)	1.917412e-03^{3} (1.630558e-04)	1.419384e-03^{2} (6.647139e-05)
	4	8.023139e-03^{2} (1.366638e-03)	2.749785e-03^{1} (4.176458e-04)	1.565746e-02^{5} (3.012736e-03)	6.478771e-02^{7} (3.556609e-03)	2.155934e-02^{6} (5.016484e-03)	8.060869e-03^{3} (1.503055e-03)	1.141551e-02^{4} (2.646230e-03)
	5	1.408376e-02^{3} (6.539680e-03)	2.610348e-03^{1} (2.089773e-03)	2.883783e-02^{5} (8.432654e-03)	5.559754e-02^{7} (1.621516e-02)	3.713536e-02^{6} (2.124380e-02)	1.239066e-02^{2} (6.679335e-03)	2.300490e-02^{4} (1.046787e-02)
	6	3.401874e-02^{5} (1.682665e-02)	1.252136e-02^{1} (2.557340e-03)	3.326390e-02^{4} (1.363092e-02)	9.616769e-02^{7} (1.854383e-02)	6.862086e-02^{6} (3.643032e-02)	2.027970e-02^{2} (1.135392e-02)	2.091867e-02^{3} (1.149312e-02)
DTLZ6	2	1.877589e-03^{5} (6.030663e-05)	1.491427e-03^{2} (9.659012e-06)	1.566703e-03^{3} (6.428278e-07)	1.566749e-03^{4} (6.724065e-07)	3.686674e-03^{7} (1.742385e-05)	1.898056e-03^{6} (1.020496e-04)	1.446830e-03^{1} (7.616147e-06)
	3	1.940649e-03^{4} (2.042044e-04)	3.577551e-03^{5} (6.104803e-04)	1.211512e-03^{1} (6.651891e-05)	2.865815e-02^{7} (6.849137e-03)	9.093707e-03^{6} (2.512411e-05)	1.816435e-03^{3} (1.462651e-04)	1.373945e-03^{2} (2.557814e-05)
	4	9.734077e-03^{3} (3.465035e-03)	3.245002e-03^{1} (3.241986e-05)	1.339053e-02^{4} (9.330006e-03)	5.331371e-02^{6} (1.270498e-02)	6.205338e-02^{7} (1.467690e-02)	9.507360e-03^{2} (2.910350e-03)	1.617094e-02^{5} (5.223090e-03)
	5	1.415423e-02^{2} (9.965304e-03)	1.929962e-03^{1} (1.583100e-03)	2.140242e-02^{3} (1.216103e-02)	4.797969e-02^{6} (3.598216e-02)	9.476773e-02^{7} (4.224034e-03)	2.354112e-02^{4} (1.219344e-02)	3.352185e-02^{5} (1.309425e-02)
	6	2.991190e-02^{2} (2.730771e-02)	5.400016e-03^{1} (3.777592e-03)	4.145664e-02^{4} (2.635875e-02)	1.102870e-01^{6} (1.011170e-01)	1.311603e-01^{7} (2.477662e-03)	4.027082e-02^{3} (2.288557e-02)	5.653649e-02^{5} (3.542186e-02)
DTLZ7	2	1.906783e-03^{4} (5.835403e-04)	1.207938e-03^{1} (2.584745e-05)	4.209567e-02^{7} (1.151821e-01)	1.828072e-02^{6} (3.646494e-03)	4.317421e-03^{5} (6.743396e-04)	1.884242e-03^{3} (3.480371e-04)	1.289989e-03^{2} (1.173963e-04)
	3	3.971671e-02^{3} (6.665155e-03)	1.829159e-02^{1} (9.208004e-04)	7.183282e-02^{6} (9.925551e-02)	4.601597e-02^{5} (4.731680e-03)	4.049999e-02^{4} (7.386388e-03)	2.147655e-02^{2} (9.746881e-04)	8.087664e-02^{7} (1.051818e-01)
	4	2.649638e-01^{7} (1.933020e-01)	5.870829e-02^{2} (3.260059e-03)	1.502439e-01^{5} (1.647542e-01)	1.623527e-01^{6} (7.905825e-03)	1.012745e-01^{3} (1.149861e-02)	5.631071e-02^{1} (4.739604e-02)	1.489029e-01^{4} (1.570384e-01)
	5	5.827856e-01^{7} (2.937364e-01)	1.788822e-01^{3} (1.165019e-01)	1.741057e-01^{2} (1.328614e-02)	3.922572e-01^{6} (1.007066e-02)	2.494687e-01^{4} (3.773586e-02)	1.365118e-01^{1} (9.239830e-02)	2.741421e-01^{5} (8.380253e-02)
	6	7.153383e-01^{7} (5.144686e-01)	4.033109e-01^{3} (2.412554e-01)	3.762309e-01^{2} (1.392944e-02)	6.306077e-01^{6} (1.961635e-02)	5.557452e-01^{5} (7.848585e-02)	1.406443e-01^{1} (5.865441e-02)	4.496572e-01^{4} (5.603505e-02)

Table B.33 – *Continuation*

MOP	Dim.	IGD$^+$-MaOEA	MOMBI3	AR-MOEA	RVEA	GrEA	SPEA2SDE	Two_Arch2
WFG1	2	9.984261e-01^{7} (1.621571e-02)	9.752719e-01^{6} (1.648003e-02)	1.435566e-01^{3} (5.596396e-02)	7.830368e-01^{5} (6.036343e-02)	1.347089e-01^{2} (4.248360e-02)	1.313623e-01^{1} (4.769777e-02)	2.882107e-01^{4} (5.861448e-02)
	3	1.168333e+00^{6} (1.425372e-02)	1.188691e+00^{7} (1.689522e-02)	5.534817e-01^{4} (6.630637e-02)	8.959644e-01^{5} (8.430181e-02)	3.743457e-01^{2} (4.668456e-02)	2.456006e-01^{1} (4.674128e-02)	5.482457e-01^{3} (5.093874e-02)
	4	1.369506e+00^{6} (1.909421e-02)	1.397440e+00^{7} (2.540937e-02)	7.986322e-01^{4} (6.183985e-02)	1.000033e+00^{5} (1.175127e-01)	5.693667e-01^{2} (8.770734e-02)	3.570794e-01^{1} (5.778684e-02)	7.959504e-01^{3} (8.377075e-02)
	5	1.534538e+00^{6} (2.673924e-02)	1.565892e+00^{7} (2.677392e-02)	9.028002e-01^{3} (7.886697e-02)	1.022781e+00^{5} (1.270306e-01)	6.481181e-01^{2} (9.840506e-02)	4.228389e-01^{1} (6.032076e-02)	9.650333e-01^{4} (8.423309e-02)
	6	1.691704e+00^{6} (2.741779e-02)	1.721845e+00^{7} (2.322193e-02)	1.088629e+00^{5} (9.309822e-02)	1.022463e+00^{3} (1.488916e-01)	7.426411e-01^{2} (8.773121e-02)	4.148099e-01^{1} (8.082625e-02)	1.059730e+00^{4} (7.804779e-02)
WFG2	2	7.972985e-02^{6} (1.454432e-02)	3.988094e-02^{1} (3.532381e-02)	6.354846e-02^{4} (3.238451e-02)	1.046108e-01^{7} (3.243505e-02)	5.453964e-02^{3} (3.409668e-02)	5.281574e-02^{2} (3.519017e-02)	7.807874e-02^{5} (3.999287e-02)
	3	1.072437e-01^{2} (1.289143e-01)	1.369386e-01^{4} (1.376217e-01)	2.236377e-01^{7} (1.437264e-01)	2.129684e-01^{6} (1.278432e-01)	1.071225e-01^{1} (1.161817e-01)	1.294572e-01^{3} (1.381686e-01)	1.809484e-01^{5} (1.415020e-01)
	4	3.985453e-01^{7} (3.466408e-01)	3.770502e-01^{4} (3.324399e-01)	3.829374e-01^{5} (3.185037e-01)	3.371626e-01^{2} (3.004887e-01)	3.440528e-01^{3} (3.189767e-01)	2.654636e-01^{1} (3.038267e-01)	3.835191e-01^{6} (3.227303e-01)
	5	6.899279e-01^{7} (5.670131e-01)	3.602381e-01^{2} (4.290866e-01)	4.274490e-01^{3} (4.568648e-01)	4.937417e-01^{4} (5.141519e-01)	3.093281e-01^{1} (3.485279e-01)	5.028578e-01^{5} (5.403979e-01)	5.260832e-01^{6} (4.962794e-01)
	6	6.603668e-01^{4} (6.542452e-01)	5.011577e-01^{1} (5.680666e-01)	6.394148e-01^{3} (6.149410e-01)	8.597063e-01^{7} (7.069565e-01)	7.004609e-01^{5} (6.362571e-01)	8.338341e-01^{6} (7.064507e-01)	6.052590e-01^{2} (5.910810e-01)
WFG3	2	1.152797e-02^{1} (1.807666e-03)	1.209778e-02^{2} (2.713718e-03)	2.013135e-02^{4} (7.693501e-03)	7.516406e-02^{7} (1.101547e-02)	2.034346e-02^{5} (4.812141e-03)	1.376243e-02^{3} (2.096653e-03)	2.304781e-02^{6} (8.374956e-03)
	3	4.316490e-02^{1} (7.756661e-03)	7.244595e-02^{5} (9.811667e-03)	1.263235e-01^{6} (1.233731e-02)	1.902844e-01^{7} (3.033326e-02)	4.632982e-02^{2} (5.211288e-03)	5.122038e-02^{3} (1.410503e-02)	6.497272e-02^{4} (7.222295e-03)
	4	1.643996e-01^{2} (5.866616e-02)	2.304333e-01^{4} (2.502890e-02)	3.472534e-01^{6} (2.107439e-02)	2.359480e-01^{5} (4.226937e-02)	1.150884e-01^{1} (2.934924e-02)	4.719783e-01^{7} (1.504013e-01)	1.738409e-01^{3} (1.897015e-02)
	5	3.402327e-01^{4} (1.300318e-01)	3.164773e-01^{3} (5.535217e-02)	5.810350e-01^{5} (8.156559e-02)	6.828762e-01^{6} (2.578632e-01)	2.440892e-01^{1} (5.702263e-02)	7.727110e-01^{7} (1.978081e-01)	2.924229e-01^{2} (4.755664e-02)
	6	4.844243e-01^{4} (2.077087e-01)	3.532273e-01^{1} (8.790708e-02)	8.729694e-01^{5} (3.334460e-02)	1.580180e+00^{7} (2.356378e-01)	3.719682e-01^{2} (7.182148e-02)	1.008372e+00^{6} (2.843666e-01)	4.392026e-01^{3} (1.173999e-01)
WFG4	2	7.098130e-03^{2} (9.924998e-04)	5.387584e-03^{1} (2.958363e-04)	7.809801e-03^{5} (6.501667e-04)	5.720368e-02^{7} (5.452779e-03)	1.070697e-02^{6} (5.119317e-04)	7.156284e-03^{3} (3.808636e-04)	7.280440e-03^{4} (7.805079e-04)
	3	8.019988e-02^{2} (2.767301e-03)	7.717562e-02^{1} (2.022474e-03)	9.467682e-02^{6} (3.714682e-03)	1.065319e-01^{7} (4.334160e-03)	8.163150e-02^{3} (2.548951e-03)	8.479305e-02^{4} (2.888075e-03)	9.438488e-02^{5} (2.720406e-03)
	4	2.021614e-01^{3} (6.580342e-03)	1.851633e-01^{1} (3.540175e-03)	2.259955e-01^{6} (7.093812e-03)	2.098381e-01^{4} (7.484031e-03)	1.943648e-01^{2} (4.792531e-03)	2.198872e-01^{5} (6.516767e-03)	2.961896e-01^{7} (7.328630e-03)
	5	3.361883e-01^{2} (1.090852e-02)	3.226175e-01^{1} (1.146458e-02)	3.713824e-01^{4} (8.582555e-03)	3.462618e-01^{3} (1.355044e-02)	3.816621e-01^{5} (9.764519e-03)	3.819037e-01^{6} (1.528085e-02)	5.284729e-01^{7} (1.393521e-02)
	6	4.455531e-01^{1} (2.554860e-02)	4.859999e-01^{3} (2.388624e-02)	4.883199e-01^{4} (1.399812e-02)	4.553627e-01^{2} (1.376721e-02)	5.278510e-01^{5} (1.364949e-02)	5.651826e-01^{6} (2.030016e-02)	7.943524e-01^{7} (3.624100e-02)

Table B.34: IGD$^+$ comparison using UDH-based reference sets.

MOP	Dim.	IGD$^+$-MaOEA	MOMBI3	AR-MOEA	RVEA	GrEA	SPEA2SDE	Two_Arch2
DTLZ1	2	1.324051e-03^{2} (1.154024e-04)	1.279141e-03^{1} (1.927749e-04)	1.405776e-03^{4} (3.458349e-04)	1.528324e-03^{5} (5.409787e-04)	1.060823e-02^{7} (2.375199e-02)	1.339401e-03^{3} (1.124702e-04)	1.687139e-03^{6} (7.458047e-04)
	3	1.382335e-02^{5} (1.166225e-03)	1.315206e-02^{4} (2.824475e-04)	1.310507e-02^{3} (4.668964e-04)	1.282997e-02^{1} (2.741686e-04)	4.633251e-02^{7} (3.176606e-02)	1.309558e-02^{2} (2.921977e-04)	1.394501e-02^{6} (5.882157e-04)
	4	2.911302e-02^{2} (1.360973e-03)	3.066007e-02^{6} (6.494343e-04)	2.999447e-02^{5} (3.616953e-04)	2.990065e-02^{4} (3.079862e-04)	1.093885e-01^{7} (7.945736e-02)	2.766327e-02^{1} (4.531053e-04)	2.958536e-02^{3} (1.212098e-03)
	5	4.176877e-02^{3} (1.917778e-03)	4.684337e-02^{6} (6.079066e-04)	4.670322e-02^{5} (4.721630e-04)	4.662515e-02^{4} (3.653019e-04)	1.336351e-01^{7} (8.594715e-02)	3.925955e-02^{1} (5.070377e-04)	4.148411e-02^{2} (7.797090e-04)
	6	5.444840e-02^{3} (2.949583e-03)	6.079399e-02^{4} (9.719294e-04)	6.133991e-02^{6} (5.180373e-04)	6.118458e-02^{5} (2.842136e-04)	1.651265e-01^{7} (9.506121e-02)	4.902414e-02^{1} (7.484000e-04)	5.099482e-02^{2} (8.440598e-04)
DTLZ2	2	1.950440e-03^{5} (1.000948e-04)	1.503621e-03^{2} (1.209360e-05)	1.574301e-03^{3} (3.130495e-06)	1.844977e-03^{4} (3.095272e-04)	3.668668e-03^{7} (2.685367e-05)	1.975921e-03^{6} (7.433082e-05)	1.432168e-03^{1} (1.000267e-05)
	3	2.176324e-02^{5} (6.284821e-04)	1.989343e-02^{3} (4.041110e-04)	1.971037e-02^{2} (5.807101e-05)	1.968697e-02^{1} (3.872437e-05)	2.181481e-02^{6} (2.089609e-04)	2.214139e-02^{7} (6.527265e-04)	2.143933e-02^{4} (4.643648e-04)
	4	4.874797e-02^{5} (1.864103e-03)	4.768373e-02^{4} (7.396472e-04)	4.648298e-02^{2} (7.847379e-05)	4.632623e-02^{1} (2.675828e-05)	4.714445e-02^{3} (7.998318e-04)	4.948563e-02^{6} (1.125331e-03)	6.150874e-02^{7} (1.472552e-03)
	5	7.078245e-02^{3} (1.857172e-03)	7.349746e-02^{5} (1.303636e-03)	6.878300e-02^{2} (1.915546e-04)	6.840746e-02^{1} (3.626676e-05)	7.470857e-02^{6} (9.823115e-04)	7.233284e-02^{4} (1.760922e-03)	1.086211e-01^{7} (2.552946e-03)
	6	9.242335e-02^{3} (3.904072e-03)	9.810024e-02^{5} (2.935386e-03)	8.878644e-02^{2} (2.650623e-04)	8.844944e-02^{1} (1.285948e-05)	1.009243e-01^{6} (1.672561e-03)	9.326010e-02^{4} (2.125345e-03)	1.522256e-01^{7} (6.258806e-03)
DTLZ5	2	1.950422e-03^{5} (1.000948e-04)	1.503603e-03^{2} (1.209344e-05)	1.574957e-03^{3} (3.315580e-06)	2.007197e-03^{6} (3.202046e-04)	3.657068e-03^{7} (4.618351e-05)	1.949309e-03^{4} (8.191604e-05)	1.432766e-03^{1} (1.195204e-05)
	3	2.089575e-03^{5} (1.533411e-04)	2.058047e-03^{4} (2.258169e-04)	1.689428e-03^{2} (6.118240e-05)	3.326089e-02^{7} (8.279955e-03)	9.321207e-03^{6} (3.357379e-04)	1.983767e-03^{3} (1.524725e-04)	1.421671e-03^{1} (3.243590e-05)
	4	1.152942e-02^{3} (1.409002e-03)	3.051279e-03^{1} (2.805665e-04)	1.928599e-02^{5} (2.434303e-03)	6.744380e-02^{7} (3.795838e-03)	2.843115e-02^{6} (6.309438e-03)	1.012374e-02^{2} (1.935487e-03)	1.422070e-02^{4} (1.799639e-03)
	5	2.193913e-02^{3} (2.783274e-03)	5.395163e-03^{1} (6.786100e-04)	2.975153e-02^{5} (3.830402e-03)	6.673571e-02^{7} (1.025156e-02)	4.632928e-02^{6} (1.100979e-02)	1.763731e-02^{2} (3.594348e-03)	2.361389e-02^{4} (6.057343e-03)
	6	3.448744e-02^{5} (5.549588e-03)	5.815605e-03^{1} (4.932972e-04)	3.221273e-02^{4} (6.259586e-03)	5.371907e-02^{6} (1.807625e-02)	5.509923e-02^{7} (9.265240e-03)	2.154794e-02^{2} (2.555320e-03)	2.881149e-02^{3} (6.014349e-03)
DTLZ6	2	1.886139e-03^{5} (5.945767e-05)	1.499132e-03^{2} (1.141841e-05)	1.570502e-03^{3} (9.903146e-07)	1.570836e-03^{4} (5.600080e-07)	3.690640e-03^{7} (1.731526e-05)	1.905746e-03^{6} (1.017125e-04)	1.451994e-03^{1} (7.982600e-06)
	3	2.039559e-03^{4} (1.935074e-04)	3.738602e-03^{5} (6.515201e-04)	1.498508e-03^{2} (3.336619e-05)	3.083256e-02^{7} (7.095574e-03)	9.565214e-03^{6} (2.982475e-05)	1.873872e-03^{3} (1.366285e-04)	1.382517e-03^{1} (2.233042e-05)
	4	1.283747e-02^{3} (2.135342e-03)	3.665911e-03^{1} (6.008399e-05)	1.614254e-02^{4} (6.721090e-03)	5.535358e-02^{6} (1.222354e-02)	6.443799e-02^{7} (1.600311e-02)	1.086656e-02^{2} (1.722762e-03)	1.678694e-02^{5} (2.739175e-03)
	5	2.307132e-02^{3} (6.264973e-03)	4.316608e-03^{1} (2.171166e-04)	3.123793e-02^{4} (5.998371e-03)	5.132062e-02^{6} (2.787541e-02)	6.708434e-02^{7} (9.494691e-03)	2.255002e-02^{2} (4.025114e-03)	3.732147e-02^{5} (1.068602e-02)
	6	3.165959e-02^{2} (8.130380e-03)	6.063604e-03^{1} (1.791191e-03)	3.238550e-02^{3} (8.636768e-03)	9.454018e-02^{7} (1.020529e-01)	6.446602e-02^{6} (1.082926e-02)	3.257577e-02^{4} (6.703368e-03)	4.608503e-02^{5} (1.367437e-02)
DTLZ7	2	1.902103e-03^{4} (5.844817e-04)	1.206305e-03^{1} (2.940717e-05)	4.183454e-02^{7} (1.144679e-01)	1.828860e-02^{6} (3.662342e-03)	4.309463e-03^{5} (6.762755e-04)	1.891868e-03^{3} (3.496320e-04)	1.291894e-03^{2} (1.183777e-04)
	3	4.137492e-02^{3} (7.405608e-03)	1.806021e-02^{1} (9.290792e-04)	6.835665e-02^{6} (9.419188e-02)	4.491262e-02^{5} (4.786289e-03)	4.159438e-02^{4} (8.330337e-03)	2.158811e-02^{2} (1.114053e-03)	7.754853e-02^{7} (9.970184e-02)
	4	2.464057e-01^{7} (1.643319e-01)	5.987417e-02^{2} (3.572561e-03)	1.455310e-01^{5} (1.395618e-01)	1.605516e-01^{6} (7.889435e-03)	1.046965e-01^{3} (1.141767e-02)	5.664126e-02^{1} (3.860982e-02)	1.371205e-01^{4} (1.355410e-01)
	5	5.096669e-01^{7} (2.616783e-01)	1.775074e-01^{2} (9.130360e-02)	1.829294e-01^{3} (1.928250e-02)	4.209783e-01^{6} (8.887140e-03)	2.058693e-01^{4} (2.737708e-02)	1.239181e-01^{1} (7.721360e-02)	2.315607e-01^{5} (7.341674e-02)
	6	7.127840e-01^{7} (5.354749e-01)	4.032815e-01^{4} (2.437134e-01)	3.412251e-01^{2} (1.296125e-02)	6.558665e-01^{6} (1.947128e-02)	5.457011e-01^{5} (7.511767e-02)	1.438864e-01^{1} (5.097089e-02)	3.910899e-01^{3} (6.952159e-02)

Table B.34 – *Continuation*

MOP	Dim.	IGD$^+$-MaOEA	MOMBI3	AR-MOEA	RVEA	GrEA	SPEA2SDE	Two_Arch2
WFG1	2	9.983230e-01^{7} (1.621803e-02)	9.751799e-01^{6} (1.647677e-02)	1.434892e-01^{3} (5.598323e-02)	7.830778e-01^{5} (6.036583e-02)	1.346816e-01^{2} (4.250254e-02)	1.313458e-01^{1} (4.771038e-02)	2.881881e-01^{4} (5.862570e-02)
	3	1.168303e+00^{6} (1.422890e-02)	1.189887e+00^{7} (1.688308e-02)	5.537384e-01^{4} (6.667339e-02)	8.978989e-01^{5} (8.419329e-02)	3.749111e-01^{2} (4.658890e-02)	2.453532e-01^{1} (4.700536e-02)	5.483238e-01^{3} (5.104881e-02)
	4	1.372020e+00^{6} (1.880165e-02)	1.409848e+00^{7} (2.595396e-02)	8.195498e-01^{4} (6.272679e-02)	1.018767e+00^{5} (1.161294e-01)	5.680620e-01^{2} (8.800181e-02)	3.637256e-01^{1} (5.795881e-02)	8.008100e-01^{3} (8.432830e-02)
	5	1.551836e+00^{6} (2.801320e-02)	1.611726e+00^{7} (2.945105e-02)	9.552283e-01^{3} (8.168211e-02)	1.059912e+00^{5} (1.330987e-01)	6.347110e-01^{2} (1.023613e-01)	4.303613e-01^{1} (6.123097e-02)	9.825506e-01^{4} (8.580492e-02)
	6	1.692933e+00^{6} (2.891967e-02)	1.766628e+00^{7} (2.304626e-02)	1.156939e+00^{5} (1.007675e-01)	1.063473e+00^{4} (1.497396e-01)	7.132287e-01^{2} (9.060379e-02)	4.161199e-01^{1} (7.978050e-02)	1.061635e+00^{3} (8.375182e-02)
WFG2	2	7.774423e-02^{6} (1.416691e-02)	3.896284e-02^{1} (3.431184e-02)	6.209511e-02^{4} (3.147449e-02)	1.040489e-01^{7} (3.162225e-02)	5.341053e-02^{3} (3.310404e-02)	5.159996e-02^{2} (3.419856e-02)	7.662012e-02^{5} (3.912907e-02)
	3	1.040326e-01^{1} (1.233149e-01)	1.338511e-01^{4} (1.307986e-01)	2.143158e-01^{7} (1.374728e-01)	2.075585e-01^{6} (1.212799e-01)	1.054314e-01^{2} (1.109109e-01)	1.257164e-01^{3} (1.320045e-01)	1.750007e-01^{5} (1.351781e-01)
	4	4.024152e-01^{6} (3.606878e-01)	4.016406e-01^{5} (3.369568e-01)	4.108211e-01^{7} (3.220677e-01)	3.612242e-01^{3} (3.048173e-01)	3.427149e-01^{2} (3.330492e-01)	2.682620e-01^{1} (3.153904e-01)	3.978826e-01^{4} (3.318905e-01)
	5	7.186262e-01^{7} (6.204375e-01)	4.210443e-01^{2} (4.466308e-01)	4.850014e-01^{3} (4.829748e-01)	5.469658e-01^{5} (5.429189e-01)	2.988388e-01^{1} (3.819363e-01)	5.269254e-01^{4} (5.865232e-01)	5.626268e-01^{6} (5.336850e-01)
	6	7.535445e-01^{3} (8.481633e-01)	6.572643e-01^{1} (6.898957e-01)	8.054604e-01^{5} (7.608907e-01)	1.068084e+00^{7} (8.766575e-01)	8.032552e-01^{4} (8.236410e-01)	1.006424e+00^{6} (9.041520e-01)	7.111678e-01^{2} (7.489061e-01)
WFG3	2	1.152178e-02^{1} (1.806088e-03)	1.209502e-02^{2} (2.715902e-03)	2.012941e-02^{4} (7.697378e-03)	7.522916e-02^{7} (1.102903e-02)	2.031614e-02^{5} (4.815808e-03)	1.377301e-02^{3} (2.099078e-03)	2.304723e-02^{6} (8.373293e-03)
	3	4.336936e-02^{1} (7.804580e-03)	7.230598e-02^{5} (1.016463e-02)	1.265424e-01^{6} (1.241872e-02)	1.928357e-01^{7} (3.108922e-02)	4.553405e-02^{2} (5.782044e-03)	4.958835e-02^{3} (1.205825e-02)	6.444861e-02^{4} (7.372261e-03)
	4	1.557595e-01^{2} (3.937167e-02)	2.282657e-01^{4} (2.767787e-02)	3.477117e-01^{6} (2.553892e-02)	2.434553e-01^{5} (3.278396e-02)	1.151659e-01^{1} (3.019059e-02)	3.920967e-01^{7} (1.358536e-01)	1.762689e-01^{3} (1.654304e-02)
	5	3.030407e-01^{3} (7.302335e-02)	3.215065e-01^{4} (3.764356e-02)	6.017774e-01^{5} (6.463194e-02)	6.165683e-01^{6} (2.011576e-01)	2.851814e-01^{1} (5.518277e-02)	6.170333e-01^{7} (1.752855e-01)	2.908928e-01^{2} (3.649698e-02)
	6	4.589439e-01^{3} (1.803103e-01)	3.563403e-01^{1} (5.373724e-02)	9.270318e-01^{5} (4.338618e-02)	1.517495e+00^{7} (2.708525e-01)	4.432061e-01^{2} (4.901491e-02)	9.310811e-01^{6} (3.146159e-01)	4.601143e-01^{4} (5.890386e-02)
WFG4	2	7.113670e-03^{2} (9.745456e-04)	5.404687e-03^{1} (3.003400e-04)	7.835687e-03^{5} (6.445107e-04)	5.734398e-02^{7} (5.465860e-03)	1.074618e-02^{6} (5.076597e-04)	7.183940e-03^{3} (3.815990e-04)	7.298549e-03^{4} (7.823154e-04)
	3	8.300866e-02^{2} (2.763610e-03)	7.948898e-02^{1} (2.116639e-03)	9.470951e-02^{6} (3.658960e-03)	1.079102e-01^{7} (4.405331e-03)	8.378223e-02^{3} (2.576967e-03)	8.760430e-02^{4} (3.128183e-03)	9.441479e-02^{5} (2.412362e-03)
	4	2.174223e-01^{3} (4.917894e-03)	2.047303e-01^{1} (3.832313e-03)	2.424847e-01^{6} (7.091242e-03)	2.286591e-01^{4} (7.370096e-03)	2.170130e-01^{2} (4.233947e-03)	2.399417e-01^{5} (6.484737e-03)	2.922046e-01^{7} (5.569928e-03)
	5	3.743669e-01^{2} (9.972570e-03)	3.487338e-01^{1} (7.246013e-03)	4.054146e-01^{5} (7.925299e-03)	3.776892e-01^{3} (9.788891e-03)	4.048932e-01^{4} (1.016860e-02)	4.284986e-01^{6} (1.321062e-02)	5.524213e-01^{7} (1.425268e-02)
	6	5.009650e-01^{1} (1.728382e-02)	5.128546e-01^{3} (1.429861e-02)	5.352279e-01^{4} (1.353231e-02)	5.024518e-01^{2} (1.162238e-02)	5.716344e-01^{5} (1.478217e-02)	6.264556e-01^{6} (1.716451e-02)	8.280933e-01^{7} (2.973892e-02)

Table B.35: IGD$^+$ comparison using Random-based reference sets.

MOP	Dim.	IGD$^+$-MaOEA	MOMBI3	AR-MOEA	RVEA	GrEA	SPEA2SDE	Two_Arch2
DTLZ1	2	1.332874e-03^{2} (1.181491e-04)	1.272934e-03^{1} (1.931908e-04)	1.405601e-03^{4} (3.529751e-04)	1.529136e-03^{5} (5.432142e-04)	1.010776e-02^{7} (2.280788e-02)	1.334800e-03^{3} (1.138604e-04)	1.707537e-03^{6} (7.741155e-04)
	3	1.371777e-02^{6} (1.150677e-03)	1.259467e-02^{2} (2.560855e-04)	1.267705e-02^{3} (4.824325e-04)	1.240388e-02^{1} (2.837062e-04)	4.914840e-02^{7} (3.372346e-02)	1.304137e-02^{4} (3.430401e-04)	1.327512e-02^{5} (5.213795e-04)
	4	2.895487e-02^{6} (1.370751e-03)	2.828882e-02^{4} (6.744534e-04)	2.803025e-02^{3} (3.760572e-04)	2.799382e-02^{2} (3.312804e-04)	1.111301e-01^{7} (7.782605e-02)	2.779764e-02^{1} (4.707867e-04)	2.841427e-02^{5} (8.331734e-04)
	5	4.265518e-02^{6} (2.266162e-03)	4.037813e-02^{2} (6.309017e-04)	4.046538e-02^{4} (4.589167e-04)	4.039197e-02^{3} (3.401296e-04)	1.365477e-01^{7} (8.545470e-02)	3.964948e-02^{1} (6.084616e-04)	4.066136e-02^{5} (6.109842e-04)
	6	5.500792e-02^{5} (3.136463e-03)	5.440579e-02^{3} (1.003673e-03)	5.515704e-02^{6} (4.468048e-04)	5.496561e-02^{4} (2.872537e-04)	1.686607e-01^{7} (9.484555e-02)	4.951583e-02^{1} (8.710182e-04)	5.131656e-02^{2} (7.900856e-04)
DTLZ2	2	1.941008e-03^{5} (1.160471e-04)	1.515882e-03^{2} (4.322632e-05)	1.605719e-03^{3} (4.135311e-06)	1.874810e-03^{4} (3.091121e-04)	3.670071e-03^{7} (3.122824e-05)	1.959902e-03^{6} (8.667445e-05)	1.444747e-03^{1} (2.568942e-05)
	3	2.185929e-02^{4} (5.951223e-04)	2.113330e-02^{3} (4.734830e-04)	2.083048e-02^{2} (7.962962e-05)	2.082696e-02^{1} (4.226757e-05)	2.236402e-02^{5} (2.729647e-04)	2.237384e-02^{6} (6.661026e-04)	2.253091e-02^{7} (5.760438e-04)
	4	5.109463e-02^{5} (1.726859e-03)	5.064084e-02^{4} (6.188774e-04)	5.029785e-02^{3} (9.515165e-05)	5.014942e-02^{2} (2.552035e-05)	4.948455e-02^{1} (6.454956e-04)	5.175553e-02^{6} (1.223239e-03)	6.324416e-02^{7} (1.527579e-03)
	5	7.745373e-02^{3} (1.612216e-03)	7.988676e-02^{5} (1.495310e-03)	7.694797e-02^{2} (1.404261e-04)	7.666158e-02^{1} (3.443344e-05)	8.193884e-02^{6} (1.374319e-03)	7.961159e-02^{4} (1.722418e-03)	1.121862e-01^{7} (2.211320e-03)
	6	1.064304e-01^{3} (3.177298e-03)	1.084327e-01^{5} (2.271152e-03)	1.021238e-01^{2} (2.192056e-04)	1.018702e-01^{1} (1.894728e-05)	1.132832e-01^{6} (1.470854e-03)	1.071483e-01^{4} (2.716053e-03)	1.574591e-01^{7} (4.105072e-03)
DTLZ5	2	1.925139e-03^{5} (1.078184e-04)	1.496443e-03^{2} (3.595464e-05)	1.504234e-03^{3} (3.764150e-06)	1.948702e-03^{6} (3.213793e-04)	3.598324e-03^{7} (4.509783e-05)	1.924679e-03^{4} (1.032593e-04)	1.346342e-03^{1} (1.566109e-05)
	3	1.948532e-03^{2} (1.044571e-04)	2.580566e-03^{5} (3.121079e-04)	1.996597e-03^{4} (8.635992e-05)	4.204664e-02^{7} (1.092477e-02)	1.068308e-02^{6} (3.600839e-04)	1.970745e-03^{3} (1.017245e-04)	1.631100e-03^{1} (4.705632e-05)
	4	1.395937e-02^{3} (1.432424e-03)	4.403851e-03^{1} (4.407041e-04)	2.647889e-02^{5} (2.952696e-03)	1.141944e-01^{7} (6.512763e-03)	3.993214e-02^{6} (9.392227e-03)	1.189324e-02^{2} (1.943622e-03)	2.083088e-02^{4} (3.399981e-03)
	5	2.870507e-02^{3} (4.389569e-03)	8.383750e-03^{1} (6.033973e-04)	4.447901e-02^{5} (6.691247e-03)	1.410373e-01^{7} (2.354658e-02)	6.817051e-02^{6} (2.203845e-02)	2.089348e-02^{2} (3.476628e-03)	4.139335e-02^{4} (1.570227e-02)
	6	5.682469e-02^{4} (1.207938e-02)	1.068024e-02^{1} (1.107683e-03)	5.673932e-02^{3} (1.337666e-02)	1.232506e-01^{7} (5.056219e-02)	9.931087e-02^{6} (2.289470e-02)	3.305920e-02^{2} (5.015523e-03)	5.925079e-02^{5} (1.674733e-02)
DTLZ6	2	1.869212e-03^{5} (8.233077e-05)	1.544319e-03^{2} (4.120117e-05)	1.641159e-03^{3} (1.221022e-06)	1.641297e-03^{4} (2.105363e-06)	3.692092e-03^{7} (1.495923e-05)	1.902288e-03^{6} (1.203625e-04)	1.472836e-03^{1} (2.888335e-05)
	3	1.957827e-03^{4} (1.258513e-04)	4.144900e-03^{5} (7.285022e-04)	1.770497e-03^{2} (3.803940e-05)	3.777473e-02^{7} (9.178944e-03)	1.138331e-02^{6} (4.505041e-05)	1.898705e-03^{3} (1.132639e-04)	1.560321e-03^{1} (2.297118e-05)
	4	1.534285e-02^{3} (2.666567e-03)	5.615821e-03^{1} (4.932848e-05)	2.052861e-02^{4} (4.224773e-03)	9.650338e-02^{6} (2.536536e-02)	1.052637e-01^{7} (3.084724e-02)	1.321639e-02^{2} (2.362828e-03)	2.547231e-02^{5} (5.524260e-03)
	5	3.352650e-02^{3} (1.099258e-02)	6.853724e-03^{1} (4.482012e-04)	4.733857e-02^{4} (1.214739e-02)	8.146856e-02^{6} (2.590994e-02)	1.097002e-01^{7} (2.463038e-02)	2.922531e-02^{2} (5.227075e-03)	6.511792e-02^{5} (2.755185e-02)
	6	5.411039e-02^{2} (1.878586e-02)	1.031013e-02^{1} (3.333820e-03)	6.107267e-02^{4} (1.884337e-02)	9.324975e-02^{5} (4.906605e-02)	1.372881e-01^{7} (3.034968e-02)	5.483429e-02^{3} (1.396433e-02)	9.673096e-02^{6} (3.696711e-02)
DTLZ7	2	1.734509e-03^{4} (1.374278e-04)	1.545322e-03^{1} (3.033962e-05)	4.249152e-02^{7} (1.142726e-01)	1.673178e-02^{6} (2.782649e-03)	5.333904e-03^{5} (4.672041e-04)	1.640142e-03^{3} (6.593245e-05)	1.617733e-03^{2} (3.752766e-05)
	3	2.199651e-02^{3} (1.101503e-03)	2.107686e-02^{1} (4.964144e-04)	6.447318e-02^{6} (8.390255e-02)	4.463080e-02^{5} (3.215543e-03)	2.954112e-02^{4} (1.099611e-03)	2.121379e-02^{2} (5.702011e-04)	7.010326e-02^{7} (8.890680e-02)
	4	1.553965e-01^{7} (1.438082e-01)	6.477184e-02^{2} (1.626277e-03)	1.213109e-01^{5} (1.059412e-01)	1.287224e-01^{6} (4.634671e-03)	6.734984e-02^{3} (2.564415e-03)	6.329523e-02^{1} (2.425189e-02)	1.110608e-01^{4} (1.046604e-01)
	5	3.223276e-01^{7} (1.959163e-01)	1.418171e-01^{3} (4.860142e-02)	1.591665e-01^{4} (5.503674e-03)	2.833535e-01^{6} (7.212775e-03)	1.206996e-01^{2} (6.123716e-03)	1.150264e-01^{1} (3.208071e-02)	1.741966e-01^{5} (3.988130e-02)
	6	5.236289e-01^{6} (4.830104e-01)	3.037824e-01^{3} (1.897730e-01)	2.626012e-01^{2} (7.884932e-03)	5.894377e-01^{7} (3.091843e-02)	3.088992e-01^{4} (3.878609e-02)	1.652441e-01^{1} (2.518098e-02)	3.159516e-01^{5} (5.190783e-02)

Table B.35 – *Continuation*

MOP	Dim.	IGD$^+$-MaOEA	MOMBI3	AR-MOEA	RVEA	GrEA	SPEA2SDE	Two_Arch2
WFG1	2	1.001477e+00^{7} (1.630828e-02)	9.781496e-01^{6} (1.657825e-02)	1.433935e-01^{3} (5.614341e-02)	7.850056e-01^{5} (6.049264e-02)	1.347614e-01^{2} (4.257131e-02)	1.312997e-01^{1} (4.798104e-02)	2.885374e-01^{4} (5.875720e-02)
	3	1.128853e+00^{6} (1.393108e-02)	1.144621e+00^{7} (1.633713e-02)	5.280810e-01^{4} (6.334890e-02)	8.576872e-01^{5} (8.130551e-02)	3.568134e-01^{2} (4.380487e-02)	2.393924e-01^{1} (4.338168e-02)	5.246940e-01^{3} (4.821700e-02)
	4	1.312102e+00^{6} (1.972542e-02)	1.339353e+00^{7} (2.465004e-02)	7.578930e-01^{4} (5.688324e-02)	9.544803e-01^{5} (1.133414e-01)	5.380146e-01^{2} (8.583217e-02)	3.457113e-01^{1} (5.446506e-02)	7.555208e-01^{3} (7.914235e-02)
	5	1.476442e+00^{6} (2.365008e-02)	1.503520e+00^{7} (2.445905e-02)	8.529205e-01^{3} (7.602074e-02)	9.824744e-01^{5} (1.211272e-01)	6.154525e-01^{2} (9.304282e-02)	4.106855e-01^{1} (5.806553e-02)	9.161894e-01^{4} (8.179707e-02)
	6	1.623595e+00^{6} (2.339209e-02)	1.656023e+00^{7} (2.435914e-02)	1.033319e+00^{5} (8.797599e-02)	9.810546e-01^{3} (1.412419e-01)	6.948639e-01^{2} (8.511378e-02)	4.077660e-01^{1} (7.744258e-02)	1.002361e+00^{4} (7.259813e-02)
WFG2	2	1.201098e-01^{7} (2.221757e-02)	5.858387e-02^{1} (5.627745e-02)	9.266904e-02^{4} (5.149201e-02)	1.070778e-01^{6} (4.959413e-02)	7.783881e-02^{2} (5.470170e-02)	7.788111e-02^{3} (5.588208e-02)	1.055211e-01^{5} (5.744494e-02)
	3	1.004977e-01^{2} (1.121734e-01)	1.198822e-01^{3} (1.217730e-01)	1.980142e-01^{7} (1.246614e-01)	1.812561e-01^{6} (1.150487e-01)	9.818299e-02^{1} (1.018460e-01)	1.202287e-01^{4} (1.198849e-01)	1.537598e-01^{5} (1.253356e-01)
	4	3.078247e-01^{7} (2.407358e-01)	2.879846e-01^{5} (2.344714e-01)	3.034893e-01^{6} (2.182923e-01)	2.650036e-01^{2} (2.093777e-01)	2.690086e-01^{3} (2.224663e-01)	2.157271e-01^{1} (2.094410e-01)	2.852393e-01^{4} (2.301068e-01)
	5	4.876104e-01^{7} (3.517879e-01)	2.636289e-01^{2} (2.736014e-01)	3.276097e-01^{3} (2.847852e-01)	3.587874e-01^{4} (3.240961e-01)	2.539693e-01^{1} (2.174399e-01)	3.665166e-01^{5} (3.359677e-01)	3.728742e-01^{6} (3.172320e-01)
	6	4.474122e-01^{4} (3.559076e-01)	3.331210e-01^{1} (3.162583e-01)	4.456732e-01^{3} (3.253875e-01)	5.490982e-01^{7} (3.917667e-01)	4.750878e-01^{5} (3.462713e-01)	5.334112e-01^{6} (3.837474e-01)	4.067203e-01^{2} (3.297194e-01)
WFG3	2	1.154052e-02^{1} (1.860163e-03)	1.196857e-02^{2} (2.737255e-03)	2.001339e-02^{4} (7.759901e-03)	7.528116e-02^{7} (1.095277e-02)	2.015768e-02^{5} (4.811837e-03)	1.370648e-02^{3} (2.116245e-03)	2.298361e-02^{6} (8.415539e-03)
	3	4.439003e-02^{1} (7.794556e-03)	7.614778e-02^{5} (1.020880e-02)	1.282474e-01^{6} (1.174663e-02)	1.987908e-01^{7} (3.048640e-02)	4.702346e-02^{3} (6.255144e-03)	4.687267e-02^{2} (9.264763e-03)	6.811676e-02^{4} (7.780912e-03)
	4	1.530096e-01^{2} (2.557910e-02)	2.418503e-01^{4} (2.940792e-02)	3.563367e-01^{7} (3.150355e-02)	2.627217e-01^{6} (4.412453e-02)	1.261904e-01^{1} (3.255183e-02)	2.520306e-01^{5} (7.159861e-02)	1.805874e-01^{3} (1.939892e-02)
	5	2.923852e-01^{1} (4.187468e-02)	3.476457e-01^{4} (3.492576e-02)	5.987221e-01^{7} (5.264326e-02)	5.480534e-01^{6} (1.184093e-01)	3.369029e-01^{3} (5.435876e-02)	4.083619e-01^{5} (8.558181e-02)	3.103157e-01^{2} (3.893291e-02)
	6	4.211688e-01^{2} (9.698000e-02)	3.744474e-01^{1} (4.976396e-02)	9.930721e-01^{6} (5.311903e-02)	1.227987e+00^{7} (1.768418e-01)	4.990083e-01^{4} (4.959961e-02)	6.000326e-01^{5} (1.685298e-01)	4.780230e-01^{3} (5.100508e-02)
WFG4	2	7.160358e-03^{3} (1.087868e-03)	5.359837e-03^{1} (2.911235e-04)	7.557483e-03^{5} (7.097654e-04)	5.730846e-02^{7} (5.612464e-03)	1.059641e-02^{6} (5.361120e-04)	7.141246e-03^{2} (4.117008e-04)	7.204909e-03^{4} (7.890218e-04)
	3	8.088780e-02^{1} (2.962819e-03)	8.299443e-02^{2} (2.338096e-03)	9.702950e-02^{6} (3.450661e-03)	1.122119e-01^{7} (4.402225e-03)	8.609215e-02^{3} (2.453195e-03)	9.027149e-02^{4} (2.963920e-03)	9.458125e-02^{5} (3.196555e-03)
	4	2.162944e-01^{2} (6.345028e-03)	2.059445e-01^{1} (4.468893e-03)	2.465787e-01^{5} (7.369801e-03)	2.346384e-01^{4} (7.652210e-03)	2.184644e-01^{3} (4.440183e-03)	2.475074e-01^{6} (8.601116e-03)	2.927510e-01^{7} (6.692486e-03)
	5	3.910944e-01^{2} (8.701388e-03)	3.603304e-01^{1} (7.609800e-03)	4.308940e-01^{5} (7.705062e-03)	4.062861e-01^{3} (1.122872e-02)	4.277826e-01^{4} (9.280090e-03)	4.496127e-01^{6} (1.558900e-02)	5.609883e-01^{7} (1.298327e-02)
	6	5.689056e-01^{1} (1.178164e-02)	5.882264e-01^{2} (1.052044e-02)	6.311322e-01^{5} (1.244041e-02)	6.101305e-01^{3} (1.294714e-02)	6.247860e-01^{4} (1.013397e-02)	6.766671e-01^{6} (1.583195e-02)	8.440672e-01^{7} (2.216884e-02)

Bibliography

[1] Søren B. Andersen and Ilmar F. Santos. Evolution strategies and multi-objective optimization of permanent magnet motor. *Applied Soft Computing*, 12(2):778 – 792, 2012.

[2] Anne Auger, Johannes Bader, Dimo Brockhoff, and Eckart Zitzler. Theory of the Hypervolume Indicator: Optimal μ-Distributions and the Choice of the Reference Point. In *FOGA '09: Proceedings of the tenth ACM SIGEVO workshop on Foundations of genetic algorithms*, pages 87–102, Orlando, Florida, USA, January 2009. ACM.

[3] Johannes Bader and Eckart Zitzler. HypE: An Algorithm for Fast Hypervolume-Based Many-Objective Optimization. *Evolutionary Computation*, 19(1):45–76, Spring 2011.

[4] Matthieu Basseur, Bilel Derbel, Adrien Goeffon, and Arnaud Liefooghe. Experiments on Greedy and Local Search Heuristics for d-Dimensional Hypervolume Subset Selection. In *2016 Genetic and Evolutionary Computation Conference (GECCO'2016)*, pages 541–548, Denver, Colorado, USA, 20-24 July 2016. ACM Press. ISBN 978-1-4503-4206-3.

[5] Vitor Basto-Fernandes, Iryna Yevseyeva, André Deutz, and Michael Emmerich. A Survey of Diversity Oriented Optimization: Problems, Indicators, and Algorithms. In Michael Emmerich, André Deutz, Oliver Schütze, Pierrick Legrand, Emilia Tantar, and Alexandru-Adrian Tantar, editors, *EVOLVE - A Bridge between Probability, Set Oriented Numerics and Evolutionary Computation VII*, pages 3–23. Springer, Cham, Switzerland, 2017. ISBN 978-3-319-49324-4.

[6] José A. Molinet Berenguer and Carlos A. Coello Coello. Evolutionary Many-Objective Optimization Based on Kuhn-Munkres' Algorithm. In António Gaspar-Cunha, Carlos Henggeler Antunes, and Carlos Coello Coello, editors, *Evolutionary Multi-Criterion Optimization, 8th International Conference, EMO 2015*, pages 3–17. Springer. Lecture Notes in Computer Science Vol. 9019, Guimarães, Portugal, March 29 - April 1 2015.

[7] Nicola Beume, Carlos M. Fonseca, Manuel Lopez-Ibanez, Luis Paquete, and Jan Vahrenhold. On the Complexity of Computing the Hypervolume Indicator.

IEEE Transactions on Evolutionary Computation, 13(5):1075–1082, October 2009.

[8] Nicola Beume, Boris Naujoks, and Michael Emmerich. SMS-EMOA: Multiobjective selection based on dominated hypervolume. *European Journal of Operational Research*, 181(3):1653–1669, 16 September 2007.

[9] Leonardo C. T. Bezerra, Manuel López-Ibáñez, and Thomas Stützle. An Empirical Assessment of the Properties of Inverted Generational Distance on Multi- and Many-Objective Optimization. In Heike Trautmann, Günter Rudolph, Kathrin Klamroth, Oliver Schütze, Margaret Wiecek, Yaochu Jin, and Christian Grimme, editors, *Evolutionary Multi-Criterion Optimization, 9th International Conference, EMO 2017*, pages 31–45. Springer. Lecture Notes in Computer Science Vol. 10173, Münster, Germany, March 19-21 2017. ISBN: 978-3-319-54156-3.

[10] Tobias Blickle and Lothar Thiele. A Comparison of Selection Schemes used in Genetic Algorithms. Technical Report TIK Report-Nr. 11, Computer Engineering and Communication Networks Lab (TIK), Swiss Federal Institute of Technology (ETH), Gloriastrasse 35, 8092 Zurich, December 1995.

[11] Lucas Bradstreet, Luigi Barone, and Lyndon While. Maximising Hypervolume for Selection in Multi-objective Evolutionary Algorithms. In *2006 IEEE Congress on Evolutionary Computation (CEC'2006)*, pages 6208–6215, Vancouver, BC, Canada, July 2006. IEEE.

[12] Karl Bringmann and Tobias Friedrich. Approximating the least hypervolume contributor: NP-hard in general, but fast in practice. *Theoretical Computer Science*, 425:104–116, March 30 2012.

[13] Karl Bringmann, Tobias Friedrich, and Patrick Klitzke. Two-dimensional Subset Selection for Hypervolume and Epsilon-Indicator. In *2014 Genetic and Evolutionary Computation Conference (GECCO 2014)*, pages 589–596, Vancouver, Canada, July 12-16 2014. ACM Press. ISBN 978-1-4503-2662-9.

[14] Karl Bringmann, Tobias Friedrich, Frank Neumann, and Markus Wagner. Approximation-Guided Evolutionary Multi-Objective Optimization. In *Proceedings of the 21st International Joint Conference on Artificial Intelligence (IJCAI 2011)*, pages 1198–1203, Barcelona, Spain, 16-22 July 2011. AAAI Press.

[15] Dimo Brockhoff. A Bug in the Multiobjective Optimizer IBEA: Salutary Lessons for Code Release and a Performance Re-Assessment. In António Gaspar-Cunha, Carlos Henggeler Antunes, and Carlos Coello Coello, editors, *Evolutionary Multi-Criterion Optimization, 8th International Conference, EMO 2015*, pages 187–201. Springer. Lecture Notes in Computer Science Vol. 9018, Guimarães, Portugal, March 29 - April 1 2015.

[16] Dimo Brockhoff, Tobias Friedrich, and Frank Neumann. Analyzing Hypervolume Indicator Based Algorithms. In Günter Rudolph, Thomas Jansen, Simon Lucas, Carlo Poloni, and Nicola Beume, editors, *Parallel Problem Solving from Nature–PPSN X*, pages 651–660. Springer. Lecture Notes in Computer Science Vol. 5199, Dortmund, Germany, September 2008.

[17] Dimo Brockhoff, Tobias Wagner, and Heike Trautmann. On the Properties of the $R2$ Indicator. In *2012 Genetic and Evolutionary Computation Conference (GECCO'2012)*, pages 465–472, Philadelphia, USA, July 2012. ACM Press. ISBN: 978-1-4503-1177-9.

[18] Dimo Brockhoff, Tobias Wagner, and Heike Trautmann. R2 Indicator-Based Multiobjective Search. *Evolutionary Computation*, 23(3):369–395, Fall 2015.

[19] Edmund K Burke, Michel Gendreau, Matthew Hyde, Graham Kendall, Gabriela Ochoa, Ender Özcan, and Rong Qu. Hyper-heuristics: a survey of the state of the art. *Journal of the Operational Research Society*, 64(12):1695–1724, 2013.

[20] R. Cheng, Y. Jin, M. Olhofer, and B. Sendhoff. A reference vector guided evolutionary algorithm for many-objective optimization. *IEEE Transactions on Evolutionary Computation*, 20(5):773–791, Oct 2016.

[21] Ran Cheng, Miqing Li, Ye Tian, Xingyi Zhang, Shengxiang Yang, Yaochu Jin, and Xin Yao. A Benchmark Test Suite for Evolutionary Many-Objective Optimization. *Complex & Intelligent Systems*, 3(1):67–81, March 2017.

[22] Tinkle Chugh, Karthik Sindhya, Jussi Hakanen, and Kaisa Miettinen. An Interactive Simple Indicator-Based Evolutionary Algorithm (I-SIBEA) for Multiobjective Optimization Problems. In António Gaspar-Cunha, Carlos Henggeler Antunes, and Carlos Coello Coello, editors, *Evolutionary Multi-Criterion Optimization, 8th International Conference, EMO 2015*, pages 277–291. Springer. Lecture Notes in Computer Science Vol. 9018, Guimarães, Portugal, March 29 - April 1 2015.

[23] Carlos A. Coello Coello and Nareli Cruz Cortés. Solving Multiobjective Optimization Problems using an Artificial Immune System. *Genetic Programming and Evolvable Machines*, 6(2):163–190, June 2005.

[24] Carlos A. Coello Coello, Gary B. Lamont, and David A. Van Veldhuizen. *Evolutionary Algorithms for Solving Multi-Objective Problems*. Springer, New York, second edition, September 2007. ISBN 978-0-387-33254-3.

[25] Carlos A. Coello Coello and Margarita Reyes Sierra. A Study of the Parallelization of a Coevolutionary Multi-Objective Evolutionary Algorithm. In Raúl Monroy, Gustavo Arroyo-Figueroa, Luis Enrique Sucar, and Humberto Sossa, editors, *Proceedings of the Third Mexican International Conference on*

Artificial Intelligence (MICAI'2004), pages 688–697. Springer Verlag. Lecture Notes in Artificial Intelligence Vol. 2972, April 2004.

[26] I. Das and J. E. Dennis. Normal-boundary intersection: A new method for generating the pareto surface in nonlinear multicriteria optimization problems. *SIAM Journal on Optimization*, 8(3):631–657, 1998.

[27] Luis Gerardo de la Fraga and Esteban Tlelo-Cuautle. Optimizing an amplifier by a many-objective algorithm based on R2 indicator. In *2015 IEEE International Symposium on Circuits and Systems (ISCAS'2015)*, pages 265–269, Lisbon, Portugal, 24-27 May 2015. IEEE. ISBN 978-1-4799-8391-9.

[28] Kalyanmoy Deb and Ram Bhushan Agrawal. Simulated Binary Crossover for Continuous Search Space. *Complex Systems*, 9(2):115–148, 1995.

[29] Kalyanmoy Deb, Samir Agrawal, Amrit Pratap, and T. Meyarivan. A Fast Elitist Non-Dominated Sorting Genetic Algorithm for Multi-Objective Optimization: NSGA-II. In Marc Schoenauer, Kalyanmoy Deb, Günter Rudolph, Xin Yao, Evelyne Lutton, Juan Julian Merelo, and Hans-Paul Schwefel, editors, *Proceedings of the Parallel Problem Solving from Nature VI Conference*, pages 849–858, Paris, France, 2000. Springer. Lecture Notes in Computer Science No. 1917.

[30] Kalyanmoy Deb and Himanshu Jain. An Evolutionary Many-Objective Optimization Algorithm Using Reference-Point-Based Nondominated Sorting Approach, Part I: Solving Problems With Box Constraints. *IEEE Transactions on Evolutionary Computation*, 18(4):577–601, August 2014.

[31] Kalyanmoy Deb, Amrit Pratap, Sameer Agarwal, and T. Meyarivan. A Fast and Elitist Multiobjective Genetic Algorithm: NSGA–II. *IEEE Transactions on Evolutionary Computation*, 6(2):182–197, April 2002.

[32] Kalyanmoy Deb, Lothar Thiele, Marco Laumanns, and Eckart Zitzler. Scalable Multi-Objective Optimization Test Problems. In *Congress on Evolutionary Computation (CEC'2002)*, volume 1, pages 825–830, Piscataway, New Jersey, May 2002. IEEE Service Center.

[33] Kalyanmoy Deb, Lothar Thiele, Marco Laumanns, and Eckart Zitzler. Scalable Test Problems for Evolutionary Multiobjective Optimization. In Ajith Abraham, Lakhmi Jain, and Robert Goldberg, editors, *Evolutionary Multiobjective Optimization. Theoretical Advances and Applications*, pages 105–145. Springer, USA, 2005.

[34] Roman Denysiuk, Lino Costa, and Isabel Espírito Santo. Many-Objective Optimization using Differential Evolution with Variable-Wise Mutation Restriction. In *2013 Genetic and Evolutionary Computation Conference (GECCO'2013)*,

pages 591–598, New York, USA, July 2013. ACM Press. ISBN 978-1-4503-1963-8.

[35] Alan Díaz-Manríquez, Gregorio Toscano-Pulido, Carlos A. Coello Coello, and Ricardo Landa-Becerra. A Ranking Method Based on the $R2$ Indicator for Many-Objective Optimization. In *2013 IEEE Congress on Evolutionary Computation (CEC'2013)*, pages 1523–1530, Cancún, México, 20-23 June 2013. IEEE Press. ISBN 978-1-4799-0454-9.

[36] Christian Domínguez-Medina, Güenter Rudolph, Oliver Schüetze, and Heike Trautmann. Evenly Spaced Pareto Fronts of Quad-objective Problems using PSA Partitioning Technique. In *2013 IEEE Congress on Evolutionary Computation (CEC'2013)*, pages 3190–3197, Cancún, México, 20-23 June 2013. IEEE Press. ISBN 978-1-4799-0454-9.

[37] Nicole Drechsler, Rolf Drechsler, and Bernd Becker. Multi-Objected Optimization in Evolutionary Algorithms Using Satisfyability Classes. In Bernd Reusch, editor, *International Conference on Computational Intelligence, Theory and Applications, 6th Fuzzy Days*, pages 108–117, Dortmund, Germany, 1999. Springer-Verlag. Lecture Notes in Computer Science Vol. 1625.

[38] Michael T.M. Emmerich and André H. Deutz. Test Problems Based on Lamé Superspheres. In Shigeru Obayashi, Kalyanmoy Deb, Carlo Poloni, Tomoyuki Hiroyasu, and Tadahiko Murata, editors, *Evolutionary Multi-Criterion Optimization, 4th International Conference, EMO 2007*, pages 922–936, Matshushima, Japan, March 2007. Springer. Lecture Notes in Computer Science Vol. 4403.

[39] Michael T.M. Emmerich, André H. Deutz, and Johannes W. Kruisselbrink. On Quality Indicators for Black-Box Level Set Approximation. In Emilia Tantar, Alexandru-Adrian Tantar, Pascal Bouvry, Pierre Del Moral, Pierrick Legrand, Carlos A. Coello Coello, and Oliver Schütze, editors, *EVOLVE - A bridge between Probability, Set Oriented Numerics and Evolutionary Computation*, chapter 4, pages 157–185. Springer-Verlag. Studies in Computational Intelligence Vol. 447, Heidelberg, Germany, 2013. 978-3-642-32725-4.

[40] Michael T.M. Emmerich, André H. Deutz, and Iryna Yevseyeva. On reference point free weighted hypervolume indicators based on desirability functions and their probabilistic interpretation. *Procedia Technology*, 16:532 – 541, 2014. CENTERIS 2014 - Conference on ENTERprise Information Systems / ProjMAN 2014 - International Conference on Project MANagement / HCIST 2014 - International Conference on Health and Social Care Information Systems and Technologies.

[41] Henrik Esbensen and Ernest S. Kuh. Design space exploration using the genetic algorithm. In *IEEE International Symposium on Circuits and Systems (ISCAS'96)*, pages 500–503, Piscataway, NJ, 1996. IEEE.

[42] Jesús Guillermo Falcón-Cardona and Carlos A. Coello Coello. A Multi-Objective Evolutionary Hyper-Heuristic Based on Multiple Indicator-Based Density Estimators. In *2018 Genetic and Evolutionary Computation Conference (GECCO'2018)*, pages 633–640, Kyoto, Japan, July 15–19 2018. ACM Press. ISBN: 978-1-4503-5618-3.

[43] Jesús Guillermo Falcón-Cardona and Carlos A. Coello Coello. Towards a More General Many-objective Evolutionary Optimizer. In *Parallel Problem Solving from Nature – PPSN XV, 15th International Conference, Proceedings, Part I*, pages 335–346. Springer. Lecture Notes in Computer Science Vol. 11101, Coimbra, Portugal, September 8–12 2018. ISBN: 978-3-319-99258-7.

[44] M. Farina and P. Amato. On the Optimal Solution Definition for Many-criteria Optimization Problems. In *Proceedings of the NAFIPS-FLINT International Conference'2002*, pages 233–238, Piscataway, New Jersey, June 2002. IEEE Service Center.

[45] Stacey L. Faulkenberg and Margaret M. Wiecek. On the quality of discrete representations in multiple objective programming. *Optimization and Engineering*, 11(3):423–440, 2010.

[46] M. Fleischer. The Measure of Pareto Optima. Applications to Multi-objective Metaheuristics. In Carlos M. Fonseca, Peter J. Fleming, Eckart Zitzler, Kalyanmoy Deb, and Lothar Thiele, editors, *Evolutionary Multi-Criterion Optimization. Second International Conference, EMO 2003*, pages 519–533, Faro, Portugal, April 2003. Springer. Lecture Notes in Computer Science. Volume 2632.

[47] Peter Fleming, Robin C. Purshouse, and Robert J. Lygoe. Many-Objective Optimization: An Engineering Design Perspective. In Carlos A. Coello Coello, Arturo Hernández Aguirre, and Eckart Zitzler, editors, *Evolutionary Multi-Criterion Optimization. Third International Conference, EMO 2005*, pages 14–32, Guanajuato, México, March 2005. Springer. Lecture Notes in Computer Science Vol. 3410.

[48] Carlos M. Fonseca and Peter J. Fleming. On the Performance Assessment and Comparison of Stochastic Multiobjective Optimizers. In Hans-Michael Voigt, Werner Ebeling, Ingo Rechenberg, and Hans-Paul Schwefel, editors, *Parallel Problem Solving from Nature—PPSN IV*, Lecture Notes in Computer Science, pages 584–593, Berlin, Germany, September 1996. Springer-Verlag.

[49] Yoav Freund and Robert E Schapire. A Decision-Theoretic Generalization of On-Line Learning and an Application to Boosting. *Journal of Computer and System Sciences*, 55(1):119 – 139, 1997.

[50] Tobias Friedrich, Karl Bringmann, Thomas Voß, and Christian Igel. The Logarithmic Hypervolume Indicator. In Hans-Georg Beyer and William B. Langdon, editors, *Proceedings of the 2011 ACM/SIGEVO Foundations of Genetic Algorithms XI (FOGA'2011)*, pages 81–92. ACM Press, Schwarzenberg, Austria, January 5–9 2011.

[51] K. Gerstl, G. Rudolph, O. Schütze, and H. Trautmann. Finding Evenly Spaced Fronts for Multiobjective Control via Averaging Hausdorff-Measure. In *The 2011 8th International Conference on Electrical Engineering, Computer Science and Automatic Control (CCE'2011)*, pages 975–980, Mérida, Yucatán, México, October 2011. IEEE Press.

[52] Crina Grosan, Mihai Olteanand , and D. Dumitrescu. Performance Metrics for Multiobjective Optimization Evolutionary Algorithms. In Teodor Maghiar, Adelina Georgescu, Mircea Balaj, Ioan Dzitac, and Ioan Mang, editors, *Proceedings of the 11th Conference on Applied and Industrial Mathematics (CAIM 2003)*, volume 1, pages 125–128. Editura Universitatii din Oradea, Oradea, Romania, May 29 - 31 2003. ISBN 973-613-330-3.

[53] Viviane Grunert da Fonseca and Carlos M. Fonseca. The Attainment-Function Approach to Stochastic Multiobjective Optimizer Assessment and Comparison. In Thomas Bartz-Beielstein, Marco Chiarandini, Luís Paquete, and Mike Preuss, editors, *Experimental Methods for the Analysis of Optimization Algorithms*, chapter 9, pages 103–130. Springer, Heidelberg, 2010.

[54] Jianmei Guo, Jia Hui Liang, Kai Shi, Dingyu Yang, Jingsong Zhang, Krzysztof Czarnecki, Vijay Ganesh, and Huiqun Yu. SMTIBEA: A Hybrid Multi-Objective Optimization Algorithm for Configuring Large Constrained Software Product Lines. *Software and Systems Modeling*, 18(2):1447–1466, April 2019.

[55] Michael Pilegaard Hansen and Andrzej Jaszkiewicz. Evaluating the quality of approximations to the non-dominated set. Technical Report IMM-REP-1998-7, Technical University of Denmark, March 1998.

[56] D. P. Hardin and E. B. Saff. Discretizing Manifolds via Minimum Energy Points. *Notices of the AMS*, 51(10):1186–1194, 2004.

[57] D. P. Hardn and E.B. Saff. Minimal Riesz energy point configurations for rectifiable d-dimensional manifolds. *Advances in Mathematics*, 193(1):174–204, May 1 2005.

[58] Raquel Hernández-Gómez, Carlos A. Coello Coello, and Enrique Alba. A Parallel Version of SMS-EMOA for Many-Objective Optimization Problems. In Julia Handl, Emma Hart, Peter R. Lewis, Manuel López-Ibáñez, Gabriela Ochoa, and Ben Paechter, editors, *Parallel Problem Solving from Nature – PPSN XIV, 14th International Conference*, pages 568–577. Springer. Lecture Notes in Computer

Science Vol. 9921, Edinburgh, UK, September 17-21 2016. ISBN 978-3-319-45822-9.

[59] Raquel Hernández Gómez and Carlos A. Coello Coello. MOMBI: A New Metaheuristic for Many-Objective Optimization Based on the $R2$ Indicator. In *2013 IEEE Congress on Evolutionary Computation (CEC'2013)*, pages 2488–2495, Cancún, México, 20-23 June 2013. IEEE Press. ISBN 978-1-4799-0454-9.

[60] Raquel Hernández Gómez and Carlos A. Coello Coello. Improved Metaheuristic Based on the $R2$ Indicator for Many-Objective Optimization. In *2015 Genetic and Evolutionary Computation Conference (GECCO 2015)*, pages 679–686, Madrid, Spain, July 11-15 2015. ACM Press. ISBN 978-1-4503-3472-3.

[61] Raquel Hernández Gómez and Carlos A. Coello Coello. A Hyper-Heuristic of Scalarizing Functions. In *2017 Genetic and Evolutionary Computation Conference (GECCO'2017)*, pages 577 –584, Berlin, Germany, July 15-19 2017. ACM Press. ISBN 978-1-4503-4920-8.

[62] Raquel Hernández Gómez, Carlos A. Coello Coello, and Enrique Alba Torres. A Multi-Objective Evolutionary Algorithm based on Parallel Coordinates. In *2016 Genetic and Evolutionary Computation Conference (GECCO'2016)*, pages 565–572, Denver, Colorado, USA, 20-24 July 2016. ACM Press. ISBN 978-1-4503-4206-3.

[63] Jeffrey Horn, Nicholas Nafpliotis, and David E. Goldberg. A Niched Pareto Genetic Algorithm for Multiobjective Optimization. In *Proceedings of the First IEEE Conference on Evolutionary Computation, IEEE World Congress on Computational Intelligence*, volume 1, pages 82–87, Piscataway, New Jersey, June 1994. IEEE Service Center.

[64] Simon Huband, Luigi Barone, Lyndon While, and Phil Hingston. A Scalable Multi-objective Test Problem Toolkit. In Carlos A. Coello Coello, Arturo Hernández Aguirre, and Eckart Zitzler, editors, *Evolutionary Multi-Criterion Optimization. Third International Conference, EMO 2005*, pages 280–295, Guanajuato, México, March 2005. Springer. Lecture Notes in Computer Science Vol. 3410.

[65] Simon Huband, Phil Hingston, Luigi Barone, and Lyndon While. A Review of Multiobjective Test Problems and a Scalable Test Problem Toolkit. *IEEE Transactions on Evolutionary Computation*, 10(5):477–506, October 2006.

[66] Simon Huband, Phil Hingston, Lyndon White, and Luigi Barone. An Evolution Strategy with Probabilistic Mutation for Multi-Objective Optimisation. In *Proceedings of the 2003 Congress on Evolutionary Computation (CEC'2003)*, volume 3, pages 2284–2291, Canberra, Australia, December 2003. IEEE Press.

[67] Christian Igel, Nikolaus Hansen, and Stefan Roth. Covariance Matrix Adaptation for Multi-objective Optimization. *Evolutionary Computation*, 15(1):1–28, Spring 2007.

[68] H. Ishibuchi, R. Imada, Y. Setoguchi, and Y. Nojima. Reference point specification in inverted generational distance for triangular linear pareto front. *IEEE Transactions on Evolutionary Computation*, 22(6):961–975, Dec 2018.

[69] Hisao Ishibuchi, Ryo Imada, Naoki Masuyama, and Yusuke Nojima. Dynamic Specification of a Reference Point for Hypervolume Calculation in SMS-EMOA. In *2018 IEEE Congress on Evolutionary Computation (CEC'2018)*, pages 701–708, Rio de Janeiro, Brazil, July 8–13 2018. IEEE Press. ISBN: 978-1-5090-6017-7.

[70] Hisao Ishibuchi, Ryo Imada, Naoki Masuyama, and Yusuke Nojima. Comparison of Hypervolume, IGD and IGD+ from the Viewpoint of Optimal Distributions of Solutions. In Kalyanmoy Deb, Erik Goodman, Carlos A. Coello Coello, Kathrin Klamroth, Kaisa Miettinen, Sanaz Mostaghim, and Patrick Reed, editors, *Evolutionary Multi-Criterion Optimization, 10th International Conference, EMO 2019*, pages 332–345. Springer. Lecture Notes in Computer Science Vol. 11411, East Lansing, Michigan, USA, March 10–13 2019. ISBN 978-3-030-12597-4.

[71] Hisao Ishibuchi, Ryo Imada, Yu Setoguchi, and Yusuke Nojima. Reference Point Specification in Hypervolume Calculation for Fair Comparison and Efficient Search. In *2017 Genetic and Evolutionary Computation Conference (GECCO'2017)*, pages 585–592, Berlin, Germany, July 15-19 2017. ACM Press. ISBN 978-1-4503-4920-8.

[72] Hisao Ishibuchi, Hiroyuki Masuda, and Yusuke Nojima. Sensitivity of Performance Evaluation Results by Inverted Generational Distance to Reference Points. In *2016 IEEE Congress on Evolutionary Computation (CEC'2016)*, pages 1107–1114, Vancouver, Canada, 24-29 July 2016. IEEE Press. ISBN 978-1-5090-0623-6.

[73] Hisao Ishibuchi, Hiroyuki Masuda, Yuki Tanigaki, and Yusuke Nojima. Difficulties in Specifying Reference Points to Calculate the Inverted Generational Distance for Many-Objective Optimization Problems. In *2014 IEEE Symposium on Computational Intelligence in Multi-Criteria Decision-Making (MCDM'2014)*, pages 170–177, Orlando, Florida, USA, 9-12 December 2014. IEEE Press. ISBN 978-1-4799-4467-5.

[74] Hisao Ishibuchi, Hiroyuki Masuda, Yuki Tanigaki, and Yusuke Nojima. Modified Distance Calculation in Generational Distance and Inverted Generational Distance. In António Gaspar-Cunha, Carlos Henggeler Antunes, and Carlos

Coello Coello, editors, *Evolutionary Multi-Criterion Optimization, 8th International Conference, EMO 2015*, pages 110–125. Springer. Lecture Notes in Computer Science Vol. 9019, Guimarães, Portugal, March 29 - April 1 2015.

[75] Hisao Ishibuchi, Yu Setoguchi, Hiroyuki Masuda, and Yusuke Nojima. Performance of Decomposition-Based Many-Objective Algorithms Strongly Depends on Pareto Front Shapes. *IEEE Transactions on Evolutionary Computation*, 21(2):169–190, April 2017.

[76] Hisao Ishibuchi, Noritaka Tsukamoto, and Yusuke Nojima. Iterative Approach to Indicator-Based Multiobjective Optimization. In *2007 IEEE Congress on Evolutionary Computation (CEC'2007)*, pages 3967–3974, Singapore, September 2007. IEEE Press.

[77] Hisao Ishibuchi, Noritaka Tsukamoto, and Yusuke Nojima. Evolutionary many-objective optimization: A short review. In *2008 Congress on Evolutionary Computation (CEC'2008)*, pages 2424–2431, Hong Kong, June 2008. IEEE Service Center.

[78] Hisao Ishibuchi, Noritaka Tsukamoto, Yuji Sakane, and Yusuke Nojima. Hypervolume Approximation Using Achievement Scalarizing Functions for Evolutionary Many-Objective Optimization. In *2009 IEEE Congress on Evolutionary Computation (CEC'2009)*, pages 530–537, Trondheim, Norway, May 2009. IEEE Press.

[79] Hisao Ishibuchi, Noritaka Tsukamoto, Yuji Sakane, and Yusuke Nojima. Indicator-Based Evolutionary Algorithm with Hypervolume Approximation by Achievement Scalarizing Functions. In *Proceedings of the 12th annual conference on Genetic and Evolutionary Computation (GECCO'2010)*, pages 527–534, Portland, Oregon, USA, July 7–11 2010. ACM Press. ISBN 978-1-4503-0072-8.

[80] Siwei Jiang and Zhihua Cai. Enhance the Convergence and Diversity for ϵ-MOPSO by Uniform Design and Minimum Reduce Hypervolume. In *Proceedings of the 2009 International Conference on Artificial Intelligence and Computational Intelligence (AICI'09)*, volume 1, pages 129–133, Shanghai, China, November 7-8 2009. IEEE Computer Society Press. ISBN 978-0-7695-3816-7.

[81] Siwei Jiang, Liang Few, Chen Kim Heng, Quoc Chinh Nguyen, Yew-Soon Ong, Allan NengSheng Zhang, and Puay Siew Tan. Adaptive Indicator-based Evolutionary Algorithm for Multiobjective Optimization Problems. In *2016 IEEE Congress on Evolutionary Computation (CEC'2016)*, pages 492–499, Vancouver, Canada, July 24-29 2016. IEEE Press. ISBN 978-1-5090-0623-9.

[82] Siwei Jiang, Yew-Soon Ong, Jie Zhang, and Liang Feng. Consistencies and Contradictions of Performance Metrics in Multiobjective Optimization. *IEEE Transactions on Cybernetics*, 44(12):2391–2404, December 2014.

[83] Siwei Jiang, Jie Zhang, Yew-Soon Ong, Allan N. Zhang, and Puay Siew Tan. A Simple and Fast Hypervolume Indicator-Based Multiobjective Evolutionary Algorithm. *IEEE Transactions on Cybernetics*, 45(10):2202–2213, October 2015.

[84] Joshua Knowles and David Corne. On Metrics for Comparing Nondominated Sets. In *Congress on Evolutionary Computation (CEC'2002)*, volume 1, pages 711–716, Piscataway, New Jersey, May 2002. IEEE Service Center.

[85] Joshua Knowles and David Corne. Properties of an Adaptive Archiving Algorithm for Storing Nondominated Vectors. *IEEE Transactions on Evolutionary Computation*, 7(2):100–116, April 2003.

[86] Joshua Knowles, Lothar Thiele, and Eckart Zitzler. A Tutorial on the Performance Assessment of Stochastic Multiobjective Optimizers. 214, Computer Engineering and Networks Laboratory (TIK), ETH Zurich, Switzerland, feb 2006. revised version.

[87] Joshua D. Knowles, David W. Corne, and Mark Fleischer. Bounded Archiving using the Lebesgue Measure. In *Proceedings of the 2003 Congress on Evolutionary Computation (CEC'2003)*, volume 4, pages 2490–2497, Canberra, Australia, December 2003. IEEE Press.

[88] Michael A. Lee, Henrik Esbensen, and Laurent Lemaitre. The Design of Hybrid Fuzzy/Evolutionary Multiobjective Optimization Algorithms. In *Proceedings of the 1995 IEEE/Nagoya University World Wiseperson Workshop*, pages 118–125, Nagoya, Japan, 1995.

[89] Bingdong Li, Jinlong Li, Ke Tang, and Xin Yao. Many-Objective Evolutionary Algorithms: A Survey. *ACM Computing Surveys*, 48(1), September 2015.

[90] Bingdong Li, Ke Tang, Jinlong Li, and Xin Yao. Stochastic Ranking Algorithm for Many-Objective Optimization Based on Multiple Indicators. *IEEE Transactions on Evolutionary Computation*, 20(6):924–938, December 2016.

[91] Fei Li, Ran Cheng, Jianchang Liu, and Yaochu Jin. A Two-Stage R2 Indicator Based Evolutionary Algorithm for Many-Objective Optimization. *Applied Soft Computing*, 67:245–260, June 2018.

[92] Fei Li, Jianchang Liu, Peiqiu Huang, and Huaitao Shi. An R2 Indicator and Decomposition Based Steady-State Evolutionary Algorithm for Many-Objective Optimization. *Mathematical Problems in Engineering*, 2018, 2018. Article number: 1435463.

[93] Ke Li, Kalyanmoy Deb, Qingfu Zhang, and Sam Kwong. An Evolutionary Many-Objective Optimization Algorithm Based on Dominance and Decomposition. *IEEE Transactions on Evolutionary Computation*, 19(5):694–716, October 2015.

[94] Miqing Li, Shengxiang Yang, and Xiaohui Liu. Shift-Based Density Estimation for Pareto-Based Algorithms in Many-Objective Optimization. *IEEE Transactions on Evolutionary Computation*, 18(3):348–365, June 2014.

[95] Miqing Li and Xin Yao. Quality evaluation of solution sets in multiobjective optimisation: A survey. *ACM Computing Surveys*, 52(2):26:1–26:38, March 2019.

[96] Wenwen Li, Ender Özcan, Robert John, John H. Drake, Aneta Neumann, and Markus Wagner. A Modified Indicator-Based Evolutionary Algorithm (mIBEA). In *2017 IEEE Congress on Evolutionary Computation (CEC'2017)*, pages 1047–1054, San Sebastián, Spain, June 5-8 2017. IEEE Press. ISBN 978-1-5090-4601-0.

[97] Arnaud Liefooghe and Bilel Derbel. A Correlation Analysis of Set Quality Indicator Values in Multiobjective Optimization. In *2016 Genetic and Evolutionary Computation Conference (GECCO'2016)*, pages 581–588, Denver, Colorado, USA, 20-24 July 2016. ACM Press. ISBN 978-1-4503-4206-3.

[98] Antonio López Jaimes and Carlos A. Coello Coello. Study of Preference Relations in Many-Objective Optimization. In *2009 Genetic and Evolutionary Computation Conference (GECCO'2009)*, pages 611–618, Montreal, Canada, July 8–12 2009. ACM Press. ISBN 978-1-60558-325-9.

[99] Francisco Luna, Gustavo R. Zavala, Antonio J. Nebro, Juan J. Durillo, and Carlos A. Coello Coello. Solving a Real-World Structural Optimization Problem With a Distributed SMS-EMOA Algorithm. In *2013 Eighth International Conference on P2P, Parallel, Grid, Cloud and Internet Computing (3PGCIC)*, pages 600–605, Compiègne, France, October 28-30 2013. IEEE Computer Society Press.

[100] Edgar Manoatl Lopez and Carlos A. Coello Coello. IGD$^+$-EMOA: A Multi-Objective Evolutionary Algorithm based on IGD$^+$. In *2016 IEEE Congress on Evolutionary Computation (CEC'2016)*, pages 999–1006, Vancouver, Canada, 24-29 July 2016. IEEE Press. ISBN 978-1-5090-0623-9.

[101] Edgar Manoatl Lopez and Carlos A. Coello Coello. An Improved Version of a Reference-Based Multi-Objective Evolutionary Algorithm based on IGD+. In *2018 Genetic and Evolutionary Computation Conference (GECCO'2018)*, pages 713–720, Kyoto, Japan, July 15–19 2018. ACM Press. ISBN: 978-1-4503-5618-3.

[102] Kent McClymont and Ed C. Keedwell. Markov Chain hyper-Heuristic (MCHH): an Online Selective Hyper-Heuristic for Multi-Objective Continuous Problems. In *2011 Genetic and Evolutionary Computation Conference (GECCO'2011)*, pages 2003–2010, Dublin, Ireland, July 12-16 2011. ACM Press.

[103] Adriana Menchaca-Mendez and Carlos A. Coello Coello. A New Selection Mechanism Based on Hypervolume and its Locality Property. In *2013 IEEE Congress on Evolutionary Computation (CEC'2013)*, pages 924–931, Cancún, México, 20-23 June 2013. IEEE Press. ISBN 978-1-4799-0454-9.

[104] Adriana Menchaca-Mendez and Carlos A. Coello Coello. GD-MOEA: A New Multi-Objective Evolutionary Algorithm Based on the Generational Distance Indicator. In António Gaspar-Cunha, Carlos Henggeler Antunes, and Carlos Coello Coello, editors, *Evolutionary Multi-Criterion Optimization, 8th International Conference, EMO 2015*, pages 156–170. Springer. Lecture Notes in Computer Science Vol. 9018, Guimarães, Portugal, March 29 - April 1 2015.

[105] Adriana Menchaca-Mendez and Carlos A. Coello Coello. GDE-MOEA : A New MOEA based on the Generational Distance indicator and ϵ-dominance. In *2015 IEEE Congress on Evolutionary Computation (CEC'2015)*, pages 947–955, Sendai, Japan, 25-28 May 2015. IEEE Press. ISBN 978-1-4799-7492-4.

[106] Adriana Menchaca-Mendez and Carlos A. Coello Coello. An Alternative Hypervolume-Based Selection Mechanism for Multi-Objective Evolutionary Algorithms. *Soft Computing*, 21(4):861–884, February 2017.

[107] Adriana Menchaca-Mendez, Carlos Hernández, and Carlos A. Coello Coello. Δ_p-MOEA: A New Multi-Objective Evolutionary Algorithm Based on the Δ_p Indicator. In *2016 IEEE Congress on Evolutionary Computation (CEC'2016)*, pages 3753–3760, Vancouver, Canada, 24-29 July 2016. IEEE Press. ISBN 978-1-5090-0623-9.

[108] Kaisa Miettinen. *Nonlinear Multobjective Optimization*. Kluwer Academic Publishers, Boston, 1999.

[109] Eneko Osaba, Javier Del Ser, Antonio J. Nebro, Ibai La na, Miren Nekane Bilbao, and Javier J. Sanchez-Medina. Multi-Objective Optimization of Bike Routes for Last-Mile Package Delivery with Drop-Offs. In *2018 21st International Conference on Intelligent Transportation Systems (ITSC'2018)*, pages 865–870, Maui, Hawaii, USA, 4-7 November 2018. IEEE.

[110] Miriam Pescador-Rojas, Raquel Hernández Gómez, Elizabeth Montero, Nicolás Rojas-Morales, María-Cristina Riff, and Carlos A. Coello Coello. An Overview of Weighted and Unconstrained Scalarizing Functions. In Heike Trautmann, Günter Rudolph, Kathrin Klamroth, Oliver Schütze, Margaret Wiecek, Yaochu Jin, and Christian Grimme, editors, *Evolutionary Multi-Criterion Optimization, 9th International Conference, EMO 2017*, pages 499–513. Springer. Lecture Notes in Computer Science Vol. 10173, Münster, Germany, March 19-22 2017. ISBN 978-3-319-54156-3.

[111] Dung H. Phan and Junichi Suzuki. Boosting Indicator-Based Selection Operators for Evolutionary Multiobjective Optimization Algorithms. In *2011 IEEE 23rd International Conference on Tools with Artificial Intelligence (ICTAI'2011)*, pages 276–281, Boca Raton, Florida, USA, 7-9 November 2011. IEEE Computer Society Press. ISBN 978-1-4577-2068-0.

[112] Dung H. Phan, Junichi Suzuki, and Isao Hayashi. Leveraging Indicator-Based Ensemble Selection in Evolutionary Multiobjective Optimization Algorithms. In *2012 Genetic and Evolutionary Computation Conference (GECCO'2012)*, pages 497–504, Philadelphia, USA, July 2012. ACM Press. ISBN: 978-1-4503-1177-9.

[113] Cynthia A. Rodríguez Villalobos and Carlos A. Coello Coello. A New Multi-Objective Evolutionary Algorithm Based on a Performance Assessment Indicator. In *2012 Genetic and Evolutionary Computation Conference (GECCO'2012)*, pages 505–512, Philadelphia, USA, July 2012. ACM Press. ISBN: 978-1-4503-1177-9.

[114] Günter Rudolph, Heike Trautmann, Soumyadip Sengupta, and Oliver Schütze. Evenly Spaced Pareto Front Approximations for Tricriteria Problems Based on Triangulation. In Robin C. Purshouse, Peter J. Fleming, Carlos M. Fonseca, Salvatore Greco, and Jane Shaw, editors, *Evolutionary Multi-Criterion Optimization, 7th International Conference, EMO 2013*, pages 443–458. Springer. Lecture Notes in Computer Science Vol. 7811, Sheffield, UK, March 19-22 2013.

[115] Ruhul Sarker and Carlos A. Coello Coello. Assessment Methodologies for Multiobjective Evolutionary Algorithms. In Ruhul Sarker, Masoud Mohammadian, and Xin Yao, editors, *Evolutionary Optimization*, pages 177–195. Kluwer Academic Publishers, New York, February 2002. ISBN 0-7923-7654-4.

[116] Hiroyuki Sato, Hernán E. Aguirre, and Kiyoshi Tanaka. Controlling Dominance Area of Solutions and Its Impact on the Performance of MOEAs. In Shigeru Obayashi, Kalyanmoy Deb, Carlo Poloni, Tomoyuki Hiroyasu, and Tadahiko Murata, editors, *Evolutionary Multi-Criterion Optimization, 4th International Conference, EMO 2007*, pages 5–20, Matshushima, Japan, March 2007. Springer. Lecture Notes in Computer Science Vol. 4403.

[117] John David Schaffer. *Multiple Objective Optimization with Vector Evaluated Genetic Algorithms*. PhD thesis, Vanderbilt University, Nashville, Tennessee, USA, 1984.

[118] Oliver Schütze, Xavier Esquivel, Adriana Lara, and Carlos A. Coello Coello. Using the Averaged Hausdorff Distance as a Performance Measure in Evolutionary Multiobjective Optimization. *IEEE Transactions on Evolutionary Computation*, 16(4):504–522, August 2012.

[119] Ke Shang, Hisao Ishibuchi, Min-Ling Zhang, and Yiping Liu. A New R2 Indicator for Better Hypervolume Approximation. In *2018 Genetic and Evolutionary Computation Conference (GECCO'2018)*, pages 745–752, Kyoto, Japan, July 15–19 2018. ACM Press. ISBN: 978-1-4503-5618-3.

[120] N. Srinivas and Kalyanmoy Deb. Multiobjective Optimization Using Nondominated Sorting in Genetic Algorithms. *Evolutionary Computation*, 2(3):221–248, Fall 1994.

[121] Yanan Sun, Gary G. Yen, and Zhang Yi. IGD Indicator-Based Evolutionary Algorithm for Many-Objective Optimization Problems. *IEEE Transactions on Evolutionary Computation*, 23(2):173–187, April 2019.

[122] K.C. Tan, T.H. Lee, and E.F. Khor. Evolutionary Algorithms for Multi-Objective Optimization: Performance Assessments and Comparisons. *Artificial Intelligence Review*, 17(4):253–290, June 2002.

[123] Lothar Thiele. Indicator-based selection. In Janusz Kacprzyk and Witold Pedrycz, editors, *Springer Handbook of Computational Intelligence*, chapter 48, pages 983–994. Springer, Berlin, Germany, 2015. ISBN 978-3-662-43504-5.

[124] Y. Tian, X. Zhang, R. Cheng, and Y. Jin. A multi-objective evolutionary algorithm based on an enhanced inverted generational distance metric. In *2016 IEEE Congress on Evolutionary Computation (CEC'2016)*, pages 5222–5229. IEEE Press, July 2016.

[125] Ye Tian, Ran Cheng, Xingyi Zhang, Fan Cheng, and Yaochu Jin. An Indicator-Based Multiobjective Evolutionary Algorithm with Reference Point Adaptation for Better Versatility. *IEEE Transactions on Evolutionary Computation*, 22(4):609–622, August 2018.

[126] Ye Tian, Ran Cheng, Xingyi Zhang, and Yaochu Jin. PlatEMO: A MATLAB Platform for Evolutionary Multi-Objective Optimization. *IEEE Computational Intelligence Magazine*, 12(4):73–87, November 2017.

[127] Ye Tian, Ran Cheng, Xingyi Zhang, Miqing Li, and Yaochu Jin. Diversity Assessment of Multi-Objective Evolutionary Algorithms: Performance Metric and Benchmark Problems. *IEEE Computational Intelligence Magazine*, 14(3):61–74, August 2019.

[128] Heike Trautmann, Günter Rudolph, Christian Dominguez-Medina, and Oliver Schütze. Finding Evenly Spaced Pareto Fronts for Three-Objective Optimization Problems. In Oliver Schütze, Carlos A. Coello Coello, Alexandru-Adrian Tantar, Emilia Tantar, Pascal Bouvry, Pierre Del Moral, and Pierrick Legrand, editors, *EVOLVE - A Bridge between Probability, Set Oriented Numerics, and Evolutionary Computation II*, pages 89–105. Springer, Advances in Intelligent

Systems and Computing Vol. 175, Berlin, Germany, 2012. ISBN 978-3-642-31519-0.

[129] Anupam Trivedi, Dipti Srinivasan, Krishnendu Sanyal, and Abhiroop Ghosh. A Survey of Multiobjective Evolutionary Algorithms Based on Decomposition. *IEEE Transactions on Evolutionary Computation*, 21(3):440–462, June 2017.

[130] Tamara Ulrich, Johannes Bader, and Eckart Zitzler. Integrating Decision Space Diversity into Hypervolume-Based Multiobjective Search. In *Proceedings of the 12th annual conference on Genetic and Evolutionary Computation (GECCO'2010)*, pages 455–462, Portland, Oregon, USA, July 7–11 2010. ACM Press. ISBN 978-1-4503-0072-8.

[131] Dũng H. Phan and Junichi Suzuki. R2-IBEA: R2 Indicator Based Evolutionary Algorithm for Multiobjective Optimization. In *2013 IEEE Congress on Evolutionary Computation (CEC'2013)*, pages 1836–1845, Cancún, México, 20-23 June 2013. IEEE Press. ISBN 978-1-4799-0454-9.

[132] Koen van der Blom, Sjonnie Boonstra, Hèrm Hofmeyer, Thomas Bäck, and Michael T. M. Emmerich. Configuring Advanced Evolutionary Algorithms for Multicriteria Building Spatial Design Optimisation. In *2017 IEEE Congress on Evolutionary Computation (CEC'2017)*, pages 1803–1810, San Sebastián, Spain, June 5-8 2017. IEEE Press. ISBN 978-1-5090-4601-0.

[133] David A. Van Veldhuizen. *Multiobjective Evolutionary Algorithms: Classifications, Analyses, and New Innovations*. PhD thesis, Department of Electrical and Computer Engineering. Graduate School of Engineering. Air Force Institute of Technology, Wright-Patterson AFB, Ohio, USA, May 1999.

[134] David A. Van Veldhuizen and Gary B. Lamont. Genetic Algorithms, Building Blocks, and Multiobjective Optimization. In Annie S. Wu, editor, *Proceedings of the 1999 Genetic and Evolutionary Computation Conference. Workshop Program*, pages 125–126, Orlando, Florida, July 1999.

[135] David A. Van Veldhuizen and Gary B. Lamont. On Measuring Multiobjective Evolutionary Algorithm Performance. In *2000 IEEE Congress on Evolutionary Computation*, volume 1, pages 204–211, Piscataway, New Jersey, July 2000. IEEE Service Center.

[136] Christian von Lücken, Benjamin Baran, and Carlos Brizuela. A survey on multi-objective evolutionary algorithms for many-objective problems. *Computational Optimization and Applications*, 58(3):707–756, July 2014.

[137] Markus Wagner and Frank Neumann. A Fast Approximation-Guided Evolutionary Multi-Objective Algorithm. In *2013 Genetic and Evolutionary Computation Conference (GECCO'2013)*, pages 687–694, New York, USA, July 2013. ACM Press. ISBN 978-1-4503-1963-8.

[138] Handing Wang, Licheng Jiao, and Xin Yao. Two_Arch2: An Improved Two-Archive Algorithm for Many-Objective Optimization. *IEEE Transactions on Evolutionary Computation*, 19(4):524–541, August 2015.

[139] Lyndon While, Lucas Bradstreet, and Luigi Barone. A Fast Way of Calculating Exact Hypervolumes. *IEEE Transactions on Evolutionary Computation*, 16(1):86–95, February 2012.

[140] D. H. Wolpert and W. G. Macready. No free lunch theorems for optimization. *IEEE Transactions on Evolutionary Computation*, 1(1):67–82, April 1997.

[141] Jin Wu and Shapour Azarm. Metrics for Quality Assessment of a Multiobjective Design Optimization Solution Set. *Transactions of the ASME, Journal of Mechanical Design*, 123:18–25, 2001.

[142] Kaifeng Yang, Michael T.M. Emmerich, Rui Li, Ji Wang, and Thomas Bäck. Power Distribution Network Reconfiguration by Evolutionary Integer Programming. In Thomas Bartz-Beielstein, Jürgen Branke, Bogdan Filipič, and Jim Smith, editors, *Parallel Problem Solving from Nature - PPSN XIII, 13th International Conference*, pages 11–23. Springer. Lecture Notes in Computer Science Vol. 8672, Ljubljana, Slovenia, September 13-17 2014.

[143] Shengxiang Yang, Miqing Li, Xiaohui Liu, and Jinhua Zheng. A Grid-Based Evolutionary Algorithm for Many-Objective Optimization. *IEEE Transactions on Evolutionary Computation*, 17(5):721–736, October 2013.

[144] Zhiwei Yang, Michael Emmerich, Thomas Bäck, and Joost Kok. Multi-objective inventory routing with uncertain demand using population-based metaheuristics. *Integrated Computer-Aided Engineering*, 23(3):205–220, 2016.

[145] Gary G. Yen and Zhenan He. Performance Metric Ensemble for Multiobjective Evolutionary Algorithms. *IEEE Transactions on Evolutionary Computation*, 18(1):131–144, February 2014.

[146] Saúl Zapotecas Martínez, Víctor A. Sosa Hernández, Hernán Aguirre, Kiyoshi Tanaka, and Carlos A. Coello Coello. Using a Family of Curves to Approximate the Pareto Front of a Multi-Objective Optimization Problem. In Thomas Bartz-Beielstein, Jürgen Branke, Bogdan Filipič, and Jim Smith, editors, *Parallel Problem Solving from Nature - PPSN XIII, 13th International Conference*, pages 682–691. Springer. Lecture Notes in Computer Science Vol. 8672, Ljubljana, Slovenia, September 13-17 2014.

[147] Qingfu Zhang and Hui Li. MOEA/D: A Multiobjective Evolutionary Algorithm Based on Decomposition. *IEEE Transactions on Evolutionary Computation*, 11(6):712–731, December 2007.

[148] Eckart Zitzler. *Evolutionary Algorithms for Multiobjective Optimization: Methods and Applications*. PhD thesis, Swiss Federal Institute of Technology (ETH), Zurich, Switzerland, November 1999.

[149] Eckart Zitzler, Dimo Brockhoff, and Lothar Thiele. The Hypervolume Indicator Revisited: On the Design of Pareto-compliant Indicator Via Weighted Integration. In Shigeru Obayashi, Kalyanmoy Deb, Carlo Poloni, Tomoyuki Hiroyasu, and Tadahiko Murata, editors, *Evolutionary Multi-Criterion Optimization, 4th International Conference, EMO 2007*, pages 862–876, Matshushima, Japan, March 2007. Springer. Lecture Notes in Computer Science Vol. 4403.

[150] Eckart Zitzler, Kalyanmoy Deb, and Lothar Thiele. Comparison of Multiobjective Evolutionary Algorithms: Empirical Results. *Evolutionary Computation*, 8(2):173–195, Summer 2000.

[151] Eckart Zitzler, Joshua Knowles, and Lothar Thiele. Quality Assessment of Pareto Set Approximations. In Jürgen Branke, Kalyanmoy Deb, Kaisa Miettinen, and Roman Slowinski, editors, *Multiobjective Optimization. Interactive and Evolutionary Approaches*, pages 373–404. Springer. Lecture Notes in Computer Science Vol. 5252, Berlin, Germany, 2008.

[152] Eckart Zitzler and Simon Künzli. Indicator-based Selection in Multiobjective Search. In Xin Yao et al., editor, *Parallel Problem Solving from Nature - PPSN VIII*, pages 832–842, Birmingham, UK, September 2004. Springer-Verlag. Lecture Notes in Computer Science Vol. 3242.

[153] Eckart Zitzler, Marco Laumanns, and Stefan Bleuler. A Tutorial on Evolutionary Multiobjective Optimization. In Xavier Gandibleux, Marc Sevaux, Kenneth Sörensen, and Vincent T'kindt, editors, *Metaheuristics for Multiobjective Optimisation*, pages 3–37, Berlin, 2004. Springer. Lecture Notes in Economics and Mathematical Systems Vol. 535.

[154] Eckart Zitzler, Marco Laumanns, and Lothar Thiele. SPEA2: Improving the Strength Pareto Evolutionary Algorithm. In K. Giannakoglou, D. Tsahalis, J. Periaux, P. Papailou, and T. Fogarty, editors, *EUROGEN 2001. Evolutionary Methods for Design, Optimization and Control with Applications to Industrial Problems*, pages 95–100, Athens, Greece, 2001.

[155] Eckart Zitzler, Marco Laumanns, and Lothar Thiele. SPEA2: Improving the Strength Pareto Evolutionary Algorithm. Technical Report 103, Computer Engineering and Networks Laboratory (TIK), Swiss Federal Institute of Technology (ETH) Zurich, Gloriastrasse 35, CH-8092 Zurich, Switzerland, May 2001.

[156] Eckart Zitzler and Lothar Thiele. Multiobjective Optimization Using Evolutionary Algorithms—A Comparative Study. In A. E. Eiben, editor, *Parallel Problem Solving from Nature V*, pages 292–301, Amsterdam, September 1998. Springer-Verlag.

[157] Eckart Zitzler, Lothar Thiele, and Johannes Bader. On Set-Based Multiobjective Optimization. *IEEE Transactions on Evolutionary Computation*, 14(1):58–79, February 2010.

[158] Eckart Zitzler, Lothar Thiele, Marco Laumanns, Carlos M. Fonseca, and Viviane Grunert da Fonseca. Performance Assessment of Multiobjective Optimizers: An Analysis and Review. *IEEE Transactions on Evolutionary Computation*, 7(2):117–132, April 2003.